STABLE ISOTOPE STUDIES IN THE CALEDONIDES OF S.W. CONNEMARA, IRELAND

by

GAWEN RICHARD TREVENEN JENKIN.

Department of Geology,
University of Glasgow.
July 1988.

Thesis submitted for the degree of Doctor of Philosophy.

ACKNOWLEDGEMENTS.

I would like to express my thanks to the following people who have helped me in some way in this research:

Professor Leake, for awarding me the project in the first place, for discussions throughout the project and for his patience during the final stages.

Tony Fallick, Joe Hamilton and Alex Halliday, without whose help and advice (not only geological) I would not have completed this project. I can never thank these three people enough (but I'll have a good go in the Aragon when we've finished the viva).

Tony Fallick is also thanked for his careful critical reading of the manuscript and pointing out some stupid errors. However the responsibility for all the remaining mistakes and tortuous English is all mine. I am grateful to Tony for pointing out the fact that paragraphs are more easily read if they are divided up into sentences and for suggesting that commas would also be a useful addition,,,,,,,,,,,,,,.

All the staff at the Scottish Universities Research and Reactor Centre who made this research possible. Special thanks to Claire Behan, Alison MacDonald, Julie Gerc, Ward Scott, Adrian Boyce, Fred Cornwallis, Julian Jocelyn (Jos), Andrew Tait, and Fred Cornwallis. Terry Donnely deserves special mention for his tireless work in keeping the lab. running, even if it meant working through his weekend. He is a hero.

The technical staff at Glasgow University Geology Department. George Bruce for his help in the lab and for magicing di-iodomethane up from nowhere. Robert MacDonald and Jim Gallagher for producing the thin sections, not the most exciting job in the world - it was appreciated. Douglas MacLean for preparing the plates and making excellent slides during this project. Bob Cumberland, Roddy Morrison and the secretaries for various things. Eddy and Jimmy for their continuing good humour!

Colin Farrow at GU Geology Department is thanked for his expert instruction in the use of computers, which made much of the data interpretation in this project possible, or at least less tedious.

Adrian Boyce, Yousef Ahmed-Said, Steve Daly, Christian France-Lanord, Rabah Laouar, Bruno Giletti, Colin Graham, Steve Hay, Andy Hogg, Jim Kay, Adrian Park, Neil Reynolds, Mike Russel, Geoff Tanner, John Valley, Mark Wood, Bernie Wood, Bruce Yardley are all thanked for discussions regarding this project at various times and in various places (and in various states of insobriety). Peter Haughton is especially thanked for his continuing interest and advice throughout the project.

Pete Harvey, Tim Brewer and the late Dennis Field of the department of Geology at Nottingham, for their altruistic teaching of geology during my degree.

Geoff Pooley (P) and Bob Quixley (Q) at the Penwith Sixth Form College for teaching me my early geology so well, with good humour throughout.

Chris Goninan at the Humphry Davy Grammar School for beating (literally) the fundamentals of chemistry into me. Colin Woolcock for his brilliant chemistry teaching at the Penwith Sixth Form College.

Phyllis, Tom and Dara O'Donoghue from Sunset Cottage, Cashel. For feeding me, drying me out and putting up with me during my stays in Connemara. Mortin Neagh for the trick with the Mr Sheen. Mark Wood was a superb field assistant in February '87 - thanks again.

My friends, especially Gill Whelan, Mark Wood, Chris Clough, Adrian Park, The Haughtons, Jo Ratchford and Tony Dixon, Christa Sawyer and Graeme Waller for doing various friendly things.

Gill Whelan and Lisa Haughton for typing some of the manuscript. Gill for sticking together the triangular diagrams.

Guinness, Primo Levi, Douglas Adams - for inspiration.

Martin Jagger, E. Elias, Prof. Leake and Geoff Tanner for providing me with additional samples.

NERC for a grant to do this project, the DHSS for continuing the funding without too much hassle. My parents and my late Grandmother Dorothy Trevenen are thanked for additional monetary support.

Katherine Young and the other staff at the Hunterian Museum who allowed me access to their Laserprinter at the last minute. Help from Simon George, Steve Hay and Mark Wood in the last few days has helped enormously.

Anyone else I have omitted.

And finally my family Mum, Dad, Morwenna, Loveday and Conan for - well for being my family! Thats a good enough reason isn't it? Love to you all.

Dedication.

This thesis is dedicated to the memory of my very dear late Grandmother

Dorothy Kathleen Trevenen

who died during the period of this research.

Declaration.

The material presented in this thesis is the result of research carried out between August 1984 and July 1988 in the Department of Geology, University of Glasgow, under the supervision of Professor B. E. Leake.

This thesis is based on my own independent research and any published or unpublished material used by me has been given full acknowledgement in the text.

Gawen Jenkin
July, 1988.

TABLE OF CONTENTS

FIGURES.

TABLES.

PLATES.

MAPS

Maps 1. and 2. are located in the pocket at the back of this thesis.

THERMODYNAMIC TERMS

Δ change of a property for a balanced reaction = (sum of properties of products) -(sum of properties of reactants). Typed bold to distinguish from isotopic Δ.

μ chemical potential of the end member(s) in the phase(s) concerned

G Gibbs energy

G° standard Gibbs energy, the standard state being some specified temperature, pressure and composition of the phase(s) concerned.

K the equilibrium constant of the reaction as written, which is the ratio of activities^n of products/reactants. (n = coefficients in reaction as written) typed bold to distinguish from Kelvin.

ρ density

V volume

S entropy

T temperature (in degrees Kelvin - K)

P pressure (in kbar)

R the universal gas constant R = 8.31441 $Jmol^{-1}K^{-1}$

[ ] concentration of a phase or end member

ISOTOPIC TERMS

δ the isotopic composition of a sample (see 2.3.1)

α the isotopic fractionation factor (see 2.3.2)

Δ_{x-y} the difference in δ values between two phases x and y

A A coefficient in the fractionation equation (see 2.4.3) unless stated otherwise.

B B coefficient in the fractionation equation.

DIFFUSION TERMS (see 2.6.3)

E activation energy

D diffusion coefficient, typed bold to distinguish from D for deuterium

D_o diffusion coefficient at infinite temperature

t time

x distance

C concentration

F fraction of approach to equilibrium

β volumetric fluid/mineral ratio

J flux of material (rate of transfer per unit area of a section, units are mass distance^{-2} time^{-1})

OTHERS

dy/dx the derivative of y with respect to x

$\left(\frac{\partial y}{\partial x}\right)_z$ when y = function(x,z) this is the partial derivative of y with respect to x when z is held constant.

$\propto$ is proportional to

UNITS

K temperature in degrees Kelvin (K=°C+273.15)

°C temperature in degrees Centigrade

kb pressure in kilobars

% percent - parts per hundred

‰ permil - parts per thousand

M molarity of a solution in moles dm^{-3} (1000cm^3)

m molality of a solution = n.moles of solute + 1 dm^3 H_2O ≈ molarity.

SUMMARY.

The Dalradian rocks of Connemara, western Ireland, are a sequence of deformed and metamorphosed sediments and basic intrusives and extrusives, which were deposited between the late Pre-Cambrian and the Lower Ordovician. The metamorphic grade increases towards the south, where migmatites are formed adjacent to an elongated belt of meta-igneous rocks (the metagabbro suite - MGS). The MGS was intruded synchronously with the peak of metamorphism and intrusion has been dated at ~490±1 Ma by Jagger *et al.* (1988). The MGS is composed of isolated outcrops of ultrabasic rocks with more voluminous gabbroic rocks and intermediate and acid gneisses. Subsequent to intrusion the MGS together with the Dalradian rocks were thrust southwards on a major thrust plane, the Mannin Thrust at ~460 Ma and were later later intruded by Caledonian granites at ~400 Ma.

The MGS is distinctive in that amphibole (mostly hornblende) is abundant throughout the suite. Some of this hornblende is apparently magmatic in origin, while some is secondary, replacing primary pyroxenes. Throughout the MGS, the Dalradian sequence, and the Caledonian granites, intense retrograde alteration of other primary minerals to secondary (mostly hydrous) minerals is commonly observed: feldspars are often sericitised and saussuritised, biotite is frequently replaced by chlorite and secondary epidote is common. In the MGS this alteration is texturally later than the hornblende formation.

This study makes use of stable isotope data from rocks in S.W. Connemara to constrain a. the origin of the water in the hornblende in the MGS and b.the origin of the fluid which caused the development of the later retrograde minerals.

MGS hornblendes which are thought to be of magmatic origin have $\delta^{18}O$ values of +6 to +8‰ and δD values of -60 to -80‰. Hornblendes which are thought to be of metamorphic origin have a more restricted range in $\delta^{18}O$ (+6.8 to +7.6‰) and δD (-65 to -73‰) values within the range for the magmatic hornblendes. Modelling of the $\delta^{18}O$ and δD ratios of the MGS magma indicates that it probably originated by mixing of a MORB- or OIB-like parental magma with ~20-30 wt.% of crustal material, which was probably mostly partial melt derived from the Dalradian metasediments. This being the case, nearly all the water in the magmatic hornblendes must have ultimately been derived from the Dalradian metasediments. The metamorphic hornblendes were probably formed from residual magmatic fluids from the MGS magma.

The chlorite, epidote and sericite in the MGS were formed as the result of infiltration of these rocks by a high δD (~-25‰), low $\delta^{18}O$ (+7 to +3‰ or lower) fluid. The MGS hornblendes did not equilibrate either oxygen or hydrogen isotopes with this fluid and are believed to have largely preserved their original $\delta^{18}O$ and δD values.

A similar high δD, low $\delta^{18}O$ fluid to that which caused the late alteration in the MGS is found to have caused the formation of chlorite, epidote and sericite throughout the whole of S.W. Connemara, including the Caledonian granites. In all of the rock types examined, the stable isotope data suggest that this high δD, low $\delta^{18}O$ fluid was not present at temperatures much above ~300°C, but continued to be present in these rocks to temperatures as low as 180°C or even lower. This fluid is also inferred to be saline throughout the entire area studied and has a very uniform $H_2O/(H_2O+CO_2)$ ratio of 0.98-0.987. It is inferred that the formation of chlorite, epidote and sericite took place during a single event in all rock types as the result of the infiltration of the whole area by a surface derived fluid. Occasional examples occur of rocks in which secondary minerals must have equilibrated with fluids with a $\delta^{18}O$ significantly <0‰, which together with the very uniform δD values of ~-20 to -25‰ measured or inferred for this fluid, is taken to indicate that this fluid was of meteoric origin.

It is suggested that the infiltration of meteoric fluid into this area took place as the result of the development of one or more meteoric convection system(s) caused by the thermal anomalies of the Caledonian granites. Convection probably took place soon after emplacement of these granites, but might have taken place as late as 300 Ma.

I would watch the buds swell in the spring, the mica glint in the granite, my own hands, and I would say to myself: "I will understand this, too, I will understand everything, but not the way *they* want me to. I will find a shortcut, I will make a lock-pick, I will push open the doors.".....

..... Enrico was in a bad mood and doubted everything. "Who says that it's actually hydrogen and oxygen?" he said to me rudely. "And what if there's chlorine? Didn't you put in salt?"

The objection struck me as insulting: How did Enrico dare to doubt my statement? I was the theoretician, only I: he, although the proprietor of the lab (to a certain degree, and then only second hand), indeed, precisely because he was in the position to boast of other qualities, should have abstained from criticism. "Now we shall see," I said: I carefully lifted the cathode jar and, holding it with its open end down, lit a match and brought it close. There was an explosion, small but sharp and angry, the jar burst into splinters, and there remained in my hand, as a sarcastic symbol, the glass ring of the bottom.

We left, discussing what had occurred. My legs were shaking a bit; I experienced retrospective fear and at the same time a kind of foolish pride, at having confirmed a hypothesis and having unleashed a force of nature. It was indeed hydrogen therefore: the same element that burns in the sun and stars and from whose condensation the universes are formed in eternal silence.

From "Hydrogen", a short story in
"The Periodic Table" by Primo Levi.

CHAPTER 1.

INTRODUCTION AND GEOLOGY

1.1 INTRODUCTION.

The purpose of this chapter is to outline the problems which this thesis attempts to examine and to describe the features of the geology of Connemara which are relevant to these problems.

1.2 THE AIMS OF THIS STUDY.

The lower Ordovician metagabbros and orthogneisses of Connemara are distinctive in that they contain abundant amphibole, some of which is apparently magmatic in origin, while much appears to be secondary after primary pyroxenes. In addition, numerous workers when describing these and other rocks of various ages from Connemara have noted that intense secondary alteration can be observed in many of these rocks: feldspars are commonly observed to be sericitised and saussuritised, primary biotite is frequently partially or totally replaced by chlorite, secondary epidote is common and secondary carbonate, prehnite, pumpellyite, talc and serpentine minerals have also been observed.

Neglecting the magmatic amphibole, such features are indicative of reaction of the rocks with hydrous fluids at temperatures at, or below, their peak temperatures, a process which may be termed retrograde hydration. Compared with the number of studies of fluid-rock interaction during prograde or peak grade metamorphism, studies of retrograde hydration are notably scarce, although petrographic evidence that such a process has taken place is abundant in many igneous and high grade metamorphic rocks.

The aims of this study are to attempt to use stable isotope geochemistry to investigate a. the origin of the water in the hornblende in the Lower Ordovician intrusives, and b. the cause(s) of the retrograde hydration event(s) in Connemara. Stable isotope measurements are well suited for investigating these aims, since as well as indicating the ultimate origin of the light stable elements in a rock, they can also potentially yield information with regard to the temperature, duration and fluid/rock ratio of an interaction event.

1.3 REGIONAL GEOLOGY.

The Connemara Massif is a Dalradian inlier on the W coast of Ireland. The inlier is unconformably overlain to the N by U. Llandoverian sediments (McKerrow and Campbell, 1960) and to the E by lower Carboniferous limestones (S evastopulo, 1981) see map 1.

1.3.1 Dalradian sequence.

The oldest Dalradian rocks in Connemara are marbles and metapelites of the Blair Atholl subgroup (Upper Appin group - Lower Dalradian) which are exposed in the core of the Connemara Antiform (map 1). The rocks are overlain by a Middle Dalradian (Argyll Group) sequence comprising tillite, quartzites, semipelites, pelites, marbles and amphibolites which can easily be correlated with the other Dalradian successions (Harris and Pitcher, 1975). Outcrops of Upper Dalradian (Southern Highland Group) psammitic wackes occur in NE Connemara.

According to Harris and Pitcher (*ibid.*) the Upper Precambrian (Vendian) - Cambrian boundary lies somewhere within the Middle Dalradian while the Cambro - Ordovician boundary is probably later than Upper Dalradian.

The metamorphic grade of most of the Connemara Dalradian is anomalously high compared to much of the Dalradian elsewhere. In general the metamorphic grade of the Dalradian succession increases southwards from garnet zone in the NW through staurolite zone, sillimanite + muscovite zone, sillimanite + K-feldspar zone to a migmatite zone in the S. Thus the isograds run approximately east-west, which is parallel to the predominant trend of bedding and major fold axes. The migmatite zone in the S formed adjacent to a major intrusive complex (see below) which probably provided the heat source which caused the southwards increase in grade (Treloar, 1985; Yardley *et al.*, 1987).

The first major phase of deformation in the Dalradian succession was D_2 which produced tight isoclinal folds and the regional schistosity (Leake, 1986). An earlier fabric is preserved in some pre- to syn- D_2 garnets (Leake, 1986; Yardley *et al.*, 1987). Staurolite (rarely with kyanite) grew after D_2 (Yardley *et al.*, 1987). Sillimanite is seen to replace early staurolite. Near to the northern margin of sillimanite this reaction apparently started around the beginning of D_3 but further S in the migmatite zone sillimanite growth largely predated D_3 suggesting a northward progression of the isotherm (Yardley *et al.*, 1987). D_3 also produced tight to isoclinal folds which locally develop a new axial planar fabric. Late D_4 folding produced large open east-west trending folds, of which the largest is the Connemara Antiform (map 1) which brings up the oldest Dalradian between younger material to N and S.

Yardley *et al.* (1987) have proposed that after early staurolite-kyanite zone metamorphism (540-600°C, ~6 kb) there is evidence of uplift prior to the thermal maximum (700-750°C, ~5.5 kb in the migmatites) and Barber and Yardley (1985) have suggested that anatectic melts in the migmatites may not have crystallised (650-700°C) until pressure fell to ~2.5 kb. Yardley *et al.* (1987) suggest on the basis of unpublished Rb-Sr data that closure of Rb-Sr exchange between leucosomes and restite (≡ crystallisation?) took place at ~480 Ma. Higher maximum temperatures (>850°C) were attained in the immediate hornfelses of the basic intrusive masses (Treloar, 1981). Yardley *et al.* (1987) also propose (their fig. 10) that a late prehnite-pumpellyite phase of metamorphism (~350°C, 3 kb) took place at ~455 Ma, presumably related to thrusting in the Delaney dome (see below).

1.3.2 The Metagabbro Suite intrusive complex.

Large volumes of magma were intruded to the S of the migmatite zone in a belt between 2 and 25 km wide which extends east-west at least 80 km from Slyne Head in the W to Galway in the E, where it disappears beneath the Carboniferous cover. The major part of the outcrop occurs to the W of Oughterard (map 1.). Isolated intrusions of similar material form the Currywongaun-Doughruagh and Dawros intrusions (Kanaris-Sotiriou and Angus, 1976; Bennet and Gibb, 1983) which occur in stratigraphically equivalent host rocks on the northern side of the Connemara antiform, indicating that the lateral distribution of this intrusive complex may have been even greater prior to erosion.

The magmatic material varies in composition from isolated outcrops of ultrabasic material, through basic gabbroic rocks to intermediate and acid gneisses. Field relations suggest that differentiation must have taken place at the present level of exposure, but probably also took place at a deeper level. It is supposed that the whole suite developed from a single magmatic episode (Leake pers. comm.) although this is difficult to prove conclusively because the field relationships between the different units have been complicated by contemporaneous deformation. It is assumed here that the whole suite is cogenetic and for convenience the suite will be referred to hereafter as the metagabbro suite (MGS).

It has been suggested (Stillman *et al.*, in Harris, 1984) that the MGS is a tectonically emplaced ophiolite. However in the Cashel district there is clear evidence that the local country rock was assimilated into molten magma (Leake and Skirrow, 1960; Evans, 1964), furthermore dykes of basic material which intrude into the surrounding schists can be recognised in some areas (my field observations) although they have invariably been disrupted by later deformation.

Zircons in the basic rocks from the Cashel district have been U-Pb dated at 510± 10 Ma (Pidgeon, 1969), however Jagger *et al.* (1988) dated zircons from the same outcrop and determined a Pb-Pb age of 490±1 Ma. The more recently determined age is likely to be more reliable, the discrepancy with the older determination can easily be attributed to the poorer analytical techniques and statistical treatment of the data that were used by Pidgeon as well as the change in the decay constants used. Amphiboles from the same sample that was dated by Jagger and from another basic rock yielded K-Ar dates of 486± 9 and 481±9 Ma respectively (Elias, 1985), while two amphiboles from the intermediate gneisses both gave similar K-Ar ages of 478± 10 Ma (*ibid.*). However zircons from acid K-feldspar gneisses in the Cashel area gave a discordant lower intercept U-Pb age of 454^{+16}_{-14} Ma (Jagger *et al.*, 1988) which is difficult to reconcile with the older K-Ar and zircon dates, especially as one of the amphibole-bearing samples was collected <100 m away from the K-feldspar gneiss sample which produced the zircons. It is likely therefore that this young age represents a local disturbance of the system, possibly late Pb loss due to low temperature alteration of the zircon.

According to Leake (1986) the MGS was intruded pre-D_2, while the disruption of early differentiates and back intrusion by later differentiates took place syn-D_2. Foliations in the gneisses were folded by D_3 and later

events (*ibid.*). However, some of the acid members of the MGS are hardly foliated suggesting that they may not have been entirely crystallised during D_3 (Leake, 1978). If this was the case then D_3 probably occurred reasonably soon after D_2 which must have been c. 490-480 Ma according to the age data given above.

1.3.3 The Ballyconneely amphibolite and the Delaney Dome Formation.

In the Delaney Dome area basic rocks of the MGS lying above the contact with the Delaney Dome Formation (DDF) have become converted to highly schistose fine grained, albite-epidote-hornblende amphibolite (the Ballyconneely amphibolite -BA, Leake, 1986) as a result of penetrative shearing. The DDF, which lies beneath the BA is a sequence of highly sheared quartzofeldspathic rocks believed on the basis of chemical data to have originally been acid volcanics (Leake and Singh, 1986). The contact between the BA and the DDF is believed to represent a major tectonic break, the Mannin Thrust (Leake *et al.*, 1983, 1984).

Newly recrystallised hornblende in the BA is lineated NNW which is the same direction as an extension lineation in fibrous quartz in the DDF, indicating that the last movement of the thrust at least occurred in this orientation. From kinematic indicators the direction of thrusting was towards the S (P.W.G. Tanner pers. comm.) and thus the minimum amount of movement on the thrust must be at least 20 km. Leake *et al.* (1983, 1984) pointed out that the Connemara Dalradian lies in anomalous geographical position SSE of the strike continuation of the other Dalradian rocks of Scotland and Ireland and south of the inferred position of the Highland Boundary Fault. They proposed that this anomalous position could be explained if the Connemara massif was carried southwards >50 km on major thrusts represented by the Mannin Thrust and other possible deeper thrusts, together with major strike slip faulting. The latter is required since it seems unlikely that the Connemara massif was thrust over the Ordovician rocks of the South Mayo Trough which lies directly to the N, since they are presently only of pumpellyite or zeolite facies. Nevertheless the Mannin Thrust must represent a major discontinuity.

The rotation of D_3 folds by shearing coupled with the folding of the thrust plane and mineral lineations by open D_4 folds constrains thrusting to be between D_3 and D_4. It is clear that thrusting had terminated by ~400 Ma because the BA is cut in the S by part of the Galway granite, furthermore Leake (1988) states that D_4 must be significantly pre-U. Llandovery (~430 Ma[1]) since Dalradian rocks which are folded by D_4 are overlain by sediments of this age at Tonalee. It has proved difficult to determine a more accurate date for the thrusting. A Rb-Sr whole rock isochron on the mylonitised DDF gave an age of 460± 25 Ma (Leake *et al.*, 1983), although it is questionable whether this age relates to the homogenisation of ^{87}Sr during thrusting. K-Ar dates on the hornblendes in the BA average 455± 10 Ma (Leake *et al.*, 1984), with the oldest sample giving 468±12 Ma. A young age on one

---

[1] The timescale of Harland *et al.* (1982) is used throughout this thesis whenever radiometric dates are related to the stratigraphic timescale.

amphibole demonstrates that some of these dates could have been partially reset towards a later event. From this evidence it seems unlikely that thrusting took place later than 450 Ma despite suggestions to the contrary by Kennan and Murphy (1987).

SSE plunging D_5 folds have been recognised in the southern side of the Delaney Dome (Leake, 1986). Interference of these folds with the D_4 Mannin Antiform probably resulted in the formation of the Delaney Dome structure.

1.3.4 The Oughterard Granite.

Bradshaw *et al.* (1969) emphasised that the Oughterard granite in E Connemara is quite unlike the other granites in Connemara. The granite typically occurs as a number of small disconnected intrusions with irregular boundaries which have no contact aureole. The western body contains abundant partially digested xenoliths of Dalradian lithologies. In places the intrusion of the granite appears to have followed late faults (possibly D_5 Leggo *et al.*, 1966). Petrographically the granite is aphyric and it is very strongly chloritised and sericitised, minor muscovite is present along with rare garnet and hornblende is restricted to one intrusion. The intrusions largely lie in the core of the Connemara Antiform and clearly truncate both D_3 and D_4 folds. The ubiquitous alteration of the granite, the small spread in Rb/Sr ratio and the initial isotopic inhomogeneity due to assimilation have meant that it has been difficult to determine a Rb-Sr intrusion age for this granite. Whole rock Rb-Sr isochrons yield dates between 407 and 532 Ma (Kennan *et al.*, 1987) or 528 and 663 Ma (Leggo *et al.*, 1966) depending on which samples are excluded from the regression line. Undoubtedly the only age which can be truly meaningful is an age of 459± 7 Ma[2] obtained by Leggo *et al.* for a K-feldspar-muscovite-whole rock isochron for one sample. This age reflects the last disturbance of the Rb-Sr system and therefore must be a minimum age of intrusion for the Oughterard granite (Leake, 1988).

1.3.5 The Galway Granite Suite

Apart from the Oughterard granite the other major Caledonian granites of Connemara are the Galway, Omey, Roundstone and Inish granites which are believed to be cogenetic and are collectively referred to as the Galway granites. All the granites in this suite are petrographically and chemically I-type granites (Chappell and White, 1974). These granites all occur in major circular to elliptical bodies with sharp curvilinear contacts and have developed contact aureoles (Leake, 1978). A number of granite, aplite and porphyry dykes and veins genetically related to the granites intrude both the granites and the surrounding country rocks. These granites are clearly post D_5 and any foliation within them can be attributed to flow during crystallisation. Rb-Sr whole rock isochrons determined by Leggo *et al.* (1966) yield ages of 398±1 Ma (Galway), 402±17 Ma (Omey), 409±80 Ma

---

[2] All Rb-Sr dates used in this thesis have been recalculated to be consistent with $\lambda\ Rb^{87} = 1.42 \times 10^{-11}\ y^{-1}$.

(Roundstone) and 418±8 Ma (Inish). Thus the Galway granites correlate in age with the younger granites of Scotland.

1.3.6 Later events.

Mitchell and Mohr (1987) have identified a diffuse swarm of arcuate mainly ENE-NE trending dolerite dykes in Connemara which cut both the Dalradian gneisses and the Galway granite, some of which show evidence of faulting prior to final solidification. Interestingly one dyke terminates against prominent N-S jointing in the Galway granite. Primary minerals in these dykes are commonly altered; plagioclase phenocrysts are strongly saussuritised, epidotised or sericitised; augite is partly chloritised and may also be altered to magnetite, prehnite, pumpellyite or antigorite; olivine is always completely replaced by serpentine and secondary calcite may also be present. The geochemistry of these dykes also reflects the effects of pervasive hydrothermal alteration. Whole rock apparent K-Ar ages for these dykes give a mean value of 247±31 Ma for 14 samples. However a number of groups of ages can be determined which Mitchell and Mohr (1987) suggest are related to more than one post intrusive resetting episode. From a broad inverse correlation between K-Ar age and degree of plagioclase alteration they suggest that the two oldest ages which are concordant at 305 Ma may reflect the age of intrusion (Late Westphalian U. Carboniferous).

At Glengowla, just W of Oughterard, a galena-pyrite-sphalerite-barite-calcite-quartz vein deposit is present in the Dalradian. This deposit was worked for Pb and Zn in the 19th century (Cole, 1922). Two K-Ar ages of clay separates from this vein are concordant at 212±2 Ma (Halliday and Mitchell, 1983). It is not certain whether this date is a time of ore formation or remobilisation of the system, however Mitchell and Halliday suggest that excess argon is not a problem in dating clays and therefore this date can be regarded as a minimum age for the deposit.

Mitchell and Mohr (1986) demonstrate that a number of mostly NE trending Tertiary dolerite dykes are present in Connemara. These dolerites are much less altered than the Carboniferous dykes. Pristine olivine is present in many samples, more altered samples contain zeolite minerals. Whole rock K-Ar ages on these dykes gave apparent ages of 59-27 Ma. Mitchell and Mohr interpret the oldest age (Paleocene-L.Tertiary) as being the emplacement age with the younger ages reflecting various degrees of post emplacement argon loss.

1.3.7 Uplift and thermal history.

Because temperature is such an important factor controlling stable isotope exchange processes (see 2.6) it is important that as much as possible is known about the thermal history of the area.

From K-Ar and Rb-Sr mineral ages Elias *et al.* (1988) show that the Connemara massif was not uplifted as a single block, but that individual blocks moved upwards independently. Cooling rates in S Connemara were found to be an order of magnitude greater than in the N. Elias *et al.* (1988) suggest that simple tilting of the area could not account for this difference.

Instead they propose that after rapid initial uplift and cooling (30°C/Ma) over the whole area at ~480-490 Ma, slower cooling took place until ~460 Ma and ~440 Ma when blocks in central and northern Connemara again underwent rapid uplift producing younger hornblende K-Ar ages in these areas. Biotite K-Ar and Rb-Sr ages (closure temperature 300± 50°C) were found to be approximately 440 Ma over the whole massif suggesting that final uplift took place as a single block at this time. Denudation in the N must have reached the present level at ~430 Ma since the Dalradian in N Connemara is overlain by late Llandoverian sediments (McKerrow and Campbell, 1960).

Later thermal events may also have affected the Connemara massif. Burial beneath 3 km or more of sediments before the end of the Wenlockian ~420 Ma could have allowed reheating of the Connemara block to take place. Elias *et al.* (1988) suggest that young (<425 Ma) biotite and hornblende K-Ar ages from the Dalradian just beneath the Silurian unconformity could reflect this, although the temperature of re-opening of hornblende to Ar (~550°C) could not have been attained in these rocks.

Intrusion of the Galway granite suite may have reheated parts of the Connemara massif. Being by far the largest intrusion the Galway granite might be expected to have the largest thermal aureole. The contact at the western end appears to be a fault and no hornfelsing is apparent (Leake, 1970a, but see 1.4.3) probably because the hornfelsed material was stoped away into the granite as it intruded (B.E. Leake pers. comm.). The contact of the Roundstone granite is also faulted. Leake (1970a) recognises recrystallisation and alteration of surrounding gneisses within 55 m of the contact (but see 1.4.3). A muscovite 2 km from the contact of the Inish granite and a biotite 4 km away both yield anomalously young K-Ar ages near to the intrusion age of the granite (Elias *et al.*, 1988) suggesting that the thermal effects of this granite extend over this distance at least. Contact metamorphic biotite is formed up to 2 km away from the Omey granite (Ferguson and Al-Ameen, 1985). These authors suggest that the temperature gradient in the aureole was very shallow (~80°C/km) because of convective circulation of fluid in the aureole. From the phase assemblages in the aureole and granite they suggest that the inner aureole developed at 2.5 kb. This suggests that a deep cover (~8 km) was present at that time which would require removal at a later date. Unfortunately no geobarometric data exist on the aureoles of any of the other Connemara granites which could corroborate this proposal[†].

The late Carboniferous and the Tertiary dyke events (Mitchell and Mohr, 1987, 1986) must also represent times at which the Connemara massif was heated. Mitchell and Mohr (1987) also identify overprinting on ages from the Carboniferous dykes at 245 and 205 Ma (note that this coincides with the age of the Glengowla mineralisation). According to Mitchell and Mohr (1986) resetting of whole rock ages purely by thermal effects would require

---

[†] Note that Ferguson and Al-Ameen assume that $P_{fluid} = P_{total}$ in their calculations, an assumption which may be incompatible with their proposal of fluid convection in the aureole (see 2.7.6).

temperatures in excess of 300°C, although these temperatures may not be required if the dykes are also undergoing mineralogical alteration (see 2.6). Felsic fractions from the Galway granite have apparent K-Ar ages of 320 to 270 Ma, while mafic fractions have apparent K-Ar ages of 399 to 253 Ma, indicating that overprinting has also taken place away from the dykes.

Upper-Middle Jurassic (or later) heating to >100°C is demonstrated by apatite fission track ages of 155±10 Ma in the Roundstone granite and 178±11 Ma in the Galway granite (Gleadow, 1978). However old (394±20, 378±26 Ma respectively) sphene FT ages for these granites suggest that locally at least heating has not been greater than 300°C since intrusion. An attempt is made to summarise the thermal history of the Cashel-Recess district of southern Connemara in fig. 1.1.

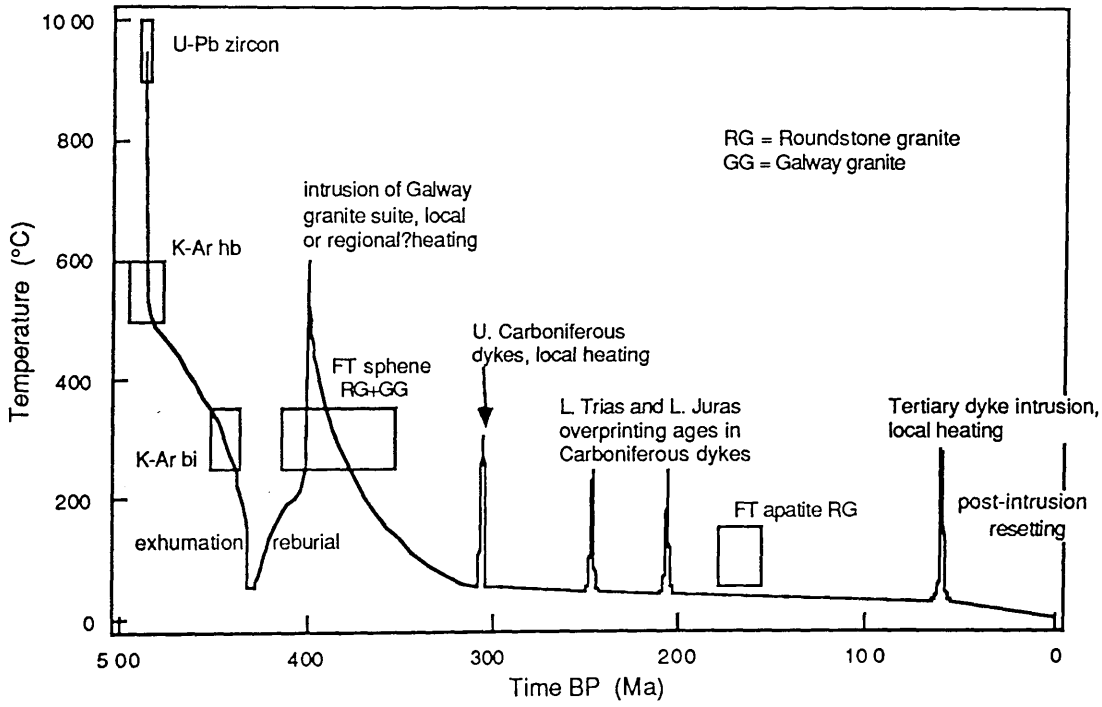

Fig. 1.1 The thermal history of the Cashel-Recess area of SW Connemara. Data sources are given in the text. The scale and magnitude of the heating during the intrusion of the Galway granite suite and later events is largely unknown. The post granite temperature peaks represent maximum regional temperatures, in the proximity of late intrusions temperatures may have been much higher.

1.3.8 Fault movements.

Because faults and shear zones can act as easy pathways for fluid flow (Kerrich *et al.*, 1984) the fracturing history of the Connemara massif is detailed here.

The earliest fault movements are those associated with the post metamorphic uplift of the area (see above) possibly as early as 460 Ma. Thrusting on the Mannin thrust also took place approximately at this time. The NW trending Maam Valley fault system in E Connemara has a movement history extending from the Ordovician to the Tertiary (Dewey and McKerrow, 1963). The NNW fault system running through Clifden and the Delaney Dome may have been initiated syn-D_5 (Leake, 1986) and

continued moving during and after emplacement of the Galway granite, as did major ESE faults at the edge of the Galway granite (Leake *et al.*, 1981 and pers. comm.). Numerous generally NE trending faults are seen to cut the Galway batholith. The Carboniferous dykes are also offset by faulting (Mitchell and Mohr, 1987).

1.4 STUDY AREAS.

In order to study retrograde hydration processes which have taken place in various rock units, possibly at different times, three areas of Connemara were chosen for detailed stable isotope studies. The largest study was carried out in the Cashel-Recess area, where over two months of fieldwork were carried out, during which the field relationships of the hydrous minerals in the Dalradian metasediments and the MGS were examined. An orientation survey was carried out in the second study area, the Delaney Dome, where the relationship of retrograde hydration to major thrusting was examined. Retrograde hydration affecting the Galway granite suite was examined in the Roundstone granite and the NW margin of the Galway granite which together with some rocks from the aureoles of these granites comprise the third study area.

The petrography and field relations of the rock units in each of these areas is described below. Locations and petrographic descriptions of analysed samples are given in A.5. The sample locations are also plotted on map 1.

1.4.1 The Dalradian succession and the Metagabbro Suite in the Cashel-Recess area.

Most of this area is covered by the large scale geological map of Leake (1970a) which is reproduced here (map 2. in pocket). A sample of intermediate gneiss from the MGS near Glinsk to the S of this area is also included in the description.

Dalradian succession.

The metasediments and amphibolites in this area belong to three formations; the Cashel, Lakes Marble and Streamstown Formations (Leake *et al.*, 1981), all of which have been assigned to the Middle Dalradian (Harris and Pitcher, 1985).

Most of the metasediments in this area belong to the Cashel formation which is a monotonous sequence of psammites, semipelites and pelites, with minor bands of calc-silicate and para-amphibolite. Where they have not been hornfelsed adjacent to the MGS the psammites (which Leake 1970a termed siliceous granulites because of their granular texture) generally contain 50-70% quartz, 25-40% sericitised plagioclase (~An_{30}) with 5-10% chloritised biotite and accessory pinitised cordierite, sillimanite, K-feldspar, magnetite, apatite, epidote, carbonate, garnet, hornblende and zircon. Unhornfelsed pelites and semipelites contain higher proportions of chloritised biotite together with sericitised plagioclase (An_{30} or An_{40}), garnet, pinitised cordierite, quartz, sericitised sillimanite and minor orthoclase, magnetite, ilmenite, pyrite, apatite and rare tourmaline (Leake 1970a). In the

field there are complete gradations from psammite through semipelite to pelite and these rock types cannot be mapped as separate units. Leake (1970a) notes that in all these rocks the plagioclase is nearly always completely sericitised and that the biotite where it is altered to chlorite contains leucoxene (TiO_2). He observes that the garnets in these rocks are often fractured and that the fractures, which are often perpendicular to the schistosity, are frequently filled with chlorite or sericite. Orthoclase in these rocks is often rather turbid in thin section (J.018, J.019).

The unhornfelsed semipelites and pelites are either schists or often migmatites with granitic leucosomes (J.018, J.019). The leucosome is generally interpreted as partial melt material which was derived *in situ*. Muscovite is frequently observed in the unhornfelsed Cashel formation in both leucosomes and paleosomes (J.018, J.019; Y. Ahmed-Said pers. comm.) both as fine grained shimmer aggregates and as large flakes. This muscovite is is usually associated with and is possibly replacing orthoclase or sometimes sillimanite or biotite, (muscovite also occurs as sericite replacing plagioclase, but the fine grain size of this sericite suggests that it formed later, at lower temperatures).

Minor bands of calc-silicate and para-amphibolite with crystallised contacts to the psammites and pelites occur throughout the Cashel Formation. According to Leake (1970a) these rocks have diverse mineral assemblages including actinolite schists, clinopyroxene-plagioclase-amphibole rocks and carbonate-phlogopite-actinolite rocks. Leake (1970a) notes that the plagioclase is often completely sericitised and that the biotite or phlogopite is often altering to chlorite, sometimes with prehnite.

Within 500-800 m of the ultrabasic and possibly the basic members of the MGS the rocks of the Cashel Formation show obvious effects of hornfelsing by the intrusion. The limit of hornfelsing by the MGS is rather indistinct, small amounts of cordierite which may have been formed at this time occur at greater distances from the MGS intrusions. The schistosity in the hornfelses has mostly been disrupted by deformation so that they now consist of disorientated lumps of relatively rigid psammitic material (and occasionally ultrabasic material) suspended in a matrix of less rigid pelitic material. The mineralogical changes that take place within the aureole are described by Leake and Skirrow (1960) and Treloar (1985) and are summarised below. Within the psammites and quartz rich semipelites cordierite and decussate biotite develop and the grain size of the quartz increases. The changes in the pelites are more marked with cordierite becoming a major constituent (J3, J.29) often with inclusions of fibrolite. Biotite decreases in abundance in the aureole and new prismatic sillimanite may develop. The regional garnet changes in composition and may become very coarse, while plagioclase becomes more calcic. Within ~15 m of the contact with the ultrabasic rocks garnet becomes unstable and the rock becomes a mixture of cordierite, prismatic sillimanite, magnetite and spinel, while rare corundum may occur. Very little leucosome material is observed in these rocks. Treloar (1981, 1985) suggests that the temperatures reached in these hornfelsed rocks was in excess of 850°C. Leake and Skirrow (1960) and Evans (1964) showed that the hornfelsed rocks differ in both major and trace element composition from the unhornfelsed Cashel formation rocks. These

authors suggested that the chemical changes could be accounted for if a granitic partial melt material has been removed from the hornfelses, so that they now represent the residue from a melting event. Some of this partial melt material may have been segregated into the Cashel microgranite sill (see below).

As with the regionally metamorphosed rocks, minerals in the hornfelsed rocks often exhibit signs of retrograde hydration. Leake and Skirrow (1960) note that cordierite is invariably totally pseudomorphed by pinite (a fine grained intergrowth of chlorite and sericite), sillimanite and plagioclase are sericitised, corundum and spinel are frequently replaced by diaspore (AlO[OH]) and garnet and biotite are chloritised and sericitised (e.g. J.3, J.29).

The Lakes Marble Formation, which is stratigraphically below the Cashel Formation, consists of calcite marbles, quartzites and amphibolites with minor pelites and semipelites. The calcite marbles are mostly calcite (60-90%) with quartz, andesine, diopside, pyrite or pyrrhotite and accessory phlogopite, sphene, K-feldspar, tremolite, apatite, clinozoisite and chlorite (after phlogopite). The band of Lakes Marble Formation which runs S of Cashel Hill, L. Emlagh and L. Emlagheask within the Cashel Formation (interpreted as a major D_2 fold hinge - the Cashel antiform by Leake, 1986) contains very little calcite marble and this lithology is only abundant in the band of Lakes Marble Formation to the north of this study area.

The quartzites in the Lakes Marble Formation contain small amounts of sericitised plagioclase and sometimes orthoclase, along with minor muscovite and chloritised biotite, apatite, zircon and magnetite (Leake, 1970a). The amphibolites have sharp contacts with the surrounding metasediments and from chemical data are most likely to be metamorphosed igneous rocks (Evans and Leake, 1960). They are presumed to represent the highly metamorphosed equivalents of the epidiorites of the Scottish Dalradian. These amphibolites are finely schistose and, in zones of syn-metamorphic movement are often striped leading them to be termed "striped amphibolites" by Evans and Leake (1960) and Leake (1970a). The amphibolites are dominantly hornblende-plagioclase rocks (E.43, GJ.130) with minor clinopyroxene, sphene, epidote, apatite, chlorite, biotite, quartz, carbonate, pyrite and ilmenite (Leake, 1970a). According to this author the plagioclase is frequently sericitised and saussuritised. In GJ.130 sericite alteration in the plagioclase is spatially associated with thin plagioclase-filled microcracks which cross cut the foliation.

The Streamstown Formation is stratigraphically below the Lakes Marble Formation and is present only in the N of the area. This Formation is a well bedded sequence of semipelitic migmatites with leucosomes thought to have been derived by *in situ* partial melting (Treloar, 1985). These rocks also exhibit retrograde hydration, e.g. GJ.238, where plagioclase is altering to sericite, and biotite is replaced by chlorite, TiO_2 and epidote. Note also that this rock contains abundant semi parallel bubble planes (Simmons and Richter, 1976) and microcracks both of which indicate past fluid flow through the sample.

The Cashel microgranite sill.

Leake (1970a) mapped a granitic sill between 3 and 10 m thick and almost 2 km long running within the hornfelsed metasediments along the northern margin of the Cashel Hill metagabbro body. The sill is composed of roughly equal amounts of turbid perthitic microcline, quartz and sericitised albite (An_{10}), with minor chloritised and epidotised biotite, sphene altering to TiO_2 apatite, allanite, ilmenite and pyrite altering to hematite (Leake, 1970a; GJ.11). A number of much smaller sills with similar compositions also occur within the hornfelses (Leake, 1970a). Because of the minimum melt-like composition of these sills and the fact that they are restricted in their occurrence to the hornfelsed metasediments (Leake, 1970a,b) suggests that they may represent segregations of the partial melt material that was removed from the metasediments during hornfelsing (Leake and Skirrow, 1960; Evans, 1964). Leake (1970b) proposed that the large sill also represents a decollement surface within the hornfelses along which the Cashel metagabbro body rotated and moved to the S, thus accounting for the anomalous orientation of the major D_3 synform trace within this body.

The Metagabbro Suite.

Leake (1958) first described rocks of the MGS in this area when he published an account of the ultrabasic and basic bodies around Cashel Hill and to the E of L. Wheelaun, which together he termed the Cashel-L. Wheelaun intrusion. It should be realised however that these bodies represent only the early members of a suite which includes intermediate and acid gneisses, and that they do not represent complete intrusions. In fact the eastern margin of the "L. Wheelaun intrusion" is actually a gradational contact to more acid gneisses. Leake described the intermediate and acid members of this suite in a later communication (1970a). The geology of the area to the south around Glinsk and Gowla was studied by Harvey (1967).

MGS nomenclature.

Rocks of the MGS are a sequence of meta-igneous rocks in which many of the primary minerals have been partially or totally replaced by a variety of secondary minerals, which means that the rocks do not easily fit into available classification schemes. Previous workers who have described the MGS within different parts of the intrusive belt have used a variety of names often based on local (sometimes textural) features to describe different rock units within their area. The result of this is that locally defined rock units may not have exact equivalents in other areas, hindering comparison of rock types over the belt. In addition, Leake's (1970a) use of the term migmatitic in his migmatitic quartz-diorite gneiss unit has caused confusion for some workers, since although it is used correctly as a textural term referring to the mixed (injection gneiss) nature of these rocks, it also can have metamorphic facies connotations.

In order to avoid a further proliferation of local names and to facilitate comparison of the rocks described in this study with those from other areas a simplified classification based solely on mineralogy is used for describing MGS rock units in this thesis. It will be shown that within the Cashel-Recess area these rock units also have distinctive textures, structures and field relationships, but as this may not be the case in other areas these features are

not included as being diagnostic of the rock units. The presence of pyroxene (ortho or clino) or the presence of very calcic plagioclase ($An_{>80}$) is diagnostic of the "ultrabasic" rocks. The "basic" rocks are defined on the presence of amphibole together with the absence of pyroxene and only minor (<5%) quartz. The "intermediate" rocks contain amphibole with significant amounts of quartz (>5%) but only minor K-feldspar (<5%), while the "acid" rocks are defined by the presence of significant amounts of K-feldspar (>5%). The terms ultrabasic, basic, intermediate and acid are used *sensu lato*, although when the rocks described by Leake (1958, 1970a) are grouped according to the classification given above, the vast majority of the SiO_2 contents of the basic, intermediate and acid rocks fall within the appropriate ranges (45-52%, 52-66%, >66% respectively), although many of the rocks which would be classified as ultrabasic have SiO_2 contents of slightly greater than 45%. The terms ultrabasic and basic are used in a similar way to Leake (1958).

Ultrabasic rocks.

As defined above these rocks contain essential pyroxene or calcic plagioclase ($An_{>80}$). Nearly all of the rocks in this group contain both of these minerals. Those rocks which do not contain pyroxene often contain amphibole with pale actinolitic patches which may represent pseudomorphs after pyroxene (see below).

Ultrabasic rocks are relatively uncommon in the Cashel-Recess area. The best examples occur in the Cashel and L.Wheelaun bodies and much of the following description is based on observations from these masses.

The ultrabasic rocks are highly variable in grain size, with groundmass grains varying from <1 mm to 5 mm or more, while oikocrysts may vary in size from several mm to many centimetres in a few rocks. The ultrabasic rocks are dominantly composed of green or brown hornblende, pyroxene and plagioclase, with rare olivine and minor biotite, epidote, quartz, apatite and opaques. The most abundant ultrabasic rock consists of approximately equal amounts of hornblende, pyroxene (usually clinopyroxene) and plagioclase. Hornblende- or pyroxene-rich rocks also occur but plagioclase-rich rocks are less common. Where they do occur the plagioclase-rich rocks generally also contain large amounts of orthopyroxene. In general the hornblende, which is usually brown, appears to be replacing the pyroxenes, olivine and plagioclase. Clinopyroxene crystals are often seen to be intimately replaced by a single hornblende crystal resulting in an intragranular implication texture (GJ.29, plate 1.), suggesting that the growth of the hornblende is being controlled by the pyroxene lattice and probably took place under subsolidus conditions.

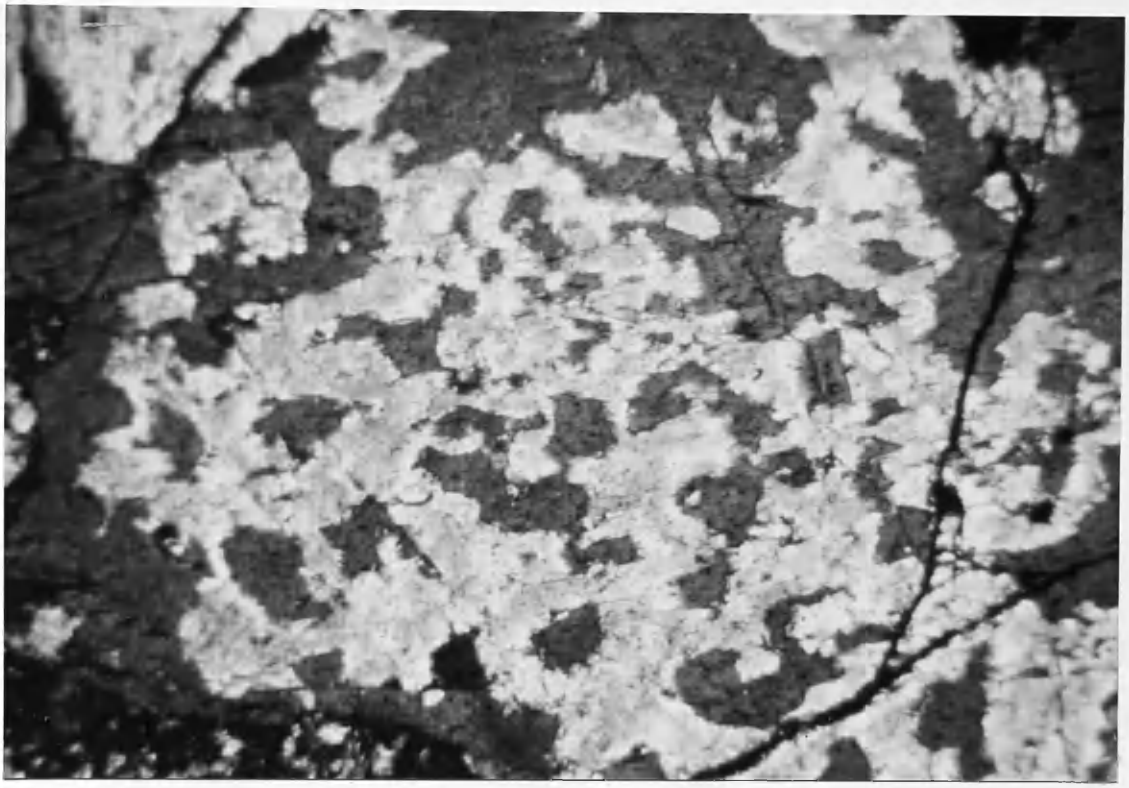

Plate 1. Actinolitic hornblende (brown) forming an intergrowth with clinopyroxene (orange). The hornblende is probably replacing the pyroxene under subsolidus conditions. Sample GJ.29 GR 836.443, L. Wheelaun body. Photograph taken under crossed polars. Width of field is approximately 800μm.

Sometimes the pyroxene twinning can still be observed. Frequently a number of pyroxene, plagioclase and biotite crystals are included in large hornblende oikocrysts, which can sometimes be up to 10 cm long and yet exhibit a good exterior crystal form. The pyroxene and plagioclase inclusions are usually rounded suggesting that they have been partially replaced by the hornblende. The biotite generally has straight edges and may itself be replacing the hornblende. The oikocrystic texture suggests that the hornblende must have grown either within a partially solid crystal mush as a heteradcumulate mineral (Wager *et al.*, 1960) or under subsolidus conditions. Rarely, a single pyroxene crystal with rounded edges may be surrounded by a margin of hornblende (GJ.39). Such a feature could be interpreted as indicating re-equilibration of an early formed crystal in a melt prior to or just after sedimentation, however other hornblendes in the same rock often include more than one pyroxene relic, so that it appears likely that all of the replacement by hornblende occurred within a mush or subsolidus. Within large hornblende oikocrysts, patches free of any inclusions of plagioclase or pyroxene may occur and these are often darker brown than the hornblende adjacent to the pyroxene, so that over lengths of ~200 μm, a faint colour zoning may be seen in places.

In places two generations of amphibole growth can be recognised (plate 2.).

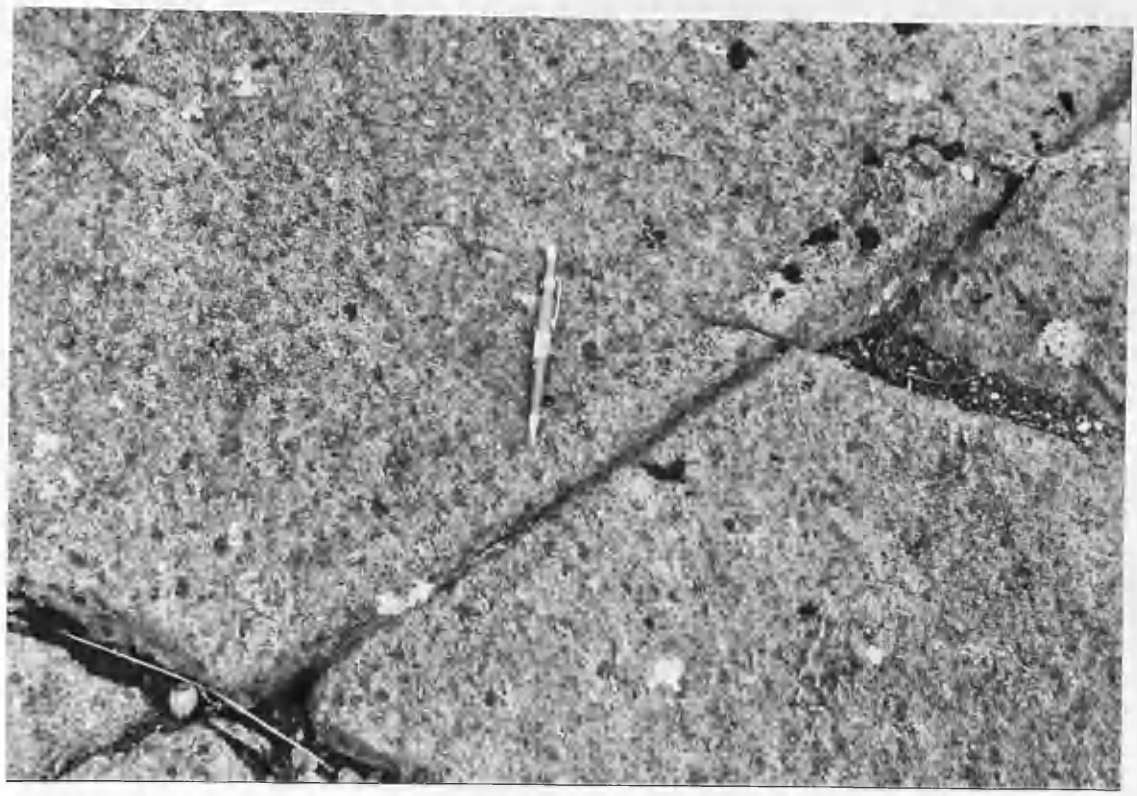

Plate 2. Altered zone (green) around a joint in fresh ultrabasic rock (brown). See text for explanation. Note also the fine epidote vein running from top left to bottom right, these veins cut across the joint and its altered margin. The pencil is 14 cm long. Locality 12. GR 844.450, L. Wheelaun body.

The unaltered rock away from the joint contains oikocrystic brown hornblende approximately 2 cm across which, as described above, appears to be growing at the expense of ortho and clinopyroxene and bytownite. In the unaltered rock these minerals are abundant in the groundmass. However within 3-4 cm of the joint the pyroxenes in the groundmass have been replaced by colourless tremolite with pine green actinolitic rims where it abuts against any remaining plagioclase. The hornblende oikocrysts are still present but the pyroxene inclusions contained within them have also been replaced by tremolite. Biotite which was deep orange in colour and fresh away from the joint is pale and partly prehnitised in the joint margin. The plagioclase, which is altered to clinozoisite throughout, is also partly sericitised near to the joint. This new sericite is unusually coarse with flakes up to 200 μm in diameter. The sericitisation is not usually intense enough to have obscured the twinning in the plagioclase. Thus some actinolitic amphibole may have formed very late, because in other rock types, prehnite may be seen associated with late chlorite.

In ultrabasic rocks without pyroxene (GJ.9) green hornblende may often contain rounded oblong shaped patches of pale fibrous actinolitic amphibole usually with dusty opaque inclusions. The hornblende around these inclusions is often riddled with quartz blebs and large opaque grains. Rather similar textures have been observed in the Glen Scaddle Complex by Mongkoltip and Ashworth (1986) where it is clear that they are the result of the replacement of clinopyroxene. Such an origin for these actinolite patches in the ultrabasic rock hornblendes seems sensible since the very calcic

nature of the plagioclase suggests that they have affinities with the other pyroxene bearing rocks.

Where orthopyroxene (bronzite-hypersthene, Leake, 1958) is present in large amounts, especially in plagioclase rich rocks, the orthopyroxene is often seen to be replaced (sometimes totally) by cummingtonite or anthophyllite (GJ.12).

Olivine is present in the ultrabasic rocks at only a few localities. Typically the olivine bearing rocks contain approximately equal amounts of olivine, orthopyroxene, clinopyroxene and hornblende with minor bytownite, phlogopite and spinel (Leake, 1958). The olivine (Fo_{80-87}, Leake, 1958) occurs as rounded grains which together with the pyroxenes and plagioclase are often enclosed within, and possibly replaced by, oikocrystic hornblende, suggesting that the hornblende grew subsolidus.

Occasionally xenoliths of ultrabasic material are observed within the ultrabasic rocks. Leake (1958) states that they are frequently bytownite-green hornblende rocks, sometimes with orthopyroxene. These xenoliths are usually fine grained with grain sizes less than 1 mm. Layering may rarely be present in the xenoliths. Leake (*ibid.*) suggests that the hornblende is secondary after clinopyroxene.

Some ultrabasic rocks contain large amounts of partially assimilated xenoliths (Leake and Skirrow, 1960). These authors describe the xenoliths as consisting of magnetite, spinel, cordierite, corundum, orthopyroxene and biotite. The cordierite is frequently pinitised, the corundum is altered to diaspore and the xenoliths are often surrounded by a thin zone of saussuritised plagioclase. Leake and Skirrow use chemical data to show that these xenoliths represent the refractory residue which was left when blocks of the Cashel Formation underwent partial melting in the magma. The ultrabasic rocks containing these xenoliths are usually bytownite-biotite rocks with minor garnet, cordierite and sometimes orthopyroxene, and apatite may be abundant (Leake, 1958). Leake describes instances where psammitic blocks have fallen into the magma and melting has taken place to form granitic pegmatites which are locally intrusive into the ultrabasic rocks, forming blocky agamtites. These pegmatites contain minor biotite (now chloritised) and muscovite (J.149).

Veins of fine grained bytownite-hornblende rock (average grain size <0.5 mm, termed ultrabasic aplites by Leake, 1958) cut the ultrabasic rocks in places. According to Leake (1958) pyroxene is absent in these veins so that the hornblende in them probably represents the first appearance of definite magmatic hornblende in the MGS. However the two veins that were sampled in this study (GJ.76, GJ.135) both contain pyroxenes and the hornblende in them appears to be secondary. In one outcrop in the L. Wheelaun mass an ultrabasic vein is cut by granitic veins and nearby both of these veins are displaced by an epidote-quartz bearing shear zone.

Leake (1958) suggests that the clinopyroxenes throughout the ultrabasic rocks are diopsidic. This proposal is supported by microprobe analyses of clinopyroxenes in the MGS in the Errisbeg area to the W of Roundstone by Bremner and Leake (1980) who found that the clinopyroxenes were

diopside/salite. Leake (1958) determined plagioclase compositions in the ultrabasic rocks using an optical method. He found that the vast majority of the plagioclase compositions fall in the range $An_{86\pm4}$. Rarely, more calcic compositions up to An_{97} were also found. Plagioclase compositions with $An_{<80}$ were associated with strong alteration of the plagioclase. These highly calcic compositions have been confirmed by microprobe determinations in the Errisbeg area by Bremner and Leake (1980).

Within the Cashel and L. Wheelaun bodies rare examples of igneous layering may be recognised in the ultrabasic rocks. In the L. Wheelaun body two layers separated by a trough structure has been preserved (plate 3.). The base of the layers is rich in orthopyroxene, opaque grains and hornblende (probably after clinopyroxene) while the proportion of megacrystic plagioclase increases towards the top.

Plate 3. Rhythmic layering within the ultrabasic rocks. Layers are separated by minor scour surfaces a few cm below the base and above the head of the hammer. GR 837.447, L. Wheelaun body.

On the northern side of Cashel Hill sequences of alternating brown and green layers occur (plate 4.).

The main differences between these bands is that the green layers are richer in clinopyroxene and poorer in plagioclase than the brown bands (fig. 1.2). There is little difference in the proportions of the other constituents.

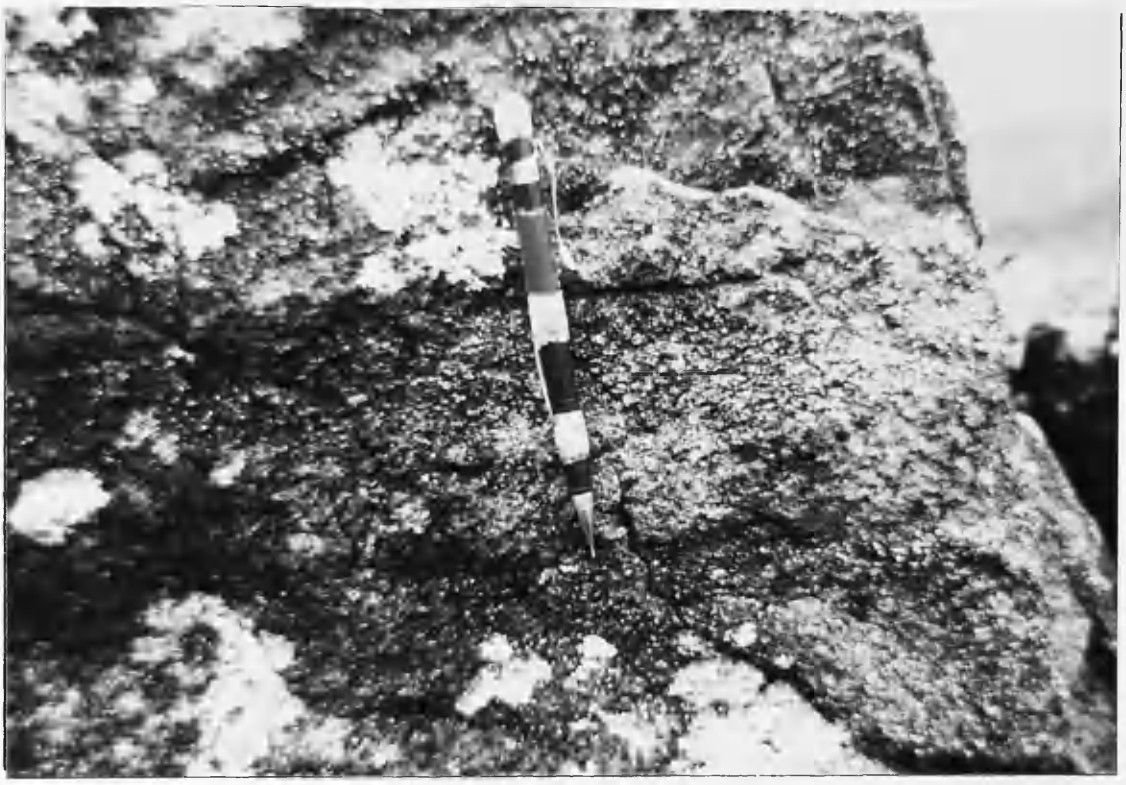

Plate 4. Alternating green and brown layers in ultrabasic rocks on the northern side of Cashel Hill. The pencil is 14 cm long. Locality 42, GR 809.446.

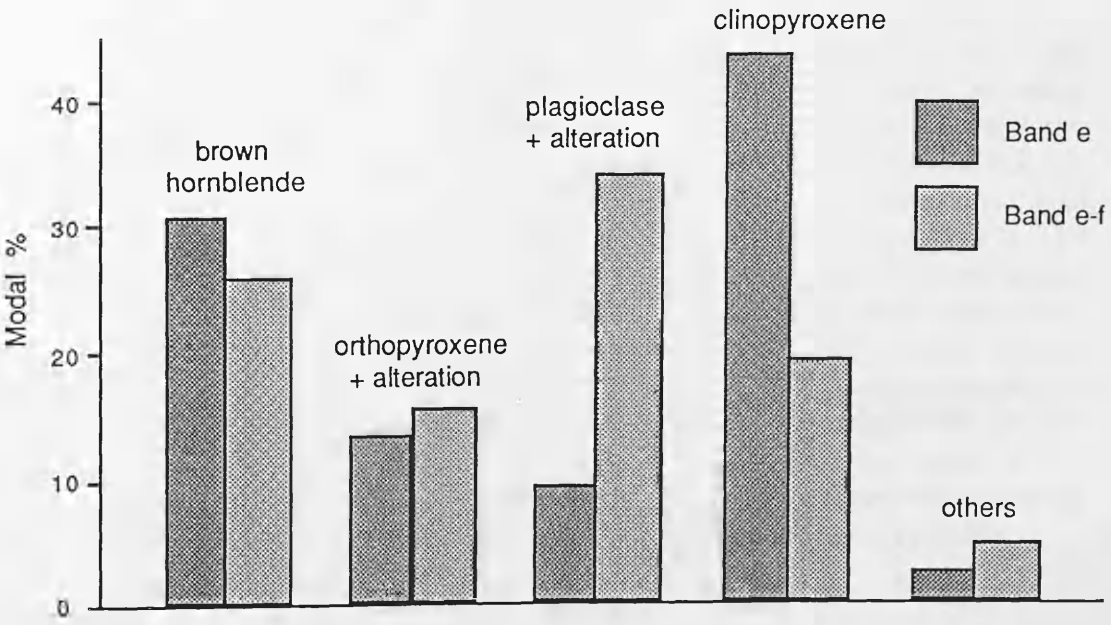

Fig. 1.2 A comparison of the modal analyses of two layers in sample GJ.166 which is shown in plate 4. Band (e) is the lower green layer, while band (e-f) is the brown layer between the two layers. The volume of alteration products of orthopyroxene and plagioclase have been included in the totals for these minerals. This procedure assumes that the volume change attending alteration is relatively small.

In the field the colour of the brown layers appears to be due to surface weathering of the orthopyroxene to produce iron oxides, the colour of which is masked in the green clinopyroxene rich layers. The hornblende is more megacrystic and oikocrystic in the green layers than in the brown layers,

where it is rather evenly disseminated, mostly occurring as rims and intergrowths with the pyroxenes, although it is oikocrystic in places. Thus the hornblende appears to have formed late in both bands and could not have been involved in the formation of the layers. The elongate prismatic orthopyroxenes often show a preferred orientation of their long axes parallel to the layers in these rocks and plagioclase crystals may also show this to a lesser extent. Because of the good preservation of the layers it seems likely that this fabric is not of tectonic origin. Cursory examination of thin sections oriented parallel to the layers suggests that there is no preferred orientation of elongate crystals within this plane. This could be taken to mean either that the crystals were deposited from a static (i.e. non flowing) melt or that they were not formed by a sedimentation mechanism. In one outcrop of ultrabasic rock in the Cashel body small structures reminiscent of sedimentary slump structures were observed.

Throughout the ultrabasic rocks, in addition to the replacement of anhydrous minerals by amphibole and amphibole by biotite, a number of other retrograde hydration reactions can be identified. The bytownite is frequently replaced by fairly coarse clinozoisite, while the biotite or phlogopite is often replaced by prehnite (chlorite after biotite is uncommon, except in the granitic pegmatites enclosed in the ultrabasic rocks). From the textural relationships of the alteration around a joint described above, the formation of clinozoisite may have taken place prior to the prehnitisation of biotite, since clinozoisite is already present in the unaltered rocks. Alternatively clinozoisite could have formed later, replacing fresh and sericitised plagioclase with equal ease. This seems unlikely because the coarseness of the clinozoisite distinguishes it from late saussurite in other MGS plagioclases (see below) and is more indicative of a high temperature origin. Plagioclase is also altered to fine sericite (GJ.29) or to chlorite (GJ.166 band e). Olivine is frequently altered to a mixture of serpentine and magnetite, or (Leake, 1958 suggests) to bowlingite (≈ chlorite+goethite?). The orthopyroxene is always much more altered than than the clinopyroxene and apart from the alteration to cummingtonite-anthophyllite, orthopyroxene is frequently seen to alter to a unidentified orangy brown material (Leake, 1958 reports that orthopyroxene is either decomposed to serpentine-amphibole or serpentine-talc-carbonate mixtures or to bowlingite, but these products have not been observed). In a few rocks (GJ.9) coarse epidote is present, apparently replacing amphibole. Ore minerals may also be altered, in GJ.29 sulphide has rims of what appears to be epidote.

Basic rocks.

The basic rocks are principally plagioclase-hornblende rocks with minor chlorite after biotite, epidote, quartz, magnetite, prehnite, pyrite, pyrrhotite, sphene, apatite and zircon. This rock type is usually medium grained with an average grain size of about 3 mm.

The plagioclase is euhedral-subhedral and commonly forms slightly larger crystals than the hornblende. According to Leake (1958) optical determinations show that nine tenths of the basic rock has plagioclase with An_{55-65}, while the remaining tenth has more basic compositions up to An_{88}. These rocks with calcic plagioclase would be classified as ultrabasic in the classification used here so that nearly all basic rocks will have plagioclases of

An_{55-65}. In comparison to the ultrabasic rocks the plagioclase in the basic rocks is always strongly altered. Fine grained sericite (flakes <20 μm diameter) is always the dominant alteration product, although fine saussurite may also be present. In many rocks the alteration is so intense that the twinning has been obscured.

The hornblende is green in colour and colour zonation is unusual. In these rocks hornblende is rarely oikocrystic, and when it is it contains only plagioclase inclusions (GJ.28). Usually the hornblende forms elongate or tabular grains, containing only very small inclusions of quartz, apatite or opaque material. However the margins of the grains are irregular so that the hornblende is anhedral. The last hornblende growth appears to have been around the edges of the plagioclase grains. Even when the plagioclase shows fairly good crystal form the contacts with the hornblende are always slightly curved, suggesting that minor replacement occurred at a late stage. Nevertheless the fact that the shape of the hornblende was influenced by the adjacent plagioclase grains only during the last stages of its growth suggests that prior to this the crystals may not have been touching, i.e. that they were suspended in a melt. The hornblende in the basic rocks may therefore be of magmatic origin. However the observation of Leake (1970a) of rare clinopyroxene cores in some hornblendes from the intermediate rocks suggests that clinopyroxene may also have been present in these rocks. The hornblende is generally fresh and may contain odd flakes of chlorite with epidote or prehnite which are probably after biotite. It is not possible to say with certainty whether this original biotite is replacing the hornblende or not. However the high concentration of pseudomorphs after biotite around the edges of hornblende grains relative to the rest of the rock indicates that the biotite may have been growing at the expense of the hornblende. The hornblende may also be altering directly to chlorite or epidote, sometimes with minor calcite.

As mentioned above, pseudomorphs of chlorite with epidote or prehnite which are clearly after biotite are common, while fresh biotite is rare. Magnetite is frequently altered along cracks to chlorite.

No layering has been observed in any of the basic rocks. However unlike the ultrabasic rocks the basic rocks are foliated over nearly the whole of their outcrop. Within the Cashel and L. Wheelaun metagabbro bodies the foliation in the basic rocks near to contacts with the hornfelsed sediments or the ultrabasic rocks, is invariably seen to be parallel to the contact and is usually more intense than the foliation away from these contacts. Such features are often seen when a viscous material is deformed around more rigid bodies, and strongly indicate that the foliation is tectonic in origin. Along the western margin of the Cashel body this foliation appears to be folded by the D_3 Cashel Synform of Leake (1970a).

In contrast to the ultrabasic rocks, metasedimentary xenoliths are not present in the basic rocks. Ultrabasic xenoliths are present, although they are rarely small (cms) and are more usually many metres in size. Thus basic rocks are later than the ultrabasic rocks. This is supported by the observation in a few localities that dykes of basic rock can be seen intruding the ultrabasic rocks. Detailed mapping S of L. Wheelaun has shown that there the two rock types may be separated by a thin, highly deformed metasedimentary

screen. The jump in plagioclase compositions and the sudden change in mineralogy between the ultrabasic and basic rocks suggests that the basic rocks are not simple differentiates of the ultrabasic rocks and that they could represent a different magma.

Intermediate rocks.

These have rather similar mineralogies to the basic rocks, but quartz is abundant (10-70%). Plagioclase is present (20-50%), while together chlorite, epidote, hornblende and biotite may form up to 20% of the rock. Accessory apatite, magnetite, pyrite and zircon are present.

The intermediate rocks are medium grained gneisses. Groundmass grains are commonly 2-3 mm across, while plagioclase megacrysts are often 3-5 mm but may be almost 1 cm across in places. A fine grained intermediate gneiss (grain size 1-2 mm) has been identified by Leake (1970a). The gneissose banding is usually caused by an alternation of quartz rich and quartz poor bands.

The plagioclase megacrysts are usually subhedral, the boundaries with the quartz are usually rounded or lobate apparently as the result of replacement of the plagioclase by the quartz. The amphibole is green and forms tabular grains often with small inclusions of apatite, quartz and opaque minerals. The amphibole is sub-anhedral and the margins sometimes partly enclose rather well shaped but small plagioclase grains, although total enclosure by hornblende is rare. Using the same arguments that were put forward for the basic rocks, it might be suggested that this hornblende was initially magmatic, but that the final growth occurred *in situ*, probably subsolidus. However Leake (1970a) notes that very rarely clinopyroxene relics may occur in the cores of some amphiboles, suggesting that they may be secondary after clinopyroxene. Chlorite with epidote or prehnite is commonly observed and as with the basic rocks this mixture is interpreted as being pseudomorphic after biotite, which is rarely seen. Leake (1970a) notes that some of this pseudomorphed biotite has previously replaced hornblende.

Like the basic rocks the intermediate rocks show abundant retrograde hydration reactions. The plagioclase is always altered to fine sericite, often with lesser saussurite. Carbonate may also be present in the altered plagioclase. The twinning is obscured in many rocks. Plagioclase may also be partly replaced by fine dusty opaque material, this has also been noted by Leake (1970a). The hornblende is often directly replaced by epidote. In a few rocks the amphibole has been completely replaced by a mixture of chlorite and carbonate (GJ.35). Magnetite is often nearly totally replaced by chlorite and pyrite may have a rim of hematite. Leake (*ibid.*) also describes opaque material altering to sphene. The quartz is frequently cut by bubble planes containing liquid vapour inclusions. Filled microcracks are also abundant and will be described separately below.

Acid rocks.

The mineralogy of the acid rocks is essentially the same as that of the intermediate rocks with the addition of K-feldspar so that they contain 30-60% plagioclase, 20-45% quartz, 15-25% K-feldspar and 7-15% chlorite and epidote pseudomorphs after biotite (Leake, 1970a). The accessory minerals

are the same as in the intermediate rocks. Hornblende is generally absent, except in the K-feldspar poor varieties, where it is being replaced by biotite (now altered) and quartz.

The acid rocks are medium grained gneisses with K-feldspar megacrysts which are often 10 mm across and may be as large as 20 mm. Within the K-feldspar are abundant rounded inclusions of plagioclase and quartz, indicating that it grew later than these minerals and partly replaced them. The K-feldspar is commonly orthoclase which is inverting to microcline. In thin section the K-feldspar often appears faintly yellow and is rather turbid, although breakdown products are not seen. Small amounts of exsolved sodic feldspar (microperthite strings) are observed. Optical determinations carried out by Leake (1970a) indicate that the plagioclase is usually An_{39-46}. The acid gneisses show similar retrograde hydration reactions to the intermediate rocks, with the possible exception that prehnite does not appear to be present as an alteration product of biotite.

The contacts between the basic and intermediate rocks and between the intermediate and acid rocks are both gradational on a scale of metres in the field. This observation coupled with the relatively continuous increase in sodium content of the plagioclase from basic to acid rocks strongly suggests that these rocks are cogenetic. However Leake (1970a) has shown that a good deal of the intermediate and acid gneisses are migmatitic (injection gneisses) intimately intruding and breaking up bodies of ultrabasic, basic and metasedimentary material. Much of this early material has been metasomatised by material from the the gneisses. According to Leake the ultimate product of this metasomatism is a quartz-plagioclase-biotite gneiss, sometimes with K-feldspar. Thus the gneisses may be polygenetic in origin.

An attempt is made to summarise the mineralogy and alteration sequence of the MGS rocks in the Cashel district in table 1.1.

Microcracks in the MGS.

Throughout the MGS sealed microcracks and larger veins are abundant. These filled microcracks can be very narrow (<5 μm in intergranular microcracks in GJ.16), while the thickest veins may be up to 1 cm wide (excluding the granitic pegmatite veins sometimes seen in the ultrabasic rocks). Most of the transgranular microcracks are between 50 and 100 μm wide. Intragranular microcracks are often seen in plagioclase when fracturing has taken place along cleavage planes, these cracks are frequently infilled by chlorite. The microcracks are not frequently seen to branch. Cross

Table 1.1 (Next page).Summary diagram of the mineralogy and alteration history of the MGS in the Cashel-Recess area. Time correlations between different rock units are rather subjective, but it is likely that the last alteration episode which formed fine sericite and chlorite took place throughout the suite at the same time.

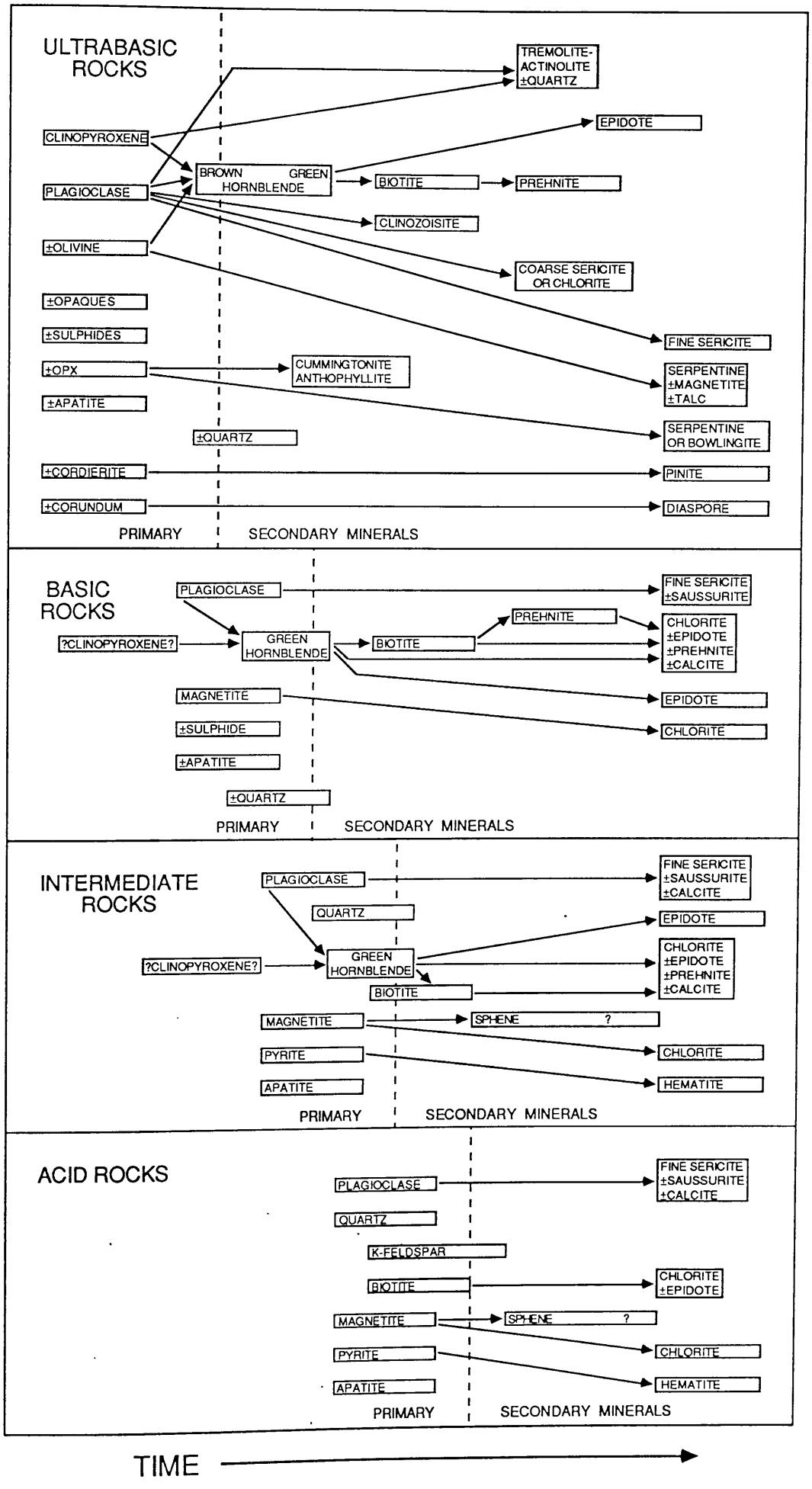
ULTRABASIC ROCKS
CLINOPYROXENE
PLAGIOCLASE
±OLIVINE
±OPAQUES
±SULPHIDES
±OPX
±APATITE
±QUARTZ
±CORDIERITE
±CORUNDUM
BROWN GREEN HORNBLENDE
TREMOLITE-ACTINOLITE ±QUARTZ
EPIDOTE
BIOTITE
PREHNITE
CLINOZOISITE
COARSE SERICITE OR CHLORITE
FINE SERICITE
CUMMINGTONITE ANTHOPHYLLITE
SERPENTINE ±MAGNETITE ±TALC
SERPENTINE OR BOWLINGITE
PINITE
DIASPORE
PRIMARY
SECONDARY MINERALS
BASIC ROCKS
PLAGIOCLASE
?CLINOPYROXENE?
GREEN HORNBLENDE
MAGNETITE
±SULPHIDE
±APATITE
±QUARTZ
BIOTITE
PREHNITE
FINE SERICITE ±SAUSSURITE
CHLORITE ±EPIDOTE ±PREHNITE ±CALCITE
EPIDOTE
CHLORITE
PRIMARY
SECONDARY MINERALS
INTERMEDIATE ROCKS
PLAGIOCLASE
QUARTZ
?CLINOPYROXENE?
GREEN HORNBLENDE
BIOTITE
MAGNETITE
PYRITE
APATITE
FINE SERICITE ±SAUSSURITE ±CALCITE
EPIDOTE
CHLORITE ±EPIDOTE ±PREHNITE ±CALCITE
SPHENE ?
CHLORITE
HEMATITE
PRIMARY
SECONDARY MINERALS
ACID ROCKS
PLAGIOCLASE
QUARTZ
K-FELDSPAR
BIOTITE
MAGNETITE
PYRITE
APATITE
FINE SERICITE ±SAUSSURITE ±CALCITE
CHLORITE ±EPIDOTE
SPHENE ?
CHLORITE
HEMATITE
PRIMARY
SECONDARY MINERALS
TIME

cutting relationships between microcracks are unusual, and when they are observed the fill assemblages of the two microcracks are similar (GJ.226). If more than one microcrack occurs in a slide they are often approximately parallel and may also be parallel to the bubble planes seen in the quartz of the host rock if it is present (GJ.6). Thus the direction of fluid flow in both structures was the same and they are probably genetically related. Some possible primary inclusions can be recognised in the quartz where it occurs in the microcracks.

Listed below are the mineral assemblages that have been observed (so far) in microcracks in the metagabbro suite.

Ultrabasic rocks	Basic rocks
chlorite	chlorite
quartz-calcite	quartz
quartz-calcite-actinolite	actinolite
quartz-cc-ep-chl-plag	quartz-calcite
	quartz-epidote
	actinolite-calcite
	actinolite-plagioclase
	quartz-chlorite-calcite
Intermediate rocks	quartz-chlorite-epidote
calcite	quartz-epidote-plagioclase
epidote	plagioclase-chlorite-actinolite
plagioclase	calcite-epidote-chlorite
quartz	
quartz-calcite	Acid rocks
plagioclase-calcite	quartz
epidote-calcite	K-feldspar-calcite-epidote
epidote-calcite-plagioclase	K-feldspar-plagioclase-epidote
	plagioclase-quartz-epidote

Throughout the MGS there appears to be a general correlation between the density of microcracking, the density of bubble planes in the host rock quartz (if present) and the intensity of the chloritisation of biotite or the sericitisation of plagioclase, strongly implying that all these features are related.

1.4.2 The Delaney Dome area.

This area has recently been described by Leake (1986), who also gives detailed geological maps of the area. Much of the following description of the area is derived from this paper.

The Delaney Dome Formation (DDF).

The DDF is a homogeneous sequence of fine grained, highly siliceous quartzofeldspathic rocks (Leake, 1986; Leake and Singh, 1986). According to Leake (1986) no structures that pre date the shearing have been identified. Typically these rocks are composed of 60-70% quartz, 10-20% orthoclase, 10% plagioclase (An_{10}) and 5% muscovite plus chlorite with accessory magnetite, epidote, sulphides and carbonate (Leake and Singh, 1986). The feldspars may

sometimes be present as megacrysts which may be relict phenocrysts (Leake, 1986). Leake and Singh (1986) note that the feldspars are often completely sericitised and saussuritised, that some of the chlorite may be secondary after biotite (some may be primary) and that where rare garnet occurs it is partially chloritised. Thus retrograde hydration has taken place in this formation. The calcite which is described as late may also be a retrogression mineral.

Within the DDF are numerous metabasic bodies (map 1.) composed of Mg-rich hornblende and highly saussuritised and sericitised plagioclase (GJ.206; Leake, 1986). Leake (*ibid.*) shows that these amphibolites are chemically distinct from the Ballyconneely amphibolite (BA) and notes that they are rather massive and usually much less foliated than either the BA or the enclosing DDF, although the margins of the bodies often possess the shear foliation that is present within the DDF. Thus it is clear that these basic bodies had been intruded before the last movement on the Mannin Thrust. Whether these bodies were intruded and amphibolitised during thrusting, or were present as a set of intrusives or extrusives in the DDF prior to thrusting has not been ascertained.

The Ballyconneely Amphibolite (BA).

This is a fine grained highly schistose albite-epidote-hornblende rock. Minor quartz is ubiquitous and accessory pyrite, sphene and zircon are present (Bremner, 1977). This author notes that biotite occurs very rarely along cleavage planes in the amphiboles (presumably replacing it), while the pyrite crystals may be mantled by hematite. The plagioclase is heavily sericitised and saussuritised and Bremner (*ibid.*) found this alteration to be so intense in the south that it was impossible to determine the composition. Using a microprobe Leake (1986) found that many samples contain a wide range in plagioclase compositions on a thin section scale. He states that the most calcic plagioclases have compositions of An_{40-50} but that these are rare and that more samples contain An_{20}, rather more An_{12-15}, while most samples contain An_{1-5}.

On the western, southern and eastern margins of the BA there is a completely gradational contact with the overlying basic rocks of the MGS which gradually become progressively more schistose and fine grained, typically over a horizontal distance of 100 m. On the northern margin the amphibolite is separated by a thrust from intermediate MGS gneisses. Geochemical studies by Bremner and Leake (1980) and others (cited in Leake, 1986) have conclusively demonstrated that the BA is the sheared equivalent of the surrounding basic rocks of the MGS. Chemical trends across the BA and into the MGS have been interpreted as indicating that the original MGS sequence overlying the thrust plane was inverted, probably on the lower limb of a major D_2 or D_3 fold (Leake, 1986; 1970b). However in detail the trends are not smooth and breaks appear to be present in the differentiation sequence, probably as a result of thrusts cutting out part of the sequence (Leake, 1986). Derivation of the BA from the basic rocks requires that grain size reduction must have occurred (new plagioclase is 0.1-0.01 mm compared with 1-5 mm in the basic rocks; Leake, *ibid.*). This must have taken place by recrystallisation as well as cataclasis because the new hornblende forms fresh acicular crystals 0.3 mm wide by 2 mm long

(Bremner, 1977) and the plagioclase has changed in composition from An_{55-65} originally to more sodic compositions. However chemical equilibrium has not been completely achieved as demonstrated by the variability of plagioclase composition within samples (see above).

Epidote veins/microcracks up to 4 mm across which cut the foliation in the BA have been identified during fieldwork for this study (GJ.203, GJ.207). Although these veins have not been noted by previous authors they must be fairly common because of the ease with which they were found during sampling.

Bremner (1977) notes that a number of old copper workings are located within the BA. He states that "the ore (pyrite) is of extremely low grade and the mineralisation is localised along fault line breccias". It is not clear which faults he is referring to.

Within the MGS just above the BA to the north of Ballinaboy, P.W.G.Tanner has observed (pers. comm.) boudinaged clinozoisite-diopside layers in a basic rock. He suggests that the latest time at which disruption of the layers could have taken place would be during thrusting in the Delaney Dome, in which case the clinozoisite must have formed syn-thrusting or earlier. A sample of this boudinaged material (T.1750) was kindly provided by Geoff Tanner for analysis in this study.

The Mannin Thrust.

Although substantial shearing has taken place throughout the BA and the DDF. Leake (1986) suggests that most movement has taken place on the Mannin Thrust. The contact between the two formations at the thrust plane is usually sharp, and there may be no difference between the rocks in the vicinity of the thrust and those further away (*ibid.*). In the north Leake notes that the a breccia of siliceous material and amphibolite may be present along the thrust plane. P.W.G.Tanner (pers. comm.) has identified a number of veins in the vicinity of the thrust plane in the north. He has observed quartz veins in the breccia, some of which are boudinaged, while others are cross cutting. At a locality within the DDF a few metres below the thrust he has observed epidote veins which appear to be concordant with the foliation but also epidote and epidote-quartz veins which definitely cut the foliation. Within the BA ten to twenty metres above the thrust plane he has collected quartz and quartz-epidote veins which are concordant with the foliation, which he has kindly supplied for analysis (T.5-T.7).

1.4.3 The Galway and Roundstone granites and their contact aureoles.

The Galway granite.

The Galway granite is a composite pluton which may extend over an area as large as 60 × 35 km (Max *et al.*, 1978). Samples analysed in this study were collected from a restricted area along the NW margin of this pluton. The following petrographic descriptions are based on these samples and may not apply to rocks of the same granite type from other parts of the pluton.

According to Max *et al.* (1978) and Leake *et al.* (1981, map 1) the samples for this study have been collected from two types of the Galway granite; the Murvey Granite which is a marginal phase and the Errisbeg Townland Granite which is a major phase which occurs throughout the pluton.

The Murvey Granite is a fine grained (2-5 mm) rather equigranular leucogranite consisting of orthoclase, plagioclase and quartz with minor (1-2%) biotite and accessory magnetite, apatite and zircon. In hand specimen the orthoclase may be slightly megacrystic in places, sometimes up to 8-9 mm across it is often pale to bright pink in colour, a feature which has also been commented on by Max *et al.* (1978). In thin section the orthoclase is rather turbid and contains minor perthite and inclusions of biotite and plagioclase. The plagioclase shows faint zoning and the cores are often altered to a very fine grained (<<5 μm diameter) sheet silicate, probably sericite, while the grain margins are often unaltered (GJ.15). Occasional large flakes of sericite (~200 μm diameter) are also present in the altered cores. The quartz often contains bubble planes of liquid-vapour inclusions. The biotite is generally fresh, although some flakes may be partially altered to chlorite, sometimes with epidote and rutile. The magnetite may show minor alteration to epidote (GJ.15).

A sample of typical Errisbeg Townland Granite from this area (BL.2085) is described by Leake (1970a). This is a megacrystic biotite adamellite consisting of plagioclase (An_{17}), megacrystic orthoclase (up to 14 mm diameter), quartz and biotite (~5%) with accessory magnetite, hornblende, apatite, zircon and sphene. The plagioclase shows normal zoning and is commonly altered to fine sericite and minor saussurite. The orthoclase is rather turbid and contains small amounts of perthite. The quartz contains fairly abundant bubble planes of liquid-vapour inclusions. The biotite is often considerably altered to chlorite, often with epidote. Some samples have been considerably altered (GJ.213) so that in hand specimen the plagioclase is apple green in colour and the orthoclase is dark pink.

In a sample of intermediate MGS rock collected ~110 m from the contact with the granite the original tabular amphibole is seen to be covered in radiating sprays of fine acicular hornblende. Since this feature has not been seen in the Cashel-Recess area it is most probably related to the effects of hornfelsing by the Galway granite. Small shear zones or veins in this sample appear to consist of a fine grained mixture of plagioclase, quartz and magnetite, a feature which has also been noticed in another sample near to the Galway granite (GJ.226) and also in one near to the Roundstone granite (GJ.7)

According to Leake (1978) the Murvey granite is a late differentiate of the Errisbeg Townland Granite, which accumulated in the space left by late stoping at the margin.

The Roundstone granite.

All of the samples from this granite come from the NE quadrant (map 1). In this area the granite is mostly an equigranular granodiorite containing plagioclase, orthoclase, quartz, biotite (~5%) and hornblende with accessory sphene, magnetite, apatite and zircon. Miarolitic cavities are present in some

samples. The plagioclase is usually strongly normally zoned, with cores of An_{28-30} and rims around An_{20} (Leake, 1970a). Fine oscillations in the zoning can be seen in many samples. The plagioclase is variably altered to fine sericite, often the cores are preferentially altered. In strongly altered samples calcite and minor saussurite may accompany the sericite and alteration may be so intense that the twinning and zoning may be almost obscured. The orthoclase is microperthitic and usually rather turbid, although this varies between samples. XRD analysis of separates of some of the more turbid samples has shown that celsian is present as a distinct phase, possibly as a result of exsolution from an originally Ba rich feldspar. Sometimes the orthoclase may be rather oikocrystic, containing rounded inclusions of quartz or plagioclase. The quartz sometimes contains bubble planes of liquid-vapour and possibly liquid-vapour-solid inclusions. The biotite and hornblende vary from being almost totally fresh to totally altered to chlorite. The pseudomorphs after biotite may also contain epidote, sphene, ilmenite, prehnite or rutile. Sometimes the magnetite grains are cracked and altering to chlorite, while the euhedral sphene may have been pseudomorphed by rutile, sometimes with calcite. Some samples contain transgranular microcracks, usually about 50 μm wide. So far calcite, chlorite-quartz, calcite-prehnite(?) and calcite-quartz assemblages have been identified in these microcracks.

For all the samples from the Roundstone granite there is seen to be a very strong correlation between the intensity of mineral alteration, the turbidity of the orthoclase, the density of bubble planes in the quartz and the density of filled microcracks, strongly indicating that all of these features are related. Thus it seems likely that the alteration of the granite was caused by fluids moving through the rock along the bubble planes and microcracks. Fresh and altered granite end members can be identified and the differences between them are summarised in the table on the next page.

In the field there appears to be a continuous gradation from fresh to totally altered granite. Altered granite and fresh granite can be found within a few metres of each other, strongly suggesting that the fluids that caused the alteration of the granite were concentrated along more permeable zones, possibly the jointing in the granite. There does not appear to be a relationship between the intensity of alteration and the distance from the granite contact.

A porphyry dyke (GJ.168) which is genetically related to the granite and runs along part of the granite contact in this area was sampled. This has a similar composition to the granite but is fine grained with plagioclase phenocrysts. The plagioclase is strongly sericitised and rather yellow in thin section, but zoning and twinning can still be identified. The orthoclase is strongly turbid and on close examination this is seen to be due to many fine tubular structures typically 10 μm long and ~ 0.25 μm wide which appear to be running parallel to the c axis. These structures are similar to some of the microtubes described by Richter and Simmons (1977) and may have originated by etching of the feldspar. The quartz is unusually free of bubble planes for such an altered rock. Chlorite with rutile and possibly ilmenite are obviously pseudomorphic after biotite, and euhedral sphene has been pseudomorphed by rutile.

	Fresh granite	Altered granite
Plagioclase	Only slightly sericitised, usually in in cores.	All strongly sericitised, some saussurite and calcite also present.
Orthoclase	Only weakly turbid in thin section. V. pale pink in hand specimen.	Strongly turbid in thin section. Dark pink-red in hand specimen.
Quartz	Almost free of bubble planes.	Many bubble planes easily identified.
Biotite	Generally fresh. Odd ribs converted to chlorite with rare sphene. Free of rutile or ilmenite.	Totally pseudomorphed by chlorite, with abundant rutile/ilmenite inclusions. Some calcite present.
Hornblende	Fresh.	Not present - totally replaced by chlorite?
Sphene	Fresh.	Totally pseudomorphed by rutile.
Magnetite	Fresh.	Altering to chlorite.
Filled microcracks.	Absent.	Common.

A sample of psammite (GJ.169) ~10 m from the contact of the granite (and from sample GJ.168) contains quartz, strongly sericitised plagioclase and chloritised biotite with minor sulphide and opaque grains. However the most noticeable feature of this sample in thin section is that the quartz contains abundant sub-parallel bubble planes which run at approximately right angles to the foliation. Since the trace of the foliation in the psammite runs parallel to the granite contact at this point (map 2) these bubble planes must be orientated at right angles to the contact. A calcite vein within this sample also has the same orientation. If the vein and bubble planes are interpreted as representing the pathways of fluid flow it is apparent that the fluid must have flowed at right angles to the granite contact (i.e. probably across it) at this point.

Sample GJ.7 ~170 m from the granite contact contains quite fresh decussate biotite growing on the hornblende. The decussate texture suggests that this biotite may have developed during heating related to the granite intrusion. Thus hornfelsing by the Roundstone granite may have extended over a wider area than previously supposed (Leake, 1970a; see 1.3.7).

A fault fill.

Also included in this section, because it is probably a late structure, is a sample of vein material (GJ.196) which was collected from an outcrop to the NW of Lettershanna Hill. The sample which consists of quartz and baryte with a later calcite infill was collected from irregular veins which cross cut the foliation in the intermediate gneisses at this point. From maps 1. and 2. it is apparent that this outcrop is within a metre or two of the fault which runs down the road. Since such vein assemblages have not been identified

elsewhere in this area, it seems reasonable to assume that the vein material is related to the fault. Unfortunately this fault does not cross cut any late structures, so that all that can be said about its age is that it is post MGS. However since a large number of the faults to the S do cut the Galway granite (map 1.) it is quite likely that this fault was also active after ~400 Ma.

1.5 THE FORMATION OF MAGMATIC HORNBLENDE AND RETROGRADE HYDRATION IN SW CONNEMARA.

From the descriptions of the three study areas given in the previous section (1.4) it is clear that the rocks in SW Connemara show abundant evidence of having experienced retrograde hydration. It is also clear that the alteration of these rocks cannot have taken place during a single event, but that at least two or possibly more periods of retrograde hydration are required to explain the long and complex sequence of alteration that is observed in these rocks.

The earliest retrograde hydration event must have taken place very soon after the intrusion of the MGS because much of the amphibole seen in the ultrabasic members formed at fairly high temperatures, which could only have been attained soon after intrusion (fig. 1.1). From the chemistries of similar amphiboles in the ultrabasic rocks to the W of Roundstone, Bremner and Leake (1970) have suggested that the brown hornblendes in the MGS could have formed at temperatures of 800-1000°C, while much of the green hornblende probably formed at temperatures less than 800 or even 700°C. At the higher temperatures the rock could not have been entirely solid. Thus the oikocrystic texture of some of the brown hornblendes could be interpreted as being due to heteradcumulate growth and they may be truly igneous in origin (i.e. crystallised in equilibrium with a melt). However the textural relationships of much of the green hornblende in the ultrabasic rocks can only be reasonably interpreted as being due to subsolidus (metamorphic) growth and this is supported by the temperature estimates of Bremner and Leake (1980) which would indicate that the rock was totally solid at the time of formation. Since there were no other hydrous minerals apart from apatite present in the ultrabasic rocks at this time (table 1.1) the hydrogen in these hornblendes can only have been supplied by hydrous fluids moving through the rock. These fluids must have passed through the rock prior to ~480 Ma since this is the time at which the MGS in the Cashel district cooled through 550°C, which is well below the hornblende formation temperature. Similarly it can be argued that the replacement of orthopyroxene by cummingtonite-anthophyllite and hornblende by biotite both must have taken place at fairly high temperatures, probably during this early hydration event.

An early high temperature hydrous retrogression has also taken place in the Dalradian migmatites in the Cashel-Recess area, because the coarse muscovite within these rocks can only have formed during cooling, if, as Treloar (1985) states the muscovite-out isograd lies within the Lakes Marble formation in the N of the area. It is possible that some of the leucosome muscovite could have crystallised magmatically. Barber and Yardley (1985) suggest that the leucosomes in migmatites further to the E did not crystallise until the pressure had fallen to ~2.5 kb. If leucosomes in the Cashel-Recess district crystallised at similar pressures it is difficult to predict whether leucosome muscovite crystallised magmatically or subsolidus, because the

granite minimum melt curve and the quartz+muscovite ⇔ K-feldspar+H_2O curves intersect around this pressure so that depending on which calibration is taken for the muscovite-out curve, muscovite could form in either way. In either case, if as textural relationships tend to indicate, muscovite did form by this reaction it must have crystallised at temperatures exceeding 600°C (Chatterjee and Johannes, 1974), unless it crystallised at very low water pressures. Thus a source of hydrogen for hydrous mineral growth seems to be required soon after the metamorphic peak within both the metasediments and the MGS.

A later lower temperature retrograde hydration of unknown age has also taken place in both of these rocks producing alteration mineral assemblages similar to greenschist or prehnite-actinolite (Liou *et al.*, 1985) facies assemblages. Within the MGS especially this alteration appears to be related to microcracks which are now filled with similar assemblages.

Within the Delaney Dome area the retrogression of basic MGS rocks to albite-epidote amphibolites is obviously associated with thrusting at ~460 Ma. Since the study of Hubbert and Rubey (1959) which indicated that thrusting mechanisms require fluid pressures close to, or greater than lithostatic, a number of studies (Fyfe and Kerrich, 1985; Negga *et al.*, 1986) have shown that thrust planes may be sources for large volumes of fluids, which can migrate into the overlying slab. Fluid production by the Mannin Thrust could represent one possible source for the fluids causing the low temperature hydration in the Cashel-Recess area. However although there is some evidence that fluids were present along the thrust plane during thrusting, a good deal of the alteration and veining of these rocks, both above and below the thrust appears to have taken place after the termination of thrusting, possibly during a distinct event. Thus a hydration event post 460 Ma is indicated in this area. Retrograde hydration has also taken place in the Galway granite suite, indicating that at least one period of alteration must have taken place after ~400 Ma, while the latest significant retrograde hydration event in the area is constrained to have taken place post 305 Ma which is the inferred intrusion date of the altered U. Carboniferous dykes described by Mitchell and Mohr (1987).

rocks beneath

After a brief introduction to stable isotope systematics in chapter 2., the stable isotope data for the three study areas described in 1.4 will be presented in chapters 3-6. In these chapters the results will be used to constrain the stable isotopic compositions and ultimately the origins of the different retrograde fluids present in these rocks from pre-480 Ma to post-400 Ma.

1.6 SUMMARY.

The regional geology of Connemara and the detailed geology of the study areas together with the evidence of retrograde alteration in Connemara have been presented in this chapter. The important points are summarised below.

1. Connemara is a Dalradian inlier which experienced an anomalously high grade of metamorphism during the Grampian Orogeny. In the S the

metamorphic peak (~700-750°C, ~5.5 kb) at ~490 Ma was followed by rapid uplift to lower pressure conditions (~650-700°C, ~2.5 kb) at ~ 480 Ma.

2. In S Connemara large volumes of magma (the MGS) were intruded into the Dalradian approximately synchronously with the peak of metamorphism.

3. Both the Dalradian sequence and the MGS rocks have experienced a complex sequence of events subsequent to the metamorphic peak, including thrusting over the Delaney Dome Formation at ~460 Ma, exhumation and reburial prior to 400 Ma, intrusion by Caledonian granites (mostly at ~ 400 Ma) and dyke intrusion during the U. Carboniferous and Tertiary, as well as local reheating events.

4. Petrographic examination of rocks from the Dalradian sequence, the MGS, from around the Mannin Thrust and from the Galway granite suite, shows that all of these rocks exhibit mineralogical changes which are indicative of reaction with hydrous fluids at or below their peak temperatures, a process which is termed retrograde hydration in this study.

5. It is clear that more than one period of retrograde hydration is required to explain the alteration observed in these rocks, since the earliest hydration event is constrained to take place pre ~480 Ma, while the latest hydration event must have taken place post 305 Ma.

6. The aims of this study are to attempt to use stable isotope geochemistry to investigate a. the origins of the water in the MGS hornblendes, and b. the origins of the fluids involved in these retrograde hydration events in order to ultimately understand the factors which cause retrograde hydration to take place.

CHAPTER 2

STABLE ISOTOPE SYSTEMATICS

2.1 INTRODUCTION

The study of the stable isotope geochemistry of terrestrial samples is principally concerned with the natural variation of the isotopic composition of six elements: hydrogen, carbon, nitrogen, oxygen, silicon and sulphur. The isotopic composition of these elements varies because their isotopes are fractionated when they take part in natural chemical and physical processes.

The purpose of this chapter is to explain the definitions used in stable isotope geochemistry, to explain the systematics which govern the variation in stable isotope ratios and to show how measured variations may be interpreted.

The methods used for the analysis of the stable isotopes measured for this study are outlined in the appendix (section A.1).

2.2 THE ISOTOPES OF HYDROGEN, CARBON, OXYGEN AND SULPHUR.

Isotopes are defined as atoms of the same element which have different atomic masses. Oxygen is an element which has an atomic number (Z) of 8. This means that all atoms of oxygen have 8 protons in the nucleus. The number of neutrons (N) in an oxygen atom nucleus can be either 8, 9 or 10 giving three isotopes of relative atomic mass A (= Z + N) of 16, 17 and 18. The different isotopes of an element are denoted by a superscript of A, for example ^{18}O is the isotope of oxygen with an atomic mass of 18.

Tabulated on the next page are the stable isotopes of the elements examined in this study along with their approximate abundances and the isotopic ratio that is usually measured.

2.3 THE δ VALUE AND THE RELATION OF δ TO α.

2.3.1 The δ value.

The stable isotope composition of a sample is reported using the δ notation defined as:

$$\delta_{SAMP} = \left[\frac{R_{SAMP} - R_{STD}}{R_{STD}}\right] \times 1000‰, \qquad (2.1)$$

where conventionally R is the atomic ratio of the heavy isotope to the light isotope (i.e. D/H, $^{13}C/^{12}C$, $^{18}O/^{16}O$, $^{34}S/^{32}S$). The δ value then is the parts per thousand (or "permil", ‰) difference in isotopic ratio between the

ELEMENT	ATOMIC NUMBER	ISOTOPES (APPROXIMATE ABUNDANCES)				ISOTOPIC RATIO MEASURED
HYDROGEN	1	H^1 (99.985)	D (0.015)			D/H
CARBON	6	^{12}C (98.89)	^{13}C (1.11)			$^{13}C/^{12}C$
OXYGEN	8	^{16}O (99.756)	^{17}O (0.039)	^{18}O (0.205)		$^{18}O/^{16}O$
SULPHUR	16	^{32}S (95.02)	^{33}S (0.75)	^{34}S (4.21)	^{36}S (0.02)	$^{34}S/^{32}S$

sample and a standard. The δ symbol is normally suffixed by the heavy isotope of the element in question. Hence a sample with a $\delta^{18}O$ value of +10‰ is enriched in ^{18}O by 10 ‰ or 1% relative to the standard. Negative δ values indicate that the sample is depleted in the heavy isotope relative to the standard.

The δ value is measured directly using a mass spectrometer (see appendix). The value of the absolute isotope ratio of a sample (R_{SAMP}) is not required for the purpose of this thesis and although it can be calculated from δ_{SAMP} and R_{STD} this has not been done here.

The standard used for reporting $\delta^{18}O$ and δD values is the internationally accepted reference standard V-SMOW (Vienna - Standard Mean Ocean Water). This is identical within the limits of analytical uncertainty to the original SMOW standard defined by Craig (1961).

The standard for reporting $\delta^{13}C$ is V-PDB (Vienna - Peedee Belemnite) defined by:

$$\delta^{13}C_{NBS\text{-}19/V\text{-}PDB} = 1.95$$

(O'Neil, 1986). As with V-SMOW the original PDB standard and V-PDB are identical.

Canyon Diablo Troilite (CDT) is the internationally accepted standard used to report $\delta^{34}S$.

---

[1] Throughout this thesis, where the letter "H" is written it is used to denote the isotope of hydrogen ^1H. The letter "D" denotes the isotope of hydrogen ^2H (deuterium). "Hydrogen"or "H_2" are used to describe the gas of the element hydrogen and does not imply any isotopic composition.

2.3.2 The α value

The isotopic fractionation that occurs during a process is defined by the fractionation factor (α) where:

$$\alpha_{A\text{-}B} = R_A/R_B, \qquad (2.2)$$

where R_A is the absolute isotopic ratio in phase A and R_B the ratio in B.

The α value rather than δ values is used to represent the fractionation between two phases, because α can be simply related to the equilibrium constant (K) for the exchange reaction. For a general isotope exchange reaction, (e.g. for oxygen isotope exchange):

$$mA^{16}O_n + nB^{18}O_m \Leftrightarrow mA^{18}O_n + nB^{16}O_m,$$

the equilibrium constant is defined as:

$$K = \frac{[A^{18}O_n]^m [B^{16}O_m]^n}{[A^{16}O_n]^m [B^{18}O_m]^n},$$

where [ ] stands for the concentration of that end member. This can be rearranged to:

$$K = \frac{[A^{18}O_n]^m / [A^{16}O_n]^m}{[B^{18}O_m]^n / [B^{16}O_m]^n}.$$

If the isotopes are randomly distributed over all possible sites or positions in A and B[1] then:

$$[A^{18}O_n] = \left(\frac{^{18}O}{^{18}O + ^{16}O}\right)_A^n$$

and

$$[A^{16}O_n] = \left(\frac{^{16}O}{^{18}O + ^{16}O}\right)_A^n.$$

This being the case, then:

$$\frac{[A^{18}O_n]^m}{[A^{16}O_n]^m} = \left(\frac{^{18}O}{^{16}O}\right)_A^{nm}$$

---

[1] This will only be the case if all the sites in which the isotopes are located in each phase have the same preference for the different isotopes, if the sites differ energetically then the partitioning will be non random. For example hydrogen in chlorite occurs in two distinct structural sites (Joswig *et al.*, 1980) and significant equilibrium hydrogen isotope fractionation is found to occur between these sites (Suzuoki and Epstein, 1976).

and similarly

$$\frac{[B\,^{18}O_n]^m}{[B\,^{16}O_n]^m} = \left(\frac{^{18}O}{^{16}O}\right)_B^{nm}.$$

Thus

$$K = \frac{(^{18}O/^{16}O)_A^{nm}}{(^{18}O/^{16}O)_B^{nm}}.$$

Since α is defined as

$$\alpha = \frac{(^{18}O/^{16}O)_A}{(^{18}O/^{16}O)_B}$$

(eqn. 2.2), it can be seen that

$$\alpha = K^{1/nm}_{\text{exchange}}. \qquad (2.3)$$

If the equation is written such that one atom is exchanged (n.m = 1), then K = α.

2.3.3. The relationship between δ values and α.

The relationship between these two values can be derived as follows: Let $R_{V\text{-}SMOW}$, R_A and R_B be the isotopic ratios in V-SMOW, A and B. From equation 2.1

$$\delta_A = \left[\frac{R_A - R_{V\text{-}SMOW}}{R_{V\text{-}SMOW}}\right] \times 1000.$$

This rearranges to

$$R_A = \left[\frac{(\delta_A + 1000)R_{V\text{-}SMOW}}{1000}\right].$$

Similarly

$$R_B = \left[\frac{(\delta_B + 1000)R_{V\text{-}SMOW}}{1000}\right].$$

Substituting these equations into equation 2.2 gives:

$$\alpha_{A-B} = \frac{R_A}{R_B} = \left[\frac{(\delta_A/1000)+1}{(\delta_B/1000)+1}\right].$$

Thus

$$\alpha_{A-B} = \left[\frac{\delta_A + 1000}{\delta_B + 1000}\right]. \qquad (2.4)$$

Values of α are normally very close to unity, usually 1.00X where X is rarely greater than 4.

2.3.4. $10^3 \ln \alpha$ and the Δ value.

Frequently instead of using α the fractionation is expressed as $10^3 \ln \alpha$ termed the "permil fractionation" (O'Neil, 1986).

$10^3 \ln \alpha$ provides a more convenient number to use than α. It is a useful mathematical fact that $10^3 \ln (1.00X) \approx X$. Faure (1977) uses this fact to derive the approximation

$$\Delta_{A-B} = \delta_A - \delta_B \approx 10^3 \ln \alpha_{A-B} . \qquad (2.5)$$

This means that the difference in δ values between two phases is approximately equal to the permil fractionation and hence $10^3 \ln \alpha$ has real meaning.

Δ_{A-B} will be equal to $10^3 \ln \alpha_{A-B}$ within the limits of analytical error if Δ and δ are less than 10^1.

The logarithmic function has theoretical significance, since studies which calculate α using statistical mechanics (e.g. Bottinga and Javoy 1973, Clayton and Epstein 1961) predict that $\ln \alpha$ should be a simple function of absolute temperature (see 2.4). Because of this, experimental studies to determine α often use a plot of $10^3 \ln \alpha$ against $1/T^2$ to derive a simple straight line or curve relationship. The fractionation is therefore often reported in terms of $10^3 \ln \alpha$ rather than α.

2.4 ISOTOPIC FRACTIONATION

The different isotopes of the light elements are fractionated because they vary slightly in their physical and chemical properties. The dominant cause of this is the very large mass differences between different isotopes of the light elements. For example ^{18}O is 12.5% heavier than ^{16}O, while D is almost 100% heavier than H. For elements of higher atomic number this mass difference is much smaller (1.2% for ^{87}Sr relative to ^{86}Sr).

Fractionation occurs during various chemical reactions and physical processes and may be divided into two types: kinetic and equilibrium fractionation.

---

[1] Unfortunately these constraints are not obeyed for most hydrogen isotope mineral-fluid fractionations. Because of this the computer programs written to calculate fluid δ values have been written using the more correct formulation relating δ to α (equation 2.4).

2.4.1 Kinetic fractionation.

Kinetic fractionation is associated with fast, incomplete or unidirectional processes such as evaporation, diffusion and dissociation and redox reactions. Fractionation during evaporation and diffusion can be explained by kinetic theory. The average kinetic energy of a gas molecule is defined:

$$K.E. = 1/2\, Mv^2 .$$

Kinetic theory states that the average kinetic energy per molecule is the same for all ideal gases at a given temperature. Hence at any temperature

$$(1/2Mv^2)_{GAS\,A} = (1/2Mv^2)_{GAS\,B},$$

which rearranges to

$$\frac{v_A}{v_B} = \sqrt{\frac{M_B}{M_A}} .$$

This means that the relative velocity of two gas species is inversely proportional to the root of their atomic masses. For example the water molecule $H_2{}^{16}O$ has an average velocity 2.7% greater than $HD^{16}O$, at any temperature. This allows the lighter molecule to diffuse faster or in a liquid enables a larger proportion of the light molecule to break through the liquid surface on evaporation. This kinetic effect on evaporation is partly the cause of the latitudinal variation in isotopic composition of meteoric water described in 2.9.

Kinetic fractionation during dissociation and redox reactions is a result of the molecules containing the heavy isotope having a higher dissociation energy than those containing the light isotope.

Kinetic fractionation processes are thought not to be important in the high temperature processes involving O and H being studied in this thesis. However kinetic effects may be important in some redox reactions involving C and S. Kinetic isotope fractionation may also take place during preparation of gases for isotopic analysis and care has to be taken to avoid this otherwise systematically biased isotopic ratios may result.

2.4.2. Equilibrium fractionation.

Equilibrium fractionation takes place whenever an isotope exchange reaction occurs between two phases. For example, the oxygen isotope exchange reaction between quartz and water can be written (such that one atom of oxygen is exchanged):

$$1/2Si^{16}O_2 + H_2{}^{18}O \Leftrightarrow 1/2Si^{18}O_2 + H_2{}^{16}O. \qquad (2.6)$$

At equilibrium, the equilibrium constant **K** for the reaction can be written:

$$K = \frac{(Si^{18}O_2)^{1/2}\,(H_2{}^{16}O)}{(Si^{16}O_2)^{1/2}\,(H_2{}^{18}O)} .$$

From equation 2.3 $K = \alpha$. At 400°C α =1.00407 and $10^3 \ln \alpha = 4.06$ (Matsuhisa *et al.*, 1979) which means that $\Delta SiO_2 - H_2O$ at 400°C is 4.06‰.

Equilibrium fractionation takes place because the different isotopes have slightly different bonding energies. It can be shown (O'Neil, 1986) that molecules containing the heavy isotope are more stable (have a lower potential energy) than molecules containing the light isotope. In isotope exchange reactions the free energy of the system is minimised by partitioning the heavy isotope between the two phases. Expressed thermodynamically this is $\Delta\mu = 0$.

Equilibrium fractionation is the only fractionation process that takes place at high temperatures for O and H isotopes. Because carbon and sulphur isotope variations may also be dependent on kinetic effects and fluid speciation, the isotope systematics of these elements are described separately in section 2.8. The next four sections evaluate the factors that may cause variation in the value of equilibrium fractionation factors for geological systems.

2.4.3. The dependence of α on temperature.

Temperature is the most important factor which causes a variation in α. The theoretical methods of calculation of α described in 2.4.6 can be used to give the following predictions of the variation of α with T. (All temperatures are in K unless otherwise specified.)

a. At high temperatures the fractionation (Δ) between two substances is predicted to decrease linearly with T^{-2} towards infinite temperature when the fractionation factors between all substances should be zero (α = 1, $10^3 \ln \alpha = 0$).

b. Near to absolute zero, with decreasing temperature, the fractionations (Δ) between all substances approach their maximum values linearly with T^{-1}.

Unfortunately in the temperature range of geological interest (300-1500K) the behaviour is transitional between these limits. Despite this it has been empirically observed that graphs of ln α versus T^{-2} give good approximations to a straight line for many systems over a temperature range of a few hundred degrees. Consequently equations of the form $1000 \ln \alpha = (A/T^2) + B$ have been used by many authors to represent experimental and theoretical results. A useful property of the fractionation factor expressed in this form is that the equations for two systems can be subtracted to remove a common component:

If

$$10^3 \ln \alpha_{(X-Y)} = A/T^2 + B$$

and

$$10^3 \ln \alpha_{(Z\text{-}Y)} = A'/T^2 + B',$$

then by subtraction

$$10^3 \ln \alpha_{(X\text{-}Y)} - 10^3 \ln \alpha_{(Z\text{-}Y)} = 10^3 \ln \alpha_{(X\text{-}Z)} = (A\text{-}A')/T^2 + (B\text{-}B').$$

Javoy (1977) suggests that the intercept term in most ^{18}O mineral-water fractionations is usually -3.7 and that this can be attributed to a constant contribution to the free energy term from water rather than the mineral. (Theory predicts that the free energy of water and hydrous minerals will have a different temperature dependence to anhydrous minerals.) If this is the case the B term should cancel when two mineral-water equations are subtracted to yield the mineral-mineral equation. Many mineral-mineral fractionation equations do indeed have a near zero intercept term.

The predictions of the variation of α with T are largely based on calculations for perfect gas systems, and numerous exceptions have been identified in mineral-fluid systems. Some systems show "crossovers" where $10^3 \ln \alpha$ changes sign as the temperature changes, for example the ^{18}O fractionation between anorthite and water (Matsuhisa *et al.*, 1979) or between zoisite and water (Matthews *et al.*, 1983a). Some fractionation curves show inflections in $\ln \alpha$ when plotted against T or T^{-1}, for instance ^{18}O fractionation between magnetite and water (Becker 1971). Graham and co-workers (1984, 1980) have shown that hydrogen isotope fractionation in the amphibole-water and epidote-water systems is independent of temperature over a range of 400-500°C.

In the light of these exceptions it seems prudent not to use the theoretical relationships of α to T to extrapolate to temperatures where no experimental data exist. The theoretical relationships can however be used for interpolation of data over small ranges of T between data points.

2.4.4 The dependence of α on pressure

Theory

As noted above (2.4.2), at equilibrium the sum of the chemical potentials for any reaction is zero:

$$\Delta\mu = 0 = \Delta G^\circ + RT\ln K, \qquad (2.7)$$

which rearranges to

$$\ln K = -\Delta G^\circ/RT. \qquad (2.8)$$

To find $\ln K$ the value of ΔG° at the P and T of interest = $\Delta G(P,T)$ needs to be calculated (see 2.4.7a). The variation of ΔG with P and T can be written:

$$d\Delta G = \Delta V dP - \Delta S dT.$$

Taking the partial derivative at constant temperature:

$$\left(\frac{\partial \Delta G}{\partial P}\right)_T = \Delta V.$$

Substituting this into eqn. 2.8 the pressure dependence of lnK at constant temperature is:

$$\left(\frac{\partial \ln K}{\partial P}\right)_T = \frac{-\Delta V}{RT},$$

where ΔV is the molar volume change for the reaction as written. If the equation is written such that one atom is exchanged, then $\alpha = K$ (eqn 2.3) and

$$\left(\frac{\partial \ln \alpha}{\partial P}\right)_T = \frac{-\Delta V}{RT}.$$

Since $1000 \ln \alpha \approx \Delta$ (the isotopic fractionation, eqn 2.5) then:

$$\left(\frac{\partial \Delta}{\partial P}\right)_T = \frac{-1000 \Delta V}{RT}, \qquad (2.9)$$

which is the equation for the pressure dependence of isotopic fractionation derived by Clayton *et al.* (1975).

Oxygen isotope fractionation

For the oxygen isotope exchange reaction:

$$1/3CaC^{16}O_3 + H_2{}^{18}O \Leftrightarrow 1/3CaC^{18}O_3 + H_2{}^{16}O$$

Clayton *et al.* (1975) estimated a maximum ΔV for this reaction of 1.9×10^{-3} cm^3 mol^{-1} which suggested that the pressure dependence of this reaction at 500°C might be 0.03 ‰ $kbar^{-1}$ at most. However experimental determination of $\partial\Delta$ for this reaction between 0.5 and 20 kbar by the same authors failed to show any detectable change in Δ with pressure. They were able to calculate an upper limit for ΔV that is consistent with their results to be 1.3×10^{-4} cm^3 mol^{-1} at 500°C. Furthermore they suggested (after Joy and Libby, 1960) that the value of ΔV for this reaction is probably quite large in comparison to ΔV for an exchange reaction between two silicate phases. Thus they concluded that a pressure effect on oxygen isotopic fractionation, even in the mantle must be negligible.

Hydrogen isotope fractionation

Apparently no previous work exists which examines the question of whether or not a pressure effect is important in governing hydrogen isotope fractionation. However preliminary research outlined here indicates that the pressure dependence of hydrogen isotope fractionation may not be negligible as is commonly supposed.

A general hydrogen isotope exchange reaction between a mineral and water can be written:

$$\text{MINERAL-OH} + 1/2D_2O \Leftrightarrow \text{MINERAL-OD} + 1/2H_2O, \qquad (2.10)$$

where the pressure dependence is as eqn. 2.9 (strictly $\Delta \neq 1000\ln\alpha$ in this case but considering the errors in estimation of ΔV this approximation is good enough at at present). It might be suspected that the contribution to ΔV from ($V_{MINERAL\text{-}OD}$ - $V_{MINERAL\text{-}OH}$) may be quite small for two reasons:

a. The hydrogen is always only a very minor constituent of all hydrous minerals, unlike oxygen, so that isotopic substitution might be expected to only produce a small change in molar volume.

b. The hydrogen is held in sites in a semi-rigid lattice which might be expected to inhibit large volume changes.

If therefore the assumption can be made that this contribution is negligible then:

$$\Delta V \approx 1/2V_{H2O} - 1/2V_{D2O}.$$

Fortunately recent work is available (Kell *et al.*, 1985a,b) which allows V_{D2O} - V_{H2O} at elevated temperatures and pressures to be calculated from density data. The calculated value is potentially very accurate since the density determinations were carried out using the same method on the same apparatus, hence systematic errors in the measurements should cancel.

Calculated values of V_{D2O} - V_{H2O} at 350, 400 and 500°C and over a range of pressure are shown in fig 2.1. Two points are apparent from this figure.

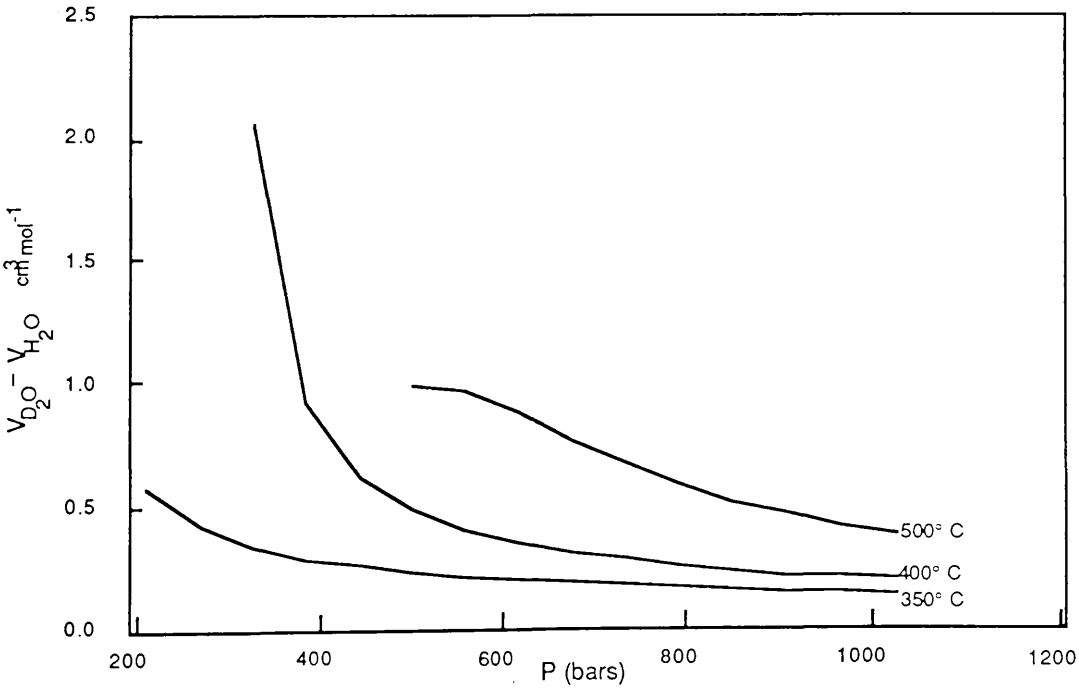

Fig.2.1 $\Delta V_{D2O\text{ - }H2O}$ plotted against pressure for three different temperatures. The data of Kell *et al.* (1985a,b) were used to calculate $\Delta V_{D2O\text{ - }H2O}$.

a. Over all points in this PT region V_{D2O} - V_{H2O} is large (3-6 orders of magnitude greater than ΔV for oxygen exchange between calcite and water at 500°C), such that calculated values of $(\partial\Delta/\partial P)_T$ are large enough

to be highly significant e.g. 2.95 ‰ $kbar^{-1}$ at 500°C, 1.026 kbar. This value has a positive sign for eqn 2.10 as written.

b. The value $V_{D2O} - V_{H2O}$ is a function of P and T, increasing with increasing temperature, but decreasing with increasing pressure.

Whether or not the value of $V_{D2O} - V_{H2O}$ decreases at higher pressures so much that the pressure dependence becomes insignificant is not possible to say. However the curves do appear to be flattening out with increasing pressure, suggesting perhaps that they might be approaching some limiting (high?) value at higher pressures.

If the assumptions made above are true, then it is apparent that pressure, as well as temperature and composition, may well be a variable controlling the magnitude of hydrogen isotope fractionation factors. Since there is as yet no experimental confirmation of this effect the conclusions made in this thesis are made under the assumption that any pressure effect is negligible. Work is currently being instigated at SURRC to search for this predicted pressure effect.

2.4.5 The dependence of α on chemical composition.

The chemical composition of both minerals and fluids may influence the values of fractionation factors. This effect is usually minor in comparison to the temperature effect but can be dominant in some systems.

A. MINERAL COMPOSITION

Oxygen isotope fractionation

The energy of a bond with an isotope depends not only on the isotope itself but also the other atoms which it is bonded to. In general bonds to ions with a high ionic potential, high charge and low atomic mass will have the highest vibration frequency and therefore the highest energy. Since we know that substitution of a light isotope by a heavier isotope reduces the bond energy it follows that to minimise the energy of a system, these more energetic bonds will preferentially incorporate the heavy isotope. The ions Si^{4+}, Al^{3+}, Fe^{2+} show a general decrease in ionic potential and charge and increase in mass. In natural systems the $\delta^{18}O$ values of minerals involving these ions decrease in the same order. In an equilibrium assemblage, quartz (Si-O bonds) is always more ^{18}O rich than feldspar (Si-O and Al-O bonds) while pyroxenes (Al-O and Fe-O bonds) are more ^{18}O depleted. Magnetite (pure Fe-O bonds) is always the most ^{18}O poor mineral in natural equilibrium assemblages. Similarly substitution of different ions within a solid solution series can cause similar changes in fractionation factors. Thus Taylor and O'Neil (1977) showed that there is a 1.7‰ fractionation between grossular ($Ca_3Al_2Si_3O_{12}$) and andratite ($Ca_3Fe_2Si_3O_{12}$) at 600°C, which can be solely attributed to the substitution of Al^{3+} by Fe^{3+}. Matsuhisa *et al.* (1979) have shown that the $\delta^{18}O$ difference between the end members of the plagioclase series is between 1.3-2.3‰. O'Neil (1986) suggests that this is probably due to the replacement of Si by Al in the coupled substitution. Some mineral series show no dependence of fractionation factor on chemistry. For example the albite-K-feldspar and muscovite-paragonite

systems show no appreciable change in fractionation with Na/K substitution (O'Neil and Taylor, 1967, 1969). This implies that the cations in these sites have only a weak influence on the energy of the Si-O and Al-O bonds in the lattice. The high coordination numbers of these cations presumably mean that any electronic effect will be spread over a number of nearby bonds.

Hydrogen isotope fractionation.

The literature concerning the relationship between chemical composition and hydrogen isotope fractionation is often apparently conflicting. Suzuoki and Epstein (1976) experimentally determined the equilibrium hydrogen isotope fractionation between a number of hydroxyl bearing minerals and water. From the data on micas and an amphibole they concluded that the magnitude of the mineral-water fractionation is related not only to the temperature but also to the mineral chemistry by the expression

$$10^3 \ln \alpha_{\text{mineral-water}} = -22.4(10^6 T^{-2}) + (2X_{Al} - 4X_{Mg} - 68X_{Fe}) + 28.2$$

where X is the mole fraction of the cation in the octahedral site. From this it is apparent that the fractionation between coexisting micas and amphiboles should be independent of T and solely related to cation composition. Suzuoki and Epstein show that the increased preference of the Al and Mg end members for D relative to the iron end member can be correlated with the lower (atomic mass/charge) ratio of these ions. However the precise reason why this should be so is not clear. It is important to note that this relationship is based only on data for one muscovite, hornblende and phlogopite and two biotites. Graham *et al.* (1984) have pointed out that this "hornblende" is probably actually an actinolite. Criticisms of the fitting of the data to derive the equation can be made and an improved equation derived from a re-evaluation of the same data is given in A.4.3.

Graham *et al.* (1984) carried out a more thorough experimental investigation of hydrogen isotope fractionation between a variety of amphiboles and water. They were able to demonstrate that the relationship proposed by Suzuoki and Epstein did not apply for the amphiboles that they investigated. Instead between 650-350°C the values of $10^3 \ln \alpha_{\text{AMPH-WATER}}$ for a tremolite and hornblende were indistinguishable within analytical error and independent of temperature. The Suzuoki-Epstein equation predicts that the two minerals should have a difference in fractionation with water in the order of 20‰ and that the fractionation should be a function of temperature.

Between 650-850°C the fractionation was found to be a function of temperature with a slope fairly similar to that estimated by Suzuoki and Epstein. The fractionations between different amphiboles are in the same direction as predicted by Suzuoki and Epstein but the magnitudes are significantly different. Graham *et al.* (1984) tentatively suggested that Na substitution into the A site could also be a factor controlling the fractionation.

Marumo *et al.* (1980) (cf 2.4.7c) have asserted that there is a correlation between $10^3 \ln \alpha_{\text{CHLORITE-WATER}}$ (=Δ) and Fe/(Fe + Mg) ratio and that Δ "does not depend on temperature explicitly". However, Graham *et al.* (1987b) state that for the data of Marumo *et al.*, the effects of temperature and Fe/(Fe

+ Mg) cannot be unambiguously separated, and taken with their own experimental data do not support the hypothesis that Fe/(Fe + Mg) ratio has an effect on fractionation.

Multiple regression analysis of the data from Marumo *et al.* (1980) by the author (A.7) shows that a better fit to the data can be obtained if $10^3\ln\alpha$ is assumed to be a function of both temperature and Fe/(Fe + Mg) ratio; rather than either of these two variables taken separately. It seems likely therefore that $10^3\ln\alpha_{CHLORITE\text{-}WATER}$ does show some dependence on chemical composition at low temperature, but at present there are not enough data to confirm that this is the case at higher temperature. Dependence of mineral-water hydrogen isotope fractionation factors on the amount of Fe substitution has been suggested by Cole *et al.* (1987) to account for the difference between experimentally determined basalt-seawater fractionations and those predicted using fractionations for Mg rich phases.

Using this newly derived equation the dependence of $10^3\ln\alpha_{CHLORITE\text{-}WATER}$ on Fe/(Fe + Mg) is found to be of the same sign and almost exactly the same magnitude as would be predicted by the Suzuoki-Epstein equation (more Fe rich compositions are more D depleted). For example shown below are values of $10^3\ln\alpha$ at 200°C predicted by the two different equations and the resulting change in fractionation per mole % of Fe:

		$10^3\ln\alpha_{CHL\text{-}WATER}$ @200°C	
		Suzuoki-Epstein equation	Regression of data of Marumo *et al.*
Fe/Fe + Mg	0.28	-93.8‰	-26.7‰
	0.51	-108.6‰	-41.7‰
difference (0.28-0.51)	0.23	14.8‰	15.0‰
‰(mole%Fe)$^{-1}$		0.64‰	0.65‰

Whether this correspondence is coincidental or not will only be determined if further data are collected on both mica and chlorite-water systems.

B. FLUID COMPOSITION

Truesdell (1974) measured the difference in oxygen isotope activity ratios (effectively equivalent to the fractionation) between pure water and 0.5-4 molal solutions of various salts commonly found in geological fluids, at temperatures between 25 and 275°C. The measured fractionations varied with temperature and were 2‰ (+ or -) at most. These findings were contrary to earlier predictions that no such effect should occur at geological temperatures.

Subsequently Graham and Sheppard (1980) measured the hydrogen isotope fractionation factors between epidote and pure water and epidote and salt solutions, enabling them to derive the fractionation between pure water and the salt solutions. They found that between 450-250°C, NaCl and

$CaCl_2$ solutions and a natural seawater all concentrated H relative to pure water. These results can be compared with Truesdell's findings at 250°C where NaCl and $CaCl_2$ solutions also concentrated ^{16}O relative to pure water. The magnitude of this hydrogen isotope fractionation varies as a complex function of temperature and solution composition and is 12‰ at its maximum value. For temperatures above 500°C the D/H fractionation for the water-brine systems examined were zero within the limits of analytical error.

The cause of this change in fractionation on addition of solutes is believed to be related to a change in structure of the solution by the solute. The ions in solution are thought to be surrounded by a "hydration shell" of oriented water molecules. Isotopic fractionation occurs between the hydration shells and the rest of the water. When the energy of vibration of the ion-hydration water bond is greater than between unassociated water molecules then water molecules containing the heavy isotopes are preferentially incorporated into the hydration shell (to reduce the system energy as for minerals, part A). Different ions may increase or decrease the bond energy and the observed solution-water fractionation is the sum of all these effects.

These solute-solvent interactions are expected to decrease with increasing temperature. Graham and Sheppard suggest that the approach by all solutions examined towards a zero fractionation relative to water at 550°C probably indicates that this is the upper temperature limit for such interactions to occur. The fact that solution chemistry can influence stable isotope fractionation has two important consequences;

a. Experimental determination of fractionation factors. In many exchange experiments to determine α dilute salt solutions were used instead of pure water, because they were found to enhance reaction rates. The isotopic fractionations measured may therefore be different from the pure water - mineral fractionation. This might explain some discrepancies between some fractionation factors determined in different laboratories. In addition, combination of mineral-"water" fractionation determined using different salt solutions, could produce erroneous mineral-mineral fractionation factors.

b. Estimation of stable isotope compositions of geological fluids. The $\delta^{18}O$ and δD values of the fluid that once coexisted with the minerals in a rock or vein are often estimated from the isotopic composition of the minerals and the appropriate fractionation factors. However it is known that geological fluids can have a wide range in salinity (usually in the range 0-40% NaCl equivalent ≈ 0-7 molal). Failure to apply a "correction" for the chemistry of the fluid could lead to erroneous estimates of fluid isotopic compositions. Truesdell (1974) shows that these errors for $\delta^{18}O$ can be up to 4‰. Graham and Sheppard (1980) point out however, that because of a lack of adequate models for the behaviour of electrolyte solutions, the quantitative prediction of fractionation factors for conditions that have not been experimentally investigated is not possible.

Recently, Kendall *et al.* (1983) demonstrated that the calcite-water oxygen isotope fractionation at 275°C is independent of water salinity for NaCl concentrations up to 4 molal, apparently contradicting Truesdell's findings. However Kazahaya and Matsuo (1986) presented experimentally determined water-salt solution fractionation factors that are almost identical to those determined by Truesdell. Because of the uncertainties in the extent of water-solute interactions and the magnitude of the resulting isotopic fractionations, such effects may be quite a major source of error in calculated fluid stable isotope compositions at the present time.

2.4.6 The dependence of α on crystal structure.

Structural effects on the isotopic properties of minerals are usually minor in comparison to the effects of temperature and chemistry. There are only two instances where structural effects are relevant to minerals that have been analysed in this study:

a. The α-β transition in quartz. Shiro and Sakai (1972) calculated that at the transition temperature (573°C) α-quartz might be enriched in $\delta^{18}O$ relative to β-quartz by ~0.8‰. Kawabe (1978) calculated the same fractionation to be 1.5‰. Experimental determinations of the quartz-water fractionation, however do not show these differences (Clayton *et al.*, 1972; Matsuhisa *et al.*, 1979). The magnitude of this fractionation obtained by calculation is probably indicative of the errors inherent in the calculation method.

b. Hydrogen bonding in OH bearing minerals. Suzuoki and Epstein (1976) predicted that hydrogen bonded minerals should concentrate H relative to non-hydrogen bonded minerals. This prediction was borne out for the AlO(OH) minerals, epidote minerals and chlorites (Graham *et al.*, 1980,1987), all of which possess hydrogen bonds and were found to have much more negative mineral-water fractionation factors than might have been predicted for non-hydrogen bonded minerals (such as micas and amphiboles) of similar cation compositions at the same temperature. The presence of hydrogen bonding may cause quite large differences in fractionation. For example Suzuoki and Epstein show that the difference between the muscovite-water and boehmite-water fractionations, which can be reasonably attributed to the difference in degree of hydrogen bonding, is in the order of 50‰ at 400°C.

2.4.7 Determination of fractionation factors.

The methods employed in the determination of isotopic fractionation factors for geological systems are briefly outlined here in order that an appreciation of the errors associated with them may be gained. Fractionation factors can be determined in 3 ways:

a. Semi-empirical calculations using spectroscopic data and the methods of statistical mechanics. This method attempts to calculate ΔG° (eqn. 2.7) over the P,T range of interest by means of partition function ratios (see O'Neil 1986). This method works well for simple molecules such as gases, but problems occur in solids where corrections have to be made for

lattice vibrations. Kieffer (1982) however, has been able to use this method to generate a self consistent set of fractionation factors for rock forming minerals. Unfortunately some of these fractionation factors are inconsistent with those derived experimentally, indicating the influence of a factor which has not been taken into account in the calculations. Richet *et al.* (1977) point out that even small uncertainties in the vibration constants used as a basis for these calculations can result in errors in $10^3\ln \alpha$ that are larger than the limits of accuracy of isotopic analyses.

At the present time, therefore, these calculated fractionation factors are best avoided, unless no other calibrations are available.

b. Experimental determinations. A number of methods are used, but all involve exchange between water and a mineral at a measured temperature and elevated pressure (but see Mayeda *et al.*,1986). The run products are then analysed and the fractionation factor derived from the results. These fractionation factors are potentially very accurate. However equilibrium is rarely attained, and the equilibrium fractionation factor has to be derived by extrapolation of the results to equilibrium (Northrop and Clayton, 1966), unfortunately this method becomes unreliable for low degrees of exchange. The error on the fractionation factor is dependent on the analytical errors. If both water and mineral are analysed then the error on the fractionation factor is the sum of the individual errors. Graham *et al.* (1987) have pointed out that hydrogen may exchange with the pressure medium through the walls of a charge, enhancing errors for hydrogen isotope fractionations.

An idea of the errors that may be associated with experimental determination can be gained by examining the calibrations performed on the same system by different laboratories using different techniques. For example there is a difference in measured $10^3\ln \alpha_{(\text{ACTINOLITE-WATER})}$ at 400°C of 10‰ between the studies of Graham *et al.* (1984) and Suzuoki and Epstein (1976). Alternatively the determinations of $10^3\ln \alpha_{(\text{QUARTZ-WATER})}$ by Matsuhisa *et al.* (1979) and Clayton *et al.* (1972) agree within experimental errors over the range 500-250°C. It is important therefore to evaluate each experimental calibration on its individual merits.

c. Observation of natural samples. Experimental determination of fractionation factors in some mineral-fluid systems has proved impossible, especially at low temperatures. This is primarily the result of slow isotopic exchange rates for these minerals. For example, Graham *et al.* (1987) found that there was no appreciable exchange of hydrogen isotopes between chlorite and water at 400°C over run periods of 5 months. For this reason some authors have attempted to examine the isotopic fractionation in natural systems where temperature and isotopic composition of fluid can be measured or well constrained. For instance Marumo *et al.* (1980) were able to measure the temperature and hydrogen isotope composition of the chlorite in a modern hydrothermal system and to estimate $10^3\ln \alpha_{(\text{chlorite-fluid})}$ between 250-130°C. The major problem with this approach is the assumption of equilibrium between mineral and fluid. Hydrothermal systems evolve with time so that the temperature and isotopic composition of the fluid in the system at

present may not be the same as it was when the minerals were deposited. The slow exchange rates of minerals at low temperature means that re-equilibration to the new conditions may not have completely taken place (e.g. see discussion in Graham *et al.* 1980 on the Wairakei hydrothermal system).

In order to obtain α over a range of temperature, calibrations by this method often involve data from a number of different hydrothermal systems (Hattori and Muehlenbachs,1982). This has the disadvantage that other factors that can affect α, such as mineralogical composition, or fluid salinity may also be different.

To summarize therefore, it is apparent that although methods a. and c. can have some distinct advantages the experimental method for determination of α is to be preferred.

Values of $10^3 \ln \alpha$ for mineral-mineral fractionations.

Since nearly all experimental determinations of fractionation factor are determined on mineral-water systems, most mineral-mineral fractionation factors have to be derived by subtraction of two mineral-water equations (2.4.3). The choice of mineral-water equations is crucial. Subtraction of incompatible equations will produce an erroneous mineral-mineral fractionation. These can exhibit false crossovers at high temperature. (NB even if the equations are compatible, the errors from both will be compounded.) For this reason calculation of $10^3 \ln \alpha_{\text{MINERAL-MINERAL}}$ should preferably use mineral-water fractionation derived using the same method, if possible carried out in the same laboratory, in order to reduce systematic errors.

The values of fractionation factors used in this study are listed in appendix (A.4).

2.5 GEOTHERMOMETRY

The equilibrium fractionation of stable isotopes between 2 phases has the following properties which could make it ideal for use in geothermometry:

a. The fractionation often varies strongly with T (2.4.3), (nearly always decreasing with increasing temperature).

b. The fractionation is effectively independent of pressure, at least in the earth's crust (2.4.4).

c. The isotopic fractionation is often large in comparison to the analytical errors (A.1), even between high temperature phases.

Although other stable isotopes have been used to determine equilibrium temperatures, oxygen isotope thermometry is by far the commonest technique used. All subsequent remarks in this section (2.5) are concerned with this method.

2.5.1 The validity of oxygen isotope thermometry.

The validity of isotope thermometers depends on:

a. The attainment of equilibrium of the phases in question.

b. That this equilibrium should be attained at a geologically recognisable time.

c. That equilibrium is subsequently preserved from that time until the present.

Most minerals will attain oxygen isotope equilibrium by isotopic exchange in geologically short periods of time at temperatures greater than about 500-600°C. Therefore all minerals in igneous rocks will be in equilibrium at their crystallization temperatures, as will medium and high grade metamorphic rocks at the metamorphic peak. Non attainment of isotopic equilibrium between minerals is common in weathering, diagenesis, or low grade metamorphism or during low temperature alteration of high grade rocks.

The degree of preservation of equilibrium between minerals in cooling igneous and metamorphic rocks is primarily a function of the rate at which these rocks cool. Thus mineral phases in volcanic rocks represent the most ideal material for thermometry since they will almost certainly have attained equilibrium in the magma chamber, while the rapid quenching on eruption means that there is a good potential for preservation of this high temperature equilibrium. On the other hand the minerals in many slowly cooled regional metamorphic or plutonic igneous rocks may have re-equilibrated to new environmental conditions during cooling, so that the isotopic temperatures may not correspond to any geologically recognisable time, such as crystallization. Alternatively it might be expected that different minerals may re-equilibrate at different rates, in which case non-equilibrium assemblages, yielding meaningless temperatures would result.

The problem of distinguishing equilibrium from non equilibrium assemblages is fundamental to the successful application of isotopic thermometry. Concordance between temperatures calculated among various mineral pairs in the same rock is the most frequently used criterion for identification of equilibrium. In the past equilibrium temperature concordance between minerals was commonly identified using $\Delta-\Delta$ plots. For three coexisting minerals (X,Y,Z) when Δ_{X-Y} is plotted vs Δ_{Y-Z} minerals with concordant temperatures should plot along a line with a slope and intercept determined by the A and B coefficients of the two fractionation equations. Bottinga and Javoy (1975) reviewed the oxygen isotope data available for igneous and metamorphic rocks at that time, and using $\Delta-\Delta$ plots to test for equilibrium were able to conclude that, "the great majority of igneous and metamorphic rocks have conserved a state of oxygen isotopic exchange equilibrium". However Deines (1977) evaluated the same body of data and concluded that "less than half the rocks analysed to date would yield concordant temperatures". This difference is partly due to the elimination of data which Deines identified as possessing spurious correlations on $\Delta-\Delta$ plots and partly because Deines also used more accurate

experimentally determined fractionation factors in his survey. Deines suggests that many of the non-concordant assemblages are the result of retrograde exchange effects. In this respect it is interesting to note that using the fractionation factors determined by the Chicago group (often considered to be the best currently available) the fractionations between some mineral pairs in many plutonic rocks yield temperatures well below the solidus (O'Neil, 1986), implying that subsolidus re-equilibration is common in such rocks. Gregory and Criss (1986) show how correlations of data on Δ–Δ plots can result from a number of different processes including various disequilibrium processes. They suggest that the use of δ_{MIN}-δ_{MIN} plots combined with modal information is the only satisfactory way to test for isotopic equilibrium.

Within the last two decades, sufficient understanding of the different factors governing the rates of isotopic exchange in rock forming minerals has become available, to enable quantitative estimates of the rates of isotopic re-equilibration in these minerals using kinetic theory. Knowledge of these rates of isotopic exchange can be used to predict whether or not valid isotopic temperatures can be obtained from a given geological system. More importantly for this study, in situations where re-equilibration has taken place the kinetic approach can be used to extract information regarding the time span and temperature range over which the isotopic re-equilibration took place. Since the igneous and metamorphic rocks studied in this project might be expected to have undergone some retrograde re-equilibration, the kinetic approach is developed in the next section (2.6).

2.5.2 Errors in equilibrium isotopic temperatures resulting from analytical errors.

Even if it can be assumed that isotopic equilibrium between phases has been preserved, calculated equilibrium temperatures will have some uncertainty associated with them because of analytical error. The magnitude of this uncertainty is estimated here.

The fractionation between two phases is usually be described by an equation of the form (see 2.4.3)

$$10^3 \ln\alpha_{X\text{-}Y} = A(10^6 T^{-2}) + B \,.$$

Since we are dealing with oxygen isotope fractionations it is reasonable to make the assumption that $10^3 \ln\alpha_{X\text{-}Y} = \Delta_{X\text{-}Y}$. The variation of the calculated equilibrium temperature with a change in Δ is given by the partial derivative:

$$\left(\frac{\partial T}{\partial \Delta_{X-Y}}\right)_{A,B} = \frac{-T^3}{2A \times 10^6} \,.$$

The uncertainty in the calculated equilibrium temperature can be estimated using a standard error equation (Taylor, 1982):

$$\sigma_T = \left|\frac{\partial T}{\partial \Delta}\right| . \sigma_\Delta \,.$$

σ_T is thus a function of both T and A as well as Δ. The uncertainty in the determination of $\delta^{18}O$ values for minerals in most laboratories is $\pm 0.1‰$ at best. Therefore $\sigma_\Delta \approx 0.14‰$.

Fig. 2.2a is a contour plot of σ_T calculated for an appropriate range of A and T assuming a fixed σ_Δ value of 0.14‰. It can be seen that for a given A value, the uncertainty increases with increasing temperature as the fractionation between phases decreases. It is important to note that this differential method only gives the standard deviation in the calculated temperature, the errors are not in fact symmetrical. Hence the calculated error at 600°C for the quartz-alkali feldspar pair (A =0.46 Matsuhisa *et al.*, 1979) is ±102°C although in actual fact the true errors resulting from $\Delta \pm \sigma_\Delta$ are 600_{-80}^{+120} °C. This is because of the steepening of the fractionation curve with increasing temperature.

It is commonly assumed by isotope geochemists that the uncertainties on the A and B coefficients are negligible. These coefficients are normally determined by carrying out a linear regression of experimentally determined Δ values against T^{-2} over a range of temperature, however the goodness of fit of the regression line to the data is rarely published. In order to estimate the errors that might be associated with the A and B coefficients, the errors calculated for a published experimental calibration are given below. The quartz-water fractionation of Matsuhisa *et al.* (1979) was chosen because this was determined using the most modern techniques available and is commonly thought of as being the most accurate calibration attainable at present.

Regression statistics for the quartz-water fractionation determined by Matsuhisa *et al.* (1979)

	Temperature range	
	800-500°C	500-250°C
No. of points	4	4
r^2	0.997	0.997
A (std.err.)	2.05 (0.079)	3.34 (0.122)
B (std.err.)	-1.14 (0.099)	-3.31 (0.337)

It can be seen that the 500-250°C line is in fact quite a poor fit to the data. Both regressions suffer from the low degree of freedom resulting from only using four data points. If the uncertainties on the regressions for other mineral-water systems are assumed to be comparable (they are probably worse) to the uncertainties on the 500-250°C line, then for a mineral-mineral fractionation derived by subtracting two mineral water fractionations (Taylor, 1982)

$$\sigma_{A_{MIN-MIN}} = \sqrt{2 \times \sigma^2_{A_{MIN-WATER}}} \approx 0.17,$$

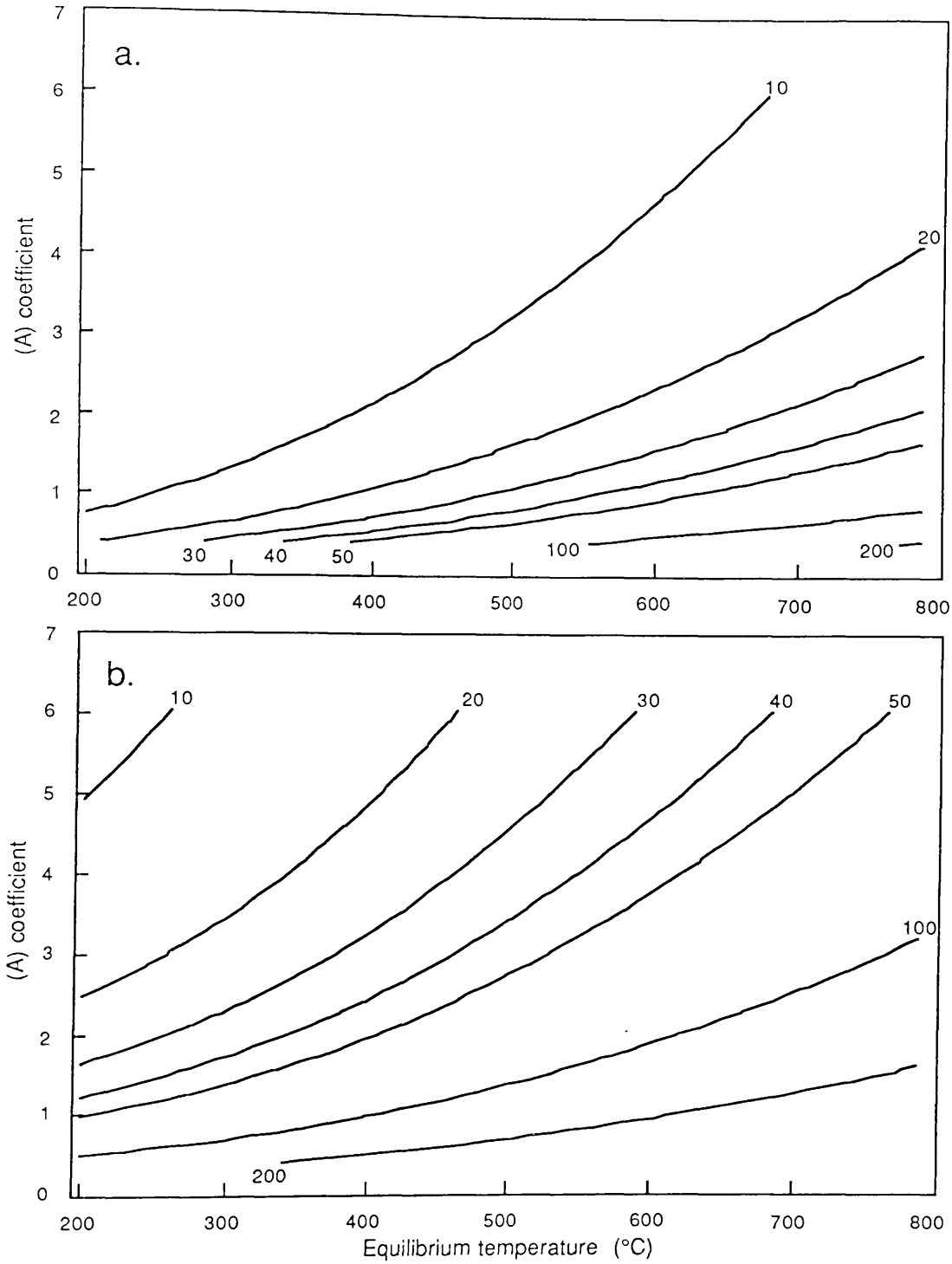

Fig.2.2. Contour plots of the uncertainty (σ_T) in the calculated equilibrium temperature for a mineral pair over a range of equilibrium temperature (T) and A coefficient in the fractionation equation, when a. all the uncertainty results from the analytical uncertainty in Δ, and σ_Δ is taken to be 0.14‰, and b. when the uncertainties on the A and B coefficients in the fractionation equation are also included (σ_A = 0.17, σ_B = 0.48‰). In both figures σ_T is independent of the actual value of the B coefficient.

and similarly $\sigma_B \approx 0.48$. The uncertainty on T can then be found using an error propagation equation:

$$\sigma_T = \sqrt{\sum_{i=1}^{i=n}\left(\frac{\partial T}{\partial x_i}\right)^2_{x_j(j\neq i)} \cdot \sigma^2_{x_i}},$$

where $x_i = \Delta$, A and B[1] . This equation was used to produce a contour plot of σ_T from the uncertainties given above (fig. 2.2b).

Most mineral pairs have A values less than or equal to 2 (e.g. quartz-epidote, quartz-albite, pyroxene-olivine, An_{60}-biotite). If A = 2 fig. 2.2b indicates that for the temperature range 300-600°C, σ_T could be 20-80°C. As A decreases σ_T rapidly increases. Mineral pairs having a value of A between 2 and 4 include pairs between a mineral with a strong affinity for ^{18}O, such as quartz, alkali feldspar and calcite and a mineral with a weak affinity for ^{18}O such as diopside, garnet or biotite. These mineral pairs could have σ_T of 10-80°C between 300 and 600°C. The only mineral pairs which have values of A greater than 4 are those in which one phase has a very strong affinity for ^{16}O such as rutile, ilmenite or magnetite and the other phase has a high affinity for ^{18}O. Temperatures calculated using these pairs may have values of σ_T = 5-50°C over the same temperature range. Unfortunately oxygen isotope analysis of oxide phases such as rutile, ilmenite and magnetite often proves to be more difficult than for other minerals and values of $\sigma\Delta$ may be > 0.14‰ for such mineral pairs!

It will be seen therefore that even if equilibrium is attained and preserved thereafter that it cannot be expected that equilibrium temperatures will be very accurate. Under some conditions, such as high temperature fractionation between a mineral pair with a small A value it is obvious that errors on the calculated temperatures will be so large that the temperature estimate will be of little use. Since these high temperature assemblages are also prone to down-temperature re-equilibration (see 2.5.1, 2.6) it is unlikely that there is any point in calculating temperatures in such rocks. The prospects for accurate thermometry in low temperature assemblages which have reached equilibrium are better, because of the increased fractionations between phases. However at very low temperatures kinetic isotope effects can become significant, setting a lower temperature limit for isotopic thermometry.

---

[1] It is realised that this approach is not statistically rigorous. It is used here only so that a rough idea can be gained of the uncertainty on T. The conditions for applying this equation include a. that the errors on x_i are independent and b. that σ_T is small in relation to T. In fact neither of these conditions may be met. A more correct statistical approach to this "calibration problem" is currently being investigated with Dr. Jim Kay of the Statistics Department Glasgow.

2.6 ISOTOPE EXCHANGE KINETICS

Isotope exchange takes place when two phases are out of isotopic equilibrium under the prevailing conditions. The 'driving force' for isotope exchange is the necessity that the system should always move towards thermodynamic equilibrium. However the path by which equilibrium is approached and the degree of equilibrium attained is governed by the kinetics of the exchange reaction. Thus a negligible amount of isotopic exchange will take place between a sample of quartz and some water at room temperature, even if they are grossly out of isotopic equilibrium, because the rate of exchange is so low under these conditions.

2.6.1 Some basic definitions

Some basic definitions of terms used in the study of geochemical kinetics are given below.

The rate or speed of a reaction is usually defined in terms of the change in concentration of the reactants in unit time, for reactions with one reactant W:

$$\text{rate} = \frac{-dC_W}{dt} ,$$

where C is the concentration of reactant at time t.

For a general reaction equation:

$$wW + xX + \ldots\ldots \Leftrightarrow yY + zZ\ldots . ,$$

the rate of reaction is

$$-\frac{1}{w}\frac{dC_W}{dt} \equiv -\frac{1}{x}\frac{dC_X}{dt} \ldots \equiv \frac{1}{y}\frac{dC_Y}{dt} \equiv \frac{1}{z}\frac{dC_Z}{dt} \ldots .$$

The rate constant k is the proportionality constant between the concentration of the reactant and the rate, in the simple case of one reactant:

$$-\frac{dC_W}{dt} = kC_W .$$

The order of a reaction is the sum of the exponents of the concentration terms in the rate equation, hence

$$-\frac{dC_W}{dt} = kC_W^2$$

is a second order reaction, where the rate depends on the square of the concentration of W. The order of a reaction can be any real number (i.e. can be fractional or negative) although it is often 0, 1 or 2 for simple reactions.

Lasaga (1981a) notes that the rate of complex reactions can depend on the concentrations of the products as well as the reactants, hence for our general equation:

$$\text{rate} = k C_W^{n_w} C_X^{n_x} \ldots C_Y^{n_y} C_Z^{n_z} \ldots$$

and the order is

$$n_W + n_X \ldots + n_Y + n_Z \ldots .$$

The units of k are the concentration to the power of -(order -1) per unit time. Hence the units of k are C t^{-1} for a zero order reaction, t^{-1} for a first order reaction and C^{-1} t^{-1} for a second order reaction.

The order of a reaction may give some indication of the mechanism of the reaction. In simple reactions the order may indicate the number of species that come together in the transition state for the slowest step of a reaction. This is not the case for more complex reactions (see Lasaga, 1981a).

Isotope exchange reactions progress towards a final equilibrium value. The rate of this type of reaction at any one time depends on the difference of the concentration of a reactant from its equilibrium concentration, so that the rate equation takes the form

$$-\frac{dC_W}{dt} = k(C_{We} - C_{Wt})^n, \qquad (2.11)$$

where C_{We} is the equilibrium concentration of W and C_{Wt} is the concentration of W at time t. It can be seen that at equilibrium $C_{We} = C_{Wt}$ and therefore the rate is zero.

Because isotope exchange reactions are equilibrium reactions they can be written as a reversible reactions such as

$$A^{16}O + B^{18}O \underset{k_-}{\overset{k_+}{\Leftrightarrow}} A^{18}O + B^{16}O,$$

where k_+ and k_- are the rate constants for the forward and reverse reactions. If following Cole and Ohmoto (1986) we assume that both the forward and reverse reactions are simple second order reactions then

$$\text{forward rate} = k_+[A^{16}O]\,[B^{18}O]$$

and

$$\text{reverse rate} = k_-[A^{18}O]\,[B^{16}O]$$

and

$$\text{overall rate} = \text{forward rate} - \text{reverse rate}$$

$$= k_+[A^{16}O]\,[B^{18}O] - k_-[A^{18}O]\,[B^{16}O].$$

At equilibrium the overall rate is zero, so that the rates of the forward and reverse reactions are equal:

$$k_+[A^{16}O]\,[B^{18}O] = k_-[A^{18}O]\,[B^{16}O]. \qquad (2.12)$$

This is an example of the principle of detailed balancing (Lasaga, 1981a). (Note that at equilibrium the exchange process does not stop, rather equilibrium is a dynamic balance). Equation 2.12 can be rearranged to

$$\frac{k_+}{k_-} = \frac{[A\,^{18}O][B\,^{16}O]}{[A\,^{16}O][B\,^{18}O]},$$

in which the right hand term can be seen to equal **K**, the equilibrium constant. Thus recalling equation 2.3 if one atom is exchanged then

$$\alpha = k_+/k_- . \qquad (2.13)$$

This equation is of great importance since it links kinetics with thermodynamics.

In isotope exchange reactions between two phases it is convenient to replace the concentration term in the simple rate equation (2.11) by another measure of the progress of the reaction which is defined in isotopic terms. This is F the fractional approach to equilibrium (Myers and Prestwood, 1951) where

$$F = \frac{n_f - n_i}{n_e - n_i}$$

and n_e = the number of atoms of the heavy isotope in one of the phases at equilibrium, n_i = the number of atoms of the heavy isotope in the same phase initially and n_f is the amount of heavy isotope present in that phase at a certain time. It is obvious that the values of n may be substituted by concentrations. Northrop and Clayton (1966) have shown that F can also be related to the α value for fractionation between the two phases, so that

$$F = \frac{\alpha_f - \alpha_i}{\alpha_e - \alpha_i} \qquad 1 - F = \frac{\alpha_e - \alpha_f}{\alpha_e - \alpha_i},$$

where α_e = the equilibrium fractionation between the two phases undergoing exchange, α_i = the initial fractionation and α_f = the final fractionation measured at a certain time. F can also be defined in terms of the δ value of one of the phases:

$$F = \frac{\delta_f - \delta_i}{\delta_e - \delta_i}, \qquad (2.14)$$

where the subscripts have the same meaning as those for n. F will vary between 0 and 1, since when no exchange has taken place $\delta_f = \delta_i$ and F = 0, while at equilibrium $\delta_f = \delta_e$ and F = 1.

For first order exchange, replacing C by (1-F):

$$\frac{-d(1-F)}{dt} = k_1(1-F),$$

where k_1 is the first order rate constant. On integration this gives

$$\ln (1-F) = -k_1 t . \qquad (2.15)$$

Hence for first order exchange a plot of ln(1-F) vs t will yield a straight line. Similarly it can be shown for second order exchange

$$\frac{F}{(1-F)} = k_2 t \,. \qquad (2.16)$$

The value of the rate constant is strongly dependent on temperature and is often found to follow the classic Arrhenius equation:

$$k = A_0 \exp(-E_a/RT), \qquad (2.17)$$

where A_0 is the pre-exponential factor, sometimes called the "frequency factor" (not surface area) and E_a is the activation energy. A_0 may be weakly dependent on temperature, although the effect of this on k is usually within the error of estimation of k (Lasaga, 1981a). E_a may also vary with temperature (Lasaga, *ibid.*). The temperature dependence of k given by (2.17) is a consequence of chemical reactions requiring a certain activation energy to be available before the reaction can take place. The Boltzmann factor exp (E_a/RT) is the fraction of molecules in the system that possess this amount of energy. The activation energy is often thought to be the activation energy for the rate-determining step (e.g. Graham, 1981) although Lasaga (*ibid.*) points out that for an overall reaction consisting of a number of steps the activation energy will be a composite of the activation energies of the elementary reactions.

Most reactions actually occur by means of a number of simple steps (elementary reactions), rather than the simple stoichiometric union of reactants and formation of products described by the reaction equation. Each of these steps will have an individual rate constant, however the overall rate constant of the reaction will depend on the rate constant of the slowest step which is termed the rate determining step (strictly this is only true for sequential reactions, see Lasaga 1981a).

This concept of rate determining step can also be applied to overall exchange processes (rate determining or limiting process), for example the factor controlling the amount of exchange in a mineral grain in a given time may be the rate of exchange of isotopes between the mineral and the fluid or it could be the rate of supply of fresh unexchanged fluid to the mineral grain.

In a sequential reaction consisting of a number of elementary reactions it is often the case that after a certain time the production of an intermediate species (reaction intermediate) by one reaction will come to be balanced by the breakdown of that intermediate by the next reaction. A state of dynamic equilibrium is thus achieved which is termed steady state. As with the rate determining step this concept can also be usefully applied to overall exchange processes, for example the isotopic composition of the intergranular fluid in a rock mass may remain constant if the rate of change in composition by exchange with the minerals in the rock is balanced by the recharge of that fluid with fresh unexchanged fluid from outside of the rock mass in question.

Isotope exchange reactions between minerals and fluid or between two minerals are examples of heterogeneous reactions in which exchange occurs between two different phases.

Two other terms that will be used in the next few sections which also require definition are transport and infiltration. Transport is the mechanism independent term which describes the actual movement of material or one particular chemical or isotopic species from one point in space to another. The term transport can also be used to describe the movement of heat in the same way. Transport will be discussed in more detail in 2.7. Infiltration is transport in the fluid phase due to the motion of the pore fluid (fluid flow) relative to the solid framework (Fletcher and Hofmann, 1974).

2.6.2 Isotope exchange mechanisms

Giletti (1985) notes that the free energy change involved in most natural isotope exchange reactions is 3-4 orders of magnitude smaller than the free energy changes observed in most common chemical reactions. Such low free energy changes could never be the driving force for chemical reactions and therefore isotope exchange must by necessity take place by other mechanisms. Isotope exchange between coexisting minerals is generally assumed to take place via an intergranular fluid phase, in which case the kinetics of all isotope exchange reactions in rocks can be described in terms of mineral-fluid exchange reactions.

Isotope exchange in mineral-fluid systems can occur by one or more of three mechanisms:

a. Diffusion.

b. Recrystallisation (solution-reprecipitation)

c. Chemical reaction forming a new phase

The diffusion and solution-reprecipitation exchange mechanisms can take place when the mineral and fluid are in chemical equilibrium, while chemical disequilibrium is required for a chemical reaction to take place. Mechanisms b. and c. have features in common and have been termed surface reactions (Cole *et al.*, 1983). Importantly experimental studies have shown (see Cole and Ohmoto, 1986 for a review) that regardless of reaction mechanism the rate of isotope exchange in mineral-fluid systems is a function of five main parameters: temperature, pressure, grain size, grain shape and solution to solid ratio.

Isotopic exchange by diffusion and by surface reactions are compared below.

2.6.3 Isotope exchange accompanying diffusion

Diffusion is defined as "the process by which matter is transported from one part of a system to another as a result of random molecular motions" (Crank,1975).

Examples of isotopic exchange in which diffusion of atoms through a mineral lattice appears to have been the dominant exchange process (termed here diffusion controlled exchange[1]) include the shifting of feldspar $\delta^{18}O$ values in the Scottish Tertiary intrusives as a result of meteoric water interaction (Forester and Taylor, 1976) and the commonly observed resetting of Rb-Sr intrusion ages during subsequent metamorphism.

An atomistic explanation of diffusion in crystals

At an atomic level, diffusion within crystals takes place by means of single atoms jumping from one point in a lattice to another. In the simple case where the individual jumps are independent of one another the diffusion flux (J) resulting from the these jumps can be described by simple random walk type equations. For example if diffusion occurs between two neighbouring lattice planes 1 and 2, the number of jumps (j_{12}) per unit time and per unit area from plane 1 to plane 2 is:

$$j_{12} = n_1 \Gamma_{12},$$

where n_1 is the number of atoms per unit area of the diffusing species on plane 1 and Γ_{12} is the jump frequency for an atom to jump from 1 to 2. Similarly:

$$j_{21} = n_2 \Gamma_{21}.$$

The net atom flux (J) between the planes is:

$$J = j_{12} - j_{21}.$$

If there is no driving force (see below) then

$$\Gamma_{12} = \Gamma_{21} = \Gamma$$

and

$$J = (n_1 - n_2)\Gamma. \qquad (2.18)$$

The atom concentrations per unit area (n) can be related to the concentration per unit volume (C) by

$$n = C\lambda,$$

where λ is the distance between neighbouring planes. Also the concentration difference can be expressed in terms of λ and the concentration gradient. Thus:

---

[1] "diffusion controlled exchange" is used here to describe isotopic exchange between a mineral and a fluid in which diffusion through the mineral is the rate limiting exchange process. It does not refer to the type of "transport controlled" reaction as defined by Berner (1981) in which growth or dissolution of a grain is rate limited by diffusion of material through the fluid phase to the fluid-mineral interface. However the term surface controlled reaction is used here in the same sense as it is defined by Berner (1981).

$$n_1 - n_2 = -\lambda(\partial n/\partial x) = -\lambda^2(\partial C/\partial x),$$

combining with (2.18) gives:

$$J = -\lambda^2 \Gamma (\partial C/\partial x), \qquad (2.19)$$

Thus it can be seen that in the absence of a driving force the diffusive flux is proportional to the concentration gradient. It should be noted however that the concentration gradient does not drive the diffusion (as is mistakenly suggested by Freer, 1981) because the diffusion of atoms between plane 1 and plane 2 will take place regardless of the concentration gradient, although a zero net flux will result if the concentration of atoms is the same on the two planes (from a thermodynamic viewpoint however it can be seen that diffusion down a concentration gradient will reduce the free energy of the system since an increase in entropy is involved, thus a "thermodynamic driving force" can be envisaged). A driving force as used here is defined (after Manning,1968) as any influence that makes the jump frequency for a jump in one direction between two given sites differ from that for a jump in the opposite direction between the same two sites. Manning (1974) lists a number of possible driving forces such as an electric field, a stress field or a temperature gradient. These driving forces are not thought to be important in this study and will be neglected henceforth.

Jump mechanisms

Manning (1968) describes a number of mechanisms by which atoms can jump from one site in a crystal to another. The vacancy mechanism is most probably the the dominant mechanism of oxygen diffusion in minerals. In this mechanism an atom jumps into a nearby vacant site, thereby leaving a new vacancy at its previous position. Hydrogen diffusion in minerals probably also takes place via a vacancy mechanism (see below under temperature dependence) but could take place by an interstitial mechanism if it is diffusing as atomic hydrogen, by virtue of its small size. Atoms jump directly from one interstitial site to another in this diffusion mechanism. At present it is not clear what form (e.g. H, H^+, OH^-, H_2O, O, O^{2-}) oxygen and hydrogen take when diffusing through silicate minerals.

The macroscopic effect of diffusion

It can be seen from the description of diffusion given above that the macroscopic effect of diffusion will be to "smooth out" any concentration gradient that exists. For example if a crystal of quartz is placed in an ^{18}O enriched fluid, we can envisage that the ^{18}O concentration at the very edge of the crystal will always be in isotopic equilibrium with the fluid (there may actually be a difference in ^{18}O concentration between the quartz and the fluid at the grain boundary due to isotopic fractionation). Thus a concentration gradient has been set up and at the first instance F = 0 (eqn 2.15). The ^{18}O (and the other oxygen isotopes) in the fluid will diffuse into the quartz crystal and the concentration gradient in ^{18}O will be reduced. At infinite time the concentration of ^{18}O and the other oxygen isotopes will be uniform across the grain and F will equal 1. Fig. 2.3 shows the flattening with time of calculated concentration profiles across a sheet shaped grain which was placed in a fluid with a fixed ^{18}O concentration. Since the oxygen

from the fluid has to diffuse further before reaching the centre of the grain, the concentration in the centre of the grain will always "lag behind" the concentration at the margin of the grain.

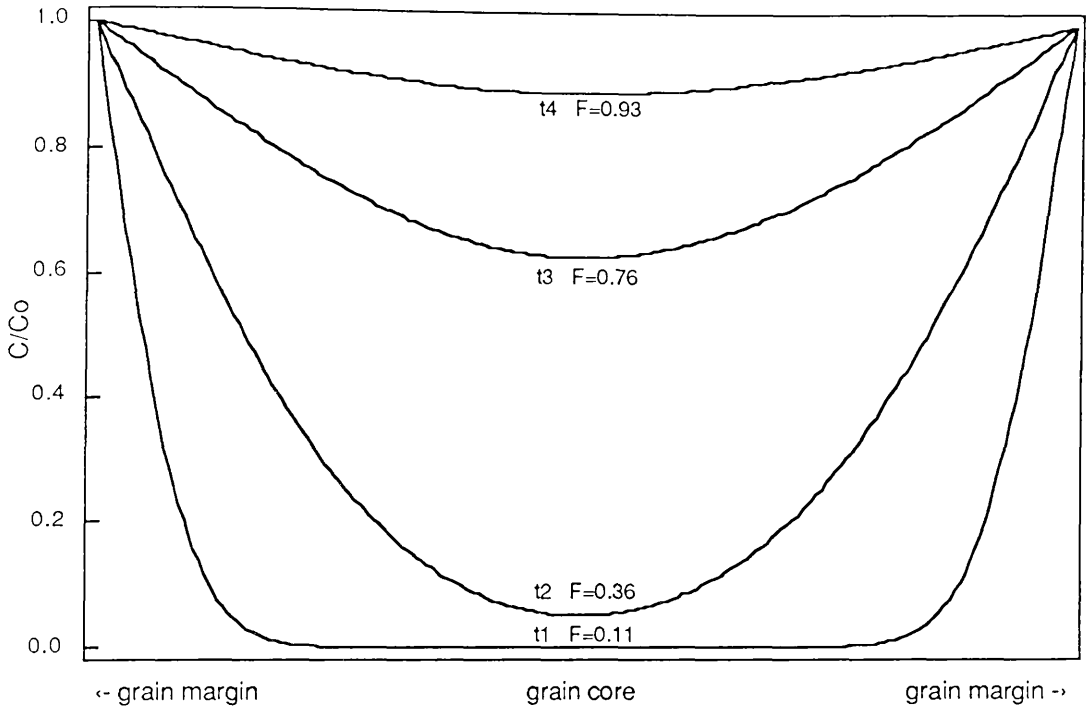

Fig.2.3 Concentration profiles at four different times (t4 > t3 > t2 > t1) across a plate shaped grain when the surface concentration is held at a fixed concentration. C/Co is the concentration of solute in the grain relative to the original concentration in the solute. Initially the grain contained no solute. No fractionation takes place at the grain boundary. F= numbers on curves are the fractional approach to equilibrium. Profiles calculated using equation 4.45 (infinite plate model) from Crank (1975). Parameters used were b (volumetric fluid/mineral ratio) = 10000, 1/2 plate thickness = 1, D = 1 and times t1 = 0.01, t2 = 0.1, t3 = 0.5, t4 = 1.0. Note this and all subsequent examples of diffusion profiles show the diffusion of a solute into a grain. The mathematical solutions to the opposite situation where solute is diffusing out of the grain are identical, provided the variables are suitably renamed. The diffusion profiles in this situation will therefore be the same shape but will be inverted.

The diffusion coefficient

The diffusion coefficient (D) is defined as the proportionality constant between the flux of material through unit area of a section of a solid and the concentration gradient measured normal to this section:

$$J = -D\,(\partial C/\partial x), \tag{2.20}$$

which is Fick's first law. It can be seen that this equation takes the same form as eqn 2.19, thus D is proportional to the square of the jump distance and to the jump frequency. Since J is not readily measurable the diffusion coefficient is usually found using the partial differential equation:

$$\frac{\partial C}{\partial t} = D\left(\frac{\partial^2 C}{\partial x^2}\right) \tag{2.21}$$

(Fick's second law), or a transformation of this equation to other coordinates. It can be seen from this equation that the units of **D** are distance^2 time^{-1}.

A number of different diffusion coefficients have been defined. The diffusion coefficient that is appropriate for the purpose of this thesis is the tracer diffusion coefficient (often written as **D***, although **D** is used here), which is defined as the diffusion coefficient measured for a tracer isotope present in a very dilute concentration in an otherwise homogeneous crystal, when there are no driving forces (Manning, 1968). If the diffusing species is present in large quantities the structure of the mineral may vary with diffusant concentration and since **D** is related to structure, **D** could also vary with concentration (this is the intrinsic diffusion coefficient). Deuterium and ^{18}O are present in such small quantities in natural samples that this should not be the case. The term "self diffusion coefficient" is sometimes used to refer to the special case of tracer diffusion where the tracer atoms are of the same species as the non-tracer atoms in the crystal.

The effect of temperature on the rate of diffusion.

The temperature dependence of the diffusion coefficient is usually given in an equation of the form

$$D = D_0 \exp(-E/RT), \tag{2.22}$$

where both the pre-exponential factor (D_0) and the activation energy for diffusion (E) are independent of temperature, but depend on the identity of the diffusing element and the composition of the diffusing crystal and can also vary with pressure.

The exponential dependence of **D** on temperature can be explained by the atomistic approach. If the diffusion occurs by means of a vacancy mechanism then it can be seen that the number of atoms jumping into adjacent vacancies (total jump frequency) will depend on a. the number of vacancies and b. the fraction of atoms which being next to a vacancy have sufficient thermal energy to go over a migration activation energy barrier and into the vacancy.

Vacancies and other point defects can be divided into two types:

a. Intrinsic defects (Schottky or Frenkel defects) are thermally generated and increase exponentially with temperature:

$$X_{Vint} \propto \exp(-\Delta H_f/2RT), \tag{2.23}$$

where X_V is the mole fraction of vacancies and ΔH_f is the energy needed to form the vacancy (Lasaga, 1981d).

b. Extrinsic defects are dependent on the amount of impurity ions in a crystal and are independent of temperature:

$$X_{Vext} \propto C_{impurity}.$$

Thus the total mole fraction of vacancies:

$$X_V = X_{Vint} + X_{Vext},$$

is partly a function of temperature. Since X_{Vint} increases exponentially with temperature, at high temperatures X_V will be dominated by intrinsic vacancies:

$$X_V \approx X_{Vint}$$

(intrinsic diffusion region), while at low temperatures extrinsic vacancies will become dominant:

$$X_V \approx X_{Vext}$$

(extrinsic diffusion regime). Because of the exponential dependence of X_{Vint} the transition between regimes occurs over a fairly short range of temperature. Lasaga (1981,d) states that most silicates of geochemical interest contain enough impurities that diffusion should take place in the the extrinsic regime under geological conditions.

When an atom jumps into a neighbouring vacancy it is jumping from one site in which it is energetically favoured to another such site. However the region in between is less energetically favoured because the atom has to push past other nearby atoms . The migration energy (ΔH_m) is the minimum energy that is required before the jump can take place. The number of atoms which possess this minimum energy increases exponentially with temperature:

$$\text{atoms with minimum migration energy} \propto \exp(-\Delta H_m/RT).$$

Thus

$$\text{total jump frequency} \propto X_V \exp(-\Delta H_m/RT),$$

so that in the extrinsic region

$$\text{total jump frequency} \propto X_{Vext} \exp(-\Delta H_m/RT)$$

and therefore $E = \Delta H_m$, while in the intrinsic region

$$\text{total jump frequency} \propto X_{Vint} \exp(-\Delta H_m/RT),$$

which on substituting (2.23) gives

$$\text{total jump frequency} \propto \exp(-\Delta H_f/2RT) \exp(-\Delta H_m/RT).$$

Thus it can be seen in the intrinsic region that $E = \Delta H_m + \Delta H_f/2$. The pre-exponential factor D_0 incorporates the squared jump distance, the number of possible jump paths and the mole fraction of defects at infinite temperature in the intrinsic region or X_{Vext} in the extrinsic region.

Equation (2.22) is an Arrhenius type relationship. Taking logarithms on both sides gives:

$$\log D = \log D_0 - E/2.303\,RT.$$

Hence a plot of log D vs. 1/T (called an Arrhenius plot) will yield a straight line, with an intercept of log D_0 at infinite temperature and a slope of -E/2.303 R. The transition from the intrinsic to the extrinsic diffusion regime will be shown by a knee on the Arrhenius plot with a lowering of E and D_0 in the extrinsic region.

The diffusion coefficients used in this study are shown on Arrhenius plots in Fig. 2.4a,b (next page). It can be seen that the slopes of the lines for both oxygen and hydrogen diffusion are fairly similar (E ≈ 15-40 kcal mol^{-1}) but the absolute values for the diffusion coefficients in different minerals may differ by several orders of magnitude at the same temperature. The diffusivity of hydrogen in different minerals is distinctly higher than for oxygen (3-4 orders of magnitude in hornblende).

The relative uniformity of activation energies may suggest that a similar diffusion mechanism may operate in all these minerals (Lasaga, 1981a, p.34). All of these diffusion coefficients were measured using hydrothermal apparatus, and water may well be important in this diffusion mechanism, since activation energies measures under anhydrous conditions are distinctly higher (>50 kcal $mole^{-1}$, e.g. Muehlenbachs and Kushiro, 1974).

Diffusion in a rock.

So far we have only been concerned with diffusion within a region of regular crystal structure. This is termed volume diffusion. However diffusion within a crystalline solid can also occur along faster routes such as grain boundaries, cleavage planes and dislocation lines (grain boundary diffusion), along free surfaces (surface diffusion) or through the fluid phase contained along the grain boundaries (see Fig. 2.5).

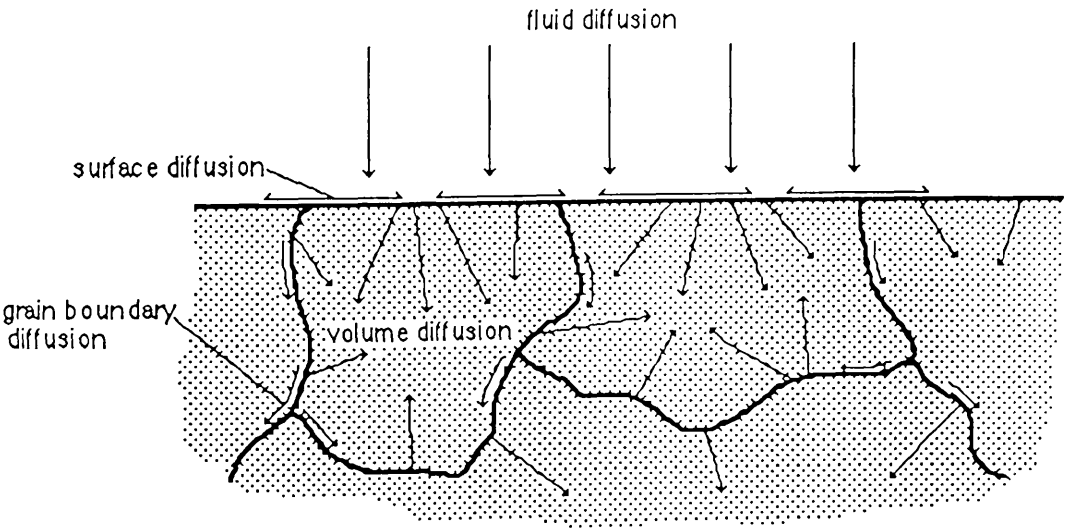

Fig.2.5 Surface, grain boundary and volume diffusion paths in a simple solid. After Manning (1974).

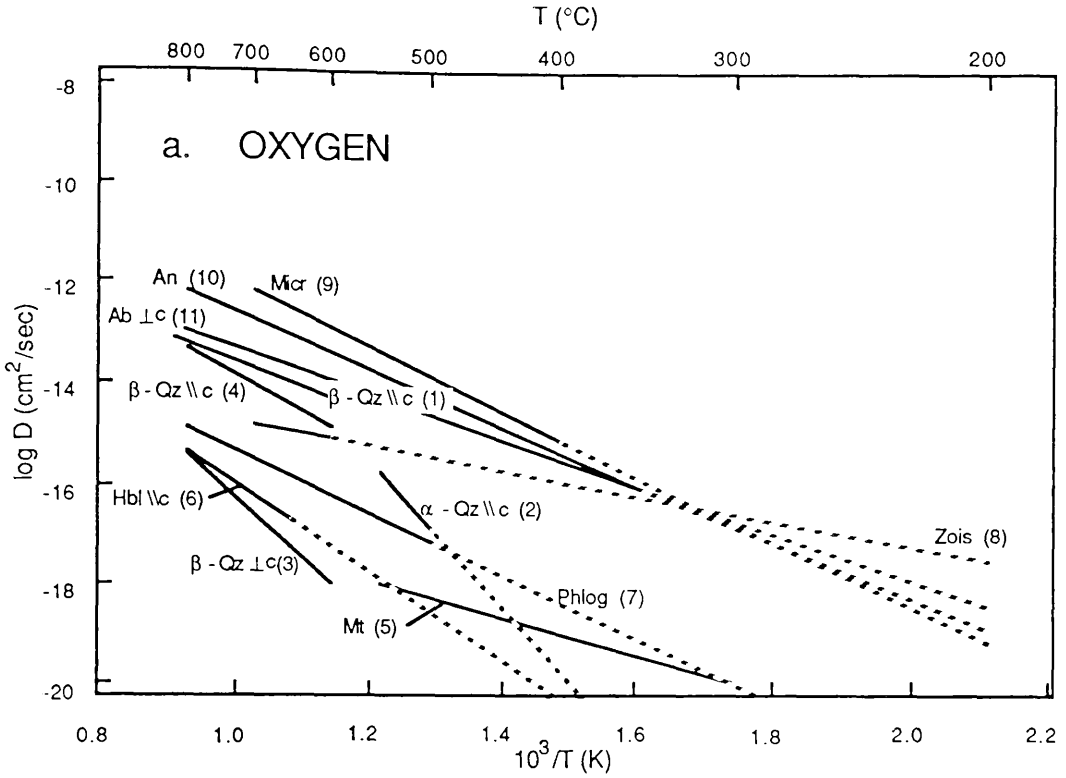

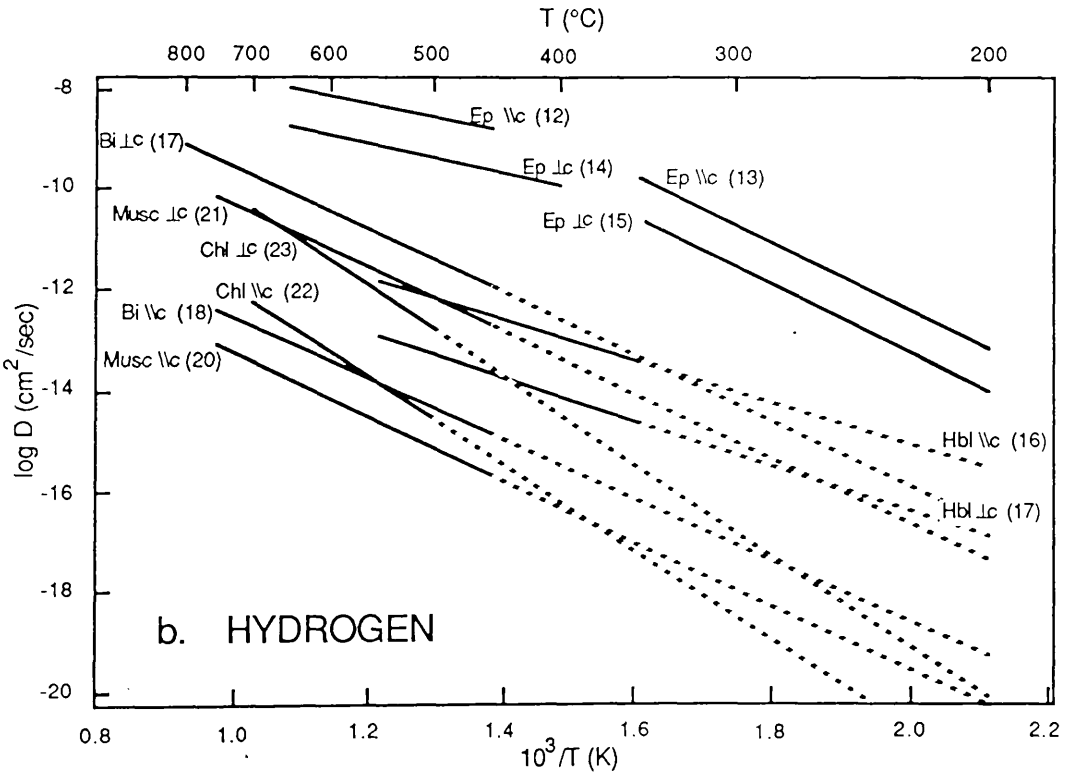

Fig.2.4. Composite Arrhenius plots of oxygen and hydrogen diffusion coefficients derived from hydrothermal experiments which are pertinent to this study. //c and ⊥c refer to transport directions in minerals i.e. parallel to the c-axis and normal to the c-axis respectively. The data sources is given in A.5. The data used to construct these lines are given in A.5 and are indexed by the number next to each line.

The density of dislocations in a crystal is measured as the number of intersections with unit area and can vary from $100/cm^2$ for nearly perfect crystals to 10^{11}-$10^{12}/cm^2$ in strongly defective crystals (Kittel, 1956, p.617).

Measurements of grain boundary diffusivities in silicates are sparse. Kovalev (1971) determined the self diffusion coefficients of Fe, Ca and S in granodiorite to be 10^{-3}-10^{-5} $cm^2\ s^{-1}$ at temperatures between 1000 and 500°C (compare with values of 10^{-12}-10^{-18} $cm^2\ s^{-1}$ for oxygen volume diffusion in silicates over the same temperature range - fig. 2.4). Unfortunately Kovalev's measurements probably included some transport by infiltration as well as diffusion so that his coefficients may be too high. Elliott (1973) suggests that grain boundary diffusion may take place in channels one or two atomic spacings thick which are highly disordered and have a high concentration of vacancies. Such a structure is similar to that of silicate glasses and therefore Fisher and Elliott (1974) have suggested that self diffusion data for silicate glasses may give a rough estimate of silicate grain boundary diffusivities. Measured diffusion coefficients in silicate glasses range from 10^{-4} to 10^{-12} $cm^2\ s^{-1}$ between 1000 and 500°C (compilation in Fisher and Elliott, *ibid.*).

No data appears to exist for surface diffusivities in silicates, although by analogy with metals the diffusion coefficient might be expected to be higher than that for grain boundary diffusion at the same temperature.

Diffusion coefficients have been obtained for most electrolytes in water at room temperature and are found to be be typically of the order of 10^{-5} $cm^2\ s^{-1}$ these may increase to ~ 10^{-4} $cm^2\ s^{-1}$ at temperatures of 500-700°C (Fletcher and Hofmann, 1974). The self diffusion coefficient of liquid water is 2.2×10^{-5} $cm^2\ s^{-1}$ (Franks, 1972).

Thus it can be seen that diffusivities at low temperatures increase in the order

volume diffusion < grain boundary diffusion < surface diffusion < fluid diffusion.

The reason for this is the increase in defect concentration and decrease in activation energies in the same way. Extrinsic defects are often much more common along grain surfaces. Atoms within a crystal lattice will be more constrained in their motion than atoms at a grain boundary, while atoms on a free surface will be less constrained and thus ΔH_f (governing the concentration of intrinsic defects) and ΔH_m (governing the motion of all defects) will decrease in this order. In simple crystals such as metals the activation energy for volume diffusion has been found to be typically twice that for grain boundary diffusion which in turn is about twice that for surface diffusion (Manning, 1974). The activation energy for diffusion in a liquid might be expected to be much lower than in solids (15-40 kcal mol^{-1} see above), and this appears to be the case with activation energies typically less than 5 kcal mol^{-1} (Lasaga, 1981a). Because of the large difference in activation energy between fluid and grain boundary and volume diffusion, at low temperatures transport through a rock mass by grain boundary diffusion dominates that by volume diffusion. However at high temperatures, because of the stronger temperature dependence and because diffusion can take place over a much greater cross sectional area normal to

the transport direction, volume diffusion may become the dominant diffusive transport process. Nevertheless volume diffusion will always be the limiting process controlling the movement of material into regions of good crystal structure.

The effect of pressure on the rate of diffusion.

Unlike the effect of temperature on the rate of diffusion, which is expected from theory and is well documented by experimentation, the dependence on pressure is poorly understood. The pressure dependence might be expected to follow an Arrhenius relationship:

$$D_P = D_0 \exp(-P\Delta V^*/RT), \qquad (2.24)$$

where ΔV^* is the activation volume for diffusion (Lazarus and Nachtrieb, 1963). The activation volume is the sum of two terms: ΔV_f, the change in volume of a crystal on the formation of a defect and ΔV_m, the lattice expansion attending an atomic jump. The first term may be negative (in the case of inward relaxation of the lattice around a vacancy) or positive (due to outward relaxation around an interstitial). The second term is always positive (Lazarus and Nachtrieb, *ibid.*). ΔV^* is nearly always positive, so that an increase in pressure should result in a decrease in the diffusion coefficient. This is the case for the inter-diffusion coefficient (D) for Fe-Mg exchange in olivine. Misener (1974) found that D at 900 and 1100°C decreases by approximately an order of magnitude as P increases from 0-35 kb. The calculated values of ΔV^* were in the range 4-7 cm^3 $mole^{-1}$. If the activation volume is similar for oxygen isotope diffusion then over a small range of pressure (< 10 kb) the pressure dependence of D would be less than the experimental error (D is believed to be accurate to a factor of 2) and therefore insignificant. However Yund and Anderson (1978) measured an apparent 10-fold increase in the oxygen diffusivity in adularia in 2M KCl solution at 650°C as the fluid pressure increased from 125-4000 bars and Giletti and Yund (1984) observed that D for oxygen exchange between quartz and water increased 10-fold with an increase in water pressure from 250-3500 bars. These results have not been confirmed by other workers however. For example Freer and Dennis (1982) observed no significant pressure effect on oxygen diffusion between 0.5 and 8 kb when albite was exchanged with water at 600°C and Dennis (1984) observed no pressure effect on oxygen diffusion in quartz between 0.1 and 1 kb. There may be several reasons for these differing results:

Ewald (1985) has proposed a two-stage model for diffusion controlled mineral fluid exchange. The first stage involves a reversible surface reaction in which the diffusing species moves from the fluid to become attached to the mineral surface, while the second stage involves the volume diffusion of this species into the mineral. Ewald suggests that it may be the initial reaction that is pressure dependent. Increasing pressure would act to decrease the molar volume of the fluid and hence increase the concentration of diffusing species, which would in turn increase the concentration of the diffusing species in the surface complex. This Ewald argues would increase the observed amount of exchange that takes place in a given time. The apparent change in diffusivity of oxygen in adularia with pressure in bulk exchange experiments described by Yund and Anderson

(1978) could thus be interpreted in terms of exchange via such a P dependent surface reaction followed by volume diffusion into the grain in which D is relatively constant (e.g. following an Arrhenius relation such as eqn 2.22). Ewald cites the results of Freer and Dennis (1982) as supporting his model. These workers used an ion microprobe method to investigate the diffusion of oxygen into albite. They found that the surface concentration of ^{18}O did indeed vary with pressure (Fig. 2.6), being lowest at 0.5 kb (~50% of the concentration in the fluid) but rapidly increasing by 1 kb (86% of the fluid concentration), thereafter slowly approaching the fluid composition with a further increase in pressure. The method of calculating D in this case takes into account the variation in the surface concentration (unlike bulk exchange experiments) and values of D calculated in this way were found to be independent of pressure within analytical error. Freer and Dennis themselves suggest that these results could be explained if a surface mechanism which is a function of pressure is operating.

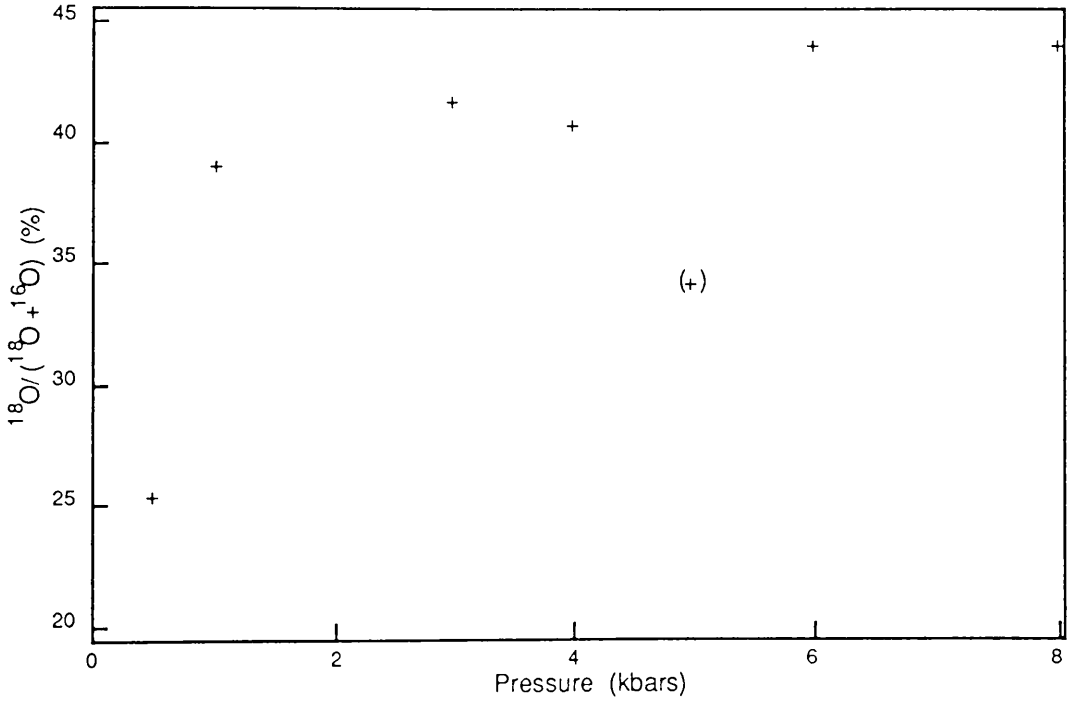

Fig.2.6 Surface concentration of ^{18}O in albite as a function of pressure after hydrothermal exchange experiments with enriched water ($^{18}O/(^{18}O + ^{16}O)$ = 44.5%). Exchange experiments were carried out at 600°C for 24-25 hours (except the 0.5 kb run ≈ 44 hr). After Freer and Dennis (1982).

Unfortunately the theoretical basis of Ewald's model is questionable. He states that the initial reaction is an equilibrium process while the volume diffusion into the grain is rate determining. The increase in rate of ^{18}O moving into the grain is thus governed by the increasing concentration of ^{18}O at the surface (see below: The effect of fluid/mineral ratio...). However if the volume diffusion of oxygen into the grain is rate limiting , then unless drastic fractionation of oxygen isotopes is taking place in the surface process (highly unlikely) then we should expect in this case that the concentration of ^{18}O (in terms of total oxygen) at the grain surface would equal the concentration in the fluid, regardless of the molar volume of the fluid. This is obviously not the case in the experiments of Freer and Dennis. However a two stage exchange process can be used to explain these results if it is

assumed that the surface reaction is rate limiting and diffusion is fast in comparison (Ewald's case 2, p.180). In this case the concentration of ^{18}O at the surface of the grain would reach a non equilibrium value controlled by the rate of movement into the grain of ^{18}O from the surface process and the movement of ^{18}O into the the grain by volume diffusion. If the forward rate of the surface reaction increases with increasing pressure then eventually the volume diffusion process would become rate limiting and the surface concentration would tend towards the concentration in the fluid. This is in accord with the observations of Freer and Dennis (1982) see Fig. 2.6, (see below: The effect of a rate limiting surface step, for the effect that this may have on the rate of exchange). The results of Giletti and Yund (1984) were also obtained using the ion microprobe method, but they found in contradiction to this theory, that even when the variation in surface concentration was taken into account that the value of D did appear to be dependent on pressure. However the results of Dennis (1984) that were also obtained by this method do not show this. It is interesting to note that the surface concentration of ^{18}O was found to be lower than the fluid concentration in both of these studies (although Giletti's group have attributed this in the past to a dilution effect from the primary 0^- beam which they have used in their experiments, see Giletti *et al.*, 1978).

Cole and Ohmoto (1986) suggested that the discrepancy between the results of Dennis and those of Giletti and Yund might be explained in terms of the defect contents of the samples. Dennis pre-annealed his samples in air at 850°C for up to a month after final polishing, while Giletti and Yund used a surface etch to try to remove surface defects due to polishing. If one method was more successful than the other in removing defects then the difference in defect content might explain the different pressure dependencies of the two samples (see below: The effect of impurities...). Giletti and Yund (1984) suggest that an increase in water pressure may increase the concentration of some impurity, such as OH^-, H^+, H_2O in the crystal, and that this could enhance the rate of diffusion. They note however that the defect that this impurity creates must be different from those naturally present (OH^- ions), and that it would have to be able to diffuse into the crystal as fast if not faster than than the oxygen bearing species if it is to have an effect. It would seem unlikely that this fast diffusing species can contain both O and H since oxygen diffusion is as fast into water rich synthetic crystals as into natural crystals and therefore a monoatomic hydrogen species is implicated.

If a solution-reprecipitation process (see 2.6.4) was also taking place in these experiments then the rate of exchange might be expected to increase with increasing pressure, as mineral solubility increases. However both Giletti and Yund (1984) and Yund and Anderson (1978) give good reasons why a solution-reprecipitation process was not important in their experiments.

The effect of grain size on the rate of diffusion controlled isotope exchange.

The rate of diffusion is not affected by grain size, however for volume diffusion into a homogeneous grain the approach to equilibrium (F) will depend on the grain size, because the distance over which diffusion has to

take place is changing. Figs, 2.7 a,b and c,d compare the calculated diffusion profiles expected in two sheet shaped grains under the same conditions, except that one of them is half the thickness of the other. For a given time the smaller grain has always achieved a closer approach to equilibrium than the larger grain, thus the rate of equilibration will be greater for a smaller grain. Hence if a fluid that is out of isotopic equilibrium with a monomineralic rock is passed along the grain boundaries, all other factors being equal a greater degree of exchange will take place in a finer grained rock than a coarse grained one. An additional factor will be that in the coarse grained rock the area of grain boundaries per unit volume will be smaller for a coarse grained rock and thus fluid transport into the rock volume, either by grain boundary flow or grain boundary diffusion may be more limited in a coarse grained rock and the rate of equilibration may be further reduced.

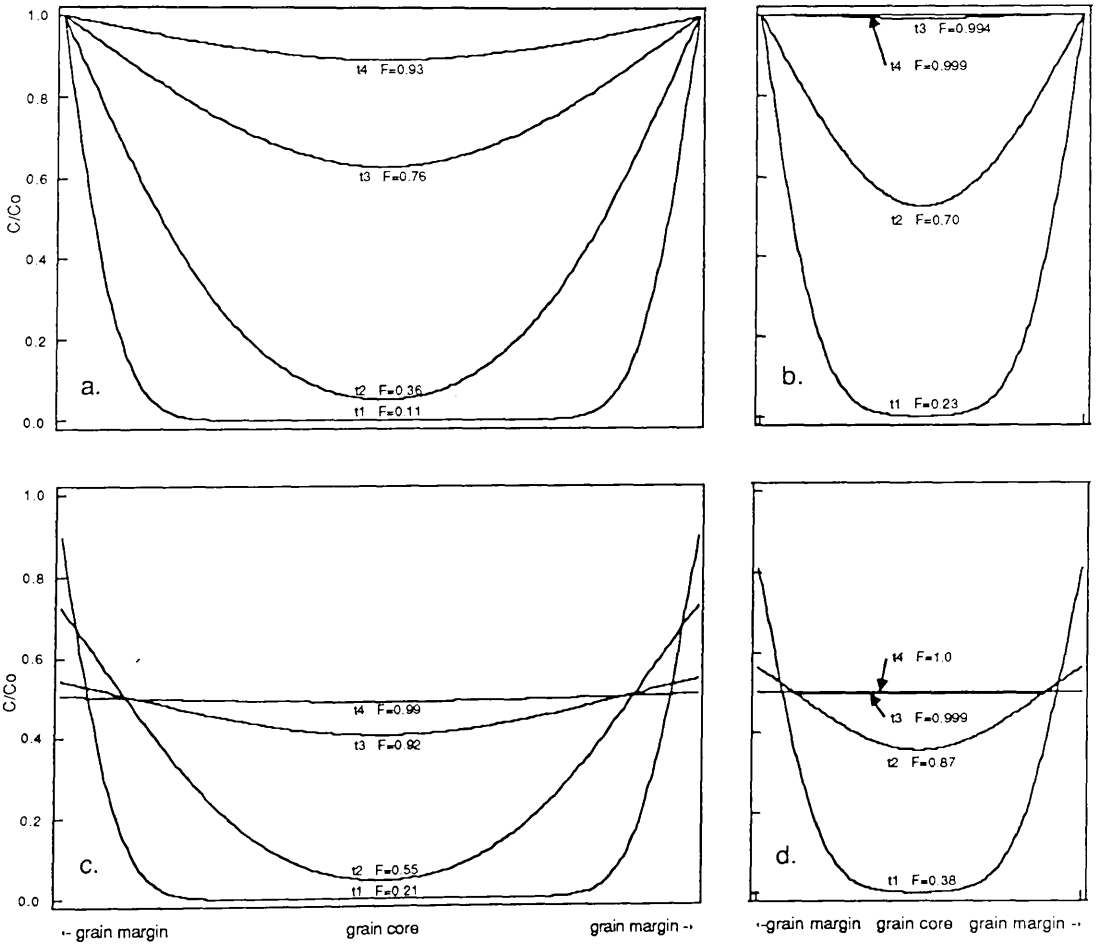

Fig.2.7 Concentration profiles at four different times (t4 > t3 > t2 > t1) across plate shaped grains for two different plate thicknesses and two fluid/mineral ratios (β). C/Co is the concentration of solute in the grain relative to the original concentration in the solute. In figs a. and c. the plate is twice the thickness of the plate in figs b. and d. In figs a. and b. the solution volume is very large so that the the solution concentration remains constant with time. In figs c. and d. the solution volume is equal to the plate volume so that both the solution composition and plate composition change with time. Initially the grain contained no solute. No fractionation takes place at the grain boundary. F= numbers on curves are the fractional approach to equilibrium. Profiles calculated using

equation 4.45 (infinite plate model) from Crank (1975). Parameters used were β = 10000 (figs a. and b.) and 1 (figs c. and d.), 1/2 plate thickness = 1 (figs a. and c.) and 0.5 (figs b. and d.), **D** = 1, and times t1 = 0.01, t2 = 0.1, t3 = 0.5, t4 = 1.0.

If it is assumed that volume diffusion is the limiting step controlling the rate of exchange, then a variation in grain size will only affect the exchange rate if transport in and out of a grain is solely by volume diffusion. If for example a grain is cracked or possesses cleavage or discordance planes then grain boundary diffusion may be the dominant transport mechanism into the the interior of the grain and the distance over which volume diffusion has to take place is effectively reduced. If planes along which grain boundary diffusion can take place are abundant within a grain the effective grain size may be fraction of the physical grain size. For example Dodson (1979) notes that Rb-Sr cooling ages (believed to be controlled by Sr diffusion) for biotites from part of the Alps are the same for biotite samples with flake diameters that vary between 0.1 and 30 cm. Either Sr exchange is not taking place by a volume diffusion mechanism, or the effective grain size for diffusion is the same for all the biotites i.e. $\leq$ 1 mm in diameter. However Giletti (1974b) has shown that Ar loss from phlogopite flakes under the same experimental conditions is inversely proportional to the grain diameter for flakes up to 646 μm across. The effective grain size for diffusion is one of the parameters used in the calculation of **D**, and Giletti found that the values of **D** calculated for different grain size fractions were the same if the physical grain size is used in the calculation, thus proving that in this case the physical grain size is equal to the effective grain size for diffusion. Similarly Foland (1974) found this to also be the case for alkali diffusion in homogeneous orthoclase grains up to 480 μm diameter.

From the limited data available it appears therefore that the effective grain size for diffusion in minerals may be of the order of a fraction of a millimetre. However it is likely that this value could be significantly reduced by, for example, the presence of exsolution structures in minerals which could provide surfaces for grain boundary diffusion (e.g. perthites in feldspars or a submicroscopic scale exsolution in amphiboles) or the opening of cleavage planes in a mineral if deformation is taking place at the same time as isotope exchange.

The effect of grain shape on the rate of diffusion controlled isotope exchange.

The diffusion coefficient is expected to vary with orientation within a crystal (diffusion anisotropy). This is because both the average squared jump distance (λ^2 which will affect D_0) and ΔH_m (which affects E) will vary with respect to lattice orientation. Ion probe examination of diffusion profiles in oriented crystals has enabled **D** to be measured with respect to different crystallographic orientations in some minerals. For example Giletti and Yund (1984) report that for quartz the diffusion coefficient for oxygen parallel to the c-axis is approximately 2-3 orders of magnitude greater than the diffusivity of oxygen normal to c.

Results from bulk exchange experiments combined with an analysis of sample stereometry may also be used to gain some information about the diffusional anisotropy in minerals by testing the the degree of fit of the data

to different diffusion models. These models are necessarily simplistic in order that mathematical solutions to them are tractable

There are three models which are often used to describe diffusion in minerals.

a. The infinite plate (or plane sheet) model (fig.2.8a). Transport of material by diffusion is assumed to take place only in one dimension, which is perpendicular to two parallel infinite planes. In practice this applies to materials in which diffusion in one direction is far more rapid than in any other direction, or to material which occurs in plates so thin that effectively all the diffusing substance enters through the plate faces and a negligible amount enters through the edges. It is important to note that in this second situation, diffusion in the mineral need not necessarily be anisotropic, the necessary criteria for the model are provided by the physical shape of the mineral.

b. The infinite cylinder model (fig. 2.8b). Transport of material by diffusion is assumed to take place radially from or to the curved surface of a cylinder which is of infinite length in its axial direction. In practice this model applies to materials in which diffusion is rapid in two directions relative to a third direction, and the diffusion coefficients in the fast directions are approximately equal. Alternatively this model may apply to grains which have an elongated cylindrical shape such that a negligible amount of material enters through the cylinder ends. Again in this situation diffusion need not necessarily be anisotropic.

c. The spherical model (fig. 2.8c). Transport by diffusion is assumed to take place at approximately equal speeds in all directions.

It might be expected that the different diffusion models could be related to the crystallographic anisotropies seen in minerals, and this is usually found to be the case. For example hydrogen transport in amphiboles may be described by the plate model in which diffusion takes place dominantly parallel to the chains (// to c, fig. 2.8a.ii) while hydrogen transport in micas is believed to take place dominantly by diffusion parallel to the layers ($\perp$c, fig. 2.8b.ii) and is therefore described by the infinite cylinder model.

It is important to note that the natural situations which these models are used to represent may often be more complex. For example transport by diffusion may be dominant in two directions so that the infinite cylinder model is applicable, however transport in the third dimension may not be insignificant. The result of this will be that **D** calculated using the cylinder model may slightly overestimate the value of the diffusion coefficient in the radial direction in the cylinder, since all diffusive transport is effectively resolved into this orientation.

A knowledge of diffusion anisotropy or at least the most appropriate diffusion model is necessary so that the appropriate grain dimension(s) can be measured in natural samples for use in diffusion calculations.

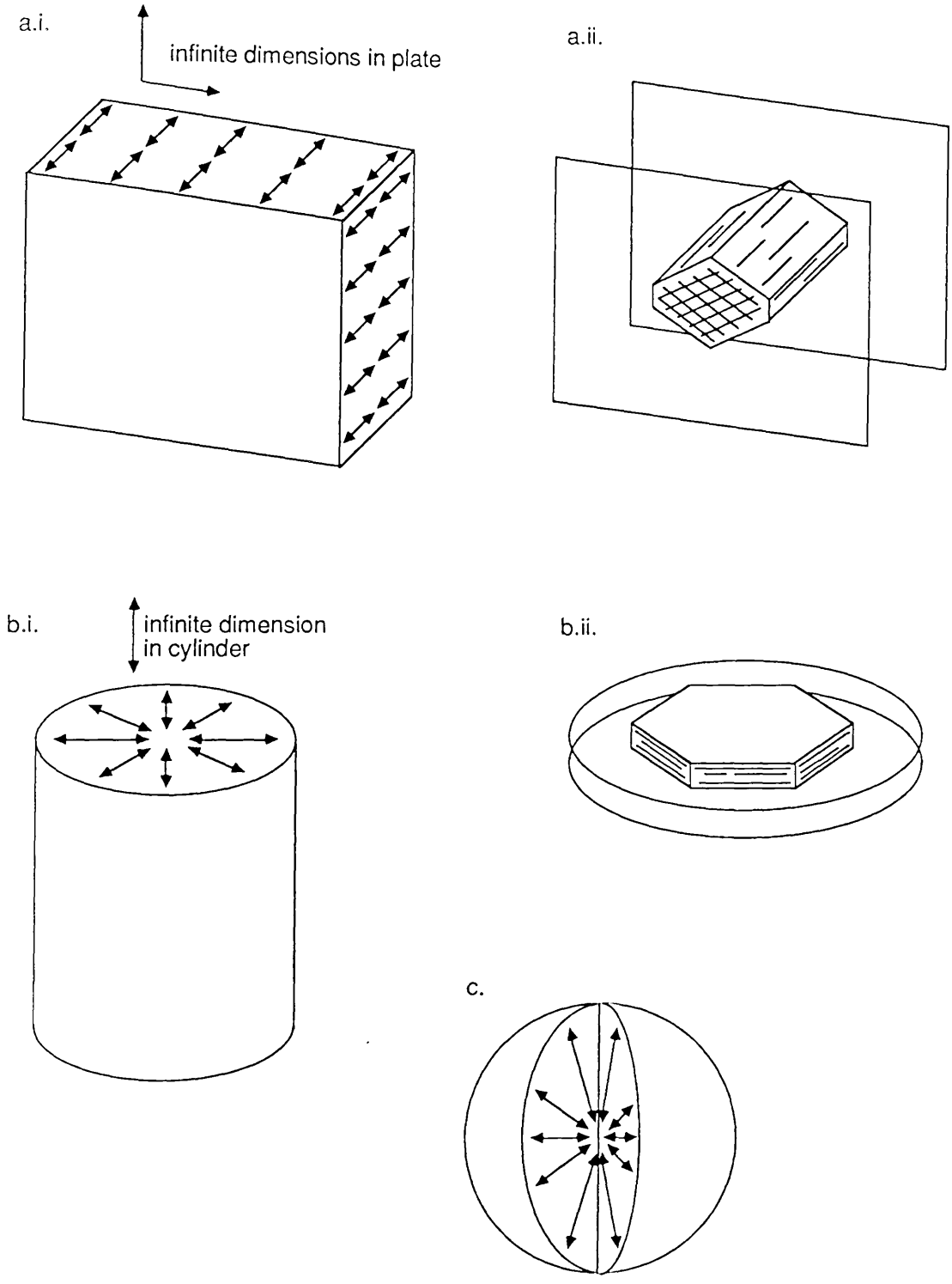

Fig.2.8 Models of diffusion geometry. The arrows show the direction(s) of transport by diffusion. a.i. The infinite plate (or plane sheet) model. a.ii. The relation of the plate faces to the crystallographic axes of an amphibole grain in which diffusion is conforming to the plate model. b.i. The infinite cylinder model. b.ii. the relation of the cylinder ends to the crystallographic axes of a mica flake in which diffusion is conforming to the cylinder model. c. The spherical model.

The effect of fluid/mineral ratio and initial fluid concentration on the rate of diffusion controlled isotopic exchange

The diffusion coefficient is not affected by the fluid/mineral ratio or the initial fluid concentration. However it will be shown here that the

fluid/mineral ratio affects the rate of diffusion controlled isotopic exchange while the concentration of the fluid does not.

The final equilibrium composition of a grain which initially contains no solute can be related to the initial fluid composition and fluid/mineral ratio using simple mass balance constraints. If the initial concentration in the solution is C_{S_0} and the volumetric solution/mineral ratio $\beta = a/l$, then since all the solute was originally in the solution the total amount of solute in the system must be aC_{S_0}. The solute content of the system at equilibrium (infinite time) must equal the original solute content of the system, hence

$$lC_{G\infty} + aC_{S\infty} = aC_{S_0},$$

where $C_{G\infty}$ and $C_{S\infty}$ are the equilibrium concentrations of solute in the grain and solution respectively. If there is no fractionation at the grain boundary ($\alpha = 1$) then the concentration in the grain at equilibrium $C_{G\infty} = C_{S\infty}$ and then

$$lC_{G\infty} + aC_{G\infty} = aC_{S_0}.$$

Dividing through by l, substituting β and rearranging gives

$$C_{G\infty}(1 + 1/\beta) = C_{S_0}$$

and

$$C_{G\infty} = \frac{C_{S_0}}{(1 + 1/\beta)}. \qquad (2.25)$$

Thus when $\beta \rightarrow \infty$, $C_{G\infty} \rightarrow C_{S_0}$ and when $\beta \rightarrow 0$, $C_{G\infty} \rightarrow 0$.

Thus the higher the fluid/mineral ratio the greater the shift in the final concentration in the grain will be for a given original concentration in the solution. Similarly the final concentration in the grain will be directly proportional to the original solution composition. These relationships can be seen by comparing the diffusion profiles in Figs 2.7a,c and b,d and Figs. 2.9a,b. In Figs. 2.7a and b the fluid/mineral ratio is high and the final equilibrium concentration in the grain tends to the initial solute concentration, while in figs. 2.7c and d, β is 1 and the equilibrium concentration by eqn (2.25) in this case is $C_{S_0}/2$. It will be noted that for a given time and grain size the fractional approach to equilibrium is greater in the grain with $\beta = 1$ than in the grain where $\beta = 10000$. Thus the exchange rate will be faster when the fluid/mineral ratio is small. This might be explained in terms of the mineral not having to shift so far in composition as the grain which was immersed in a larger volume of solution (Cole and Ohmoto, 1986), although this cannot be the full explanation since if only the initial solution concentration is varied (and therefore the final grain concentration and degree of shifting) as in Figs 2.9 a,b the value of F is is found to be the same. The fact that both of the grains start with the same initial diffusion gradient, yet the grain in which $\beta = 1$ needs only half the amount of solute to diffuse in to achieve the same value of F as the other grain must also be important. Cole *et al.* (1983) show that as the W/S (mass) ratio increases the rate of exchange becomes less dependent on it until at

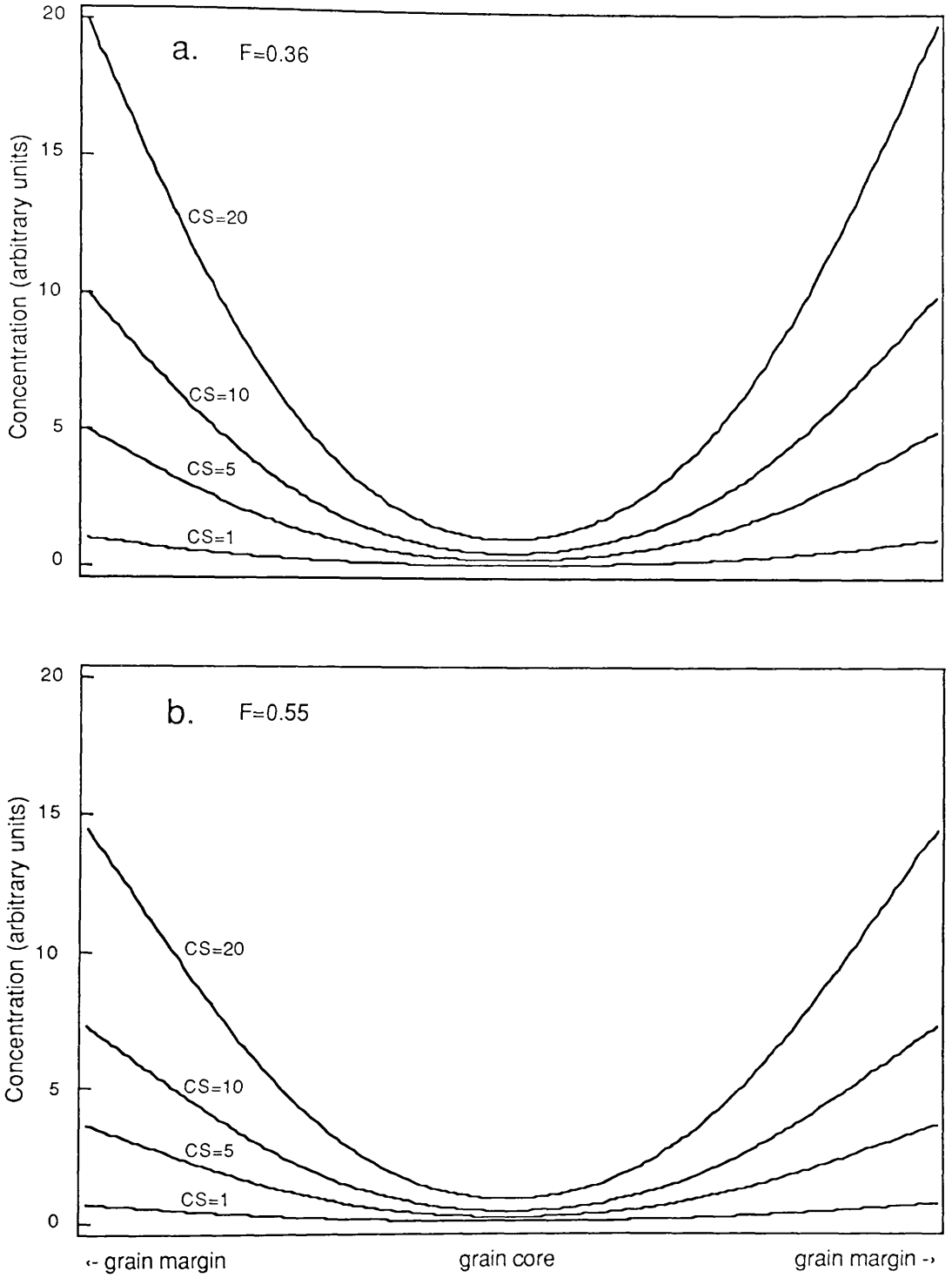

Fig.2.9 Concentration profiles across plate shaped grains for four initial solution concentrations and for two fluid/mineral ratios (β), all at the same time after the initiation of diffusion. In fig. a. the solution volume is very large so that the the solution concentration has remained constant with time. In fig. b. the solution volume is equal to the plate volume so that both the solution composition and plate composition have changed with time. The initial solution concentrations are given on the curves. Initially the grains contained no solute. No fractionation takes place at the grain boundaries. The fractional approach to equilibrium is the same for all curves with the same β value. Profiles were calculated using equation 4.45 (infinite plate model) from Crank (1975). Parameters used were β = 10000 (fig. a.) and 1 (fig. b.) and 1/2 plate thickness = 1, **D** = 1, and time = 0.1 (both figs).

high fluid/mineral ratios (generally greater than 10 by mass) the rate becomes independent of W/S (mass) ratio.

That the rate of exchange does not depend on the solution concentration does not mean of course that the absolute measured values of the shifts will not differ for exchange with solutions of different concentrations over the same time.

The effect of impurities on the rate of diffusion controlled isotope exchange.

If the diffusion of oxygen and hydrogen in silicates under geological conditions does take place in the extrinsic regime then the diffusion coefficient should be related to the impurity content of the mineral in question. Dennis (1984) has suggested that the diffusivity of oxygen in quartz might be linearly related to Al content. The only data which can be used to test this hypothesis are those of Giletti and Yund (1984). These workers measured the diffusivity of three quartz samples with OH^- contents differing by nearly 3 orders of magnitude, Na contents by one order of magnitude and Al contents by a factor of two, but found that the diffusion coefficients of the samples were not significantly different within the errors of measurement. From these limited results it could be suggested that the dependence of diffusivity in individual minerals on impurity content might be much less than the (orders of magnitude) differences between different minerals, although more data are obviously required.

The effect of a rate limiting surface step on the rate of diffusion controlled isotopic exchange

The effect of a rate limiting surface step such as proposed by Freer and Dennis (1982) and described above (the effect of pressure...) and by Arita *et al.* (1979) on the rate of isotopic exchange in which diffusion is the dominant exchange process may be examined by solving equations 4.50 and 4.53 from Crank (1975). These equations describe the diffusion of solute into a sheet when the rate of uptake is directly proportional to the difference between the surface concentration at any time (C_s)and the surface concentration that would be in equilibrium with the surrounding fluid (C_o). Mathematically this means that the boundary condition at the surface is

$$-D\left(\frac{\partial C}{\partial x}\right) = k(C_o - C_s) = J_s ,$$

where k is the rate constant for the surface reaction (units = length. $time^{-1}$) and J_s is the flux of solute at the surface.

Since the sheet is infinite the change in total amount of the solute (M_{total}) per unit cross sectional area with time is equal to the surface flux, thus

$$\left(\frac{\partial M_{total}}{\partial t}\right)_A = J_s = k(C_o - C_s) ,$$

in which case

$$\left(\frac{\partial C_{total}}{\partial t}\right)_A = k\frac{(C_o - C_s)}{l} ,$$

where l is the plate thickness. It can be seen that this equation has the form of a first order reaction which is moving towards a steady state equilibrium (eqn 2.11). It is not implied here that the surface reaction is a first order reaction (although this may be the most likely possibility). This case is used here to demonstrate the kind of effect that a surface rate step might have, purely because a solution is readily available.

Diffusion profiles and values of F calculated using this boundary condition are shown in figs. 2.10a,b.

Fig 2.10a shows the diffusion profiles that will result if the parameters that are used are the same as in fig 2.7a, except that in this case $k/\mathbf{D} = 1$ (in situations where there is no surface process operating this can be treated as if the surface process is infinitely fast, in which case $k/\mathbf{D} = \infty$). It can be seen that when a surface process is operating, the degree of exchange for a given time is reduced relative to the situation where no surface process is involved. In addition the diffusion profiles are much flatter when k is small.

The effect of different values of k for the same grain when all other parameters are constant is shown in fig. 2.10b. It can be seen that as $k/\mathbf{D}$ increases the value of F increases. At high values of $k/\mathbf{D}$ (>100) the diffusion profile approximates very closely to that when no surface process is operating ($k/\mathbf{D} = \infty$).

The effect of radiation damage on diffusion controlled isotopic exchange

Halter *et al.* (1988) show that illites and chlorites from within a uranium deposit have undergone retrograde H-isotope and K-Ar exchange with later fluids to a much greater extent than the same minerals from barren country rock away from the deposit. They attribute this enhanced susceptibility to (presumably diffusional) exchange to the catalytic effect of the radiation field, most probably by means of its damaging effect on the crystal lattice. Such effects were only seen in samples with a whole rock U content >100 ppm which is well above the maximum value for samples in the Cashel-L.Wheelaun intrusion (~6 ppm Y.Ahmed-Said pers. comm.), so that it is unlikely that such radiation effects will be important in this study.

Diffusion models

Various mathematical solutions of the diffusion equations have been used in the past to model geological processes.

Dodson (1973,1979) has formulated a mathematical model which allows the "closure" temperature of a mineral to be calculated. The closure temperature is defined for geochronological systems as "the temperature of the system at the time given by its apparent age". This definition reflects the fact that at temperatures near to the temperature of crystallisation the daughter products from radioactive decay diffuse out of a mineral as fast as they are produced (fig. 2.11). At lower temperatures because of the decrease in **D** with falling temperature (eqn. 2.22) the mineral enters a transitional range in which some of the daughter products accumulate in the mineral while some are lost. At lower temperatures still, the loss of daughter products becomes negligible. This concept of closure temperature can also be

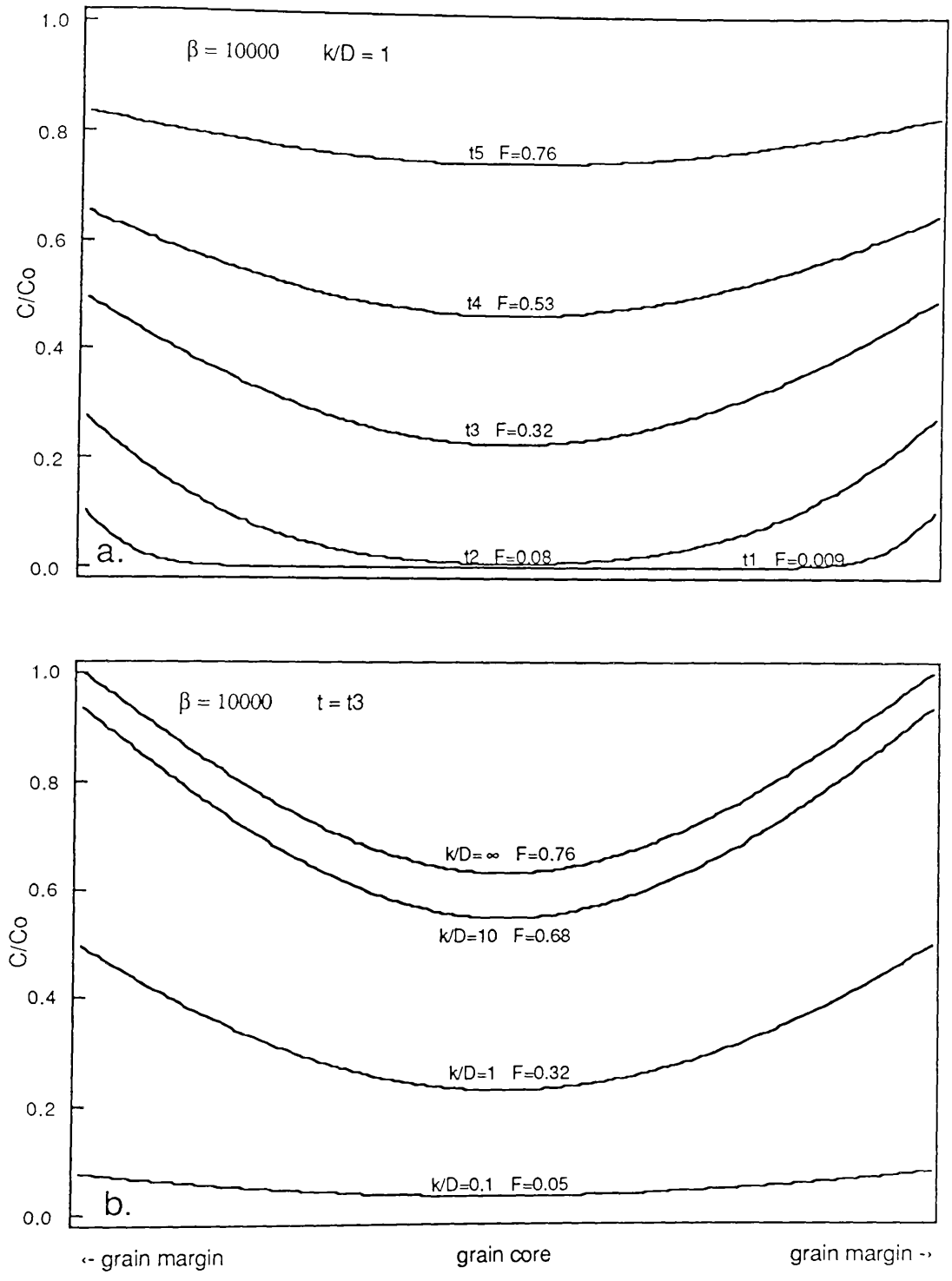

Fig.2.10 a. Concentration profiles at five different times (t5 > t4 > t3 > t2 > t1) across a plate shaped grain in which movement across the solution to solid interface is rate limiting. The initial solution and grain concentrations, the β value, grain size, diffusion coefficient and times at which the profiles are calculated are all the same as in fig. 2.7a (except that a profile at t5 is not shown in 2.7a). The rate constant for the surface reaction is 1, thus k/**D** = 1. No fractionation takes place at the grain boundary. F= numbers on curves are the fractional approach to equilibrium. Profiles and F values were calculated using equations 4.50 and 4.53 from Crank (1975). Parameters used are as in fig. 2.7a except t5 = 2. Fig. 2.10b shows the diffusion profiles across the same grain under the same conditions at time t3 for varying values of k/**D**.

successfully applied to the re-equilibration of stable isotopes between phases in a cooling rock (fig. 2.11). At high temperatures with small changes in temperature re-equilibration occurs rapidly throughout the rock. As the rock cools to lower temperatures the diffusivity of the minerals decreases. Re-equilibration will take place between minerals immediately at the grain surfaces, but equilibration will take longer between grain interiors because of the greater time necessary for diffusion into the grain. As the temperature drops still further the change in bulk isotopic composition of the grain with time becomes negligible and the isotopic composition of the grain becomes "frozen in" at a false equilibrium. Thus the closure temperature can be defined in this case as the temperature at which exchange of the species in question effectively ceases. The mathematical solution for calculating closure temperature described by Dodson (eqn. 23, 1973) assumes that the cooling history can be approximated by a linear increase in 1/T over the transitional temperature range. Thus the cooling rate of the rock needs to be estimated. Additionally isotopic exchange is assumed to take place with a semi-infinite reservoir of pore fluid (or a large quantity of adjacent mineral in which diffusion is rapid). This assumption may be violated in some natural situations.

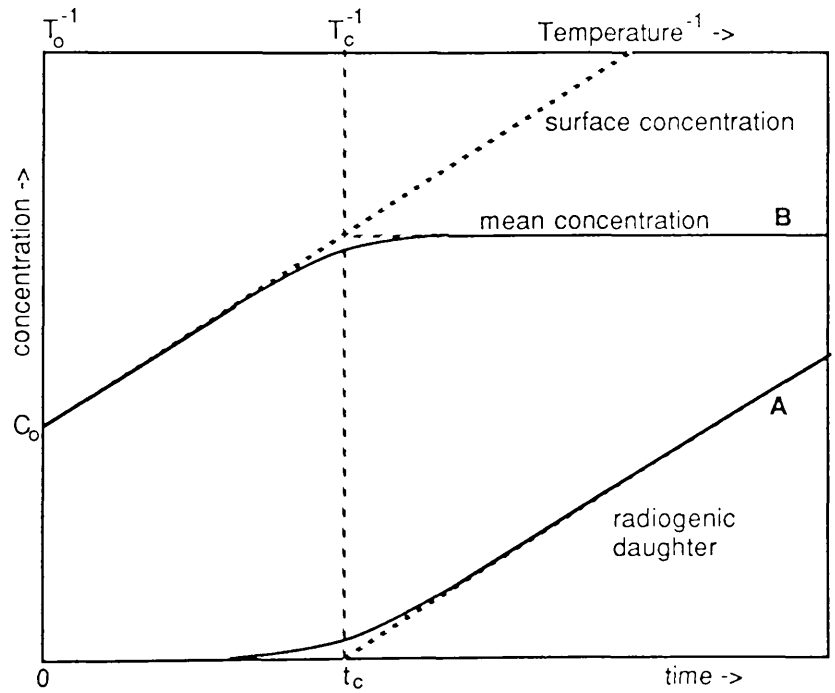

Fig.2.11 The relationship between geochronological closure temperature (A) and the closure temperature of isotopic exchange (B) for identical parameters assuming 1/T increases linearly with time. The concentration refers to either the concentration of a radiogenic daughter product in the mineral (A) or the mean concentration of one of the exchanging isotopes in the mineral (B). T_C is the closure temperature as defined and t_C is the apparent age of the geochronological system. After Dodson (1973, fig. 2).

Each mineral in a rock will have a different closure temperature (indeed each grain will, since closure temperature is a function of grain size, normally an average grain size is used in the model). A consequence of this is that different minerals within a cooling rock will equilibrate at different rates and down to different temperatures.

Giletti (1986) uses this model to examine the effect of slow cooling of a rock on the resulting mineral-mineral oxygen isotope fractionations and the apparent "equilibration" temperatures calculated from them. He found for example that in a rock composed of quartz, feldspar and hornblende with a grain size of 1 mm, which was cooled at 10°C/Ma, that the minimum difference in apparent temperature between quartz-feldspar and feldspar-hornblende pairs will be 115°C. For a cooling rate of 1000°C/Ma the apparent temperature difference could be up to 400°C. He was able to conclude from his analysis that consistency in oxygen isotope equilibration temperatures from slowly cooled high-grade metamorphic or igneous rocks should not be expected. While geothermometry may not be possible in such rocks Giletti shows that the cooling rate of the rock might possibly be derived from such non-equilibrium assemblages.

The closure temperature will increase with increasing cooling rate. When the cooling rate is so rapid that the closure temperature exceeds the formation temperature of a mineral, then the mineral starts out as an closed system. Thus when two minerals crystallise together at a temperature below their blocking temperatures, the calculated equilibration temperature should actually be that be that at which they formed. Oxygen isotope equilibration temperatures will only be meaningful if this criterion is met (cf 2.5.2).

Another consequence of the closure temperature model is that minerals in slowly cooled rocks should exhibit isotopic zonation. This in itself is indicative of disequilibrium (e.g. Wada, 1988). The closure temperature model only deals with mean concentrations in a grain and the corresponding closure temperature. However Dodson (1986) shows how the variation in concentration in a grain (termed by him the closure profile) may be calculated for a given set of conditions. If minerals in rocks are isotopically zoned, then it is important that care is taken to ensure that mineral separates prepared from these rocks are representative. Processes involved in mineral separation (A.1.10) could easily bias the final separate to have a greater concentration of cores or rims. Alternatively separation of cores and rims could be carried out deliberately to try to demonstrate that zonation is present (e.g. Wada, 1988). In the future developments in microbeam measurement of isotopes in natural samples may make it possible to measure such closure profiles directly.

The Dodson closure temperature model is only appropriate for certain geological situations. Specifically it only applies to steadily cooling rocks where the reservoir for exchange is semi-infinite. Recently Cole *et al.* (1983) have used solutions to the diffusion equations that were given by Crank (1975) to model diffusion controlled exchange. These solutions have the advantage that fluid/rock ratio is a variable in the calculation and is not assumed to be infinite. These solutions apply to isotopic exchange under isothermal conditions and thus may be more appropriate to modelling isotopic exchange in geothermal systems for example.

In order to gain qualitative estimates of the rates of diffusion controlled oxygen and hydrogen isotope exchange in the minerals that have been analysed in this project, a computer program to solve the diffusion equations given by Crank (1975) was developed. This program solves the

diffusion equations to find the time it will take a grain of a mineral to reach a given degree of exchange with the surrounding fluid. Some solutions for minerals relevant to this study are given in fig 2.12, where the time the mineral takes to achieve 10% and 90% exchange is plotted against temperature, which is of course, the main factor controlling exchange rates.

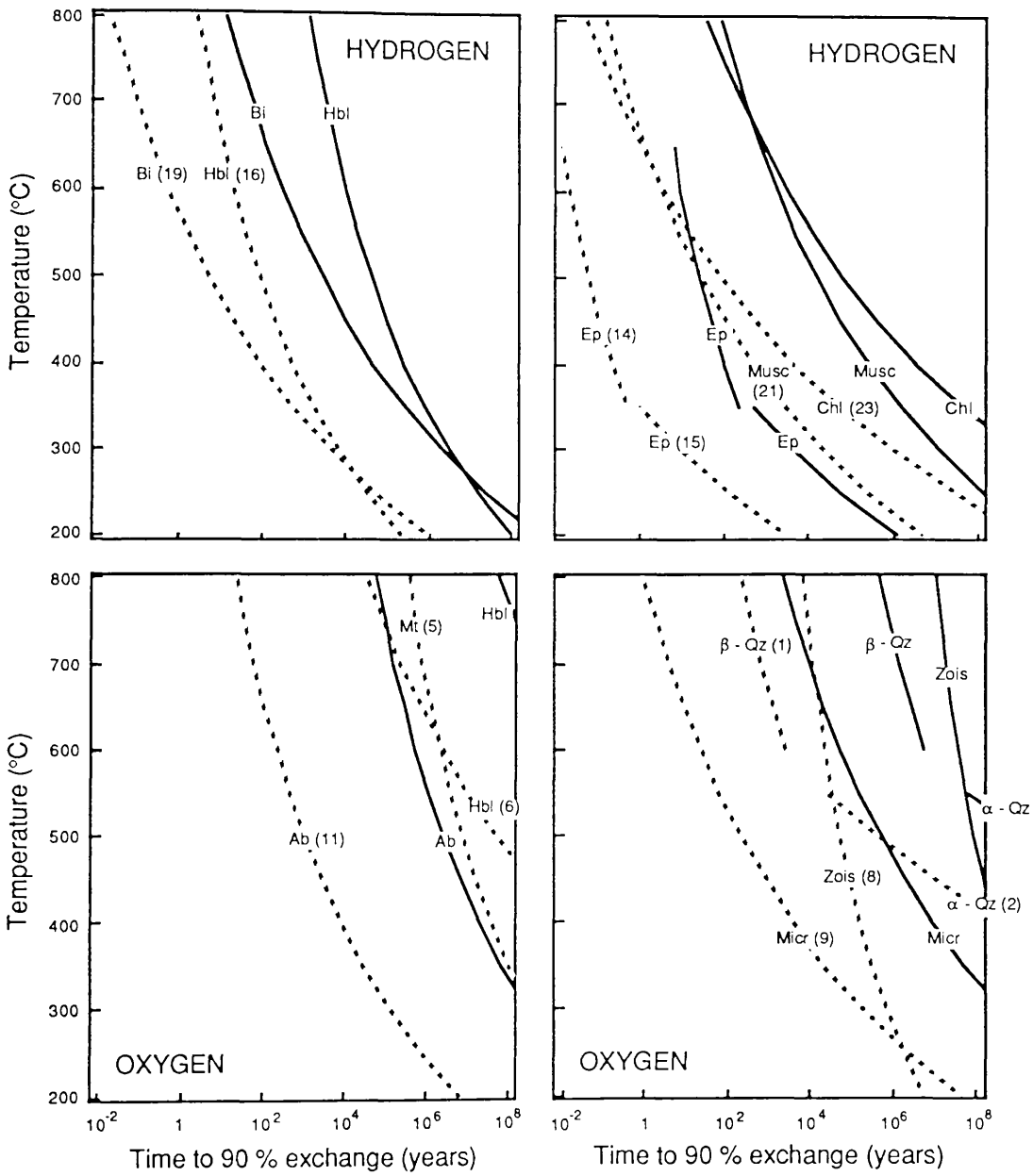

Fig 2.12a and b (next page). Times required for various minerals to reach a.90% (F=0.9) and b. 10% (F=0.1) isotopic exchange with the surrounding fluid. The upper curve for each mineral (solid line) is for exchange in a grain with an effective diffusion length (1/2 plate thickness or cylinder or sphere radius) of 1 mm with a fluid/mineral mass ratio of 10, while the lower (dashed) curve for each mineral is for a grain with effective diffusion length of 0.05 mm and a fluid/mineral mass ratio of 0.1. These values of effective diffusion length and fluid/mineral mass ratio probably bracket these values for minerals in SW Connemara, except in unusual circumstances. The diffusion data used to calculate the curves is given in A.5 and is indexed by the number next to the lower curve in fig 2.12a.

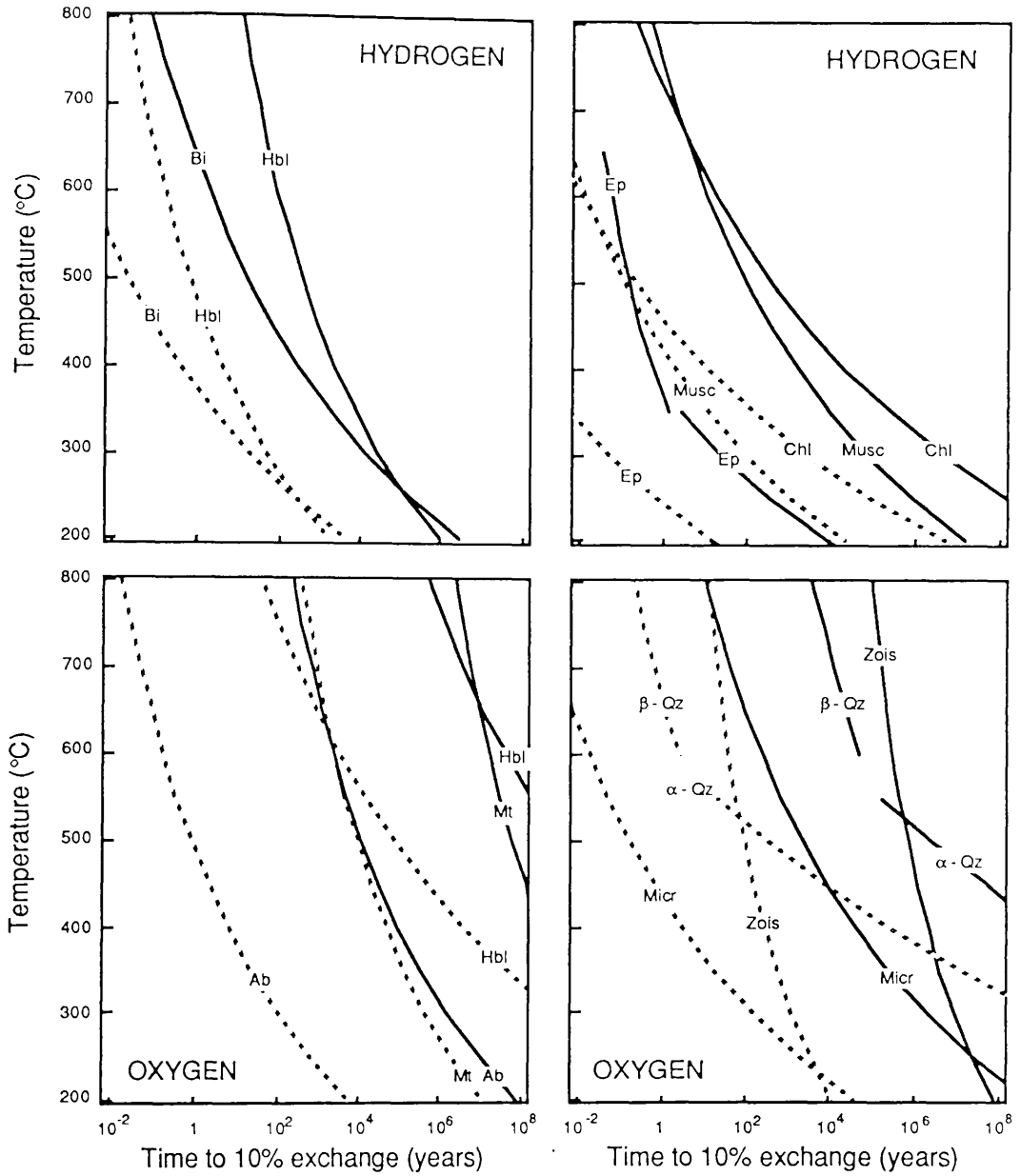

2.6.4. Isotope exchange accompanying surface reactions

Surface reactions as defined by Cole *et al.* (1983) comprise both chemical reactions resulting in phase changes and solution-reprecipitation reactions which involve recrystallisation of phases already present. In both of these reaction mechanisms the site of precipitation of new mineral material may not be adjacent to the site of dissolution of the reacting material, so that mass transport has to take place between these sites via the fluid phase. Transport in the fluid may take place either by infiltration or by diffusion. Both of these processes are thought to be fast relative to the solution and precipitation reactions at the mineral surfaces (Lasaga, 1981a). Thus the feature that these mechanisms share in common is that a reaction at the fluid-mineral interface is thought to be rate limiting (Cole *et al., ibid.*).

Isotope exchange accompanying chemical reactions

An example of isotopic exchange accompanying chemical reaction is the oxygen isotope exchange in alkali feldspars which is seen to take place with Na-K exchange (O'Neil and Taylor, 1967). The rate of oxygen isotope exchange with alkali feldspars was found to be much enhanced when alkali exchange was taking place relative to the rate when the feldspars were placed in solutions with which they were in chemical equilibrium, suggesting that the chemical reaction was actually causing isotope exchange to take place.

Isotope exchange in chemical reactions takes place synchronously with the main chemical reaction. Bonds are broken and reformed in the chemical reaction allowing isotope exchange also to take place. New phases formed in the chemical reaction are therefore believed to be in isotopic equilibrium. The coexisting fluid is also expected to equilibrate during the reaction since most reactions either take place via the fluid phase or directly involve it. Thus whenever new phases form e.g. at metamorphic isograds or during retrograde alteration, it is expected that they and the fluid in the rock will be in equilibrium at that time.

Isotope exchange in this case takes place only because of the movement of the chemically reacting phases towards thermodynamic equilibrium. The isotope exchange reaction effectively rides "piggy back" on the chemical reaction, since as noted in (2.6.2) the free energy change of the isotope exchange reaction is not large enough to drive a reaction itself. The need for the chemical system to move towards equilibrium may therefore be thought of as the "driving force" behind isotope exchange in this case. The principles of equilibrium thermodynamics which allow the conditions under which chemical reactions in a rock will take place to be estimated are well described in the literature (e.g. Powell, 1978) and will not be covered here.

Much debate has taken place concerning the the mechanism by which chemical exchange reactions such as cation exchange takes place within large crystals. O'Neil and Taylor (1967) proposed a mechanism for Na-K exchange in alkali feldspars whereby exchange takes place by means of fine scale recrystallisation at a reaction front which moves through the crystal. Local dissolution and redeposition (solution-precipitation) is envisaged to take place in a fluid film at the interface between exchanged and unexchanged feldspar. For this mechanism to be viable the fluid film at the reaction front must be in direct communication and in isotopic and chemical equilibrium with the bulk solution. Such communication was envisaged to take place along cracks and imperfections within the crystal (possibly by fast grain boundary diffusion).

Such a mechanism is partially supported by the results of Schliestedt *et al.* (1986) who showed that for the cation exchange reaction:

$$2NaSi_3O_8 + CaCl_{2(aq.)} \Rightarrow Ca_2Al_2O_8 + 4SiO_2 + 2NaCl_{(aq.)}$$

the amount of oxygen isotope exchange is equivalent to the amount of cation exchange, consistent with a reaction mechanism for oxygen isotope exchange in which the product feldspar is deposited in chemical and isotopic equilibrium with the solution. For this reaction the solid volume

is reduced (ΔV_S = -9.3 cm^3 mol^{-1}) and voids and channels were observed to have formed in the reacting feldspar. These channels would act as easy pathways for fluid to gain access to reach O'Neil and Taylor's "reaction front". However in the reverse reaction the feldspar volume increases, leading to the formation of an armouring surface of Ab-rich feldspar which apparently inhibits the access of solution to the interior of the grain, since the isotope and cation exchange rates are not coupled for this reaction. The differing rates of exchange were found to be consistent with a diffusional mechanism of movement of oxygen and cations into the bulk of the feldspar. However for the alkali exchange reaction:

$$NaCl_{(aq.)} + KAlSi_3O_8 \Leftrightarrow NaAlSi_3O_8 + KCl_{(aq.)}$$

studied by O'Neil and Taylor, although ΔV_S is 8.6 cm^3 mol^{-1} (negative for the forward reaction), the oxygen isotope exchange rates were found to be similar for both the forward and reverse reactions. Thus in this situation access of fluid to the reaction front does not appear to be affected by the increase in volume in the reverse reaction.

It is unfortunate that the term "solution-precipitation" has been used to describe the reaction mechanism for cation exchange proposed by O'Neil and Taylor, since it has lead to confusion with the term "solution-reprecipitation" which has been used to describe recrystallisation without a phase change, a process with a totally different driving force. Cole *et al.* (1983) have used these terms interchangeably leading them to imply that the mechanisms have the same cause.

Isotope exchange accompanying recrystallisation (solution-reprecipitation)

Oxygen isotope exchange has been found to accompany recrystallisation of carbonates in water (O'Neil *et al.*, 1969; Anderson and Chai, 1974), quartz in NaF solutions and pure water (Clayton *et al.*, 1972; Matthews *et al.* 1983) and a number of other minerals in various fluids. As in chemical reactions the fact that bonds are being broken and reformed in the recrystallisation process allows the low free energy isotope exchange reaction to also take place. The driving force causing recrystallisation of phases already present in a rock is the reduction in surface free energy. This can result from a decrease in the grain surface area. Thus recrystallisation usually results in the increase in average grain size in the rock. In a chemically closed system the increase in size of some grains requires a decrease in the size of others. Since small grains have a greater surface area/mass ratio they are more unstable (and therefore more soluble) than larger grains of the same material. Therefore material is dissolved from small grains and reprecipitated on larger grains. Eventually the smallest grains are eliminated. The result of this process is that the total number of grains in the system decreases and the average grain size increases. This phenomenon was first observed by Ostwald (1900) and has come to be called "Ostwald ripening".

Grain coarsening is common in prograde metamorphism; however Chai (1974) suggests that continued coarsening will be limited during retrograde cooling, firstly because the rate of grain growth decreases with increasing grain size and the rock is already coarse at the metamorphic peak, and

secondly because the recrystallisation rate will be decreasing due to falling temperature. Therefore isotope exchange due to grain coarsening in retrograde cooling is expected to be minimal.

Different parts of a grain may possess different surface free energies, because of their different specific surface areas (surface area/volume). Thus sharp grain edges with high curvature will be unstable relative to rounded edges and crystal facets, thus material is preferentially dissolved from sharp edges and deposited on crystal facets. A variation of surface free energy within grains also explains why recrystallisation is important in the process of crack healing as described by Smith and Evans (1984).

Crack healing involves the local transport of material as it reforms a fractured lattice or grain boundary. Smith and Evans (*ibid.*) distinguish crack healing from crack sealing which involves material in sealing the crack that has been transported some distance via the pore fluid (Batzle and Simmons, 1976). This process involves chemical gradients (a chemical reaction process as defined above) which are not necessary for crack healing. Crack healing and crack sealing occur in many geological environments and often result in the formation of secondary fluid inclusions (Roedder, 1984) along sub planar or curved planes that correspond to the position of the original crack (termed bubble planes by Simmons and Richter, 1976).

Crack tips have a high specific surface area which causes them to have a large surface free energy relative to other parts of the crack. Crack tips are therefore highly unstable and will gradually change shape, first by pinching off into a tubular structure and then by forming isolated bubbles. As this process continues the crack tip regresses leaving a bubble plane. The transformation from a planar crack to an array of spherical voids results in a net reduction in the total interfacial energy in the system, even when the total volume of void space remains constant (Smith and Evans, 1984). From the abundance of bubble planes in some rocks, most notably in the quartz it appears that much material must have passed through either a crack healing or crack sealing process and has therefore been reprecipitated in isotopic equilibrium with the fluid in the fracture. Furthermore Sprunt and Nur (1979) have suggested from cathodoluminescence data on quartz grains from granites that many sealed fractures may not contain secondary inclusions and be indistinguishable from the host quartz except under cathodoluminescence, in which case the volume of re-equilibrated material may be even greater.

For recrystallisation to take place, material has to be dissolved from small grains or unstable portions of grains and transported to larger grains or more stable parts of the same grain and then precipitated. This process is therefore dependent on the mineral being soluble in the fluid. It is important to note however that the system need not be out of chemical equilibrium as implied by Cole *et al.* (1983), all that is necessary is that the mineral should have a finite solubility in the fluid. However the rate will usually be dependent on the solubility (Lasaga 1981a, p.55). Matthews *et al.* (1983a) suggest that the effects of solubility on recrystallisation rate may be considered in terms of a simple kinetic model in which the rate of recrystallisation is proportional to the difference $X_A - X_\infty$, where X_A is the

solubility and X_∞ is the equilibrium solubility of the mineral and that this can be given by

$$X_A - X_\infty = X_\infty [\exp.(2\sigma V S_A/3RT) - 1] ,$$

where σ is the surface free energy of the solid with respect to the solution, V is the molar volume of the solid and S_A is the specific surface area. Thus if this assumption is correct the rate of exchange will be proportional to the equilibrium solubility. Chai (1974) notes that the recrystallisation rate of calcite increased at the same temperature with increasing solubility in various solutions. However Lasaga (1981a. p.55-56) shows that the dependence of recrystallisation rate on solubility cannot be accurately predicted unless the reaction mechanism is known. Unfortunately this is not usually the case.

A rate law for surface isotope exchange reactions

Northrop and Clayton (1966) and Cole *et al.* (1983) have derived a rate law which is applicable to a variety of isotope exchange reactions. Starting from the assumption that the exchange reaction is second order they show that it can be described by the pseudo-first-order rate expression:

$$r_+ = \frac{-\ln(1-F)(W)(S)}{(W+S)t} , \qquad (2.26)$$

where r_+ is a rate constant for the forward reaction, F is the fractional approach to equilibrium and W and S are the number of isotopically exchangeable atoms (e.g. atoms of O or H) in the fluid and solid phases.

A pseudo-first-order reaction is one which is actually 2nd order with two reactants so that

$$\frac{-dC_w}{dt} = k\, C_w\, C_x ,$$

however the concentration of one reactant is so high initially (C_X°) that the rate is effectively controlled by the concentration of the other reactant i.e.

$$\frac{-dC_w}{dt} \approx k\, C_x^\circ\, C_w = k' C_w ,$$

where $k' \equiv k\, C_X^\circ$. In this case the concentration of the light isotope varies so little because of its high abundance, that the effect of its concentration change on the rate can be ignored.

Thus plots of ln(1-F) versus time should yield straight lines for isotope exchange reactions. In practice many diffusion dominated exchange reactions do not conform to this rate model, but most exchange reactions taking place by surface processes are found to.

Cole and Ohmoto (1986) point out that r_+ is not strictly a "rate constant" for the isotope exchange reaction. The rate constant for the forward reaction (k_+) is usually a simple function of r_+ and some appropriate constants, e.g the surface area of solid (A) is a necessary factor in heterogeneous reactions.

The effect of temperature on the rate of surface controlled isotope exchange reactions.

As stated in (2.6.1) the dependence of the rate constant on temperature usually follows the Arrhenius equation (eqn. 2.17) and therefore depends exponentially on -1/T. Rate constants are therefore often plotted on Arrhenius plots of log k vs. 1/T which have slopes of $-E_a/2.303R$ and an intercept at infinite temperature of log A_0. Fig (2.13) shows an Arrhenius plot of some rate constants (r_+) for oxygen isotopic exchange derived by Cole *et al.* (1983) using eqn 2.26 and which are pertinent to this study.

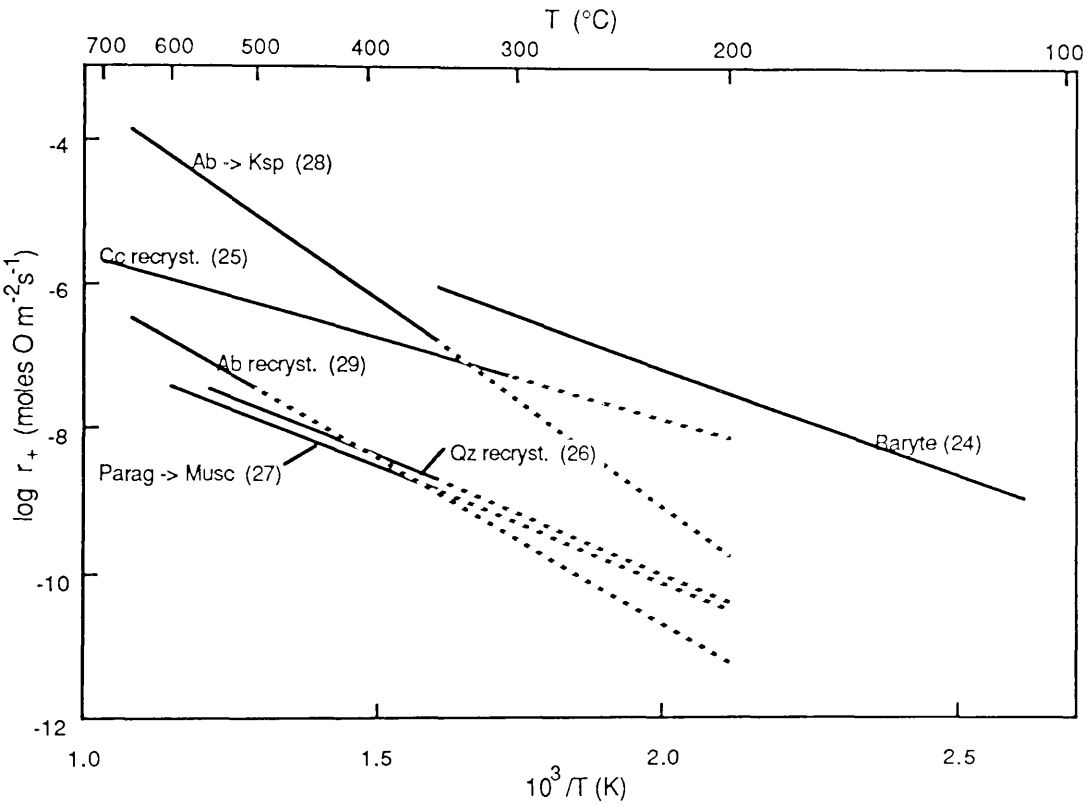

Fig.2.13 A composite Arrhenius plot of some rate constants for oxygen isotope exchange reactions that took place by chemical reaction or recrystallisation. The data used to construct these lines is given in A.5, and is indexed by the number next to each line.

It can be seen that the rate constants for different reactions can vary by up to four orders of magnitude at the same temperature. At temperatures less than 300°C the relative rates are:

baryte > calcite > Na/K-feldspars > quartz > paragonite ,

while above 300°C the relative rates are the the same except that isotope exchange in feldspar cation exchange reactions is faster than in calcite recrystallisation.

The activation energies (E_a) fall in a relatively restricted range of approximately 10-25 kcal mol^{-1}. This range of activation energies is consistent with a reaction mechanism in which reactions at the mineral-

fluid interface are rate controlling, termed "surface controlled" (Lasaga, 1981a, p.34).

It should be noted that the activation energy for a diffusion controlled reaction calculated from kinetic data relates to the same discrete atomic jump as the activation energy for diffusion, thus these two values should be the same. This has been found to be the case for diffusion controlled exchange reactions where the activation energy has been calculated from the same data using both kinetic and diffusion equations (Graham, 1981).

The effect of pressure on the rate of surface controlled isotope exchange reactions.

Matthews *et al.* (1983a) found that the rate of isotopic exchange between quartz and water increased with increasing pressure until approximately 6-9 kb, but above these pressures the degree of exchange remains constant as a function of pressure. There is good evidence that recrystallisation was the dominant mechanism by which isotope exchange took place in these experiments. Matthews *et al.* (*ibid.*) suggest that this increase in rate is related to the increased solubility (see above) of quartz over this pressure range (Walther and Helgeson, 1977). Above this pressure range they suggest that another exchange mechanism may be operating. From the observations of Matthews *et al.* it might be suggested that any pressure effect on the rate of isotope exchange taking place by recrystallisation may be related to the change in mineral solubility with pressure.

No data appear to exist concerning the effect of pressure on isotope exchange attendant on chemical reactions. As with recrystallisation the rate will probably be some function of pressure because of its effect on fluid composition.

The effect of grain size on the rate of surface controlled isotopic exchange.

If a reaction at the fluid-mineral interface is rate limiting then the rate of reaction will be dependent on the surface area/volume ratio of a mineral. Thus for the same mass of material the rate of exchange will increase with decreasing grain size. If the mineral particles are spherical and the total volume is V, then

$$\text{number of particles} = 3V/4\pi r^3,$$

where r is the particle radius and therefore

$$\text{total area of particles} = 4\pi r^2 \times \text{number of particles} = 3V/r.$$

Thus the rate will be inversely proportional to the grain radius. It should be noted however that grain size and grain shape may change as the reaction progresses (e.g. in Ostwald ripening) so that the rate may often vary as a complex function of grain size as the reaction proceeds.

The effect of grain shape on the rate of surface controlled isotopic exchange

Grain shape may affect the exchange rate in two ways. Firstly the grain shape will affect the surface area/volume ratio. Elongated needle shaped grains or flattened plate shaped grains will have a higher surface area than a

spherical grain of the same volume, and therefore will exchange more rapidly. Secondly irregular shaped or fractured grains with areas of high curvature will be more prone to recrystallisation than perfect grains showing crystal facets because of their higher surface free energy.

The effect of fluid/mineral ratio on the rate of surface controlled isotope exchange reactions

Cole *et al.* (1983, p.1690) show how eqn 2.26 can be modified to incorporate the grain size and β, the volumetric fluid/mineral ratio so that it may be applicable to surface reactions. For a spherical grain Cole *et al.* (*ibid.*) derive the expression:

$$r_+ = \frac{-\ln(1-F)(W/S)X_S r\rho_S}{3[1+(W/S)]t} ,$$

where W/S is the fluid/solid molar ratio of the exchanging element, r is the grain radius, ρ_S the density of the solid and X_S is the moles of exchanging element per gram of solid. Rearranging to a more familiar form (cf eqn. 2.15):

$$\ln(1-F) = -r_+\left\{\frac{3[1+(W/S)]}{(W/S)X_S r\rho_S}\right\}t ,$$

allows the relation between k_+ and r_+ to be seen more clearly. k_+ in this situation would equal r_+ multiplied by the terms in the curly bracket. It can be seen however that r_+ is of more general use since it is independent of grain size and fluid/mineral ratio in the system.

β can be shown to be related to W/S by

$$\beta = (W/S)[(X_S \rho_S)/(X_W \rho_W)] ,$$

where X_W and ρ_W are the corresponding quantities for the fluid as defined for the solid. From the above equations it can be seen that the smaller the value of β (or W/S) the greater the change in (1-F) will be for a given time, and thus the greater is the rate.

As with the case of fluid/mineral ratio in diffusion controlled exchange the reason for its effect on the exchange rate is not intuitively obvious, although it can be seen in the same way that if the fluid/mineral ratio is small, then the mineral does not have to shift so far in composition. In a similar way to diffusion controlled exchange Cole *et al.* (1983) show that as the W/S ratio increases the rate of exchange becomes less dependent on it until at fluid/mineral ratios greater than 10 by mass the rate becomes independent of W/S ratio.

Surface reactions in a rock

Cole *et al.* (1987) show that the isotopic exchange accompanying mineralogical alteration of basalt by seawater may also be described in terms of a surface reaction model. Exchange was found to follow a first order rate law and rate constants to range from 10^{-8} to $10^{-9.5}$ moles of oxygen/m^2 of solid surface/sec for temperatures of 500° to 300°C. The activation energy

was calculated to be 11.5 kcal mol^{-1}. Thus the rate constants are similar in magnitude to those for several mineral-fluid isotope exchange reactions (fig. 2.13).

The effect of impurities on the rate of surface controlled isotopic exchange.

Cole *et al.* (1983) note that rate constants for quartz recrystallisation derived from the results of Clayton *et al.* (1972) are separated into two populations which differ by an order of magnitude. This difference in exchange rate has apparently resulted from the use of two different quartz starting materials, and must therefore be related to a difference in either the specific surface area or the composition of the quartz itself. It would not be unlikely that a variation in defect concentration could accelerate or retard a surface process by means of a catalytic or poisoning effect, although it cannot be proven in this case. Obviously if one mineral can vary so much in exchange rate the same may be true of other minerals.

2.6.5 A comparison of surface controlled and diffusion dominated isotopic exchange.

Cole *et al.* (1983) have modeled the degree of isotopic exchange attained by surface controlled reactions and that attained by diffusion dominated exchange in similar mineral-fluid systems under the same conditions. Some of their results (with minor modification[1]) are shown in fig. 2.14 where the fraction of exchange as -ln(1-F) is plotted against time.

Fig. 2.14a shows the surface controlled oxygen isotope exchange which takes place with the cation exchange reaction:

$$\text{Paragonite} + KCl_{(aq.)} \Rightarrow \text{Muscovite} + NaCl_{(aq.)}$$

at 300°C. the curves were calculated by Cole *et al.* (*ibid.*) using an equation for the plate model similar to eqn. 2.27.

The diffusion coefficient of oxygen in paragonite has not been measured, however D_{oxygen} is available for phlogopite and for the purpose of the present discussion this is used as an order of magnitude approximation to that in paragonite. The oxygen isotope exchange which takes place by diffusion between phlogopite and water at 300°C calculated using eqn. 4.37 from Crank (1975) is shown in fig. 2.14b.

---

[1] The curves in fig. 2.14b have been recalculated using a computer program that solves eqn. 4.37 of Crank (1975) numerically. Values of F calculated using this program were always found to be slightly lower than those for the same mineral grain given by Cole et al. (1983). No reason for this discrepancy is apparent, although it seems that Cole et al. used a graphical method to derive their solutions. In addition to this these authors have used the plate thickness in their model, although the half plate thickness should have been used (Crank, 1975). This error does not account for the discrepancy described above however, because this is still found for the albite data, where Cole et al. correctly used the grain radius.

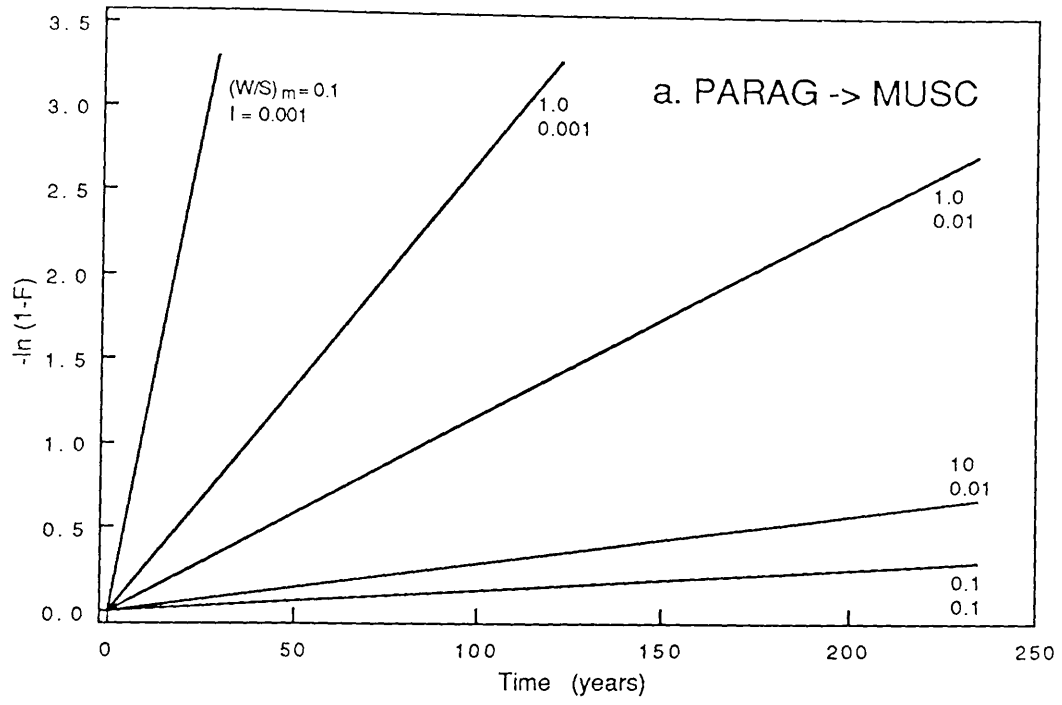

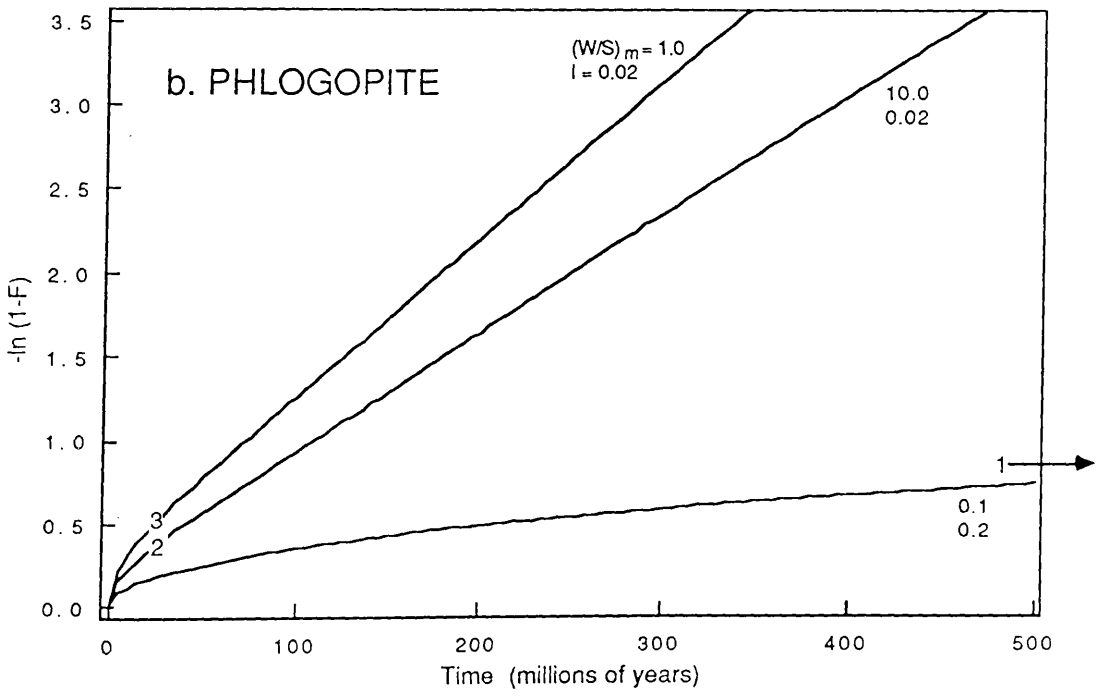

Fig.2.14 The fraction of oxygen isotope exchange as ln(1-F) versus time (first order plot) for a. the surface controlled cation exchange reaction of paragonite to muscovite compared with b. the diffusion controlled exchange of phlogopite with water, both at 300°C. Similar values of $(W/S)_M$ (fluid to solid mass ratios) and grain sizes (as plate thickness -l in cm) are used in both plots. The top number next to each curve is $(W/S)_M$ and the lower number is l. The rate constant used in a. and the diffusion coefficient used in b. are given in A.5. The fractionation factor used in b. is given in A.4. The numbers 1, 2 and 3 on the curves in b. refer to fig. 2.15. Figure partly after Cole *et al.* (1983).

Similar values of fluid/mineral (mass) ratios and grain sizes are used in both models. It can be seen from both figures that the time required to attain a certain degree of exchange for both exchange mechanisms is less for lower

fluid/mineral ratios at constant grain size and greater for larger grain sizes at constant fluid/mineral ratios, as has already been demonstrated. The most important difference between these two mechanisms is that the time for a given fraction of exchange is several orders of magnitude larger for diffusion dominated exchange than for exchange via a surface reaction (note the change in x-axis scale between figs a and b). A paragonite grain 0.01 cm thick which is altering to muscovite in a system with a mineral/fluid mass ratio of 1 reaches 90% exchange in approximately 200 years while a similar grain in which exchange is taking place by diffusion will require millions of years to undergo a similar amount of exchange. Cole *et al.* (*ibid.*) suggest on the basis of the exchange data summarised in their paper that such a difference in exchange rates between surface controlled and diffusional exchange will be general and that systems experiencing surface controlled exchange will reach isotopic equilibrium well before exchange by diffusion can become significant. The rate of exchange in a mineral-fluid system may thus depend critically upon whether the fluid is in chemical equilibrium with the rock or not. Cole *et al.* conclude that "oxygen isotopic exchange reactions between fluids and rocks in natural systems may proceed in two steps: the first through a surface-controlled mechanism when the fluids and minerals are out of chemical equilibrium, and then through a diffusional mechanism once the systems attain chemical equilibrium". (Note that this is not entirely true since it has been shown above that recrystallisation can take place even when fluid and mineral are in chemical equilibrium).

Another feature that will also be noticed from fig. 2.14 is that the shapes of the curves are different. Exchange by the surface controlled model takes place by a pseudo-first order process, so that plots of -ln(1-F) vs time will be linear (see equations 2.15, 2.26). The fraction of exchange which takes place by diffusion is a complex function of time because of the varying order of exchange as discussed below.

The order of diffusion-dominated exchange.

Crank (1975, p.37) shows that the amount of diffusing substance entering a semi-infinite medium having a uniform initial concentration and the surface of which is maintained at constant concentration is proportional to the square root of time. Diffusion into a grain may be described in this way if:

a. The grain is effectively a semi-infinite medium. This is the case during the time prior to the concentration profiles meeting at the centre of the grain.

b. The fluid/mineral ratio (β) is high enough such that the surface concentration remains effectively constant.

Thus if these conditions are satisfied

$$F=k\sqrt{t}\ .$$

Such a relationship is known as the parabolic rate law (e.g. Fletcher and Hofmann, 1974).

Only one author appears to have attempted to estimate an empirical order of reaction for isotope exchange from experimental data. Graham (1981) attempted to fit hydrogen isotope exchange data for the systems zoisite-H_2O and muscovite-H_2O to various rate expressions. The best approximation to a linear correlation was given by plotting F/(1-F) vs time, consistent with second order kinetics (eqn 2.16). Graham acknowledges however that this may not be a unique solution and it is not clear if it was attempted to fit the data to parabolic rate kinetics.

A prediction of the order of exchange that may actually apply in natural situations may be made by plotting the degree of exchange calculated for three of the phlogopite grains shown in fig. 2.14b (curves 1,2,3) against various rate expressions (fig 2.15a,b,c and 2.14b). The position of the numbers on the curves indicate the approximate time at which the concentration profiles meet at the centre of the grain which is when the grain ceases to be semi-infinite. The phlogopite grain in curve 1 is effectively semi-infinite over the whole time range. It can be seen that none of the curves is straight lines on a zero order plot (F vs t, fig. 2.15a), however when the model data is plotted on a parabolic rate plot (F vs $\sqrt{t}$, fig. 2.15b) it can be seen that the grain with the highest fluid/mineral ratio (curve 2, $W/S_M = 10$, $\beta \approx 20$) shows a good linear correlation in the semi-infinite region. Curve 3 which has a lower fluid/mineral ratio ($\beta \approx 2$) shows only a fair correlation in this region, while curve 1 ($\beta \approx 0.2$) is obviously curved. This effect is due to the change in surface concentration which takes place with the smaller mineral/fluid ratios. Interestingly on a first order plot (fig. 2.14b) both curves 2 and 3 appear to give good correlations after the grain has ceased to be semi-infinite. On a second order plot (F/(1-F) vs t, fig. 2.15c) it is interesting to note that curve 1 shows a fair correlation, although all curves in the semi-infinite region are slightly convex upwards. It is possible that Graham's (1981) empirical fit of the data to second order kinetics could actually be the result of diffusion into grains in the semi-infinite region combined with small β values.

In conclusion it is suggested that it may be possible to approximate diffusion-dominated exchange to various simple rate expressions, although further work is needed to define the regions over which these approximations could apply. Such approximations may be of considerable use in simplifying numerical models of diffusion controlled exchange. In hydrothermal systems for example, where β may be high (especially for H) and the characteristic transport distance for diffusion ($\sqrt{[Dt]}$, Fletcher and Hofmann, 1974) is less than the grain size, the rate of exchange may approximate very well to a parabolic rate law.

Fig 2.15 (next page). Curves 1, 2 and 3 from fig. 2.14b replotted in terms of a. F vs. time (zero order plot), b. F vs. $\sqrt{}$time (parabolic rate plot) and c. F/(1-F) vs. time (second order plot). Linear correlations on any of these plots might suggest that exchange conforms to the corresponding rate expression. The position of the numbers on the curves (including 2.14b) indicates the approximate time at which the concentration profiles (calculated using eqn. 4.45 from Crank, 1975) meet at the centre of the grain.

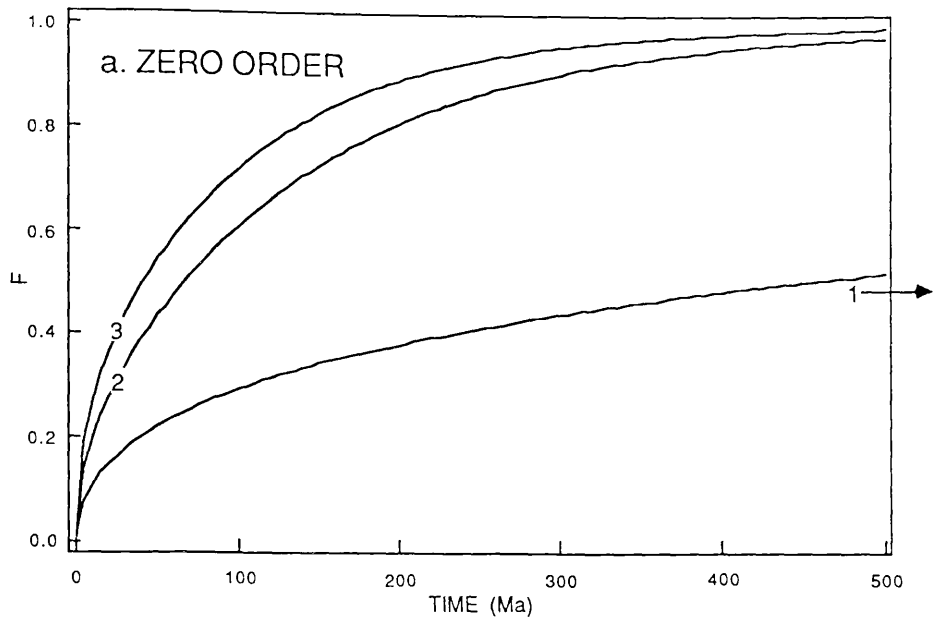
a. ZERO ORDER
F
TIME (Ma)
1
2
3

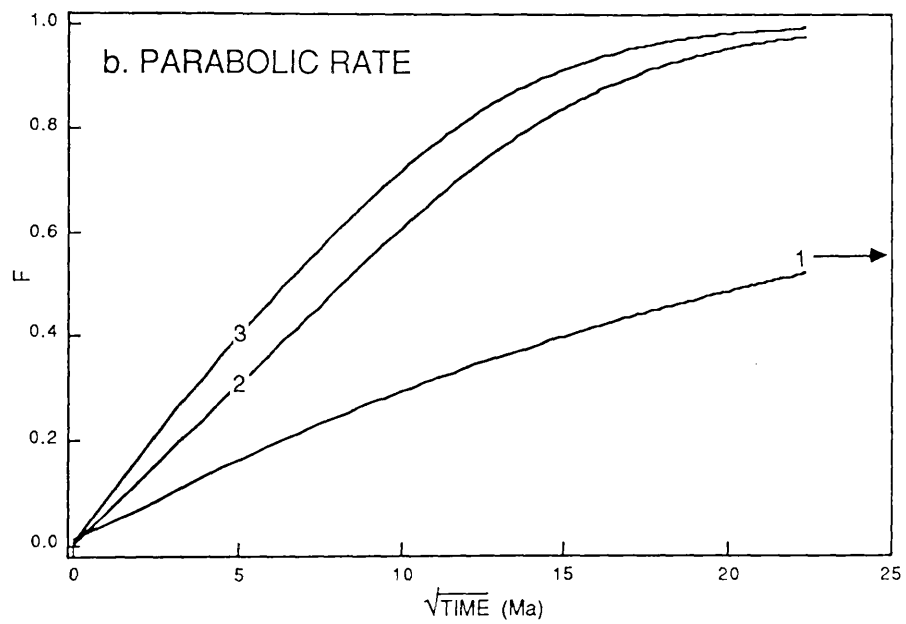
b. PARABOLIC RATE
F
√TIME (Ma)
1
2
3

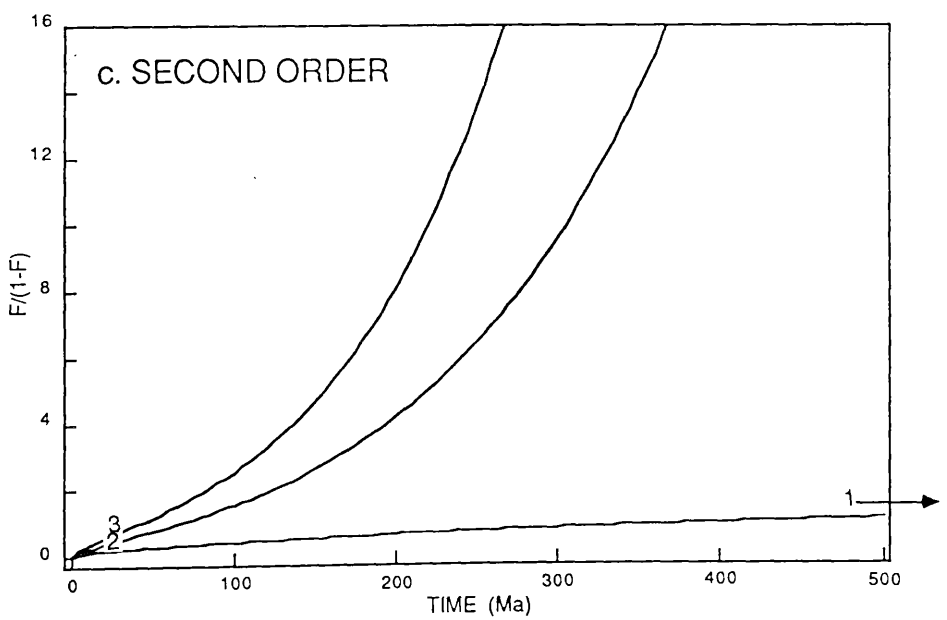
c. SECOND ORDER
F/(1-F)
TIME (Ma)
1
2
3

2.7 FLUID - ROCK INTERACTION.

A major field of stable isotope geochemistry is that which is concerned with the use of stable isotopes in investigating fluid-rock interaction. This is because stable isotope studies can potentially yield information with regards to the temperature, duration and fluid/rock ratio of the interaction event, as well as indicating the origin of the fluid (2.9). As noted by Gregory and Criss (1986) many rocks from ordinary lithospheric environments fail tests for closed system conditions and display the isotopic characteristics of systems that have been open to fluids. Because of this an understanding of the systematics of stable isotopes in fluid-rock interaction will find general application in the interpretation of a wide variety of rocks, not just those which are obviously associated with hydrothermal systems. In fact the assumption that all rocks have undergone some sort of fluid-rock interaction may be a profitable stand-point from which to interpret stable isotope data. With this point in mind, some of the principles governing the variation in stable isotope ratios during fluid-rock interaction are outlined below.

2.7.1 Major factors governing the isotopic effect of fluid infiltration.

If a fluid infiltrating a rock is out of isotopic equilibrium with the minerals in that rock under the prevailing conditions, then the minerals and the fluid will tend to change in isotopic composition in order to establish isotopic equilibrium. The amount of change that has to take place in the composition of the exchanging phases in order to reach equilibrium is governed by mass balance constraints, while the actual amount of change towards this equilibrium composition over the duration of infiltration is governed by kinetic effects. The actual mechanism by which the fluid moves through the rock will also be shown to influence the isotopic effect that fluid infiltration has.

2.7.2 Mass balance constraints in fluid-rock interaction.

The general statement of a mass balance relationship in isotopic terms is:

$$\delta SYSTEM_i = \delta SYSTEM_f = \delta SYSTEM_e \text{ ,}$$

where the subscripts i, f and e stand for the initial, final and equilibrium states of the system. In this case the system comprises the volume of rock that we are observing plus the total amount of fluid that passes through that volume of rock during the infiltration event. The initial state of the system is that prior to fluid infiltration, the final state is that after fluid infiltration and the equilibrium state refers to the system when isotopic equilibrium between fluid and rock is attained (at infinite time for stable isotope exchange taking place by first order or parabolic rate kinetics, although a state which is very close to equilibrium may be attained in a finite time). The mass balance relationship together with equilibrium fractionation factors may be used to calculate the δ value which any phase in a system will have in the equilibrium state. The change (or shift) in δ value of a phase from the initial to the equilibrium state is the maximum

shift that can occur, in practice the shift may be less than this because of kinetic effects in which case the final state is not the equilibrium state.

The specific formulation of the mass balance relationship is dependent on the conceptual model of the system. Various models of fluid-rock systems have been proposed:

a. Taylor's closed system (Taylor, 1977; Criss and Taylor, 1986). This is the closed system referred to by most geochemists. The system consists of a body of rock which is maintained at a constant temperature and is connected to a reservoir of fluid which is continually circulated through the rock until equilibrium is achieved (fig. 2.16a). The fluid/rock ratio is the ratio of fluid and rock in the two compartments. Few natural systems can be represented by this model, in geothermal systems, for example, much of the hydrothermal fluid may not be recycled. Nevertheless this closed system model is a useful approximation to some systems and the mass balance constraints (derived below) demonstrate the factors that are important in fluid-rock interaction in more complicated systems.

b. Natural closed system. The amount of fluid that can actually be contained in a given rock mass at one moment is that which can be contained in the pore space (<0.1% in crystalline rocks, Criss and Taylor, 1986). In natural closed system the fluid in the system is represented only by the pore fluid (2.16b). Thus fluid/rock ratios will always be very small. Such a system can be treated as a limiting case of Taylor's closed system model.

c. Taylor's open system (Taylor, 1977; Criss and Taylor, 1986). This is often termed a single pass model. As noted above the amount of fluid that can be contained in a rock at any one time is very small. In Taylor's open system infinitely small increments of fluid are introduced into the rock which is held at a fixed temperature,each increment is allowed to attain equilibrium and then is replaced by a new increment of fluid (fig. 2.16c). The fluid/rock ratio is a time integrated value depending on the number of increments which pass through the rock. Such a model may be more analogous to natural hydrothermal systems and situations where fluid is only moving in one direction. However on a large scale in natural systems, temperature is not constant.

d. Natural open system. In natural fluid systems the porosity of the rock is nearly always very low, and fluid is not usually recycled, as in Taylor's open system. However in natural systems the fluid that passes through a rock at high temperature may also have previously passed through and equilibrated with rock at a lower temperature (2.16d)

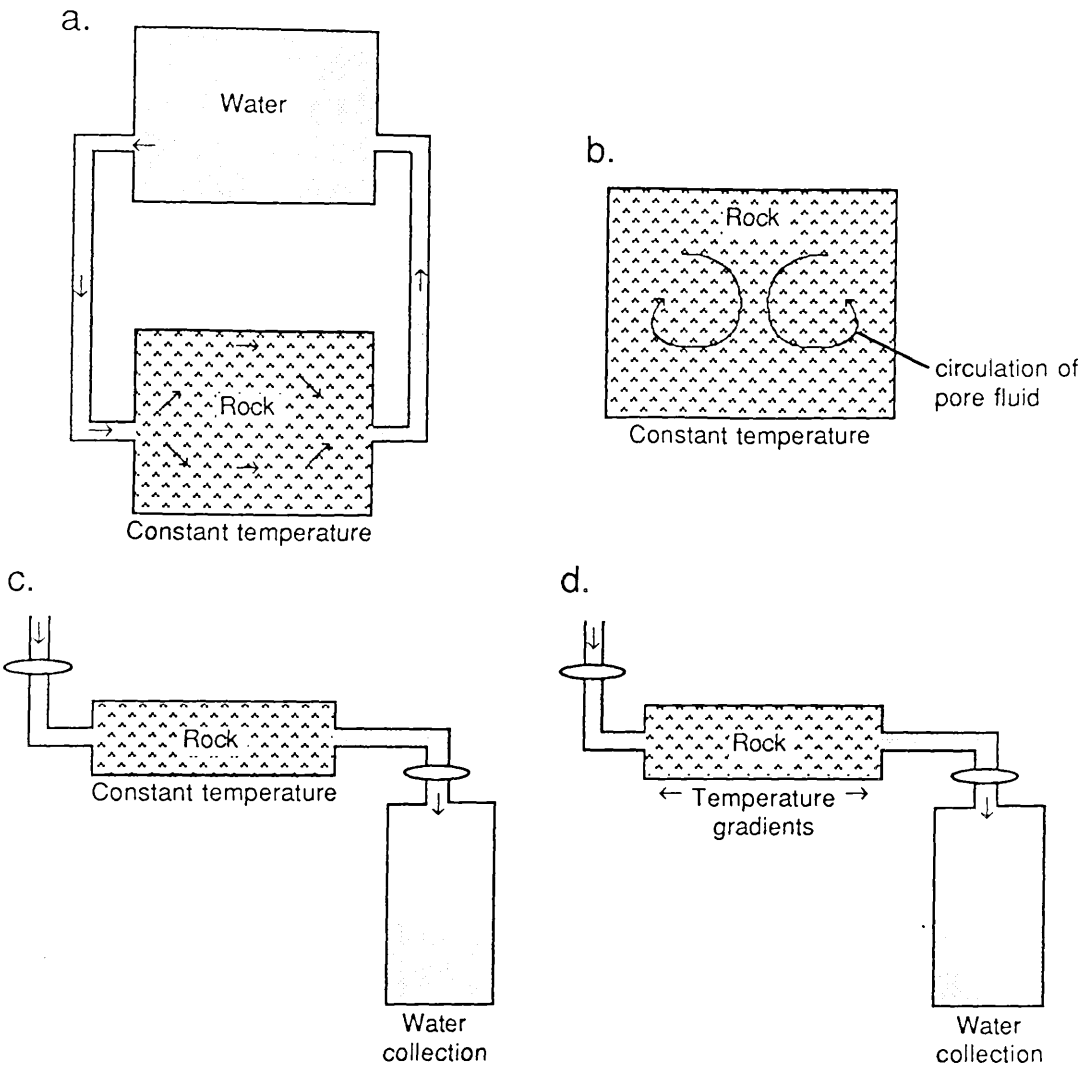

Fig 2.16 Models of fluid-rock interaction. a. Taylor's closed system, b. natural closed system, c. Taylor's open system, d. natural open system.

Mass balance constraints in Taylor's closed system.

The most simple situation that can be examined is the infiltration of fluid into a monomineralic rock, for which the mass balance relationship is:

$$\delta W_i X_W + \delta M_i X_M = \delta W_e X_W + \delta M_e X_M \ , \qquad (2.28)$$

where W and M stand for the fluid and mineral respectively and X stands for the mole fraction in the system of the element in question (e.g. O or H) in the subscripted phase. The assumption is made here that X_M and X_W do not change during infiltration, X_M and X_W could change if isotope exchange takes place by a chemical reaction mechanism (e.g. the mole fractions of H could change if a hydration reaction is taking place). These mole fractions can easily be converted to weight or volume fractions using the appropriate constants. Eqn. 2.28 can be rearranged to give:

$$\frac{X_W}{X_M} = \frac{\delta_{Me} - \delta_{Mi}}{\delta_{Wi} - \delta_{We}} \ . \qquad (2.29)$$

Thus for a natural system if it can be assumed that equilibration had taken place and the δ terms can be estimated (δ_{We} can be substituted by $\delta_{Me} - \Delta_e$, where Δ_e is the equilibrium mineral-fluid fractionation at the temperature of infiltration) then X_W/X_M - the atomic fluid/rock ratio can be estimated.

Equation 2.28 can also be rearranged to give:

$$\delta_{Me} - \delta_{Mi} = \frac{(\Delta_e - \Delta_i)\left(\frac{X_W}{X_M}\right)}{\left(1 + \left(\frac{X_W}{X_M}\right)\right)} \qquad (2.30)$$

(where $\Delta_i = \delta_{Mi} - \delta_{Wi}$), which relates the shift in δ value in the mineral which is necessary to attain equilibrium ($\delta_{Me} - \delta_{Mi}$), to the difference between the initial and equilibrium fractionations between the mineral and fluid ($\Delta_e - \Delta_i$) and to the fluid/rock ratio. Similarly it can be shown that:

$$\delta_{We} - \delta_{Wi} = \frac{(\Delta_i - \Delta_e)}{\left(1 + \left(\frac{X_W}{X_M}\right)\right)} \; . \qquad (2.31)$$

From these two equations it can be seen that if the fluid is in isotopic equilibrium with the mineral prior to infiltration ($\Delta_e = \Delta_i$) then no shift in the composition of either the mineral or the fluid will occur, regardless of the fluid/rock ratio. If ($\Delta_e \neq \Delta_i$) then the magnitude of the shift is also seen to be a function of the fluid/rock ratio; if $X_W \rightarrow 1$ (or $X_W/X_M \rightarrow \infty$), then ($\delta_{Me} - \delta_{Mi}$)$\rightarrow$($\Delta_e - \Delta_i$) and ($\delta_{We} - \delta_{Wi}$)$\rightarrow$0. Such a system is sometimes termed a fluid dominated or controlled system because the isotopic composition of the minerals is effectively controlled by the composition of the infiltrating fluid. Conversely if $X_W \rightarrow 0$ then ($\delta_{Me} - \delta_{Mi}$)$\rightarrow$0 and ($\delta_{We} - \delta_{Wi}$)$\rightarrow$($\Delta_e - \Delta_i$). Such a system is often termed a rock dominated system. Natural closed systems will usually behave as rock dominated systems. The shift in isotopic composition in a mineral is therefore directly proportional to the fluid/rock ratio and the degree of initial disequilibrium.

If the fluid is infiltrating a polymineralic rock then an additional constraint can be placed on the calculations if it is assumed that the minerals in the rock are in isotopic equilibrium prior to infiltration as well as at the equilibrium state of the system. In this case the shift ($\delta_{Me} - \delta_{Mi}$) of any one mineral will be the same as the shift of all of the other minerals in the rock, this can be shown for two minerals M1 and M2 if:

$$\Delta_{(1\text{-}2)e} = \delta_{M1e} - \delta_{M2e} \; ,$$

then

$$\delta_{M1e} = \Delta_{(1\text{-}2)e} + \delta_{M2e} \text{ and } \delta_{M1i} = \Delta_{(1\text{-}2)e} + \delta_{M2i} \; ,$$

then

$$\delta_{M1e} - \delta_{M1i} = (\Delta_{(1-2)e} + \delta_{M2e}) - (\Delta_{(1-2)e} + \delta_{M2i})$$

$$= \delta_{M2e} - \delta_{M2i} .$$

imilarly it can be shown that the shift of the whole rock will be the same as the shift of any of its constituent minerals.

Equations 2.29, 2.30, 2.31 can therefore be modified to apply to a rock if M is now taken to refer to the rock and $(\Delta_e - \Delta_i)$ is that value for any of the mineral-water fractionations in the rock. Thus it can be seen as shown above for a monomineralic rock that the shift needed to attain equilibrium upon infiltration in a polymineralic rock is a function of the initial difference from equilibrium and the fluid/rock ratio. Since the shift in any mineral is the same as the shift in the whole rock, then this will also depend on these same factors. It is important to note that the shift required in a mineral is independent of its abundance in the rock.

Mass balance constraints in Taylor's open system.

In this system each increment of fluid that passes into the rock will be isotopically dominated by the rock. As the rock slowly changes in isotopic composition so also will the increments of fluid that have equilibrated with it. Taylor (1977) shows that the fluid/rock ratio in an open system can be related to the fluid/rock ratio in a similar closed system by:

$$(X_W / X_R)_{OPEN} = \ln\left[(X_W / X_R)_{CLOSED} + 1\right] .$$

The calculated shifts of a mineral vs. fluid/rock ratio for Taylor's closed and open system models are compared in fig. 2.17. It can be seen that for a given fluid/rock ratio, the shift in the mineral is always greater in the open system.

Mass balance constraints in natural open systems.

The mass balance constraints in natural open systems can usually only be determined by numerical methods and are dependent on a number of parameters (temperature gradients, fluid flow rates etc.). Ohmoto (1986) demonstrates that the fluid/rock ratio required to cause a given shift in a natural open system may be many times that for either of Taylor's models.

Fluid/rock ratios of different elements.

Because of the different abundances of the light elements in fluids and rocks the fluid/rock ratios of these elements in the same fluid rock system may vary greatly. Tabulated below are the moles of oxygen and hydrogen kg^{-1} (molarity) in pure water, the molarity of C and S in geological fluids (after Ohmoto, 1986) and the molarity of these elements in various rock forming minerals.

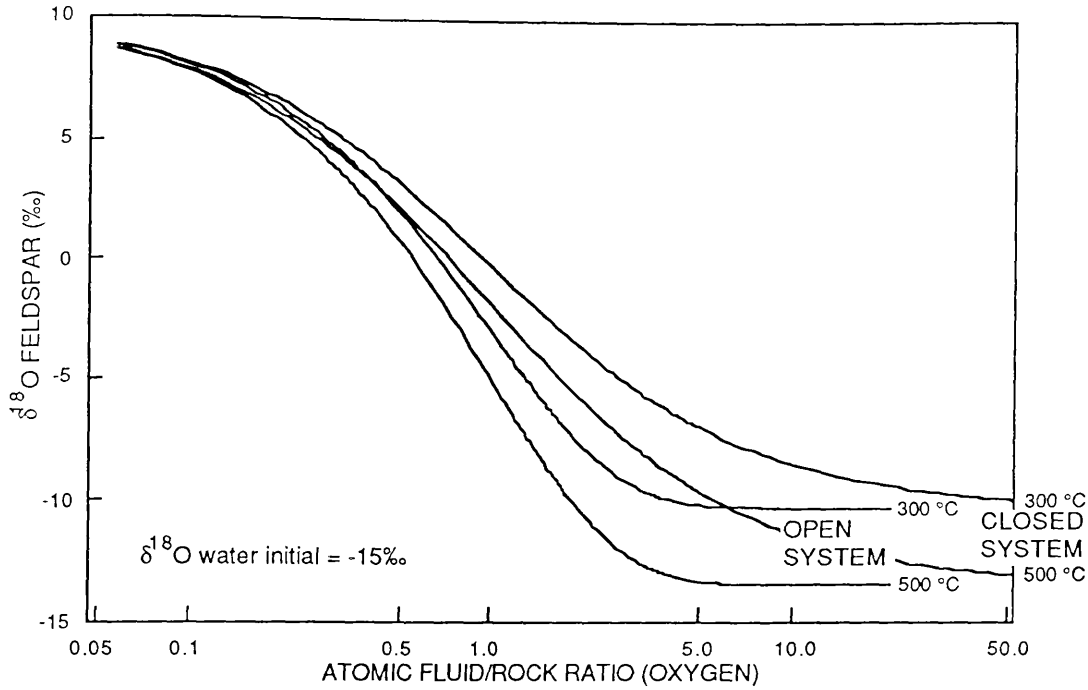

Fig. 2.17 The calculated shift in $\delta^{18}O$ of a monomineralic alkali feldspar rock (δ_i = +10‰) which is infiltrated by a meteoric fluid (-15‰), plotted against the atomic fluid/rock ratio (O) for Taylor's open system and closed system models. Note the logarithmic scale on the x-axis. Feldspar-water fractionation factor used was that of Matsuhisa *et al.* (1979).

Substance	moles O kg^{-1}	Substance	moles H kg^{-1}
H_2O	55.5	H_2O	111.0
SiO_2	33.3	Clinochlore	14.4
$NaAlSi_3O_8$	30.5	Muscovite	5.0
$CaCO_3$	30.0	Pargasite	2.4
$MgFeSiO_4$	23.2	Epidote	1.5
Fe_3O_4	17.3		
Substance	moles C kg^{-1}	Substance	moles S kg^{-1}
Fluid	0.01-1	Fluid	0.1-0.0001
Graphite	83.3	FeS_2	16.7
$CaCO_3$	10.0	FeS	11.4

It can be seen that if one kg of rock is in filtrated by 1 kg of fluid that the atomic water/rock ratio of oxygen will be ≈ 2, while if the same rock contains 5 wt.% of amphibole and no other hydrous mineral the atomic water/rock hydrogen ratio will be ≈ 900. Thus the system can be rock dominated for one element and fluid dominated for another. Obviously far more significant shifts in rock δD compared to rock $\delta^{18}O$ can result for a given amount of fluid infiltration. If a sequence of rocks with similar composition is infiltrated by varying amounts of fluid under the same conditions, X_W (hydrogen) will approximate to 1 at a much lower (fluid/rock) mass ratio than X_W (oxygen), in which case if equilibrium is rapidly attained most of the shift in hydrogen isotope composition of the

rock will occur before any measurable shift in $\delta^{18}O$ occurs. Such behaviour results in an "L-shaped " array of points on a δD vs. $\delta^{18}O$ plot for rocks of similar initial compositions which have experienced a range of fluid/rock ratios (Fig. 2.18).

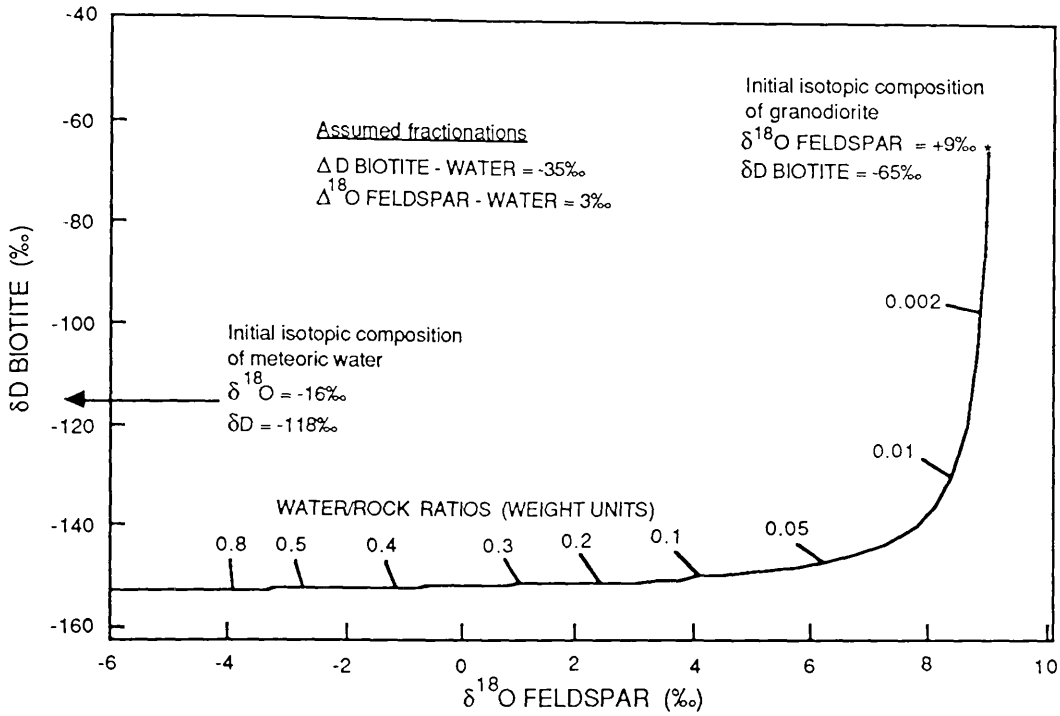

Fig. 2.18 Calculated values of biotite δD and feldspar $\delta^{18}O$ that would be produced at various fluid/rock ratios by infiltration of a typical granodiorite (65 wt.% feldspar, 25 wt.% quartz, 10 wt.% biotite) by a meteoric fluid at 400°C, assuming that Taylor's closed system model applies. The quartz and biotite are assumed to be inert to oxygen isotopic exchange. After Taylor (1977).

$X_{W(hydrogen)}$ is always higher than $X_{W(oxygen)}$ during fluid-rock interaction except under extreme circumstances. The relative values of $X_{W(carbon)}$ and $X_{W(sulphur)}$ are less predictable, being strongly dependent on rock type and fluid composition. For 1 kg of rock containing 1 wt.% calcite (or 0.12 wt.% graphite) which is infiltrated by 1 kg of fluid the atomic fluid/rock ratio for carbon will be in the range 10 to 0.1, similarly if the rock contains 1 wt.% of pyrite the fluid/rock ratio for sulphur will be in the range 0.6 to 0.0006. Thus in general the ranking may be approximately:

$$X_{W(hydrogen)} >> X_{W(oxygen)} \approx X_{W(carbon)} > X_{W(sulphur)}.$$

2.7.3 Kinetic effects in fluid-rock interaction.

In natural systems equilibration takes a finite amount of time. The actual shift that will occur in a given amount of time can be related to the calculated equilibrium shift by involving a rate expression, for example recalling eqn. 2.15 for first order exchange:

$$\ln(1-F) = -k_1 t \ ,$$

where k_1 is the first order rate constant and (1-F) is:

$$1 - \left(\frac{\delta_{Mf} - \delta_{Mi}}{\delta_{Me} - \delta_{Mi}} \right)$$

in the case of an exchanging mineral, where the subscript f refers to the δ value of the mineral at time t. Therefore

$$1 - \left(\frac{\delta_{Mf} - \delta_{Mi}}{\delta_{Me} - \delta_{Mi}} \right) = \exp^{-k_1 t},$$

which on rearrangement gives

$$\delta_{Mf} - \delta_{Mi} = (1 - \exp^{-kt}) (\delta_{Me} - \delta_{Mi}),$$

which means that the actual shift after a given time is a function of the rate constant and the equilibrium shift which was derived in 2.7.2. Similar expressions can be derived for other orders of exchange including:

$$\delta_{Mf} - \delta_{Mi} = (\sqrt{kt}) (\delta_{Me} - \delta_{Mi})$$

for a parabolic rate and

$$\delta_{Mf} - \delta_{Mi} = [kt/(1+kt)] (\delta_{Me} - \delta_{Mi})$$

for a second order reaction.

Each mineral in a rock will have a different rate constant (and possibly exchange order) so that each mineral in a rock will exchange at a different rate. Unless enough time has elapsed for the equilibrium state to be reached in all minerals in a rock which is being infiltrated a disequilibrium assemblage will result, and this is usually the case.

2.7.4 The nature of the fluid flow and its effect on fluid-rock interaction.

Fluid-rock interaction will also be dependent on the actual way in which the fluid flows through the rock. Two end member situations may be defined (Valley, 1986). Pervasive flow is when the fluid flow is independent of structural and lithologic control and occurs along grain boundaries. Flow may be very slow in this case allowing plenty of time for exchange reactions to take place. In addition the surface area of rock exposed to the fluid will be large, enhancing exchange reactions. Channelised flow takes place when fluid flow is concentrated in certain highly permeable parts of the rock mass e.g. along faults, veins, microcracks or more permeable units. In a flow channel the fluid may flow very rapidly and less exchange with the rock may occur because of this, although the effective fluid/rock ratios will increase because the fluid is coming into contact with less surface area of rock. Away from the channels the effective fluid/rock ratio will be decreased compared with the pervasive flow case. If channelised flow is taking place isolated units in which minor closed system rock-dominated exchange is taking place could occur in close proximity to areas in which open system fluid-dominated exchange is taking place.

2.7.5 Fluid-rock interaction - natural systems.

The outline of the principal factors controlling the effect of fluid-rock interaction given in the previous three sections is purposefully simplistic and by no means rigorous, it is intended merely to demonstrate the complexity of this process.

The final position of equilibrium that the minerals in a rock will evolve towards can usually be calculated from mass balance constraints, however this requires a knowledge of the most appropriate system model, the fractionation factors at the conditions of infiltration, the fluid/rock ratio and the composition of the infiltrating fluid.The fractionation factors are functions of temperature, while the fluid/rock ratio is a function of flow rate and time. The composition of the infiltrating fluid will be a function of the original composition of the fluid and the sum of all the fluid-rock reactions that have already taken place prior to the arrival of the fluid at the rock which we are examining. In a natural system all of these factors may vary with time.

The actual shift that will occur in a mineral is a function of a rate expression, time and the degree of disequilibrium. In natural situations as explained above the the position of equilibrium towards which the system is evolving may be changing with time. As outlined in section 2.6 the factors which may govern the the kinetics of fluid-rock isotope exchange reactions include temperature, the chemistry of the fluid phase and its influence on the exchange mechanism, grain size and fluid/rock ratio.

The degree of channeling of the fluid flowing through a rock may significantly affect the nature and distribution of effects that we see from fluid rock interaction in the field. Samples collected from within channels may show large differences in their isotope compositions from those collected where only pervasive flow has taken place.

Obviously modelling of a natural system which is dependent on a number of inter-related parameters is extremely difficult, and many approximations have to be made. The most successful attempt to date is that of Gregory and Criss (1986) and Criss *et al.* (1987) who have attempted to derive some solutions for the isothermal case by solving $n_{(phases)}$ rate equations together with a mass balance equation using an eigenvector method. By factoring out time and presenting the results on δ - δ plots the authors are able to simulate the disequilibrium arrays seen in many natural systems.

2.7.6 Causes of fluid infiltration.

Fluid flow can occur by two mechanisms:

A. Unidirectional fluid flow.

This results from a spatial variation in hydrostatic head and is described by Darcy's law:

$$J_F = -\frac{\kappa}{\nu}(\nabla P - \bar{\rho} g) \quad , \qquad (2.32)$$

where $\overline{J}_F$ is the fluid flux vector (g cm^{-2} sec^{-1}), κ the permeability (cm^2), ν the kinematic viscosity (cm^2 sec^{-1}), $\overline{\nabla} P$ the pressure gradient, $\overline{\rho}$ the fluid density (g cm^{-3}) and g is the gravitational acceleration (Etheridge *et al.*, 1983). Thus the fluid flux is directly proportional to the permeability and the pressure gradient and inversely proportional to the viscosity. The most important variables are the permeability and the pressure gradient. Laboratory permeabilities (Brace, 1980) of metamorphic and intrusive igneous rocks are in the range 10^{-17} to 10^{-12} cm^2 (10^{-9} to 10^{-4} darcy), but Brace (1980,1984) has emphasised the importance of the scale of measurement and suggests that permeabilities on a drill hole or crustal scale are higher, ranging from 10^{-14} to 10^{-9} cm^2 (10^{-6} to 10^{-1} darcy) because of the presence of throughgoing fractures and microcracks. The applicability of such measurements to deeper rocks is debatable, Etheridge *et al.* (1984) have suggested that high fluid pressures during regional metamorphism may result in permeabilities of the order of 10^{-14} to 10^{-11} cm^2 (10^{-6} to 10^{-3} darcy) which are at the high end of those measured in the laboratory.

Such uni-directional fluid flow may take place in situations where rock units are undergoing devolatilisation during prograde metamorphism, either on a regional scale (Graham *et al.*, 1987) or local scale (Matthews and Kolodny, 1978), or as a result of overthrusting (Fyfe and Kerrich, 1985; Negga *et al.*, 1986). Exsolution of a water rich fluid from an oversaturated magma may result in unidirectional fluid flow away from the intrusion (Nabelek *et al.*, 1984).

B. Fluid convection.

If within a body of fluid, the fluid at the base is heated such that it is less dense than the fluid at the top, the system will be gravitationally unstable and thermally induced convection of the fluid will result. In a fluid saturated rock convection can also occur, although it will be obvious from eqn. 2.32 that permeability will also be an additional factor. Etheridge *et al.* (1983) show that the conditions necessary for the initiation of convection in a permeable horizontal slab heated from below are described by the equation:

$$Ra = \frac{\kappa \gamma g \Delta T h}{\nu k_m} \quad , \qquad (2.33)$$

where Ra is a dimensionless Rayleigh number, γ is the thermal expansion coefficient of the fluid, h is the slab thickness and k_m is the thermal diffusivity. Values of Ra > ~40 indicate that convection should take place. Assuming a geothermal gradient of 50°C km^{-1} and typical properties for an aqueous fluid, this equation predicts (Criss and Taylor, 1986) that convection will be possible in a 100 m thick layer for permeabilities > 10^{-8} cm^2 (1 darcy), in a 3 km layer if the permeability exceeds 10^{-11} cm^2 (10^{-3} darcy) and in a 100 km layer if the permeability exceeds 10^{-14} cm^2 (10^{-6} darcy). Valley (1986) notes however that eqn. 2.33 does not contain a term for the compressibility of the fluid which will also affect the density contrast, although the importance of this effect will partly depend on whether the fluid is under lithostatic pressure, where the fluid pressure is controlled by the weight of

overlying rock or hydrostatic pressure where the fluid pressure relates to the weight of overlying fluid ($P_{H2O} \approx 1/3\ P_{Lithostatic}$).

The transition from hydrostatic to lithostatic fluid pressure is important in governing the depth to which surface derived fluids can be carried down into the crust by convection. Convective circulation of meteoric water and seawater into the upper 6 km of continental and oceanic crust has been demonstrated by many stable isotope and other studies (Criss and Taylor, 1986; Muehlenbachs, 1986 and references therein). In these shallow permeable environments values of P_{H2O} are approximately equal to the hydrostatic pressure and rocks have sufficient strength to hold the fluid conduits open. At greater depth the difference between $P_{Lithostatic}$ and $P_{Hydrostatic}$ exceeds the yield strength of the rock, the rock fails, and the fluids are compressed to lithostatic pressure. Obviously surface derived fluids cannot pass up this pressure gradient and this transition represents a lower depth limit for the infiltration of surface derived fluids. The yield strength of the rock will depend on both its intrinsic strength and temperature as well as porosity to some extent. Thus the deepest penetration of surface fluids might be expected to occur in cold brittle crust. The deepest known infiltration of possible (?) meteoric fluids into the crust (~12 km) occurs in the Precambrian gneisses of the Kola Peninsula (Kozlovsky, 1981), supporting this hypothesis.

The question of whether or not convection can occur in fluid under lithostatic pressure is highly controversial. Etheridge *et al.* (1983) have suggested on the basis of eqn. 2.33 that large convection cells greater than 10 km in diameter may occur in lithostatically pressured fluid in the deep crust during regional metamorphism. This process requires the presence of an impermeable layer which isolates deep convection from shallow hydrostatic fluids. As noted above Valley (1986) points out that no account is taken in eqn. 2.33 of the fluid compressibility and he suggests that taking this into account will reduce the density contrast which drives the convection. Indeed he suggests that for some common geothermal gradients and realistic fluid compositions, density will be greatest at the bottom of a lithostatically pressured layer, making convection impossible. Nevertheless some studies might provide evidence to support the case for deep convection. The large fluid/rock ratios apparently involved in some regional metamorphic areas (Ferry, 1984; Fleck and Criss, 1985) are unreasonable if a simple unidirectional flow is assumed, whereas recirculation of the fluid by convection could explain these observations. Chamberlain and Rumble (1987) have recognised localised "hot spots" associated with upward fluid flow in a regional metamorphic terrain in central New England. These hot spots may represent the best evidence yet for such deep convection.

2.8 CARBON AND SULPHUR ISOTOPE SYSTEMATICS.

There are important differences in chemical and isotopic behaviour between C and S systems and H and O systems. These differences mean that additional factors have to be taken into account when when estimating the source of C and S in carbon and sulphur bearing minerals. These differences

and their relevance to the estimation of the sources of C and S in the calcites and baryte analysed in this study are outlined below.

2.8.1 Carbon and sulphur isotope systematics compared to oxygen and hydrogen isotope systematics.

The major causes of O- and H-isotope variations in nature are vaporisation and condensation, fluid mixing and isotopic exchange reactions. In contrast the major causes of C- and S-isotope variations are redox reactions involving the isotopic species (Ohmoto, 1986). This is because:

a. C and S occur in nature in many different valence states. Both oxidised and reduced species may be present in some geological environments.

b. Many mechanisms, both biological and non-biogenic control the variations in the redox state of S and C.

c. Large kinetic isotope effects are associated with many redox reactions, particularly with reduction.

d. Large equilibrium fractionation factors exist between the oxidised and reduced species. Compounds with higher oxidation states tend to be enriched in the heavier isotopes. Thus under equilibrium conditions $\delta^{13}C_{carbonates} > \delta^{13}C_{graphite} > \delta^{13}C_{methane}$ and $\delta^{34}S_{sulphates} > \delta^{34}S_{SO2} > \delta^{34}S_{sulphides}$.

(After Ohmoto, 1986).

In contrast to O- and H- which dominantly occur as one species (H_2O) within geological fluids C and S can occur as a number of species (CO_2, CH_4, H_2S, SO_4^{2-}). This makes the estimation of the equilibrium isotope composition of the fluid which coexisted with analysed minerals far more complicated for C and S. The isotopic composition of the fluid for these elements is the weighted average of the isotopic compositions of all the species present, for example

$$\delta^{13}C_{\Sigma C} = \delta^{13}C_{CO2}.X_{CO2} + \delta^{13}C_{H2CO3}.X_{H2CO3} + \delta^{13}C_{HCO3^-}.X_{HCO3^-} + \delta^{13}C_{CH4}..X_{CH4}.$$

Thus the isotopic composition of the fluid can only be estimated if the speciation of the fluid is known. The speciation of the fluid is a function of pH, the oxygen fugacity and temperature. However it will be shown below that some simplifications can be made under certain conditions.

2.8.2 Approximations in determining the the source of carbon in carbonates.

The $\delta^{13}C_{\Sigma C}$ value of a fluid may be diagnostic of its source. In most cases only carbonate minerals are analysed which means that both the temperature and speciation of the fluid have to be known before the $\delta^{13}C_{\Sigma C}$ value of the fluid can be calculated. However Ohmoto (1986) suggests that the rates of C isotope exchange between dissolved carbonate species (ΣCO_2) and CH_4 in geological fluids may be extremely slow, so that under most geological conditions isotopic equilibrium may not be established at temperatures below ~250°C. The isotopic exchange rates between carbonate

species (CO_2, HCO_3^- etc.) that have been measured in the laboratory suggest that equilibrium will be rapidly established between these species under geological conditions (Ohmoto, 1986).

These kinetic data can be used to make approximations in the calculation of equilibrium fluid compositions at low temperatures (~ <250°C) because if no carbon isotope equilibration takes place between ΣCO_2 and CH_4 during the journey from the source then $\delta^{13}C_{\Sigma CO2}$ and $\delta^{13}C_{CH4}$ will each be the same as the initial compositions that were in equilibrium with the source. Thus only one of these values (usually $\delta^{13}C_{\Sigma CO2}$) needs to be calculated in order to estimate the source composition. The carbonate speciation is controlled by pH and temperature, however in practice a further approximation can be made because in most geological fluids at temperatures above about 100°C the amount of HCO_3^- is negligible compared to the amount of $H_2CO_3^*$ (= CO_2(aq.) + H_2CO_3). Thus the following approximation can usually be made: (Ohmoto, 1986)

$$\delta^{13}C_{\Sigma CO2} = \delta^{13}C_{carbonate} - \Delta_{carbonate\text{-}H2CO3^*}.$$

2.8.3 Sulphur isotope systematics in the formation of baryte.

The one sample which has been analysed for its sulphur isotope composition in this study is a vein baryte and therefore only the sulphur isotope systematics of sulphate ion formation, equilibration and precipitation are described here.

Sulphate ion formation.

Sulphate which is being precipitated as baryte may originate either from seawater (the main reservoir of oxidised sulphur on earth) or from the oxidation or leaching of sulphides in rocks which a fluid has previously passed through. Ohmoto and Rye (1979) suggest that sulphates produced by the oxidation of sulphides should show $\delta^{34}S$ values essentially identical to those of the initial sulphides, i.e. no fractionation occurs in this process.

Pyrite and chalcopyrite may decompose by reaction with H_2O at elevated temperatures. These decomposition reactions may be either:

a. Reactions that produce Fe-oxides, such as

$$6FeS_2 + 11\ H_2O \Rightarrow 3Fe_2O_3 + 11H_2S + SO_2$$

or,

b. Acid dissolutions, such as

$$4FeS_2 + 4\ H_2O + 6H^+ \Rightarrow 4Fe^{2+} + 7H_2S + SO_4^{2-}.$$

Reactions producing iron oxides were investigated by Grinenko and Grinenko (1967) who observed that $\delta^{34}S_{H2S}$ values were 1 to 3‰ enriched relative to the pyrite value between 350 and 550°C, as a result of kinetic isotope effects. Thus by mass balance the $\delta^{34}S_{sulphate}$ produced will be -11 to -33‰ relative to that of the reacting pyrite. However for the acid dissolution reaction Ohmoto and Archer (unpublished data in Ohmoto

and Rye, 1979) found that the $\delta^{34}S_{H2S}$ values were -1‰ relative to the pyrite, and thus $\delta^{34}S_{sulphate}$ should be ~ +7‰ relative to the pyrite.

Sulphide ion equilibration.

If both sulphide and sulphate ions occur in a fluid then as with carbon bearing species these species may or may not re-equilibrate isotopes as conditions change. Ohmoto (1986) suggests that for neutral to acid fluids the sulphide and sulphate ions are not likely to equilibrate at temperatures less than 150°C unless the residence time of the fluid is very long (>10^5 years). If isotopic equilibrium is achieved then only the bulk fluid sulphur isotope composition ($\delta^{34}S_{\Sigma S}$) will be related to the source and the speciation of the fluid needs to be determined.

Sulphate ion precipitation.

Kusakabe and Robinson (1977) found that the sulphur isotope fractionation between HSO_4^- and $BaSO_4$ was less than the experimental detection limit of 0.4‰ between 110 and 350°C. Sakai (1968) suggests that there will be very little fractionation between sulphate species under hydrothermal conditions at temperatures greater than 100°C.

2.9 δ VALUES OF TERRESTRIAL RESERVOIRS.

2.9.1 The hydrogen and oxygen isotope compositions of natural waters.

Ocean waters

The H- and O- isotope compositions of present day ocean waters are relatively uniform with δD = +5 to -7, $\delta^{18}O$ = + 0.5 to -1.0‰ (Craig and Gordon, 1965; fig 2.19). In the proximity of ice sheets these values may be more depleted because of dilution by low D and ^{18}O meltwater (Sheppard, 1986a). Seas with restricted access to the open oceans may also differ from these values. In arid areas restricted seas such as the Mediterranean are enriched in D and ^{18}O due to evaporation of H and ^{16}O-rich vapour (*ibid.*). Other restricted seas such as the Black sea are depleted in D and ^{18}O because of a large contribution from meteoric run-off (*ibid.*).

The question of whether or not the isotopic composition of the ocean has varied significantly over geological time is of critical importance to isotope geochemists. Unfortunately the composition of ancient ocean water can only be estimated by indirect means which give rather equivocal results.

The pre-glacial composition of the ocean can be calculated by adding in an appropriate contribution for the ice caps which are strongly depleted in D and ^{18}O. Prior to ice cap growth, the mean composition of the ocean is calculated to have been δD = -7, $\delta^{18}O$ = -1 (Shackleton and Kennet, 1975).

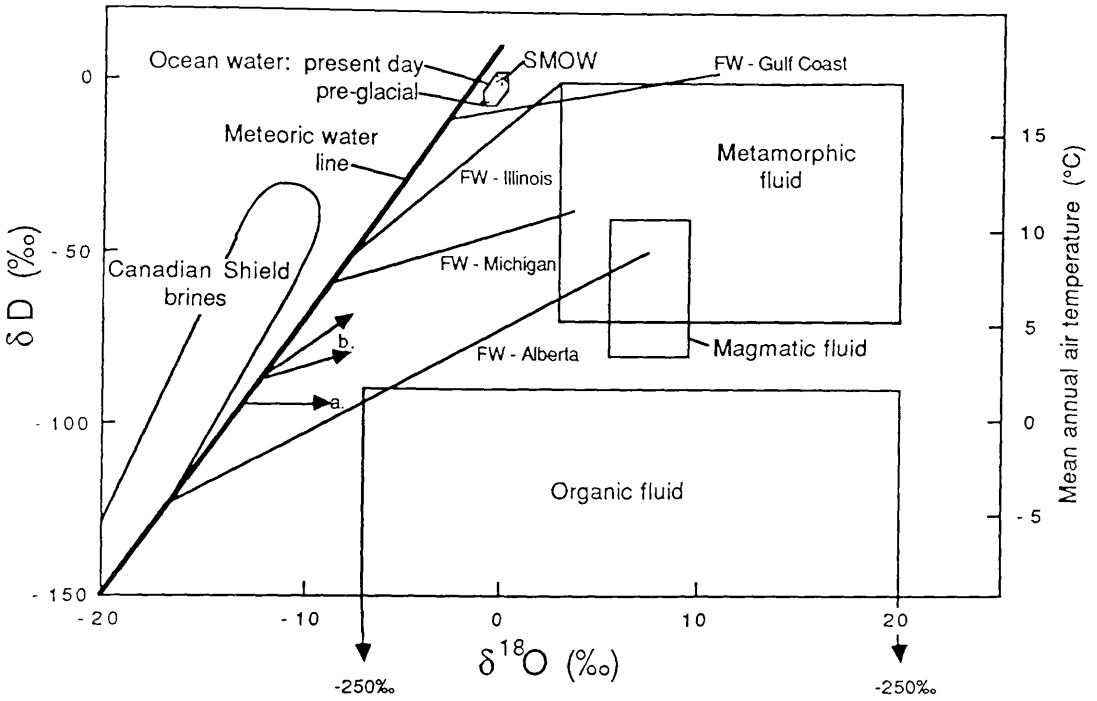

Fig. 2.19 δD - $\delta^{18}O$ diagram showing the compositions of terrestrial fluids. The meteoric water line (MWL) and the field for ocean waters are present day compositions, the calculated pre-glacial mean ocean water composition is also shown. The compositions of formation waters (FW-) from four sedimentary basins are shown by regression lines to the data, it should be noted that there is considerable scatter of data around these lines. Also shown are the isotopic trends that would result from a. meteoric waters undergoing exchange with ^{18}O rich minerals, and b. vapour loss from meteoric waters by boiling or evaporation. The temperature scale on the right hand axis gives the mean annual air temperature at which the corresponding composition of meteoric water on the MWL is precipitated, according to the relationship of Dansgaard (1961). See text for data sources.

Analyses of minerals which are thought to have been precipitated in equilibrium with seawater reveal trends in ^{18}O with time (see references in Sheppard, 1986a). These can be interpreted in a number of ways:

a. Precipitation of minerals from oceans of constant $\delta^{18}O_{value}$ but whose temperature decreased with time from ~ 70°C at 3400Ma.

b. Oceans of constant temperature, but increasing $\delta^{18}O_{value}$ from ~ -8 to -12‰ in the Archaean to ≈ 0 at the present day.

c. Post depositional effects which become increasingly intense with age.

d. A combination of any of the above.

Samples of ancient ocean crust which has been altered by seawater may be less prone to post-depositional effects and on the basis of a number of ^{18}O studies of ophiolites Muehlenbachs (1986) suggests that the $\delta^{18}O_{value}$ of seawater has not changed significantly over time. Indeed he suggests that ^{18}O buffering of seawater by interaction with ocean crust may have been important in keeping the $\delta^{18}O_{value}$ of seawater constant.

The δD of ancient ocean water may also have varied with time. Factors which may have influenced the past hydrogen isotope composition include reaction with oceanic crust (causing D enrichment of the ocean), the extent of recycling of the D-depleted material in the ocean crust back to the oceans, mantle degassing (D-depletion) and preferential loss of ^1H from the atmosphere (Kokubu *et al.*, 1961). The relative importance of these factors is poorly understood however.

Sheppard (1986a) taking into account all the arguments tentatively proposes that since ~2500Ma the $\delta^{18}O$ value of the oceans has been between 0 and -3‰ and the δD value has been between 0 and -25‰.

Meteoric waters.

These are waters that originated as precipitation (rain, snow, ice, river, lake and low temperature groundwaters). The H- and O- isotope compositions of meteoric waters cover a very wide range and are strongly correlated (fig. 2.19), being related by the equation:

$$\delta D = 8\,\delta^{18}O + 10 \qquad (2.35)$$

(Craig, 1961a; Yurtsever and Gat, 1981). Most meteoric waters which have not undergone extensive evaporation plot within a band ±1‰ $\delta^{18}O$ from this line which is termed the meteoric water line (MWL). The composition of the mean annual precipitation is found to be strongly correlated with the mean annual air temperature (Dansgaard, 1964), the equation relating these two variables being:

$$\delta^{18}O = 0.695\,T(°C) - 13.6\,. \qquad (2.36)$$

Because of this relationship there is a broad correlation of isotopic composition with latitude, the highest $\delta^{18}O$ and δD values being found in equatorial regions and the lowest at the poles, e.g. $\delta D \approx -440$, $\delta^{18}O \approx -55$ in Antarctica (Epstein *et al.*, 1970). Ocean currents and the meteorological system exert more regional influences on the isotopic composition of precipitation, e.g. the warming influence of the Gulf stream means that heavier meteoric water is precipitated in Britain ($\delta^{18}O \approx -6$‰) than in continental areas of similar latitude (≈ -14‰ in Michigan). The altitude of precipitation also exerts a strong influence because of the temperature effect, both regionally and on a local scale. The distance which the air mass has to travel from an ocean and the intensity of precipitation are also important.

These variations in isotopic compositions are caused by fractionation effects during evaporation and condensation. Nearly all atmospheric water is evaporated from the oceans, and during this evaporation process the fractionation factors are such that the vapour is enriched in the the light isotopes. Kinetic fractionation which also takes place enhances this depletion in of the heavy isotope in the vapour (Craig and Gordon, 1965). When condensation takes place the liquid phase is enriched in the heavy isotopes, so that the first material precipitated is similar in isotopic composition to ocean water. The continuing removal of heavy isotopes from the air mass results in the progressive enrichment of the light isotope in the residual water vapour. Thus later precipitation from the air mass (at

lower temperatures) has progressively lower δD and $\delta^{18}O$ values. This process is well described by a Rayleigh fractionation equation (Broecker and Oversby, 1971).

From this discussion it will be seen that the composition of ancient meteoric waters will be dependent on the composition of ocean water in the past, if this is assumed to have remained relatively constant then ancient meteoric water may have followed the MWL. Data from fossil meteoric-hydrothermal systems allows the composition of ancient meteoric waters to be estimated. Sheppard (1986a) reviews the data from a number of systems and is able to conclude that the data support the hypothesis that the composition of ancient meteoric waters may plot very near to the present MWL.

Using various geological data and certain assumptions, the stable isotope composition of the surface water (i.e. marine or meteoric water) which was present above the Connemara massif through time, has been estimated and is shown in figure 2.20.

Formation waters.

Formation water is the water which is found in the pore space of sediments. Connate water is a special type of formation water that is trapped in the sediment at the time of formation (Sheppard, 1986a) and therefore if no exchange reactions have taken place the isotopic composition of connate waters should be equal to that of seawater. Formation waters from sedimentary basins can be sampled in boreholes and are found to vary both in isotopic composition and salinity. In each basin the $\delta^{18}O$ and δD show a broad positive correlation (fig. 2.19). Regression lines to the data have lower slopes than the MWL. The most $\delta^{18}O$ and δD depleted waters plot near to the MWL and in general both the salinity and temperature of the waters tend to increase with increasing content of heavy isotopes. Because the δD value of the low salinity fluids for each basin appears to correlate with latitude Clayton *et al.* (1966) argued that the formation waters are dominantly of meteoric water origin, although a diagenetically modified seawater could also be present. The positive shift in $\delta^{18}O$ values in hotter, more saline waters is usually explained by exchange of the the water with ^{18}O rich sedimentary materials. The δD increase is less well understood.

Fig. 2.20 (next page). Estimated $\delta^{18}O$ and δD of surface waters for the Connemara massif from 500 Ma to the present. The blocks marked S are the times when the Connemara massif is thought to have been inundated by marine water. The numbers to the right of these blocks are the maximum and minimum $\delta^{34}S$ values for seawater sulphate during these times according to Claypool *et al.* (1980). The information used, and the assumptions made in the construction of this diagram are summarised in the appendix (A.6).

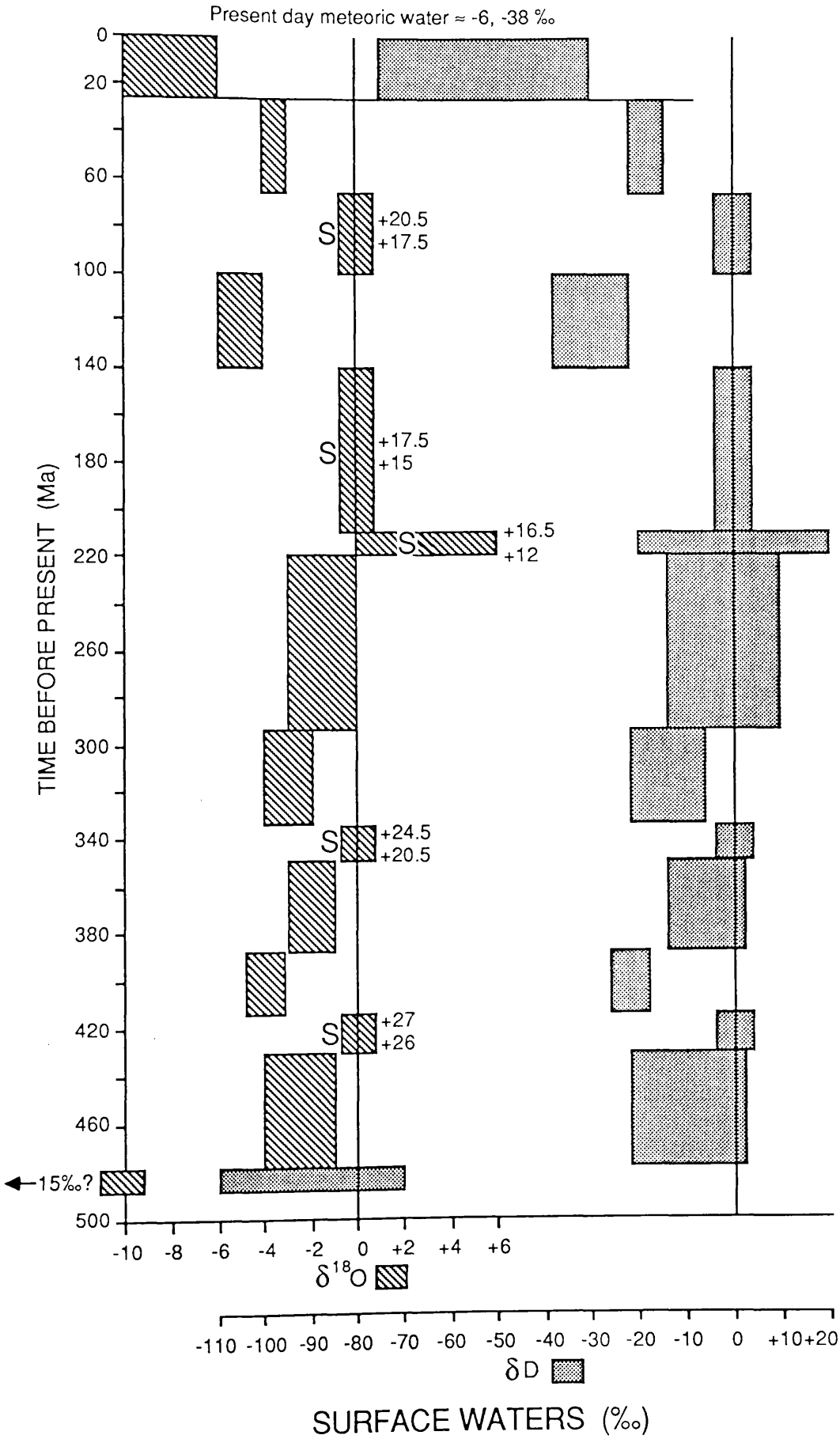
Present day meteoric water ≈ -6, -38 ‰
TIME BEFORE PRESENT (Ma)
0
20
60
100
140
180
220
260
300
340
380
420
460
500
S
+20.5
+17.5
S
+17.5
+15
S
+16.5
+12
S
+24.5
+20.5
S
+27
+26
←15‰?
-10 -8 -6 -4 -2 0 +2 +4 +6
δ18O
-110 -100 -90 -80 -70 -60 -50 -40 -30 -20 -10 0 +10+20
δD
SURFACE WATERS (‰)

Magmatic fluids.

Magmatic water is defined as the water that is in equilibrium with igneous rocks or magma at high temperatures. The H- and O- isotope compositions of magmatic waters are calculated from the compositions of fresh igneous minerals and the mineral - H_2O fractionation factors at high temperature (700-1200°C). Using normal values for igneous rocks of $\delta D \approx -50$ to -95‰ and $\delta^{18}O \approx +5.5$ to +10‰ (see 2.7.3) magmatic waters are calculated to have compositions in the range $\delta D \approx -40$ to -80‰ and $\delta^{18}O \approx +5.5$ to +9.5‰.

Under certain circumstances the composition of magmatic water could differ from this range e.g. in high $\delta^{18}O$ rocks or magmas that have undergone devolatilisation.

Metamorphic fluids.

The isotopic compositions of metamorphic fluids are usually calculated from the isotopic composition of the rocks at the temperature of interest. Application of fractionation factors to a range of meta-sedimentary and meta-igneous rocks at metamorphic temperatures yields a wide range of possible compositions of metamorphic waters from $\delta D \approx 0$ to -70‰ and $\delta^{18}O \approx +3$ to +20‰. This field also includes the high δD fluids that could result from dehydration of oceanic crust (Sheppard, 1986a). Obviously this range is large because of the wide variety of rocks used, a "local" metamorphic fluid with a more restricted range can usually be defined in most situations. The partial overlap between formation waters and metamorphic waters is to be expected, since there is really a continuum between diagenesis and low grade metamorphism.

An interesting type of metamorphic (?) fluid which has only been recently identified (Frape *et al.*, 1984) is represented by the groundwater which is present within the crystalline rocks of the Canadian Shield. On a $\delta^{18}O$ vs. δD plot the compositions of the more saline groundwaters are extremely unusual in that they plot above and to the left of the MWL (fig. 2.19). The origin of these groundwaters is not clear, although Frape *et al.* (*ibid.*) suggest that very low temperature equilibration with host rock minerals may be controlling the oxygen isotope composition of the brines. Fluids which plot above the MWL are very rare. Another situation where they have been identified is in the pore space of submarine basalts, where the stable isotope composition appears to be controlled by very low temperature hydration reactions with seawater in a rock dominated system (Lawrence and Gieskes, 1981).

The magmatic and metamorphic water fields are useful for reference when discussing the variation in isotopic composition of a sequence of very different rock types. Calculation of equilibrium water compositions can effectively "normalise out" isotopic differences in rocks due to temperature or chemical compositional differences.

Hydrothermal fluids.

These are hot aqueous fluids of any origin (Sheppard, 1986a). Hydrothermal fluids developed by the infiltration of seawater or meteoric water into hot

rocks (seawater- and meteoric-hydrothermal fluids) commonly have nearly the same δD value as the original fluid, but exhibit a large positive shift in $\delta^{18}O$. This feature is generally attributed to oxygen exchange with the enclosing rocks in a rock dominated system. The magnitude of the shift is usually found to increase with an increase in temperature of the fluid, because the mineral-water fractionation factors decrease with increasing temperature and also because the rate of oxygen isotope exchange increases with temperature. Fluid salinities also tend to increase with temperature. The lack of any appreciable shift in the δD of the water is because the system is water dominated for hydrogen (2.7.2).

Loss of the light isotopes by high temperature evaporation or boiling of hydrothermal fluid near to the surface results in a increase in the $\delta^{18}O$ and δD of the fluid (fig. 2.19). The slope of the evaporation trajectory is strongly dependent on the mechanism of vapour separation (Truesdell *et al.*, 1977) but is always less than that of the meteoric water line and usually between 2 and 5.

Hydrothermal fluids as defined above can also be igneous or metamorphic fluids.

Organic fluids.

Organic fluids have recently been defined as a fluid whose D/H ratio is derived by a reaction involving organic matter (Sheppard and Charef, 1986). The hydrogen isotope composition of organic fluids may range from -90 to -250‰. The oxygen isotope composition is probably controlled by equilibration with the local reservoir rocks.

Exotic fluids.

These are defined by Sheppard (1986a) as being any fluid that is foreign to the system or introduced from another environment. Thus hydrothermal fluids derived from surface waters (ocean or meteoric waters) are exotic. In the study of some systems it can be demonstrated that a fluid is not native to the system, although its ultimate origin cannot be identified and it is therefore termed exotic.

2.9.2 The hydrogen isotope composition of igneous rocks

Igneous rocks at the earth's surface.

Taylor and Sheppard (1986) note that the majority of igneous rocks at the earth's surface have δD values between -50 and -95‰. Rocks with values outside this range generally require some unusual process to have operated during their formation or subsequent history.

Commonly rocks with lower δD values have undergone subsolidus interaction with very low δD meteoric fluids (e.g. granites in the British Tertiary Volcanic Province; Taylor, 1977; Forester and Taylor, 1976 or the Skaergaard intrusion; Taylor and Forester, 1979) or assimilated country rock altered by low δD meteoric water (e.g. the Seychelles batholith; Taylor 1977).

Low δD rocks can also be the result of loss of a D-rich fluid by degassing of a water saturated magma (B.E.Taylor, 1986). This results in a residual magma which is both D and H_2O depleted (Nabelek *et al.*, 1983).

Arfedsonites from alkalic rocks in the Precambrian Ilimaussaq intrusion of Greenland are amongst the most D depleted minerals recorded (Sheppard, 1986b) with δD ranging from -172 to -207‰. This extreme D depletion cannot be attributed either to degassing or to interaction with low δD meteoric waters, however Sheppard (*ibid.*) suggests that organic-rich sediments in the source region may have been the cause.

Rocks with δD > -50‰ can result from interaction with high δD fluids, such as seawater or high δD meteoric fluids. Oceanic crust which has been subjected to hydrothermal alteration by seawater at mid-ocean ridges shows such high δD alteration (Stakes and O'Neil, 1982; Heaton and Sheppard, 1977) although examples of granitic rocks which have been altered by high δD fluids are conspicuously absent from the literature.

Deuteric alteration of a rock by a high δD fluid produced by exsolution from a water saturated melt may locally produce high δD alteration (Nabelek *et al.*, 1983; Brigham and O'Neil, 1985) although complementary areas of D depleted rock should also be present in such situations.

Examples also occur of igneous rocks which exhibit high δD values which are not easily attributed to subsolidus alteration. Sheppard and Harris (1985) suggest that high δD granites on Ascension Island were formed by infiltration of seawater or meteoric water directly into a subvolcanic complex. Wickham and Taylor (1985) have suggested that high δD granites (δD muscovite ≈ -30‰) of the Trois Seigneurs Massif in the Pyrenees were generated by melting of sedimentary material that was being fluxed by seawater. This interpretation of the data is not unequivocal and Sheppard (1986b) has suggested that an underlying thrust zone could be an alternative source for the high δD fluids.

The best examples of igneous rocks which appear to have inherited anomalously high δD signatures from their source include back-arc basalts from the Lau Basin and Mariana Trough (δD = -32 to -46‰; Poreda, 1985), amphibole bearing cumulate nodules in calc-alkali volcanics in Grenada (-26 to -37‰; Graham *et al.*, 1982) and amphibole bearing xenoliths in volcanic rocks from NE Japan (-23 to -36‰; Kuroda *et al.*, 1977). An explanation of the origin of these high δD values is connected with the wider discussion of the δD of the mantle and is given in the next section.

The hydrogen isotope composition of the mantle.

Large scale heterogeneity of the mantle has been demonstrated by a number of trace element and radiogenic element studies (Zindler *et al.*, 1984; Allegre *et al.*, 1983; White and Patchett, 1984) and on the basis of these studies Kyser (1986) suggests that at least three major reservoirs exist in the mantle:

a. an undepleted or undegassed reservoir that is the nearest to primordial of the reservoirs.

b. a relatively depleted portion such as that which is sampled by MORB.

c. a reservoir, usually occurring underneath continents, which has been influenced by subducted material.

The hydrogen isotope composition of MORB has been well characterised e.g. δD = -71 to -84‰ and ≈ 0.2 wt.% H_2O (Craig and Lupton, 1976), $\delta D \approx$ -80‰, 0.15 wt.% H_2O (Kyser and O'Neil, 1984) or δD = -71 to -91‰, 0.11 to 0.25 wt.% H_2O (Poreda *et al.*, 1986). Such values are probably characteristic of the source.

Phlogopites from kimberlites and xenoliths within kimberlites have δD values of -58 to -79‰, while three amphiboles from mafic and ultramafic nodules in alkali basalts have a restricted range of δD (-49 to -54‰; Boettcher and O'Neil, 1980). Amphibole megacrysts from alkali basalts sampled by Boettcher and O'Neil show a much wider variation in δD (-113 to +8‰) but the extreme values can probably be attributed to dehydration and oxidation during and after ascent and eruption (Graham and Harmon, 1983). These phlogopites and amphiboles are believed to result from a mantle metasomatism process involving a migrating hydrous fluid (e.g. Boettcher and O'Neil, 1980). The stable isotope composition of these minerals is therefore imaging the source of these fluids, which might be either a. the underlying slowly degassing mantle or b. an exotic source, possibly a subduction zone. The broad agreement of these values (-49 to -79‰) with those given by Poreda *et al.* (1986) for ocean ridge basalts (-61 to -74‰) from the Kolbeinsey and Reykjanes ridges which are believed to be samples of an enriched (undegassed?) plume source centred on Iceland suggests that they may be imaging a relatively primordial mantle source. Minor depletion of such a source ≈ -70‰ to produce slightly more depleted MORB ≈ -80‰ could be envisaged. It is not possible however to rule out the involvement of subduction derived fluid in these metasomatic fluids.

The anomalously high δD values of back arc basalts from the Lau Basin and Mariana Trough (-32 to -46‰) and from nodules in calc-alkali volcanic rocks in Granada and Japan (-23 to -37‰) referred to above are distinctly different from the values apparently obtained from a MORB source or an undepleted source. These high δD values can most easily be attributed to the influence of high δD fluids from nearby subduction zones (Poreda, 1985; Graham and Harmon, 1983). The recent calibration of the hydrogen isotope fractionation between chlorite and water (Graham *et al.*, 1987) implies that chlorite in oceanic crust which has been hydrothermally altered by seawater may have $\delta D \approx$ -30 to -40‰. Since chlorite is expected to contain a large proportion of the hydrogen in subducting ocean crust this means that a dehydrating slab will probably be producing fluid with a $\delta D \approx$ -30 to -40‰, supporting the hypothesis.

To summarise therefore it appears that the three major mantle reservoirs identified by Kyser (1986) can be tentatively assigned δD values of ≈ -70‰

for the undepleted reservoir, ≈ -80‰ for the depleted MORB source and ≈ -30‰ for mantle overlying subduction zones.

2.9.3. The oxygen isotope composition of igneous rocks.

Igneous rocks at the earth's surface.

The large majority of igneous rocks at the earth's surface have a restricted range of $\delta^{18}O$ from +5.5 to +11.0‰. As is the case with hydrogen isotope variations, rocks with values outside this range require a special process during their formation or subsequent history.

Rocks with lower $\delta^{18}O$ values are invariably the result of subsolidus interaction with low $\delta^{18}O$ meteoric fluids and are usually easily identified because they also exhibit low δD values. However at low latitudes it may be possible to have meteoric fluids with δD values similar to, or higher than, those of normal igneous rocks (fig. 2.19). Such fluids will still have lower $\delta^{18}O$ values than normal igneous rocks, so that interaction of these waters with a normal igneous rock could result in a rock with normal δD values, but ^{18}O depletions.

Variations in $\delta^{18}O$ values of igneous melts by degassing, as described above for hydrogen isotopes, are unlikely, because the rock will always be the major reservoir of oxygen and will therefore be resistant to changes in $\delta^{18}O$.

Oxygen isotope mineral-fluid fractionation factors at high temperatures are small ($\Delta_{MINERAL-FLUID}$ ≈ +1 to +2‰) so that high temperature alteration of ocean crust (average MORB = +5.7‰) by seawater should result in low $\delta^{18}O$ rocks. and this is indeed found to be the case in both dredged samples from mid ocean ridges (Stakes and O'Neil, 1982; Muehlenbachs and Clayton, 1972) and ophiolites (Heaton and Sheppard, 1978; Gregory and Taylor, 1981).

Certain rocks have low $\delta^{18}O$ values which cannot be attributed to subsolidus alteration and must have been intruded as low $\delta^{18}O$ magmas, for example the Seychelles granite pluton (Taylor, 1977). Taylor and Sheppard (1986) suggest that the most likely mechanisms for the production of such low ^{18}O magmas are

a. Oxygen isotope exchange between a normal ^{18}O magma and country rocks that had previously been hydrothermally altered and depleted in ^{18}O.

b. Assimilation or partial fusion of hydrothermally altered ^{18}O depleted country rocks by the magma.

c. Direct influx of low $\delta^{18}O$ water into the magma.

High $\delta^{18}O$ (+11 to +14‰) granites have now been recognised in a number of areas (S.E. Australia, O'Neil *et al.*, 1977; the Himalayas, Debon *et al.*, 1986;

the Variscan Province, Sheppard, 1986b; and the Caledonides, Harmon, 1984). The common factor which is causing these high $\delta^{18}O$ values appears to be the partial melting and assimilation of varying amounts of high $\delta^{18}O$ material.

The oxygen isotope composition of the mantle.

From theory it might be expected that oxygen isotope fractionations at mantle temperatures might be small and therefore that MORB and more primordial mantle sources should have similar oxygen isotope compositions. However Muehlenbachs and Kushiro (1974) measured an apparent reversal in the oxygen isotope fractionation between basalt melt and orthopyroxene at 1275°C, with Δ = -0.5‰ at 1500°C, and Kyser *et al.* (1981) have suggested that olivine becomes substantially (1-2‰?) more ^{18}O-rich than basaltic liquid above 1200°C (however see Gregory and Taylor, 1986 for an alternative point of view). Thus melting events in the mantle above 1200°C should produce ^{18}O depleted melts and ^{18}O enriched residues. Fresh MORB samples show a very restricted range of $\delta^{18}O$ values of 5.7 ±0.3‰ and Kyser (1986) reasons that undepleted mantle should have lower $\delta^{18}O$ values if MORB is a residuum from initial melting. Kyser suggests that some low $\delta^{18}O$ (5.2-6‰) continental basalts and xenoliths from Hawaii may originate from this mantle reservoir. According to Kyser higher $\delta^{18}O$ values (6-7‰) in some continental xenoliths, andesites and boninites could represent either

a. A refractory ^{18}O-rich residuum from previous partial melting which has been metasomatised to enable melting to take place.

   or

b. Mantle which has been enriched in ^{18}O either by addition of subducted high ^{18}O material or high ^{18}O fluid from a subducting slab.

In summary therefore it appears that the mantle is heterogeneous in $\delta^{18}O$, ranging from ~ +5 to +7‰. Although the specific reasons for these variations are not yet entirely clear, it is suggested that metasomatised subcontinental mantle could be at the high end of this range, while primordial mantle may be near the lower end, with the MORB source in between.

2.9.4. The hydrogen and oxygen isotope composition of sedimentary rocks.

The hydrogen isotope composition of most sedimentary rocks falls in the relatively restricted range of ≈ -40 to -85‰ (Taylor, 1977) as a result of the hydrogen isotope equilibration of clay minerals with low temperature surface waters.

Sedimentary rocks show an extremely wide range of oxygen isotope compositions. Carbonates and silica minerals deposited in equilibrium with seawater or very low temperature diagenetic fluids have extremely high $\delta^{18}O$ values (+25 to +35‰) because their composition is controlled by very low temperature mineral-water fractionations in a fluid dominated system.

Similarly shales and mudstones have high values (+13 to +20‰) because of their content of clay minerals which generally form in low temperature equilibrium with meteoric water or seawater. The composition of detrital quartz present in sedimentary will reflect the isotopic composition of the original source (≈ +14 to +8 or less for igneous and metamorphic rocks) because of its resistance to low temperature exchange. Thus sandstones will tend to have lower $\delta^{18}O$ values than other sediments.

2.9.5. The hydrogen and oxygen isotope composition of metamorphic rocks.

In general, it is expected that the isotopic composition of metamorphic rocks should reflect the composition of their precursors. This is often found to be the case, for example marbles often show $\delta^{18}O$ values of +20 to +25‰, similar to unmetamorphosed limestones and metagabbros may preserve original values of ≈ +6‰. However two processes; devolatilisation and fluid infiltration are known to alter the composition of rocks during metamorphism.

Prograde metamorphism of rocks frequently involves the liberation of "volatile" elements which are produced by the breakdown of low temperature minerals. This effect is pronounced in metasediments which often have a high concentration of volatiles. Devolatilisation generally involves dehydration (loss of water) but decarbonation and desulphidation can also be important.

The effects of devolatilisation on the isotopic composition of metamorphic rocks can be modeled by one of two end member processes:

a. Batch Volatilisation. This is a closed system process in which all the evolved fluid equilibrates with the rock at one time. The effect that this will have on the isotopic composition of the rock can be calculated from simple mass balance constraints. However volatilisation reactions produce large volumes of fluid which must necessarily be almost immediately expelled from the rock, since the porosity of most metamorphic rocks is negligible. Therefore true batch volatilisation is unlikely although it can give a reasonable approximation to the observed effects in some rocks (Valley, 1986).

b. Rayleigh volatilisation. This is an open system process in which infinitely small increments of fluid are evolved, each of which equilibrates with the rock prior to removal and the production of the next increment. The isotopic shift in a rock due to Rayleigh volatilisation is given by:

$$\delta_{Rf} - \delta_{Ri} = 1000\,(X^{(\alpha - 1)} - 1) \qquad (2.37)$$

(Broecker and Oversby, 1971), where X is the mole fraction of the element of interest that remains in the rock after volatilisation. Rayleigh fractionation may closely approximate the isotopic effects of dehydration and decarbonation (Valley, 1986).

Valley (1986) suggests that the effect of dehydration reactions on the $\delta^{18}O$ value of a rock will always be small (« 1‰), however larger negative shifts

of 3 to 6‰ can occur in a decarbonating calc-silicate mixture. Valley (*ibid.*) suggests that the effect of Rayleigh fractionation on the hydrogen isotope composition of a dehydrating rock may be much larger, possibly depleting the rock by a few tens of permil.

2.9.6. The carbon isotope composition of terrestrial reservoirs.

Atmospheres and oceans.

The $\delta^{13}C$ value of CO_2 in the atmosphere is about -7‰. Dissolved carbonate (mostly as HCO_3^-) in the oceans has $\delta^{13}C$ values near 0‰. Taking into account the small quantities of other carbonate species present this value appears to represent an equilibrium fractionation with atmospheric CO_2, using the fractionation factors of Emrich *et al.* (1970) or Deines *et al.* (1974).

Limestones.

Modern marine limestones have a restricted range of $\delta^{13}C$ from -1 to +2‰ (Ohmoto, 1986) with an average of +1‰, suggesting that they are in isotopic equilibrium with the dissolved carbonate in the oceans. The average $\delta^{13}C$ value of marine limestones shows secular variations during the Phanerozoic, between -1 and +2‰ (Veizer *et al.*, 1980). These variations are probably a result of fluctuations in the global $C_{carbonate}/C_{organic}$ ratio.

Freshwater limestones tend to have rather lower $\delta^{13}C$ values than marine limestones because of a larger content of low $\delta^{13}C$ organic carbon.

Fluids passing through limestones will become saturated in dissolved carbonate. Ohmoto (1986) suggests that under most geological conditions the $\delta^{13}C$ values of the fluid will differ by only a few permil from that of the limestone.

Marbles.

Theoretically decarbonation reactions can produce strong depletions in ^{13}C during the prograde metamorphism of limestones, especially if it follows a Rayleigh fractionation process. However Valley (1986) shows that most limestones from contact metamorphic aureoles show ^{13}C depletions towards values of ~ -4 to -7‰ which are more consistent with the infiltration of magmatic like fluids than with decarbonation reactions. Alteration of the original $\delta^{13}C$ composition of limestones in regional metamorphism may take place by decarbonation and/or infiltration, or by re-equilibration with low $\delta^{13}C$ organic material at high temperatures (Valley and O'Neil, 1981).

Organic matter.

Organic carbon has $\delta^{13}C$ values of -10 to -30‰ with an average near to -22‰. These low values are the result of large kinetic isotope effects which occur during photosynthesis. Thermal decomposition of organic matter can produce CO_2, CH_4, higher hydrocarbons and residual kerogen. The CO_2 may be very similar in isotopic composition to the parent material (Ohmoto and

Rye, 1979), but the CH_4 may have very depleted $\delta^{13}C$ compositions typically -55 to -35‰, thus leaving a ^{13}C rich residue ~ -25 to -10‰ which may be present in high grade metasediments (Ohmoto, 1986).

The mantle.

The $\delta^{13}C$ values of diamonds from kimberlites show a very wide range from -35 to +5‰, but the vast majority cluster in a much smaller range of -5±2 (Deines, 1980). Carbonates from carbonatites and kimberlites also show a wide range in $\delta^{13}C$ but average values are similar at -5.1±1.4‰ and -4.7±1.2‰ respectively (Deines and Gold, 1973). Similarly the mantle sampled by MORB and OIB appears to have values near to -5‰ (Kyser, 1986). The average composition of crustal carbon appears to be ≈ -7‰ (Fuex and Baker, 1973), if mantle degassing is the sole source of crustal carbon this will also be the average $\delta^{13}C$ value of the mantle. From this broad agreement of estimates of mantle composition from a number of different rocks, it seems likely that most of the mantle has such a composition, although large local heterogenies may well exist.

Igneous rocks at the earth's surface.

Fuex and Baker (1973) showed that carbon in granitic, mafic and ultramafic rocks is present in two forms - as carbonate which is fairly abundant (0-0.76% in granites, 53 ppm-2% in mafic/ultramafic rocks) and in a non-carbonate form which is less abundant (32-360 ppm in granites and 26-150 ppm in mafic/ultramafic rocks). The carbonate carbon in all these rocks is relatively ^{13}C rich ≈ -7±2‰ (except a camptonite dyke which has values +1 to +3‰ and which may represent an unusual mantle source -my comment). Because of their similarity to average mantle compositions these values around -7‰ are most probably original igneous values, either of original carbonate or of oxidised graphite. The non-carbonate carbon has very depleted values of -20 to -27‰. Fuex and Baker (*ibid.*) attribute this composition to a mantle source, however comparison with more recent estimates of mantle $\delta^{13}C$ compositions (see above) suggests an alternative source is required. A similar form of carbon has been identified in basaltic glass and this has been attributed to sample contamination. B.E. Taylor (1986) suggests that contamination may be the source of the low $\delta^{13}C$ values in the rocks examined by Fuex and Baker (1973).

2.9.7 The sulphur isotope composition of seawater and local reservoirs.

The sulphur isotope composition of seawater.

Seawater contains about 10% of the sulphur in the crust and the hydrosphere (Ohmoto, 1986) and is therefore a very important reservoir of sulphur. Seawater contains ~900 ppm sulphur, which occurs almost exclusively as sulphate with a $\delta^{34}S$ of +20‰. The sulphur isotope composition of seawater has been shown to undergo global fluctuations between extremes of +10 to +35‰ over the last 1000 Ma (Claypool *et al.*, 1980). The $\delta^{34}S$ values of seawater during the periods in which the Connemara massif was submarine are shown in fig. 2.20.

The sulphur isotope compositions of local reservoirs.

Sulphur isotope data already exists which allows relatively precise definition of the $\delta^{34}S$ of most rock units in Connemara, so that all the possible variations in crustal reservoirs are not described here.

Dalradian metasediments.

The sulphur isotope composition of seawater sulphate during the Middle Dalradian when most of the Connemara metasediments were deposited is very high, typically +28 to +31‰ (Claypool *et al.*, 1980), or even as high as +35 (Hall *et al.*, 1988). Sulphides now present in these metasediments probably formed from this sulphate by bacteriogenic reduction. According to Ohmoto (1986) observed (not equilibrium) fractionations between sulphate and bacteriogenic sulphides typically range from 15 to 60‰, with an average of 40‰. Hall *et al.* (1988) suggest that the fractionation might have been near to the bottom of this range (15 to 25‰) during bacteriogenic reduction of sulphate in the nearly stratigraphically equivalent Easdale Slate Fm. of the Middle Dalradian of Argyll.

Sulphide formation by this mechanism would result in relatively heavy (+10 to +20) $\delta^{34}S$ values for the pre-metamorphic sulphide present in the Connemara Dalradian. Furthermore Hall *et al.* (1988) also showed that greenschist grade metamorphic pyrite could inherit its sulphur isotope composition from its diagenetic pyrite precursor. Alternatively if desulphidation (e.g. Ferry, 1981) takes place during the higher grade metamorphism in Connemara this would tend to increase the $\delta^{34}S$ value of the residual sulphide still further, so that in either case it is likely that the Connemara schists possess sulphide with very heavy $\delta^{34}S$ values. This proposal is supported by the high $\delta^{34}S$ values of primary sulphides from the Cashel microgranite sill (+9.61) and the Oughterard granite (+6.2 to +16.0‰) analysed by Laouar (1987), since both granites are believed to contain a large contribution of local (Dalradian) metasedimentary material on the basis of their high initial Sr ratios.

Metagabbro suite.

Meteorites have a remarkably uniform sulphur isotopic composition of $\delta^{34}S = 0.2 \pm 0.2$‰ (Thode *et al.*, 1961) and that it is usually assumed that uncontaminated mantle material has similar values. Ohmoto (1986) suggests that it is unlikely that the $\delta^{34}S$ value of mantle rocks extends outside the range of -3 to +2‰, although local heterogenies are known to occur (Chaussidon *et al.*, 1987). Fractionation of S isotopes at mantle melting temperatures is likely to be less than 0.5‰ (Ohmoto and Rye, 1979) so that mantle derived melts should have a similar range of composition to the mantle.

No sulphur isotope data exists for the metagabbro suite; however it is suggested that the $\delta^{34}S$ values will vary between uncontaminated mantle values and and the composition of material which has been assimilated by this magma. The ultrabasic parts of the MGS have assimilated material at the present level of exposure (Leake, 1958; Jagger, 1985) and Jagger (*ibid.*) suggests that the radiogenic isotope compositions of all rocks in the suite

may also record crustal assimilation at a deeper level. Assimilation of metasedimentary material at the present level would result in $\delta^{34}S$ values between the compositions of the end members (mantle and local metasediments) the exact values depending on mass balance constraints. Jagger (*ibid.*) suggests that any deeper crustal contaminant may be represented by a Lewisian amphibolite like lithology. Both Archaean gneisses and sediments are expected to have $\delta^{34}S$ values near to 0‰ (Monster *et al.* 1979), so that contamination by these rock types should affect the sulphur isotope composition of a mantle derived magma very little.

Caledonian granitoids.

As noted previously those granites which contain a large sedimentary component (the Oughterard granite and the Cashel microgranite sill) have enriched $\delta^{34}S$ values. Sulphides in the other (more voluminous) granites analysed by Laouar (1987), the Galway, Roundstone and Inish granites have a limited range of $\delta^{34}S$ from +0.6 to +4.2‰ consistent with a dominantly igneous source for these granites.

2.10 SUMMARY.

The principles which govern the variation of stable isotope ratios in terrestrial rocks have been presented in this chapter. The important points are summarised below.

1. Equilibrium isotope fractionation between different phases is the major factor controlling the variations in the ratios of the stable isotopes of O and H in high temperature processes. Variations in C and S stable isotope ratios commonly result from redox reactions.

2. The equilibrium fractionation between phases (α) is strongly dependent on temperature. The pressure dependence of oxygen isotope fractionation is negligible, but hydrogen isotope fractionation may be weakly pressure dependent. The value of α may also be dependent on phase composition.

3. A critical evaluation of the errors associated with calculated equilibrium isotopic temperatures shows that even if it is assumed that isotopic equilibrium between phases has been preserved, the errors on the temperature estimates may be so large that the temperature estimate may be of little value.

4. It is now widely recognised that many rocks contain mineral assemblages which are out of stable isotope equilibrium. The stable isotope compositions of such rocks can only be meaningfully interpreted if the kinetics of stable isotope exchange are understood. In mineral-fluid systems stable isotope exchange can occur by one or more of three mechanisms, namely diffusion, recrystallisation and chemical reaction. In all of these mechanisms the same factors (temperature, pressure, grain size, grain shape, grain/solution chemistry and solution to solid ratio) are important in controlling the rate of exchange. Temperature is the most important factor since the exchange rate is found to be

exponentially dependent on temperature. Pressure appears to have only a minor indirect effect on exchange rates, although it may become a more important factor in controlling diffusion at very low pressures. In general both increasing grain size and solution to solid ratio act to decrease stable isotope exchange rates.

5. The isotopic variations which result from fluid-rock interaction are shown to be dependent on both mass balance and kinetic effects, as well as the nature of the fluid flow. Predictions of the isotopic effects of fluid infiltration are difficult because the results are strongly model dependent. Different stable isotopes are shown to behave very differently in the same system as a result of their different abundances in rocks and geological fluids.

6. Because C and S can occur as a number of species in geological fluids the estimation of the isotopic composition of the fluid in equilibrium with C and S bearing minerals requires a knowledge of the speciation of these elements in the fluids. However it is shown that simplifying approximations can be made under certain conditions.

7. The O, H, C and S stable isotopic compositions of many terrestrial reservoirs are found to be distinctive. As a result of this stable isotope ratios are of great value when examining the interactions between different reservoirs.

CHAPTER 3.

THE CASHEL - RECESS STUDY AREA - PART 1

THE DALRADIAN SEQUENCE.

3.1 INTRODUCTION.

In chapter 1. it was shown that the rocks within the Dalradian sequence contain a variety of hydrous minerals. Some of these minerals such as the biotite and cordierite in the metasediments or the hornblendes in the amphibolites were obviously formed during prograde or peak metamorphism. Other minerals such as the chlorite replacing biotite, or the pinite replacing cordierite, must have been formed at a later time. From chemical data for the metasediments it would appear that during intrusion of the MGS, partial melts were formed and extracted from the aureoles surrounding the MGS intrusions (1.4.1). Thus it can be seen that hydrous fluids (including partial melt) have been present within the Dalradian sequence at different times. Since fluids possess the property of being able to flow quite rapidly under a pressure gradient, it is possible that these fluids present in the Dalradian sequence could have flowed across the boundary with the MGS, either before, or after they were present in the Dalradian. Thus the stable isotope data for either of these rock units cannot be viewed in isolation and a knowledge of the stable isotope composition of the fluids that were present in the other unit is necessary for a full interpretation of the data.

With this point in mind the purpose of this chapter is to examine the stable isotope data for the Dalradian sequence in order to estimate the stable isotope ratios of the fluids present at different times. This may allow the origins of these fluids to be constrained and provide the necessary background to chapter 4., in which the stable isotope data for the MGS rocks in this area are presented. The origins of the fluids in the Cashel-Recess area are discussed further in chapter 4., in the light of the data from the MGS.

3.2 OXYGEN ISOTOPE DATA.

3.2.1 Description of data.

All the oxygen isotope data for the Dalradian rocks in this study area are presented in fig 3.1. Also shown in this diagram are some additional whole rock data for the igneous and metasedimentary rocks near to the contact of the Cashel body, determined by Jagger (1985). It can be seen that although the whole rock samples are highly variable in isotopic composition the lowest values (~+7‰) occur in some of the ultrabasic rocks at the margin of the Cashel body, while the highest values (+9 to +11) occur in the migmatised sediments nearly 1 km from the Cashel body. These metasediments lie just within the hornfelsed zone of Ahmed-Said (1988), but since they still contain leucosome material it is probable that the whole rock composition has not been markedly changed by loss of partial melt material. The hornfelsed metasediments just adjacent to the contact have

lower $\delta^{18}O$ values (~+8.8‰) than the migmatised sediments away from the contact but have similar values to some of the more ^{18}O rich contaminated ultrabasic rocks, and also the psammite screen within the Cashel body. The highest whole rock $\delta^{18}O$ is found within the microcline granite sill lying to the north of the Cashel body. The $\delta^{18}O$ values of quartz separates are everywhere higher than the whole rock value for the host rock (by 2.5-5.5‰) except for the vein quartz from within the microcline granite sill. The two hornblende separates from amphibolites in the Lakes Marble Formation have remarkably similar $\delta^{18}O$ values (~7.6‰). The distance of sample GJ.130 from the MGS rocks is not known exactly because it is separated from the Cashel body by a major fault. According to Leake (1970a) this amphibolite is structurally below the continuation of the Cashel body.

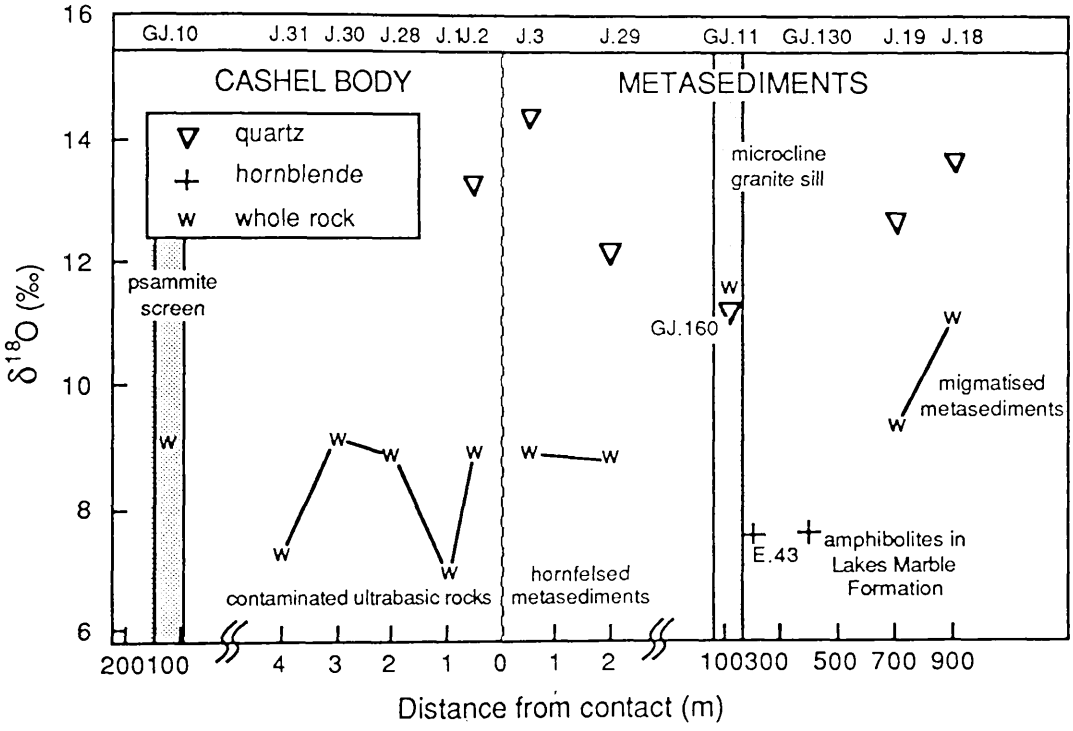

Fig. 3.1 Oxygen isotope data for the Dalradian rocks plotted against distance from the contact with the Cashel metagabbro body. The whole rock data for ultrabasic rocks and hornfelses within 2 m of the contact is from Jagger (1985). N.B. note the non-linear horizontal scale of this diagram!

3.2.2 Oxygen isotope composition of equilibrium fluids.

The limits of the $\delta^{18}O$ value of the fluid which would be in equilibrium with the quartz in the metasediments and the hornblendes in the amphibolites are shown as a function of temperature in fig. 3.2. If it assumed that diffusion is the dominant isotope exchange mechanism in these minerals then some idea of the temperature down to which continued equilibration of these minerals with the surrounding fluid could take place, can be gained by reference to fig. 2.12. From this diagram it would seem unlikely that the quartz in these rocks, which is generally fairly coarse (0.5-1 mm) will undergo appreciable exchange by diffusion with the surrounding fluid at temperatures below about 500° C. Removal of small quartz grains (<180 μm diameter) during mineral separation will tend to

increase the likelihood that the quartz that was analysed last equilibrated with a fluid above 500° C. Thus the quartz in these rocks was probably last in equilibrium with a fluid with a $\delta^{18}O$ between +10 and +14‰. Although the hornblende in the amphibolites is much finer grained than the quartz (≈0.2-0.4 mm //c) the slower diffusion of oxygen in amphibole means that detectable equilibration of oxygen isotopes with the surrounding fluid below about 600°C is extremely unlikely. Thus from fig. 3.2 it might be suggested that the amphiboles last equilibrated with a fluid with a $\delta^{18}O$ of +9 to +10 prior to closure, although there is probably a large uncertainty on these figures because the Bottinga-Javoy amphibole-water fractionation is semi-empirical (no experimental calibrations exist). Thus it would appear that the $\delta^{18}O$ of the fluid present within the rocks when these minerals last equilibrated at high temperatures was variable, both between the amphibolites and metasediments and also within the metasediments themselves. Since samples J.029 and J.003 were collected only 1.5 m apart it can also be stated that the fluid must have been heterogeneous on this scale. Thus it can be suggested that there was no pervasive flow of fluid between different rocks at high temperatures, such as has been suggested to take place in the Pyrenees (Wickham and Taylor, 1985). The quartz and hornblende define apparent equilibration temperatures (the temperature at which the curves intersect on fig. 3.2) in the range of 480-330°C. This of course is meaningless, since it is known that the minerals were present at higher temperatures, and can be attributed to the minerals closing to oxygen diffusion at higher temperatures in equilibrium with fluids of different oxygen isotope compositions. Thus the apparent equilibrium at these low temperatures is a false equilibrium.

3.3 HYDROGEN ISOTOPE DATA.

3.3.1. Description of data.

The δD values of mineral separates from the Dalradian rocks in the Cashel-Recess district are summarised in fig. 3.3. The hornblendes have δD values within the range of the biotites, while the chlorites and muscovite have rather higher values. The hydrogen isotope compositions of the hornblende separates are measurably different by ~9‰, in contrast to their $\delta^{18}O$ values.

3.3.2 Hydrogen yields of "biotites" and "chlorites".

The hydrogen yields and inferred water contents of the biotites and chlorites from the Dalradian metasediments are plotted against δD in fig. 3.4 It can be seen that three of the "biotite" separates have water contents greater than would be expected if they were pure biotites, indicating that they must contain some proportion of a hydrous mineral with a water content greater than 7 wt.%. This is most probably chlorite because biotite is observed to be altering to chlorite in a number of samples. If it is assumed that chlorite is the only contaminant, then the contribution of chlorite to the total hydrogen released from the sample can be estimated (fig 3.4), indicating that

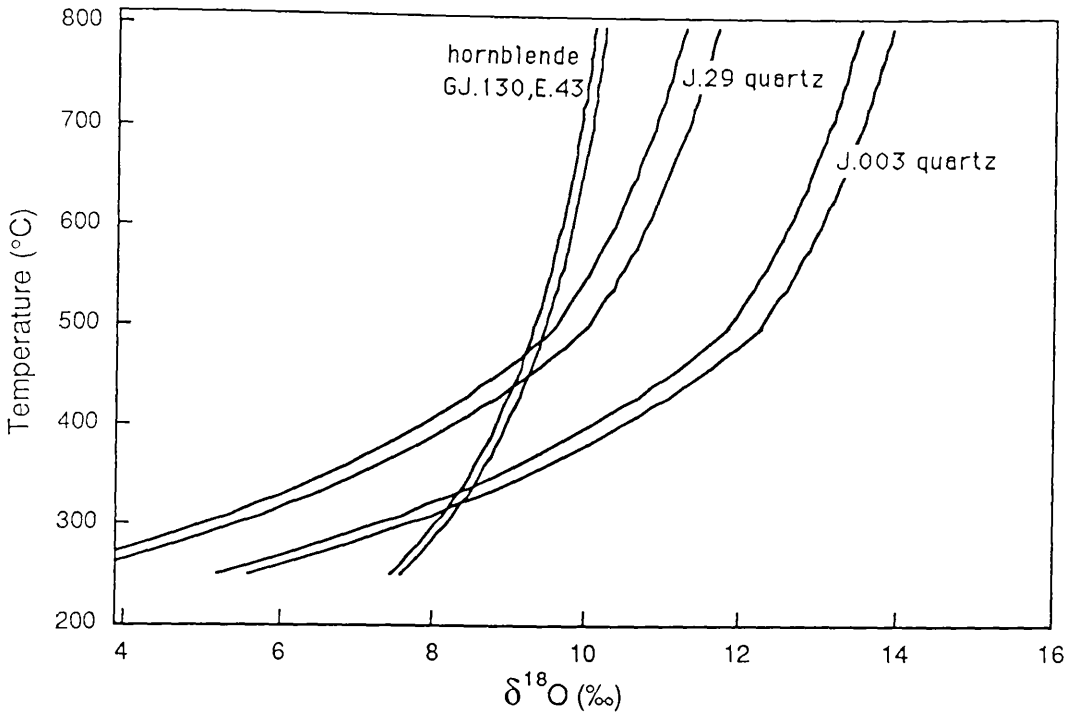

Fig. 3.2 $\delta^{18}O$ value of fluid in equilibrium with quartz within the metasediments (the two samples represent the extreme limits of $\delta^{18}O$ variation) and with hornblendes within amphibolites shown as a function of temperature. Each pair of curves corresponds to the upper and lower limits resulting from analytical uncertainty (1 σ_{n-1}). The fluids are presumed to have a fractionation behaviour similar to pure water. The quartz-water fractionation used is that of Matsuhisa *et al.* (1979), while the amphibole-water fractionation was calculated from the quartz-water equation of Bottinga and Javoy (1973) and the quartz-amphibole equation of Javoy (1977).

in the most altered sample up to 75% of the hydrogen released could have come from chlorite. However despite this, Ahmed-Said (1988) was able to obtain reasonable probe analyses of biotite on these separates, although the analyses are rather unbalanced and cannot be made to total 16 cation/22 (O), either because of low K, or high Si and Al. Examination of the separates with a binocular microscope did not show any chlorite to be present, and in thin section no visible replacement by chlorite was observed (Ahmed-Said, pers. comm.). The most altered sample (AY.50) however, is noticeably paler than the other biotite samples and contains many inclusions of rutile (?) needles, which are oriented at angles of 120° in basal sections.

The fact that chlorite or any other alteration product cannot be observed optically suggests that the partial alteration of the biotite has taken place on a very fine scale, possibly along individual layers in the biotite lattice (e.g. Veblen and Ferry, 1983).

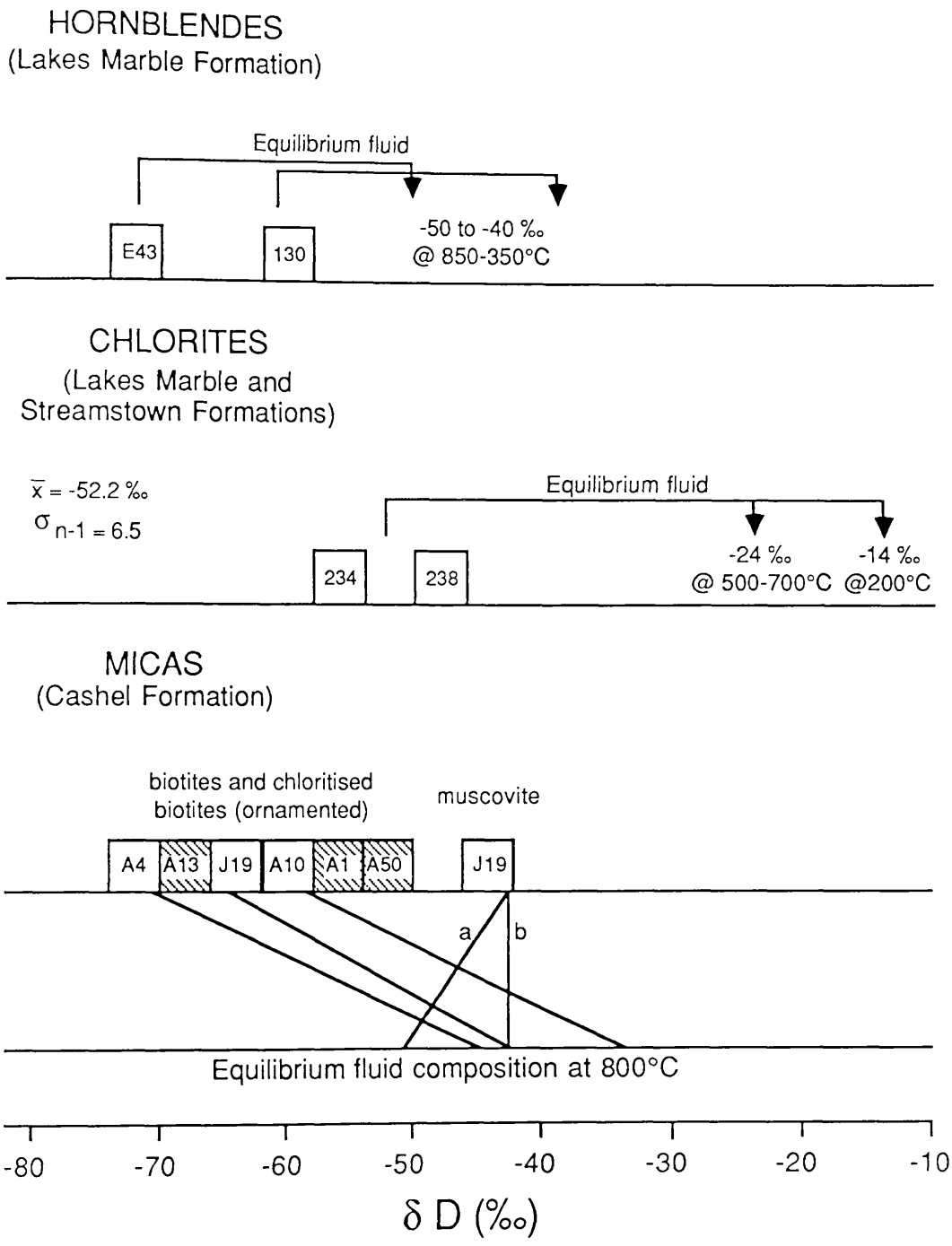

Fig. 3.3 Summary diagram of the δD values of mineral separates from the Dalradian rocks. Also shown are the equilibrium fluid compositions at various temperatures. See text and fig 3.5 for the source of the fractionation factors used. The lines labeled a. and b. indicate the δD of the fluid in equilibrium with a pure muscovite and a natural muscovite containing about 10% Fe, respectively.

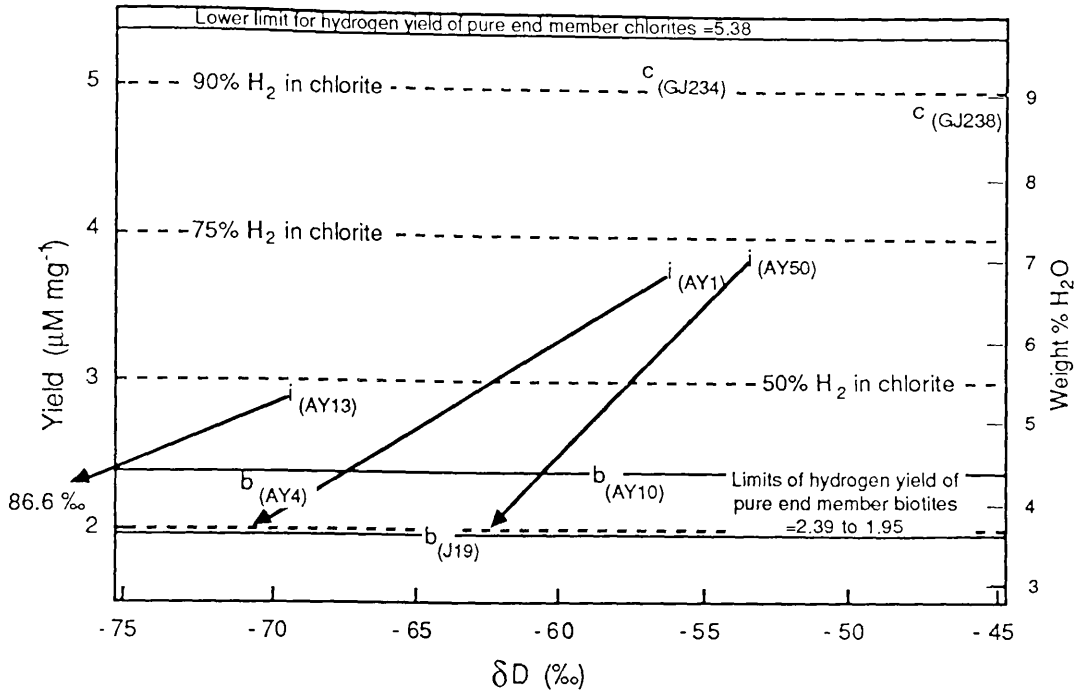

Fig. 3.4 Hydrogen isotope composition vs. hydrogen yield for "chlorites" and "biotites" from the Dalradian metasediments. b = fresh biotite, i = biotite which appears fresh but has high water content and c = chlorite which appears to contain only minor residual biotite. Also shown are the estimated molar proportion of hydrogen which was evolved from chlorite and the projection lines to pure biotite compositions which were calculated assuming mixing between a biotite end member yielding 2 μM mg^{-1} hydrogen and a chlorite end member with δD = -50‰ yielding 6μM mg^{-1} hydrogen. It should be noted that these projection lines do not follow the mixing lines between chlorite and biotite, which are curved on this plot.

The two most altered "biotites" have higher δD than the others, consistent with a significant chlorite content. Whether or not a biotite-chlorite intergrowth fractionates hydrogen in the same way as a mechanical mixture of the appropriate quantities of the two pure end members (i.e. ideal mixing) is debatable, since the fractionation is dependent on the detailed structure. However a simple projection to end member biotite δD values assuming ideal mixing (fig. 3.4) indicates that the biotite in two of the chlorites could have δD values within the range for the three pure biotites. The biotite in the chloritised biotite with the lowest δD value is indicated to have a much lighter δD value. A complicating factor in this procedure is that any unaltered biotite may have partially or totally equilibrated hydrogen isotopes with the fluid causing the chloritisation. Thus the low δD value indicated for the biotite in AY.13 could represent the δD value of the original biotite, or it could represent the δD of the biotite after it had equilibrated with the chloritising fluid.

The two "chlorites" analysed, in contrast to the biotites, have lower water contents than any pure stoichiometric chlorites. However, both of these chlorites are seen to contain ribs of residual biotite material in thin section, so it is likely that the low yields can be explained by the presence of minor

biotite in the samples as well as some minor muscovite identified by XRD in GJ.234.

3.3.3 Hydrogen isotope composition of fluids in equilibrium with hydrous minerals.

The hydrogen isotope composition of the fluid which would have been in equilibrium with the hydrous minerals at geological temperatures is shown in figures 3.3 and 3.5. In the same way as in section 3.1.2 it is possible to use fig 2.12 to gain some idea of the lower temperature limit below which diffusion controlled exchange becomes unimportant. Thus it would appear that the relatively fine grained hornblendes could have equilibrated hydrogen isotopes with a grain boundary fluid within a few hundred years or less even at temperatures as low as 300°C. However this does not affect the estimation of equilibrium fluid composition because according to Graham *et al.* (1984) the hornblende-water fractionation is independent of temperature at least to 350°C which is the lowest temperature at which it has been calibrated. Thus the hornblendes appear to have equilibrated with fluids of δD =-40 to -50‰ at some temperature (fig. 3.5).

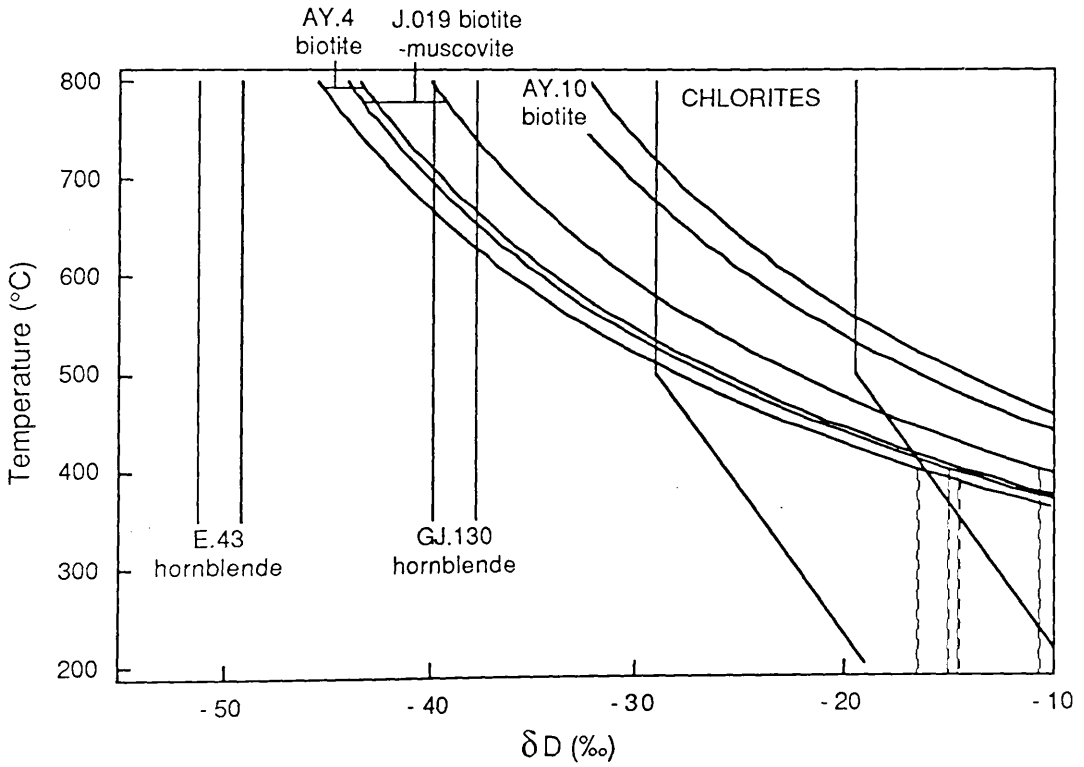

Fig. 3.5 δD value of fluid in equilibrium with hydrous minerals in the Dalradian rocks as a function of temperature. Each pair of curves correspond to the upper and lower limits of δD which result from analytical uncertainty (1 σ_{n-1}) except for the chlorite curves which correspond to the fluid in equilibrium with the two samples analysed. The amphibole-water fractionation used was that of Graham *et al.* (1984), while the chlorite-water fractionation is that of Graham *et al.* (1987). A modified Suzuoki-Epstein equation is used to construct the mica curves. The vertical dashed lines show the way in which the fractionation behaviour of the micas may change below the temperature range for which the fractionation was calibrated by Suzuoki and Epstein (1976). See text for further details of mica-water fractionation.

The fine chlorites (flake diameter = 0.3-0.4 mm) which are pseudomorphing biotite should also theoretically be able to re-equilibrate with pore fluids, if they are present, to low temperatures (fig. 2.12) possibly as low as 300°C, although chlorite closure is always predicted to occur at slightly higher temperatures than hornblende closure under the same conditions. Thus it can be stated that whatever the temperature of last equilibration the chlorites must have equilibrated with a fluid with a δD of a least -29‰, while if fluid was present at low temperatures (300°C) equilibration is likely to have taken place, in which case the the δD of this fluid would have been in the range of -25 to -15‰ (fig. 3.5). Thus whatever the exact temperature of equilibration, the δD of this fluid is distinctly different from the fluid in equilibrium with the hornblendes.

A modified Suzuoki-Epstein equation (A.4.3) is used here to calculate the δD of the fluid in equilibrium with the micas. Microprobe analyses of five of the biotites have been given by Ahmed-Said (1988). The octahedral site compositions recalculated from this data are relatively constant (mole fractions: Al ≈ 0.14, Ti ≈ 0.07, $Fe^{2+(?)}$ ≈ 0.49, Mn ≈ 0.003, Mg ≈ 0.29) except for one sample (AY.13) which is nearest to the Cashel body and has distinctly higher Mg (0.34) and lower Fe^{2+} (0.44). This difference can be attributed to the effect of heating by the Cashel body, since Ahmed-Said (1988) showed that there is a general increase in Mg and decrease in Fe in biotite towards the Cashel body. Unfortunately the biotite in J.019 has not been chemically analysed. However it is likely that the composition of this biotite can be approximated by that of the biotite from sample AY.13 which comes from less than 400 m away. The δD of the fluid in equilibrium with the three fresh biotites (see 3.1.3) at 800°C is connected by tie lines to the fluid compositions in fig. 3.3. Because of the uncertainty of the δD of the biotite end member in the partially chloritised biotite no equilibrium fluid is calculated for these samples. A diagram of this type will show the effect of the difference in in chemistry between the biotites on the equilibrium fluid δD. In fact, the chemical differences between the biotites only cause slight differences in the magnitude of fractionation of hydrogen with a fluid at any temperature, so that taking into account the chemical differences only effects a 1‰ reduction in the range of equilibrium fluid compositions relative to the range of biotite δD. Thus the variation of biotite δD is not due to equilibration of biotites with different chemistries with the same fluid, but is due to a small (~10‰) variation in the δD of the different rocks. Because the chemical analyses of these biotites are slightly unbalanced (3.1.3) the octahedral Al may be slightly underestimated, the result of this is that the equilibrium fluid for these biotites could be slightly lighter than shown.

The chemical composition of the muscovite is also not known. In fig. 3.3 the δD of the fluid in equilibrium with the muscovite is shown, assuming that either the muscovite is a pure Al muscovite or that the muscovite has a similar fractionation with the fluid as the natural muscovite analysed by Suzuoki and Epstein (1976), which contains about 10% Fe in the octahedral site. Since it is not uncommon for muscovite to contain appreciable quantities of Fe (Guidotti, 1984) it is supposed that the fractionation measured for this natural muscovite may be more appropriate for the

Connemara muscovite, although confirmation of this awaits chemical analysis. Using the fractionation for natural muscovite the δD of the equilibrium fluid at 800°C is exactly the same as that which is indicated by the coexisting biotite in the same rock, suggesting that these minerals are in equilibrium at this temperature. However because the effect of mica chemistry on the fractionation does not vary with temperature (Suzuoki and Epstein, 1976) the difference in equilibrium fluid δD between samples will be the same at any temperature. Thus it can only be inferred that this biotite and muscovite have equilibrated at some temperature, and that this equilibrium has been preserved since that time. Unfortunately because of the uncertainty in the muscovite composition and in the application of the Suzuoki-Epstein equation itself this conclusion has to be viewed with some scepticism.

The effect of temperature on the equilibrium fluid composition for the three fresh biotites (and therefore the muscovite) is shown in fig. 3.5. The solid curves for the micas were constructed assuming that the modified Suzuoki-Epstein equation (A.4.3) applied to the micas, even below the temperature range in which it was calibrated by Suzuoki and Epstein. This is in fact thought not to be the case and it is suggested that the fractionation becomes almost independent of temperature below 400°C as shown by the dashed lines (see 4.4.2 for further details). From reference to fig 2.12 it would appear that although both the biotite and the muscovite are fairly coarse grained (flake diameters ~1 mm) it is theoretically possible for hydrogen isotope equilibration of these minerals with grain boundary fluid to continue down to temperatures as low as 300°C if fluid was present, with the muscovite closing to diffusion at slightly higher temperatures than the biotite. Equilibration of these minerals with significant volumes of fluid at this sort of temperature would appear highly unlikely if the mica-water fractionation followed a Suzuoki-Epstein equation below 400°C, because the equilibrium fluid would have unreasonably high (positive) values of δD. If however the mica-water hydrogen isotope fractionation does become independent of temperature below ~400°C, then it can be seen from fig. 3.5 that the micas in AY.4 and J.019 could have equilibrated at ~300°C with the high δD fluid that equilibrated with the chlorite. It can be seen however that the biotite in AY.10 could only have equilibrated with the high δD fluid at temperatures >550°C. Equilibration of the biotites at low temperatures with the high δD fluid that equilibrated with the chlorite, is considered unlikely because the fresh biotites would have had to have undergone hydrogen isotope exchange with, but not reacted with a fluid that was causing chloritisation elsewhere. A much more likely situation is that these micas last equilibrated at high temperatures (>600°C) with a fluid with a δD of ~-40‰, similar to that in equilibrium with the hornblendes. A corollary of this is that fluid would have to be absent, or present in only small quantities in the unchloritised rocks at lower temperatures. Support for this hypothesis comes from the observation that rocks in which chloritisation has taken place show signs of fluid infiltration (e.g. bubble planes in quartz and microcracks as well as the hydration of biotite itself), while rocks containing the fresh biotite generally do not, suggesting that the fluid which caused the chloritisation was never present within unchloritised rocks.

Salt effects.

If mineral-water hydrogen isotope fractionation is taking place at temperatures less than 550°C the effect of the solute concentration and composition in the fluid may become important (2.4.5.B). Because the fluid chemistry is not yet known all that can be said is that the δD of the calculated equilibrium fluid may be slightly lighter than that given above, which is calculated assuming that the fluid is pure water. If the fluid is significantly saline the equilibrium composition could be as much as 10‰ lighter.

3.4 FLUID INCLUSION DATA.

3.4.1 Volatile chemistry.

The results of partial chemical analyses of the volatiles released from splits of a sample of vein quartz (GJ.160) from the microgranite sill, together the results of the hydrogen isotope analyses of the water released during each run are presented in fig. 3.6 (analytical details are given in A.1.4).

The most striking feature of the chemistry of the volatiles is that the variation in the $H_2O/(H_2O+CO_2)$ ratio of the different splits from the sample is much less than the variation in either the $NC/(H_2O+NC)$ or $NC/(CO_2+NC)$ ratio. Four out of the five splits have $H_2O/(H_2O+CO_2)$ ratios in the range 0.96-0.975. The higher $H_2O/(H_2O+CO_2)$ ratio of ~0.985 in the remaining sample can be attributed to accidental loss of some of the CO_2 during measurement, so that it seems likely that all of the splits had a very similar $H_2O/(H_2O+CO_2)$ ratio. The NC content on the other hand varies greatly between the different fractions of the same sample, from 0-5% overall or 0-2.4 $\mu M\ mg^{-1}$ in terms of yield. The relative constancy of the $H_2O/(H_2O+CO_2)$ ratio coupled with the variability in the NC content is best explained by mixing of variable proportions of two components, one NC rich (possibly pure NCs) and the other NC poor (probably no NCs) which also has a constant $H_2O/(H_2O+CO_2)$ ratio. The nature of this rather sporadic NC rich component is not immediately obvious. Non-condensible gases in geological materials are most usually CH_4, N_2 or Ar, while lesser quantities of other noble gases can also occur. If the NCs were methane from fluid inclusions it might be expected that the δD would correlate with NC content, since equilibration of the water with methane would leave it strongly enriched ($10^3 ln\alpha_{H2O\text{-}CH4}$ = 60-75‰ between 200 and 700°C; Bottinga, 1969a). Mass balance calculations show that equilibration with 5% methane would increase the water δD by ~3.5‰ if δD_{SYSTEM} remained constant. Thus the fact that the two samples with the highest NC content have the lowest δD would tend to argue against methane being an important constituent in the NC rich component, unless hydrogen isotopes were not equilibrated or substantially exchanged between these species. In addition methane in fluid inclusions is generally associated with graphitic host rocks (Yardley *et al.*, 1983) which do not appear to be present in this area. Thus it is likely that the NC component is composed of nitrogen and/or argon, although the presence of methane cannot be completely

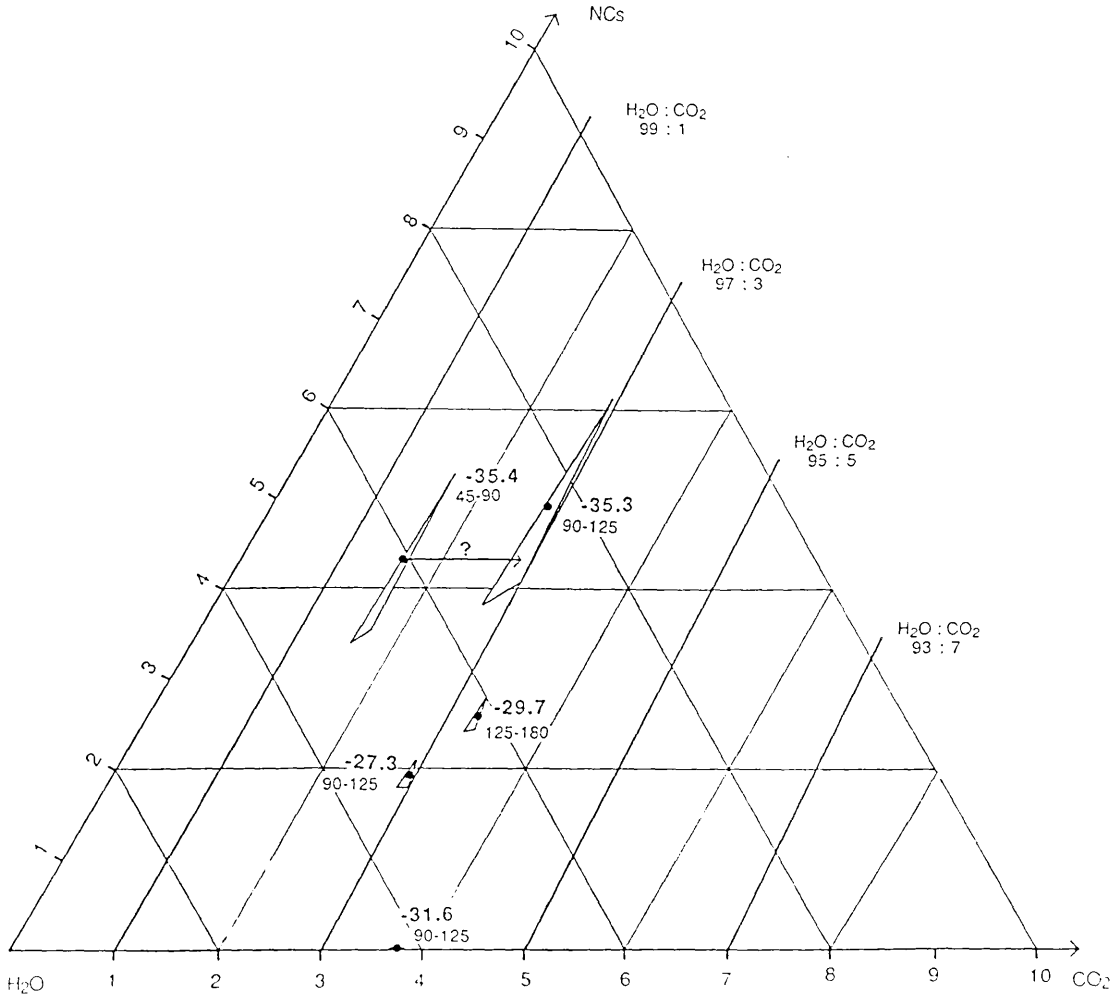

Fig. 3.6 Gas composition and δD of water of material released by decrepitation of different splits of a quartz vein (GJ.160) from the microcline granite sill. The triangles around the points are the 90% confidence limits on the gas chemistry and take into account both reading errors and the uncertainty in the calibration line used. The grain sizes of the splits are also shown. It should be noted that only the water rich apex of the compositional triangle is shown.

excluded. There are three possibilities for the origin of a N_2/Ar NC component:

1. From a leak in the extraction line.
2. From a layer of absorbed gas on the sample.
3. From within fluid inclusions.

The first possibility is not favoured, since although a minor intermittent leak was known to be present in the line at the time of the earlier runs, these runs have lower (even zero) NC contents compared to the samples analysed during later runs when the line was known to be very airtight. Furthermore, monitoring of the amount of NCs collected with time during

the run showed that most, if not all of the NC gases were released within a few minutes of the initiation of the heating of the sample, indicating that the NCs must be associated with the sample. The second possibility, that the NCs were evolved from an absorbed layer on the sample is also thought to be unlikely since although the large sample size used in these runs provides a much larger surface area for absorption of atmospheric gases than hydrous mineral samples, the degassing procedure used is generally thought to remove most absorbed volatiles, especially inert gasses because these can only be adsorbed. In addition, a plot of NC yield vs. approximate sample surface area (fig. 3.7) does not show a simple linear correlation of yield to surface area, with the best fit line running through the origin, or having an intercept on the yield axis as would be expected if evolution of NCs from a surface layer was the major cause of NC variation. The third possibility, that the NCs released by the samples must come from fluid inclusions within them also has its problems however. The fact that the NC content is highly variable between samples indicates that the NC filled inclusions would have to be very sparsely distributed i.e on the order of one per gram of sample which would then imply that they would have to be very large in order to contain the required quantities of NCs. If the inclusions are assumed to contain 2 μM of pure nitrogen with a density of 0.5 g/cm^3 (the value given for nitrogen inclusions in Norwegian migmatites with a similar PT uplift path to Connemara; Touret and Dietvorst, 1983) the calculated inclusion size is found to be an order of magnitude greater than the largest grain size of quartz analysed (1.1×10^{-4} cm^3 relative to 2.4×10^{-5} cm^3)[1]. Thus for the present the nature of the NC component has to remain unexplained until further information on its composition can be obtained. Irrespective of this problem the constancy of the $H_2O/(H_2O+CO_2)$ ratio for different splits of the same sample suggests that this ratio is a real feature of the fluid present within this sample.

3.4.2 δD of fluid inclusions.

The δD of the water released by the different splits is relatively homogeneous. The two lowest values may be rather suspect because both of these splits would probably have been prone to contamination with the minor water blank (A.1.3) associated with the analysis, which would tend to reduce the δD (run 4489 because of the low overall yield of water, run 4493 because of the very large surface area of the sample). Thus it may be tentatively suggested that the δD of the water within the inclusions is near to -30‰. The water contents of the sample splits are found to vary between 0.094 and 0.079 wt.% H_2O, decreasing regularly with grain size of the splits

---

[1] The original purpose of using a range of rather finer grain sizes than is often used for fluid inclusion analysis was to see whether more than one generation of inclusion could be distinguished by means of their different size distributions, and also to try to filter out extremely large (usually late) inclusions which would tend to dominate the gas composition. It would seem that this procedure has been partly successful by excluding the possibility of large inclusions!

just as would be expected if the water was being evolved from fluid inclusions within the sample.

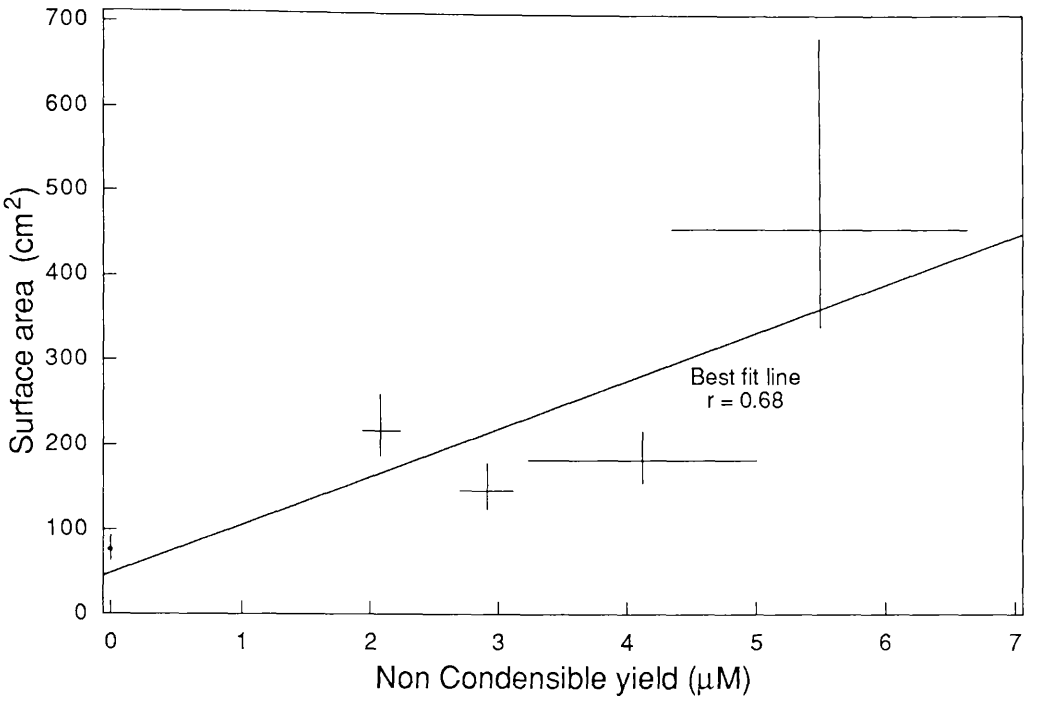

Fig. 3.7 Total yield of NCs vs. the approximate surface area for the different splits of quartz sample GJ.160. Surface areas were calculated assuming that grains were spheres with a diameter equal to the median, maximum and minimum of the grain size range (best estimate, minimum and maximum surface areas respectively).

3.5 DISCUSSION.

3.5.1 Dalradian amphibolites.

Both of the hornblendes within the amphibolites have $\delta^{18}O$ values of ~+7.6‰. Since plagioclase is the only other major constituent of the rock, and at equilibrium the plagioclase will always concentrate ^{18}O relative to amphibole (Bottinga and Javoy, 1975) it would seem likely that the $\delta^{18}O$ value of the whole rocks is >8‰. This value is significantly higher than the $\delta^{18}O$ values of normal basaltic rocks which are usually near to +6‰ (2.9.3) indicating that the amphibolites have been enriched in ^{18}O by some process. Similar ^{18}O enrichments in ortho-amphibolites in regional metamorphic terranes have also been observed by O'Neil and Ghent (1975). There are a number of mechanisms by which such ^{18}O enrichment could have occurred in Connemara:

a. Contamination by high $\delta^{18}O$ sedimentary material, during intrusion or extrusion.

b. Post intrusion/extrusion hydrothermal alteration at low temperatures by sedimentary pore fluids or seawater. Graham (1976) shows that the metabasites in S.W. Scotland which may be lateral equivalents, were variably spilitised prior to metamorphism.

c. Oxygen isotope exchange with a high $\delta^{18}O$ fluid at high temperatures. This mechanism would require the high $\delta^{18}O$ fluids to have flowed through the amphibolites or their precursors by some mechanism. Graham *et al.* (1987a) show that greenschist facies metabasites in S.W. Scotland have had their $\delta^{18}O$ values shifted to ~+9‰ as a result of infiltration by fluids produced by dehydration reactions deeper within the metamorphic pile. There appears to be no reason why fluid from the metasediments should flow through the amphibolites. The apparent lack of equilibration between the amphiboles and the quartz in the metasediments indicates that the fluid/rock ratios could never have been very high at high temperature.

d. Oxygen isotope exchange with the surrounding metasedimentary rocks without fluid infiltration during metamorphism. The fact that the amphibole within the amphibolites does not appear to be in equilibrium with the quartz in the metasediments could be cited as evidence against this hypothesis, although it could be reconciled if only partial equilibration was achieved. Oxygen isotope exchange without the aid of fluid movement would have to take place by means of diffusion and it is questionable whether even at high temperatures and over long time periods that this process could have taken place rapidly enough for exchange to take place throughout the amphibolites.

The δD of the amphiboles is not incompatible with the derivation of the hydrogen in the amphibolites from fluids in the surrounding metasediments, as long as fluid/rock ratios are relatively large so that the hydrogen in the amphiboles is dominated by the fluid. This might seem at variance with the condition that ^{18}O enrichment by fluid infiltration from the metasediments could only have taken place under conditions of low fluid/rock ratio, until it is recalled that a high fluid/rock ratio for hydrogen does not necessarily indicate a high fluid/rock ratio for oxygen. The relatively low δD values of the amphiboles might be used to argue against pre-metamorphic hydrothermal alteration as a cause of the high $\delta^{18}O$ values since the δD of rocks altered by such processes are usually fairly high, because most of the hydrogen in these rocks is present as chlorite which fractionates about 30‰ below the fluid (Graham *et al.*,1987b) which would be 0‰ for seawater. However unlike the $\delta^{18}O$ of rocks, which is generally little affected during prograde metamorphism (2.9.5), the δD would tend to be reduced during dehydration reactions so that this possibility cannot be excluded. Similarly although the rock δD would probably be increased by reaction with fluids produced by dehydration lower in the pile, it is also possible that this high δD signature could then be subsequently be removed by dehydration within the rock in question.

Thus although ^{18}O enrichment has almost certainly taken place at some time during the history of the amphibolites it would appear that with the available data it is not possible to identify the process by which enrichment took place.

3.5.2 Whole rock $\delta^{18}O$ variations.

The variation of the whole rock oxygen isotope composition in the Dalradian metasediments is most easily interpreted as resulting from extraction of partial melt material from the hornfelses, a process which has been suggested to have taken place by a number of authors (Leake and Skirrow, 1960; Evans, 1964; Jagger, 1985). Granitic partial melts formed in equilibrium with a residuum containing a large proportion of mafic minerals would be expected to be enriched in ^{18}O compared to the residuum even at the high temperatures at which melting takes place. The exact magnitude of the enrichment is difficult to specify, but is probably less than 2‰ (Taylor and Sheppard, 1986, p.236). Jagger (1985, p.157) has suggested that there is limited radiogenic isotope evidence that disequilibrium partial melting might have taken place within the aureole of the Cashel body. Some theoretical evidence that oxygen isotope disequilibrium could occur during partial melting can be found by examination of figs. 2.4 and 2.12 which show that it might be possible for biotite and possibly other mafic minerals not to have equilibrated oxygen isotopes if melt extraction took place over a short time span ($<10^4$ y). However the effect of biotite not equilibrating oxygen isotopes with the melt would be to cause a very slight reduction in melt $\delta^{18}O$ which would probably be negligible compared with the equilibrium situation at low degrees of partial melting. Thus the ^{18}O depletion of the hornfelsed metasediments relative to the migmatised sediments further away which have suffered little or no loss of partial melt is explained by the loss of significant quantities of ^{18}O rich partial melt. Some caution should be emphasised here however because both the samples of hornfelsed metasediments show obvious petrographic evidence of later low temperature alteration (pinitisation of cordierite, chloritisation of biotite) which could have modified the whole rock $\delta^{18}O$ value. Indeed the concordance of $\delta^{18}O$ values of these two whole rock samples would not be predicted in view of the chemical and modal differences between samples (cordierite is the dominant mineral in J.003 and SiO_2 = 56%, while in J.29 quartz is dominant and SiO_2 = 64%; chemical data from Jagger, 1985).

The psammite screen within the Cashel body has a similar low $\delta^{18}O$ value to the hornfelsed metasediments at the contact. However it is questionable whether a rock of this composition could represent the residuum left after significant melt has been removed. It is possible therefore that the $\delta^{18}O$ lowering of this rock could have taken place by subsolidus exchange with the surrounding ultrabasic rock.

The high $\delta^{18}O$ value of the microcline granite sill is compatible with its suggested origin as a large segregation of partial melt material (Jagger, 1985), since its $\delta^{18}O$ value is higher than that of the migmatised sediments (original material) and thus forms the ^{18}O enriched complement to the hornfelsed metasediments (residual material) that is required by mass balance. Thus it might be suggested that the oxygen isotope composition of any partial melt material which was assimilated by the MGS magmas would have been ~+11.5‰. However it should be noted that the albite and biotite

in this rock show signs of intense low temperature alteration which once again may have caused some modification of the whole rock $\delta^{18}O$ value.

3.5.3 Quartz $\delta^{18}O$ variations.

The marked variation of quartz $\delta^{18}O$ values by up to 2‰ within a distance of 2.5 m at the contact of the Cashel body is quite remarkable in view of the fact that these rocks have experienced at least one and possibly two events which would tend to act to homogenise mineral $\delta^{18}O$ values. Firstly the formation of partial melts within the hornfelses might be expected to result in the convergence and ultimately homogenisation of mineral $\delta^{18}O$ values over a scale of a few metres, as long as the melt was not immediately extracted, since the melt should act as a pathway for very fast fluid diffusion of isotopes to take place between rocks. If movement of these partial melts took place through the (now solidified?) ultrabasic rocks at the contact and into the MGS magma, this might also be expected to homogenise mineral $\delta^{18}O$ values in the ultrabasic rocks at the margins of the intrusion. Secondly Jagger (1985, p.157) has proposed on the basis of Sr and Nd isotope data (on the same samples from the contact of the Cashel body that are analysed here), that mass transfer of these elements from the Cashel body into the metasediments took place at some time after intrusion. It is presumed here that this mass transfer took place via a fluid phase, in which case fluid flow must have taken place through the contact zone. As long as this fluid efflux took place above ~500°C (the approximate closure temperature of the quartz) then its effect should also have been to cause quartz $\delta^{18}O$ values to converge and finally homogenise.

Thus the inhomogeneity of the quartz $\delta^{18}O$ around the contact zone suggests either that homogeneity was achieved at high temperatures and subsequently destroyed, or that homogeneity was never achieved. If homogeneity in mineral $\delta^{18}O$ between samples was never achieved this would require that melt extraction would have had to have take place from the hornfels very rapidly. Possibly melt extraction was so rapid that isotopic equilibrium was not achieved between minerals and melts even on a hand specimen scale. Such a disequilibrium partial melting process was suggested by Jagger (1988) as an alternative to fluid efflux from the Cashel body as a mechanism to explain the radiogenic isotope distribution in the hornfelses. Thus if disequilibrium partial melting did take place, fluid efflux would not be required to explain the radiogenic isotope variation in the aureole and thus need not have taken place. If this was the case any original stable isotope inhomogeneity in the aureole would have been preserved. This explanation of the present inhomogeneity requires that the quartz $\delta^{18}O$ in the metasediments was originally inhomogeneous over a distance of 1.5 m prior to hornfelsing, a condition which would seem unlikely and cannot be substantiated with the present data.

If on the other hand homogeneity of quartz $\delta^{18}O$ <u>was</u> achieved at high temperatures (i.e. above 500°C) either by equilibration via partial melts, by exchange with a fluid derived from the Cashel body or by some other process, some later process must have taken place which disrupted the

homogeneity on a local scale. A possible mechanism by which originally homogeneous quartz compositions could be caused to diverge is by down-temperature re-equilibration in closed systems with different modal compositions. Thus the larger $\Delta_{quartz\text{-}whole\ rock}$ fractionation in J.003 relative to J.029 can be explained in terms of the larger proportion of mafic minerals and smaller proportion of quartz in J.003 which would cause the quartz $\delta^{18}O$ value to increase more on cooling because of mass balance effects. A test of this is that $\Delta_{quartz\text{-}garnet}$ for example should be similar in the two rocks.

In conclusion therefore, it would appear that taken at face value the quartz $\delta^{18}O$ data from the aureole of the Cashel body are not consistent with either a. the prolonged presence of partial melt material forming an interconnecting network in the rock or b. with an efflux of fluid from the Cashel body high temperatures as was implied by Jagger (1985). Possibly these data might indicate very rapid extraction of melt took place from hornfelses, which could have resulted in isotopic disequilibrium between melt and residuum. Alternatively retrograde cooling effect can be invoked to explain the present inhomogeneity and therefore the possibility that mineral $\delta^{18}O$ homogenisation took place by some process or other cannot be excluded. Unfortunately with the present data it is very difficult to choose between these very contrasting possibilities.

Turning now to the quartz vein in the microcline granite sill it is noteworthy that its $\delta^{18}O$ value is lower than that of the host rock, since the quartz within this rock would normally be expected to have a higher $\delta^{18}O$ value than the whole rock and thus isotopic disequilibrium is implied. This is despite the fact that the presence of coarse K-feldspar within this vein tends to suggest that it is genetically related to the sill. The fact that the $\delta^{18}O$ value of this quartz is lower than that of the quartz in the metasediments indicates that it was not deposited from fluid which had equilibrated with these rocks, supporting an association with the enclosing sill. The low $\delta^{18}O$ value of the quartz could be explained if it is supposed that the vein was deposited from the residual fluid which was formed during crystallisation of the sill. The $\delta^{18}O$ of this fluid would have been dominated by melt and crystallised material in the sill (dominantly quartz and alkali feldspar) and since all of these phases concentrate ^{18}O relative to water it seems likely that the residual fluid and the quartz that formed from it would be relatively ^{18}O depleted.

3.5.4 Hydrogen isotope variation.

From the evidence presented in 3.1.4 it appears that at least two distinct fluids can be identified within the metasediments, a fluid of $\delta D \approx -40$ to -50‰ in equilibrium with the amphiboles and probably also with the micas at high temperatures and a retrograde fluid of >-30‰ which caused chloritisation of the biotite, probably at low temperatures. A fluid with a δD of -30‰ has also been identified within a quartz vein associated with the microgranite sill. At present it is not clear whether or not any of these fluids could have been genetically related. One model which relates peak

metamorphic and retrograde fluids is described below and tested using the available isotopic data.

Recently Cartwright (1988) has proposed a model for the origin of retrograde hydrous fluid in high grade metamorphic rocks, in which water is partitioned into partial melts at the peak of metamorphism and then concentrated by segregation of these melts and finally released as the melts crystallise. It would seem possible that the high temperature (coarse muscovite forming) retrogression observed within the migmatites could have resulted from such a process. It is also conceivable that water derived by exsolution from bodies of partial melt around the MGS could have caused some of the subsolidus amphibolisation within these rocks, although this would require fluid flow to have taken place across the contact (see previous section). Furthermore direct assimilation of partial melts by the MGS intrusions may have increased the water content of the MGS magma, thus stabilising magmatic amphibole in the later differentiates. With these points in mind the hydrogen isotope data are used to estimate what the δD of the water contained within the partial melts would have been.

It is presumed here that even if the melt was extracted from the rock very rapidly that it will have equilibrated hydrogen isotopes with the residual biotite. From fig. 2.12 it seems that this should theoretically be the case, since at >800°C the biotite should equilibrate by diffusion on a timescale of 10^{-1} years. Estimates of the hydrogen isotope fractionation between water and hydrous melts are reviewed by B.E. Taylor (1986, p.191) who finds that in general $\Delta_{H2O\text{-}melt}$ is positive and probably around 20‰ for acid magmas. Using this value, and the modified Suzuoki-Epstein fractionation for the fresh biotites, $\Delta_{biotite\text{-}melt}$ is found to be $\approx$ -4‰ at 850°C which becomes slightly more negative at lower temperatures (-6‰ at 700°C). Slightly higher Mg and lower Fe in biotites near to the contact would cause this fractionation to become slightly more positive. Ideally in order to estimate the δD of the partial melt it would be useful to know the δD of biotite in rocks which have lost partial melts as well as those which have not because the mass balance constraints specify that the δD of the biotite in equilibrium with the melt will change slightly as some of it breaks down, while the way in which the biotite δD varies is dependent on the mechanism of melt extraction (batch or fractional melting). Unfortunately no analyses of biotite δD are available for rocks which have obviously lost partial melt. However, under low degrees of partial melting the biotite will remain the dominant reservoir of hydrogen and therefore shift very little in δD especially as the fractionation between biotite and melt is so small, so that the approximation can be made that $\delta D_{melt} \approx \delta D_{biotite}$ for the biotite δD in rocks which have not obviously lost partial melt. Thus the partial melts would probably have had a δD of ~-60 to -70‰. Hydrogen isotope analysis of the biotite within the microcline granite sill might confirm this prediction, but regrettably it is strongly chloritised.

Two points need further explanation since at first sight they might appear to contradict this conclusion regarding the partial melt δD. Firstly, it was

found that the large retrograde muscovite flakes within the migmatite leucosome in sample J.019 have a δD of -42‰. The fact that this value is not the same as that calculated for the partial melt does not necessarily preclude the water for muscovite growth as being supplied by crystallisation of the leucosome material since it was also shown that this muscovite was in hydrogen isotope equilibrium with the biotite in the restite in which case its original hydrogen isotope composition could have been modified by re-equilibration with the much larger hydrogen reservoir of the biotite. According to fig. 2.12 this re-equilibration could have easily been accomplished in less than 10^2 years at temperatures around 600°C. The second point is that the fluid present within the fluid inclusions in the quartz vein from the microgranite sill has a δD of ~-30‰, which is significantly higher than the predicted bulk melt δD. However this can be explained in the same way as the anomalous oxygen isotope composition of the vein was explained, i.e. that the vein material is interpreted as forming from the last highly fractionated residuum which is left over after crystallisation of the sill when most of the hydrogen had partitioned into the biotite in the sill and the melt exsolved small quantities of hydrous fluid which was enriched in δD by ~20‰. From this it would be predicted that the high δD and relatively low $\delta^{18}O$ fluid that formed this vein should be volumetrically insignificant within the metasediments. Thus it is suggested that although the fluid causing the chloritisation of the biotite has a similar high δD composition this fluid could not have been produced by exsolution from crystallising partial melts because of its widespread occurrence, a conclusion in accord with the observation that chloritisation is associated with the development of fine sericite, rather than coarse muscovite and therefore seems to have developed at much lower temperatures later in the history of Connemara.

The only other plausible mechanism by which the high δD fluid which caused the chloritisation within the Dalradian metasediment could have been generated is by hydration reactions involving the residual grain boundary fluid which reacted with biotite and plagioclase during cooling of these rocks. This hypothesis can be tested using simple mass balance equations to calculate the amount of chlorite and sericite that could be produced by such a process.

If the metasediments are assumed to have had an unusually high porosity of 0.1% (Rice and Ferry, 1982 suggest that the porosity will usually be considerably less than this value for normal metamorphic rocks) then the amount of pore fluid that would have been present in a reference volume of 100 cm^3 of rock would be 0.1 cm^3. If it is assumed that this fluid was pure liquid water and that the chlorite formed at ~300°C then the minimum density of the fluid prior to chlorite formation would have been ~0.7 (fig. 4.3 of Shepherd *et al.*, 1985), so that the mass of this water in the reference volume would have been between 0.1 and 0.07 g. Therefore between 5.5×10^{-3} and 3.9×10^{-3} M of H_2 would have been available in each reference volume of 100 cm^3 to form chlorite or sericite. Using hydrogen contents and densities of 6 μM mg^{-1} and 2.5 μM mg^{-1} and densities of 3 and 2.8 for chlorite and sericite respectively, then this amount of hydrogen could be calculated to form either 0.3-0.22 $cm^3/100$ cm^3 of chlorite or 0.76-

0.56 $cm^3/100\ cm^3$ of sericite. Modal analyses of 41 Cashel Formation rocks in the Cashel-Recess area given by Ahmed-Said (1988, p. 77) show that the amounts of chlorite and sericite in the Dalradian metasediments are between three and twenty times these values, indicating that the fluid causing development of these minerals could not have been derived by such a process.

Thus it must be concluded that there appears to be no mechanism by which the water in the chlorite and sericite in the Dalradian metasediments could have been derived from within these rocks and an external source is implied. The origin of this high δD fluid is discussed further in 4.7.3. in the light of evidence for the origin of a similar high δD fluid in the MGS.

3.6 SUMMARY.

The stable isotope data for the Dalradian rocks in the Cashel-Recess study area have been presented in this chapter. The major conclusions that can be drawn from this data are summarised below.

1. The metasediments have δD and $\delta^{18}O$ values within the range for normal metamorphic rocks, but the Dalradian amphibolites are enriched in ^{18}O compared to a normal basaltic precursor. This ^{18}O enrichment in the amphibolites could have been caused by a number of processes, but with the available data it is not possible to suggest which of these processes did cause the ^{18}O enrichment.

2. The water contents of some apparently pure biotites are anomalously high, indicating that these biotites may be altered to chlorite on a submicroscopic scale.

3. The hornblendes in the Dalradian appear to have equilibrated with a "metamorphic" fluid with a δD ≈-40 to -50‰ and a $\delta^{18}O$ of +9 to +10‰. The quartz in the metasediments must have last equilibrated with a similar metamorphic fluid with a $\delta^{18}O$ ≈+10 to +14‰. The unaltered micas in the metasediments probably also equilibrated hydrogen isotopes with the same fluid at high temperatures (>600°C), in which case the fluid in the metasediments at high temperatures would have had a δD ≈-45 to -30‰. The petrographically later chlorites must have equilibrated with a fluid with a distinctly higher δD (>-30‰). The partial melts produced during hornfelsing are estimated to have had a δD ≈-60 to -70‰ and a $\delta^{18}O$ ≈ +11.5‰.

4. The fluid present within a quartz vein from the microgranite sill has a $H_2O/(H_2O+CO_2)$ ratio of 0.96 to 0.975 and a δD of ~-30‰. This fluid is estimated to have had a $\delta^{18}O$ ≈ +9 to +10‰.

5. Whole rock $\delta^{18}O$ variations in the metasediments can be interpreted as the result of variable degrees of partial melt extraction from the rocks adjacent to the ultrabasic and basic MGS intrusions, consistent with the results from previous studies (Leake and Skirrow, 1960; Evans, 1964; Jagger, 1985) which suggest that such a process took place during the

intrusion of the MGS. The high $\delta^{18}O$ value of the microcline granite sill to the north of the Cashel body is consistent with this sill representing a large segregation of partial melt material as has been suggested by Jagger (1985).

6. The quartz $\delta^{18}O$ data from the aureole of the Cashel body is not consistent with either a. the prolonged presence of partial melt material forming an interconnecting network in the rock, or b. with an efflux of fluid taking place from the Cashel body. However this data might be interpreted to indicate that partial melts were extracted from the aureole rocks so rapidly that isotopic equilibrium between melt and hornfelses was not attained prior to melt extraction. Alternatively this data could also be interpreted as the result of down temperature closed system re-equilibration during in chemically different samples.

7. The fluid which deposited the quartz vein cutting the microcline granite sill was probably exsolved during the final stages of crystallisation of this sill. Consideration of the amounts of this fluid that would have been produced within the metasediments indicates that this fluid could not have caused the widespread chloritisation observed in the metasediments, although this fluid has a similar δD value to that which caused the chloritisation.

8. Using mass balance constraints it is shown that the late chlorite and sericite in these rocks could not have been generated by hydration reactions involving the residual grain boundary fluid during cooling. In the absence of any other mechanism by which the fluid which formed the chlorite and sericite could have been derived from within the metasediments, an external source is implied for this fluid.

CHAPTER 4.

THE CASHEL-RECESS STUDY AREA - PART 2.

THE METAGABBRO SUITE (MGS).

4.1 INTRODUCTION.

In chapter 1. it was shown that the rocks of the MGS contain primary hydrous minerals but also exhibit a complex sequence of retrograde replacement by a variety of secondary hydrous minerals, indicating the presence of hydrous fluid within these rocks after intrusion. At present the origins of the water in the primary minerals and in this retrograde fluid are unknown. It is also unclear whether the whole of the retrograde hydration sequence developed during one episode of alteration as a result of reaction at different temperatures with a single fluid, or whether different hydrous minerals developed from different fluids of different origins at distinctly different times. Thus a multitude of possible explanations for the cause(s) of retrograde hydration involving various sources of fluid can be envisaged. It might be suggested, for example, that all of the fluid causing retrograde hydration could have been derived from the MGS magma, and that hydration took place during initial cooling, in which case the observed alteration could represent an extreme example of deuteric alteration by igneous fluids (Wager, 1932). Alternatively some of the water for hydration could have been derived from the adjacent Dalradian rocks (but see chapter 3. for some constraints), or possibly the water could have been derived from more distant sources such as a major thrust plane underlying the area, or possibly from the hydrosphere.

The purpose of this chapter is to examine the stable isotope data on rocks within the MGS with a view to constraining both the stable isotopic composition of the melts which precipitated the primary hornblende and biotite and the fluid(s) causing retrograde hydration and the conditions under which hydration took place, since such information should be useful in elucidating the sources of water in these different hydrous minerals.

4.2. HYDROGEN ISOTOPE RATIOS - ALL DATA.

Hydrogen isotope compositions of all the MGS mineral separates analysed for δD are summarised in fig. 4.1. The relation of the δD variations within mineral groups to rock type, rock alteration and mineral composition are discussed in 4.3. For the present discussion these details are not necessary, since major conclusions regarding the composition of the fluid that equilibrated with the different minerals and the temperature at which equilibration took place can be reached on the basis of the hydrogen isotope data alone.

Fig 4.2 shows the estimated δD of the fluid in equilibrium with the hornblendes, chlorites and epidotes as a function of temperature. From this diagram, it can be seen that provided the hornblendes last equilibrated with a fluid within the temperature range for which hydrogen isotope

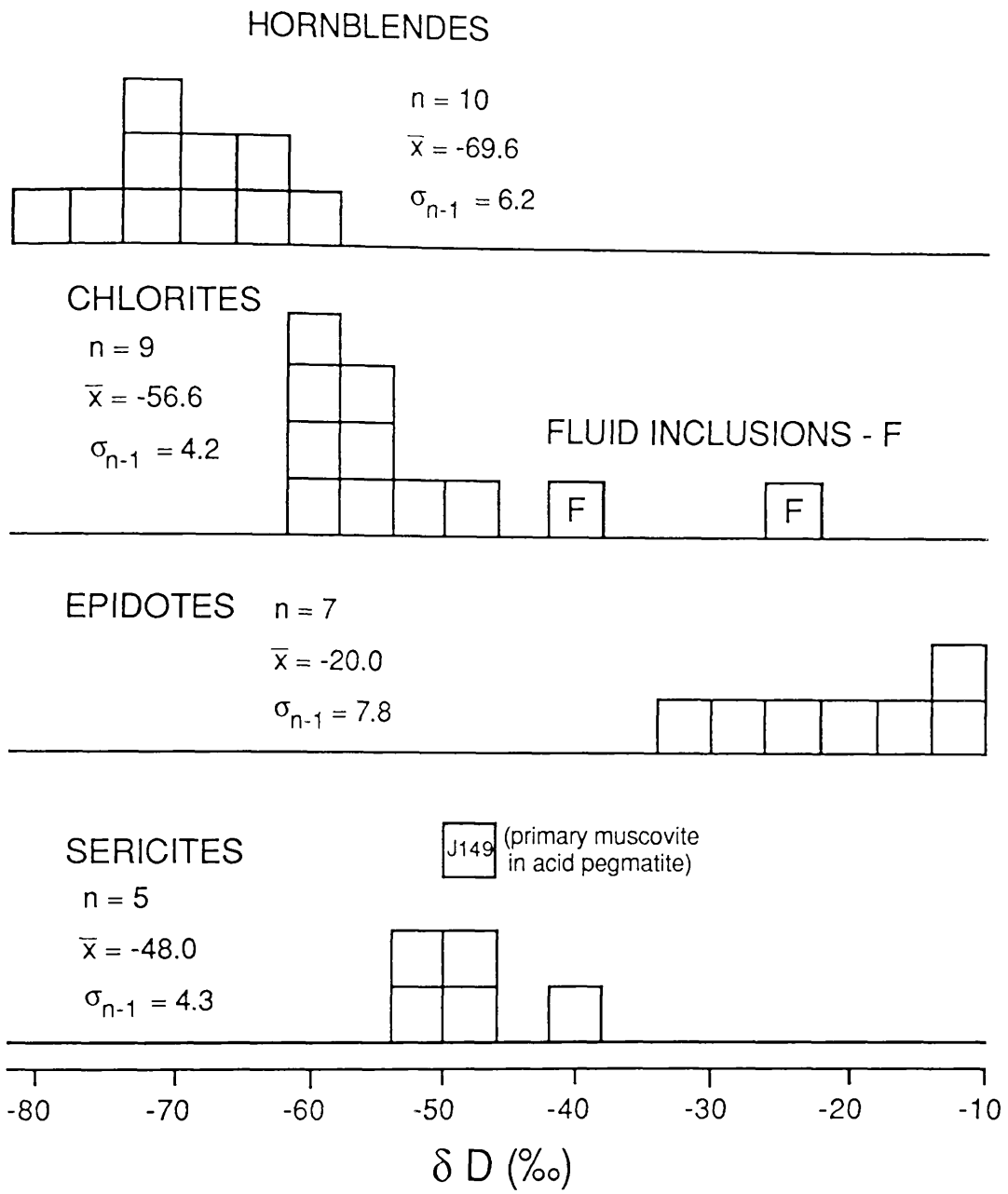

Fig. 4.1. Summary diagram of hydrogen isotope data for rocks in the MGS in the Cashel-Recess study area. Each box represents a mineral from a different sample.

fractionation between hornblende and water has been calibrated (850-350°C) it is clear that regardless of temperature or fluid salinity, the hornblende within the MGS must have last equilibrated with a fluid with a distinctly lighter δD value than the chlorites. The difference in estimated fluid compositions is ~20‰ on average at temperatures >500°C, increasing to ~30‰ at 200°C. The only way in which the fractionation between the amphiboles and chlorites could be interpreted as an equilibrium fractionation is if equilibration took place at some temperature below 350°C at which $\Delta_{amph\text{-}water}$ was in the order of -40‰. This is considered unlikely because (a). even fine grained hornblendes will not equilibrate hydrogen isotopes with pore fluid at temperatures below 200°C within periods < 1 million years (fig. 2.12) and these mostly coarse hornblendes may effectively close to diffusion at temperatures as high as 300°C; and, (b). it is unlikely

that the amphibole-water fractionation would become more negative by as much as 20‰ over a temperature drop of at most 150°C, especially since most other hydrogen isotope mineral-water fractionations are either independent of temperature or become more positive with declining temperature below 300°C (fig. 9. in O'Neil, 1986a). Thus it can be concluded from fig. 4.2 that the hornblendes and chlorites within the MGS are not in H isotope equilibrium and that the hornblendes equilibrated with a fluid with a $\delta D < -40‰$, while the chlorites equilibrated with a fluid with a $\delta D > -40‰$ (hereafter referred to as the high δD fluid). The exact δD of these two fluids can only be inferred if information is available on the equilibration temperature and fluid and mineral chemistry, factors which are presently unknown.

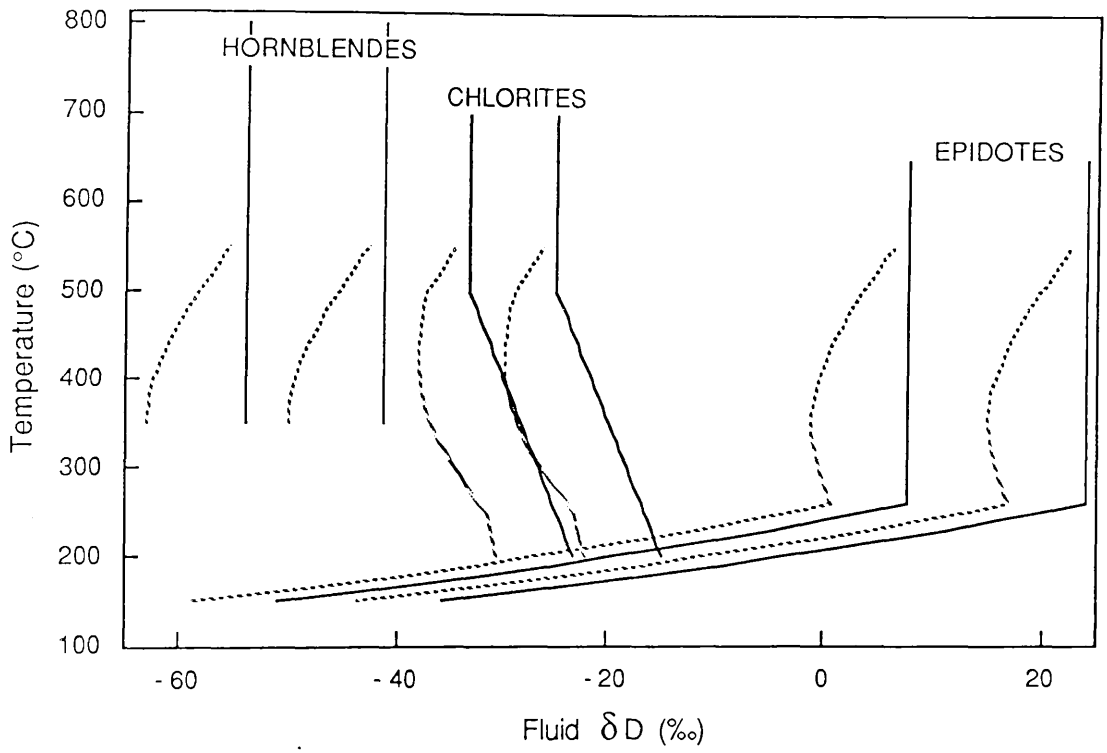

Fig. 4.2. Calculated hydrogen isotope compositions of fluid in equilibrium with the hornblendes, chlorites and epidotes within the MGS as a function of equilibration temperature.Each pair of curves represent the fluid in equilibrium with minerals with δD values $\pm 1\ \sigma_{n-1}$ from the mean composition shown in fig. 4.1. Solid lines show the fluid δD assuming that it fractionated hydrogen isotopes with the minerals in the same way as pure water, dashed lines show equilibrium fluid δD assuming that it fractionated hydrogen isotopes in the same way as a 4m NaCl solution. The fractionation factors used were from: Graham *et al.* (1984) - hornblende-water, Graham *et al.* (1980) - epidote-water, Graham *et al.* (1987b)- chlorite-water and Graham and Sheppard (1980) - 4m NaCl-water. This fractionation is not calibrated between 250 and 20°C and therefore the fractionations shown below 250°C should be regarded as highly uncertain.

Like the chlorites, the epidotes in the MGS can also only be interpreted as being in equilibrium with a fluid which has a distinctly higher δD than that which the amphiboles equilibrated with unless recourse is again made to amphibole equilibration at very low temperatures. The temperature at which the epidotes equilibrated with the fluid can be constrained to be less than 260°C because above this temperature the equilibrium fluid

composition would be unreasonably high (>0‰) unless extreme salt effects (2.4.5.B) reduced the epidote-fluid fractionation to very small values.

Provided the composition of fluid in equilibrium with the chlorite does not change significantly below 200°C the curves for the fluid in equilibrium with the chlorites and epidotes on fig. 4.2 will intersect at temperatures between 160 and 200°C, regardless of the salinity which is assumed for the fluid. This apparent equilibration temperature can be interpreted in one of three ways:

1. It is the temperature at which these minerals formed as a result of chemical reactions caused by the presence of the fluid.

2. It is the temperature at which chlorite and epidote last equilibrated during cooling from some higher temperature.

3. It is a false equilibrium, having no significance.

Petrographic evidence indicates that both of these minerals formed at the same time, but a formation temperature of <200°C would appear to be rather low for such an assemblage and a robust oxygen isotope equilibration temperature (see 4.5.2) indicates epidote formation at ~300°C, so this interpretation is not favoured. If these minerals were formed around 300°C then the interpretation of the apparent chlorite-epidote hydrogen isotope equilibration temperature as a cooling temperature would seem sensible. However, from examination of fig. 2.12 although even coarse epidotes could theoretically equilibrate with the pore fluid at temperatures as low as 200°C within less than a million years, it would appear unlikely that the fairly coarse chlorites in these rocks could re-equilibrate by diffusion with the pore fluid at temperatures below 300°C, even over periods of millions of years. Thus equilibration of hydrogen isotopes between these two minerals at 160-200°C during cooling seems unlikely and the apparent equilibration temperature is interpreted as being that of a false equilibrium.

It is clear, however, that the epidotes must have re-equilibrated hydrogen isotopes with some reservoir after formation at ~300°C, because according to the fractionation factors given by Graham *et al.* (1980) epidotes which last equilibrated at any temperature above 260°C with the high δD fluid which the chlorites equilibrated with at ~300°C would have much lighter hydrogen isotope ratios by up to 30‰ than those observed. As discussed above, H isotope exchange with both the hornblendes and the chlorites would be severely limited below 300°C, so that these minerals could not have been the exchanging hydrogen reservoir. However the fine grain size of the sericite (flakes often < 10 μm in diameter) would tend to facilitate hydrogen isotope exchange down to low temperatures (fig. 2.12), so that this mineral could represent the hydrogen reservoir with which the epidotes exchanged. Closed system re-equilibration of hydrogen isotopes between sericite and epidote during cooling would require the sericite to have originally been significantly heavier than it is at present, in order to account for the positive shift in epidote δD. Unfortunately the fractionation behaviour of muscovite below ~400°C is not well known (see 4.4.2), but unless the fractionation undergoes a reversal below 400°C, it would appear unlikely that the sericite in equilibrium with the high δD fluid at 300°C was

appreciably heavier than it is at present. Therefore it would seem that the sericite could not have been the reservoir with which the epidote equilibrated. The only other plausible exchange reservoir is free pore fluid within the rock. Mass balance constraints require that this fluid would have to have had a relatively high δD (greater than or equal to the that which is in equilibrium with the chlorite) and that it should be present in sufficient quantities to cause the ~30‰ shift in epidote δD. Thus the shift in epidote δD could have been achieved either by equilibration with a fluid with a similar δD to that which equilibrated with the chlorite, under conditions of relatively high fluid/epidote hydrogen ratios, or, a fluid of with a higher δD (up to 0‰?), under lower fluid/epidote hydrogen ratios. The only δD value that has actually been measured for fluid from fluid inclusions in these rocks is -25‰ which would tend to support the first alternative. Whatever the exact composition of this very late fluid, it has to be concluded that a high δD fluid was present within these rocks over a period during which temperature fell from at least 300°C (quartz-epidote vein temperature - see below), to temperatures below 200°C, or even as low as 160°C (fig. 4.14), when the epidotes closed to hydrogen isotope exchange.

It would seem therefore, that neither the amphibole, chlorite or epidote within the MGS rocks were in hydrogen isotope equilibrium with each other, when they passed through their closure temperatures. This disequilibrium is not due to these minerals originating from different rocks in which they have equilibrated with fluids of different δD, since a number of the separates of different minerals were obtained from the same hand specimen. Therefore the hydrogen isotope disequilibrium is on a mineral grain scale (fig. 4.3).

Examples of within rock disequilibrium are illustrated on δ–δ plots in fig. 4.4. Fig 4.4a shows that the amphibole and chlorite within these rocks could never have been in equilibrium at any temperature between 200 and 1000°C. This figure shows that either the chlorite is D enriched, or the amphibole is D depleted, by at least 20‰ relative to the equilibrium fractionation. Fig 4.4b shows the low apparent equilibrium temperatures for two chlorite-epidote pairs in these rocks, which as explained above can only be reasonably interpreted as false equilibrium temperatures. Similarly, although fig. 4.4c demonstrates that the epidote-amphibole pairs within these rocks could have equilibrated at temperatures around 150°C, these temperatures are also interpreted as a false equilibrium temperatures, for the same reasons as for the chlorite-epidote pairs.

Such examples of within rock disequilibrium provide unequivocal evidence that the hydrogen isotope composition of the pore fluid within the MGS varied with time. When the hornblendes last equilibrated with the pore fluid it must have had a $\delta D < -40‰$, yet when the chlorites and epidotes equilibrated with the pore fluid it must have had a $\delta D > -40‰$.

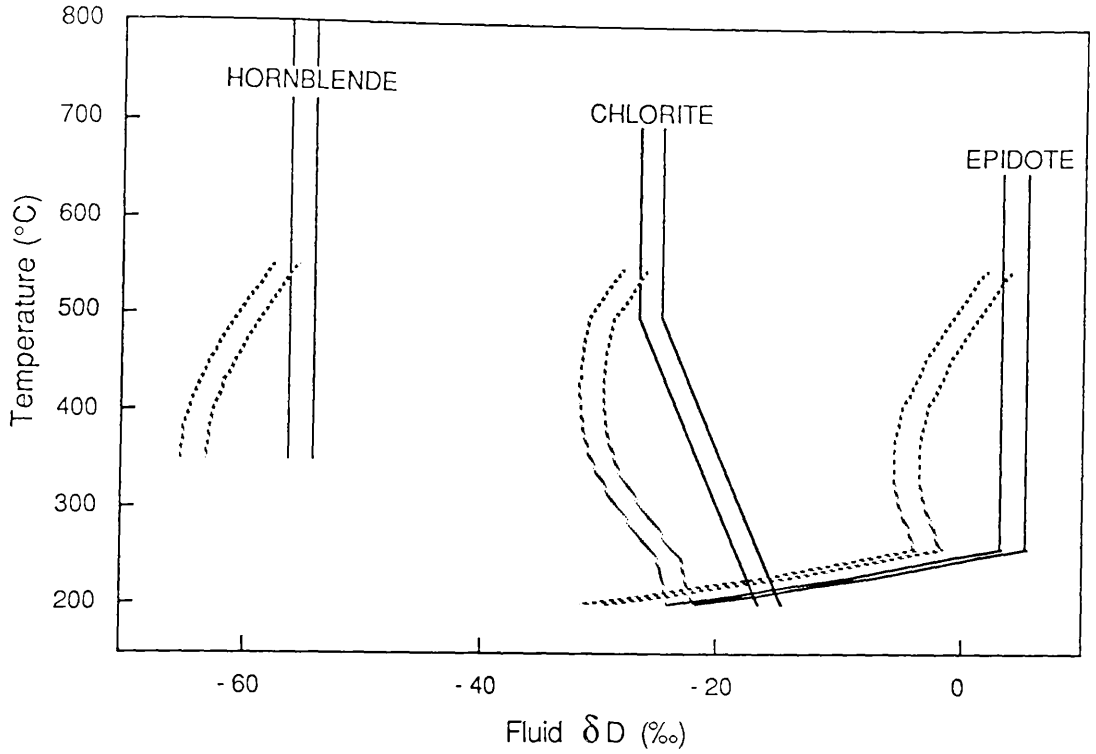

Fig. 4.3. Calculated hydrogen isotope compositions of fluid in equilibrium with the hornblende, chlorite and epidote within a single rock sample from the MGS (GJ.060) as a function of equilibration temperature. In this diagram each pair of curves correspond to the errors due the uncertainty in the hydrogen isotope analysis of the mineral. The solid and dashed curves correspond to a fluid behaving like pure water and a 4m NaCl solution respectively. The fractionation factors used are the same as in fig. 4.2.

Since the chlorites and epidotes are petrographically later than the hornblende, it seems sensible to conclude that the fluid that these minerals equilibrated with was present in the rock at a later time than the fluid with which the hornblende equilibrated. The alternative situation is that the fluid that equilibrated with the hornblendes, was present in the rock at a later time than the high δD fluid that equilibrated with the chlorites and epidotes. This situation can be shown to be untenable since, over the same time period, the closure temperatures of the hornblendes are well above those of the epidotes. Thus in this case resetting of the hornblende δD would also be expected to be accompanied by resetting of the epidote δD, which is obviously not the case.

Fig. 4.4. (next page) δ–δ plots for hydrogen isotope compositions of a. amphibole-chlorite, b. amphibole-epidote and c. chlorite-epidote pairs from individual rock samples in the MGS. Isothermal lines (lines along which the mineral compositions should lie if they are at equilibrium at that temperature), were drawn using the assumption that $10^3 \ln\alpha_{min\text{-}min} = \Delta_{min\text{-}min}$ (i.e. the lines have a slope of 1). In fig. 4.4a the isotherms for temperatures above 700°C were constructed assuming that the chlorite-water fractionation does not vary above 700°C. Fractionation factors used are those given in fig. 4.2. The salinity of the fluid does not affect the positions of the isotherms on these diagrams because such effects cancel when mineral-mineral fractionations are considered.

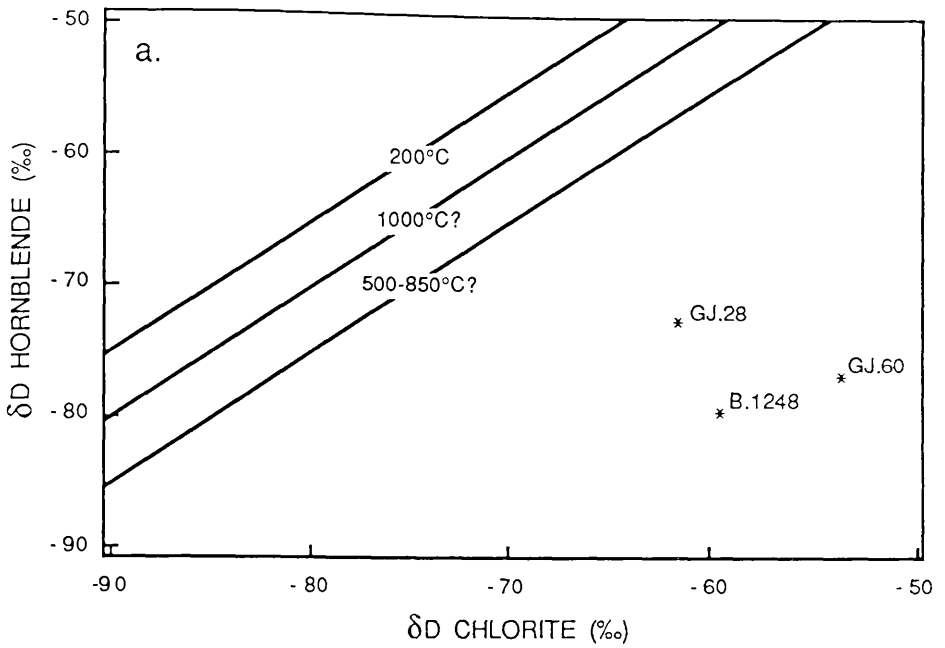
a.
200°C
1000°C?
500-850°C?
GJ.28
GJ.60
B.1248
δD HORNBLENDE (‰)
δD CHLORITE (‰)
-50
-60
-70
-80
-90
-90
-80
-70
-60
-50

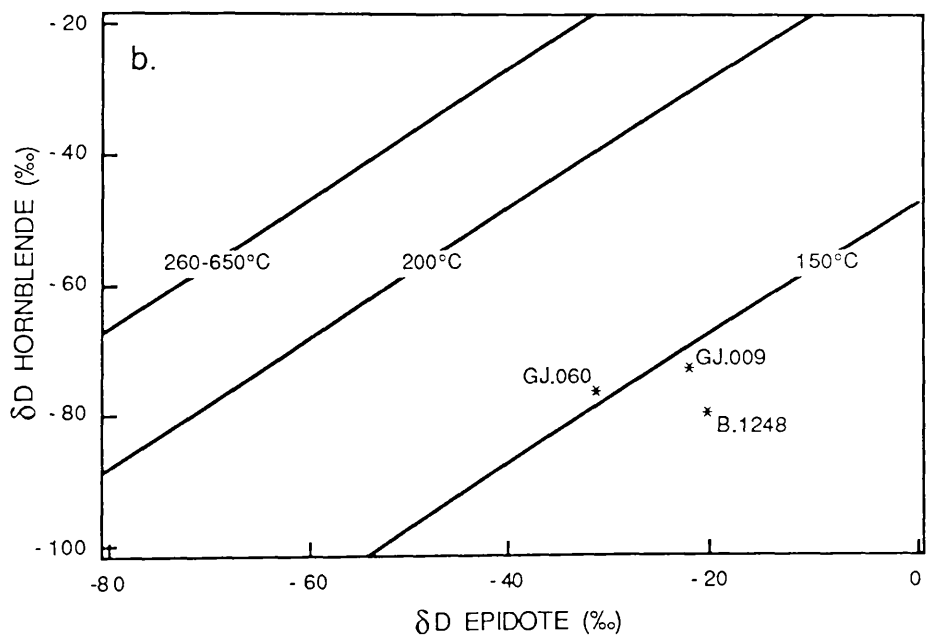
b.
260-650°C
200°C
150°C
GJ.060
GJ.009
B.1248
δD HORNBLENDE (‰)
δD EPIDOTE (‰)
-20
-40
-60
-80
-100
-80
-60
-40
-20
0

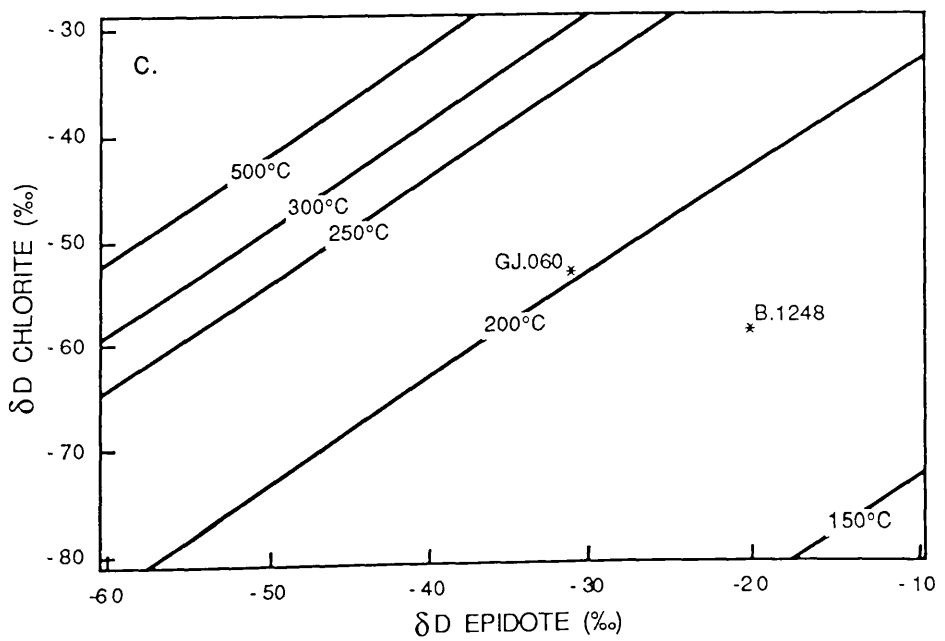
c.
500°C
300°C
250°C
200°C
150°C
GJ.060
B.1248
δD CHLORITE (‰)
δD EPIDOTE (‰)
-30
-40
-50
-60
-70
-80
-60
-50
-40
-30
-20
-10

It could also be suggested that all of these hydrous minerals formed during one event, in equilibrium with the early fluid of < -40‰, but that the chlorites and epidotes then re-equilibrated with the high δD fluid at a later time. Assuming that this later re-equilibration was to take place by volume diffusion, this suggestion can also be shown to be unlikely. According to fig. 2.12a the chlorite closure temperature to hydrogen diffusion in some of these rocks may be equal to, or even higher, than that of the hornblendes under the same conditions. If this was the case, then it would be unlikely that the chlorites would have all re-equilibrated with the fluid while the hornblendes had not. Therefore it can be concluded that the chlorites cannot have re-equilibrated with the later high δD by diffusion, in which case, equilibration with the high δD fluid must have taken place by a fast surface reaction. Since the chlorite itself is the product of a chemical reaction, it is difficult not to conclude that it was during this reaction that equilibration with the high δD fluid took place.

The fact that the petrographically early hornblendes which last equilibrated with the low δD (> -40‰) fluid, did not re-equilibrate hydrogen isotopes with the later high δD fluid, indicates that the hornblendes did not chemically react with the high δD fluid and also places some constraints on the temperature-time conditions at which the high δD fluid could have been present in the rock. This is because if it can be assumed that the hornblendes only exchanged H isotopes by diffusion, then the temperature-time conditions must lie on curves similar to those shown for hornblende in fig. 2.12. The position of the curves will depend on the effective grain size for diffusion and the degree of exchange, as well as fluid/mineral ratio, none of which are known at present. Nevertheless the degree of exchange can be assumed to be less than 90%, since re-equilbration has obviously not taken place. In addition, the effective grain size for diffusion is probably rather less than the physical grain size (up to 3-4 mm long) of the hornblendes (see 2.6.3). Therefore the upper time-temperature conditions may well be approximated by the upper hornblende curve in fig. 2.12a. If this is the case then at 300°C, the suggested temperature of epidote-chlorite formation (and thus presence of the high δD fluid in the system), the duration of fluid presence is constrained to be less than ~1 million years. Alternatively this fluid could have been present in the rocks at higher temperatures, but for a shorter time period. Since this fluid appears also have been present during cooling (because epidote re-equilibration has been shown to have taken place), the times for fluid presence at 300°C could be somewhat less.

From the association of sericite alteration in plagioclase with secondary chlorite and epidote, it is assumed that the sericite also developed at the same time and temperature (~300°C) as the chlorite and epidote. Thus the sericite will have equilibrated with the high δD fluid at some point, although as noted above, the fine grain size of the sericite means that it is likely that it last equilibrated hydrogen isotopes with the pore fluid at some temperature below its formation temperature. Unfortunately the hydrogen isotope fractionation between muscovite and water has not been calibrated below 400°C, so that the estimation of the δD of the fluid in equilibrium

with the sericites at lower temperatures is rather subjective. The estimation of the fluid δD is also further complicated by the fact that the Fe content of the sericites, which may also affect the fractionation (Suzuoki and Epstein, 1976), is unknown. Nevertheless, the fluid in equilibrium with a range of muscovite composition which might bracket the composition of the natural sericite is predicted to have a relatively high δD value (> -40‰) at 450°C (fig. 4.5). Therefore, unless the muscovite-water fractionation undergoes a reversal at lower temperatures, it seems unlikely that the sericites did not equilibrate with the high δD fluid. Projection of the Suzuoki-Epstein fractionation curve to lower temperatures, would indicate that these sericites were in equilibrium with a very high δD fluid (>0‰) at temperatures as high as 300°C, or slightly lower temperatures if salt effects are important. These estimates of equilibrium fluid composition are unrealistically high, since chlorites in the same rocks appear to be recording equilibration with fluids of <-15‰ (fig. 4.2), around 300°C. Therefore it seems likely that the fractionation behaviour of muscovite changes at temperatures below ~450°C. Some indication that this is the case is given by the 400°C data given by Suzuoki and Epstein which seem to indicate that the fractionation is increasing less at lower temperatures. From a consideration of the δD of fluid inclusions and coexisting sericite in a single rock (see 4.4.2), it would appear that at some temperature below 400°C the combined effect of fluid salinity and muscovite composition is to make the sericite-fluid fractionation approximately 20-25‰. Thus it can be concluded that the sericites did last equilibrate with the high δD (~-25‰) fluid which was in equilibrium with the chlorites and epidotes, although the exact temperature of last equilibration is not known (fig. 4.5).

The primary muscovite (J.149) from a granitic pegmatite of presumed metasedimentary origin (1.4.1 ultrabasic rocks) within the ultrabasic rocks of the L. Wheelaun body has a similar δD value to the later sericites. This could be explained in one of two ways (fig. 4.5); either (a.) this muscovite has equilibrated with the high δD fluid under the same conditions as the sericites, or (b.) this muscovite equilibrated at high temperatures (>500°C) with a lower δD fluid. High δD fluid was present at some time within this rock, because the primary biotite that coexisted with the muscovite is now chloritised. It is questionable, however, whether this coarse (up to 1 cm diameter flakes) muscovite could have re-equilibrated with the high δD fluid over a reasonable timescale (fig. 2.12). Re-equilibration could possibly have taken place if the effective grain size for diffusion was much less than the physical grain size (i.e. < 1 mm), as has been noted by Dodson (1973). If this muscovite <u>is</u> retaining the signature of equilibration of a lower δD fluid from higher temperature, the presence of such a low δD fluid within this pegmatite is not unexpected. This is because such low δD fluid was causing the growth of metamorphic hornblendes at in the surrounding MGS rocks (4.2, 4.6.2) at high temperatures, while metasedimentary derived melts would be expected to have had relatively low (~ -60 to -70‰) bulk δD values (3.5.4) in any case. Without further knowledge of the effective grain size for diffusion of hydrogen in coarse

muscovites it is impossible to predict whether or not the muscovite last equilibrated with a high δD fluid.

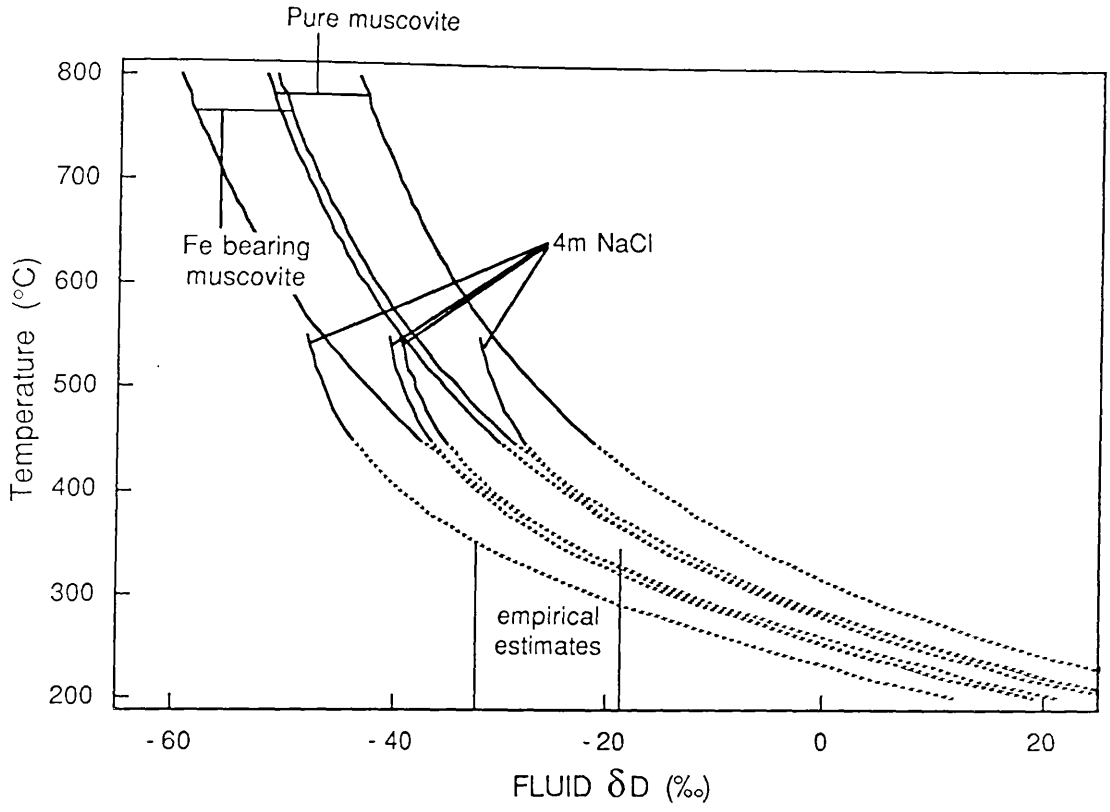

Fig. 4.5. Estimated δD of the fluid in equilibrium with the sericites in the MGS as a function of temperature. The curves for fluid in equilibrium with muscovite at temperatures >450°C use the modified fractionation factor (A.4.3) based on the Suzuoki-Epstein (1976) equation for a pure muscovite and the fractionation equation given by Suzuoki and Epstein (*ibid.*) for an Fe bearing natural muscovite with ~10% Fe (their eqn. 1). Curves below 550°C labeled '4m NaCl' show the δD of the fluid in equilibrium with these muscovites assuming that the fluid fractionated hydrogen isotopes in the same way as a 4m NaCl fluid, calculated using data from Graham and Sheppard (1980). These curves are projected to lower temperatures using the same fractionation equations (dashed lines). The solid curves at temperatures below 350°C show the empirical estimates of the δD of the fluid in equilibrium with the sericites at some point in this temperature range on the basis of fluid inclusion data given in 4.4.2, the effects of composition of the sericite and the fluid salinity on the fractionation are taken in to account in these empirical curves. Each pair of curves represents the fluid in equilibrium with minerals with δD values $\pm 1\ \sigma_{n-1}$ from the mean composition shown in fig. 4.1.

The water from two quartz samples from the MGS had δD values of -40.7 and -27.1‰ respectively (fig 4.1). As explained below in 4.4.2 the lower δD value is believed to be spurious, while the value of -27.1‰ for the other sample is believed to represent hydrogen isotope ratio of the high δD fluid which is inferred from mineral data to have caused the late retrogression in these rocks.

4.3 WITHIN-GROUP VARIATION IN HYDROGEN ISOTOPE COMPOSITIONS.

So far the hydrogen isotope data have been interpreted using the mean δD values for each mineral. It is clear however, that each mineral shows hydrogen isotope variations around this mean value which are significantly greater than analytical error. This section examines the hydrogen isotope data in terms of features such as rock type, rock alteration and mineral composition in order to attempt to identify the important factors controlling the within-group variation.

4.3.1 Within-group variation in hornblende δD.

The δD values of hornblende separates are related to sample number and to a number of features of the rock from which they originated in fig. 4.6.

The relation of hornblende δD to paragenesis.

One factor which might have controlled the δD of the hornblendes when they formed is whether they formed metamorphically or are igneous in origin. As discussed in 1.4.1 and 1.5 it is actually very difficult to distinguish between hornblendes formed by these two modes of origin, although in general it would seem that definite metamorphic hornblende is restricted to the ultrabasic rocks. Fig. 4.6c shows that the four hornblende samples which might be, or are definitely, of metamorphic origin have a limited range of δD (-73.2 to -65.4‰) which is within the range of δD for the other hornblendes which are inferred to be of igneous origin. Graham *et al.* (1984) have shown that the hornblende-water hydrogen isotope fractionation is independent of temperature in the range 350-850°C. Since this is also probably the temperature range in which hydrogen isotope exchange of hornblende with the surrounding medium is likely to have ceased, it can be concluded that the small range in δD of the metamorphic hornblendes must be due to the homogeneity of the hydrogen isotope composition of the fluid with which they equilibrated.

The hornblendes which are apparently of igneous origin range in δD from -80 to -60‰. From the limited data available it is not possible to be sure whether the amphibole δD is actually showing any significant variation amongst rock types, although it might be suggested that the hornblende in the intermediate rocks has lighter δD values than the hornblende in the cogenetic basic rocks. It is possible that such a difference in δD could have been caused by by magmatic differentiation in which D was preferentially fractionated into primary hornblende. Hydrogen isotope fractionation between hydrous minerals and melts is known to be a function of temperature, hydrogen speciation of the melt, and the chemical structure and composition of the melt (B.E. Taylor, 1986), as well as perhaps the composition of the mineral (Suzuoki and Epstein, 1976), but very little quantitative data are available. The only available datum on the hydrogen isotope fractionation between hornblende and melt is that given by Friedman *et al.* (1964), who measured a fractionation of 4.4‰ between a hornblende and rhyolitic glass (0.26 wt.% H_2O) in a natural rhyolite flow. If

this fractionation can be applied to hornblendes in the MGS, then the decreasing δD with the intrusion sequence could be explained by primary hornblende precipitation. However the melt which precipitated the MGS hornblendes, must have had a different chemistry, temperature and and probably water content from the rhyolite melt. Because of this, it is not possible to come to any definite conclusion as to whether the difference in δD between the basic and intermediate rocks is due to amphibole fractionation or not.

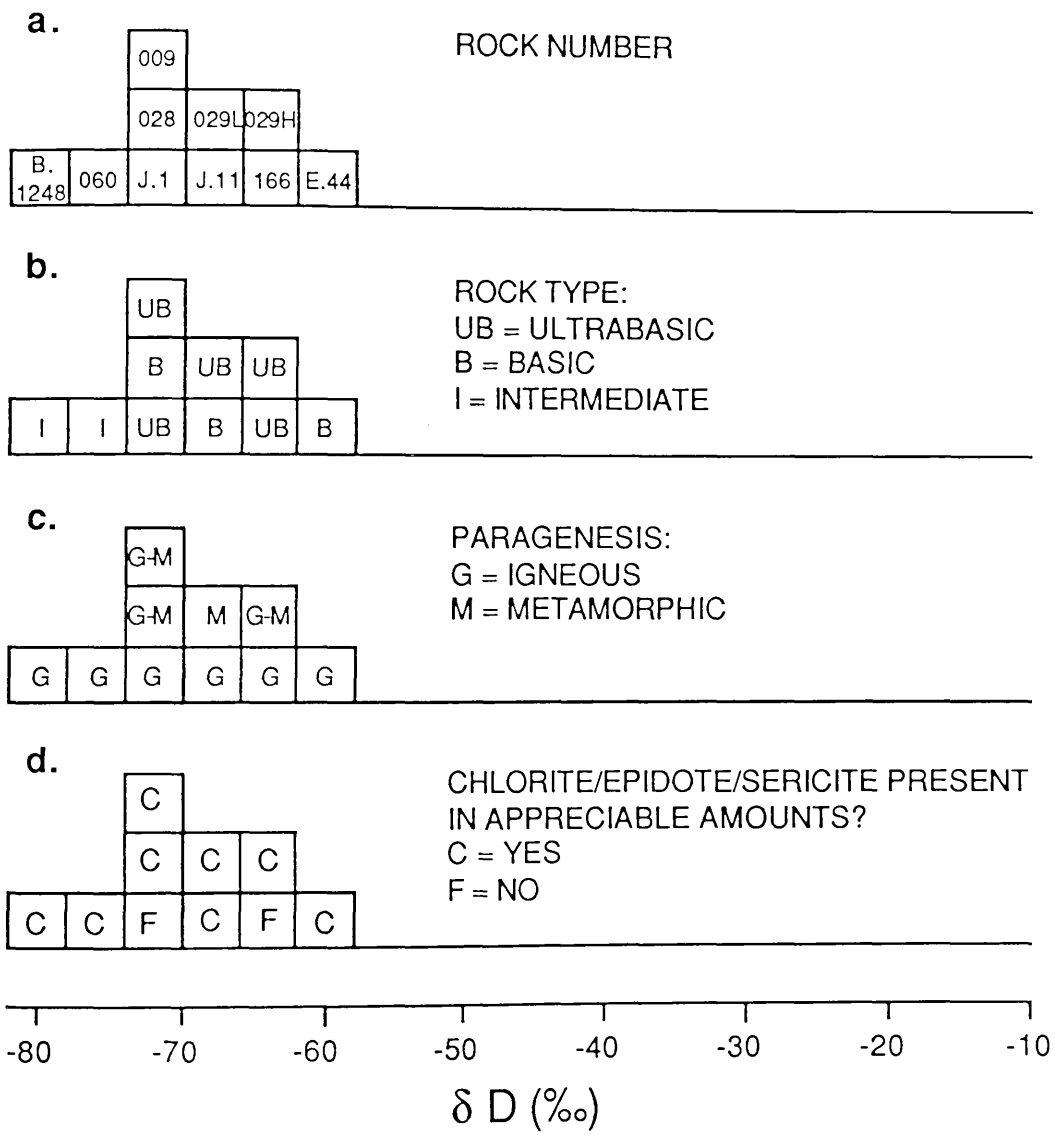

Fig. 4.6. δD of hornblendes from the MGS as a function of different features of the rock. In each histogram the sample position maps directly to the same position in the other histograms. In 4.6a the rock number for each sample is shown, 4.6b shows the rock type for each sample, 4.6c shows the inferred paragenesis of the hornblende, 4.6d shows whether or not the rock contains appreciable amounts of chlorite, epidote or sericite. Sample numbers with no prefix are those collected during this study which have a prefix GJ.. The hornblende from GJ.166 comes from band(e) a hornblende-pyroxene rich igneous layer in the sample.

The relation of hornblende δD to hornblende chemistry.

Suzuoki and Epstein (1976) suggested that the amphibole-water fractionation should be a function of the chemistry of the octahedral site, while Graham *et al.* (1984) suggested that the composition of the A-site cation could also be important in governing the fractionation. Some evidence that compositional effects may not be very important in controlling the hornblende δD in the MGS comes from the δD data on light and dense hornblende separates from a single rock (GJ.29). These two separates are chemically distinct (A.2.4), and can be correlated with the different hornblendes observed in thin section. The light fraction is presumed to represent the pale actinolitic hornblende which is replacing the pyroxene (plate 1.), while the heavy fraction contains more green or brown hornblende which corresponds to the pyroxene-free hornblende seen in thin section. Some of this pyroxene free hornblende may be primary. Although the early hornblende may have originally had a different δD value, it is presumed here that it rapidly re-equilibrated with the metamorphic fluid which caused the growth of the actinolitic hornblende. Thus any difference in δD between the two separates should be a result of the chemical composition alone. However despite the difference in chemistries, a two tailed t-test of duplicate hydrogen isotope analyses of the separates indicates that they are not significantly different in δD, even at very low confidence levels. This would suggest that variations in hornblende chemistry in this compositional range are not important in controlling the hornblende-fluid fractionation. However the Suzuoki-Epstein equation would predict that the light fraction should only be 1.9‰ richer in D than the heavy fraction, so the fact that the two separates have the same δD cannot be used as evidence to refute the Suzuoki-Epstein equation.

The water contents of the MGS hornblendes are plotted against δD in fig. 4.7. It can be seen that all but two of these hornblendes have higher hydrogen contents than any pure stoichiometric calcic hornblendes. This high hydrogen content must be due either to the hornblende structure containing excess hydrogen in some way (e.g. as H_3O^+ in the A-site; Hawthorne, 1981, or possibly as NH_4^+ in the A-site) or alternatively the presence of a hydrogen-rich impurity in the hornblendes. The second explanation is preferred, since XRD analysis of the GJ.29-L separate indicates that minor chlorite is present. However this chlorite could not be observed in the separate, either with a binocular microscope, or in thin section at the highest magnification (× 400), indicating that the chlorite must be very finely disseminated. This might be corroborated by the fact that attempts to remove the chlorite contaminant from the separate by steeping in 4M HCl for up to 8 days were unsuccessful. No obvious hydrous contaminant was observed with a binocular microscope in any of the hornblende separates, and it is considered likely that these samples also contain submicroscopic chlorite. If the contaminant is chlorite, it can be calculated that the amount necessary to cause the increase in hydrogen yield is very small (fig. 4.7 - a 30% contribution to the total hydrogen translates to ~8 wt.% ≈ 8 volume % of chlorite). The presence of chlorite in the separates would tend to increase the measured δD value relative to that of the pure hornblendes, because the

chlorites all have heavier δD values than the hornblendes. The shift in δD that a chlorite contaminant would cause can be calculated using mixing equations based on those described in 4.6.1. If it is assumed that the chlorite contaminant has a δD similar to that of an "average" MGS chlorite (≈ -57‰; fig. 4.1), and that the pure chlorite and hornblende have water contents of 10.8 and 2.16 wt.% H_2O respectively, then it can be calculated that the δD value measured for all but one of the hornblende separates will not be significantly (i.e. >2‰) greater than the δD value of the pure hornblende. These calculations show that chlorite contamination in the hornblende separate from GJ.028 could have increased the measured δD value by ~5‰ relative to the pure hornblende.

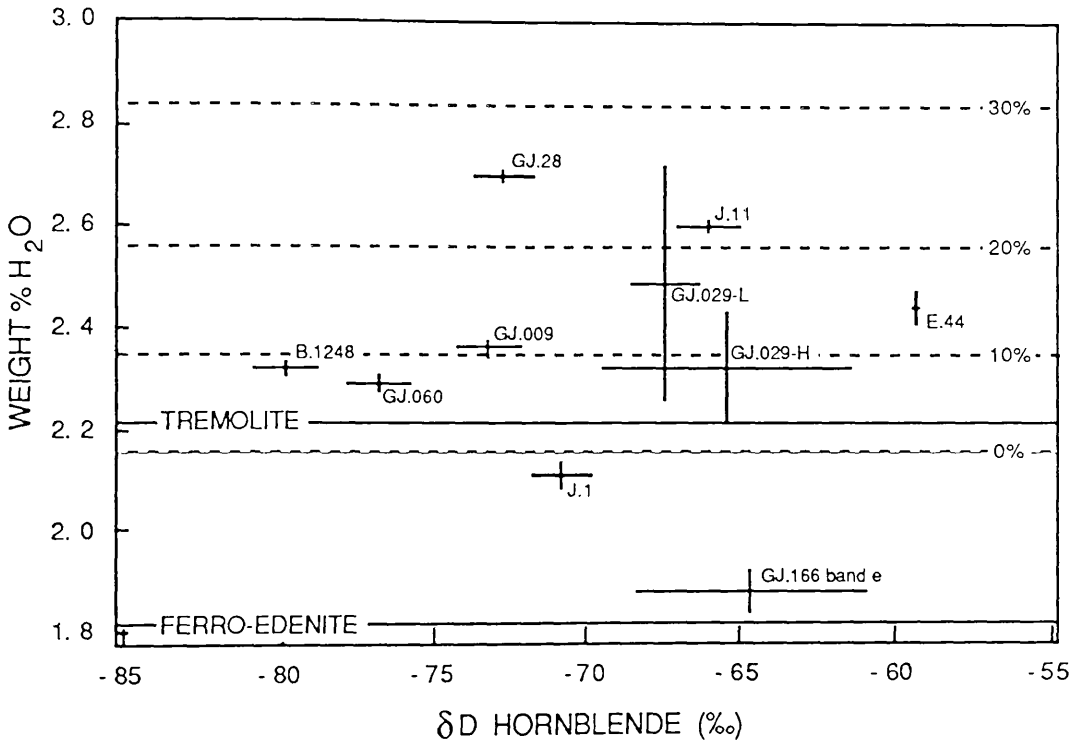

Fig. 4.7 δD plotted against estimated water content for hornblendes from the MGS. The lines labeled tremolite and ferro-edenite are the calculated water contents of pure stoichiometric tremolite and ferro-edenite which together bracket the range in possible water contents of the calcic amphiboles. The lines labeled with percentages are the calculated % of hydrogen which has been derived from chlorite assuming that chlorite is the only contaminant and that the chlorite has a hydrogen yield of 6 μM mg^{-1} (10.8 wt% H_2O) and the hornblende has a yield of 1.2 μM mg^{-1} (2.16 wt% H_2O).

The presence of chlorite contamination appears to be related to whether or not the rock has been affected by the high δD fluid (4.2), since as explained in the next section the two hornblendes which have apparently normal hydrogen contents (J.1 and GJ.166 band(e)) appear to be the only samples which have not been exposed to the high δD fluid. The recognition of fine chlorite within the hornblende is important as such alteration has been suggested to reduce the effective grain size for diffusion in hornblendes (Onstott and Peacock, 1987). A smaller effective grain size for diffusion could make the hornblendes more prone to re-equilibration with the late fluids. Neglecting the two samples which are thought to have not been

affected by the high δD fluid (J.1 and GJ.166 band(e)) and the hornblende from GJ.28 there may appear to be a vague correlation of δD with water content, which if it was real, would indicate that chloritisation of the hornblende was an important factor in controlling the degree of exchange with the late high δD fluid (see below).

The relation of variation in hornblende δD to exchange with the high δD fluid.

In 4.2 it was shown that a high δD fluid which was not in H isotope equilibrium with the hornblendes was present in chlorite/epidote/sericite bearing MGS rocks at temperatures of 300° to ~160°C, and possibly at higher temperatures. It is conceivable that part of the hydrogen isotope variation in both the igneous and metamorphic hornblendes could be due to partial hydrogen equilibration with this fluid. The strong correlation of the degree of chloritisation of biotite, the sericitisation of plagioclase and the alteration of biotite or hornblende to epidote with the abundance of bubble planes in these rocks, suggests that the chief factor controlling the extent of development of these retrograde minerals is the supply of fluid. It would follow therefore, that rocks which do not contain these alteration minerals but do contain their precursors, must have never been exposed to large amounts of high δD fluid. If this was the case then it would be expected that the hornblendes within the rocks with relatively unaltered biotite and plagioclase should have exchanged least with the high δD fluid. Exchange with the high δD fluid would tend to cause D enrichment in the hornblendes. Therefore if significant amounts of exchange had taken place in the hornblendes in more altered rocks, this might be indicated by these hornblendes having higher δD values than the hornblendes the less altered rocks. Fig. 4.6d shows the δD of the hornblendes in relation to to the presence or absence of chlorite, epidote or sericite in the enclosing rock. It can be seen that hornblendes from the two freshest samples fall in the middle of the range of δD of all the hornblendes, suggesting that the δD of the other hornblendes, or at least those with with lighter δD values have not been greatly altered by exchange with the high δD fluid.

The maximum value of F (the fractional approach to equilibrium - see 2.6.1) can be estimated by assuming that the most D rich hornblende (E.44) has had its δD value increased from the lowest value for a hornblende in the basic rock (GJ.28) and that the hornblende which would be in equilibrium with the high δD fluid would have a δD of -48‰ (i.e. high δD fluid ≈ -25‰ and is pure water fractionating ~23.1‰ heavier than the coexisting hornblende - Graham *et al.*, 1984), so that:

$$F = \frac{-59.2 + 70.8}{-48 + 70.8} \approx 0.51 \ .$$

This maximum value of F would be reduced if the hornblende which would have been in equilibrium with the fluid had a higher δD, because of salt effects reducing the magnitude of the equilibrium fractionation (see below).

If hydrogen isotope exchange of the hornblendes with the high δD fluid was diffusion controlled (see 2.6), then if all other controlling parameters were equal, the degree of exchange (F) attained in a given time would be expected to be inversely proportional (though not linearly) to the grain size of the mineral. However this would only be the case if the physical grain size of the mineral was equal to the effective grain size for diffusion. In order to test this hypothesis, that grain size might be an important factor controlling the δD variation in the MGS hornblendes, the maximum, minimum and average hornblende half c-axis lengths were estimated in thin section and are plotted against δD in fig. 4.8. Where the minimum c-axis lengths were estimated to be less than the grain size of the separate used for mineral separation, the grain size of the mineral separate was used as the minimum grain size, since grains smaller than the separate size will have been excluded from the analysis. The data points for the hornblendes in J.1 and GJ.166 band(e) are not included in the curves because from the previous discussion, it would seem likely that these hornblendes were never exposed to the high δD fluid, so that there is no reason why the data for these samples should lie on any trend seen for the other samples. Fig. 4.8 shows that there is a vague trend of increasing δD with decreasing grain size, which could indicate that exchange with the high δD fluid could have been greater in the finer grained hornblendes, assuming that all the hornblendes had initially had similar δD values. However, if the relatively high δD of the hornblende in GJ.166 can be considered as pristine, it is clear that some relatively high δD hornblendes were present prior to any exchange with the high δD fluid, so that the high δD values in the fine hornblendes cannot be unequivocally interpreted as being due to exchange with the high δD fluid.

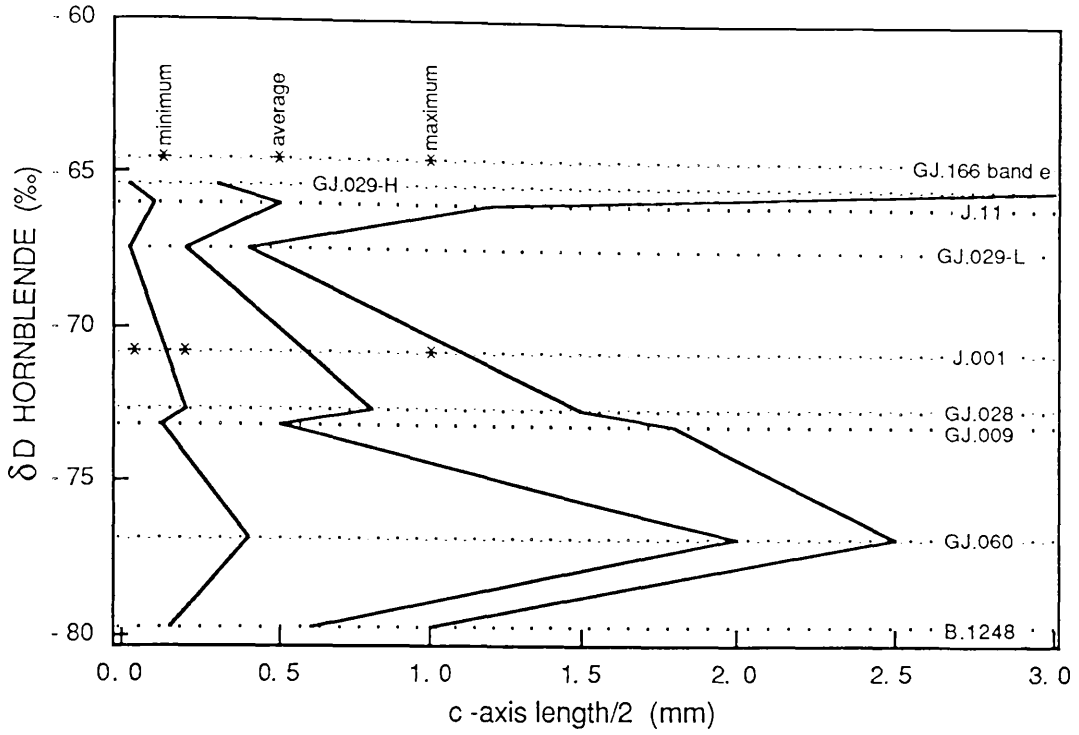

Fig. 4.8 Estimates of maximum, minimum and average half c-axis lengths of MGS hornblendes from the Cashel-Recess area, plotted against δD value. The grain sizes were measured in thin section and where the minimum c-axis length in thin section is less than the minimum grain size of the separate the half size of the minimum separate size is substituted for the minimum grain size, for reasons given in the text.

4.3.2 Within-group variation in chlorite δD.

The chlorites have a very restricted range in δD from -61.4 to -48.8‰. Because the chlorite-water fractionation appears to be only weakly dependent on temperature between 500 and 200°C (Graham *et al.*,1987b), this homogeneity in chlorite δD must reflect the relative homogeneity in δD of the high δD fluid across the area. The δD values of chlorite separates are related to the rock number and to the rock type in fig. 4.9.

Relation of chlorite δD to rock type.

It can be seen that there is no clear distinction between the δD values of chlorites from different rock types, indicating that rock type is not an important factor in controlling chlorite δD.

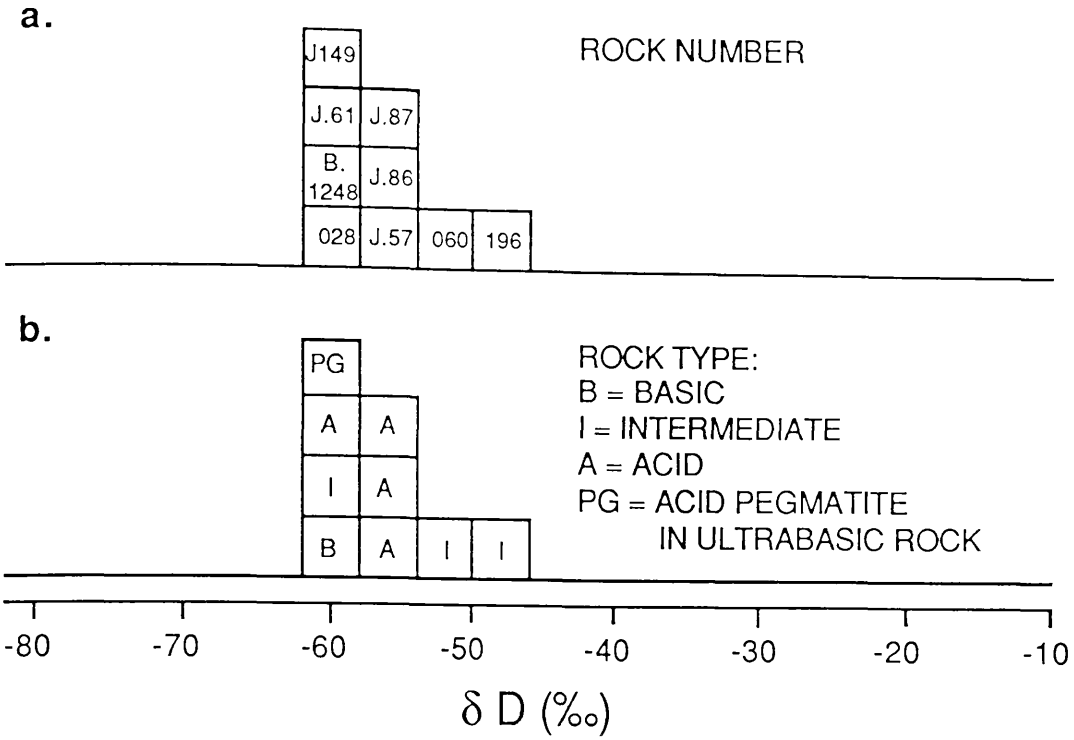

Fig. 4.9 δD of chlorites from the MGS as a function of rock type. In each histogram the sample position maps directly to the same position in the other histograms. In 4.8a the rock number for each sample is shown, while the 4.8b shows the rock type for each sample Sample numbers with no prefix are those collected during this study, which have a prefix GJ..

Relation of chlorite δD to water content.

The hydrogen yield of the chlorites is plotted against δD in fig. 4.10 (compare with fig. 3.4). It can be seen that like the chlorites in the Dalradian metasediments described in chapter 3., many of these MGS "chlorites" gave low hydrogen yields compared with pure stoichiometric chlorites. This indicates that these chlorites probably contain significant quantities of an impurity with a low H content. This impurity is most likely to be unchloritised biotite, which the chlorite is seen to be replacing in thin section, although some H free material such as rutile or quartz could also be present. It might be questioned whether it was correct to have assumed in 4.2 that these "chlorite" separates fractionated hydrogen with the coexisting fluid in the same way as pure chlorite (Graham *et al.*,1987b). Two points can made to justify this assumption. Firstly it can be seen that samples J.86 and J.87 which came from the same outcrop have δD values which are identical within experimental error, yet have significantly different hydrogen contents. If it is assumed that the δD of the fluid which caused chloritisation was homogeneous on an outcrop scale, then it can be seen that while the different samples may have significant differences in the proportion of chlorite present, this does not appear to have affected the δD of the samples. Therefore either the material which is contaminating the chlorite contains no hydrogen (although no such contaminant was observed in any quantity), or, the the contaminant is biotite which has a δD value which is not much more negative than the chlorite which is replacing it. Secondly it can be seen that the range of δD of the more chlorite rich separates encompasses

the δD values of the less chloritised samples. Therefore, even if the less chlorite rich samples had been excluded from the discussion in 4.2, the conclusions drawn from the H isotope data would not have been any different.

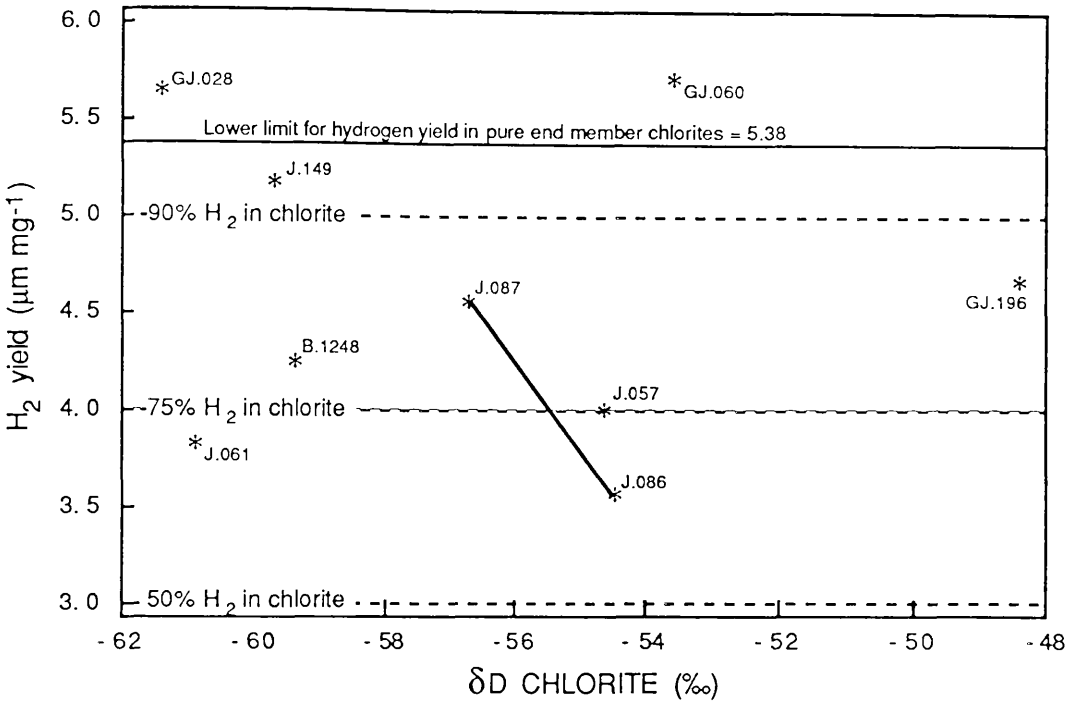

Fig. 4.10. δD plotted against hydrogen yield for chlorite separates from the MGS. Also shown are the estimated proportion of hydrogen which was evolved from chlorite assuming mixing between a biotite end member yielding 2 μm mg^{-1} hydrogen and a chlorite end member yielding 6 μm mg^{-1} hydrogen. The two samples joined by a tie line come from the same outcrop.

It is interesting to note from the discussion above, that if the contaminant in the chlorite separates is unchloritised biotite, that it must have δD values similar to that of the chlorite which is replacing it. It is unlikely that the biotite originally had such high δD values (-65 to -55‰) since biotites which originally crystallised in H isotope equilibrium with the igneous hornblende in the MGS might be expected to have had δD values similar to, or lower than than the coexisting hornblendes (O'Neil and Ghent, 1975; Kuroda *et al.*, 1986), unless they were very Mg rich, which is unlikely in the intermediate and acid rocks. The fact that the estimated δD of the unchloritised biotite is significantly higher than that of the hornblendes, suggests that it may have undergone hydrogen isotope exchange to higher values, presumably with the high δD fluid. Unfortunately there is no information on the biotite-water hydrogen isotope fractionation below 400°C which could be used to substantiate this suggestion.

4.3.3 Within-group variation in epidote δD.

The epidotes have a wide range of δD from -31.1 to -10.8‰ and have by far the largest within-group variance of δD any of the MGS minerals. The δD values of epidote separates from the MGS are related to rock number and rock type in fig. 4.11.

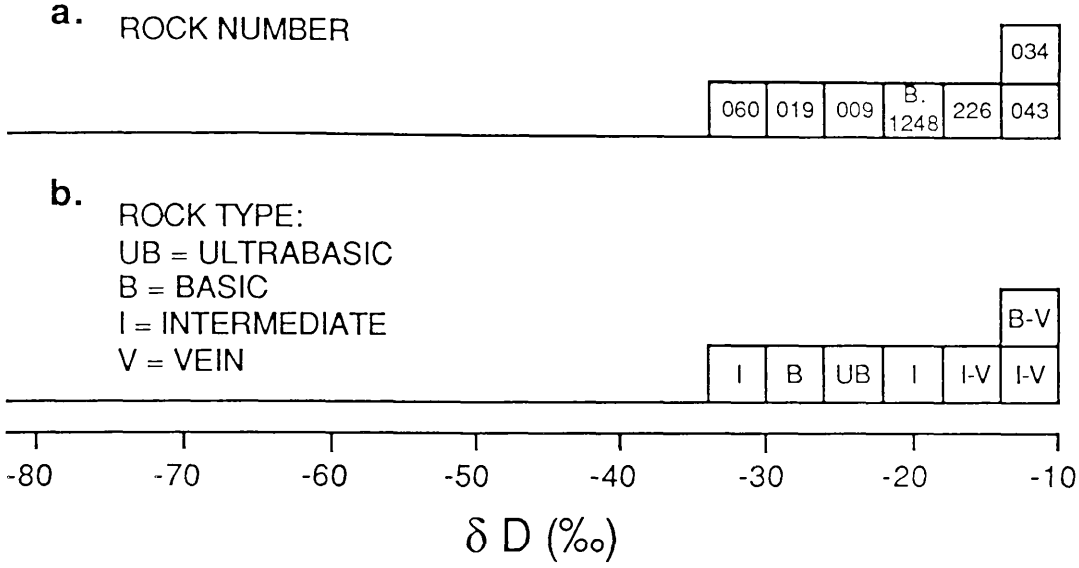

Fig. 4.11 δD of epidotes from the MGS as a function of rock type. In each histogram the sample position maps directly to the same position in the other histograms. In 4.11a the rock number for each sample is shown, while the 4.11b shows the rock type for each sample Sample numbers with no prefix are those collected during this study, which have a prefix GJ..

Relation of epidote δD to epidote chemistry.

In order to examine the effects on δD of the hydrogen content of the MGS epidotes, these two variables are plotted against each other in fig. 4.12. It can be seen that three of the epidotes have hydrogen contents which are probably within the range for pure stoichiometric epidotes when the analytical errors are taken into account. The other four epidotes have rather higher hydrogen contents which must be due to contamination with some other hydrogen-rich phase. Possibly this could be fluid in fluid inclusions, or small amounts of chlorite. No fluid inclusions have been observed in the epidotes and it seems more likely that the contaminant is chlorite, especially since epidote is often seen growing with chlorite in thin section. If the contaminant is chlorite, only very small amounts are required to account for the increase in hydrogen content (fig. 4.12 - a 30% contribution of hydrogen from chlorite translates to ~7 wt.% or ≈ 7 volume % chlorite), so that its presence could have have been overlooked during binocular microscope examination of the mineral separates for purity with. Because all chlorite equilibrated with the high δD fluid has lighter δD values (fig. 4.1), the effect of the presence of chlorite on the measured δD of the epidote will be to reduce it relative to that of the pure epidote. Projection lines to pure epidote end members are shown in fig. 4.12. It can be seen that if the high hydrogen yield of some of these epidotes is due to the presence of

chlorite, then the δD values of the pure epidotes may be even heavier, by up to 10‰ in some samples. Nevertheless it can be seen that the variation in δD measured for the epidote separates cannot be attributed to variation in the amounts of chlorite present, because the spread in δD calculated for the pure epidotes is not significantly less than the spread for the mineral separates.

The low hydrogen yields of two of the epidote separates (B.1248 and GJ.226) can probably be attributed to the presence of small quantities of quartz in the separates.

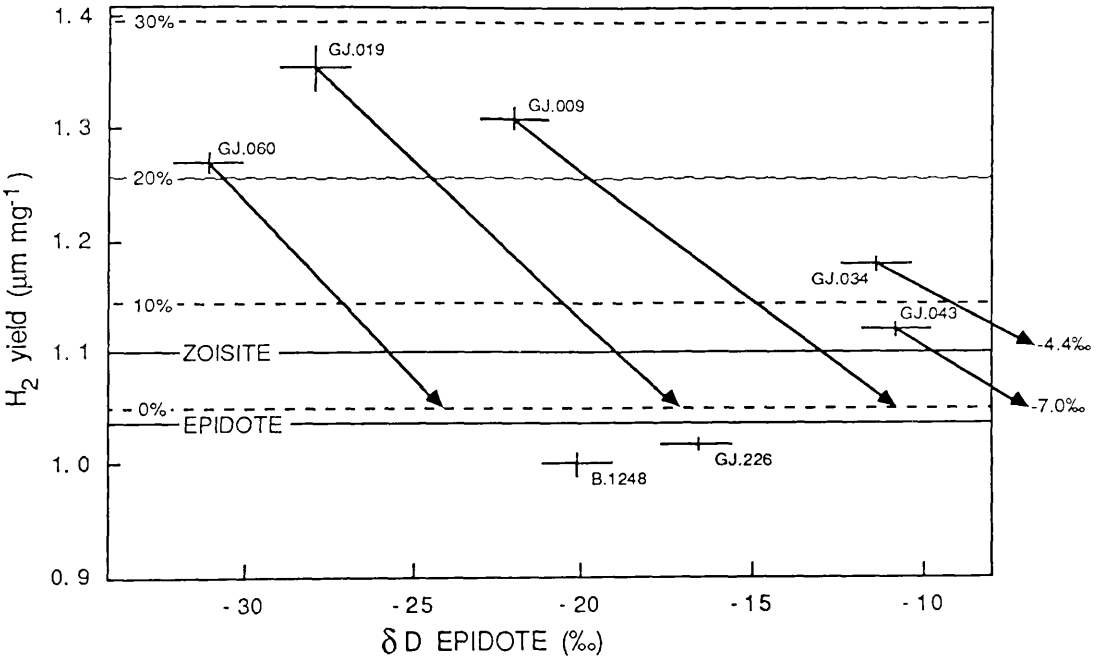

Fig. 4.12 δD plotted against yield of hydrogen for epidotes from the MGS. The lines labeled EPIDOTE and ZOISITE are the calculated water contents of pure stoichiometric epidote and zoisite which together bracket the range in possible water contents of the epidote minerals. The lines labeled with percentages are the calculated % of hydrogen which has been derived from chlorite and the arrows are projection lines to pure epidote compositions. Both were constructed assuming that chlorite is the only contaminant, that the chlorite has a δD = -57‰ and a hydrogen yield of 6 μM mg^{-1} and the epidote has a yield of 1.05 μM mg^{-1}. It should be noted that the projection lines do not follow the mixing lines between chlorite and epidote, which are curved on this plot. The error crosses show the analytical uncertainty in each of the variables.

In fig. 4.13 the δD is plotted against the content of the Fe end member for the four epidotes which have been analysed with an electron microprobe. It can be seen that there is no relationship between Fe content and δD.

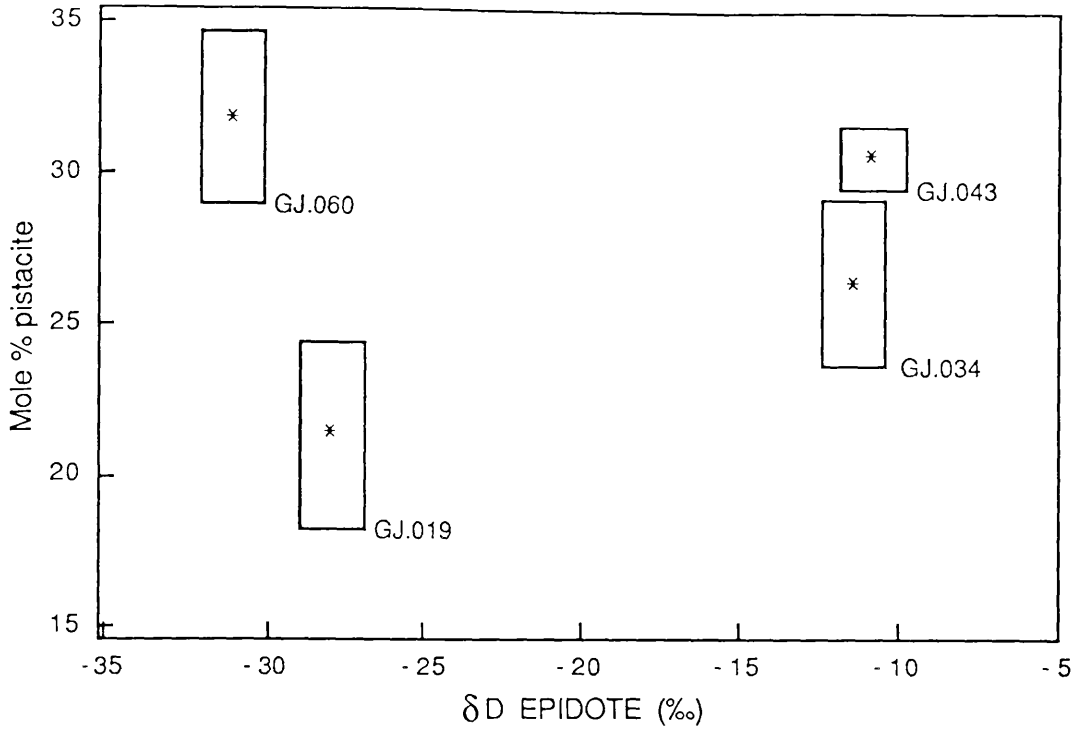

Fig. 14.13 δD plotted against mole % of pistacite ($Ca_2Fe_3Si_3O_{12}OH$) for four MGS epidotes. The boxes around the points correspond to ±1 standard deviation (σ_{n-1}) for each of the variables.

The relation of epidote δD to the conditions of exchange with the high δD fluid.

From the discussion in 4.2, it would appear that all the epidotes must have exchanged hydrogen isotopes with a high δD fluid at temperatures below 260°C, prior to passing through their closure temperatures. This being the case, the wide range in δD of the epidotes could be explained in terms of exchange with this fluid, with differences between samples in either

a. fluid salinity.

b. fluid δD.

c. temperature at which equilibration last took place (≈closure temperature).

d. fluid/rock ratios.

or a combination of these variables.

If closure temperature and fluid δD were the same for all the epidotes and fluid/rock ratios were high everywhere, then it would seem unlikely that salt effects alone could have been the cause of the 20‰ variation between epidotes, because no salt effect of such a magnitude has yet been identified.

Variation in fluid δD at constant salinity, temperature and high fluid/rock ratio is also considered as an unlikely cause of variation in epidote δD. This is because the fluid would need to vary by up to ~20‰

between samples (fig. 4.14), yet the epidotes with the highest and lowest δD values are located only 250 m apart. It seems unlikely that the fluid could vary so much in hydrogen isotope composition over such a small distance at the same instant, especially since both samples show evidence that the late fluid infiltrated through the rocks and has not been locally derived (see 1.4.1). In addition, the relative homogeneity in chlorite (4.3.2) and sericite (see below) δD also indicate that the fluid had a relatively constant δD at the closure temperatures of these two minerals.

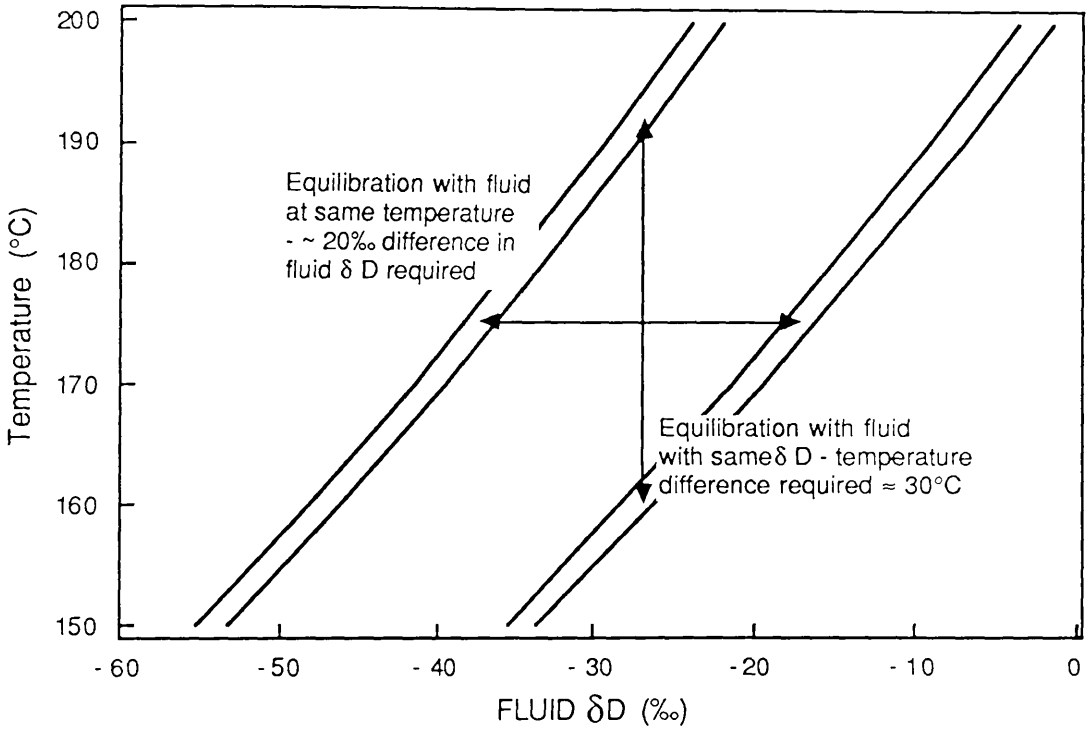

Fig. 4.14 δD of fluid in equilibrium with the two epidotes from the MGS with the lowest and highest δD values, at low temperatures, plotted as a function of temperature. Each pair of curves corresponds to the variation due to analytical uncertainty in the measurement of δD. It is assumed that the fluid is fractionating hydrogen isotopes in the same way as pure water. As long as the salt effects were the same in each sample the both curves would move horizontally by approximately the same amount at the same temperature. Therefore the temperature or fluid δD difference that would be required to explain the difference in epidote composition will not be affected. The epidote-water fractionation of Graham *et al.* (1980) was used to calculate the curves.

If fluid salinity and δD were the same for all samples, and fluid/rock ratios were high throughout, a 30°C difference in the temperature at which the epidotes in different samples last equilibrated with the fluid could account for the difference in δD between the most D depleted and D enriched samples (fig. 4.14). If this was the case the D depleted sample would have closed at higher temperatures. If the epidotes equilibrated with a pure water fluid with a δD =-25‰ then the most D rich sample is calculated to have last equilibrated at ~160°C (or 154°C if the value of -4.4‰ is used for this epidote; see fig. 4.12). If the fluid was saline this could increase or decrease the equilibrium temperature depending on the sign of the salt effect. In 4.4.2 it is estimated that the magnitude of the salt effect at the temperature at which the chlorites last equilibrated with the high δD fluid

was ~12‰ ($\Delta_{water\text{-}fluid}$). Because solute-solvent interactions vary as a function of temperature (Graham and Sheppard, 1980), it is not possible to assume that this was the magnitude of the salt effect at the temperature at which the epidote last equilibrated. Nevertheless according to Graham and Sheppard (*ibid.*) H isotope salt effects appear to decrease with decreasing temperature below ~ 300°C, so that this value might be used as an upper limit for the salt effect at the temperature of epidote equilibration. Using 12‰ as the value of the salt effect, the most D rich sample is calculated to have last equilibrated at 182°C with a fluid with a $\delta D = -25‰$.

If the water/epidote ratio is high throughout, a 30°C difference in closure temperature between different epidotes could only be accomplished by a change in the effective grain radius by a factor of more than 2 (fig. 4.15).

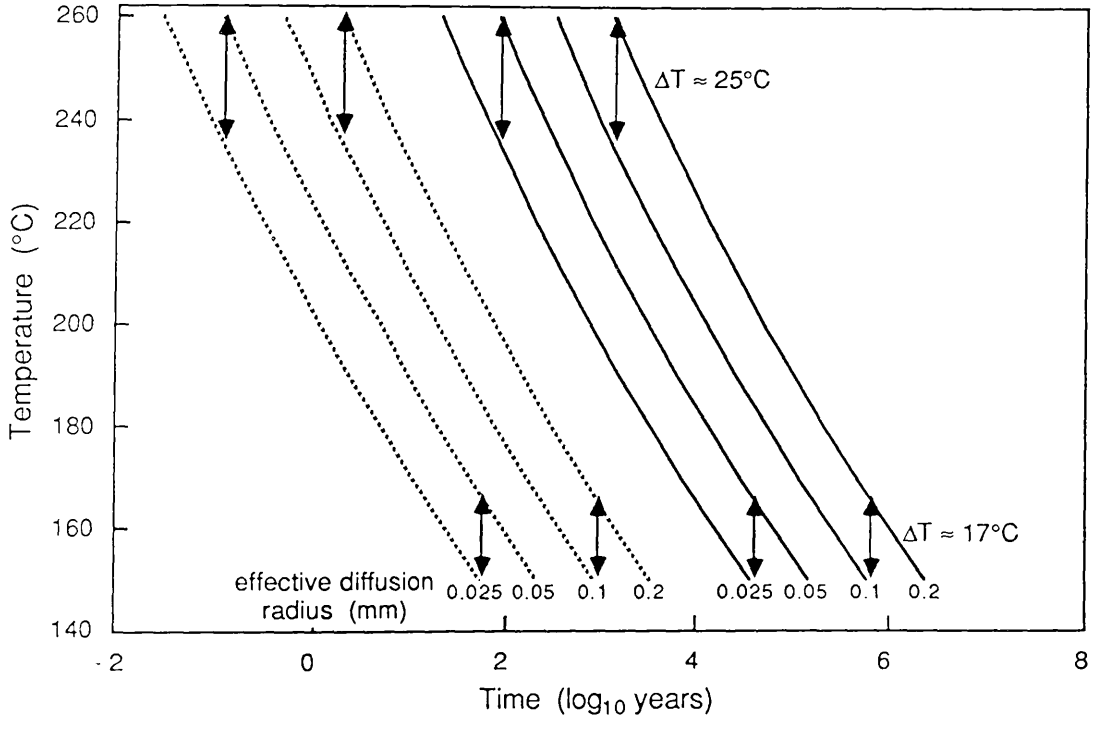

Fig. 4.15 Time required for epidote grains of different effective diffusion radii to reach 5% (F=0.05, dashed lines) and 90% (F=0.9, solid lines) hydrogen isotope exchange with the surrounding pore fluid plotted against temperature. Curves calculated using equations (5.33,5.34) from Crank (1975) assuming a cylindrical diffusion geometry. The diffusion parameters used are given in A.5.1 [15]. From the definition of closure temperature given in 2.6.3 a grain closes to diffusion when exchange effectively ceases (i.e. $F \rightarrow 0$ over the time period in question). This figure shows that the difference in temperature at which grains of different sizes reach a certain value of F in a given time period is independent of either F or the time period and is only dependent on grain size. Thus the difference in closure temperature between the grains of different sizes will always be a constant value, whatever the actual conditions of closure, provided the exchange conforms to the boundary conditions of Crank's model.

From fig. 4.16 it may be seen that, excluding sample GJ.34, the epidotes do in fact show an approximately twofold reduction in average physical grain radius from the low δD to the high δD samples, a correlation which could be taken to indicate that differences in closure temperature between grains were the cause of δD variations in the epidotes. However the variation in grain size used for mineral separation (fig. 4.16) may mean that the δD of

the separate could be different from that of the "average grain", in which case this correlation may be of dubious significance. This interpretation of the grain size δD correlation also assumes that the physical grain size of the epidote grains approximates to the the effective grain size for diffusion, which may not necessarily be the case, although the fine average grain size of the epidotes increases the likelihood of this being the case (2.6.3 the effect of grain size...).

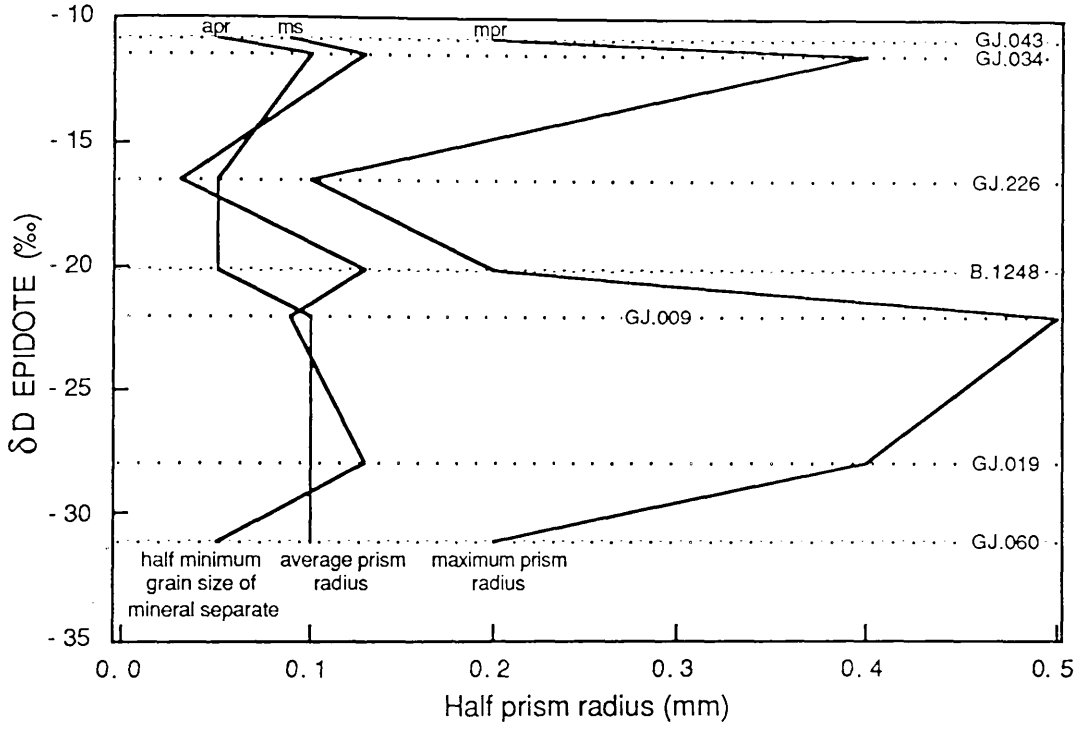

Fig. 4.16 Estimated maximum and average prism radius and half minimum grain size of mineral separates for MGS epidotes plotted against δD. The maximum and average prism radii were estimated from thin sections. In practice it is often difficult to distinguish the orientation of the epidote grains in thin section and in these cases these measurements are for the half widths of all grains observed in thin section.

If fluid salinity, δD and temperature were the same for all samples during exchange with the high δD fluid, then variations in fluid/epidote hydrogen ratio could also have caused the variation in epidote δD. In this case, epidotes which experienced higher fluid/epidote ratios during the period in which exchange took place would show the greatest shifts in δD (fig. 2.17). Recent studies suggest that it is likely that microcracks may remain zones of high permeability and porosity, even after the main phase of sealing has taken place (Hay *et al.*, 1988 and pers. comm.), so that time integrated fluid/epidote ratios might be expected to have been high in the microcracks. On the other hand, the only fluid which would have been available for H isotope exchange with the epidotes within rocks is that which was present along grain boundaries, the volume of which would have been small at any one time. The rate of recharge of this fluid with fresh unexchanged fluid would probably have been very low, because of the low permeability of narrow grain boundaries, so that the time integrated fluid/epidote ratio for the epidotes within rocks is expected to have been much lower that that for the epidotes within the microcracks. Thus if the fluid/epidote ratio is the

dominant factor in controlling the shift in epidote δD it would be predicted that epidotes with the highest δD values should occur in microcracks. This is exactly what is observed (fig. 4.11), strongly supporting this hypothesis.

Thus it would appear that variations in either closure temperature, or fluid/epidote ratio could have caused the δD variation in the epidotes. At present it is difficult to choose between these possibilities, although this might not be necessary since it is possible that the δD variation could also have been caused both factors working together.

4.3.4 Within-group variation in plagioclase (sericite) δD.

The δD values of plagioclase separates from the MGS are related to rock number and rock type in fig. 4.17. Like the chlorites, the plagioclase samples have a restricted range of δD which, excluding one sample, is almost within the range of analytical error. It is assumed here that the bulk of the hydrogen released from these plagioclase samples is derived from the sericite which it is seen to be altering to in thin section. XRD analysis of the plagioclase from GJ.29 has confirmed that the main alteration mineral is mineralogically muscovite and not some other sheet silicate mineral.

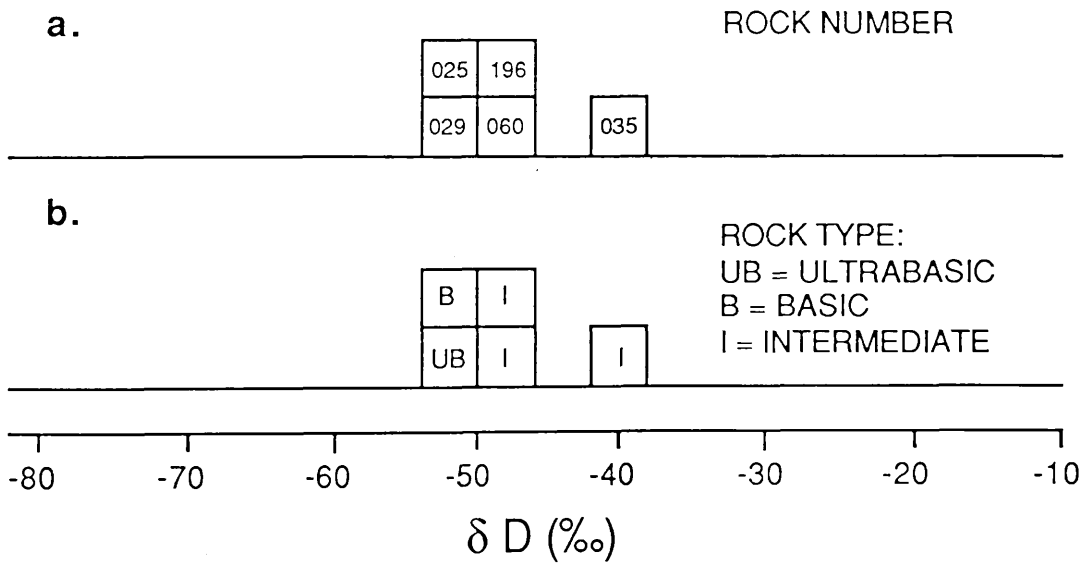

Fig. 4.17 δD of plagioclase separates from the MGS as a function of rock type. In each histogram the sample position maps directly to the same position in the other histograms. In 4.17a the rock number for each sample is shown, while the 4.17b shows the rock type for each sample Sample numbers with no prefix are those collected during this study, which have a prefix GJ..

The relation of sericite δD to rock type.

Because of the small number of samples analysed it is not possible to say with any confidence whether or not there is a relationship between δD and rock type.

The relation of sericite δD to intensity of alteration of plagioclase.

The hydrogen yield and estimated weight % of muscovite of the plagioclase separates is plotted against δD in fig. 4.18. From this figure it can be seen that the δD of the sericite is independent of the intensity of alteration of the plagioclase. Estimated muscovite contents vary from 30-70 wt.%, underlining the importance of hydration in the late retrogression.

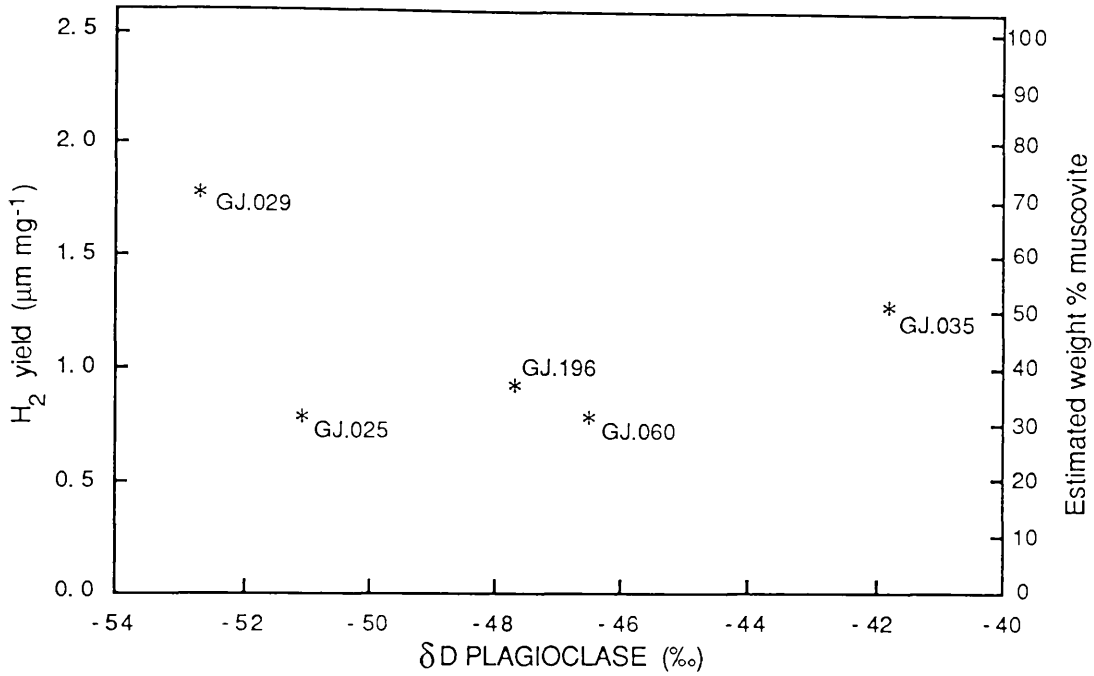

Fig. 4.18 δD plotted against hydrogen yield for plagioclase separates from MGS. The right hand axis shows the estimated weight % of muscovite in the separate calculated assuming that muscovite yields 2.51 μM H_2 mg^{-1} and that the plagioclase does not contain any hydrogen. The hydrogen yields of GJ.60 and GJ.35 have been corrected to take account of the quartz present in the separate.

The relation of sericite δD to the conditions of exchange with the high δD fluid.

From the discussion in 4.2 it would appear likely that the high δD fluid was present in these rocks in the temperature range 300-160°C (although it is apparent from the previous section that fluid/rock ratios could have varied between samples). The fine grain size of the sericites would tend to facilitate hydrogen isotope exchange with this fluid down to low temperatures, so that it is likely that the sericites last equilibrated with the high δD fluid at some temperature below their formation temperature. From H isotope data on sericite and fluid inclusions from the same sample, described in the next section, it would appear likely that the sericite-fluid fractionation in this area was probably -20 to -25‰ and fairly independent of temperature. Therefore the small variation in sericite δD can be attributed to variation in fluid δD, or to salt effects of less than 10‰, supporting the arguments in the previous section that large variations in these variables could not have been responsible for the large variations in epidote δD.

4.4.1 Volatile chemistry.

The results of partial chemical analyses of the volatiles released by heating two quartz separates from intermediate rocks in the MGS are presented in fig. 4.19. In thin section the quartz in both of these samples was observed to contain abundant bubble planes of secondary fluid inclusions. It can be seen that the volatiles from these two samples have a very restricted range of $H_2O/(H_2O+CO_2)$ ratio of 0.98-0.985, but very large differences in $NC/(H_2O+NC)$ or $NC/(CO_2+NC)$ ratios, similar to the volatiles in the quartz samples from the microgranite sill described in chapter 3. In this case, the very high NC content measured for the quartz sample from GJ.60 can be attributed to an air leak which was believed to have been present in the extraction line during the run. The CO_2 measurement would have been unaffected by this leak, while the H_2O could have been very slightly increased by continued addition of air to the hydrogen between measurement of the NCs and the total NCs + H_2. Thus the $H_2O/(H_2O+CO_2)$ ratio of 0.98 for this sample should be considered a maximum value. If the $H_2O/(H_2O+CO_2)$ ratio of this sample is taken to be very near to 0.98 then it can be seen that both of these samples have distinctly higher $H_2O/(H_2O+CO_2)$ ratios than the quartz samples from the microgranite sill, which have ratios of 0.96-0.975 (fig. 3.6).

4.4.2 δD of fluid inclusions.

The δD values of the two quartz samples are also shown on fig. 4.19. The high δD value of the water in quartz from GJ.196 is almost, within the limits of experimental error, the same as the δD value of -24.4‰ for the water released from calcite in the vein running through this sample (6.3.2) suggesting that the bubble planes in the quartz were formed at the same time as the vein. Sample GJ.196 has been intensely chloritised and sericitised indicating that it has been affected by the high δD fluid (4.2). The high δD value of the water released from the quartz suggests that it may be a relatively undiluted sample of the high δD fluid inferred to have been present in the rock from mineral δD data. If it assumed that the δD of the water released from the this quartz is that of the high δD fluid that caused the late alteration in this rock, then some inferences can be made about a. the fluid salinity and b. the sericite-fluid fractionation, (fig. 4.20).

Fig. 4.20a compares the calculated δD of pure water in equilibrium with the chlorite in this rock as a function of temperature with the actual δD of the water in the fluid inclusions in the quartz and the calcite vein in this rock. It can be seen that at any temperature, the actual δD of the fluid is distinctly lighter than the calculated δD of the pure water in equilibrium with the chlorite, indicating that there must be a salt effect which reduces the chlorite-fluid fractionation relative to the chlorite-water fractionation. At the preferred temperature of chlorite equilibration with the high δD fluid of

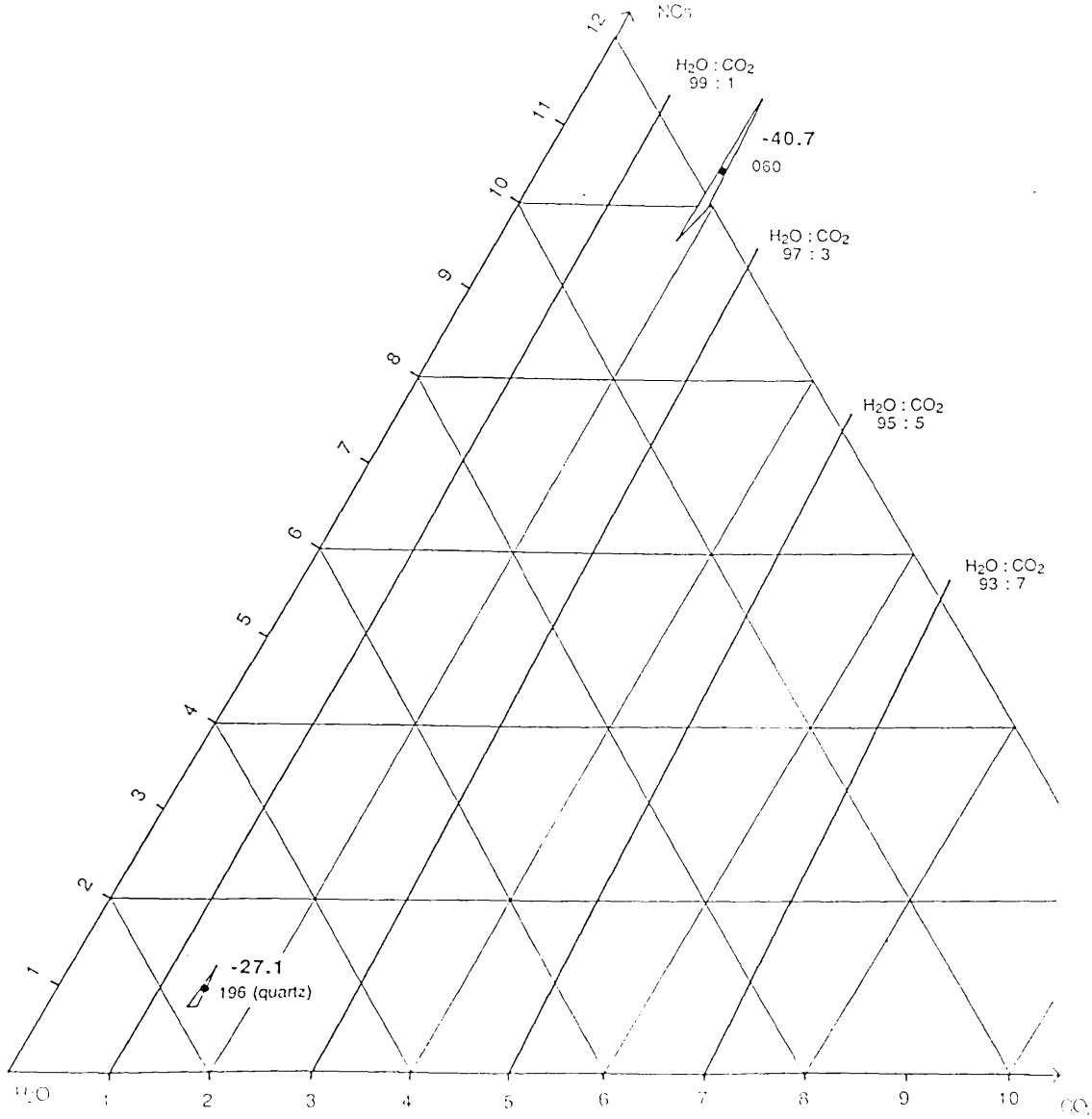

Fig. 4.19 Gas composition and δD of water of volatiles released by heating of quartz separates from the MGS. The triangles around the points are the 90% confidence limits on the gas chemistry and take into account both the reading errors and the uncertainty in the calibration line used. It should be noted that only the water rich apex of the compositional triangle is shown.

~300°C the salt effect is inferred to have been of the order of 12‰, similar to that measured between 4 m NaCl and pure water at this temperature by Graham and Sheppard (1980). The chlorite-water fractionation of Graham *et al.* (1987) may only be strictly applicable to Mg-chlorites, yet preliminary chemical data on chlorites from one ultrabasic rock (GJ.49) and one acid rock (GJ.62) suggests that the chlorites may contain appreciable Fe ($Fe_t/[Fe_t+Mg]$ is ~0.37 and 0.59 respectively). The effect of Fe substitution may be to increase the magnitude of the chlorite-water fractionation (2.4.5 A) so that the salt effect could be even larger than 12‰.

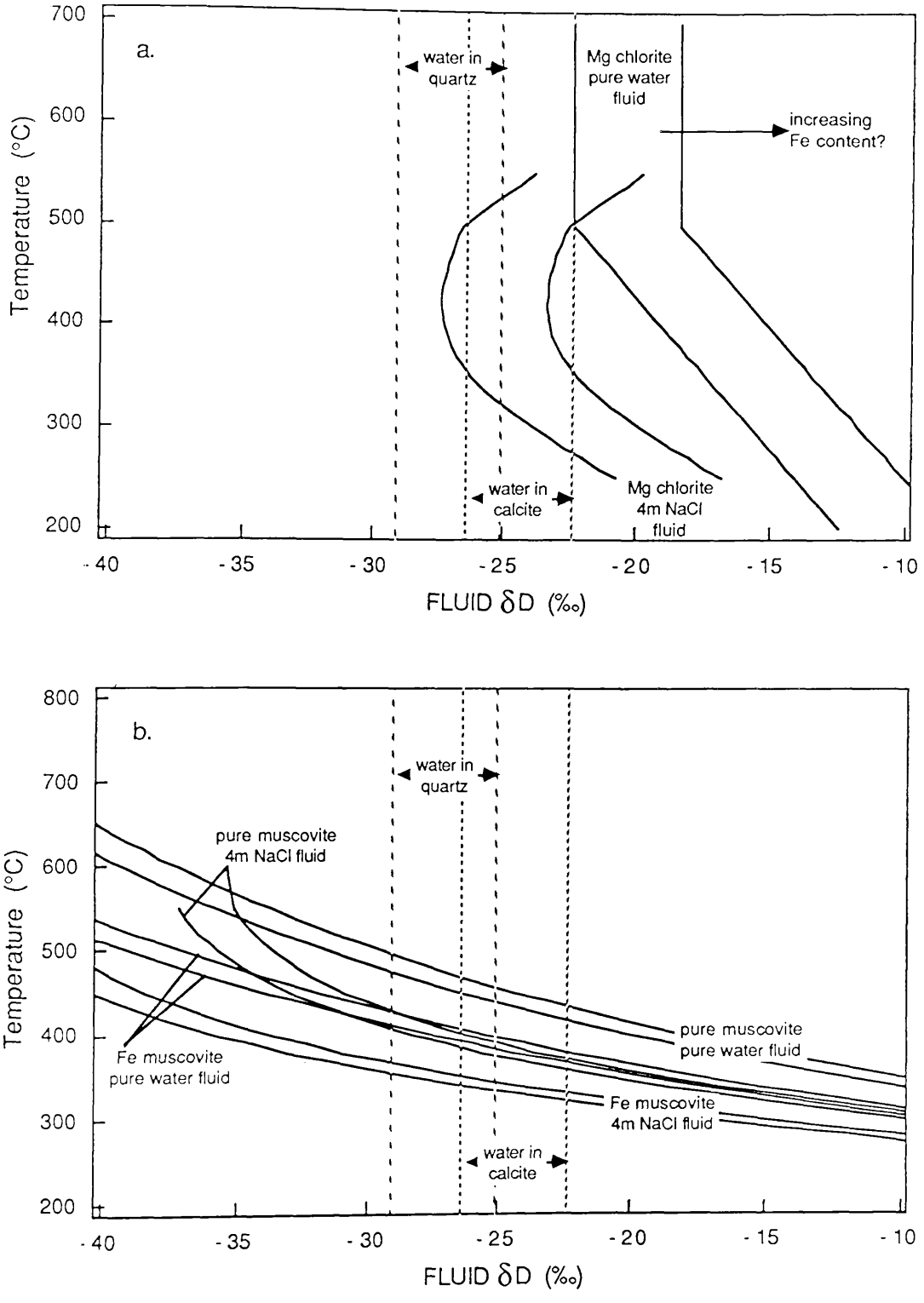

Fig. 4.20 Calculated δD of fluid in equilibrium with a. chlorite and b. sericite in GJ.196 as a function of temperature, assuming that the fluid fractionates hydrogen isotopes in the same way as pure water and a 4m NaCl solution. Also shown are the measured δD values of the water from the quartz in the rock and the calcite vein which is cutting the rock. Each pair of curves correspond to the errors due to analytical uncertainty in the hydrogen isotope analysis. Fractionation factors used were from Graham *et al.* (1987) - chlorite-water, Suzuoki and Epstein (1976)- muscovite-water and Graham and Sheppard (1980) - 4m NaCl-water. This fractionation is not calibrated between 250 and 20°C and

therefore fractionations below 250°C should be regarded as highly subjective. The two curves for fluid in equilibrium with the muscovite are for a pure muscovite and a natural muscovite with ~10% Fe (eqn 1 in Suzuoki and Epstein; 1976). This range in muscovite composition is assumed to bracket the compositional range in the sericites from the MGS.

Fig. 4.20b compares the measured δD of the fluid in the fluid inclusions with the calculated δD of pure water in equilibrium with the sericite in GJ.196 over a range of temperature, assuming that the fractionation follows the Suzuoki-Epstein equation to low temperatures. It can be seen that over the likely range of equilibration temperatures for the sericites (160-300°C), the estimated δD of the fluid in equilibrium with the sericites is heavier than that in the fluid inclusions, even when salt effects are taken into account. Thus the muscovite-water fractionation must change its temperature dependence below 400°C as suggested by Suzuoki and Epstein (1976). From fig. 4.20b it can be seen that the measured sericite-fluid fractionation is of the order of -20 to -25‰. This is approximately the magnitude of the sericite-pure water fractionation at 450-400°C. Therefore if salt effects are in the region of 12‰ (or possibly less because of the probable lower temperature of sericite equilibration compared to that of chlorite), then the muscovite-pure water fractionation can be inferred to increase by a maximum of 12‰ in the temperature drop between 400°C and the temperature at which the sericites equilibrated with the fluid. This suggestion is supported by the data of Marumo *et al.* (1980), who observed that the sericite-fluid hydrogen isotope fractionation in an active geothermal system was found to be approximately constant at -23 to -27‰, over the temperature range 250-130°C.

Water from the other quartz sample (GJ.60) has a significantly lower δD value (-40.7‰) than the water from GJ.196. However this low value can only be interpreted as a minimum δD for the sample, since the total yield of hydrogen from the sample was very low, so that that blank effects which tend to lower the measured δD may have been significant (A.1.4).

4.5 OXYGEN ISOTOPE DATA.

4.5.1. Hornblendes.

Oxygen isotope ratios for the MGS hornblendes are presented on a $\delta^{18}O$ vs. δD plot in fig. 4.21. It can be seen from this figure that the $\delta^{18}O$ for the hornblendes which are thought to be of metamorphic origin (fig. 4.6) have a limited range in $\delta^{18}O$ (+6.8 to +7.6‰) which falls within the range of $\delta^{18}O$ of the other hornblendes (+6 to +8‰) which are inferred to be of igneous origin. Thus the metamorphic hornblendes appear to have a more restricted range in both δD and $\delta^{18}O$ compared to the igneous hornblendes.

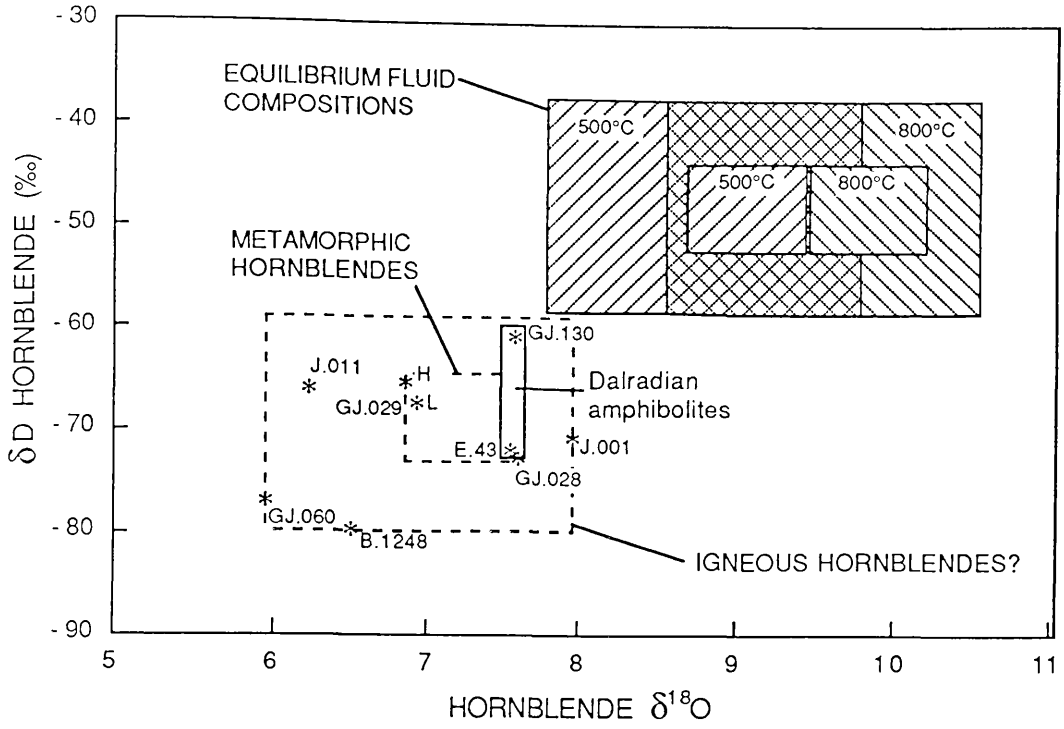

Fig. 4.21 $\delta^{18}O$ vs δD plot for hornblendes from the MGS. The fields for the water in equilibrium with the metamorphic (small boxes) and igneous hornblendes (large boxes) at temperatures between 500 and 800°C are also shown. δD data for hornblendes not shown on this diagram were also used in calculating the igneous water field. Fractionation factors used were the hydrogen isotope fractionation of Graham *et al.* (1984) and an oxygen isotope fractionation calculated from the quartz-water equation of Bottinga and Javoy (1973) and the quartz-amphibole equation of Javoy (1977). No corrections have been made for salt effects on the fractionation. The stable isotopic composition of the two hornblendes from the Dalradian amphibolites are also shown for reference.

The magmatic hornblende with the heaviest $\delta^{18}O$ value (+8‰) comes from an ultrabasic rock which occurs only 1 m away from the contact with the country rock and contains many partially assimilated pelitic xenoliths, so that the high $\delta^{18}O$ value of this hornblende can most easily be attributed to crystallisation from an ^{18}O enriched melt. The lower $\delta^{18}O$ values in the basic and intermediate rocks are consistent with this explanation since these rocks do not appear to have assimilated metasedimentary material. The 0.5‰ increase in hornblende $\delta^{18}O$ from the basic rocks to the intermediate rock could reflect an increase in melt $\delta^{18}O$ due to magmatic differentiation. Such an increase in melt $\delta^{18}O$ could have taken place if hornblende, magnetite and biotite were the dominant fractionates from the basic magma, although if plagioclase was a major fractionate a depletion in melt $\delta^{18}O$ might be expected (Taylor and Sheppard, 1986, p.236).

Because hornblende-melt ^{18}O fractionations are likely to be small (<2‰) but negative (*ibid.*), it can be inferred that all of the magmatic hornblendes must have crystallised from a melt with a $\delta^{18}O > +6‰$. Such $\delta^{18}O$ values are higher than those for unmetasomatised uncontaminated mantle derived basic melts (2.9.3), indicating that all of the MGS magma must have been ^{18}O enriched by some process during or prior to intrusion.

From fig. 4.21 it can be seen that the $\delta^{18}O$ of the fluid that was in equilibrium with the metamorphic hornblendes at likely closure temperatures of between 800 and 500°C (fig. 2.12) was between +8 and +10‰, while the $\delta^{18}O$ of the fluid which was in equilibrium with the magmatic hornblendes was between +7 and +10.5‰, over the same temperature range. Thus both hornblendes probably last equilibrated with fluids which have $\delta^{18}O$ values within the ranges of both magmatic and metamorphic fluids (fig. 2.19).

Oxygen isotope ratios of the two chemically distinct hornblende separates from the same rock (GJ.29-L, GJ.29-H) are not statistically different, even at the 80% confidence level, according to a two tailed t-test. Therefore it can be concluded that the effect of chemical differences between the metamorphic hornblendes on the calculated $\delta^{18}O$ value of the equilibrium fluid will not be significant.

4.5.2. Quartz-epidote oxygen isotope thermometry.

In order to attempt to determine the temperature at which the high δD fluid which caused the growth of chlorite, epidote and sericite was present in the MGS, coexisting quartz and epidote were separated from a microcrack (GJ.34) and analysed for $\delta^{18}O$. These microcrack minerals are the only minerals formed during the late retrogression which pass the necessary requirements for a valid oxygen isotope thermometer in that:

a. They are observed to be intergrown, indicating that they grew at the same time in isotopic equilibrium with the same fluid.

b. Both minerals have low diffusion coefficients for oxygen, so that they are unlikely to have re-equilibrated oxygen isotopes during cooling.

c. They are pure minerals which can be easily separated from minerals formed earlier in the paragenetic sequence.

$\Delta_{qtz\text{-}ep}$ was found to be +6.36 ± 0.23‰ (1σ), which using the quartz-epidote fractionation of Matthews and Schliestedt (1984) corresponds to an equilibration temperature of 297 ± 13°C (1σ). The uncertainty was calculated using the error propagation equation given in 2.5.1 to incorporate the uncertainty in Δ and β (the mole fraction of pistacite in the epidote A.2.4). The main sources of error in this temperature estimate are probably the uncertainties in the fractionation coefficients, which unfortunately cannot be evaluated because the fractionation equation is semi-empirical (*ibid.*). In order to attempt to correct for these other errors it is considered reasonable to double the error estimate on the equilibrium temperature to ±26°C.

An alternative calibration of the quartz-epidote oxygen isotope thermometer, based on fractionations observed in natural quartz-epidote pairs, is given by Hattori and Muehlenbachs (1982). This calibration gives a higher equilibration temperature of 367±42°C. The calibration of Matthews and Schliestedt (1984) is preferred here because although it is semi-empirical, it is based on experimental data (zoisite-water fractionation of

Matthews *et al.*, (1983c) and the grossular-andratite fractionation of Taylor and O'Neil, 1977) and incorporates the effect of epidote Fe content. The Hattori and Muehlenbachs (1982) calibration does not take account of the epidote Fe content and is strongly dependent on data from Troodos (Heaton and Sheppard, 1976), for which the estimated equilibrium temperature appears to be anomalously high, since similar temperatures have been inferred for much smaller quartz-epidote fractionations by Stakes and O'Neil (1982).

Thus it is concluded that the quartz and epidote in this microcrack crystallised at 297±26°C. This temperature can only be interpreted as the lower limit for the upper temperature at which the high δD fluid was present in the MGS because the microcrack could have been open at higher temperatures, and only become sealed during cooling. Thus the high δD fluid is inferred to have first been present in the MGS rocks at some temperature > 300°C.

4.5.3 Epidotes.

The $\delta^{18}O$ values of four epidotes were measured in order to constrain the $\delta^{18}O$ composition of the high δD fluid which is inferred to have caused epidote growth in the MGS (4.2). Because the extent of Fe substitution in the octahedral site may affect the epidote-fluid fractionation (Matthews and Schliestedt, 1984), the chemistry of the epidote separates was determined using an electron microprobe (A.2.4) and is plotted against the $\delta^{18}O$ values in fig. 4.22. The very good correlation of these variables over a wide range of both $\delta^{18}O$ and Fe content strongly suggests that the epidote-fluid fractionation may in be related in some way to the Fe content. The fact that the δD of the epidotes shows no correlation with Fe content (fig. 4.13), and hence $\delta^{18}O$, supports the proposal made in 4.3.3 that epidote δD was controlled by post-crystallisation exchange effects.

Because of the strong correlation of $\delta^{18}O$ with Fe content in the epidotes, an epidote-water fractionation which takes account of the epidote Fe content, was calculated from the empirical quartz-epidote fractionation of Matthews and Schliestedt (1984) and the 250-500°C quartz-water fractionation of Matsuhisa *et al.* (1979). The $\delta^{18}O$ of the fluid in equilibrium with the epidotes calculated using this fractionation equation is shown as a function of temperature in fig. 4.23. From this diagram it can be seen that using this fractionation equation, the calculated equilibrium fluid $\delta^{18}O$ for each epidote lies along a distinctly different curve, indicating that none of these epidotes are in oxygen isotope equilibrium. It can also be seen that the there is a relationship between the the position of the curve and the Fe content of the epidote so that at any temperature, the most Fe poor and ^{18}O rich epidote appears to be in equilibrium with the most ^{18}O rich fluid, while the most Fe rich and ^{18}O poor epidote appears to be in equilibrium with the most ^{18}O poor fluid.

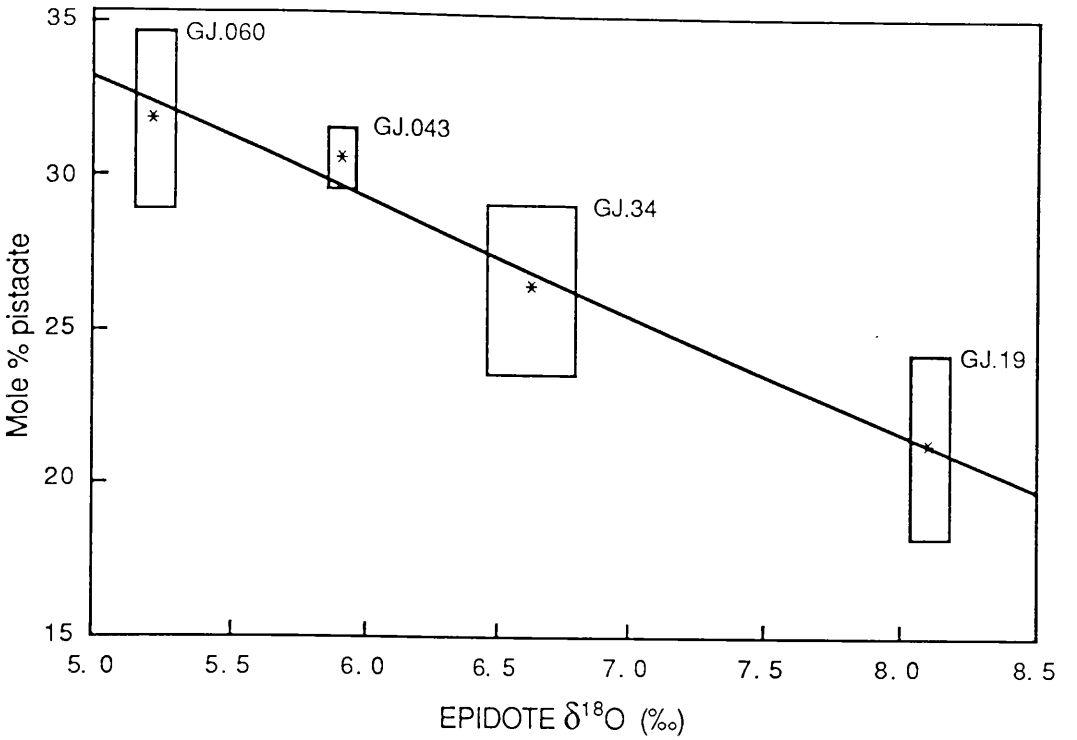

Fig. 4.22 Epidote $\delta^{18}O$ vs. mole % pistacite ($Ca_2Fe_3Si_3O_{12}OH$) in epidote. The boxes around the data points are $\pm$ 1 σ_{n-1} for each variable. The line through the data is a reduced major axis regression line described by the equation % pistacite = 52.3 -(3.82 $\times$ $\delta^{18}O$).

One explanation of this relationship is that all the epidotes did actually equilibrate with a fluid of similar $\delta^{18}O$ at a similar temperature, but that the fractionation equation does not adequately take account of the variation in Fe contents of the epidotes. This would cause the the curves to be displaced from one another in proportion to their Fe contents, instead of all lying in approximately the same position, as would be the case if the epidotes had equilibrated oxygen isotopes with a fluid with a similar $\delta^{18}O$ at a similar temperature. Although this fractionation equation is semi-empirical, it is considered unlikely that it could be in error by as much as 1‰, and it is therefore suggested that the differences in the positions of the curves are real.

If the fractionation equation is correct then the difference in the position of the curves can be explained in a number of ways:

a. All the epidotes equilibrated with a fluid with the same $\delta^{18}O$ at the same temperature, but variations in salinity between fluids caused the epidote-fluid fractionation to vary between samples, causing them to appear not to be in equilibrium.

b. The epidotes equilibrated oxygen isotopes with a fluid with approximately the same $\delta^{18}O$ value as that which the epidote in GJ.34 equilibrated with at 300°C (~+6.1‰), but at different temperatures ranging from ~230 to 410°C (fig. 4.22 arrow b).

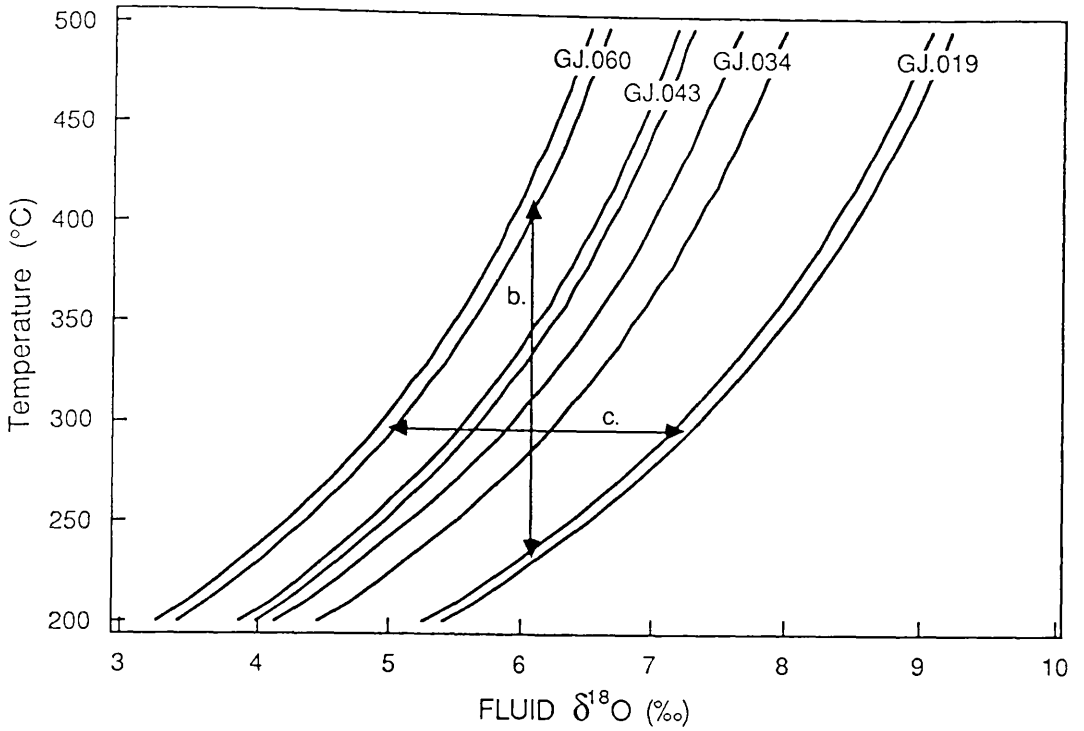

Fig. 4.23 Calculated $\delta^{18}O$ of fluid in equilibrium with the four epidotes from Fig. 4.22 as a function of temperature. Curves calculated using a fractionation equation derived from other fractionation equations (see text). Each pair of curves corresponds to the upper and lower limits resulting from analytical uncertainty ($1\ \sigma_{n-1}$). No corrections are made for salt effects, so that the absolute horizontal positions of the curves may be slightly different, although the relative differences at any temperature will remain. Arrows labeled b and c correspond to explanations of the different positions of the curves described in the text. These two arrows cross at the fluid $\delta^{18}O$ and equilibration temperature inferred for the quartz-epidote filled microcrack described in the previous section (GJ.34).

c. The epidotes equilibrated oxygen isotopes at the same temperature as the epidote in GJ.34 (~300°C) but the fluid varied in $\delta^{18}O$ from ~+5 to +7.2‰ (fig. 4.22 arrow c).

d. Different epidotes equilibrated at different temperatures and with fluids of different $\delta^{18}O$.

From the relative homogeneity in chlorite and sericite δD it was concluded in 4.3.4 that variations in the salt effect on mineral-fluid hydrogen isotope fractionations must have been relatively small (<10‰ in δD). Therefore it is considered that variations in the salt effect alone are unlikely to have caused the variation in epidote $\delta^{18}O$.

If the epidotes equilibrated with a fluid with a similar $\delta^{18}O$ value (~+6.1‰), but at different temperatures, then it is apparent that the most Fe rich epidote must have equilibrated at the highest temperature and the most Fe poor epidote at the lowest temperature. Because epidotes have relatively low diffusion coefficients for oxygen it is probably safe to make the assumption that that the equilibration temperature approximates very closely to formation temperature, so that it would appear that in this case the the epidote Fe content would be positively correlated with formation

temperature. Numerous studies (e.g. Holdaway, 1972; Raith, 1976; Bird and Helgeson, 1981; Liou *et al.*, 1983) have all indicated that in systems containing Fe oxides if all other parameters are constant, then the Fe content of epidote will increase with either an increase in fO_2 or a decrease in temperature. Thus the Fe variation in the epidotes is opposite to that which would be expected if the epidotes formed from the same fluid at different temperatures, and the only way in which the variability in epidote Fe content can be explained in this case is if the fluid at higher temperatures had a much higher fO_2. However it is impossible to account for the $\delta^{18}O$ - Fe correlation in the epidotes without inferring some fO_2 variation in the fluid. This is because in the situation (c.) in which all the epidotes are assumed to have equilibrated at ~300°C with fluids of differing $\delta^{18}O$, since T is constant, only a variation in fluid fO_2 can account for the variation in epidote Fe content. Thus it has to be concluded that the fluid fO_2 varied between different rocks during epidote formation and therefore assumptions about fluid fO_2 variability or constancy cannot be used to choose between hypotheses b and c.

Thus with only the information available it is impossible to choose between hypothesis b. in which all the epidotes formed from a fluid with constant $\delta^{18}O$ and the most Fe rich epidotes formed from the hottest most oxidising fluid, or hypothesis c. in which all of the epidotes formed at the same temperature from a fluid with variable $\delta^{18}O$, with the most ^{18}O poor fluid being most oxidising, or hypothesis d. a combination of b. and c.

Regardless of which of these options is correct, it can be seen from fig. 4.23 that it is likely that all of the epidotes must have equilibrated with a fluid with $\delta^{18}O$ <7‰. This $\delta^{18}O$ value is distinctly lower than that of the fluid calculated to be in equilibrium with the MGS hornblendes at likely closure temperatures (+7 to +10.5‰ at 500-800°C, 4.5.1). Only if the hornblendes equilibrated down to unreasonably low temperatures could some of the hornblendes and epidotes be in equilibrium with the same fluid. Thus it can be concluded that the hornblendes and epidotes are not in oxygen isotope equilibrium and that the the fluid causing chlorite, epidote and sericite growth in the MGS was ^{18}O depleted, as well as D enriched, relative to the fluid that last equilibrated with the MGS hornblendes.

4.5.4 Within-rock oxygen isotope disequilibrium.

In the previous section it was shown that the epidotes in the MGS do not appear to be in oxygen isotope equilibrium with the hornblendes. From the $\delta^{18}O$ values of mineral separates from a single hand specimen, it can be shown that like the hydrogen isotope disequilibrium between these two minerals, the oxygen isotope disequilibrium is on a grain scale, because mineral separates from a single hand specimens are not in oxygen isotope equilibrium (fig. 4.24). In this figure the $\delta^{18}O$ value of the fluid in equilibrium with the hornblende in this rock is seen to be different from the fluid in equilibrium with the epidotes at any temperature, conclusively proving that these minerals are not in equilibrium. In this rock the pore fluid is inferred to have had a relatively high $\delta^{18}O$ value of ~+8‰ between the closure temperature in the hornblende (possibly as high as 700-800°C)

and closure in the quartz (~400-500°C fig. 2.12) and then decreased to < +6‰ when the epidote formed at 300-420°C (fig. 4.23).

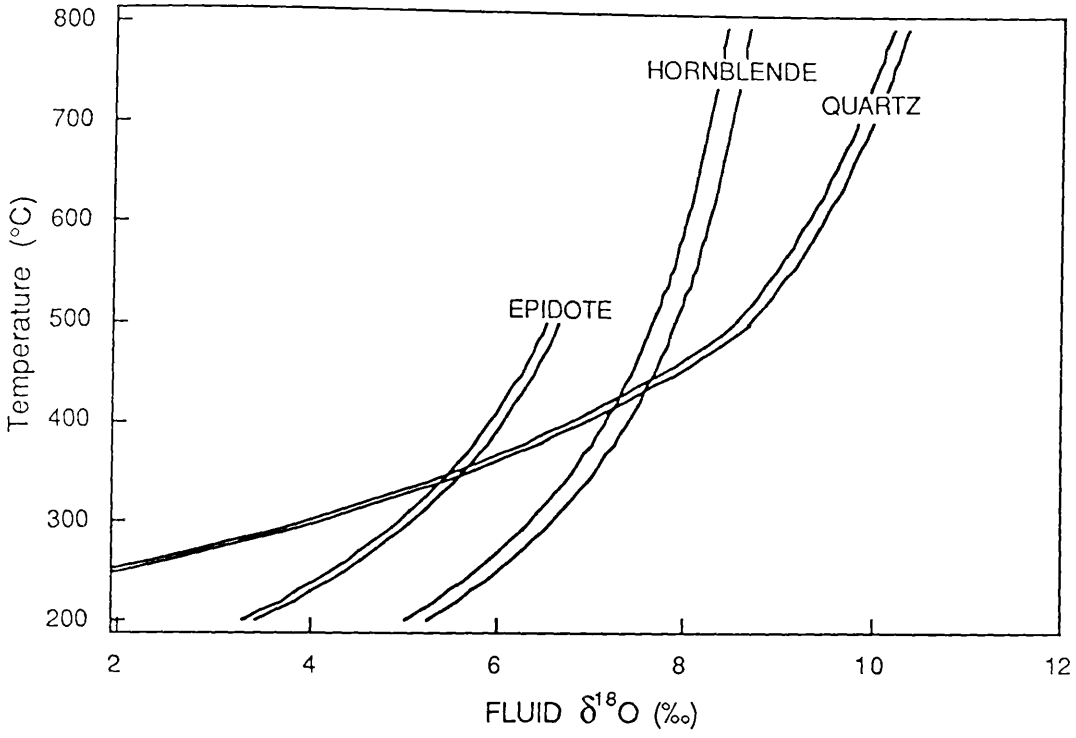

Fig. 4.24 $\delta^{18}O$ value of fluid in equilibrium with the hornblende, epidote and quartz in sample GJ.60 shown as a function of temperature. Each pair of curves corresponds to the upper and lower limits resulting from analytical uncertainty ($1\ \sigma_{n-1}$). Fractionation factors used for hornblende and epidote are the same as those used in figures 4.21 and 4.23 respectively, the quartz-water fractionations are from Matsuhisa *et al.* (1979). No corrections are made for salt effects.

4.5.5 Oxygen and carbon isotope data for calcites.

Because only two calcite samples from the MGS have been analysed, these results are not presented here, but are given in 6.6, where they are compared with the results from calcites from other areas.

4.6 THE ORIGIN OF WATER IN HORNBLENDES.

4.6.1. Magmatic hornblendes.

Introduction.

The high abundance of hornblende in the MGS has been commented on by a number of authors (e.g. Leake, 1970b; Bremner and Leake, 1980). Textural relations (1.4.1) indicate that much of this hornblende must be magmatic in origin, either as a primary precipitate or as a secondary replacement after olivine or pyroxenes before crystallisation was complete. Thus the water in these hornblendes must have been derived from the MGS magma. Even if the textural criteria used to identify magmatic hornblende are not correct, and all the hornblende in the MGS did develop metamorphically, it would seem unlikely that the water in these hornblendes could have been derived

from anywhere but the magma. This is because hornblende occurs throughout the MGS intrusion, even in areas such as that to the W of Roundstone which are many km from the nearest outcrop of metasedimentary material and it would appear unlikely that fluid from the metasediment would flow over such distances for no apparent reason.

It might be intuitively predicted that precipitation of hornblende from a basaltic melt would require a high water content in the magma. Leake (1970b) has cited the presence of calcic plagioclase in the MGS as evidence of a high P_{H2O} in the magma, while Bremner and Leake (1980) suggest that the calcic compositions of the clinopyroxenes might also be a result of crystallising from a magma with a high P_{H2O}. Experimental studies at 5 kb (the approximate pressure of hornfelsing in the Cashel aureole; Treloar, 1981) indicate that hornblende can be a major precipitate from basaltic melts both at $P_{H2O} = P_{total}$ (Helz, 1973) and at lower water fugacities ($fH_2O \approx 0.6$ $f$pure H_2O; Holloway and Burnham, 1972). However in neither of these studies are the predicted phase relations analogous to those observed in the MGS. In these experimental studies the plagioclase is found to crystallise at lower temperature than the clinopyroxene and most of the hornblende. However, in the ultrabasic MGS rocks, plagioclase is observed to form cumulate textures with pyroxene and is present as inclusions in oikocrystic hornblende, while in the basic rocks plagioclase also appears to have crystallised before hornblende. It is suggested that the observed phase relations in the MGS rocks could only have been obtained if crystallisation took place from a hydrous magma with $P_{H2O} << P_{total}$, so that plagioclase was stable at higher temperatures (Burnham and Davies, 1974). Lowering P_{H2O} might be expected to also lower the upper temperature at which hornblende is stable (Yoder and Tilley, 1962), although some minor reduction of P_{H2O} has been shown to actually increase the upper stability of hornblende (Holloway and Burnham, 1972; Allen and Boettcher, 1978). After reviewing the literature on experimental studies of hornblende stability in which $P_{H2O} < P_{total}$, Helz (1982) concluded that at pressures between 5 and 10 kb amphibole stability is insensitive to decreasing fluid X_{H2O} down to values of 0.3 to 0.4 (where here fluid is the fluid phase in equilibrium with the melt). Thus the partial pressure of water in the MGS magma could have been quite small and hornblende would still have been stable. Presumably early crystallisation of anhydrous phases would have enriched the melt in water, so that P_{H2O} would have risen during crystallisation, stabilising hornblende at lower temperatures.

Because it is not possible to accurately estimate P_{H2O} for the MGS magma it is difficult to estimate the water content of the melt. Water saturated basaltic melts ($P_{H2O} = P_{total}$) at 5 kb contain ~8.5 wt.% H_2O (Hamilton *et al.*, 1964 ≡ 24 mole % H_2O!), so that if P_{H2O} is < 1/2 P_{total} (?), the maximum water content of the melt must have been ~ 4 wt.%. The minimum water content in the magma which would be necessary to supply all the water present in the magmatic hornblende and biotite in the MGS can be roughly estimated to be up to 2 wt.% H_2O, if it assumed that the most hornblende rich rocks crystallised in closed system conditions (hornblende contains ~2 wt.% H_2O). If these hornblende rich rocks were cumulates (i.e. only part of the original system) the water content of the melt need not have been so high. Biotite, which is more water rich than hornblende, is only present in subordinate amounts in the ultrabasic and basic rocks, although it is often

present in greater proportions than hornblende in the intermediate and acid rocks. However, these rocks usually contain low total amounts of hornblende and biotite, so that the minimum water content in these rocks is probably not any higher.

The water in the MGS magma could have originated from two sources:

a. The magma source rocks.

b. From the rocks through which the MGS magma intruded prior to crystallisation.

Very little is known about the water contents of basaltic magmas in equilibrium with their source rocks. Yoder (1976) suggests that melts in equilibrium with a mantle source will be water undersaturated. However, since water saturation at mantle PT conditions would require the melt to contain 10-20 wt.% H_2O (Hamilton *et al.*, 1964; Hodges, 1974) even if the melts were undersaturated they could still theoretically contain large amounts of water. Water contents of quenched basaltic glasses can provide minimum estimates of the water contents of different basaltic rock types. Glasses of subduction related basalts from the Mariana arc and trough are relatively water rich with 0.6-2.0 wt.% H_2O (Garcia *et al.*, 1979; Poreda, 1985). Glasses of other basaltic magma types generally contain less water (OIB < 1 wt.% H_2O and mostly 0.4-0.8 wt.% H_2O, MORB mostly 0.1-0.4 wt.% H_2O; B.E. Taylor, 1986). These values may be minimum estimates because the water content could have been controlled by the maximum solubility which decreases with decreasing pressure (Hamilton *et al.*, 1964), so that these values might represent water saturation at the extrusion pressure. However, the fact that the glasses from different magma types do have different water contents would suggest that these water contents are not on the saturation curves, at least for OIB and MORB, so that these water contents may be good estimates of water contents of the magmas at their sources.

Thus it would appear that the water in the MGS magma (?2 wt.% H_2O) could only have been totally derived from its source if the source was subduction related. If the magma was generated in other tectonic regimes an additional source of water would be required.

Addition of water to the MGS magma after leaving its source could have taken place by 3 mechanisms:

a. bulk assimilation of water rich material.

b. assimilation of water rich partial melts.

c. assimilation of water rich fluids.

Field evidence indicates that some addition of water to the ultrabasic magma may have taken place at the present level of intrusion, prior to crystallisation, by mechanisms a. and b. It is clear from the radiogenic isotope data of Jagger (1985) that some marginal assimilation of metasedimentary material took place at the present level.

According to Leake and Skirrow (1960) and Evans (1964), the hornfelsed metasediments around the ultrabasic rocks have lost partial melt material during hornfelsing. Some of this partial melt material appears to have been segregated into granitic sills (1.4.1), but it is possible that some may also have been assimilated into the MGS magma in a similar manner to that envisaged by Patchett (1980). This author envisaged that partial melt produced by hornfelsing around basaltic intrusions in the mid crust flowed into the magma when later intrusive pulses fractured the peripheral chill. Jagger (1985) has suggested that such a process could have been enhanced by the syntectonic nature of MGS intrusion.

The presence of partially assimilated xenoliths of pelitic material in some of the ultrabasic rocks indicates that some assimilation may have taken place as a bulk assimilation process. However it is likely that this metasedimentary material was hornfelsed and water poor prior to incorporation in the melt, so that true bulk assimilation is unlikely to have taken place, although if the partial melt produced from these hornfelsed rocks was also assimilated by the magma, the combined effect might have been the same as true bulk assimilation.

Addition of water by mechanisms a. and b. to the basic and later differentiates of the magma at the present level would seem unlikely, because the hornfelsed zones of these rock types are relatively narrow and no partially melted xenoliths are present in these rocks. Thus assimilation of water rich material into these rock types could have only taken place at a deeper level. It is likely that most assimilation at a deeper level took place prior to crystallisation of the early members, when temperatures were highest, so that the more differentiated rock types could have inherited magmatic water assimilated at an early stage. Leake (1970a) suggests that the magma from which the intermediate and later rock types rock types were derived from had probably assimilated metasedimentary material, because the volume of later differentiates appears to be larger than would be produced by an uncontaminated basic magma.

From a consideration of the Sr and Nd isotope ratios of the ultrabasic and basic rocks Jagger (1985) suggested that apart from Dalradian metasedimentary material another plausible contaminant at a deeper level might be lower crustal material, which could be represented by lithologies like Lewisian amphibolite.

The water content of bulk Dalradian metasediment cannot be derived from whole rock chemical analyses of the Dalradian rocks, because of the hydrating nature of the late chlorite-sericite forming retrogression in these rocks. However the water content may be estimated from the average modal analysis of unhornfelsed metasediment given by Ahmed-Said (1988, p.77). If it assumed that volume % muscovite/biotite $\approx$ wt.% muscovite/biotite (calculations show this to be accurate to ~5%), and that biotite and muscovite contain 4 wt.% H_2O, then the water content of these rocks at the peak of metamorphism can be estimated to be 1.9±0.6 wt.%. If the water content of the contact hornfelses (which have lost partial melt material) are estimated from Ahmed-Said's (1988) data in the same way, then the water content of the partial melt material can also be estimated from the mass balance relationship:

$H_2O_{UM} - xH_2O_{PM} = (1-x)H_2O_{MGS}$

where UM=unhornfelsed metasediment, PM = partial melt of UM contact hornfelses and x is the mass fraction of UM which melts. The degree of partial melting in the contact hornfelses is estimated by Ahmed-Said (1990) to be 30-40% on the basis of trace element modelling. Using these values for x, the water content of the partial melt is estimated to be [illegible] wt.%, while maximising and minimising the errors on H_2O_{UM} and H_2O_{MGS} gives upper and lower limits of 7.34 and 2.14 wt.% respectively. These estimates are consistent with water contents that would be predicted from experimental data. Johannes (1985, fig.2.3) shows that granitic melts must contain at least 2 wt.% H_2O at the conditions at which partial melting took place (~5 Kb, 850-900°C?; Treloar, 1981), while Cartwright (1988, fig.4) shows that the maximum water content of a granitic melt under the same conditions will be ~ 9-9.5 wt.%. The bulk water content of a Lewisian amphibolite lithology would be between 0 and ~2 wt.% H_2O, depending on its amphibole content. Thus if the parental basaltic magma to the MGS magma was not water rich (i.e. not derived from a subduction related source) it is apparent that partial melt material, bulk metasediment or Lewisian amphibolite like material would all have increased the water content of the melt during assimilation and could therefore represent plausible end members in some contamination process.

It is considered unlikely that direct assimilation of water rich fluid by the magma could have taken place at any level, because although such fluid may have been produced during hornfelsing, it would either have flowed away from the intrusion (down the thermal and pressure gradients) or been assimilated by the water undersaturated (see above) partial melts that were forming in the hornfelses. Furthermore the inhomogeneity of quartz $\delta^{18}O$ values at the contact of the Cashel body is also inconsistent with direct assimilation of this fluid (3.5.3).

Thus from a consideration of the water content of the possible water sources alone it is not possible to identify the source of the water in the MGS magma. However it is possible to conclude that only if the parental magma was subduction related would it be possible for all the water in the MGS magma to have been derived from the magmatic source. If the parental magma was derived from any other source then contamination with some water rich material is required. Materials which could represent this contaminant could include partial melts derived from Dalradian metasediments or bulk Dalradian metasediments or Lewisian amphibolite like lithologies.

Stable isotope constraints.

To attempt to further constrain the origins of the water in the magmatic MGS hornblendes and the origin of the MGS magma itself, the H and O abundances and isotopic ratios have been estimated for the unfractionated MGS magma, for all possible parental magma types and all materials which could have contaminated these magmas, and are tabulated in table 4.1.

Table 4.1 Estimates of δD, Wt.% H_2O, $\delta^{18}O$ and Wt.% O for the unfractionated MGS magma and various end member components which could have been involved in its formation.

Unfractionated MGS magma

δD: -70±5 determined using an assumed hornblende-melt fractionation of 0‰ (4.3.1) and the δD values of two hornblendes (J.001, GJ.166 band e) which are thought to have not been affected by high δD fluid (4.3.1) and are from ultrabasic rocks so that their values should reflect the δD of a relatively unfractionated melt.

Wt.% H_2O: BE=2.0, UL=4.0, LL=0.8 relate to $P_{H2O} \approx 0.25$, 0.5 and 0.1 relative to P_{total}, consistent with phase relations, see previous subsection.

$\delta^{18}O$: +7 determined using a mineral-melt fractionation of -1‰ and the value of ~+6‰ (the lowest value of the MGS hornblendes) as an estimate of hornblende $\delta^{18}O$ in the most unfractionated and uncontaminated MGS magma.

Wt.% O: 46 guestimate only.

End member: Subduction related basalt

δD: -30±5 see 2.9.2

Wt.% H_2O: BE=1.0, UL=2.0, LL=0.5 see previous subsection.

$\delta^{18}O$: +7 see 2.9.3

Wt.% O: 45 calculated for average arc basalt from Ewart (1976), recalculated to contain 2 wt.% H_2O.

End member: MORB basalt

δD: -80±5 see 2.9.2

Wt.% H_2O: BE=0.25, UL=0.4, LL=0.1 see previous subsection.

$\delta^{18}O$: +6 see 2.9.3

Wt.% O: 44.5 calculated for ocean floor tholeiite from Bender *et al.* (1978), recalculated to contain 0.25 wt.% H_2O.

End member: OIB basalt

δD: -70±5 see 2.9.2

Wt.% H_2O: BE=0.6, UL=0.8, LL=0.4 see previous subsection.

$\delta^{18}O$: +5 see 2.9.3

Wt.% O: 44 calculated for estimated parental basalt for Kilauea tholeiites, Hawaii, from Bence *et al.* (1980), recalculated to contain 0.6 wt.% H_2O.

End member: Bulk Dalradian metasediment (Cashel formation).

δD: -60±10 see fig.3.3

Wt.% H_2O: 1.9±0.6 see previous subsection.

$\delta^{18}O$: +10±1 see fig.3.1

Wt.% O: 48 guestimate - slightly more basic than partial melt.

End member: Partial melt from Dalradian metasediment (Cashel formation).

δD: -65±5 see 3.5.4

Wt.% H_2O: BE=3.75, UL=7.35, LL=2.14 see previous subsection.

$\delta^{18}O$: +11.5 see 3.5.2

Wt.% O: 3.75 wt.% H_2O = 49, 7.34 wt.% H_2O = 50.5 calculated using analysis of microcline microgranite sill given by Leake (1970b) recalculated using 3.75 or 7.34 wt.% H_2O.

End member: Fluid from Dalradian metasediment (Cashel formation).

δD: -40±5 see fig.3.5

Wt.% H_2O: 100 presumes a pure water fluid.

$\delta^{18}O$: +11±1 see fig.3.2

Wt.% O: 89 presumes a pure water fluid.

End member: Bulk Lewisian amphibolite

δD: -52	apparently only available
Wt.% H_2O: 0.6	values for Lewisian amphibolite
$\delta^{18}O$: +8	-from Kay (1979)
Wt.% O: 46	guestimate only

BE = best estimate, UL = upper limit, LL = lower limit.

The δD, $\delta^{18}O$ and wt.% H_2O of these different end members are compared with those of the MGS in figs. 4.25a-f. Also shown on these diagrams are mixing lines between different pairs of parental magma types and contaminants. These simple two component mixing lines were calculated using the relationships

$$C_{MIX} = (X_1 \times C_1) + (X_2 \times C_2)$$

and

$$\delta_{MIX} = [(X_1 \times C_1 \times \delta_1) + (X_2 \times C_2 \times \delta_2)] \; / \; C_{MIX}$$

where C = wt.% H_2O or O, X = weight fraction of end member and δ = δ value and the subscripts MIX, 1, and 2 refer to the mixture and the two end members respectively[1] .

[1] These equations use the approximation that δ values can be treated in the same way as the concentration of a trace element in a mixing process. This is not strictly true, but the approximation is very good (<0.01‰ difference) for mixing between materials within the range known for geological materials.

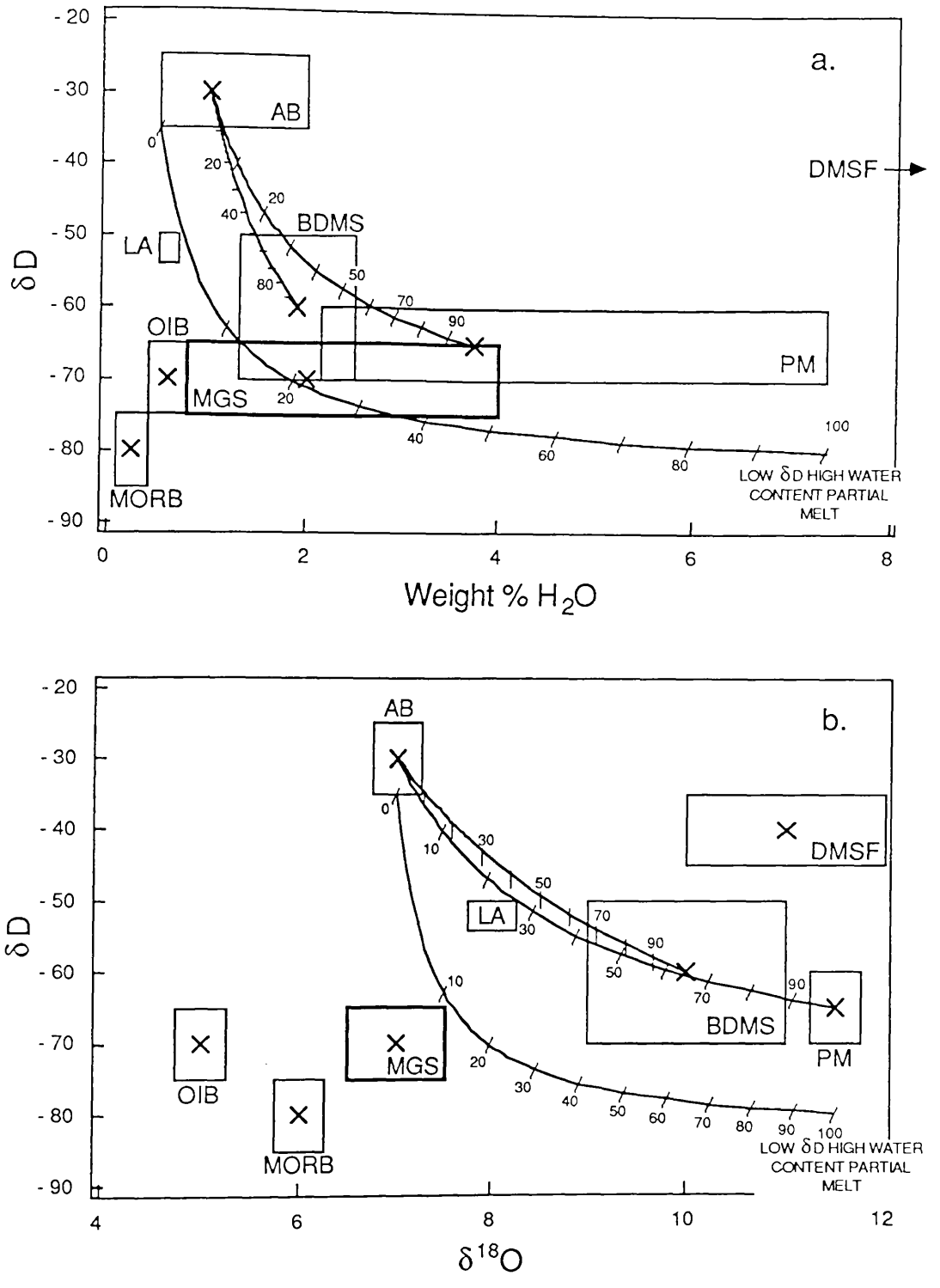

Fig. 4.25 a-f. Wt.% H_2O vs. δD (figs a, c, and e) and $\delta^{18}O$ vs. δD (figs b, d and f) for the MGS magma and hypothetical end members (described in table 4.1) which may have been involved in formation of the MGS magma. Two end member mixing curves between different end members are shown in each figure. Crosses in boxes are best estimates of the compositions, while the area covered by the boxes represent the uncertainties in the estimated values, except for the box for the Lewisian amphibolite end member which only encloses the analytical uncertainty for the data given by Kay (1979). Abbreviations: MGS = unfractionated MGS magma, AB = subduction related basalt end member, OIB = Ocean Island Basalt end member, MORB = Mid Ocean Ridge Basalt end member, LA = Lewisian Amphibolite end member, BDMS = Bulk Dalradian metasediment end member, DMSF = Dalradian metasedimentary fluid end member and PM = partial melt end member. The numbers on ticks on

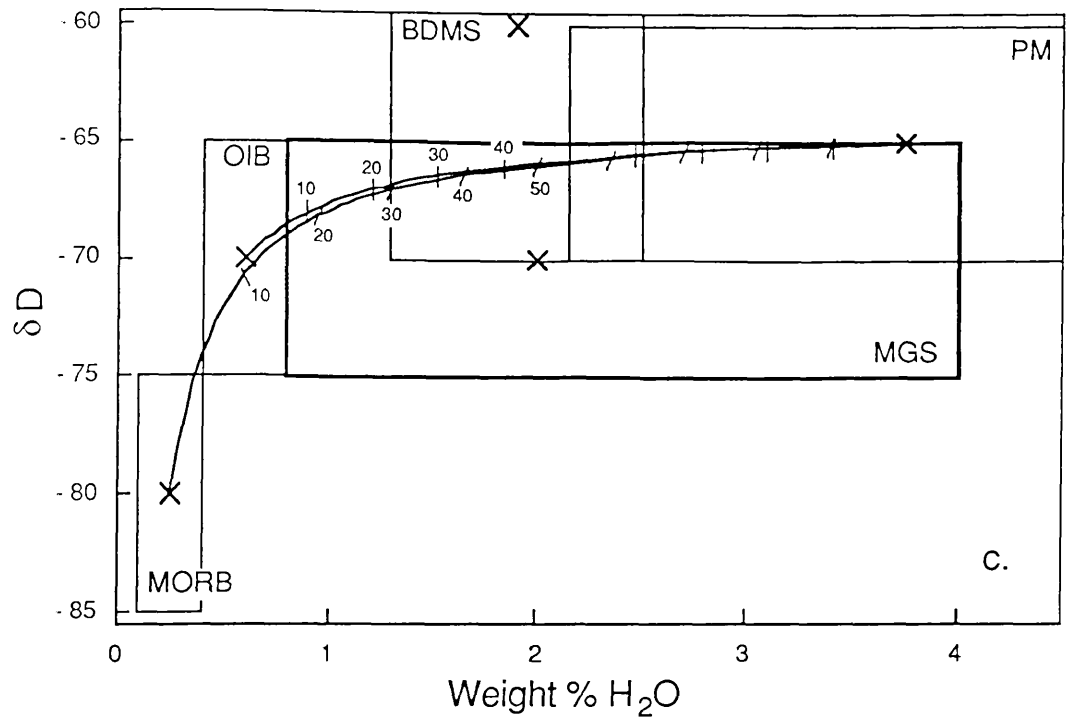

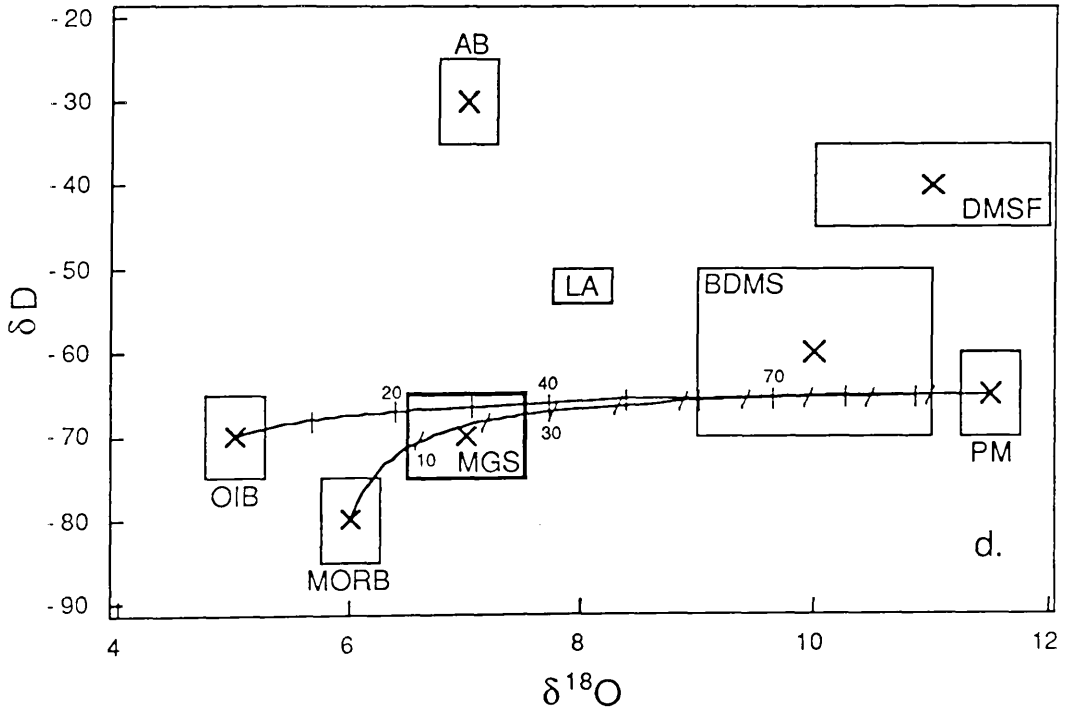

the mixing lines between end members are wt.% of the crustal contaminant in the mixture. Note the change in scale between figs a, c and e.

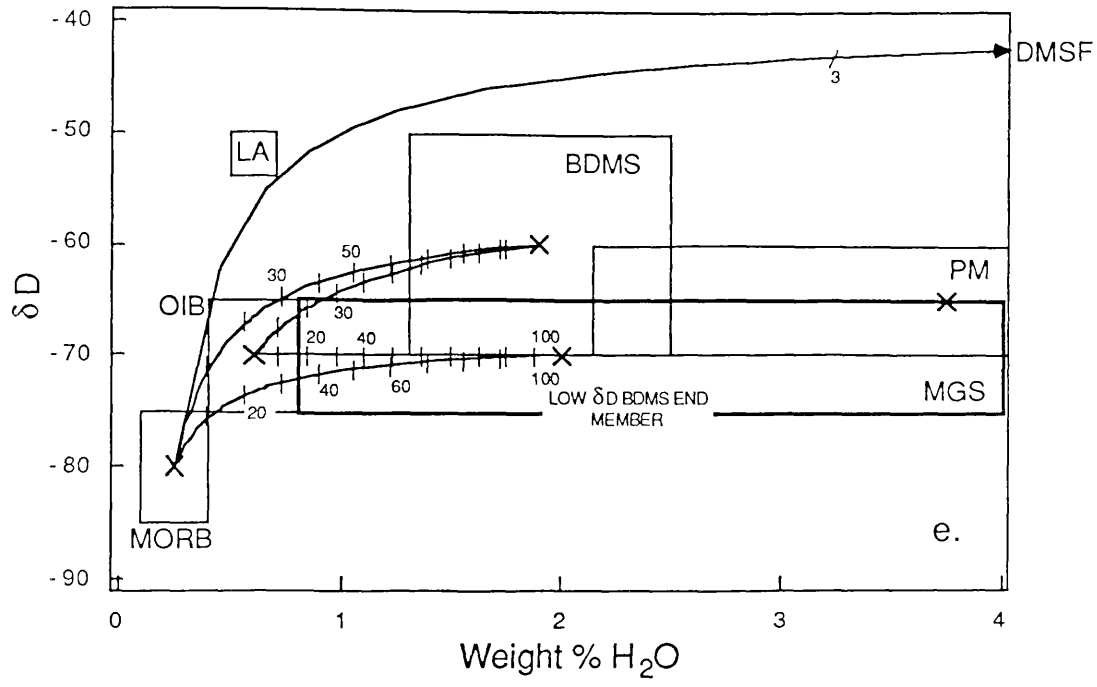

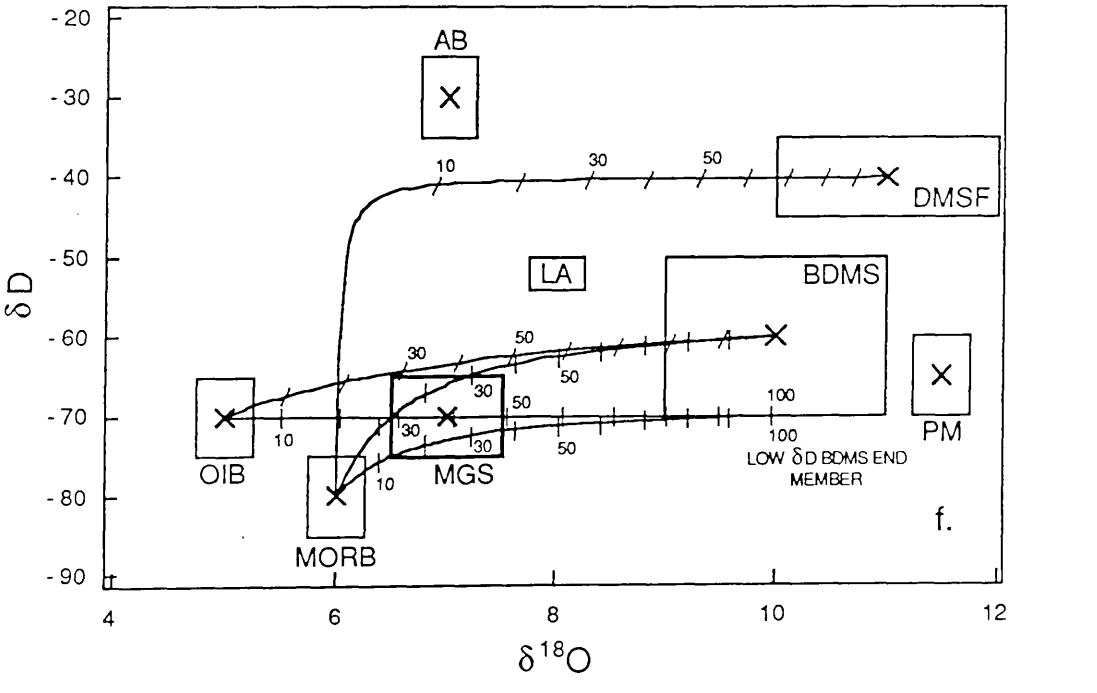

From figs.4.25a and b. it can be seen that it is unlikely that the parental basaltic magma to the MGS magma was similar to the subduction related end member. This is because, although the subduction related end member could have supplied much, or possibly all, of the water in the MGS magma, the high δD of the subduction related end member means that mixtures with any of the possible contaminants always have δD values significantly higher than the MGS magma. Even if the δD of the subduction related and partial melt end members are lowered and the water content contents are minimised and maximised respectively it can be seen that it is still not possible to obtain a mixture with δD and $\delta^{18}O$ values similar to that of the MGS magma.

In figs.4.25c and d. the effect of mixing of MORB or OIB like parental magmas with partial melt material produced within the Dalradian metasediments is examined. It can be seen from fig.4.25d that addition of between 20-35 wt.% of partial melt end member to an OIB like magma could produce a magma with a $\delta^{18}O$ and δD similar to that of the MGS, while if the parental magma was MORB like 10-15 wt.% of partial melt would produce a magma similar in $\delta^{18}O$ and δD to the MGS magma. From fig.4.25c it can be seen that such mixtures would have water contents mostly within the range estimated for the MGS magma, although slightly lower than the best estimate. If the partial melt had a water content nearer to the upper limit than the best estimate, then mixing curves (not shown), indicate that mixing of similar quantities of partial melt end member to those given above, with MORB or OIB like parents would yield a melt with the same $\delta^{18}O$ and δD values but with water contents of 0.9-2.0 wt.% H_2O and 1.9-2.8 wt.% H_2O respectively. Obviously a perfect fit for the $\delta^{18}O$, δD and wt.% H_2O values of the MGS magma could be obtained from mixing an OIB parent with partial melt if the water content of the partial melt was slightly higher than the best estimate, while a perfect fit from mixing a MORB parent with partial melt could be obtained if the water content of the partial melt was near its upper limit. Alternatively if the actual water content of the MGS magma was slightly lower than the best estimate then perfect fits could also be obtained.

The effect of mixing OIB- or MORB-like parents with with bulk Dalradian metasediment or fluid derived from the Dalradian metasediments is demonstrated in in figs.4.25d and e. It can be seen that addition of even very small amounts of the fluid present within the Dalradian metasediments at high temperatures, would increase the δD of these parental magmas well above that estimated for the MGS magma. This provides strong evidence that no significant flow of fluid took place from the metasediments into the MGS magma at high temperatures. It can also be seen that contamination of an OIB-like parent with the best estimate bulk Dalradian metasediment could not have produced the MGS magma, because the δD of mixtures with the appropriate water content would have been too high. Addition of ~20 wt.% of the best estimate bulk Dalradian metasediment to a MORB parent could have possibly formed the MGS magma, but the water content of the magma would be at the low end of the range for the MGS magma. If the δD of the bulk metasediment was 10‰ lower, at the bottom of the estimated range, then melts with δD similar to that of the MGS magma could have been produced from both parental magma types. However only mixtures of an OIB-like parent with 30-50 wt.% of bulk Dalradian metasediment would have δD, $\delta^{18}O$, wt.% H_2O values similar to those estimated for the MGS magma, although the water contents are near the low end of the estimated range (especially since the amount of assimilation is unlikely to have been as much as 50% by weight). Melts produced by mixing with a MORB like parent do not fall in the MGS field on a $\delta^{18}O$-wt.% H_2O plot at the degrees of contamination indicated on the δD-$\delta^{18}O$ plot.

It is possible, of course, that more than two end members may have been involved in the production of the MGS magma. The possibility that the

MGS could have been produced by mixing between 3 end members can be evaluated using the same x-y plots. The range of possible values that can be produced by mixing between 3 end members is bounded on an x-y plot by the curves for two end member mixing running between each pair of end members. This is because as the weight fraction of one end member $\rightarrow 0$ the three end member system reduces to a two end member system.

It has already been shown that it is impossible for fluid derived from the Dalradian metasediments to have mixed with a parental basalt end member since mixing with this fluid would have rapidly changed the melt δD to ~-40‰. For the same reason it is thought unlikely that this fluid could have been involved in 3 end member mixing. Similarly it has also been shown that a subduction related magma could not have been mixed with any crustal end member to give a mixture with a similar δD to the MGS, so that this end member is also considered not to have been important in any 3 end member mixing process. Thus the only possible combinations for 3 end member mixing are between either a MORB or OIB like parental basaltic melt and two of either the Lewisian amphibolite end member, the bulk Dalradian metasediment end member, or the partial melt end member. Figs.4.26a-d show δD-wt.% H_2O and δD-$\delta^{18}O$ plots with bounding curves for 3 end member mixing between the possible combinations of these end members. Bounding curves for OIB and MORB end members mixing with bulk Dalradian metasediment and Lewisian amphibolite end members are not shown because no combinations of these end members fall within the field for the MGS magma on both plots. It can be seen from these diagrams that the MGS magma could have been produced by mixing of OIB- or MORB-like end members with ~20-30 wt.% of crustal material, made up mostly of partial melt material with smaller amounts of bulk Dalradian metasediment or Lewisian amphibolite end members.

Conclusions.

From consideration of the estimated δD, $\delta^{18}O$ and wt.% H_2O of the MGS magma and the materials which could have been involved in its formation it is possible to conclude that

1. The end member that is thought to represent a basaltic melt produced in the vicinity of a subduction zone cannot have been a parental magma to the MGS magma.

2. Fluid present within the Dalradian metasediments during MGS intrusion was not involved in hydrating the magma.

3. Possible parental magmas to the MGS magma could have been similar to the OIB or MORB end members defined above. Possible crustal contaminants for these magmas could be represented by the Lewisian amphibolite, bulk Dalradian metasediment or partial melt end members.

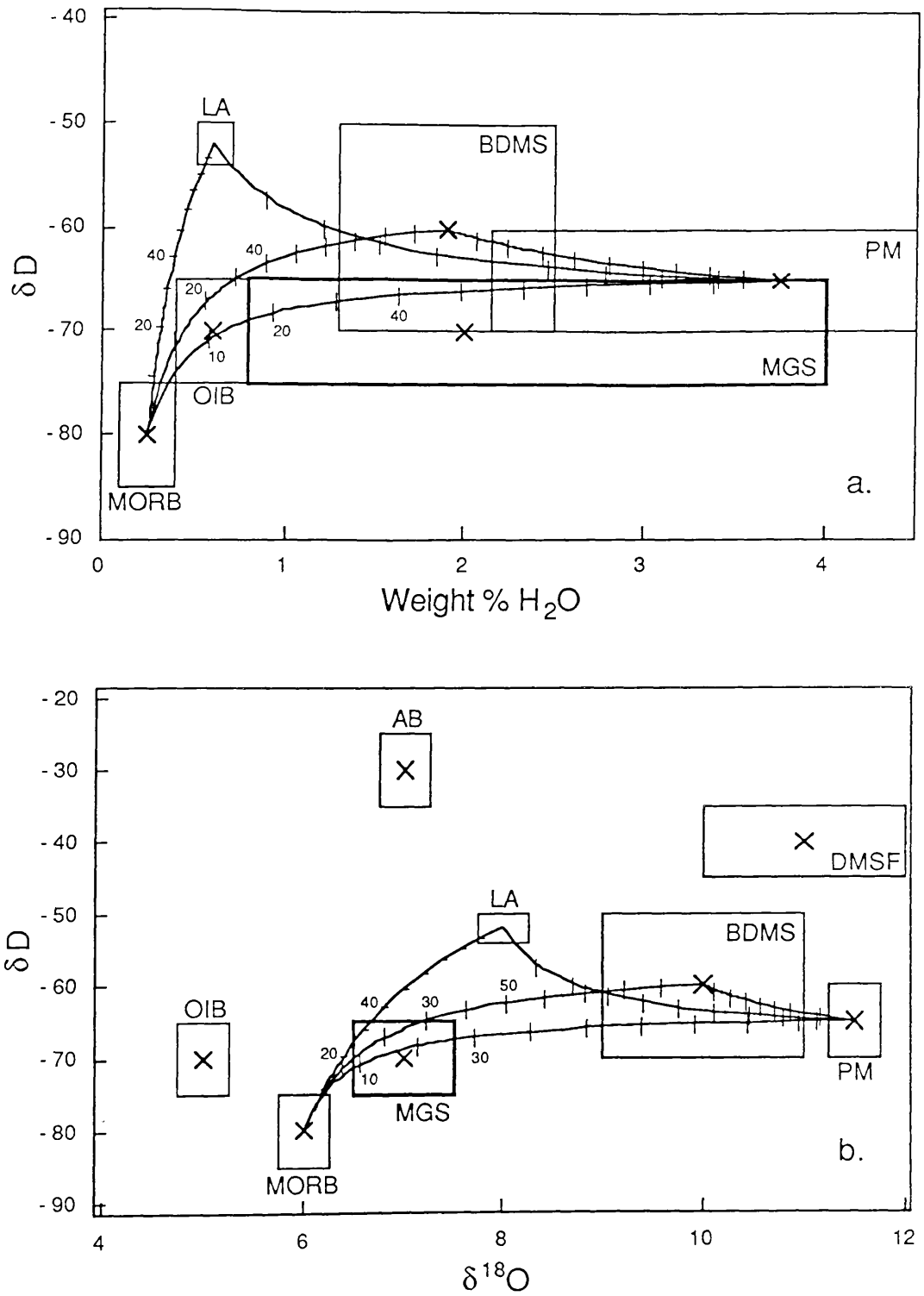

Fig. 4.26 a-d. Wt.% H_2O vs. δD (figs a and c) and $\delta^{18}O$ vs. δD (figs b and d) for the MGS magma and hypothetical end members (described in table 4.1) which may have been involved in formation of the MGS magma. Two end member mixing curves between different end members, which bound areas which are possible with three end member mixing, are shown in each figure. The abbreviations used are the same as those used in fig. 4.25.

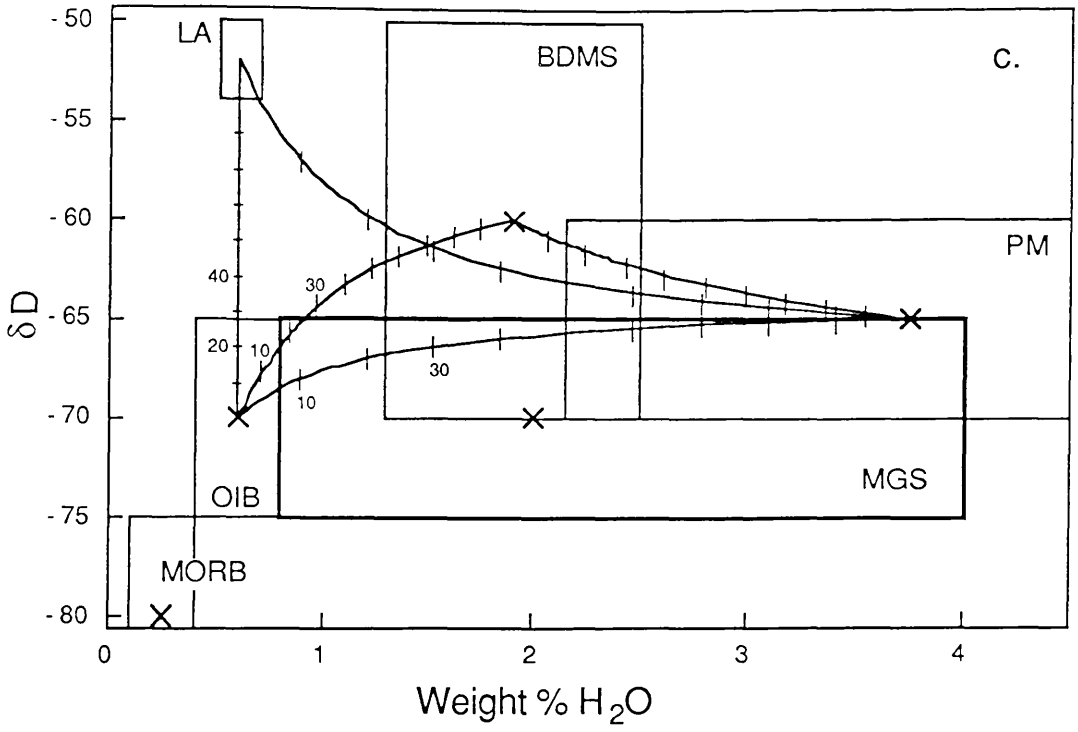

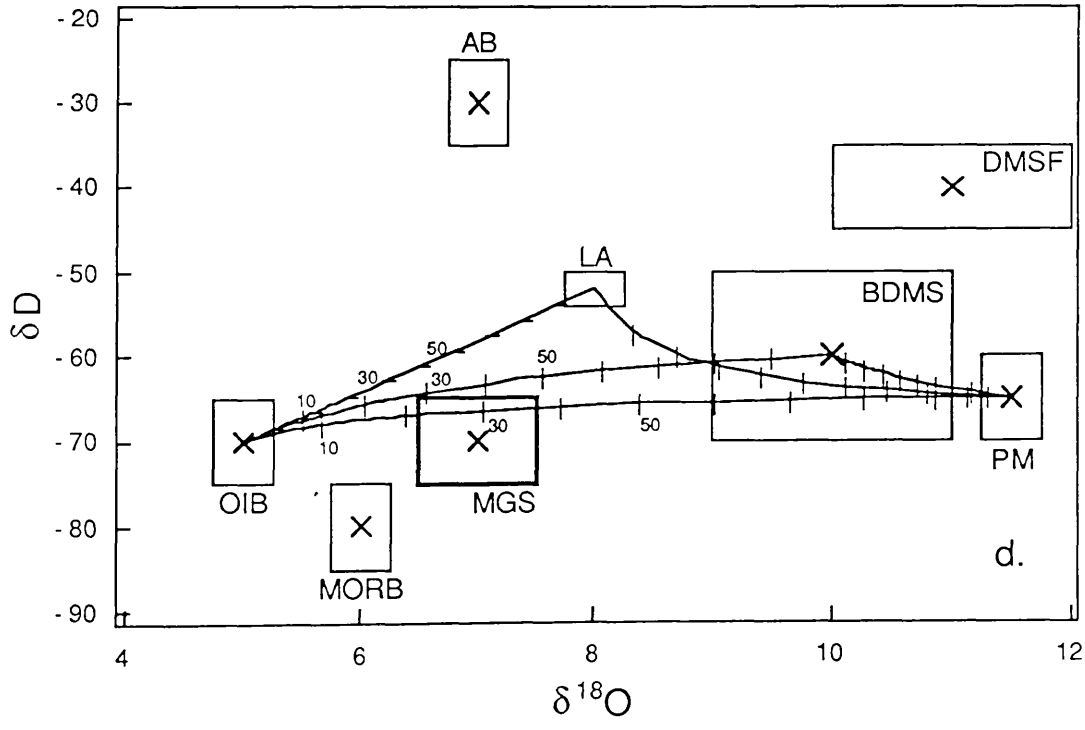

4. Although various combinations between end members are possible, the best fits to the estimated values of δD, $\delta^{18}O$ and wt.% H_2O for the MGS magma are obtained by mixing a MORB or OIB like parental magma with 20-30 wt.% of crustal material. This crustal material would be mostly material derived from partial melting of Dalradian metasediments, together with smaller amounts of bulk metasediment (this would be consistent with the field observations), or with a Lewisian amphibolite like end member.

5. If the principal end members involved in forming the MGS magma were those given above, then it can be concluded that nearly all of the water in the magmatic MGS hornblendes was ultimately derived from the Dalradian metasediments, both at the present level and at a deeper level.

6. Most plausible mixtures (even those involving the most water rich partial melt end member possible) have water contents near the low end of the estimated range for the MGS magma, indicating that its water content may have been as low as 1 wt.%. If this was the case P_{H2O} would have been ~0.12 P_{total}, which would explain the discrepancy between the observed phase relations and those observed in experimental studies for basalts crystallising under conditions of high P_{H2O}.

It should be noted that these conclusions would not be significantly different if all the hornblendes which have been identified as magmatic were actually formed metamorphically. This is because the hydrogen present within the hornblendes was almost certainly derived from the magma (see introduction to this section) and should have a δD similar to the magma even if they were metamorphic, because the amount of hydrogen now present in the hornblendes is similar to that estimated to have been contained within the melt on petrologic grounds.

Conclusion 4. compares well with the results of 2 end member mixing calculations using Sr and Nd isotope data, carried out by Jagger (1985), who concluded that the combination of end members that produced a mixture with Sr and Nd isotope ratios nearest to those of the primitive MGS magma was an "enriched mantle source" mixing with 25(Nd)-30(Sr) wt.% of Connemara Dalradian metasediment. Jagger did not model mixing involving a partial melt end member. However, Sr abundances and $^{87}/^{86}Sr_i$ ratios in the microgranite sill N of the Cashel body, which may be representative of the partial melt end member, are similar to those in the metasediments (*ibid.*), so that at least in terms of Sr the MGS magma could equally well have originated by mixing of an 'enriched mantle source" with 25-30 wt.% partial melt material, although there might be some discrepancy using Nd data. Jagger's "enriched mantle source" might be expected to be more comparable in terms of trace elements to the OIB end member than the MORB end member used in this thesis, indicating perhaps that a magma similar to the OIB end member may have been parental to the MGS magma.

The fact that the subduction related end member can be excluded as a parental end member for the MGS magma might be taken to indicate that the MGS was not developed over a subduction zone as has been suggested by Yardley and Senior (1982) and Thompson (1985), but was produced in another tectonic setting (e.g. Lambert and McKerrow, 1976; Dewey and Shackleton, 1984). Furthermore the fact that presence of magmatic hornblende can be attributed to assimilation of partial melt in the mid crust and not to a high water content in the source also negates the argument used by Yardley and Senior (1982) that the MGS was developed in an arc setting because the mineralogy is similar to that of cognate xenoliths from arc volcanics (Arculus and Wills, 1980).

However many magmatic rocks which can be plausibly attributed to a subduction related origin do have δD similar to the MGS hornblendes (e.g. biotites in porphyry copper stocks on the Pacific margin of N America; Sheppard *et al.*, 1971 or Japanese granitoids; Kuroda *et al.*, 1986). Therefore it seems possible that subduction related magmas may not always have high δD values similar to the subduction related end member described above. Presumably if the hydrogen contribution of the melt from the high δD subducting slab was relatively small, perhaps because the degree of melting was high, or because the subcontinental mantle had been metasomatised by fluids with mantle δD, then the δD of the melt produced may have been nearer more normal mantle values (-70‰?).

Thus it would be unwise to conclude from this evidence that the MGS magma was not ultimately related to subduction, although the case for this hypothesis is weakened.

4.6.2. Metamorphic hornblendes.

Some hornblendes within the ultrabasic rocks show clear textural evidence that they formed by subsolidus reactions and are therefore metamorphic in origin (e.g. plates 1 and 2). The stable isotope ratios of the metamorphic hornblendes measured so far are not diagnostic of their origin. Fig. 4.21 shows that these hornblendes last equilibrated with a fluid with a δD and $\delta^{18}O$ indistinguishable from that in equilibrium with the magmatic hornblendes so that it is logical to suggest that these metamorphic hornblendes were formed from small amounts of residual magmatic fluid left over after crystallisation had taken place, which had its isotopic composition controlled by equilibration with the large volumes of magmatic hornblende within the surrounding rock. However the δD and $\delta^{18}O$ values of the fluid in equilibrium with these hornblendes is also similar to those of the fluid in equilibrium with the surrounding metasediments indicating that this fluid could also have caused hornblende growth. Alternatively, since it is often observed that ultrabasic rock has been amphibolised where it has been intruded by quartzofeldspathic veins (e.g. GJ.29) which are presumably metasedimentary melts, the hydrogen for hornblende formation may have been derived from these melts in a closed system reaction (i.e. $\delta D_{hornblende} = \delta D_{melt}$). Although both of these mechanisms are feasible near to the contact with the metasediment it would appear unlikely that they could account for the presence of metamorphic hornblende in areas many km away from any metasedimentary material, such as the area to the W of Roundstone. Furthermore as pointed out previously, quartz $\delta^{18}O$ variations at the margin of the Cashel body are inconsistent with large amounts of high temperature fluid flow across the contact. Thus the first explanation is preferred here.

The association of some actinolite with late prehnite and chlorite (plate 2.) suggests that this amphibole may have formed during the late retrogression event, in equilibrium with the high δD fluid. Unfortunately none of this actinolite has yet been analysed for its hydrogen isotope

composition If this actinolite did grow in equilibrium with the high δD fluid it is predicted that it should have a δD of > -50‰, if the hydrogen isotope fractionation of Graham *et al.* (1984) between actinolite and water does not change drastically below 350°C, the lower temperature at which it was calibrated.

4.7 THE ORIGIN OF THE HIGH δD FLUID CAUSING CHLORITE, EPIDOTE AND SERICITE FORMATION.

4.7.1 Introduction.

It has already been shown in this chapter that chlorite, epidote and sericite in the MGS developed as a result of hydration reactions involving a fluid with a high δD (probably ~-25‰). It has also been shown that this fluid:

a. had a lower $\delta^{18}O$ than the fluid that was in equilibrium with these rocks at high temperatures.

b. must have been saline to some extent.

c. had $H_2O/(H_2O+CO_2)$ ratios of 0.98-0.985 (i.e. 2-1.5 mole % CO_2).

d. was present in these rocks in some quantity between temperatures of 300°C (or greater) and 180°C (and possibly as low as 160°C).

4.7.2 Internal vs. external origin for the high δD fluid in the MGS.

There are two major possibilities for the origin of the high δD fluid, either it could have been produced internally within the MGS, from the residual magmatic fluids by some fractionation process (i.e. it was "deuteric"), or alternatively it could have been derived from some reservoir external to the MGS (i.e. exotic). It is clear from the association of chlorite/epidote/sericite with with microcracks and bubble planes (often showing a subparallel orientation in a single sample), that the high δD fluid was locally infiltrative and therefore not derived from that particular rock mass. However on the scale of the whole MGS intrusion, it is possible that this fluid could have been derived from other parts of the MGS, most probably the later differentiates. The water content of the MGS magma would have increased with magmatic differentiation, provided that the amount of water that was precipitated in primary minerals was less than the water content of the magma at any time. If the water content of the MGS magma was initially near to 1 wt.% (4.6.3), then unless greater than 50 volume % of the hornblende was precipitated through the entire sequence, the water content of the magma would have increased in the later differentiates. It would seem likely therefore, that at some point the later differentiates would have become water saturated and exsolved a water rich fluid. Some evidence that such a fluid was actually formed comes from the observation of Leake (1970a) that country rocks within a few km of the intermediate gneisses appears to have been infiltrated by metasomatic fluids which caused the growth of andesine and quartz in these rocks. Leake (*ibid.*, p. 225) also notes that in the Cashel-Recess area, the hornblende in the

intermediate and acid rocks is much more chloritised than in the adjacent basic rocks, and suggests that this indicates an association between the fluid causing chloritisation and the later differentiates. The question of whether the high δD fluid was derived internally (i.e. from these residual magmatic fluids, within the MGS intrusion as a whole), or is exotic and was derived from a source external to the MGS can be examined using isotopic and mass balance constraints.

Isotopic constraints.

The hydrogen isotopic composition of a fluid which equilibrated with the intermediate or acid magmas is likely to have D enriched by ~ 20‰ (B.E. Taylor, 1986). Therefore the δD of the exsolved fluid is likely to have been <-50‰, the exact δD depending on the mechanism of fluid separation from the melt (e.g. Nabelek *et al.*, 1983). It is likely that within the MGS, the δD of this fluid would have been altered by equilibration with the large volume of hydrogen contained within the MGS hornblendes prior to closure. Therefore it is suggested that this fluid could have had a δD as high as -50 to -30‰ (fig. 4.2). The δD values of the metamorphic hornblendes in the MGS are in accord with this suggestion (4.6.2). If this fluid also caused the late chlorite/epidote/sericite-forming retrogression, the δD of this fluid would need to be modified to higher δD values (~-25‰) by some process. Steam separation from this fluid could increase the δD of the remaining fluid (fig. 2.19) and this cannot be excluded on isotopic grounds, but is considered unlikely since it could only have taken place at very shallow depths on the boiling curve (< 1 km at 300°C; Haas, 1971). Examination of the fluid inclusions could rapidly show whether or not this is the case. Alternatively formation of low δD chlorite and sericite by hydration reactions could have increased the δD of the remaining fluid. Because of the high abundance and high water content of chlorite, most of the hydrogen in minerals formed in the late retrogression is contained in this mineral. Because of this, it is considered that the effect of hydration reactions on the fluid δD can be approximated to that resulting from the formation of chlorite alone.

The δD of the chlorite formed during a hydration reaction will depend on the rate at which it re-equilibrates with the fluid after formation. Two end member situations can be envisaged:

1. If the chlorite continuously re-equilibrates H isotopes with the fluid as fast as it is formed then the final δD of the chlorite and fluid can be calculated from the simple mass balance and fractionation equations

$$\delta D_{fluid(X)} = \delta D_{fluid(i)} - (1\text{-}X) \times 10^3 \ln\alpha_{chlorite\text{-}fluid}$$

and

$$\delta D_{chlorite(X)} \approx \delta D_{fluid(X)} + 10^3 \ln\alpha_{chlorite\text{-}fluid}$$

where X is the fraction of hydrogen remaining in the fluid after chloritisation (i.e. X decreases with increasing chloritisation), $\delta D_{fluid(X)}$ and $\delta D_{chlorite(X)}$ are the δD values of the fluid and chlorite at a certain

value of X and $\delta D_{fluid(i)}$ is the initial δD of the fluid (i.e. when X = 1). This is a simple batch fractionation process.

2. If the chlorite that has already formed does not re-equilibrate H isotopes with the fluid as chloritisation proceeds, then the δD values of the fluid and any further chlorite that forms from it, evolve to higher δD values following a Rayleigh fractionation equation

$$\delta D_{fluid(X)} = 10^3 (X^{(\alpha-1)}-1) + \delta D_{fluid(i)}$$

(cf eqn. 2.37) and

$$\delta D_{chlorite(X)} \approx \delta D_{fluid(X)} + 10^3 \ln\alpha_{chlorite\text{-}fluid}$$

where the symbols are the same as defined above, except that in this case $\delta D_{chlorite(X)}$ only refers to the δD of the infinitely small amount of chlorite formed at that value of X, rather than all the chlorite formed in the system. This process is often termed a fractional equilibrium process.

The calculated δD of the chlorite and fluid that would result from a hydration reaction with a fluid of δD = -48‰ (the average δD of the fluid in equilibrium with the hornblendes at high temperature; fig. 4.2) by either of these processes is shown in fig. 4.27. The calculations do not take account of the fact that the chlorite is usually replacing biotite or sometimes hornblende (i.e. the chlorite precursor is assumed to be anhydrous). Because biotite or hornblende are likely to have had lower δD values than the initial fluid, the effect of ignoring the contribution of the hydrogen from these minerals to the system is to move all the curves to slightly higher δD values.

Fig. 4.27 shows that the δD of the first chlorite that formed from the fluid with δD = -48‰ would be ~-78‰. In the batch fractionation process, as further chlorite is formed, it re-equilibrates with the fluid and the δD values of the chlorite and fluid move to higher values along the two straight curves shown. It can be seen that if ~75% of the fluid that was present initially was incorporated into chlorite, then the end result would be that the fluid would have a δD of ≈ -25‰ and the chlorite a δD ≈ -57‰, similar to the δD values actually observed in the MGS. If the contribution of hydrogen from the precursor biotite or hornblende is also taken into account then a rather greater proportion of the fluid originally present would have to be incorporated into chlorite to achieve the same effect. In 4.2 it was suggested that if the chlorite formed at ~300°C, then it would be unlikely that it would re-equilibrate hydrogen isotopes with the pore fluid by diffusion after formation. Thus although a batch fractionation process could produce a high δD fluid by chloritisation, this process is unlikely to have caused the formation of the high δD fluid in the MGS unless chloritisation took place at higher temperatures than supposed, enabling rapid hydrogen isotope re-equilibration with the fluid.

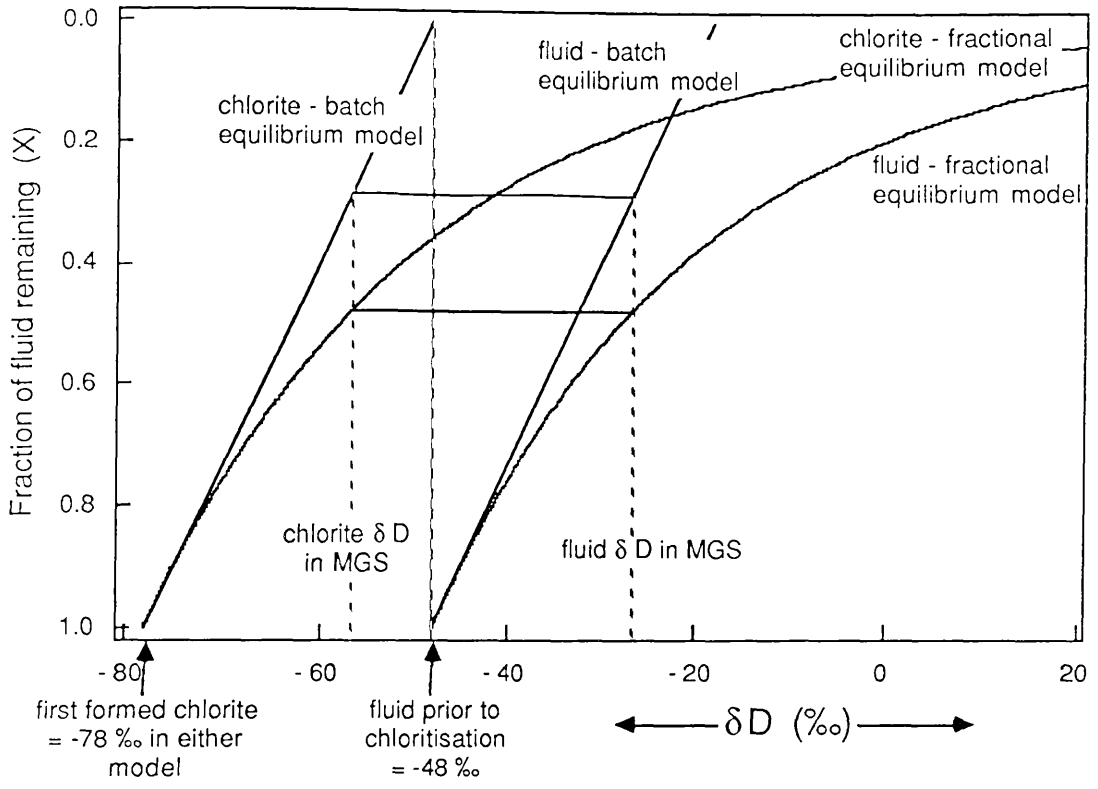

Fig. 4.27 Calculated δD of chlorite produced by a hydration reaction from a fluid with δD of -48‰ as a function of the amount of this fluid which is incorporated into chlorite, assuming either a batch equilibrium or fractional equilibrium process. The δD of the remaining fluid is also shown.

If, as would seem likely, the chlorite did not appreciably re-equilibrate with the fluid as it formed, then the first formed chlorite with a δD of -78‰ would be preserved. Later formed chlorites would have heavier δD values and the δD of the chlorite forming at any time and the δD of the fluid in equilibrium with it would follow the curved lines shown in fig. 4.27. It can be seen that if ~55 % of the fluid that was initially present was incorporated into chlorite, the δD of the remaining fluid would be similar to that of the high δD fluid present in fluid inclusions. However in this case, although the δD of the chlorite which last formed from this fluid would be similar to that observed in the MGS all the earlier formed chlorite would have lower δD values. The frequency distribution and mean of the δD values of chlorites formed by this process are compared with those actually measured for chlorites in the MGS in fig. 4.28.

It can be seen that the two distributions and means are distinctly different suggesting that the high δD could not have been produced by such a process. The frequency distribution of chlorite δD produced by fractional equilibration could differ from that shown depending on the size of the system. The distribution given in fig. 4.28 is for a large (>hand specimen) sized system. In such a system, the fluid causing chloritisation is envisaged to be progressively moving through the rock mass, so that the chlorite in each hand specimen forms from a fluid with a relatively constant δD and is

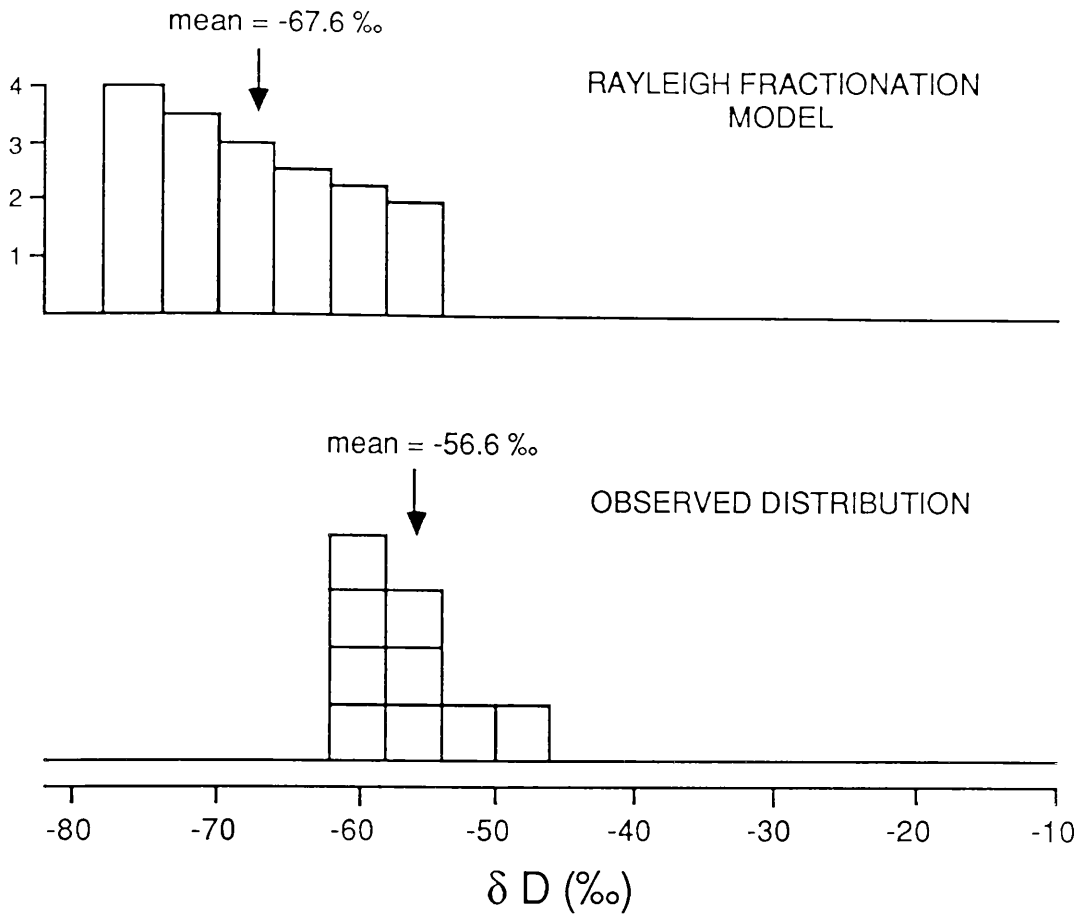

Fig. 4.28 Frequency distribution and mean of δD of chlorite produced during the fractional equilibrium process shown in fig. 4.27 which resulted in the formation of a fluid with a δD of -26.6‰, compared with the actual δD values of chlorites from the MGS.

therefore homogeneous on a hand specimen scale. In this system, the variations in chlorite δD occur between hand specimens. If on the other hand the system is envisaged to be on a hand specimen scale (i.e. the fluid causing chloritisation is present in the same hand specimen throughout the duration of chloritisation), then although the chlorite δD may vary on a grain scale, the chlorite δD measured for each sample will be the average of all the grains in the sample. Therefore the chlorite δD will be similar in all samples, provided the degree of chloritisation is the same. In either case the mean δD of all the chlorite produced will be similar and as noted above this mean value is distinctly different from that actually observed in the MGS. Furthermore the δD of the chlorites that were sampled is very homogeneous across the Cashel-Recess area, indicating that the fluid was homogeneous on this scale. Thus the high δD fluid could only have been obtained from a residual magmatic fluid by a fractional equilibrium process if the Cashel-Recess area was part of a much larger system, in which fluid δD was varying on a greater scale. This is considered to be extremely unlikely because the presence of a similar high δD fluid is also indicated by epidotes in the Delaney Dome area over 10 km to the west, a distance which is a significant fraction of the size of the whole MGS outcrop.

Thus from an examination of the H isotopic data it can be concluded that it is unlikely that the high δD fluid was formed from a residual magmatic fluid. This could only be the case if either steam separation was taking place, or chloritisation took place at higher temperatures than envisaged, so that a batch fractionation process could take place.

Mass balance constraints.

It was suggested in 4.6.1 that the water content of the MGS magma must have been quite low (~1-1.5 wt.% H_2O). If this magma crystallised as a closed system and the water in the chlorite, epidote and sericite was derived from the magma, then it would be expected that the average water content of all rock types, weighted in terms of their abundance, should equal this value. If the magma did not crystallise in a closed system, but lost water during crystallisation, for example as a result of vapour loss during eruption at a higher level, then the average water content would be less than this value. Alternatively if the MGS rocks had water added to them after crystallisation, then the average water content should be greater than that inferred for the MGS magma. Fig. 4.29 shows the water contents determined by Leake (1958,1970a) for a number of samples of MGS rocks claimed to be representative of the different rock types in the area. Since these samples were chosen for the purpose of showing the differences in chemistry due to magmatic variations, it is likely that they may be fresher (i.e. contain less chlorite/epidote/sericite alteration) than many of the MGS rocks, so that the water contents of these rocks may slightly underestimate those in the average MGS rocks. In practice it is actually rather difficult to calculate the weighted average water content of the MGS rocks because of the uncertainty in the proportions of the different rock types. However this is found not to be necessary, because it can be seen from fig. 4.29, that the water content of nearly all these samples is higher than that inferred for the MGS magma. Thus as long as these samples are representative of the MGS as a whole, it would appear unlikely that the total amount of water contained in all the hydrous minerals in the MGS rocks could all have been supplied by the MGS magma. Hence an external source is required for some of the water. This additional water must have been added to the magma after crystallisation, because otherwise the water content of the magma would have been higher, so that this additional water must be located within the subsolidus hydrous minerals (i.e. the chlorite/ epidote/sericite). Therefore it is possible to conclude that, provided the water content of the MGS magma has been correctly estimated, the water in the late retrograde minerals was derived from a source external to the MGS.

Thus from both the isotopic and mass balance constraints, it would seem unlikely that the high δD fluid was derived internally within the MGS and therefore it must be concluded that the high δD fluid is exotic to this rock unit.

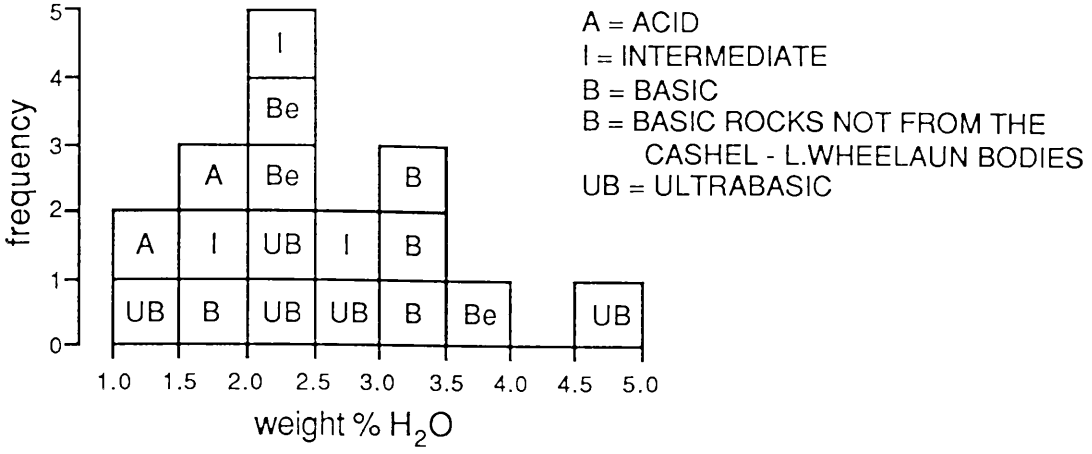

Fig. 4.29 Total water content of MGS rocks from the Cashel-Recess area. The analyses are those given in Leake (1958,1970a).

4.7.3. Internal vs. external origin for the high δD fluid in the Cashel-Recess area.

In the previous section it was concluded that the high δD fluid which caused chlorite/epidote/sericite growth in the the MGS was derived from a source external to the MGS. Since the hydration reactions forming these minerals have taken place throughout the MGS, even in bodies that appear to be totally surrounded by Dalradian metasediments, it is concluded that the high δD fluid must have either been derived from the Dalradian metasediments, or passed through them on the journey from a more distant source. The presence of chloritised biotites, with δD values ≈ -50‰ (fig. 3.3), within the Dalradian metasediments indicates that a high δD fluid was also present within these rocks at low temperatures. It seems reasonable, in the light of the previous conclusion, to correlate this high δD fluid with that causing the late retrogression in the MGS. Like the high δD fluid in the MGS, the high δD fluid in the metasediments appears to have been infiltrative, at least on a local scale, since chloritisation and sericitisation appear to be spatially associated with oriented bubble planes or microcracks. In 3.5.4 it was shown that there was no reasonable mechanism by which the water in the chlorite and sericite in the Dalradian metasediments could have been derived internally from within these rocks and it was suggested that the high δD fluid was exotic to the metasediments. Thus if the high δD was exotic to both the MGS and the Dalradian metasediments, it must be concluded that the high δD fluid was derived from a source external to the Cashel-Recess area altogether.

4.7.4 Depth at which the high δD fluid was present in the MGS.

Prior to any discussion on the origin of the exotic high δD fluid in the Cashel-Recess area, it would be useful to have some idea of the depth at which infiltration took place. Some indication of the pressure conditions under which chlorite, epidote and sericite growth took place may be gained from examination of the phase equilibria in the MGS. It should be noted

however, that there are problems attendant on this approach to the estimation of P-T conditions for low grade metamorphic assemblages. Slow reaction kinetics at low temperatures can lead to disequilibrium mineral assemblages (as demonstrated by the hydrogen isotope disequilibrium), or to equilibrium domains being very small (Cho and Liou, 1987). In addition, the effect of mixed component volatiles, fO_2 variations and mineral solid solution on mineral stability are often only qualitatively known. Nevertheless, if mm scale chemical equilibrium is assumed, then an estimate of the maximum pressure at which the late alteration of the MGS took place can be gained from the mineralogy of prehnite bearing assemblages.

Prehnite is occasionally present in the alteration assemblage prehnite-actinolite-chlorite±clinozoisite in some ultrabasic rocks (e.g. GJ.103). These minerals are not usually observed to be contiguous but are often seen to occur within a fraction of a mm of each other in thin section. Such an assemblage is diagnostic of the prehnite-actinolite facies defined by Liou *et al.* (1985) for metabasites. These authors present a petrogenetic grid for mineral assemblages in the NCMASH system with excess chlorite, quartz and albite (their fig. 2), which might be used to estimate the P-T conditions at which this alteration assemblage developed. If M is taken to be equal to MgO+FeO then the NCMASH system approximates very well to the compositions of the ultrabasic rocks, which according to the analyses of Leake (1958) have >94 wt.% of their oxides in this system. Both quartz and plagioclase are present in GJ.103 so that it might be considered reasonable to apply this grid to the assemblage in this rock. It should be noted that this plagioclase is a relict igneous phase and therefore highly calcic. However, since the plagioclase is still the only major Na bearing mineral in the rock, it is considered that its presence should make no difference to the phase relations derived assuming an albite excess, except that the bulk composition of the alteration mineralogy will be driven away from the Ca apex of the ACM triangle used by Liou *et al.* (*ibid.*). If the application of this petrogenetic grid is valid, then conditions at which the assemblage prehnite-actinolite-chlorite±clinozoisite is stable can be constrained to be 230-400°C, with a maximum P_{fluid} of 2.2 kb at 340°C. If it is assumed that the temperature of alteration was everywhere near to 300°C (the quartz-epidote oxygen isotope temperature derived in 4.5.2), then the maximum fluid pressure would have been ~1.8 kb.

The NCMASH system does not take into account the effect of the presence of Fe^{3+}, or of CO_2 in the fluid, both of which may be present in natural systems. Liou *et al.* (1985) show that the introduction of ferric iron into this system will displace the upper stability limit of the prehnite-actinolite facies to lower pressures. However the ultrabasic rocks contain little Fe^{3+} (Leake, 1958) and the reduction in maximum P_{fluid} at 300°C that this causes is likely to have been minimal (fig. 4, *ibid.*). Cho and Liou (1987) show that the presence of even small amounts of CO_2 in the fluid will drastically alter the pressure maximum of the prehnite actinolite facies, although this effect has not been quantified. The high δD fluid is believed to contain at least 1.5 mole % CO_2 and small amounts of calcite observed in GJ.130 indicate that some CO_2 was present in the fluid altering this rock.

Thus this prehnite bearing assemblage could have formed at pressures considerably less than 1.8 kb.

Bruton and Helgeson (1983) have proved that it is justified to apply equilibria calculated at a given fluid pressure (P_{fluid}) and temperature, to all systems where P_{fluid} applies, regardless of whether the system is lithostatically or hydrostatically pressured. Thus, in either case, this maximum fluid pressure can be used to place an upper limit on the depth at which this assemblage formed. If the fluid was lithostatically pressured and $\rho_{rock} = 3.0$, then this assemblage could have formed at <~6 km, while if the fluid was hydrostatically pressured, even if it was assumed that $\rho_{fluid} = 1.0$ at all depths (it is actually likely to reduce with depth because of the effect of increasing T; *ibid.*) the assemblage could have formed at depths of up to 17 km. This upper depth limit is deeper than any known hydrostatic system and therefore provides no constraint on the depth at which the assemblage formed if it formed in a hydrostatic system. Thus it can be tentatively concluded from the phase relations that the high δD fluid infiltrated the MGS at depths of less than 6 km if it was lithostatically pressured, while if it was hydrostatically pressured it could have infiltrated at depths of up to ~10 km which is thought to be the maximum depth at which fluid can be hydrostatically pressured. If the fluid was hydrostatically pressured then $P_{fluid} \approx$ <0.1× depth (in km) and therefore must have been less than ~1 kb. The minimum depth at which prehnite-actinolite facies mineral growth could have taken place is as shallow as 1.5 km, since minerals of this facies have been observed to form in active geothermal systems at this depth (e.g. the Cerro Prieto system; Bird *et al.*, 1984). It is hoped that further refinement of the pressure estimate will shortly be obtained from fluid inclusion data.

4.7.5. The origin of the high δD fluid in the Cashel-Recess area.

The δD value of this exotic fluid is unlikely to have been significantly altered by exchange since leaving its source because the fluid/rock ratios for hydrogen will always be high during fluid infiltration. The homogeneity in fluid δD across the area indicated by the chlorite and sericite data supports this proposal. Thus the δD value of this fluid (~-25‰) can be used to constrain its possible origins. Reference to fig. 2.19 shows that fluids with such a high δD value must either be ultimately of surface (meteoric or seawater) origin or be derived from a certain type of metamorphic source.

The high δD fluid is distinctly lower in δD than present day seawater. The only way in which the high δD fluid could have been derived from a seawater source is if either the δD of seawater was lower in the past, as has been suggested by some authors (Ohmoto, 1986; Sheppard, 1986a), or the the seawater δD was lowered by some process, prior to infiltrating the area. Processes which can significantly lower fluid δD are very unusual and as noted above the homogeneity in fluid δD argues against the δD having been changed by some process. Therefore if seawater in the past was not significantly different in δD from that at present, it would be concluded that a seawater origin for this fluid would be unlikely. However, because of the

uncertainty in the δD of the oceans through time it is not possible to exclude the possibility that the high δD fluid could have been derived from a seawater source. Measurement of the fluid inclusion salinities may provide evidence to show whether or not this was the case. If the fluid were of meteoric origin, then the $\delta^{18}O$ value of the fluid at its source can be calculated to be ~-4.5‰ using Craig's (1961a) equation for the meteoric water line (eqn. 2.35). Because fluid/rock ratios for oxygen are always much smaller than for hydrogen, unlike the fluid δD, the $\delta^{18}O$ value of a fluid is expected to change during infiltration, shifting towards the equilibrium fractionation with the rock under the conditions of infiltration. Thus the positive $\delta^{18}O$ values indicated by the epidotes for the high δD fluid in this area (fig. 4.23) do not mean that a surface water source can be excluded. The fact that the $\delta^{18}O$ value of the high δD fluid is lower than that which would be in equilibrium with the hornblende and quartz in one rock (fig. 4.24) shows that oxygen isotope equilibrium was not totally achieved between the high δD fluid and the MGS minerals and indicates that prior to any oxygen isotope exchange the the high δD fluid must have had a lower $\delta^{18}O$ value. A low $\delta^{18}O$ (<+7‰) value for the high δD fluid would tend to indicate a surface water source, although certain types of metamorphic fluid could also have $\delta^{18}O$ values as low as +3‰. Surface waters are strongly oxidised relative to all igneous rocks, so that the fO_2 variations inferred for the high δD fluid in 4.5.3 could be the result of variable degrees of reaction between an oxidising fluid and a reduced rock. It was noted in 4.3.5 that if all the epidotes had equilibrated with the high δD fluid at approximately the same temperature then the fluid must have varied in $\delta^{18}O$ between samples and that the most ^{18}O poor fluid must have had the highest fO_2 while the most ^{18}O rich fluid must have had the lowest fO_2. Such a correlation between fluid $\delta^{18}O$ and fO_2 is exactly what might be expected if a low $\delta^{18}O$, high fO_2 surface water infiltrated high $\delta^{18}O$, low fO_2 rocks under conditions of varying fluid/rock ratio. Thus if all the epidotes did equilibrate oxygen isotopes with the fluid at approximately the same temperature, then their $\delta^{18}O$-Fe^{3+} correlation (fig. 4.22) provides strong support for a surface water origin for this fluid.

It is now commonly accepted that there is no viable mechanism by which hydrostatically pressured surface water can migrate up the pressure gradient into the lithostatically pressured fluid regime (Valley, 1986). Therefore if the high δD fluid was of surface water origin, it must be concluded that the retrograde alteration took place in a hydrostatically pressured regime. Within this regime the only way in which large volumes of surface water can be moved into rocks at depth is by convective circulation of pore waters. Convective circulation has frequently been found to take place around cooling intrusives at high levels. However a localised heat source may not always be required to cause convection because the gravitational instability of a convection cell is also a function of the height of the cell (2.7.6), so that convection could also take place in a deep cell with only a moderate thermal gradient (e.g. Russel, 1978). The post MGS Galway granite intrusions potentially could have acted as heat sources to drive convective hydrothermal systems which brought down meteoric water or seawater into

the Cashel-Recess area. The recognition that retrograde hydration processes have taken place in the Galway and Roundstone granites (1.3.4) provides additional support for this suggestion. It can be seen from fig. 2.20 that meteoric water of $\delta D \approx -25‰$ may have been present at the surface at the time of intrusion of these granites, suggesting that the high δD fluid could have originated by such a process. However it was noted in 1.3.6 that some retrograde hydration has taken place in later Lower Carboniferous dykes so it is possible that fluid infiltration could have taken place at a later time. It can be seen from fig. 2.20 that waters with relatively heavy δD values were probably present at the surface during much of the post Ordovician history of the Connemara massif, so that the coincidence of δD values between the high δD fluid and the surface waters at ~400 Ma does not unequivocally prove that, if the high δD fluid was of surface water origin, it infiltrated at this time.

Metamorphic fluids with high δD values include high temperature formation fluids in sedimentary basins (fig. 2.19) and fluids produced during prograde metamorphism of low grade pelitic rocks (Rye *et al.*, 1976). Formation fluids in sedimentary basins may be rather reducing because of reactions with organic matter which is often (but not always) present, while these fluids can also have extremely high $\delta^{18}O$ values due to equilibration with carbonate or clay minerals. Because the high δD fluid is known to be oxidising and to have relatively low $\delta^{18}O$ values derivation from such a source is not favoured, especially since it is difficult to envisage a mechanism for the downward migration of formation fluids from a basin into the underlying basement.

Because all sheet silicate-fluid hydrogen isotope fractionation factors are negative by about 20-30‰ at low metamorphic grades, it is often supposed that the fluids produced from dehydration of clay minerals during prograde metamorphism have relatively high δD values (e.g. Rye *et al.* ,*ibid.*; Negga *et al.*, 1983). The Dalradian rocks of Connemara had all passed through their peak metamorphic temperatures by the time the high δD fluid infiltrated the MGS, so that dehydration reactions in these rocks could not have produced the high δD fluid. However relatively low grade rocks are known to be present below the Mannin Thrust in the Delaney Dome area. Since Leake (1986) has suggested the Mannin Thrust may extend beneath much of Connemara, these low grade rocks may extend beneath the Cashel-Recess area at some depth. Overthrusting of low grade rocks by basement provides the opportunity to produce a high δD fluid as a result of downward heating by the overlying slab, while overpressuring of this fluid due to thermal expansion provides a mechanism by which this fluid can be forced into the overlying rocks. Such a thrust related model has been suggested to explain the origin of the infiltrative high δD fluid in the La Lauziere metamorphic complex by Negga *et al.* (1983). The major problem with such a model for the origin of the high δD fluid in the Cashel-Recess area is that the Delaney Dome formation, which is exposed below the Mannin Thrust in the Delaney Dome area, is a sequence of relatively anhydrous quartzo-feldspathic rocks which are unlikely to have produced significant quantities

of fluid during progradation. However it is not impossible that the rocks beneath the Mannin Thrust could vary in composition laterally, while Leake (1986) has suggested that the Mannin Thrust could be underlain by younger thrusts, which could bring in different lithologies beneath the area. In 1.4.2 it was shown that there is some petrographic evidence that fluid movement took place within the Delaney Dome area, both prior to and after thrusting, so for this reason it is suggested that a thrust related origin for the high δD fluid in the Cashel-Recess area cannot be ruled out at this stage.

In conclusion therefore, it is suggested that with the available evidence it is not possible to unequivocally identify the source of the high δD fluid in the Cashel-Recess area. However it is clear that this fluid was derived from a source external to this area. The most likely source for this fluid appears to have been surface waters and it is possible that these could have been brought down into these rocks by convection around the 400 Ma Galway granites. However it is not possible to exclude a thrust related origin for the high δD fluid with the present data. In order to attempt to distinguish between these two origins, work was carried out to investigate the isotopic characteristics of the fluids causing retrograde alteration in the Delaney Dome area and in the Galway and Roundstone granites. The isotopic data for rocks from these two areas are presented in the next two chapters.

4.8 SUMMARY.

The stable isotope geochemistry of MGS rocks from the Cashel-Recess study area has been described in this chapter. The major conclusions that can be drawn from these data are summarised below.

1. The MGS hornblendes last equilibrated with a fluid with a δD <-40‰ while all of the later retrograde hydrous minerals last equilibrated with a fluid with a δD > -40‰ (probably near to -25‰), the "high δD fluid". Thus the MGS hornblendes are not in hydrogen isotope equilibrium with any of the later hydrous minerals. The hornblendes are also not in equilibrium with the fluid present in the fluid inclusions in the MGS rocks.

2. The chlorite, epidote and sericite in the MGS formed at low temperatures (~300°C) by mineral reactions caused by the presence of the high δD fluid. The chemistry of the high δD fluid, and the time period during which it was present in the rocks were such that the the hornblendes did not re-equilibrate hydrogen isotopes with this fluid.

3. The hydrogen isotope disequilibrium between the hornblendes and the later retrograde minerals can be observed in mineral separates from the same hand specimen, indicating that hydrogen isotope disequilibrium must be on a mineral grain scale.

4. The maximum possible degree of exchange (F, see 2.6.1) for the hornblendes with the high δD fluid is estimated to be ~0.5. However, it is likely that the degree of exchange was actually much less than this, and that the δD values of the hornblendes have probably not been

significantly increased by exchange with the high δD fluid. This is because hornblendes which are believed not to have been exposed to the high δD fluid do not have lower δD values than the other hornblendes which were exposed to this fluid. Thus it is thought that some of the δD variation between samples may still reflect magmatic or high temperature metamorphic variations.

5. Although both the chlorite and epidote in the MGS have equilibrated with a fluid with a high δD value, it appears that the epidote must have re-equilibrated with this fluid after its formation during cooling, possibly down to temperatures as low as 160°C.

6. The homogeneity in chlorite and sericite δD across the area indicates that the high δD fluid was relatively homogeneous in terms of salinity and δD. Thus the high δD fluid probably had a δD value of ~-25‰ which is the value measured for the water in fluid inclusions in one sample. The epidotes show a relatively large variation in the δD and this can be attributed either to variations in closure temperature between grains because of variations in grain size, or to variations in fluid/epidote hydrogen ratios between samples during exchange at low temperature.

7. Partial chemical analyses of the volatiles in two quartz samples indicates that the high δD fluid may have had a relatively restricted range in of $H_2O/(H_2O+CO_2)$ ratio of 0.98-0.985.

8. Quartz-epidote oxygen isotope thermometry for a microcrack fill material indicates that the high δD fluid was present in these rocks at temperatures of 300°C and possibly at higher temperatures.

9. An inverse correlation of epidote $\delta^{18}O$ with Fe^{3+} content can be interpreted in a number of ways, but it must be inferred that the fluid fO_2 varied between samples. If all the epidotes equilibrated oxygen isotopes at approximately the same temperature, then fluid $\delta^{18}O$ was inversely correlated with fluid fO_2.

10. Oxygen isotope ratios of magmatic hornblendes show that the MGS magma must have been relatively ^{18}O enriched relative to normal basaltic melts, while the hornblende δD values show that the magma δD was <-70‰. Modelling of the δD and $\delta^{18}O$ ratios using two and three end member mixing equations shows that the MGS magma could not have been derived from a high δD subduction related source. This modelling also shows that fluid present within the Dalradian metasediments during MGS intrusion was not assimilated into the MGS magma. These mixing calculations show that the MGS magma was most likely to have originated by mixing of a MORB or OIB like parental magma with 20-30 wt.% of crustal material, which was probably mostly partial melt derived from the Dalradian metasediments. This being the case, nearly all of the water in the magmatic hornblendes must have ultimately been derived from the Dalradian metasediments.

11. Observation of the phase relations in the MGS and the mixing calculations both indicate that the P_{H2O} in the MGS magma may have been significantly less than P_{total}, possibly as low as 0.1 P_{total}, at least in the early differentiates.

12. Isotopic and mass balance constraints indicate that the high δD fluid causing chlorite, epidote and sericite growth must have been derived from a source external to the MGS. Correlation of the high δD fluid in the MGS with the high δD fluid in the Dalradian metasediments, which was shown to be exotic to that rock unit in chapter 3., implies that the high δD fluid must have been exotic to the whole of the Cashel-Recess area.

13. Consideration of the phase equilibria of prehnite containing alteration assemblages formed by infiltration of the high δD fluid into the MGS suggests that the maximum P_{fluid} during infiltration was ~1.8 kb.

14. The high δD value of the fluid which caused chlorite, epidote and sericite growth in the MGS indicates that it must have been either a surface derived fluid (meteoric or seawater), or a metamorphic fluid produced by rocks undergoing prograde metamorphism. Mechanisms can be envisaged by which fluids of either origin could have been infiltrated into the Cashel-Recess area, although a surface derived origin would appear to be more likely. The origin of the high δD fluid will only be discerned by examination of rocks from outside of this area.

CHAPTER 5.

THE DELANEY DOME STUDY AREA.

5.1 INTRODUCTION.

In chapter 1 it was noted that rocks in the Delaney Dome area show petrographic evidence that hydrous fluids were present during and after, and possibly before movement on the Mannin Thrust (MT). Theoretical considerations indicate that fluid pressures on the thrust plane during thrusting should have been close to, or greater than lithostatic (Hubbert and Rubey, 1959). It was suggested in chapter 4 , that a possible source for the fluids present during thrusting could have been rocks beneath the MT which produced fluids by dehydration reactions. It was hypothesised that these fluids could have migrated across the thrust plane, into the overlying slab, and caused the chlorite/epidote/sericite forming retrogression in the Cashel-Recess district. However, much of the alteration and veining in the Delaney Dome area appears to have taken place after thrusting and it is possible that the fluids causing this alteration may have originated from a different source from the fluid present during thrusting.

The purpose of this chapter is to use stable isotope data for the minerals in the this area to find out whether:

a. the fluids present at different times were derived from the same, or different sources.

b. the stable isotope ratios estimated for the fluid(s) give some indication of their origin.

c. the fluids present during thrusting are similar to the late high δD fluid in the Cashel-Recess area, and could therefore have migrated into the overlying slab and caused the chlorite/epidote/sericite forming retrogression in the Cashel-Recess district.

Because this area was only examined in a preliminary orientation survey, and because hydrogen isotope ratios are usually the best indicators of fluid sources, only mineral and fluid inclusion δD values have been measured in this area at present.

5.2 MINERAL HYDROGEN ISOTOPE DATA.

The mineral hydrogen isotope values are related to sample number and to rock type in fig. 5.1 and the structural relations of the epidotes are also shown. The mineral δD values are plotted against calculated water contents in fig. 5.2 and the estimated δD of the fluid in equilibrium with some of these minerals is shown as a function of temperature in fig. 5.3.

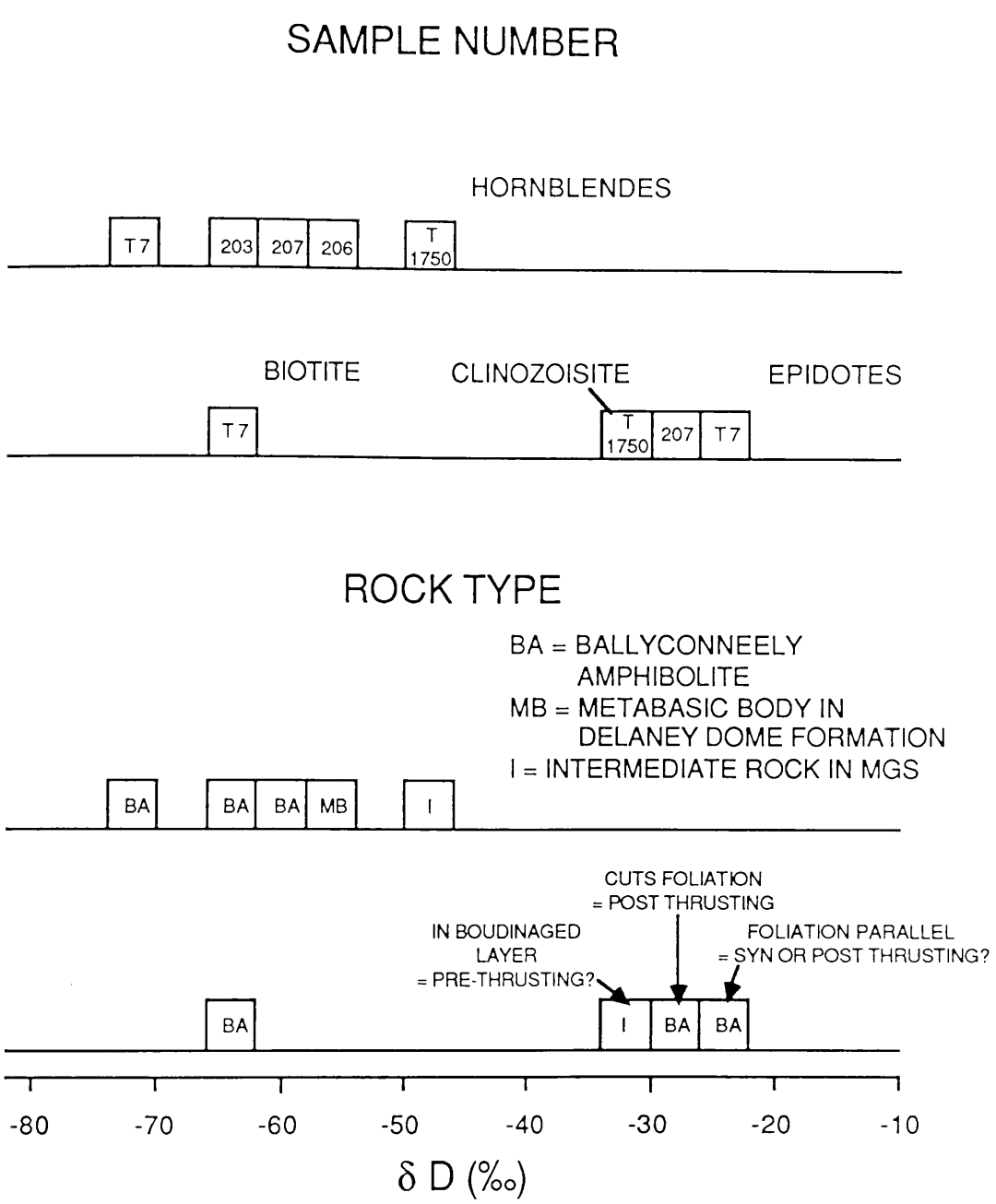

Fig. 5.1 δD of mineral separates from the Delaney Dome area as a function of rock type, the structural relations of the epidotes are also indicated. In each histogram the sample position maps directly onto the same position in the other histogram. Sample numbers with no prefix are those collected during this study which have a prefix GJ..

5.2.1. Water contents of minerals.

It can be seen from fig. 5.2 that, like the mineral separates from the Cashel-Recess district, some of the hornblende separates and the biotite separate from this area have water contents greater than the calculated limits for the pure stoichiometric minerals. This could be interpreted as being due either to the presence of excess hydrogen in the mineral structure, or to the presence of small amounts of chlorite or or other hydrogen-rich minerals within the separate. As far as could be discerned with a binocular microscope the separates were free of any such contaminant, although it is possible that chlorite could be present as a fine grained intergrowth in the

same manner as was suggested for the hydrous minerals in the Cashel-Recess district. If the excess hydrogen was due to the presence of chlorite in the mineral, then by analogy with the hornblendes and biotites in the Cashel-Recess district, the presence of excess hydrogen would imply that these minerals had been exposed to a hydrous fluid at low temperatures. If all the excess hydrogen in these minerals was present in chlorite with a δD = -50‰ and a water content of 10.8 wt.%, then the change in measured δD relative to the pure minerals, that this would have caused is calculated to have been less than the experimental error in all cases.

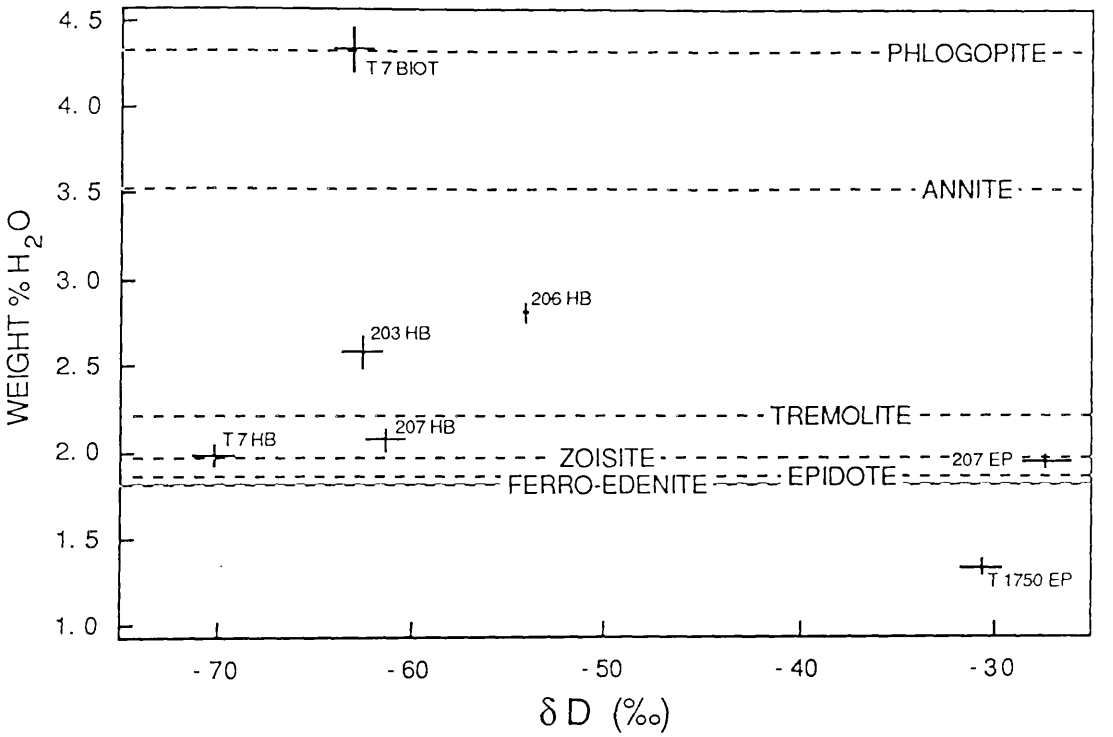

Fig. 5.2 δD of mineral separates from the Delaney Dome area plotted against water content calculated from the hydrogen yield measured during hydrogen isotope analysis. The water contents are indicated for stoichiometric minerals which have the highest or lowest water content of all biotites (s.l.), calcic hornblendes and epidotes which therefore bracket the possible range in water content for pure stoichiometric minerals of these groups. The data points for the hornblende from T.1750 and the epidote from T.7 are not shown because these separates were contaminated with large quantities (~50 vol.%) of plagioclase and quartz respectively which could not be removed by mineral separation. The presence of these contaminants should not affect the measured δD but will affect the yield. Abbreviations used: Bl = biotite, HB = hornblende and EP = epidote/clinozoisite.

The hydrogen content of the clinozoisite from T.1750 is significantly lower than that expected for a pure clinozoisite. This could either be due to the presence of a anhydrous mineral in this sample, or to incomplete extraction of hydrogen from the sample. The first case is likely because it proved difficult to totally separate the clinozoisite from the diopside in this sample and some diopside was detected in the separate by XRD analysis.

5.2.2. δD values of minerals.

Ballyconneely amphibolite (BA) and MGS.

From fig. 5.1 it can be seen that the BA hornblendes have a relatively large spread in δD values, similar to the spread for hornblendes from the MGS in the Cashel-Recess area (fig. 4.1). Since the BA is believed to have developed from basic rocks of the MGS (1.4.2), the δD of the hornblendes in the BA would be expected to be the same as those in the basic rocks in the Cashel-Recess district, unless the hornblendes in the BA have exchanged with an external fluid either during or after thrusting. By comparing fig. 4.1 with fig. 5.1 it can be seen that the three BA hornblendes have δD values within the range for hornblendes from the basic rocks in the Cashel-Recess area. Recrystallisation of the MGS hornblendes and relatively high temperatures (>380°C for albite-epidote amphibolite facies; Liou *et al.*, 1985) during formation of the BA would mean that the hornblendes would have re-equilibrated hydrogen isotopes with any fluid that was present during thrusting. Therefore this similarity in δD of the hornblendes between the two areas must indicate that the δD of the fluid present in the BA during thrusting was the same as that in equilibrium with the hornblendes in the Cashel-Recess district. Therefore it can be concluded that there could not have been pervasive movement of significant quantities (i.e. bulk fluid/rock mass ratios > 0.05, see 2.7.2) of high δD fluid through the BA during thrusting. If significant quantities of fluid did move pervasively through the BA during thrusting then it must be concluded that the fluid had a δD of ~-50 to -40‰ (figs. 5.3, 5.1), assuming that salt effects were negligible at the temperatures at which thrusting took place.

The epidote mineral δD values are in the range of δD values for epidotes in the Cashel-Recess district and indicate that there must have been a high δD fluid present in these rocks at some time (fig. 5.3). From this figure it can be seen that the equilibration temperature for hydrogen in these epidotes must have been below ~250°C because otherwise the epidotes would have been in equilibrium with a fluid with an unreasonably high δD value (>0‰). If, (as would seem likely from the study of Graham and Sheppard, 1980), the closure temperatures for the Delaney Dome epidotes were similar to those from the Cashel-Recess district (~200-160°C), then the Delaney Dome epidotes could also have last equilibrated with the high δD fluid similar to that present in the Cashel-Recess district (~-25‰). If equilibration had taken place at such temperatures, it would probably have been at temperatures below the formation temperature for the epidotes, especially since two of these epidotes (*s.l.*) formed prior to or during thrusting (fig. 5.1). If this was the case, then the epidotes would have been re-equilibrating with the pore fluid during cooling. The shape of the epidote-water fractionation curve of Graham *et al.* (1980) requires that if the pore fluid had a constant δD during cooling from >260°C to the closure temperature, then the epidote will always be re-equilibrating to more heavy δD values as temperature falls. If epidote closure temperature was a function of grain size, then some

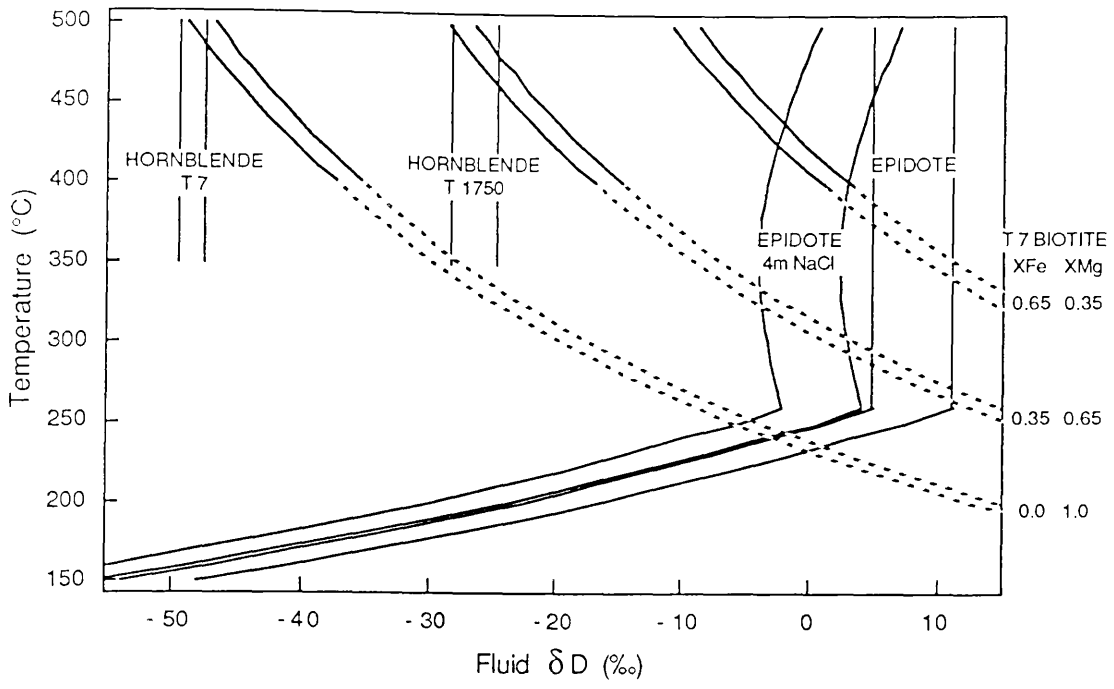

Fig. 5.3 Estimated δD of the fluid that would be in equilibrium with various minerals from the Delaney Dome area as a function of temperature. The curves labeled epidote correspond to the fluid in equilibrium with minerals $\pm 1\sigma_{n-1}$ from the mean value of epidote mineral δD. It is assumed, on the basis of the two data points for clinozoisite given by Graham *et al.* (1980), that clinozoisite has the same hydrogen isotope fractionation behaviour as epidote at all temperatures. The other pairs of curves correspond to the errors due to the uncertainty in the hydrogen isotope analysis of the mineral. The two curves for hornblende are for the two hornblendes with the most extreme values of δD. The three curves for the biotite correspond to the fluid in equilibrium with the biotite assuming different octahedral site occupancies shown and are dashed below the experimentally calibrated range. The curve labeled "epidote 4m NaCl" is for the fluid in equilibrium with the epidote minerals assuming that the fluid fractionates hydrogen isotopes in the same way as a 4m NaCl solution, all other curves are for the fluid in equilibrium with various minerals assuming that the fluid fractionates hydrogen isotopes in the same way as pure water. The biotite curves were calculated using a modified Suzuoki-Epstein equation (A.4.3), while the other fractionation factors used are the same as those used in fig 4.2.

evidence that this may have been the case comes from the observation that there is an inverse correlation between epidote grain size and δD (fig. 5.4, c.f 4.3.3). Thus it is possible that high δD fluid may may also have been present in this area at temperatures above the closure temperature for the epidotes.

The upper temperature at which the high δD fluid could have been present in this area is constrained by the δD data for the hornblende in the enclosing rocks, because as noted above the BA hornblendes have not equilibrated with a high δD fluid. Thus the high δD fluid could only have been present within these rocks at temperatures and times over which the hornblende could not totally equilibrate with it. The fine grain size of the hornblendes in these rocks means that they lie near to the lower curves for hornblende in fig. 2.12, so that if the fluid was present for $> 10^4$ years then the maximum temperature must have been <300°C, while shorter times

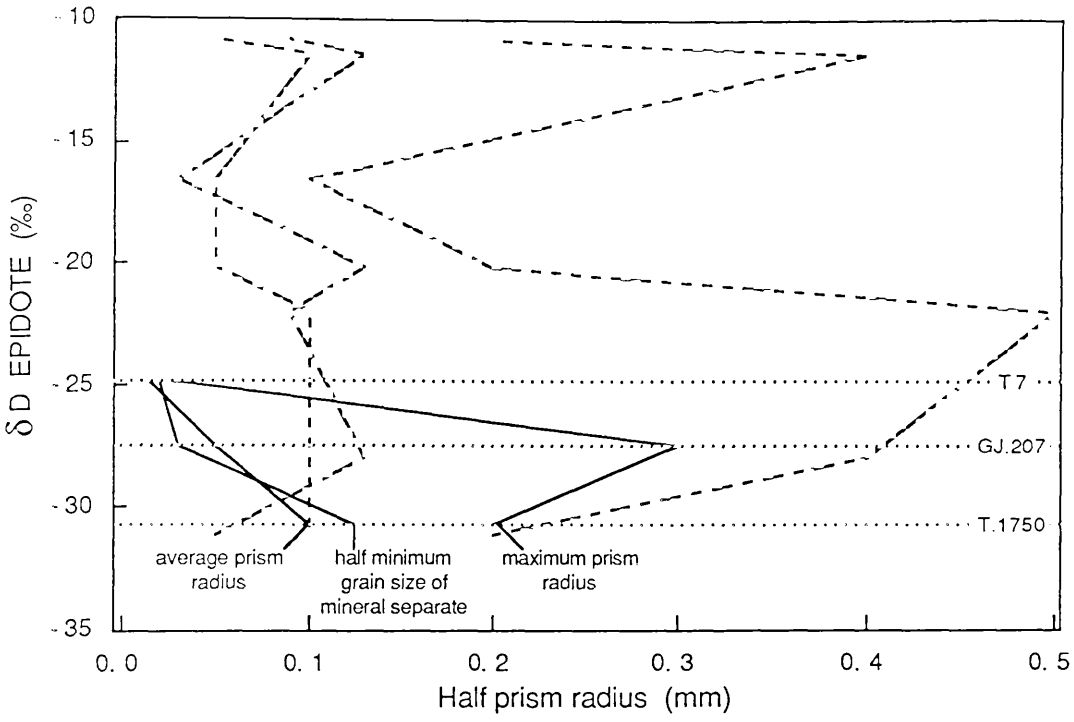

Fig. 5.4 Estimated maximum and average prism radius and half minimum grain size of mineral separate for the epidotes and the clinozoisite from the Delaney Dome area plotted against δD. The maximum and average prism radii were estimated from thin sections. In practice it is often difficult to distinguish the orientation of the epidote grains in thin section and in these cases the these measurements are for the half widths of all grains cut by the thin section. The grain sizes curves for the epidotes from the Cashel-Recess area (fig. 4.16) are shown for reference (dashed lines).

would mean that the fluid could have been hotter, or longer times would require that the fluid was colder. The hornblende from the MGS above the BA (T.1750) has the highest δD of all the hornblendes measured in this study. Following the arguments given above, it is unlikely that this δD value is an original value for a MGS hornblende and therefore the high δD value of this hornblende must reflect a larger degree of exchange (or possibly total equilibration) with the high δD fluid in this hornblende, compared to the other hornblendes. Thus variation in hornblende δD in this area could be attributed to varying degrees of exchange with this late high δD fluid. However the differences in degree of exchange with this fluid cannot be solely caused by differences in in grain size of the hornblendes, because there is no correlation between grain size and δD (fig. 5.5), although apart from the hornblende in T.7 all the BA hornblendes are fine grained relative to the hornblendes in the Cashel-Recess area. Possibly differences between samples in fluid/rock ratios or the temperature-time conditions at which the high δD fluid was present, could explain the δD differences between the hornblendes.

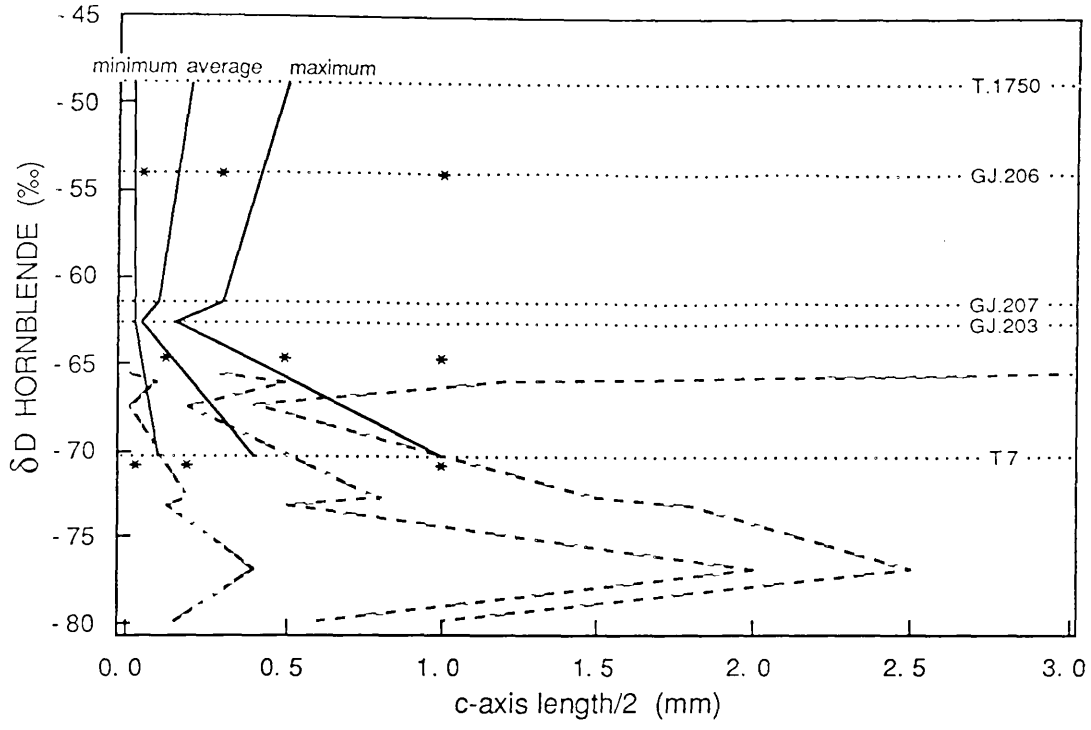

Fig. 5.5 Estimates of maximum, minimum and average half c-axis lengths measured in thin section of hornblendes from the Delaney Dome area plotted against δD value. The grain sizes curves for the hornblendes from the Cashel-Recess area (fig. 4.8) are shown for reference (dashed lines). Where the minimum c-axis length in thin section is less than the minimum grain size of the separate the half size of the minimum separate size is substituted for the minimum grain size, for reasons given in 4.3.2.

The biotite in sample T.7 has not been analysed chemically, so that the mineral-fluid hydrogen isotope fractionation cannot be accurately estimated. Nevertheless it can be seen from fig. 5.3 that unless the biotite was actually a pure phlogopite (which its density of >3.0 measured during mineral separation does not indicate), then it cannot be in hydrogen isotope equilibrium with the the same fluid that the hornblende in this rock equilibrated with at temperatures less than or equal to the temperatures for thrusting (?500°C max). This is despite the fact that both of these minerals appear to have formed at the same time. Fig. 5.3 shows that the biotite must have equilibrated with a fluid with a higher δD. This can be interpreted as the result of partial or complete exchange with the high δD fluid that equilibrated with the epidote minerals. Such hydrogen isotope exchange of biotite with the high δD fluid, either prior to or during chloritisation, was also inferred for biotites in the Cashel-Recess district (4.3.3). The curves for the δD of the fluid in equilibrium with the biotite shown in fig. 5.3 are calculated assuming that the biotite-fluid fractionation follows a Suzuoki-Epstein relationship at low temperatures. This is probably not the case, in fact it is likely that the fractionation may become independent of temperature below ~400-450°C, as was suggested previously for muscovite (4.2.2). Thus the biotite could have totally equilibrated with a high δD fluid of -25‰ at some temperature below 400°C if X_{Mg} in the octahedral site was ~0.7. It is interesting that the biotite in T.7 appears to have equilibrated with the high δD fluid to a greater extent than the hornblende, because the biotite

actually has a greater effective diffusion length than the hornblende (half flake diameter compared with half c-axis length for the hornblende) and at low temperatures grains of similar sizes should have similar exchangeabilities (fig. 2.12). Therefore if exchange was taking place by diffusion, the biotite should have exchanged less than the hornblende. Possibly the greater degree of exchange in the biotite could be due to an enhanced rate of exchange in the biotite because some ion exchange was taking place with the high δD fluid, or the incipient chloritisation reaction was allowing an increased rate of hydrogen isotope exchange.

Basic intrusions in the Delaney Dome Formation (DDF).

The δD has been measured for one hornblende separate from one of the basic bodies in the DDF. The interpretation of this δD value is difficult because it is not clear either how much the hornblende has exchanged with the high δD fluid, or where the hydrogen in this hornblende originated from (1.4.2). If the basic bodies were present in the DDF prior to thrusting, then the hydrogen could either have been derived from pre-thrusting hydrous alteration minerals in these bodies, or the basic bodies could have been unaltered (i.e. anhydrous) prior to thrusting and the hydrogen could have been derived from fluids present during thrusting. Alternatively if these basic bodies were only intruded during thrusting, then the hydrogen could either have been derived from the magma, or the fluids in the surrounding DDF. Even if the basic bodies were originally hydrous prior to thrusting or were intruded as hydrous magmas it is likely that the hornblende in them formed during thrusting because it is thought that these rocks had not been metamorphosed prior to thrusting. Therefore it is considered reasonable to make the assumption that the hornblende in this sample should have equilibrated with the fluids present in the DDF during thrusting, especially since this sample was collected from the margin of one of the basic bodies. Thus this hornblende would indicate that the δD of the fluid present in the DDF during thrusting was ~-30‰ (figs. 5.1, 5.3) provided that the fluid/hornblende hydrogen ratios were large enough that the δD of the hornblende was controlled by that of the fluid and that the hornblende has not subsequently exchanged with the late high δD fluid. If the fluid/hornblende ratios were lower, then the δD of the fluid would have been nearer to that of the hornblende itself, i.e -54‰, while if the hornblende had had its δD value increased after thrusting by exchange with the high δD fluid, then the δD of the fluid during thrusting must have been lower than -30‰.

5.3 FLUID INCLUSION DATA.

5.3.1. Origin of quartz veins.

Samples of quartz from two foliation parallel quartz veins (T.5,T.6) from the BA just above the MT were chosen for analysis of their volatile chemistry and the δD of the water that they contained. It is envisaged that these foliation parallel quartz veins (and the epidote-quartz vein in T.7) could have formed during thrusting as a result of transient overpressuring (P_{fluid}

$> \sigma_{N\ minimum} = \sigma_{vertical}$) which forced the foliation apart and allowed deposition of the quartz from a supersaturated fluid from the surrounding rock. Thus the fluid present in the fluid inclusions in these quartz veins might represent a sample of the fluid present during thrusting. Planes of secondary inclusions which could contain fluids present after thrusting may also be present in these samples. These veins have not yet been examined in thin section, so that the ratio of fluid contained in primary inclusions to fluid contained in secondary inclusions cannot be estimated. An alternative mechanism by which these quartz veins could have formed is by later post thrusting fracturing, in which the fracture orientation followed the foliation because it was a plane of pre-existing weakness. Without detailed structural and textural studies of the quartz veins from the whole area it is not possible to unequivocally choose between these two origins for these quartz veins. Nevertheless the fluid contained within the fluid inclusions can provide information on the fluid present at some time in this area.

5.3.2 Volatile chemistry.

The results of partial chemical analyses of the volatiles released by heating different splits of crushed quartz with different grain sizes from the two quartz veins are shown in fig. 5.6.

It can be seen that, like the splits from the quartz vein in the microcline granite sill described in 3.4.1, the splits of quartz from these two veins have a relatively narrow range in $H_2O/(H_2O+CO_2)$ ratio compared to the ranges in either $H_2O/(H_2O+NC)$ or $NC/(CO_2+NC)$ (NC = non condensible gases at -196°C). If the most CO_2 rich split from T.6 is excluded, the other samples have $H_2O/(H_2O+CO_2)$ ratios in the range 0.964-0.983 (1.9 mole % variation in CO_2), while the $H_2O/(H_2O+NC)$ ratio varies from 0.94-0.998 (5.7 mole % variation in NCs) and the $NC/(CO_2+NC)$ ratio varies from 0.05-0.78. As with the volatiles from the quartz samples described in 3.4.1 this relative constancy in the $H_2O/(H_2O+CO_2)$ ratio, together with the variability in in NC content, is best explained by mixing of variable proportions of an NC rich component with an NC poor component with a relatively constant $H_2O/(H_2O+CO_2)$ ratio. The same arguments concerning the nature of the NC rich component that were presented in 3.4.1 can also be made here. Thus, because there is no apparent correlation of δD with NC content, which suggests that methane was not an important constituent in the NC rich component, it is inferred that this component is dominantly composed of N_2 or Ar. Similarly there are three possibilities for the origin of this N_2/Ar NC component.

1. From a leak in the extraction line.

2. From a layer of absorbed gas on the sample.

3. From within fluid inclusions.

The first possibility is considered unlikely, because the line was known to be very airtight over the two week period during which six of the splits were analysed and runs where high amounts of NCs were measured were interspersed with those where only very small amounts of NCs were

measured. Furthermore as described in 3.4.1 much, if not all, of the NC gas measured for these samples was released within a few minutes of the initiation of heating of the sample, indicating that the NCs must be associated with the sample.

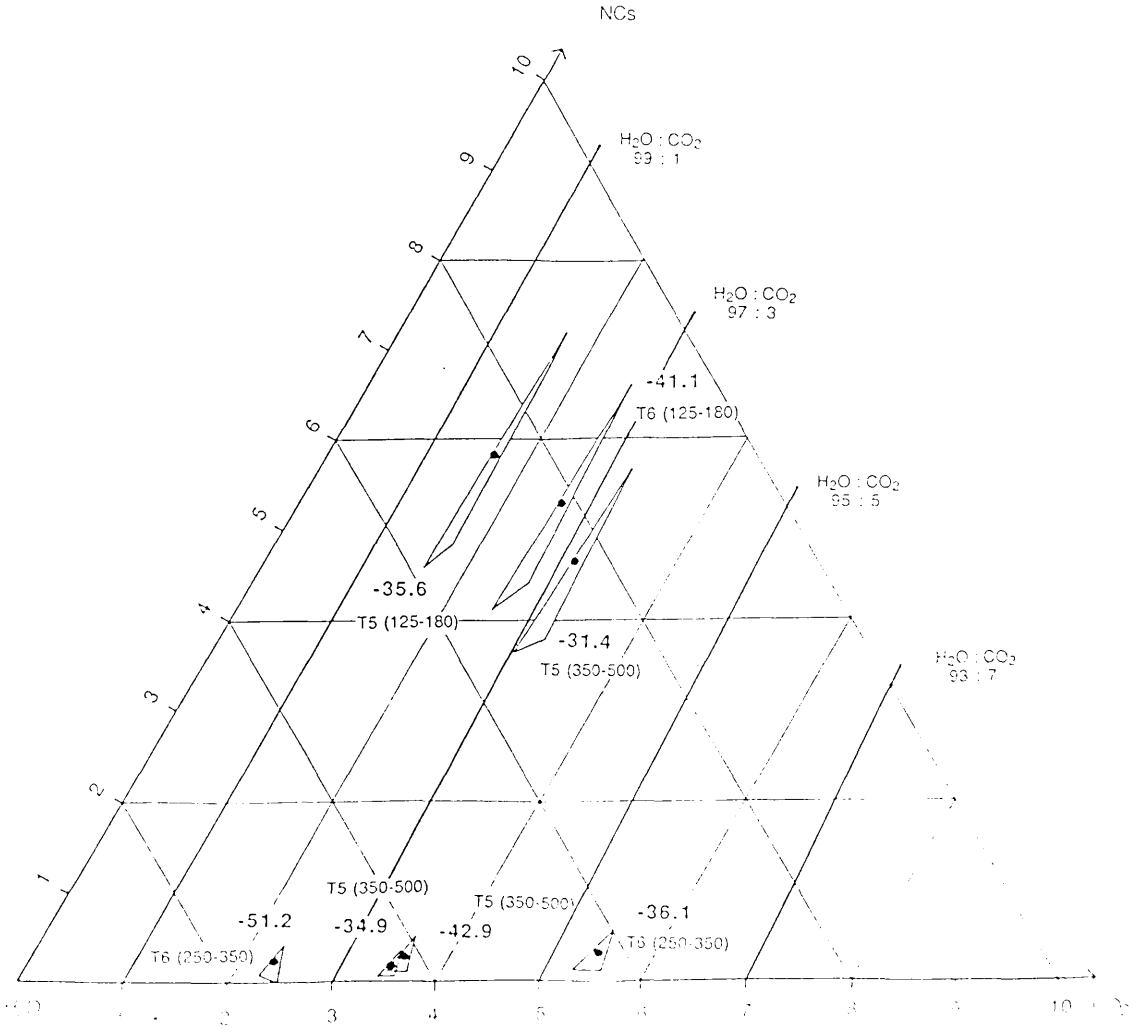

Fig. 5.6 Gas composition and δD of water of volatiles released by heating quartz from the Ballyconneely Amphibolite. The triangles around the points are the 90% confidence limits on the gas chemistry and take into account both the reading errors and the uncertainty in the calibration line used. It should be noted that only the water rich apex of the compositional triangle is shown.

The second possibility, that the NCs were evolved from an absorbed layer on the sample, is also thought to be unlikely for the same reasons that were given in 3.4.1. In fact on a plot of NC yield vs. approximate surface area (not shown) these samples have an even lower correlation coefficient than sample GJ.160 in fig. 3.7 and also have a best fit line intercept on the surface area axis. The third possibility, that the NCs released came from fluid inclusions within the samples, also has problems associated with it, because as described in 3.4.1 the inclusions would have to be very sparsely distributed and therefore very large. As with the quartz sample in 3.4.1 it can be calculated that for any reasonable density of nitrogen in the

inclusions, the inclusions would be larger than the grain size used in some of the runs, although they might just be accommodated in some of the grains in the coarsest splits analysed (500-350 μm).

The only other possible explanation for the NC variation could be that the NCs are contained in very small inclusions in all the splits of these samples (N_2 rich inclusions are commonly observed to be very small; e.g. Yardley *et al.*, 1983) which decrepitated in some runs, but not in others, possibly as a result of different heating rates or heating to different final temperatures in different runs. Thus it must be concluded that the nature of the NC rich component has to remain unclear, until such time as the fluid inclusions in these samples are examined petrographically. However, irrespective of this problem, the constancy in $H_2O/(H_2O+CO_2)$ ratio for different splits of these two samples suggests that this ratio is a real feature of the fluid present within the sample. Comparison with figs. 3.6 and 4.19 shows that the range of $H_2O/(H_2O+CO_2)$ ratio in these BA samples (~0.985-0.96) encloses the ranges determined for the quartz from the vein in the microgranite sill in the Cashel-Recess area (0.96-0.975) and the quartz from the intermediate MGS rocks in the Cashel-Recess area (0.98-0.985).

5.3.3 δD of fluid inclusions.

The δD values of the water released from these different splits are also shown on fig. 5.6. It can be seen from this figure that there is no apparent correlation between δD and either grain size, or volatile chemistry and that there is no appreciable difference in δD of the water between the two samples (T.5 average = -36.2 ± 4.8, T.6 average = -42.8 ± 7.7, or -38.6 ± 3.5 excluding the -51.2‰ value; errors are ± σ_{n-1}). The reason for the variation in δD between different splits of the same sample is not entirely clear, but may simply be the result of more than one generation of fluid inclusion being present in the sample. Possibly a high δD component is represented by the value of -31‰ in one of the coarse splits from T.5, while a low δD component may be represented by the value of -51‰ in one of the finer fractions from T.6. If this was the case, then the fact that the volatile chemistry does not correlate with δD would tend to indicate that the two components do not have drastically different volatile chemistries.

The average δD values for these samples are distinctly lower than the value of -25‰ suggested for the "high δD fluid" which caused chlorite/epidote/sericite growth in the Cashel-Recess area in 4.4.2. Therefore, if it is assumed that the dominant inclusions in this vein are primary inclusions, these data do not indicate that a high δD fluid was present during the formation of these veins. If, as is thought likely, these veins were formed approximately syn-thrusting then these data do not indicate that a high δD fluid was present in the BA during thrusting, in agreement with the conclusion reached from consideration of the hornblende data in 5.2.2.

The water contents of these splits range between 0.07 and 0.04 wt.%, decreasing slightly with the decrease in grain size, just as would be expected if the water was contained in fluid inclusions.

5.4 DISCUSSION - FLUIDS IN THE DELANEY DOME AREA.

In the previous two sections it was shown using hornblende and fluid inclusion data for the BA, that the δD of the fluid present in this rock unit during thrusting was between -50 and -38‰ (hornblende) or between -36 and -43‰ (fluid inclusions). The δD of the hornblende from a metabasic body in the DDF suggests that the δD of the fluid present in this rock unit during thrusting was less than or equal to -30‰. Thus these data do not indicate that a high δD fluid was pervasively present in these rocks during thrusting. Therefore the data from this area do not support the model proposed in the previous chapter, in which the high δD fluid in the Cashel-Recess district was derived from a source beneath the MT during thrusting. However it is not possible to exclude the possibility that the high δD fluid was derived from a source beneath the MT, but did not migrate into the overlying rocks until after movement in the MT zone had ceased. Indeed the low permeability of rocks undergoing ductile deformation during thrusting would be expected to significantly retard the passage of fluids through the thrust plane during thrusting. Therefore the upward passage of pore fluids from beneath the thrust could have been delayed until movement stopped, when the rocks passed back into the brittle regime. If, as suggested by Leake (1986), the MT is underlain by younger thrusts, then it is possible that fluid production could still have been taking place at a deeper level after movement had ceased on the MT zone.

The fact that all the epidotes and clinozoisite examined have relatively high δD values attests to the pervasive presence within these rocks of a high δD fluid at low temperatures. It is considered reasonable to correlate this low temperature, high δD fluid with that identified in the Cashel-Recess district, although further fluid inclusion data are needed before this correlation can be considered firm. If this high δD fluid is the same as that in the Cashel-Recess district, then it can be inferred that this fluid must have infiltrated an area of MGS and Dalradian metasediment at least 20 × 5 km (map 1.). It is likely that the influx of high δD fluid into the Delaney Dome area was associated with the late epidote veins which cross cut the thrust foliation. This will only be confirmed by measurement of the δD of material with a higher closure temperature for hydrogen than epidote (e.g. chlorite, amphibole or inclusions in quartz) from in or around these veins. The early formed pre-and syn-thrusting epidote and clinozoisite could not have formed from the the high δD fluid, but have now had their δD overprinted by this late fluid. The fluid which deposited these veins was probably locally derived. Therefore it might be expected that the $\delta^{18}O$ values of this epidote and clinozoisite, which should be much more resistant to post formation isotopic exchange than the δD values, would be different

from that of the later foliation cutting epidotes if the fluid which formed these later veins was derived from an exotic source.

Thus it may be concluded that although a high δD fluid did infiltrate this area, it was not present until after thrusting. This would tend to indicate that this fluid was not thrusting related. However, with the data available, it is not possible to exclude a model for the origin of the high δD fluid in which it is derived from a source beneath the MT, but its infiltration into the area was delayed until after thrusting. Further constraint on the origin of the high δD fluid in SW Connemara can only be obtained from examination of the isotopic characteristics of the retrograde alteration minerals in the Galway and Roundstone granites which are presented in the next chapter.

5.5 SUMMARY.

The hydrogen isotope data for minerals from the Delaney Dome study area have been presented in this chapter. The major conclusions which can be drawn from this data are summarised below.

1. Fluids present at different times in this area were derived from different sources.

2. Fluids present during thrusting had δD values in the range -36 to -50‰ (BA) and <-30‰ (DDF) and were probably internally derived from within these rock units.

3. After thrusting the area was pervasively infiltrated by a high δD fluid at temperatures that were probably less than ~300°C.

4. Some hornblendes in this area may have partially, or totally equilibrated with the late high δD fluid and one biotite is also thought to have equilibrated with this fluid to a significant extent. Both the epidotes and the clinozoisite have exchanged with this fluid during cooling, probably to temperatures <200°C.

5. The high δD fluid in this area can probably be correlated with that identified in the Cashel-Recess area. If this is the case, then the high δD fluid must have infiltrated an area of at least 20 × 5 km of MGS and Dalradian metasediments.

6. The data from this area shows that the high δD fluid did not infiltrate the area until after thrusting, which would tend to indicate that it was not thrusting related. However it is not possible to exclude a model for the origin of the high δD fluid in which it is derived from a source beneath the MT. The source of this fluid may only be elucidated by examination of the retrograde alteration in the Galway granites.

CHAPTER 6.

THE GALWAY AND ROUNDSTONE GRANITES AND THEIR CONTACT AUREOLES.

6.1 INTRODUCTION.

In chapters 4. and 5., it was shown that a high δD fluid of exotic origin infiltrated both the Cashel-Recess area and the Delaney Dome areas at some time after ductile deformation in the Mannin Thrust zone had ceased. In the previous chapter it was shown that it is not possible to exclude an origin for this fluid whereby it was produced as a result of overthrusting, although there is no positive evidence that this was the case. The alternative origin for this high δD fluid suggested in chapter 4., was that it was derived from a surface source (probably meteoric), as a result of convective circulation around the Galway granites. This was because it is well known that high level intrusive bodies frequently initiate convective circulation of pore fluid within the surrounding rocks (e.g. Taylor, 1977; Taylor and Forester, 1979). These and other studies have also shown that, during the later stages of cooling, the convective cell can collapse into the bodies themselves. Petrographic evidence that retrograde hydration has taken place within the Galway granite suite (1.4.3), indicating that hydrous fluids were present in these bodies at some time after crystallisation, is consistent with such a model.

The purpose of this chapter is to use stable isotope data from the Galway and Roundstone granites to estimate the stable isotopic and chemical composition of the fluids causing retrograde hydration in these bodies. If the fluid causing alteration in these granites can be shown to have a similar δD value and chemistry to the distinctive high δD fluid identified in the surrounding rocks, it would suggest that fluid in the granites was derived from the same source and imply that the high δD fluid must have infiltrated the area post ~400 Ma. If this was the case, then the possibility of a thrusting related origin for the high δD fluid in Connemara could be eliminated, while the alternative model in which the fluid was derived from the surface as a result of convection around, and through the Galway granites would be supported. If, on the other hand, the fluid causing alteration in the Galway granites is found to be distinct from that causing alteration in the country rocks, then an internal origin for the fluid causing alteration in the granites would be implied and the infiltration of the high δD fluid into the country rocks could be constrained to have taken place prior to ~400 Ma.

6.2 HYDROGEN ISOTOPE DATA.

6.2.1 Water contents of minerals and rocks.

The hydrogen isotope data for mineral separates and whole rock samples are plotted against calculated water contents in fig. 6.1. It can be seen from

this figure that, like many of the hornblendes and biotites from the Cashel-Recess area, or the Ballyconneely amphibolite, the hornblende in GJ.002 and the biotite in GJ.015 both have a greater water content than the calculated limits for the pure stoichiometric minerals. Following the same arguments that were outlined in 5.2.1, this excess hydrogen is interpreted as being due to the presence of small amounts of fine grained, possibly submicroscopic, chlorite within these minerals. The presence of this chlorite alteration is thought to reflect the infiltration of hydrous fluid into these samples.

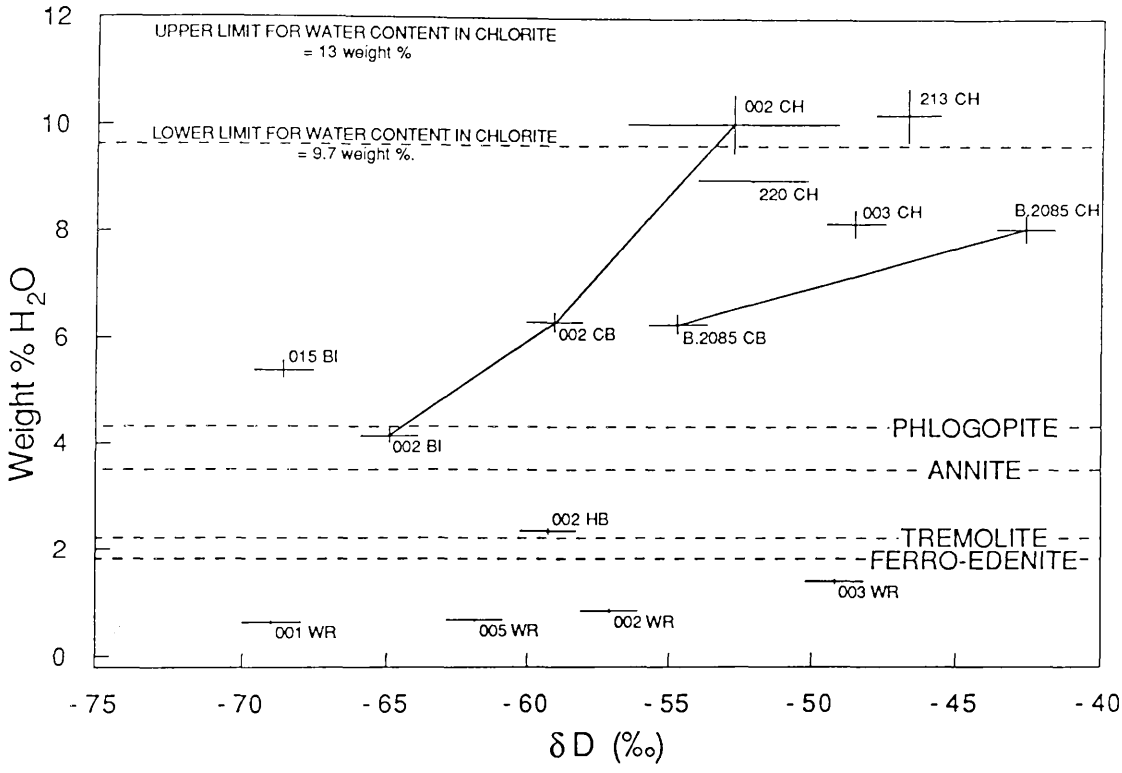

Fig. 6.1 δD of mineral separates and whole rock samples from the Roundstone and Galway granites plotted against water content calculated from the hydrogen yield measured during hydrogen isotope analysis. The water contents are indicated for stoichiometric minerals which have the highest or lowest water contents of all biotites (*s.l.*), calcic amphiboles and chlorites and which therefore bracket the possible range of water contents for pure minerals in these groups. The tie-lines join different chlorite, chloritised biotite or biotite separates from the same samples. Abbreviations used: BI = biotite, CB = chloritised biotite, CH = chlorite, HB = hornblende.

The difference between the measured δD and the δD of the pure mineral that that would result from the presence of this chlorite can be calculated by assuming that the chlorite has a δD of ~-49‰ (the "average" δD of the chlorite in the granites) and a water content of 10.8 wt.%. For the hornblende, this difference is calculated to be less than the error in the determination of δD, but the biotite separate may be as much as 13‰ heavier than the pure biotite that it contains. Biotites which are visibly chloritised can be seen to have higher water contents and δD values than the fresh biotites, but lower δD values and water contents than the separates that appear to be pure chlorite. The chloritised biotite separate from GJ.002 lies below a straight line running between the chlorite and biotite rich separates from the same sample. This is what would be expected if the

chloritised biotite was a mechanical mixture of the two end members, since mixing curves on this plot will always be concave upwards. The whole rock data also lie along a concave upwards curve, with the δD increasing with increasing water content. This suggests that these rocks lie along a mixing curve between a high δD, high water content end member and a low δD, low water content end member. The higher water content of the high δD samples can be seen to be due to the greater abundance of secondary hydrous minerals (mostly chlorite and sericite) in these samples.

6.2.2 δD values of whole rock samples.

The δD values of whole rock samples from a traverse across the margin of the Roundstone granite are shown in fig. 6.2. The $\delta^{18}O$ values of these whole rock samples are also shown on the same diagram. It can be seen that the whole rock δD varies by 20‰ within this granite. The δD correlates very well with the degree of alteration of the granite, with the sample with the highest δD being the most altered (i.e. nearest to the altered granite end member described in 1.4.3), while the sample with the lowest δD (GJ.001) is petrographically the freshest granite. Since chlorite is the most abundant hydrous mineral in the most altered sample (GJ.003) and chlorite has a very high water content, the whole rock δD value approximates very well to that of the chlorite. The high δD value indicated for the chlorite suggests that the chlorite in this rock has equilibrated with a high δD fluid. Because biotite is the only hydrous mineral present in any quantity in the least altered sample, the whole rock δD value probably approximates to the biotite δD in this sample. Such a δD value is not unusual for biotite in a granitic rock (Taylor and Sheppard, 1986).

The δD values of two whole rock samples from the MGS adjacent to the Roundstone granite are also shown for reference. The δD value of -59‰ for GJ.009 reflects the fact that it contains hornblende (δD = -74‰) and epidote (δD = -22‰), which has equilibrated with the high δD fluid (figs. 4.6, 4.11). Sample GJ.008 contains both chlorite and hornblende and it is likely that the δD value of -54‰ for this sample is intermediate between the δD values of the chlorite and the hornblende, with the chlorite being more D rich. Thus it seems likely that the chlorite in this sample has also equilibrated with the high δD fluid that infiltrated the MGS rocks further to the north.

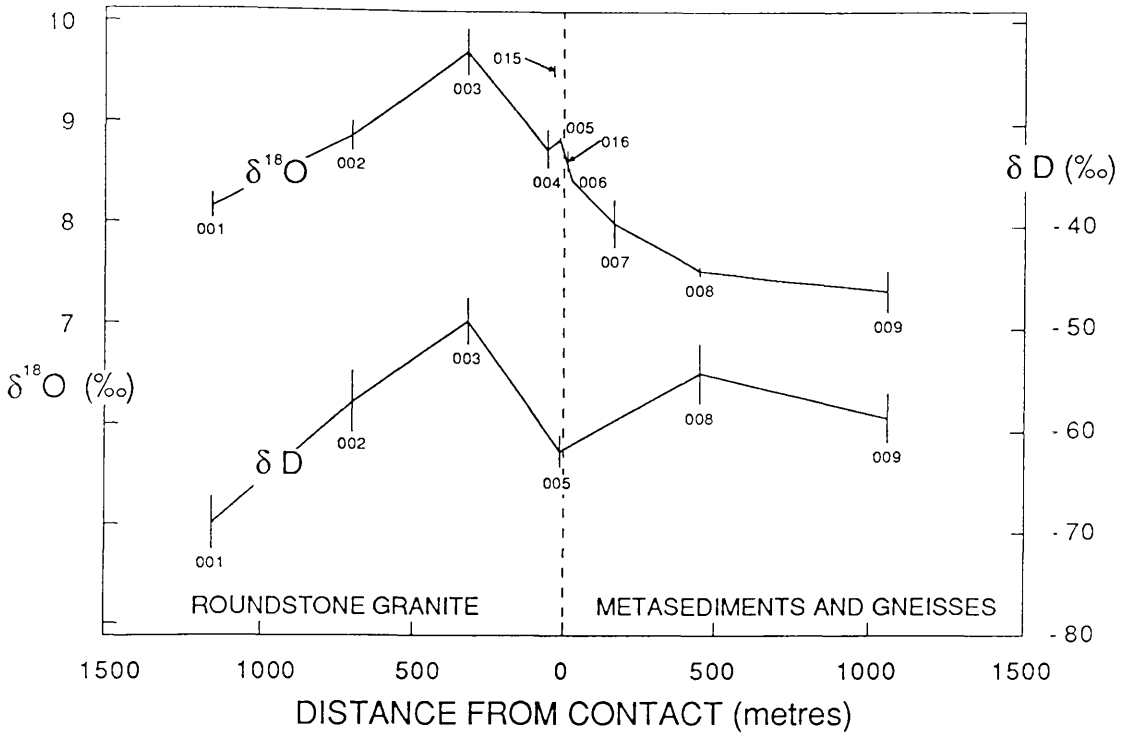

Fig. 6.2 Whole rock δD and $\delta^{18}O$ values for samples in a traverse across the contact of the Roundstone granite. Whole rock $\delta^{18}O$ values are also shown for two samples from the contact of the Galway granite. The vertical error bars at each point correspond to ± 1 σ_{n-1} of the value as estimated from replicate analyses of the samples. All samples were collected during this study and are prefixed by GJ..

6.2.3 δD values of mineral separates.

The δD data for mineral separates from the Galway and Roundstone granites are summarised in fig. 6.3.

It can be seen from this diagram that, as suggested in the previous section from whole rock data, the chlorites in both of these bodies do indeed have relatively high δD values (mean of 5 chlorites = -48.5‰ σ_{n-1} = 4.2). The high δD values of these chlorites indicate that they equilibrated with a high δD fluid (> -30‰?) at some temperature (fig. 6.4). The presence of a high δD fluid in these samples is confirmed by the high δD values measured for the water contained in fluid inclusions in the quartz in the strongly chloritised samples (fig. 6.3). Thus a fluid with a high δD must have been present in these granites at some time.

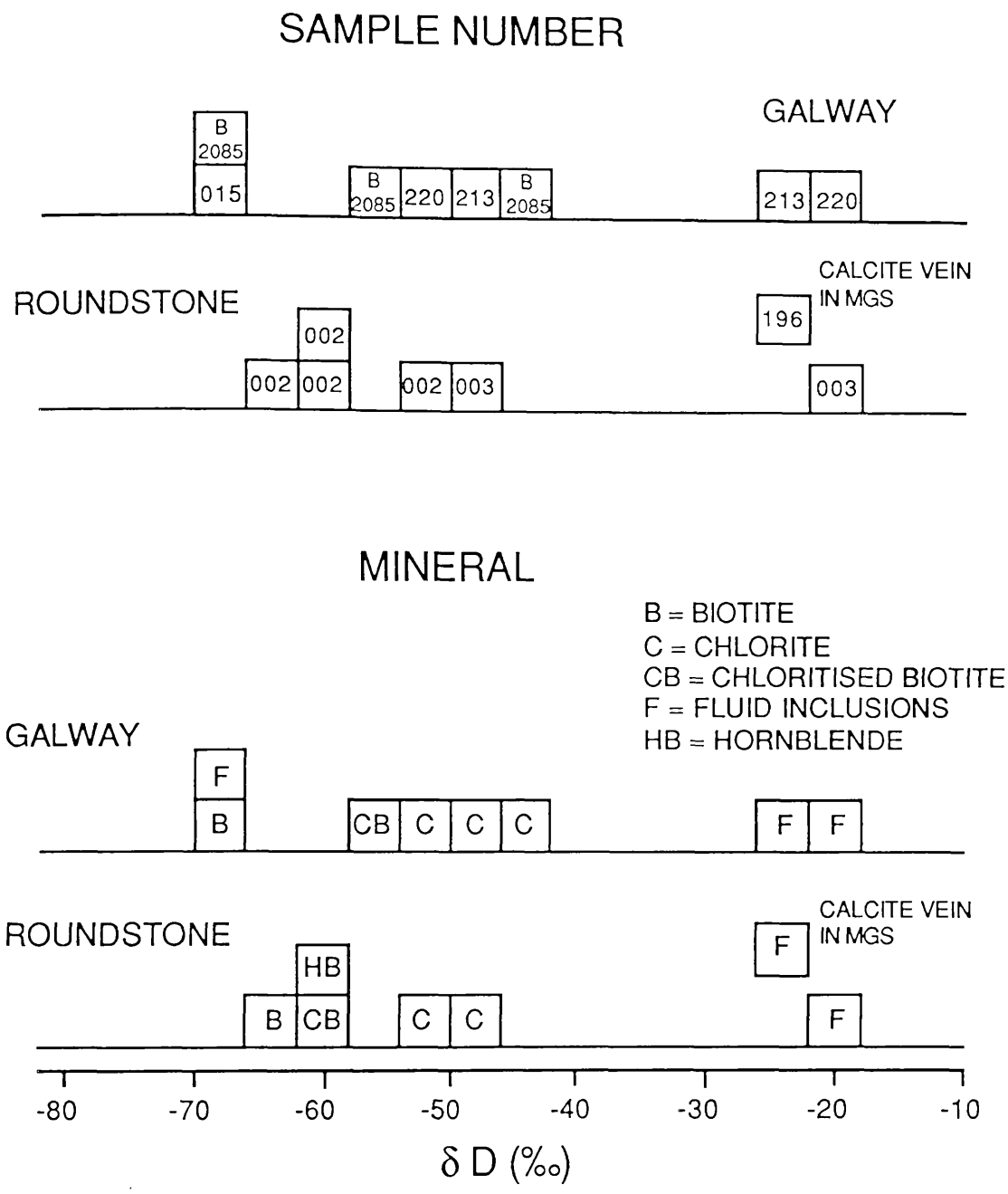

Fig. 6.3 Summary diagram for hydrogen isotope data for mineral separates from the Galway and Roundstone granites. Each box represents a mineral from a different sample. The data for minerals from each granite are shown separately for the purposes of comparison. The sample position in the top two histograms map directly onto the same position in the bottom two histograms.

The hornblende from a partially chloritised sample from the Roundstone granite (GJ.002) apparently last equilibrated with a fluid with a $\delta D \approx -38‰$, if salt effects at the temperature of equilibration were small (fig.6.4). Thus this hornblende cannot have equilibrated with the high δD fluid causing chloritisation in this rock, although partial exchange could have taken place. The fact that the hornblende has not equilibrated with this fluid suggests, firstly that the fluid did not react with the hornblende, and secondly that the high δD fluid could not have been present in this rock at

high temperatures, or for long times (c.f. the arguments presented in 4.2 regarding the lack of equilibration in the MGS hornblendes). The hornblende in this rock is fairly fine (<2 mm \\c), so that temperatures of chlorite formation are not likely to have been much greater than 300°C, unless the high δD fluid was present in this rock for a period much less than 1 million years (fig. 2.12a).

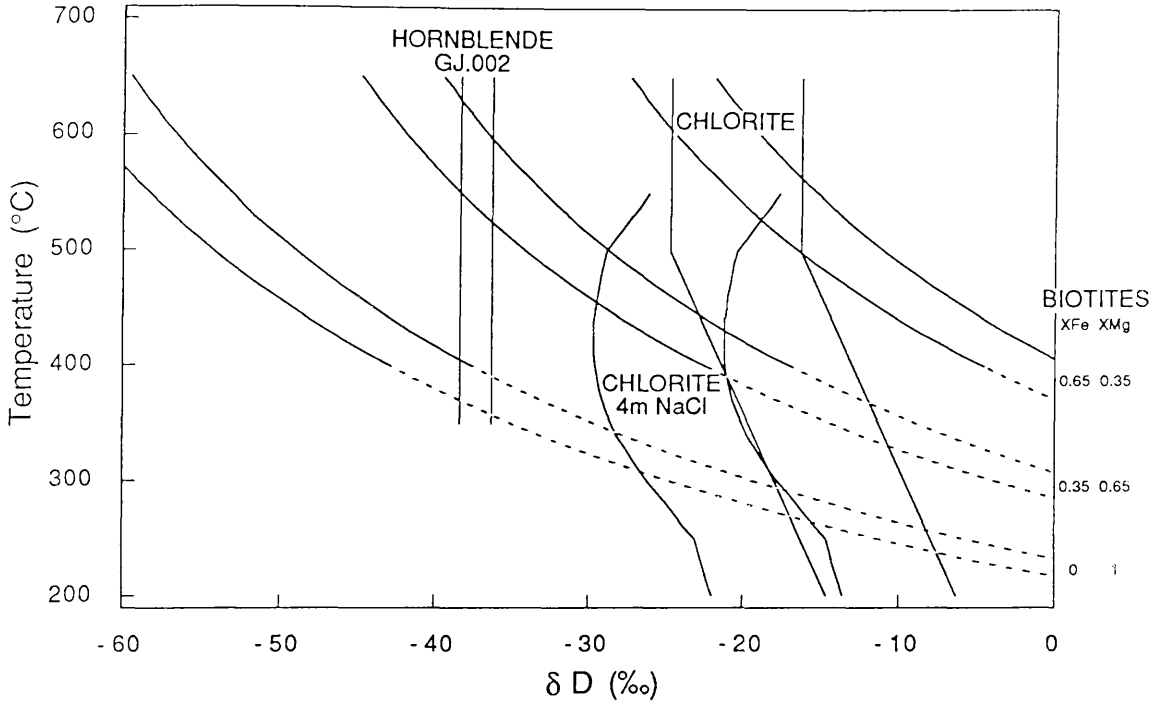

Fig. 6.4 Estimated δD of the fluid that would be in equilibrium with the hornblende in GJ.002 and chlorites and biotites from the Galway and Roundstone granites as a function of temperature.Each pair of curves for chlorite and biotite represent the fluid in equilibrium with minerals with δD values ± 1 σ_{n-1} from the mean compositions of these minerals from both granites. The pair of curves for the hornblende in GJ.002 correspond to the uncertainty resulting from the analytical uncertainty in the hydrogen isotope analysis. The biotite curves are dashed below the experimentally calibrated range. The curves labeled "chlorite 4m NaCl" is for the fluid in equilibrium with the chlorites assuming that the fluid fractionates hydrogen isotopes in the same way as a 4m NaCl solution. All other curves were drawn assuming that the fluid fractionates hydrogen isotopes in the same way as pure water. The biotite curves were calculated using a modified Suzuoki-Epstein equation (A.4.3), while the other fractionation factors used are the same as those used in fig. 4.2.

The biotites in these granites have a more negative δD than the chlorites, and as discussed above (6.2.1) the biotite in GJ.015 may be even more negative than the measured value. Unfortunately these biotites have not been chemically analysed, so that the mineral-fluid hydrogen isotope fractionations for these minerals cannot be accurately estimated. The equilibrium fluid curves for three different biotite compositions are shown in fig. 6.4. It should be noted that these curves should probably become sub-vertical below ~400°C (see 5.2.2). It can be seen from this diagram that if the biotites contain ~35% Fe^{2+} and 65% Mg^{2+} in the octahedral site, then they could have equilibrated with the same fluid that equilibrated with the hornblende at temperatures near to crystallisation temperatures. However this interpretation is not unique, since biotites with the same chemical

composition could also have equilibrated with with a high δD fluid at lower temperatures. Thus if the biotites do have the suggested chemical composition, the δD values cannot be unequivocally interpreted as the result of high temperature equilibration with an "igneous fluid", but might reflect a later low temperature equilibration with the high δD fluid, as has been suggested for the biotite in the Ballyconneely amphibolite (5.2.2), or the biotites in the MGS (4.3.2). If the biotites are much more Mg rich than this (>65% Mg^{2+}) and the curves do become sub-vertical below ~400°C, then the biotite could not have equilibrated with the high δD fluid, but must have equilibrated with a fluid with a lower δD. Alternatively if the biotites contain much more than 35% Fe^{2+} in the octahedral site it can be seen that they could only have equilibrated with a high δD fluid. Therefore until the biotites have been chemically analysed it is not possible to give an unequivocal interpretation of their δD compositions.

6.3 FLUID INCLUSION DATA.

6.3.1 Volatile chemistry.

The results of partial chemical analyses of the volatiles released by heating quartz separates from altered (as defined in 1.4.3) granite samples are presented in fig. 6.5. In thin section the quartz in all these samples (except perhaps B.2085) was observed to contain abundant bubble planes of secondary inclusions. In 1.4.3 it was noted that the intensity of bubble plane development correlated very well with the degree of chloritisation of biotite in the granites, so it is likely that the fluid contained in these inclusions was that which caused the chloritisation. The NC/H_2O ratio of the gas released by heating a vein calcite (GJ.196) thought to be associated with a fault cutting the MGS is also shown in this diagram. It can be seen that, excluding the quartz from B.2085, the samples have a very narrow range in $H_2O/(H_2O+CO_2)$ ratio of 0.982-0.987 and including the calcite, all but two of the samples have a narrow range of $H_2O/(H_2O+NC)$ ratios between ~0.985 and 0.995. However two samples have much higher NC contents which cause the overall variations in NC/(H_2O+NC) and NC/(CO_2+NC) ratios to be much larger than the variations in $H_2O/(H_2O+CO_2)$ (excluding B.2085). This large variation in NC content between splits of the same sample (GJ.213) is similar to that observed for quartz samples from the microgranite sill, the MGS and the Ballyconneely amphibolite (figs. 3.6, 4.19, 5.6 respectively). The same arguments concerning the reasons for the NC variation between splits of the same sample that were presented in 3.4.1 and 5.3.2 also apply in this case. Thus the NC variations cannot be attributed to either leaks in the extraction line, surface absorption of NCs on the samples, or to the presence of NC bearing inclusions in the sample and therefore the reasons for the variation are not clear. Despite this, the constancy in $H_2O/(H_2O+CO_2)$ ratios and the difference of this ratio from samples in other rock types (see below) suggests that this ratio is a real feature of the fluid present within the samples and has genetic significance. It is possible that the lower $H_2O/(H_2O+NC)$ values seen in most of the samples may also be a real feature of the fluid in the sample, although this cannot be proven.

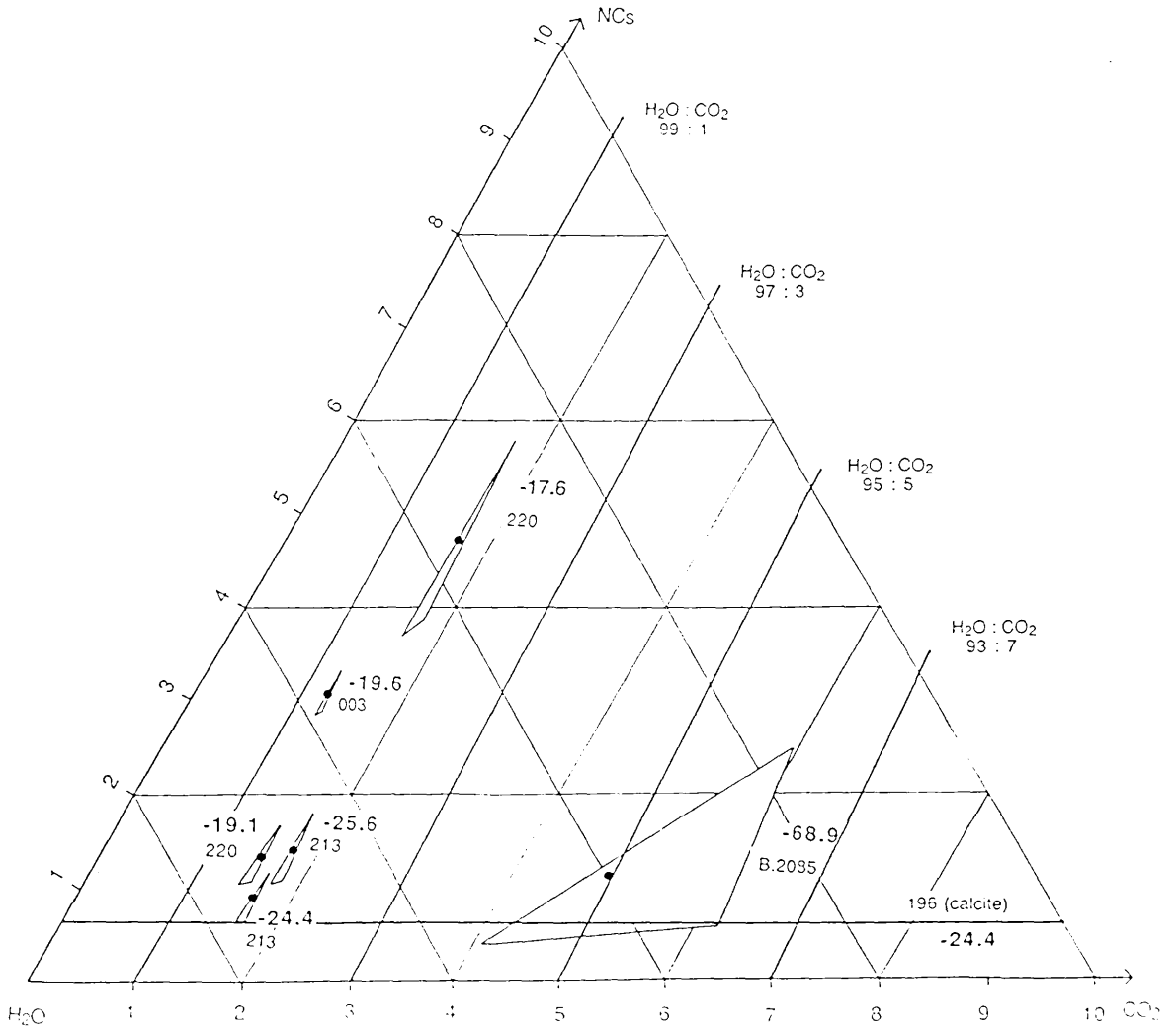

Fig. 6.5 Gas composition and δD of water of volatiles released by heating quartz separates from the Galway and Roundstone granites and calcite from a late fault cutting the MGS. The triangles around the points are the 90% confidence limits on the gas chemistry and take into account both the reading errors and the uncertainty in the calibration line used. It should be noted that only the water rich apex of the compositional triangle is shown.

The constancy in $H_2O/(H_2O+CO_2)$ ratio between different granite samples coming from over 10 km apart, in two different granite bodies is very striking and strongly suggests that the high δD fluid in the two bodies had a common origin. Comparison with figs. 3.6, 4.19 and 5.6 shows that the $H_2O/(H_2O+CO_2)$ ratios of the fluid in these granites (0.982-0.987) is very similar to that for the fluid in quartz from intermediate rocks in the Cashel-Recess area (0.98-0.985) and to the higher values for the fluid in quartz in the Ballyconneely amphibolite (~0.985-0.96). However the $H_2O/(H_2O+CO_2)$ ratio is distinctly higher than that measured for fluid in the quartz in the microgranite sill in the Cashel-Recess area. (0.96-0.975).

The gas obtained from the quartz from the sample B.2085 is anomalous, both in terms of its volatile composition and its water δD value. The δD

value is lower than that of the chlorite and probably any of the hydrous minerals in the sample, indicating that the water could not be in equilibrium with any of the hydrous phases, since all mineral-fluid hydrogen isotope fractionation factors are negative at high temperatures (O'Neil, 1986, fig. 9). The very low absolute yields of all gases from this sample (A.2.3) means that the volatile ratios will be subject to large errors, especially if one of the gases were preferentially absorbed in the extraction line relative to the others. Thus the low $H_2O/(H_2O+CO_2)$ ratio of this sample could be explained as a result of loss of very small amounts of H_2O during the extraction procedure, possibly by absorption on glass surfaces, or in the U-furnace. If the water that was absorbed was isotopically heavy relative to the remaining water then such a process could also explain the low δD measured for this sample. Alternatively because the amount of hydrogen released from the sample was so small the δD of this sample could have been lowered by the addition of a small, but very D depleted, blank derived from the platinum crucible as described in A.1.3. Whatever the cause of the difference between the volatile composition and water δD in this sample and the other samples, the low absolute yield of gases make it highly unlikely that the the measured values are actually those of the fluid inclusions in the sample.

6.3.2 δD of the water in the fluid inclusions.

The δD values of the water released in each experimental run are also shown in fig. 6.5. As noted above the low δD value for the quartz in B.2085 is probably spurious. The other samples have a very narrow range in δD and do not show any correlation with the chemistry. The differences in δD between different splits of the same sample for the quartzes from the Galway granite is well within the error limits for the determination of δD in mineral samples, and indicates that a high degree of confidence can be placed in the precision of these analyses.

The δD of the water in the vein calcite from MGS (GJ.196) is indistinguishable from that of the fluid inclusion water in the altered granites and the water in fluid inclusions in quartz in the enclosing MGS rock (4.4.2). Because the fluid inclusions in the calcite have not yet been studied in detail, it is not possible to say whether the bulk of the water was contained in primary or secondary inclusions. Thus it is not possible to definitely say whether the calcite actually precipitated from a high δD fluid, or was permeated by a high δD fluid after formation. The first case is more likely because:

1. The MGS rock which is cut by the vein shows very intense alteration which has been definitely linked with the infiltration of a high δD fluid (chapter 4.), strongly suggesting that the vein was a conduit through which the high δD fluid infiltrated the area.

2. If the fluid inclusions in the calcite were formed by the high δD fluid moving through the vein after crystallisation (i.e.secondary), then it is likely that the calcite would have equilibrated oxygen isotopes with this

fluid by a solution-reprecipitation process (2.6.4). If this was the case then baryte would also be expected to have equilibrated oxygen isotopes with this fluid, because baryte exchanges oxygen isotopes almost an order of magnitude faster than calcite at any temperature by a solution-reprecipitation process (fig. 2.13). However it is shown in 6.4.3 that this the baryte did not equilibrate with the same fluid with which the calcite equilibrated at any temperature. Thus a primary origin is implied.

Regardless of the exact time relations between the fluid inclusions and the calcite, the presence of a high δD fluid in the calcite, dates the presence of high δD fluid in this vein to be syn-vein formation at the earliest. Therefore high δD fluid may have been present in this area quite late in the geological history (1.4.3).

Tabulated below are the (mean) δD values for chlorite and fluid and the apparent fractionation between these two phases, for samples in which the δD of both phases has been measured.

Sample	δD_{fluid}	$\delta D_{chlorite}$	$\Delta_{fluid\text{-}chlorite}$	$10^3 ln\alpha_{fluid\text{-}chlorite}$
GJ.003	-19.6	> -48.5[2]	<28.9	<29.9
GJ.220	-18.4	> -52.1[2]	<33.7	<34.9
GJ.213	-25.0	-46.7	21.7	22.5
GJ.196	-27.2 (q[1])	> -48.5[1,2]	<21.6	<22.5
GJ.196	-24.4 (cc)	> -48.5[1,2]	<24.4	<25.3

[1]quartz and chlorite in the rock which is cut by the calcite vein.

[2]these values are minima because these chlorites probably contain some biotite (fig. 6.1) so that the δD of the chlorite could be heavier.

It can be seen that three of the measured fractionations are are less than 28‰, which is the water-chlorite fractionation at 500-700°C according to Graham *et al.* (1987b). Because the water-chlorite fractionation increases at lower temperatures (~38‰ at 200°C, *ibid.*) all of the measured fractionations will be less than the predicted fractionation below ~300°C. The water-chlorite fractionation of Graham *et al.* (*ibid.*) may only apply to Mg-chlorites, yet these chlorites, coming from granitic rocks, will probably contain appreciable Fe. If Fe bearing chlorites fractionate differently from pure Mg-chlorites it is likely that the water-chlorite fractionation will be greater in Fe bearing chlorites (A.7). Thus the fact that at least some of the measured fractionations are less than the predicted fractionation cannot be explained in terms of chemical variation in the chlorite and therefore can only be due to a salt effect reducing the fluid-mineral fractionation (cf. 4.4.2). Because the hornblende in GJ.002 has not equilibrated hydrogen isotopes with the high δD fluid, it is unlikely that chloritisation took place at temperatures much above ~300°C (6.2.3). At temperatures below or equal to 300°C the water-chlorite fractionation would have been >= 35‰ which is greater than all the measured fractionations and salt effects can be calculated to have been >1.3‰ and possibly as much a 16.4‰. Thus it can be inferred that the high δD fluid must have been saline. The difference in measured fluid-chlorite fractionations between samples could be the result of differences in the salt effect between samples. However, other factors, such

as variation in the purity of the chlorites, or differences in re-equilibration of chlorite during cooling, could also explain these differences, and variations in fluid salinity cannot necessarily be inferred.

6.4 OXYGEN ISOTOPE DATA.

6.4.1 Whole rock data.

The $\delta^{18}O$ values for whole rock samples from a traverse across the contact of the Roundstone granite were shown together with the δD values for these samples in fig. 6.2 Two whole rock analyses from either side of the contact of the Galway granite are also shown on this diagram.

The whole rock $\delta^{18}O$ values in the Roundstone granite vary between +8.2 and 9.7‰ and show a very good positive correlation with the whole rock δD value. Thus if it can be assumed that the granite was originally homogeneous in whole rock $\delta^{18}O$ value then it would appear that alteration of the rock by the high δD fluid has increased the whole rock $\delta^{18}O$ value as well as the δD value. Because the $\delta^{18}O$ values of some of these rocks have been increased by interaction with the high δD fluid, the $\delta^{18}O$ value of the least altered sample (GJ.001) is probably nearest to that of the granite prior to interaction with this fluid. The $\delta^{18}O$ value of +8.16‰ for this sample is consistent with the I-type nature (Chappell and White, 1974) of this granite inferred from other chemical and petrographic criteria (1.3.5).

The whole rock $\delta^{18}O$ value for GJ.015 from the margin of the Galway granite is similar to that of the most altered sample from the Roundstone granite (GJ.003). However this sample is much less altered than GJ.003, since it contains a good deal of fresh biotite. Therefore the high $\delta^{18}O$ value of this sample cannot be attributed to interaction with the high δD fluid and must be a feature of the unaltered rock. This is not unreasonable since the GJ.015 was collected from the Murvey phase of the Galway granite, which is an evolved leucogranite. This would be expected to have a higher $\delta^{18}O$ than the more basic Roundstone granite, if they were both derived originally from the same source.

The $\delta^{18}O$ values of the MGS rocks adjacent to the Roundstone granite appear to show a decrease in $\delta^{18}O$ away from the contact of this granite. This may partly be the result of sampling different rock types, since GJ.009 is an ultrabasic-basic MGS rock, while all the other rocks are intermediate MGS rocks. Alternatively this whole rock $\delta^{18}O$ variation could be the result of interaction of fluids associated with the granite with those rocks nearest to the granite. This hypothesis cannot be tested without more detailed sampling and analysis of mineral separates from these rocks.

The data plotted on fig. 6.2 suggest that the whole rock samples from the margin of the Roundstone granite show a relatively smooth variation in $\delta^{18}O$ and δD with distance from the contact. However measurement of whole rock $\delta^{18}O$ values at closely spaced intervals shows that this is not in

fact the case (fig. 6.6). This figure shows that whole rock $\delta^{18}O$ values can vary by up to 2‰ over distances of 40 m, or 1‰ over 15 m. Once again, the samples with the higher $\delta^{18}O$ values can be seen to be more altered. Thus the $\delta^{18}O$ enrichment in the granite appears to be restricted to the altered zones in the granite and shows no relationship with distance from the contact. Field evidence (1.4.3) indicates that the intensity of the the alteration in the Roundstone granite is highly variable over a scale of metres, and therefore it is suggested that the high δD fluid was concentrated along more permeable zones in this granite and was not pervasively present in the margin.

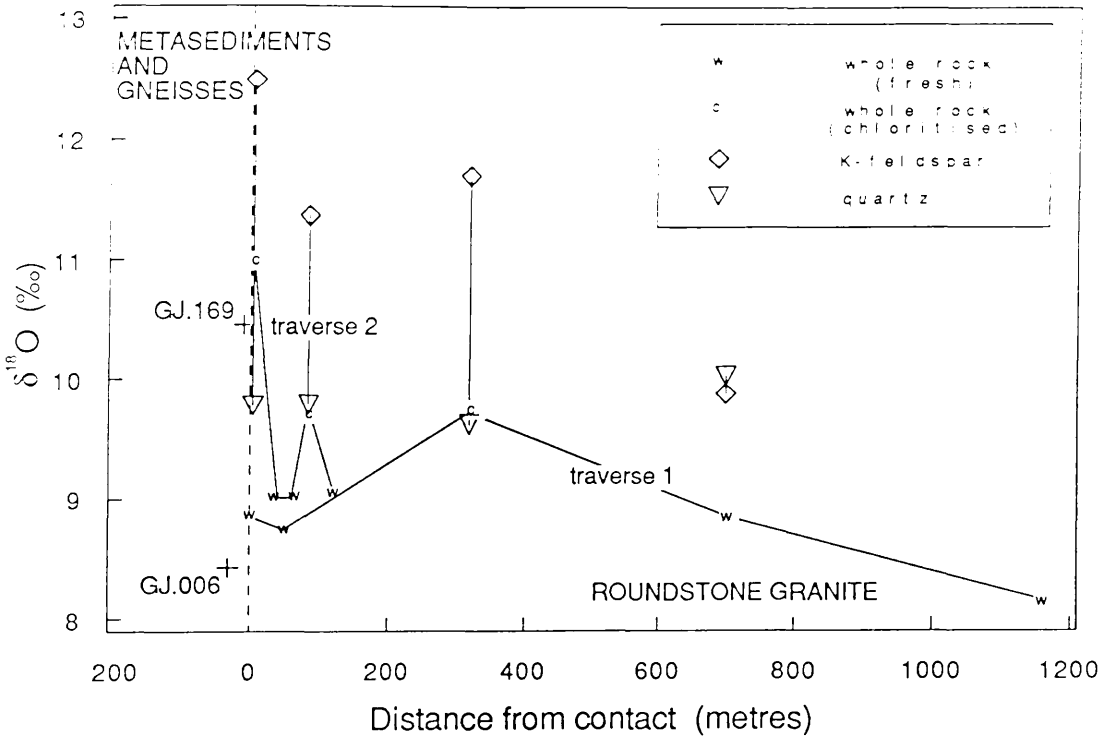

Fig. 6.6 Whole rock and quartz and K-feldspar $\delta^{18}O$ values for two traverses at the margin of the Roundstone granite. The whole rock data for the longer traverse is repeated from fig. 2.2. The $\delta^{18}O$ values for whole rock samples of the country rock just adjacent to the contact are also shown. The distinction between altered (chloritised) and fresh granite samples is only qualititative and is based on the degree of chloritisation of biotite observed in thin section.

6.4.2 Mineral separate data.

The $\delta^{18}O$ values for quartz and K-feldspar separates from four samples from the Roundstone granite are also shown on fig. 6.6. It can be seen that the $\delta^{18}O$ values of the quartz from the altered rocks (average = 9.69‰, σ_{n-1} = 0.09) are probably not significantly different from the $\delta^{18}O$ value of the quartz in the less altered rock (GJ.002, quartz = 10.03‰), once analytical uncertainty has been taken into account. This implies that either the quartz in the altered rock has has not undergone appreciable oxygen isotopic exchange with the high δD fluid, or that some equilibration has taken place, but the $\delta^{18}O$ value of the equilibrated quartz is not greatly different from

that of the quartz initially. In either case, the relative constancy in quartz $\delta^{18}O$ across the margin of the granite would suggest that the quartz was originally homogeneous in $\delta^{18}O$ over the length of the traverse prior to reaction with the high δD fluid. This would support the assumption made in 6.4.1, that the granite was originally homogeneous in $\delta^{18}O$, since the granite varies little in modal composition along the length of the traverse.

Unlike the quartz, the K-feldspar $\delta^{18}O$ values are highly variable and show a relatively good correlation with the variations in whole rock $\delta^{18}O$ values and the intensity of alteration in the rock. Thus the most petrographically altered samples have the highest whole rock $\delta^{18}O$ values and contain the most ^{18}O rich K-feldspar. This relationship implies that the increase in whole rock $\delta^{18}O$ in the altered rocks may be partly caused by the ^{18}O enrichment of the K-feldspars. Examination of the relative $\delta^{18}O$ values of the quartz and K-feldspar in the altered rocks shows that the K-feldspar must have been enriched in ^{18}O <u>after</u> crystallisation of these rocks. This is because the quartz - K-feldspar fractionations in the altered rocks are all negative and therefore cannot represent an equilibrium fractionation (Matsuhisa *et al.*, 1979). Such disequilibrium mineral pairs can only be produced by differential rates of exchange in the two minerals when exchanging with a reservoir which would cause a shift in their isotopic composition. The large variations in K-feldspar $\delta^{18}O$ values between different rocks (>2.5‰), together with the small variations in quartz $\delta^{18}O$ values strongly suggest that these disequilibrium pairs are the result of the K-feldspar having exchanged oxygen isotopes with a reservoir which variably enriched its $\delta^{18}O$ value, while the quartz did not appreciably exchange with this reservoir. This proposal is consistent with the available kinetic data which indicate that oxygen isotope exchange between quartz and fluid always takes place at a much slower rate than between alkali feldspar and fluid, both in diffusion controlled (fig. 2.12), and surface controlled exchange (fig. 2.13, Cole *et al.*, 1983). Since the greatest ^{18}O enrichments in the K-feldspar correlate with the intensity of alteration of the rock, it is reasonable to assume that the reservoir with which the K-feldspar exchanged was the high δD fluid which has already been shown to have caused the alteration in these rocks.

The $\delta^{18}O$ data for other mineral separates from three of the rocks from the Roundstone granite are shown together with the quartz and K-feldspar data in fig. 6.7. To aid in the interpretation of these data the mineral fractionations that would be expected if oxygen isotope equilibrium between phases had been "frozen in" at either 500 or 600°C are also shown by the lower curves.

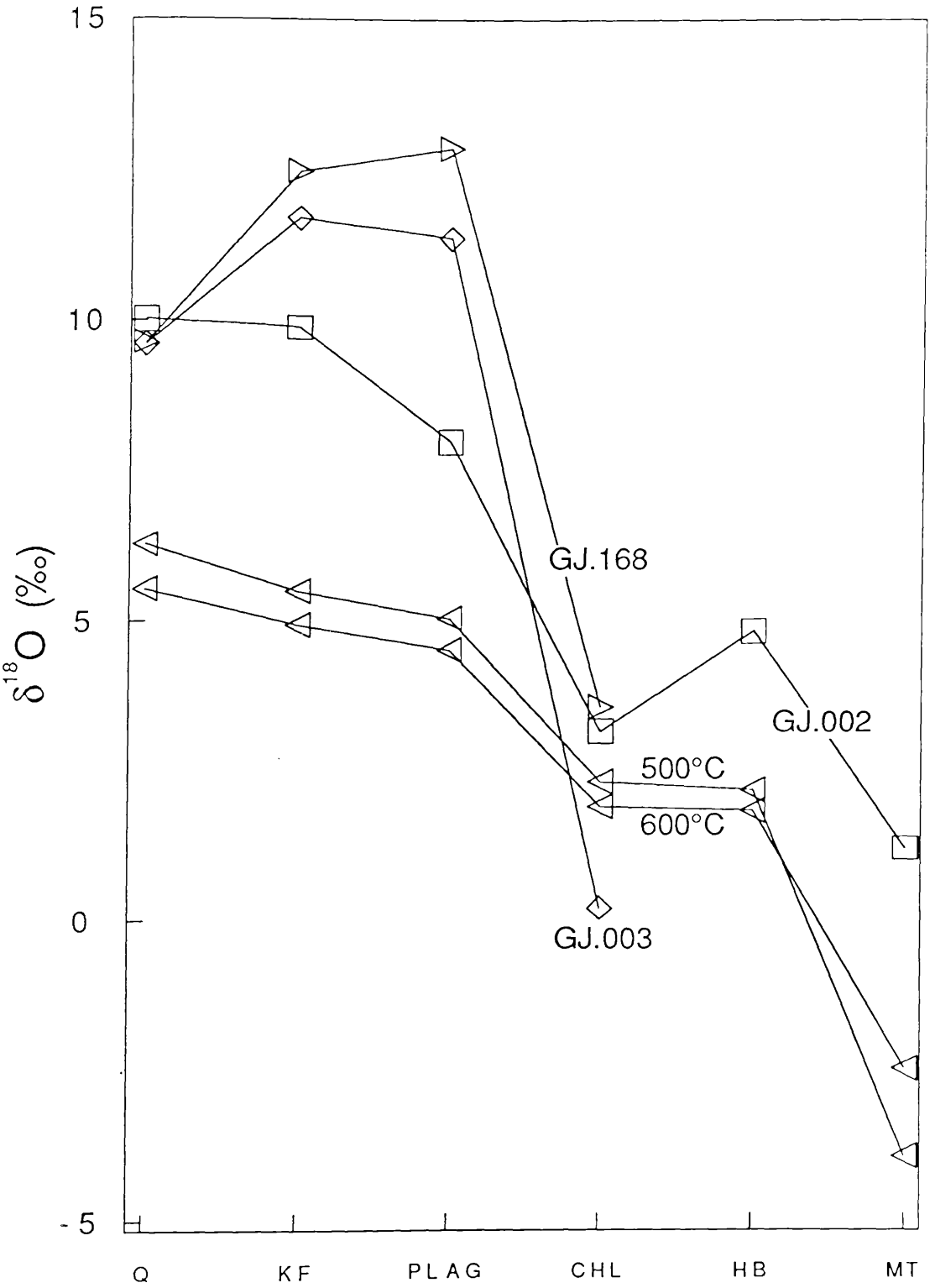

Fig. 6.7 $\delta^{18}O$ data for mineral separates from three samples from the Roundstone granite. The plagioclase $\delta^{18}O$ values for GJ.003 and GJ.168 were not measured but calculated by mass balance from the $\delta^{18}O$ data for the whole rock and the other mineral separates and the modal analyses. The calculated values and their uncertainties (resulting from the uncertainties in all the $\delta^{18}O$ data, but not the modal analyses) are GJ.003 = +11.36±0.76‰, GJ.168 = +12.87±1.29‰. The curves labeled 500°C and 600°C show the calculated fractionations between the different phases at 500 and 600°C.

The absolute $\delta^{18}O$ values for the minerals on these curves have no significance, since they depend on the whole rock $\delta^{18}O$ value. The curves are placed at lower $\delta^{18}O$ values to avoid confusion with the data curves. These model curves were calculated using the following fractionation equations: The quartz-water, K-feldspar-water (assuming behaves the same as albite - O'Neil and Taylor, 1967) and plagioclase-water (assuming plagioclase is An_{25}) equations of Matsuhisa *et al.* (1979), the magnetite-water equation of Matthews *et al.* (1983b), a hornblende-water equation derived from the equations of Bottinga and Javoy (1973) and Javoy (1977) and a chlorite-water fractionation derived from the data of Onuma *et al.* (1972). See A.4.2 for further details.

It can be seen from fig. 6.7 that in the more altered rocks the plagioclase-quartz fractionations are negative, as well as the quartz - K-feldspar fractionations. Negative quartz-plagioclase fractionations are also non-equilibrium fractionations and can be explained in the same way as the non-equilibrium quartz - K-feldspar fractionations, i.e. by enrichment of the plagioclase in ^{18}O as a result of interaction with the high δD fluid. This is because both of these minerals have similar fractionation behaviours and susceptibilities to oxygen isotope exchange. The $\delta^{18}O$ value of the plagioclase separates may also have been increased somewhat by the presence of calcite with high $\delta^{18}O$ values (12.38±0.12‰ in GJ.003) as a breakdown product in the plagioclase.

In the less altered sample (GJ.002) both the quartz - K-feldspar and quartz-plagioclase fractionations are positive. However these fractionations are unlikely to represent equilibrium fractionations. The quartz - K-feldspar fractionation is too small to represent an equilibrium fractionation at subsolidus temperatures. On the other hand, the quartz-plagioclase fractionation is such that it would have had to have been achieved at temperatures so low (<<400°C), that the quartz would have been unlikely to have equilibrated within any reasonable length of time. The high $\delta^{18}O$ value of the K-feldspar is more readily explained if it is interpreted as showing a slight ^{18}O enrichment as a result of partial exchange with the high $\delta^{18}O$ fluid. Similarly the apparently low $\delta^{18}O$ value of the plagioclase can be more easily explained as the result of the presence of significant quantities of relatively ^{18}O depleted sericite (=muscovite) in the sample (the hydrogen yield from this separate indicates that it could contain as much as ~36 wt.% muscovite).

The quartz - K-feldspar $\delta^{18}O$ fractionation measured for one mineral pair from the Galway granite (sample GJ.015) is also too small to represent an equilibrium fractionation (quartz = +9.53‰, K-feldspar = +9.46‰, Δ = 0.07). Following the same arguments that are given above, it is suggested some ^{18}O enrichment must also have taken place in the K-feldspar in this rock. This is despite the fact that this rock is relatively unaltered (most of the biotite has not been chloritised). Thus some oxygen isotope exchange may have also taken place in rocks which show only limited evidence of mineralogical alteration. The observation that the $\delta^{18}O$ value of K-feldspar has been increased in this granite, shows that this is a common feature of the alteration in both the Galway and Roundstone granites.

The quartz-chlorite fractionations measured are significantly greater (by as much as 6‰) than those which would be expected if the chlorite had

equilibrated with the quartz at 500-600°C. This reflects the fact that the chlorite formed at lower temperatures in equilibrium with the high δD fluid (because it formed by a chemical reaction from biotite), which the quartz did not equilibrate with. The $\delta^{18}O$ of the chlorite from GJ.003 is more than 3‰ lower than the $\delta^{18}O$ values of the other two chlorites analysed. This might be attributed to the presence of significant amounts of ilmenite in the separate, since this mineral was observed to be growing in the chlorite in thin section. If this ilmenite was in oxygen isotope equilibrium with the chlorite when the chlorite formed, then it would have had a lower $\delta^{18}O$ value and therefore lowered the $\delta^{18}O$ of the separate. However no peaks corresponding to ilmenite were identified in the XRD trace for this sample indicating that it forms less than 5-10% of the separate, in which case it would have had to have had an unreasonably low $\delta^{18}O$ value (<-20‰) in order to lower the chlorite $\delta^{18}O$ from ~3‰ to 0.2‰. Thus the difference in chlorite $\delta^{18}O$ between samples may be a result of differences in fluid $\delta^{18}O$ between samples (see below).

In contrast to the fractionations between other mineral pairs, the fractionations between quartz, magnetite and hornblende in GJ.002 are very similar to those shown by the model curves for equilibration at 500-600°C. Using the quartz-magnetite fractionation equation of Matthews *et al.* (1983b) the apparent equilibration temperature between these two phases can be calculated to be 560±15°C. This temperature is below the granite solidus, so that taken at face value, these data would suggest that some re-equilibration must have taken place in the solid state. However in the light of theoretical studies it is unlikely that such an apparent equilibration temperature will have any real significance (e.g. Giletti, 1986). Nevertheless, the fact that the fractionations between these minerals are similar to those that would be expected at high temperatures, suggests that the oxygen isotope ratios in these minerals have probably been inherited from high temperatures. This would be consistent with diffusion data (figs. 2.4, 2.12) which indicate that all of these phases should pass through their closure temperatures at relatively high temperatures (>500°C?).

The $\delta^{18}O$ value of the high δD fluid can be estimated from the $\delta^{18}O$ values of the phases which appear to have equilibrated with this fluid. Estimation of the $\delta^{18}O$ of the fluid that equilibrated with the plagioclase is complicated by the fact that the separates of this mineral are not pure plagioclase but contain variable amounts of the alteration products (mostly calcite and sericite). For this reason no attempt is made here to estimate the $\delta^{18}O$ of the fluid that equilibrated with the plagioclase and the $\delta^{18}O$ of the fluid is estimated by looking at the oxygen isotope compositions of the other phases which appear to have equilibrated with this fluid (K-feldspar, chlorite and calcite in GJ.003) which can be obtained as relatively pure separates.

Unfortunately the chlorite-water oxygen isotope fractionation has not been experimentally calibrated, because of the extremely slow rates of oxygen isotope exchange between chlorite and water (Matthews *et al.*, 1983a). Therefore the only fractionation equations available for this system have been derived either by theoretically based calculations, or empirically,

by observation of natural assemblages. Both of these methods may have large uncertainties associated with them (2.4.7) and, because of this, two fractionation equations derived using these different approaches are used here to estimate the $\delta^{18}O$ value of the fluid in equilibrium with the chlorite. (fig. 6.8).

The fractionation equation given by Wenner and Taylor (1971) was derived empirically, from the oxygen isotope fractionations (measured by Garlick, 1969) between coexisting quartz, chlorite and ilmenite from biotite and lower garnet grade pelitic schists. Such empirically derived fractionations are prone to be inaccurate because they do not take into account the variable degrees of retrograde exchange experienced by different minerals (see Giletti, 1986). Some evidence that retrograde exchange has taken place in the minerals analysed by Garlick (1969) comes from application to these minerals of the quartz-chlorite fractionation equation derived from these data by Wenner and Taylor (1971). This equation gives unreasonably low quartz-chlorite equilibration temperatures of 330-360°C for these rocks, indicating that some differential retrograde exchange has probably taken place in these rocks (or that the fractionation derived by Wenner and Taylor; *ibid.*, is not internally self consistent). For this reason the other chlorite-water fractionation equation used here is preferred. This equation was derived by multiple regression of fractionations calculated from the reduced partition functions of Onuma *et al.* (1972) for temperatures between 100 and 472°C. Such theoretically derived fractionation equations have the advantage over the empirically based fractionations in that they are not biased by retrograde effects; nevertheless these fractionations can have large errors associated with them because of the uncertainties in the input data used. Despite the fact that these two fractionation equations have been derived in different ways it can be seen from fig. 6.8 that fluid $\delta^{18}O$ values calculated for the same sample using both of these equations are fairly similar. This relatively good agreement between the fractionations derived by these different methods means that an increased degree of confidence can be placed in these equations, since it is unlikely that both are completely inaccurate.

The chlorite curves shown in fig. 6.8 show that the fluid from which this mineral formed must have had a fairly low $\delta^{18}O$ value (<6‰), assuming the chlorite formed below 500°C. At 300°C, which is the suggested upper temperature at which chloritisation probably could have taken place (6.2.3), the fluid in equilibrium with the chlorite in GJ.168 has a $\delta^{18}O$ value of ~+2 to +3‰. The lower $\delta^{18}O$ value of the chlorite in GJ.003 means the estimated $\delta^{18}O$ of the fluid in equilibrium with this chlorite is lower than that in equilibrium with the chlorite in GJ.168 at the same temperature. For both of these chlorites to have equilibrated with a fluid of the same $\delta^{18}O$, they would have had to have equilibrated at temperatures at least 75°C apart (if they equilibrated with a fluid with $\delta^{18}O$ = -2‰) and possibly as much as 200°C apart (if they equilibrated with a fluid with $\delta^{18}O$ = +2‰, fig. 6.8). If the chlorite did form at 300°C, then the chlorite in GJ.003 would have equilibrated with a fluid of ~0 to -1‰, while the chlorite in GJ.168 could not have equilibrated with the same fluid until the temperature had fallen to ~200-170°C. This situation would be highly improbable because the rates of

oxygen isotope exchange between fluid and chlorite at these temperatures would probably be so low (Matthews *et al.*, 1983b) that chlorite would not appreciably re-equilibrate oxygen isotopes with the fluid after it formed. Thus either the chlorites formed over a range of temperatures, or else the chlorite formed at the same temperature and the fluid which caused its formation was heterogeneous in $\delta^{18}O$ between samples. Possibly examination of the chlorite chemistry could indicate which of these possibilities was the case.

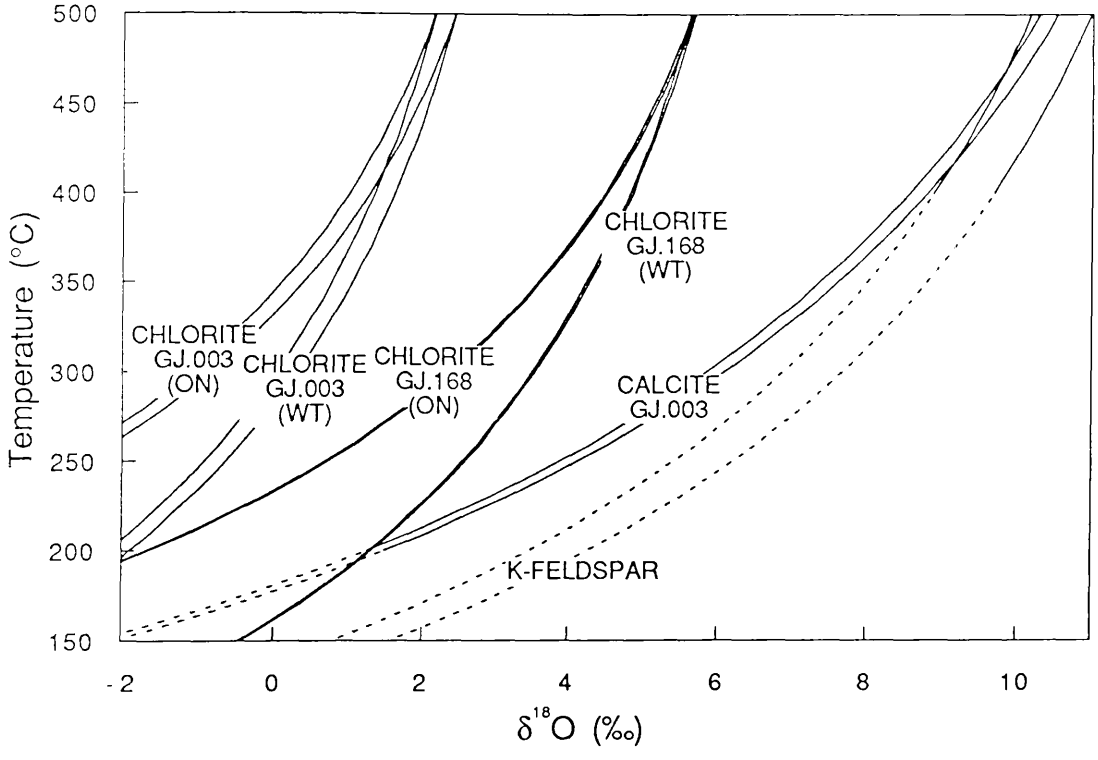

Fig. 6.8 Estimated $\delta^{18}O$ of the fluid in equilibrium with the chlorites and K-feldspars in GJ.003 and GJ.168 and the calcite in GJ.003, shown as a function of temperature assuming that the fluid fractionated oxygen isotopes in the same was as pure water. The pair of curves labeled "K-feldspar" correspond to the fluid in equilibrium with the K-feldspar in GJ.003 and GJ.168. All the other pairs of curves show the estimated $\delta^{18}O$ of the fluid in equilibrium with a single mineral separate, with the two curves bracketing the uncertainty in the calculated fluid $\delta^{18}O$ due to the uncertainty in the oxygen isotope analysis of that separate. All curves were calculated assuming that the fluid in equilibrium with these minerals fractionated oxygen isotopes in the same way as pure water. The sources of the fractionation equations used were: K-feldspar-water; Matsuhisa *et al.* (1979), chlorite-water; Wenner and Taylor (1971) - labeled "W+T" and a recalculation of the data given by Onuma *et al.* (1972) - labeled "ON", calcite-water: a recalculation of the data given by O'Neil, Clayton and Mayeda (1969). See text and A.4.2 for further details. The K-feldspar and calcite fluid curves are dashed below the experimentally calibrated range.

The calculated $\delta^{18}O$ values of the fluid in equilibrium with the K-feldspars in GJ.003 and GJ.003 and the calcite in GJ.003 are also shown in fig. 6.8. It can be seen that at any temperature, the fluid in equilibrium with these minerals is significantly heavier than the fluid in equilibrium with the chlorites in the same rocks. Thus it can be concluded that the K-feldspars and calcites in these rocks did not equilibrate oxygen isotopes with the pore fluid at the same temperature as the chlorite. Both calcite and K-feldspar have been shown to undergo very rapid oxygen isotope exchange

with hydrous fluids even at low temperatures, in contrast to chlorite, which is very resistant to post formational oxygen isotope exchange. This being the case, the chlorite must have equilibrated with the fluid prior to the equilibration of the K-feldspar and calcite with the fluid. The alternative situation in which the calcite and K-feldspar equilibrated with the fluid at a higher temperature than the chlorite (i.e. before its formation) is untenable, because the calcite and K-feldspar would have undoubtedly equilibrated with the fluid which formed the chlorite.

It follows from this argument that during the formation of the chlorite, the calcite and K-feldspar must have been in equilibrium with the fluid that formed the chlorite. The $\delta^{18}O$ of this fluid is shown by the chlorite curves in fig. 6.8. If the chlorite formed at ~300°C from a fluid with $\delta^{18}O$ = +3‰, then the $\delta^{18}O$ value of the K-feldspar during chlorite formation can be calculated to have been ~+7.8‰ using the fractionation of Matsuhisa *et al.* (1979). This value is significantly lower than the $\delta^{18}O$ which the K-feldspar is likely to have had prior to exchange with this fluid. If the K-feldspar previously equilibrated with the quartz at 500-600°C prior to the high δD being present in the rock, then the K-feldspar would have originally have had a $\delta^{18}O$ of ~+8.7 to 9.1‰. Thus the K-feldspar must have initially had its $\delta^{18}O$ lowered as a result of exchange with the high δD fluid. The chlorite formed by replacement of biotite and the $\delta^{18}O$ of this biotite prior to reaction with the fluid can also be estimated by assuming that it previously equilibrated with the quartz in this rock at high temperature. If the biotite had ceased exchanging by ~500-600°C then its $\delta^{18}O$ value can be estimated to have been ~+4.8 to 5.7‰. This value is higher than that of the chlorite which replaced the biotite (~+3‰). During exchange at 300°C the plagioclase probably behaved similarly to the K-feldspar, while no other phases in the rock appear to have appreciably exchanged with the high δD fluid. Thus it can be seen that at 300°C, the $\delta^{18}O$ values of <u>all minerals</u> which exchanged with this fluid were <u>reduced</u>, and therefore the $\delta^{18}O$ of the whole rock was also reduced. If this fluid reduced the $\delta^{18}O$ of all exchangeable minerals in the granite at 300°C, then by the laws of mass balance the $\delta^{18}O$ value of the fluid must have originally been lower than +3‰ prior to infiltration into the granite. This strongly suggests that this fluid was of surface derived origin, which is consistent with the hydrogen isotope data and the mineral data from the fault fill material described in 6.4.3.

If the K-feldspar $\delta^{18}O$ values were ~+7.8‰ during chloritisation at 300°C, then the $\delta^{18}O$ of this mineral must have been significantly <u>increased</u> between that time and the present day. There are two extreme possibilities for the way in which this could have happened:

1. equilibration of the K-feldspar (and calcite) after chlorite formation, but at the same (i.e. 300°C) or slightly lower temperature, with a fluid with a much higher $\delta^{18}O$.

2. equilibration of the K-feldspar (and calcite) after chlorite formation at much lower temperatures, with a fluid with a similar $\delta^{18}O$ value to that which equilibrated with the chlorite.

In order to increase the $\delta^{18}O$ of the K-feldspar to as much as 12.5‰ at 300°C the $\delta^{18}O$ of the fluid would would eventually have to increase to at least 7.7‰. This is the minimum increase in fluid $\delta^{18}O$ required and could only apply if fluid/rock ratios were infinitely high. If, for example, the fluid $\delta^{18}O$ was +8‰, then the fluid/K-feldspar oxygen ratios that would be required to cause the shift in K-feldspar $\delta^{18}O$ from 7.8 to 12.5‰, can be calculated (using the equations given in 2.7.2), to be 16.9 for a closed system or 2.9 for a open system. If the fluid was +10‰ then the fluid/K-feldspar oxygen ratios required to cause the same shift would be reduced to 2.1 for a closed system and 1.1 for an open system. Since the plagioclase probably behaved in a similar way to the K-feldspar and together these minerals make up ~ 2/3 of the granite fluid/rock oxygen ratios would have been ≈ 2/3 of the fluid/K-feldspar ratios. Thus even if the fluid $\delta^{18}O$ increased to as much as 10‰ after chlorite formation rather high fluid/rock ratios would be required to account for the shifts in K-feldspar $\delta^{18}O$ values.

These is no reason why the $\delta^{18}O$ of the fluid in this rock should have increased from <=+3‰ to such values >8‰ after chloritisation. Indeed there are only a limited number of mechanisms which could have caused any $\delta^{18}O$ increase in the fluid. If the fluid was internally derived within the granites, then only chloritisation reactions or equilibration with K-feldspar in other rocks could have caused a $\delta^{18}O$ increase in the fluid. Chloritisation reactions could have acted to increase fluid $\delta^{18}O$ if the biotite which reacted to form the chlorite was more ^{18}O enriched than the chlorite produced. However this process could not have increased fluid $\delta^{18}O$ values to greater than the $\delta^{18}O$ values of the biotite if $\Delta_{chlorite\text{-}fluid} \approx 0$‰ at 300°C. Thus this process could not have increased fluid $\delta^{18}O$ values to much more than ≈ 6‰ (see above) in the granites. If prior to infiltrating this rock, the fluid had exchanged oxygen isotopes with other feldspars within the granite, which had not been previously ^{18}O depleted, then this process could have increased the fluid $\delta^{18}O$. If the feldspars in the granite originally had a $\delta^{18}O$ of ≈ +9‰ and if feldspar/fluid ratios were tending to infinity, then the maximum increase in fluid $\delta^{18}O$ by this process would be to ~7.5‰ if the fluid was coming from hotter rocks (500°C) or ~5.3‰ if the fluid was coming from rocks with the same temperature (300°C). Thus such processes could not have increased the fluid $\delta^{18}O$ enough to have caused the $\delta^{18}O$ shift in the K-feldspars at 300°C.

If the fluid was not internally derived from the granite but had come from a more distant source then similar mechanisms could have acted to increase the fluid $\delta^{18}O$ in other rock units. From fig. 3.1 it can be seen that quartz in the Cashel Formation has $\delta^{18}O$ values between +12 and +14‰, in which case biotites in these rocks probably have $\delta^{18}O$ values of +8 to +9‰. Reactions of small volumes of a fluid with large amounts of this biotite

could conceivably have raised the $\delta^{18}O$ of the fluid to ~+8‰. Thus this process could just have increased the fluid $\delta^{18}O$ enough to have caused the $\delta^{18}O$ shift in the K-feldspars. However this this possibility is considered unreasonable because such a fluid would have had to have reacted with the biotite in the metasediments under conditions of very low fluid/rock ratios, yet been present in the Galway granites in very large quantities to produce the $\delta^{18}O$ shift in the K-feldspar (high fluid/rock ratios). From the hydrogen isotope data for the chlorites and fluid inclusions in the granite, and the oxygen isotope data for the chlorite and the minerals in a vein in the MGS, it would appear likely that the fluid causing chloritisation in the Galway granites originated from a meteoric source (6.5). This being the case then if the fluid causing the $\delta^{18}O$ shift in the K-feldspar was also derived from the same source, and traveled to the granite by the same path, there is no reason why the later fluid should have become more ^{18}O enriched than the earlier fluid (<=+3‰). If anything the opposite effect would be expected because the continued exchange of the rocks on the infiltration path with meteoric fluid would progressively lower the $\delta^{18}O$ of the rocks, hence reducing the capacity of these rocks to shift the $\delta^{18}O$ of the fluid to higher values.

Thus there does not appear to be a plausible mechanism by which the fluid $\delta^{18}O$ value could have been increased to as much as the +8‰ at 300°C, and it can be concluded that the $\delta^{18}O$ enrichment of the K-feldspar in the Galway granites must have taken place at a lower temperature.

If the $\delta^{18}O$ enrichment of the K-feldspar took place at lower temperatures, it can be seen that the $\delta^{18}O$ of the fluid that would be required to produce this enrichment will become progressively lower as temperature falls, because of the increase in the value of $\Delta_{K\text{-feldspar-fluid}}$. From fig. 6.9 it can be seen that the minimum fluid $\delta^{18}O$ required (i.e. with infinite fluid/K-feldspar ratios) to shift the $\delta^{18}O$ of the K-feldspar in GJ.168 up to 12.5‰ is ~6.3‰ at 250°C, ~4.3‰ at 200°C and 1.7‰ at 150°C. In order that the fluid rock ratios should not be unrealistically high (<10 in an open system) the actual fluid $\delta^{18}O$ values would have to be at least 0.3‰ higher than these values.

The only mechanisms which could have caused the fluid $\delta^{18}O$ to have increased at temperatures <300°C, are the same as those which could have caused fluid $\delta^{18}O$ enrichment at 300°C, described above. However these mechanisms become increasingly less efficient in increasing fluid $\delta^{18}O$ with falling temperature for two reasons

1. As temperature falls the magnitude of the K-feldspar - water and chlorite-water fractionations increases, so that the upper limit to which chloritisation reactions, or exchange with K-feldspar can shift the fluid $\delta^{18}O$ decreases.

2. If the chloritisation reaction has a similar activation energy to other mineralogical reactions, then all other factors being equal, the effect of

the temperature falling from 300 to 200°C will be to decrease the reaction rate by approximately an order of magnitude (fig. 2.13). If the temperature falls a further 50°C then the reaction rate will decrease by another order of magnitude. Similarly it can be seen from fig. 2.12 that if the temperature fell to 200°C that the rate of diffusion controlled oxygen isotope exchange between K-feldspar and fluid would decrease by approximately two orders of magnitude.

Thus as temperature falls, although the $\delta^{18}O$ of the fluid required to cause the $\delta^{18}O$ increase in the K-feldspar becomes lower, the probability of the fluid having its $\delta^{18}O$ value increased by any process also decreases. Consequently it is considered likely that the $\delta^{18}O$ of the fluid that caused the $\delta^{18}O$ increase in the K-feldspar in the Galway granites was probably not much greater than the $\delta^{18}O$ of the fluid that caused the chloritisation in the same rocks. If this was the case, then the increase in $\delta^{18}O$ of the K-feldspar must have been caused by a fluid with a $\delta^{18}O$ of <=+3‰. Since exchange with the K-feldspar would have lowered the fluid $\delta^{18}O$ somewhat, depending on fluid/K-feldspar ratios, the final $\delta^{18}O$ of the fluid after equilibration must have been <=+2.7‰ even if the fluid/K-feldspar ratios were very high (≈ 10 in an open system).

It can be seen from fig. 6.8 that for the K-feldspar in GJ.168 to have equilibrated with a fluid with a $\delta^{18}O$ of <=+2.7‰, equilibration would have had to have taken place at temperatures <180°C, if the fractionation curves of Matsuhisa *et al.* (1979) can be extrapolated to such low temperatures. If the K-feldspar underwent its positive shift by exchange in a closed system with fluid/rock ratios of ~3 then the $\delta^{18}O$ of the fluid after equilibration would have been <~+2‰ in which case equilibration would have had to have taken place at 160°C. Similarly closed system fluid/rock ratios of ~1 would require the feldspar in GJ.168 to have equilibrated down to temperatures of 125°C! The K-feldspar in these rocks is fairly coarse (1-2 mm diameter in GJ.168, oikocrysts 2 mm or more in diameter in GJ.003), so that if the the effective grain size for diffusion was equal to physical grain size, oxygen isotope equilibration by diffusion down to such temperatures by diffusion alone would be unrealistic (fig. 2.12). However it is possible that the presence of microperthite and celsian exsolution could have acted to substantially reduce the effective grain size for diffusion. It is also possible that some oxygen isotope exchange with the fluid could have taken place by a solution-reprecipitation process, or that the exsolution process itself could have enhanced the rate of oxygen isotope exchange. The tiny microtubes observed in the K-felspar in GJ.168 (1.4.3) may be evidence that solution-reprecipitation was taking place in this sample at least. The development of a fine network of interconnecting fluid filled tubes in this feldspar would have greatly reduced the diffusion length.

There is some evidence from $\delta^{18}O$ measurements on natural K-feldspar which indicates that it can equilibrate oxygen isotopes with the pore fluid in rocks down to low temperatures. From studies of hydrothermal systems by Clayton *et al.* (1968) and Clayton and Steiner (1975) it would appear that detrital K-feldspar has undergone a high degree of exchange with the

hydrothermal fluid at temperatures possibly as low as 150°C. Wenner and Taylor (1976) measured the $\delta^{18}O$ compositions of quartz and K-feldspar from the Precambrian St. Francois mountain terrane. They found that, like the granites analysed in this study, some of the rocks were ^{18}O enriched, and that the degree of ^{18}O enrichment showed a correlation with the increasing intensity of "brick red" alteration in the K-feldspars. Coexisting quartz and K-feldspar were typically found not to be in oxygen isotope equilibrium due to ^{18}O enrichment in the K-feldspars. These authors argue that considering the possible sources of fluid in that area, the alteration of the K-feldspars may have taken place at temperatures as low as 100 or even 50°C. They also noted that O'Neil and Taylor (1967) had found experimentally that feldspars which had been subjected to oxygen isotope and cation exchange at high temperatures became transformed to a much more reactive condition. Wenner and Taylor (1976) suggested that if the feldspars had previously been exposed to a hydrothermal fluid, such a "pre-treatment" could explain why the feldspars were able to exchange to low temperatures. Such an explanation could also apply to the feldspars in the Roundstone granite because it is likely that the K-feldspars in this granite exchanged with fluid present in the rock at temperatures of ~300°C prior to the exchange at lower temperatures.

Thus, if the assumptions made above are all correct, it can be concluded from this discussion that the feldspars in the Galway granites must have undergone ^{18}O enrichment by exchange with a fluid with a $\delta^{18}O$ (<+3‰) at very low temperatures. Since the curves for the calcite in GJ.003 are similar to the K-feldspar curves, it can be inferred that the calcite also equilibrated with this fluid down to low temperatures. The relative positions of the curves indicate that the calcite may have ceased equilibration with this fluid at a slightly higher temperature than the K-feldspar. Therefore there must have been fluid present in some parts of these granites down to very low temperatures. The exact temperature to which equilibration is required to have taken place is dependent on the fluid/rock ratios operative in the rocks in which the feldspar $\delta^{18}O$ values have been increased. However, even if fluid/rock ratios were infinitely high, equilibration temperatures as low as 180°C are required in some rocks. On the other hand, if fluid/rock ratios were only moderately high, very low equilibration temperatures would be required. Because the likelihood of any exchange process being capable of causing fluid-mineral equilibration decreases rapidly with temperature (because the rates follow an Arrhenius relationship), it is likely that fluid/mineral oxygen ratios were probably quite high during this low temperature alteration of the feldspars.

The interpretation given above was made by assuming that the fluid fractionated oxygen isotopes in the same way as pure water. It has already been shown from the hydrogen isotope data (6.3.2) that the fluid <u>was</u> saline and therefore these conclusions may have to be modified somewhat, depending on what the oxygen isotope salt effect of the solutes in the fluid were. The exact salinity of the fluid and the composition of the salts in the fluid are not known, although it was observed that the hydrogen isotope salt effect was similar to that which would be produced by a 4m NaCl solution. Examination of the oxygen isotope salt effects measured by Truesdell (1974) reveals that three salts that are often most abundant in

geological fluids (NaCl, $CaCl_2$, KCl) all have similar effects on the fractionation behaviour of the fluid at the same temperature. The presence of one of these three salts (but not $MgCl_2$) in a fluid causes the mineral-fluid fractionations to be larger than the corresponding mineral-water fractionation at temperatures above ~150°C and to be less than the mineral-water fractionation below ~150°C. If it is presumed that a. the major salts in the fluid which caused the alteration in the granites were these three salts, and that b. the fractionation behaviour of a fluid containing a mixture of these salts is the sum of the fractionation effects of the individual salts (Sofer and Gat, 1972), then the effect of the fluid being saline on the isotopic relationships described above can be demonstrated by making the assumption that the mineral-fluid fractionations corresponded to that of one of these salt solutions. For example, the curves for the $\delta^{18}O$ of the fluid in equilibrium with the same minerals shown in fig. 6.8, when the fluid is a 4m NaCl solution are shown in fig. 6.9. Such a solution had the most extreme salt effects of all the solutions investigated by Truesdell (*ibid.*) so that it is quite likely that the actual equilibrium fluid curves for these minerals from the Roundstone granite lie somewhere between the curves shown in figs. 6.8 and 6.9, unless the fluid was extremely saline.

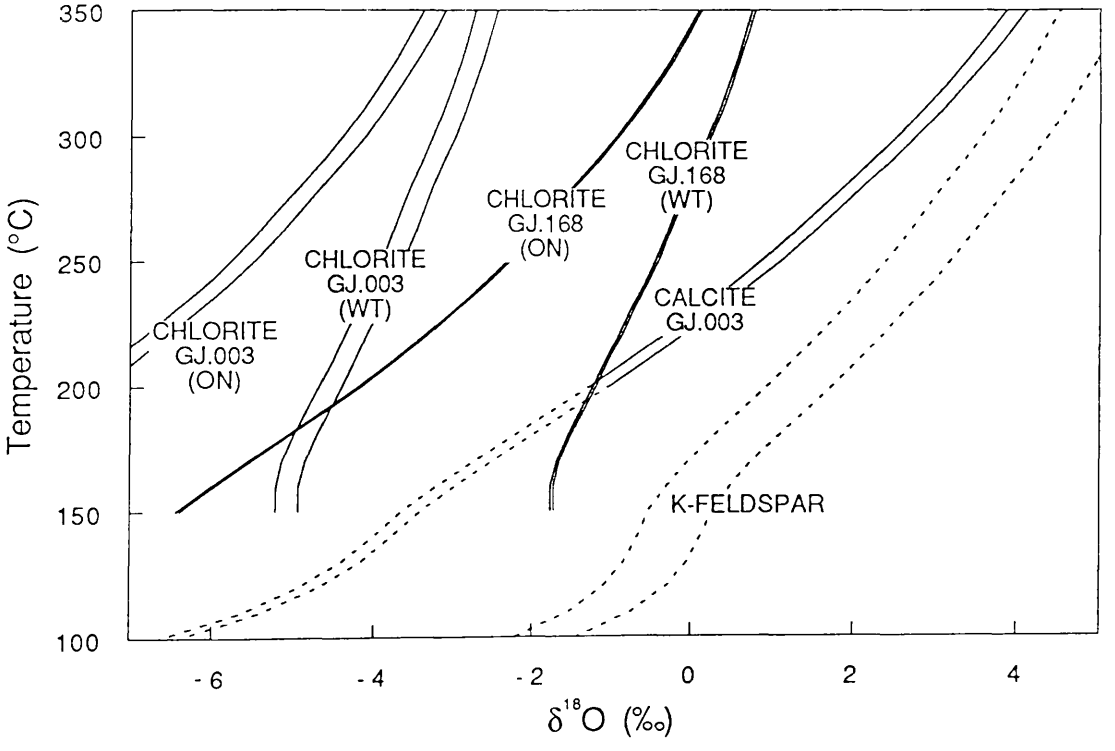

Fig. 6.9 Estimated $\delta^{18}O$ of the fluid in equilibrium with the chlorites and K-feldspars in GJ.003 and GJ.168 and the calcite in GJ.003, shown as a function of temperature assuming that the fluid fractionated oxygen isotopes in the same way as a 4m NaCl solution. The curves are labeled in the same way as the curves in fig. 6.8. The curves were derived by adding the 4m NaCl solution-water fractionation curve of Truesdell (1974) to the curves shown in fig. 6.8.

If the fluid which caused the alteration in the Roundstone granite did fractionate oxygen isotopes in the same way as a 4m NaCl solution, then using the same arguments that were used in the discussion of fig. 6.8, the following points can be inferred from fig. 6.9.

1. The fluid in equilibrium with the chlorite in GJ.168 at its likely formation temperature (~300°C) would have had a $\delta^{18}O$ less than or equal to 0‰. This would indicate that this fluid must have been derived from a surface source. Since it is likely that this fluid would have undergone a positive $\delta^{18}O$ shift on its journey from the surface, it is probable that this fluid was originally of meteoric origin. If the chlorite in GJ.003 formed at 300°C the $\delta^{18}O$ value of the fluid which it would have equilibrated with is ~ -3 to -5‰. Therefore this chlorite must have been formed from a fluid of meteoric origin. Because the δD value of a fluid is very resistant to change during fluid-rock interaction (2.7.2), the $\delta^{18}O$ value of a meteoric fluid prior to undergoing any $\delta^{18}O$ shift can be estimated from the δD of the fluid using Craig's (1961a) equation for the present day meteoric water line. From the δD value of -19.6‰ measured for the water in the fluid inclusions in the quartz in GJ.003 the original $\delta^{18}O$ of the meteoric fluid from which this fluid was derived can be estimated to be ~-3.7‰. This value is not significantly different from the $\delta^{18}O$ value inferred from the chlorite, suggesting that the fluid which formed this chlorite may have been relatively unaltered meteoric fluid. Alternatively the fluid may have undergone some positive $\delta^{18}O$ shift, in which case the chlorite must have formed at a rather higher temperature than 300°C.

2. At 300°C the K-feldspar would have been ^{18}O depleted relative to its initial $\delta^{18}O$ value (~<=+5‰ compared to ~9‰ initially) if it equilibrated with the fluid present at that temperature. Thus the K-feldspar must have undergone later ^{18}O enrichment to account for the presently observed high $\delta^{18}O$ values. The mechanisms described above for increasing the fluid $\delta^{18}O$ after chlorite formation could conceivably have caused a $\delta^{18}O$ increase in the fluid to the value of ~4‰ which would have been necessary to produce the ^{18}O enrichment at 300°C. However since in this case it is certain that the fluid was of meteoric origin, such a later ^{18}O enrichment in the fluid would appear to be improbable, if relatively unshifted meteoric fluid had previously infiltrated these rocks (see above). Thus it is likely that the fluid $\delta^{18}O$ did not increase with time and that, therefore, the ^{18}O enrichment in the K-feldspars must have been caused by fluids with a $\delta^{18}O$ of less than or equal to 0‰.

3. If the ^{18}O enrichment in the K-feldspars was caused by fluids with a $\delta^{18}O$ less than or equal to 0‰, then it can be seen from fig. 6.9 that even if fluid/rock ratios were infinitely high, the K-feldspar would have had to have equilibrated oxygen isotopes with the fluid to temperatures as low as 170°C (GJ.003) or 140°C (GJ.168).

4. Since the curves for the calcite from GJ.003 are similar to the K-feldspar curves in fig. 6.9, it can be inferred that the calcite also equilibrated with this fluid down to low temperatures. As in the case in which the fluid was presumed to be pure water, the relative positions of the curves

indicate that the calcite may have ceased equilibration with this fluid at a slightly higher temperature than the K-feldspar.

It can be concluded from this discussion that the $\delta^{18}O$ values of the fluid causing the alteration in the granites, and the temperatures at which alteration took place, cannot be exactly estimated from the mineral separate $\delta^{18}O$ data unless the fluid salinities are known. However if the fractionation behaviour of the fluid that caused this alteration was somewhere between that of a pure water fluid and a 4m NaCl solution it can be concluded that:

1. The fluid which caused the alteration had a low $\delta^{18}O$ value, very probably indicating that it was of a surface derived origin (probably meteoric).

2. The ^{18}O enrichment in the K-feldspars was probably caused by equilibration with this same fluid at very low temperatures (<200°C), indicating that this fluid was also present in these rocks during cooling. The K-feldspar enrichment probably took place under conditions of high fluid/rock ratios.

Estimation of fluid salinity, by fluid inclusion studies, would greatly facilitate the interpretation of this data.

6.4.3 Oxygen isotope data for vein minerals in a fault fill.

The $\delta^{18}O$ values of the quartz, baryte and calcite from a vein within the MGS (GJ.196, see 1.4.3) were measured in order to estimate

1. the temperature of vein formation.

2. the $\delta^{18}O$ of the fluid from which these vein minerals were precipitated.

Estimation of these variables for this vein is important, because in 6.3.2 it was shown that the δD of the water in the fluid inclusions in the calcite is ~-24‰. This indicates that the calcite was very probably precipitated from a high δD fluid, similar to that which caused the alteration in the enclosing MGS rock and the fluid which caused alteration in the Galway granites. It may be that the fluid that precipitated the minerals in this vein can also be shown to have had a similar $\delta^{18}O$ and been present at the same temperature as the high δD fluid causing alteration in these different rock types. This would then provide good additional evidence to correlate the fluid which was present in this fault with the fluid causing alteration in the granites, or the fluid causing alteration in the MGS, or both.

The $\delta^{18}O$ values of the quartz, baryte and calcite are tabulated in A.2.2. The $\delta^{18}O$ value of the water that would be in equilibrium with these minerals is shown as a function of temperature in fig. 6.10. The following interpretation of the isotopic relationships assumes that the fluid which precipitated the minerals in this vein fractionated oxygen isotopes in the same way as pure water.

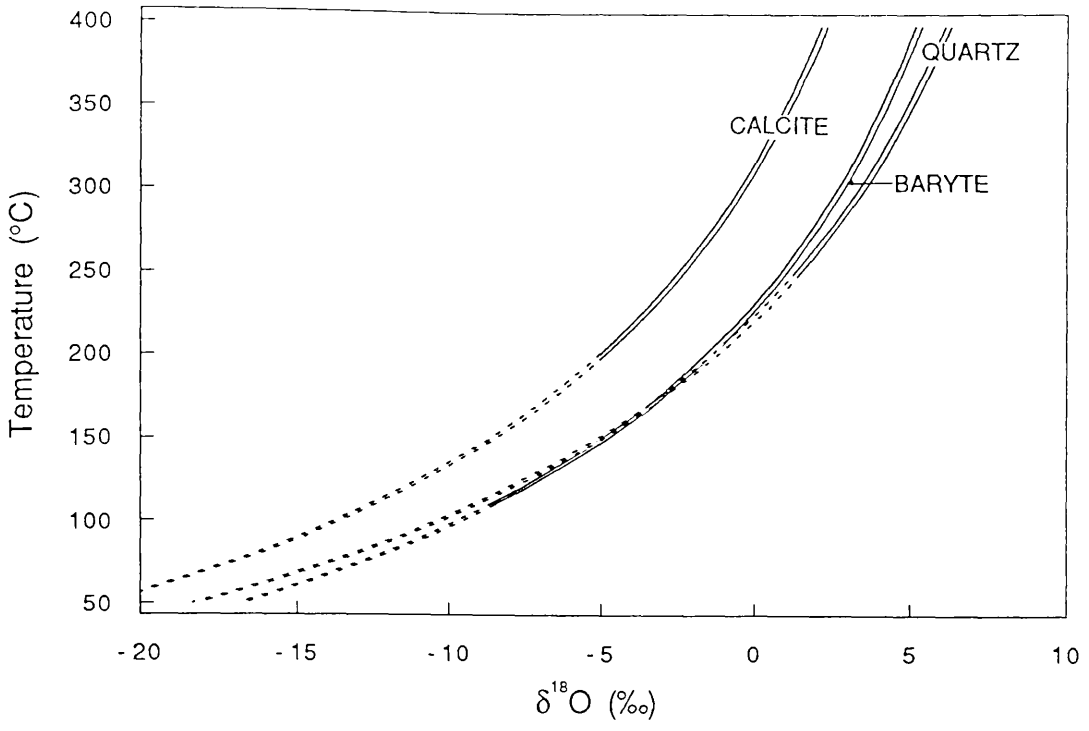

Fig. 6.10 Estimated $\delta^{18}O$ of the fluid in equilibrium with the minerals in the vein in GJ.196 as a function of equilibration temperature, assuming that the fluid fractionates oxygen isotopes in the same way as pure water. Each pair of curves corresponds to the uncertainty resulting from the error in the oxygen isotope analysis. The curves are dashed where they are projected below their experimentally calibrated range. The baryte-water and quartz-water fractionation equations used were from Kusakabe and Robinson (1977) and Matsuhisa *et al.* (1979) respectively. The calcite-water fractionation equation was recalculated from the 200-700°C data of O'Neil, Clayton and Mayeda (1969) after correction of the measured fractionations for the effect of the presence of NH_4Cl in the experimental runs (see A.4.2).

It can be seen from this figure that the fluid $\delta^{18}O$ curves for the baryte and quartz intersect, indicating that they could be have been in oxygen isotope equilibrium at that temperature. However the curve for the fluid in equilibrium with the calcite does not intersect with the other two curves at any reasonable temperature for calcite formation or equilibration. This indicates that the calcite could not have equilibrated oxygen isotopes with the other two minerals at any temperature.

The reason for the calcite not being in equilibrium with the other two phases must be because it equilibrated either with a different fluid with a different $\delta^{18}O$ and/or it equilibrated at a different temperature from the other two minerals. The textural relations for this vein are consistent with this hypothesis, because the calcite in this vein appears to have formed later than the quartz and baryte (1.4.3). Regardless of the temperature at which the quartz and baryte did actually equilibrate with the fluid in the vein it can be seen from fig. 6.10 that the calcite could only have equilibrated with a fluid with the same $\delta^{18}O$ if the calcite equilibrated with this fluid at a higher temperature than the quartz and baryte did (by at least 20°C even if the calcite did not equilibrate until 70°C). This situation is considered to be highly unlikely, because later vein filling materials usually form at the same, or lower temperature than the earlier formed minerals. Thus it is assumed here that the calcite equilibrated with fluid in the vein at the same,

or at a lower temperature than the temperature at which the quartz and baryte equilibrated with fluid in the vein. This being the case, it can be seen from fig. 6.10 that regardless of the exact temperature at which the quartz and baryte equilibrated with fluid in the vein, the calcite must have equilibrated with a fluid with a significantly lower $\delta^{18}O$ (by at least 2.7‰ even if the calcite equilibrated with the fluid @ 50°C). If the quartz and baryte did last equilibrate with the fluid in the vein at their apparent equilibration temperature, then the calcite must have equilibrated with a fluid with a $\delta^{18}O$ at least 3.5‰ lower than the fluid which equilibrated with the quartz and baryte. Thus it can be concluded that the fluid in this vein must have varied in $\delta^{18}O$ with time.

The intersection of the quartz and baryte curves defines an apparent equilibration temperature for these two minerals of 166±18°C (this error value assumes that σ_Δ = 0.14‰ and does not take into account the errors on the fractionation coefficients - 2.5.2). The $\delta^{18}O$ of the water in equilibrium with these two minerals at this temperature is -3.7‰. Such a fluid $\delta^{18}O$ value would indicate that a meteoric water component must have been present in this fluid (fig. 2.19). The fact that the calcite in this vein must have equilibrated with a fluid with a $\delta^{18}O$ at least 2.7‰ lower than that which equilibrated with the quartz and the baryte casts some doubt on the interpretation of this apparent equilibration temperature for the quartz and baryte as being the actual equilibration temperature. This is because experimental studies have shown that baryte can exchange oxygen isotopes extremely rapidly with saline solutions by a solution-reprecipitation process (fig. 2.13), but that quartz is very resistant to oxygen isotope exchange at low temperatures (3 orders of magnitude slower than baryte by a solution reprecipitation process - fig. 2.13, and very slow by diffusion - fig. 2.12). Thus it is possible that the baryte could have partially re-equilibrated with the lower $\delta^{18}O$ fluid during calcite precipitation, while the quartz did not appreciably exchange with this fluid. Hence the measured $\delta^{18}O$ value for the baryte can only be interpreted as a minimum value. It can be seen from fig. 6.10 that the slopes of the fluid curves for the quartz and baryte are very similar so that even a small depletion in the $\delta^{18}O$ of the baryte would greatly alter the position of the intersection of these curves, and therefore the apparent equilibration temperature. If, as is likely (but not proven), the quartz and baryte were also precipitated from a high δD fluid as well as the calcite, then an upper temperature limit of ~300°C can be placed on the formation temperature of the quartz and baryte. This is because it was shown in 4.2 that it is unlikely that a high δD fluid was present in the MGS at temperatures much above 300°C. If the baryte had had a $\delta^{18}O$ only 0.7‰ heavier prior to any exchange with the fluid that deposited the calcite, then the quartz and baryte could have been in equilibrium at 300°C. If this was the case, then the $\delta^{18}O$ of the fluid that would have been in equilibrium with the quartz and baryte at 300°C can be estimated from the quartz curve in fig 6.9 and is ~+3.5‰. Since it is thought that the calcite could not have formed at a higher temperature than the quartz and baryte, the maximum temperature for calcite formation must also be ~300°C. At this temperature the calcite would have been in equilibrium with a fluid with a $\delta^{18}O$ of

~-0.4‰. If the assumptions made above are correct, then this is the maximum $\delta^{18}O$ that the fluid which the calcite formed from could have had. It is likely that the calcite actually formed at a lower temperature, in which case the fluid $\delta^{18}O$ would have been lower.

The low $\delta^{18}O$ value estimated for the fluid which deposited the calcite implies that it contains some water of a surface derived origin. If it is assumed that seawater $\delta^{18}O$ values were not significantly different from 0‰ in the past, then the fact that the $\delta^{18}O$ value of the fluid that deposited the calcite is probably significantly less than 0‰ indicates that this fluid was very probably of meteoric origin. Because the δD value of a fluid is very resistant to change during fluid-rock interaction (2.7.2), the $\delta^{18}O$ value of a meteoric fluid prior to undergoing any $\delta^{18}O$ shift can be estimated from the δD of the fluid using Craig's (1961a) equation for the present day meteoric water line. From the δD value of -24.4‰ measured for the water in the fluid inclusions in the calcite, the original $\delta^{18}O$ of the meteoric fluid from which the calcite forming fluid was derived can be estimated to be ~-4.3‰. Since this meteoric fluid could only have undergone a positive $\delta^{18}O$ shift during infiltration through the MGS, this value can be regarded as a minimum value for the $\delta^{18}O$ of the fluid which deposited the calcite. If the fluid had undergone no $\delta^{18}O$ shift prior to deposition of the calcite, then the minimum temperature of calcite deposition can be estimated from the calcite-fluid fractionation to be ~210°C. Since it has already been suggested previously that the quartz and baryte must have formed at a higher temperature than the calcite, this temperature must also represent the minimum temperature for quartz and baryte deposition. The fact that the apparent equilibration temperature for the quartz and baryte is lower than this temperature can be attributed to the effect of minor oxygen isotope exchange between the baryte and the fluid which precipitated the calcite.

Thus it can be concluded from this discussion that

1. If it is assumed that the quartz and baryte formed at the same or higher temperature than the calcite, then all the vein minerals must have formed in the temperature range 210-300°C.

2. The fact that the quartz and baryte yield an apparent equilibration temperature lower than 210°C can be attributed to the baryte having exchanged oxygen isotopes to some extent with the fluid that deposited the calcite.

3. The fluid which deposited the quartz and baryte must have had a $\delta^{18}O$ value between -0.6 and +3.5‰, if these minerals formed between 210-300°C. This fluid must have contained a component of a surface derived fluid.

4. The later calcite must have been formed from a fluid with a $\delta^{18}O$ distinctly (~3.7 to 3.9‰) lower than that which formed the quartz and baryte with a $\delta^{18}O$ of -4.3 to -0.4‰. This fluid almost certainly contained a component of meteoric water.

5. From conclusions 3. and 4. it can be concluded that the $\delta^{18}O$ of the fluid in the vein must have fallen with time. It is suggested here that this may have been due to an increase in the meteoric water component in this fluid.

The interpretation given above was made by assuming that the fluid fractionated oxygen isotopes in the same way as pure water. It has already been shown from the hydrogen isotope data (6.3.2) that the fluid was saline and therefore these conclusions may have to be modified somewhat, depending on what effect the salts in the fluid had on the oxygen isotope fractionation behaviour of the fluid. Following the same arguments that were presented in 6.4.2, it is suggested that the most extreme salt effects possible for this fluid might be approximated by the salt effect produced by a 4m NaCl solution. The $\delta^{18}O$ curves for the fluid in equilibrium with the minerals in the vein when the fluid is a 4m NaCl solution, are shown in fig. 6.11.

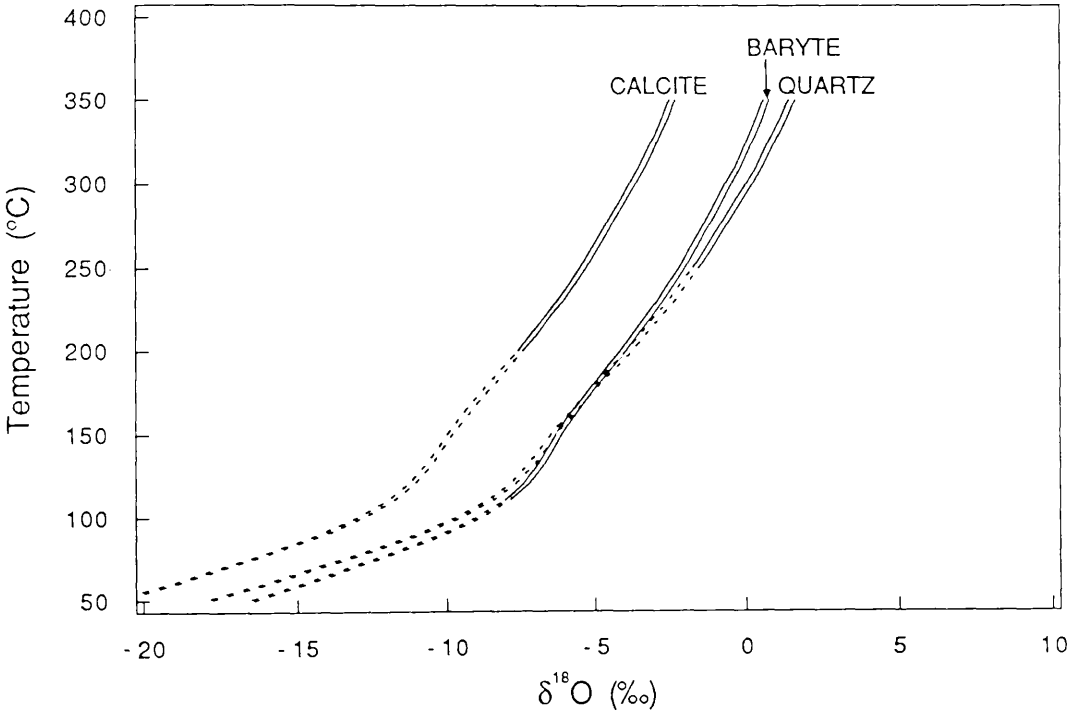

Fig. 6.11 Estimated $\delta^{18}O$ of the fluid in equilibrium with the minerals in the vein in GJ.196 as a function of equilibration temperature, assuming that the fluid fractionates oxygen isotopes in the same way as a 4m NaCl solution. Each pair of curves correspond to the uncertainty resulting from the uncertainty in the oxygen isotope analysis. The curves are dashed where they are projected below their experimentally calibrated range. The curves were derived by adding the 4m NaCl solution-water fractionation curve of Truesdell (1974) to the curves shown in fig. 6.10.

It can be seen from fig. 6.11 that the baryte and quartz curves still intersect on this diagram at 166°C, defining an apparent equilibration temperature. This is because mineral-mineral fractionations are independent of fluid salinity. Furthermore, comparison of figs. 6.9 and 6.10 shows that the differences in the $\delta^{18}O$ values between the curves at the same temperature are the same in each diagram. Thus, using the same arguments that are given above, it can be seen that the calcite must have formed from a fluid with a distinctly lower $\delta^{18}O$ value than the quartz and baryte, regardless of

the magnitude of any oxygen isotope salt effect. It can be seen, however, that the absolute $\delta^{18}O$ values of the fluid in equilibrium with the minerals in the vein would be much lower if the fluid fractionated oxygen isotopes like a 4m NaCl solution. Thus if the calcite formed at 300°C from such a fluid, the fluid would have had a $\delta^{18}O$ of -3.7‰ (compare with -0.4‰ in fig. 6.10). Even if the calcite was formed at 350°C from a 4m NaCl solution it would still have been deposited from a fluid with a negative $\delta^{18}O$ (-2.3‰). Thus if salt effects were anything like those produced by a 4m NaCl solution, the fluid would have such a negative $\delta^{18}O$ value that it could only have originated from a meteoric source. Following the same reasoning that was applied above, the minimum temperature at which the calcite was deposited can be estimated by assuming that the fluid had a $\delta^{18}O$ of -4.3‰. A temperature of ~280°C is estimated if the fluid behaved like a 4m NaCl solution, so that in this case the temperature of calcite formation may be constrained within 20°C.

Obviously the temperatures of mineral formation and the $\delta^{18}O$ values of the fluid that deposited the minerals in this vein cannot be estimated exactly from the oxygen isotope data alone. Nevertheless, if the fractionation behaviour of the fluid that deposited these minerals was somewhere between that of a pure water fluid and a 4m NaCl solution, then the minimum temperature of vein formation and the maximum fluid $\delta^{18}O$ are constrained to be ~210°C and +3.5‰ respectively. It can be seen that estimation of fluid salinity and mineral deposition temperatures, by fluid inclusion studies, would greatly facilitate the interpretation of this data.

6.5 SULPHUR ISOTOPE DATA FOR A VEIN BARYTE.

The $\delta^{34}S$ value of baryte from a vein infill in a fault cutting the MGS (1.4.3, 6.4.3) was found to be +12.6‰(CDT). Since there is no sulphur isotope fractionation effect during sulphate precipitation (2.8.3), this value will be the same as that of the sulphate in the fluid which deposited the baryte.

It has previously been suggested from the oxygen and hydrogen isotope data, that the minerals in this vein were deposited from a surface derived fluid (6.4.3), most probably a meteoric fluid. A $\delta^{34}S$ value of +12.6‰ is extremely low for a sulphate precipitated from a seawater source. If the fluid in this vein was seawater derived, and no sulphur was added to this fluid from any other source, it can be seen from fig. 2.20 that the only time at which this baryte could have been deposited was ~210-220 Ma, during the Rhaetic. It should be noted that this is the timing of the Glengowla mineralisation in E. Connemara (1.3.6). The surface waters during the Rhaetic were evaporated marine waters in a sabkha environment (fig. 2.20, A.6). The $\delta^{18}O$ of the fluid which precipitated the quartz and baryte (-0.6 to +3.5‰, 6.4.3) could be consistent with an evaporated marine source (e.g Pierre *et al.*, 1984) for the fluid in this vein. The δD value of the fluid which deposited this vein (≈-25‰?) might also be consistent with an evaporated marine origin, although the seawater would have had to have been very strongly evaporated to to produce such negative δD values (Sofer and Gat,

1975). However the calcite, which was deposited very soon after the quartz and baryte in this vein, must have been deposited from a meteoric source, if the fluid was at all saline (6.4.3). The $\delta^{18}O$ of this meteoric water, prior to any isotopic exchange with rocks, has been estimated from the δD value of the fluid inclusions in the calcite to be ~-4.3‰ (6.4.3). Using this value with Dansgaard's (1964) relationship between the $\delta^{18}O$ of meteoric water and air temperature, indicates that the mean annual air temperature at the meteoric water source may have been in the region of 13°C. This is well below the temperature required for evaporite deposition, indicating that the baryte could not have been deposited from evaporated seawater during the Rhaetic.

If, as is likely, the baryte was deposited from a meteoric derived fluid, then the sulphur in the fluid, like the carbon (6.6), must have been incorporated into the fluid from the rocks that it passed through on its journey from the surface. The $\delta^{34}S$ of the aqueous sulphate, produced by reaction of meteoric water with the sulphides in the exposed rocks, would depend in detail on the mechanism of the reaction. The highly oxidising nature of meteoric fluids suggests that the sulphides would probably have been oxidised, in which case the $\delta^{34}S$ value of the sulphate produced would have been lower than that of the initial sulphides (2.8.3). If this was the case, the $\delta^{34}S$ value of +12.6 for this baryte could reflect derivation of the sulphur from the presently exposed rocks. Most of the sulphur would have to be derived from the Dalradian metasediments ($\delta^{34}S$ = +10 to +20‰?, 2.9.7), but some could also have been derived from the MGS ($\delta^{34}S$ = 0 to +10‰?, 2.9.7). A source of sulphur external to the presently exposed rocks in the Cashel-Recess district is not required.

6.6 OXYGEN AND CARBON ISOTOPE DATA FOR CALCITE FROM THE MGS AND THE ROUNDSTONE GRANITE.

The $\delta^{13}C$ and $\delta^{18}O$ values of all the calcites analysed in this study are plotted against one another in fig. 6.12.

These calcites all come from rocks which have undergone retrograde hydration as the result of infiltration of a high δD fluid. The calcite in these samples is texturally associated with other alteration minerals (sericite, chlorite), and it is assumed here that these calcites were all formed during the retrograde hydration of these rocks. The analysed samples include:

a. two calcite separates from MGS rocks (GJ.060. GJ.035).

b. late vein calcite filling a fault which cuts the MGS (GJ.196, cf. 6.4.3).

c. three calcite bearing separates of slightly differing density from one sample of the Roundstone granite (GJ.003, cf. 6.4.2).

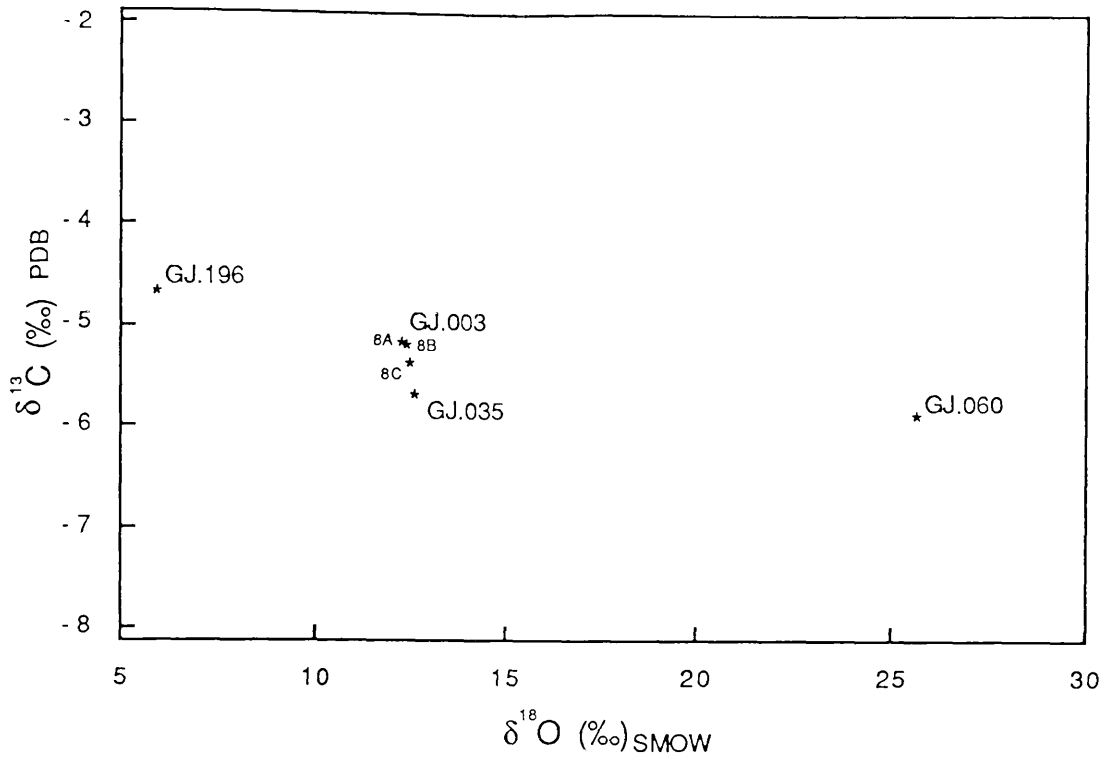

Fig. 6.12 $\delta^{18}O$ plotted against $\delta^{13}C$ for calcites from the MGS and the Roundstone granite.

It can be seen that these calcites have a very restricted range of $\delta^{13}C$ values of ~1.2‰, whereas the range in $\delta^{18}O$ values of ~19.7‰ is extremely large. There is a slight inverse correlation between the two variables, so that the most ^{18}O rich sample is also the most ^{13}C depleted. Thus the samples do not exhibit a polythermal trend (Valley, 1986) which would be the result of the equilibration of the calcites at different temperatures with a fluid with the same $\delta^{13}C$ and $\delta^{18}O$ values (Rye and Williams, 1981).

The large variation in $\delta^{18}O$ values between samples could be explained as the result of either (fig. 6.13):

a. equilibration with fluids with the same $\delta^{18}O$ at different temperatures.

b. equilibration with fluids with differing $\delta^{18}O$ at the same temperature

c. equilibration with fluids with differing $\delta^{18}O$ at different temperatures.

It has already been shown that the calcites in GJ.196 and GJ.003 must have both equilibrated with ^{18}O depleted (probably meteoric derived) fluids, and that these samples must have equilibrated oxygen isotopes with these fluids at different temperatures (6.4.2, 6.4.3). Thus the difference in the $\delta^{18}O$ values of the calcites between these two samples can be explained as the result of equilibration with fluids with similar $\delta^{18}O$ values (0 to -4‰) and salinities in fluid dominated systems at different temperatures (>210°C in GJ.196 and < 200°C in GJ.003). The similarity of the $\delta^{18}O$ values of the calcites in GJ.003 and GJ.035 suggests that the oxygen isotope composition of GJ.035 may also

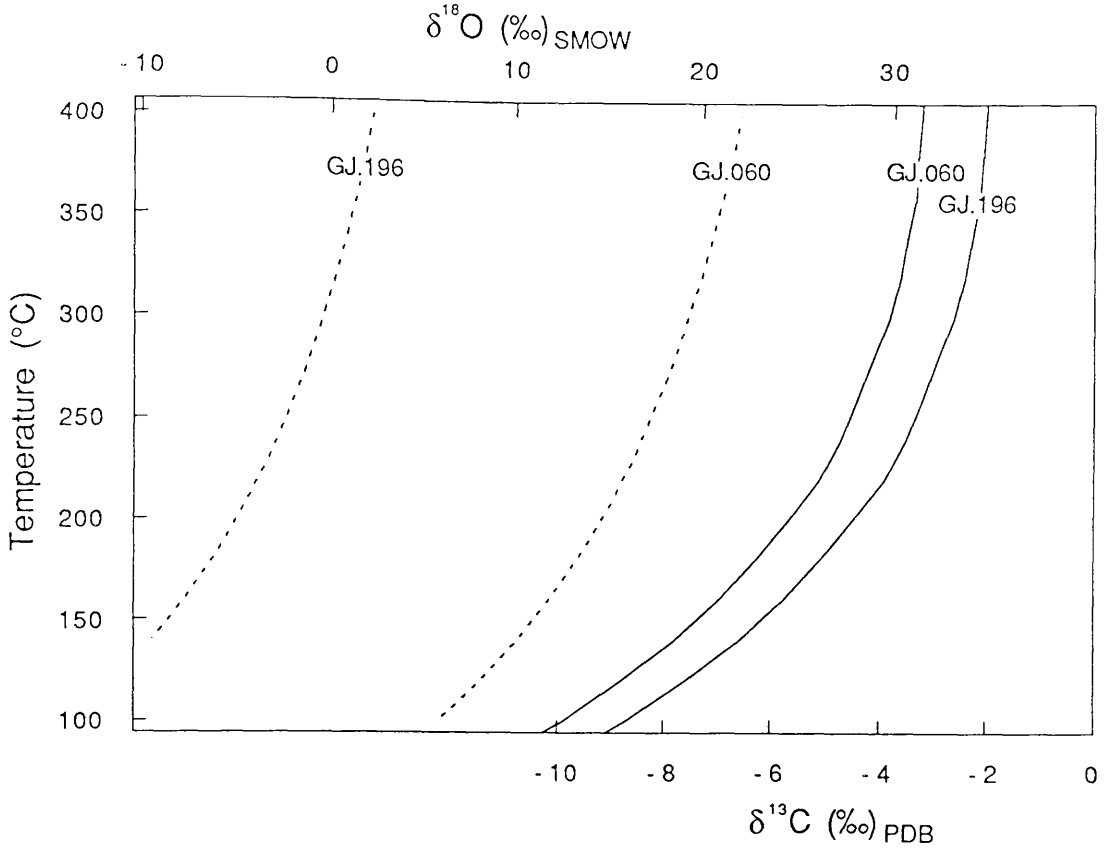

Fig. 6.13 Calculated $\delta^{13}C$ (bottom scale, solid curves) and $\delta^{18}O$ (top scale, dashed curves) of the fluid in equilibrium with the calcites with the highest and lowest $\delta^{13}C$ and $\delta^{18}O$ values measured, shown as a function of equilibration temperature. The fluid $\delta^{18}O$ values were calculated assuming that the fluid fractionated in the same way as pure water (and therefore that the presence of carbonate species in the fluid did not affect the fractionation behaviour), using the modified calcite-water fractionation based on the data of O'Neil, Clayton and Mayeda (1969), see A.4.2. The fluid $\delta^{13}C$ values were calculated using the assumption that all the carbon in the fluid is present as carbonate ($H_2CO_3^*$), since little or no CH_4 was indicated by the volatile analyses of the fluid inclusions. The $\delta^{13}C$ value of the carbonate in the fluid is assumed to be very close to that of gaseous CO_2 at the same temperature (Ohmoto, 1972) so that the calcite-fluid fractionation can be approximated by the calcite-CO_2 fractionation. The calcite-CO_2 fractionation data of Bottinga (1969) was used.

have resulted from equilibration with a low ^{18}O fluid to low temperatures. If the high $\delta^{18}O$ of the calcite in GJ.060 is also to be explained in this way, then this calcite would have to have equilibrated oxygen isotopes with a pure water fluid with a $\delta^{18}O$ of ~0‰, down to ~60°C (using the modified calcite-water fractionation - see A.4.2). Such a temperature may seem unreasonably low for calcite equilibration, although it should be noted that equilibration does take place at such low temperatures in diagenetic environments (Veizer, 1983). However this is the maximum temperature required, because this calculation makes the assumption that fluid/rock ratios were infinite. It is likely however that the $\delta^{18}O$ values in this rock were never as low as in GJ.196 or GJ.003 since the epidote in this rock indicates fluid $\delta^{18}O$ values of ~+5‰ for a pure water fluid at 300°C (fig. 4.23) and the chlorite ($\delta^{18}O$ = +4.3‰) indicates that the fluid was ~+3‰ during chlorite formation. If the $\delta^{18}O$ of the fluid infiltrating this rock did not

change from ~+5‰ during cooling the calcite need only have equilibrated oxygen isotopes with this fluid down to temperatures of ~100°C. However, it was noted in 4.3.3 that the epidote in this rock stopped equilibrating hydrogen isotopes at ~190°C. This apparent closure temperature for the epidote could either represent:

a. The actual closure temperature of the epidote as a result of the decrease in the diffusivity of hydrogen in the epidote.

or

b. The temperature at which the volume of the fluid, within, or moving through the rock ceased to be large enough to cause a significant change in epidote δD with further equilibration.

This second case is considered to be the more likely, because other MGS epidotes in veins nearby appear to have exchanged hydrogen isotopes down to lower temperatures and there is only a poor relationship between grain size and δD which would support the first possibility (4.3.3). If the second possibility were the case, then there could not have been sufficient quantities of water present in this rock below ~190°C to exchange with the calcite. If the calcite in this rock last equilibrated with a fluid at 190°C, then the minimum fluid $\delta^{18}O$ that would be required would be ~+13‰ if fluid/rock oxygen ratios were infinite. Such a $\delta^{18}O$ value is higher than nearly all of the fluid $\delta^{18}O$ values estimated in this thesis and there is no apparent reason why the $\delta^{18}O$ of the fluid should have increased to such a high value after fluid with a $\delta^{18}O$ of +3 to +5‰ had been present in this rock (cf. discussion in fig. 6.8). Thus this hypothesis is considered unlikely and at present the high $\delta^{18}O$ of this calcite has to remain unexplained. It is only a remote possibility that this calcite could have derived its high $\delta^{18}O$ value during very low temperature exchange with present day meteoric water during minor weathering of this rock.

In contrast to the $\delta^{18}O$ data for these calcites, the homogeneity in $\delta^{13}C$ values of these calcites can only be explained as the result of either:

a. equilibration with fluids with approximately the same $\delta^{13}C$ at approximately the same temperature.

b. equilibration with fluids with varying $\delta^{13}C$ over a range of temperature, with the fluid becoming more negative with decreasing temperature.

Examination of fig. 6.13 shows that if the fluids with which the calcites equilibrated carbon isotopes had exactly the same $\delta^{13}C$ value, then because of the steepness of the fluid curves, the calcites could still have equilibrated carbon isotopes over a temperature range of as much as 100°C, if equilibration took place at temperatures >250°C. However if the fluid $\delta^{13}C$ varied by only 1.2‰ between samples, then the calcites could have equilibrated carbon isotopes at exactly the same temperature. It can also be seen from fig. 6.13 that, even if the calcites equilibrated carbon isotopes between ~350°C and 150°C, the maximum $\delta^{13}C$ difference between the the fluids that equilibrated with the two calcites with the most extreme $\delta^{13}C$

values is still only ~5‰. Thus the carbon isotope data indicate that the fluids with which the calcites equilibrated with must have had fairly similar values.

The oxygen isotope data may provide some information on the range of carbon isotope equilibration temperatures, since it has already been shown that oxygen isotopes equilibrated at varying temperatures from >210°C (GJ.196) to <180°C (GJ.003, GJ.035) and possibly down to very low temperatures (GJ.060). However these calcites probably did not form over this temperature range. It is considered much more likely that the calcites formed synchronously with the other alteration minerals in these rocks at temperatures near to 300°C. Thus the lower oxygen isotope equilibration temperatures given above are probably temperatures at which oxygen isotope re-equilibration ceased. Whether or not the calcites would have equilibrated carbon isotopes with the fluid to the same temperature as they equilibrated oxygen, is dependent on the mechanism by which stable isotope exchange took place.

There are no kinetic data available on the rate of carbon isotope exchange between calcite and fluid during solution-reprecipitation, but it might be expected that it would be similar to that of the oxygen isotope exchange. Thus if exchange took place by a solution reprecipitation process, the carbon isotopes in the calcites might be expected to have equilibrated with the fluid present to approximately the same temperatures as the oxygen isotopes. If this was the case, the $\delta^{13}C$ of the fluid with which the calcites equilibrated carbon isotopes at lower temperatures would have had to have been lower (fig. 6.13). The minimum difference in $\delta^{13}C$ required between GJ.196 and GJ.003 is only ~1‰, but much larger differences might be required for the fluid in GJ.060, depending on what temperature this calcite equilibrated down to. There is no apparent reason why the $\delta^{13}C$ values of the fluid present in different rocks should have been lower at lower temperatures. Possibly the fluid $\delta^{13}C$ values could have differed between different samples, because they came from different rock types, while the correlation of fluid $\delta^{13}C$ value with equilibration temperature that would be necessary, could be merely coincidental. This is considered to be unlikely, so that this model in which carbon equilibration took place at different temperatures is not preferred.

The limited high temperature kinetic data for oxygen and carbon diffusion in calcite (Kronenberg *et al.*, 1984) suggests that at low temperatures the diffusion of oxygen in calcite might be at least two, and possibly many more orders of magnitude faster than the diffusion of carbon. Therefore if the calcites exchanged oxygen isotopes after formation by diffusion, the $\delta^{13}C$ values of the calcites would be unlikely to have been affected by this process. If this was the case, the $\delta^{13}C$ values of the calcites would reflect the $\delta^{13}C$ of the fluid that the calcite formed from, and the homogeneity in calcite $\delta^{13}C$ values would indicate that all the calcites formed from fluids with very similar $\delta^{13}C$ values (~-4‰) if they formed at ~300°C.

Possibly $\delta^{13}C$ measurements on the CO_2 contained in the fluid inclusions in these rocks could indicate whether or not the fluid $\delta^{13}C$ value varied between samples. However this would be difficult analytically because of the small CO_2 contents of the fluid. Without this information, it can be suggested that the $\delta^{13}C$ value of the fluids depositing these calcites may have been very similar (diffusion controlled oxygen exchange), although it is not possible to exclude the possibility that the $\delta^{13}C$ values of the fluids varied with temperature.

The $\delta^{13}C$ values of the calcites are not diagnostic of the source of the carbon. A value of ~-5‰ is similar to the value estimated for mantle carbon (2.9.6). Thus the carbon could have been derived from the igneous rocks containing the calcites, provided the carbon isotope fractionation between the igneous carbon (in whatever form) and the calcites was not too large. For example, Stakes and O'Neil (1982) suggests that vein calcites with a $\delta^{13}C$ of ~-4‰ in altered rocks from mid-ocean ridges, contain carbon which is principally of magmatic origin. However the $\delta^{13}C$ values of the marbles in the Lakes Marble Formation and the other marble formations may well be rather lower than the average value of marine carbonates (~+1‰, 2.9.6) if decarbonation reactions have taken place within them. Thus carbon in the fluid with a $\delta^{13}C$ value of ~-4‰ might also have been derived from dissolution of some of the marble formations.

It is clear from the oxygen isotope data, that the fluid which deposited the calcite in GJ.196 must have been of meteoric origin and the same is probably true of the fluid which deposited the calcite in GJ.003. If this was the case for all the fluid which deposited calcites, then the carbon in these calcites must have been added to the fluid on the journey between the source and the present rocks. This is because meteoric waters contain only small amounts of carbon (average river water $\approx 1 \times 10^{-3}$ M carbon, maximum $\approx 5 \times 10^{-3}$ M; Livingstone, 1963), while the fluid in the fluid inclusions, which is presumed to be that which deposited the calcite, contains much more carbon (~1-2 mole % $CO_2 \approx$ 0.5-1 M carbon; 6.3.1, 4.4.1). Thus provided the fluid did not pass through any other rock types during its journey from the source, it would be reasonable to conclude that the carbon in the calcites must have been derived from the enclosing magmatic rocks. However, this may not have been the case, since magmatic rocks also contain low carbon contents. According to Hoefs (1978) granitic and basic igneous rocks contain between 200 and 1100 ppm CO_2 and between 110 and 270 ppm of elemental carbon, which translate to maximum and minimum carbon molarities of $1.4\text{-}4.8 \times 10^{-2}$ M. These values may be maxima, because much of the carbonate carbon in the rocks analysed by Hoefs (*ibid.*) may be secondary and derived from an external source. Because of the low carbon content of magmatic rocks, each weight of fluid would have had to have scavenged the carbon (presumably by breakdown of minerals containing trace carbonate and oxidation of reduced carbon) from ~10-100 weights of rock to attain its present carbon content. The relatively unshifted oxygen isotope values inferred for the fluid which deposited some of these calcites, suggests that the rock/fluid oxygen ratios for a mass of fluid must have been much lower than this. This would tend to indicate that the carbon could not have been derived solely from the magmatic rocks and that the fluid must have

derived its carbon from a more carbon rich source, possibly the marble units in the Dalradian (or possibly an overlying sedimentary basin??).

It might be possible to test whether or not the carbon in secondary carbonates in the rocks at the present level, was derived from within these rock units, or from a more distant source by measuring the $\delta^{13}C$ values of carbonates associated with the late alteration in the metasediments. The carbon in the pelitic rocks (away from the marble horizons) may well have had a significantly lower $\delta^{13}C$ value than the carbon in the magmatic rocks. This would be reflected in the $\delta^{13}C$ of the alteration carbonate, if the carbon was locally derived.

6.7 THE ORIGIN OF THE HIGH δD FLUID CAUSING ALTERATION IN THE GRANITES.

From the data presented in the previous sections, the following features of the fluid which caused the retrograde hydration in the Galway and Roundstone granites have been inferred:

1. The fluid had a high δD of ~-20 to -25‰ (6.2.3, 6.3.2).
2. The highest temperature at which the fluid was present in these rocks was probably not much greater than ~300°C (6.3.2). In some rocks the fluid was present down to temperatures <180°C, probably in large quantities.
3. The fluid was very homogeneous in $H_2O/(H_2O+CO_2)$ ratio (0.982-0.987) in both granites (6.3.1).
4. The fluid was saline to some extent (6.3.2).
5. The fluid was not pervasively present in the granites, but must have been channelised (6.4.1).
6. The fluid had very low $\delta^{18}O$ values, between +3 and -5‰, depending on salt effects and equilibration temperatures (6.4.2).

There are two major possibilities for the origin of this high δD fluid. Either it could have been produced internally within these granite bodies, as a result of fluid phase exsolution during crystallisation (i.e. it was "deuteric"), or alternatively, it could have infiltrated into these granites from an external source.

It is clear, from the association of the more altered granite samples with the areas of most intense bubble plane and microcrack development, that the fluid which caused this alteration was locally infiltrative. However this fluid could merely have been derived from other parts of the granites, so that this textural evidence of infiltration does indicate that this fluid was externally derived.

The presence of miarolitic cavities in some samples of the Roundstone granite (1.4.3) indicates that fluid phase exsolution may have taken place within this granite (e.g. see Cox, Bell and Pankhurst, 1979). The effects of

fluid exsolution on the oxygen and hydrogen isotope ratios of minerals in granitic bodies have been described by Nabelek *et al.* (1983) and Brigham and O'Neil (1985). These authors show that the chlorite produced by reaction of exsolved fluid with primary biotite is D enriched (by ~20‰) and ^{18}O depleted (by ~2.5‰), relative to the unaltered biotite. Thus the δD and $\delta^{18}O$ values of the chlorites in the Roundstone granite would not be inconsistent with the chlorite having developed as a result of interaction with a deuteric fluid.

However three lines of evidence suggest that such a fluid produced during crystallisation of the granites could not have caused the alteration in these granites.

1. Because vapour phase exsolution takes place during crystallisation of the granites, the fluid produced by this process would have initially been present in these rocks at high temperatures (>600°C). There is no evidence from the samples examined in this project that the fluid causing alteration was present at such high temperatures. The upper temperature limit for the presence of this fluid in these rocks was estimated to be ~300°C (6.2.3). Measurement of fluid inclusion filling temperatures from altered rocks may be used to confirm this estimate in the future. Furthermore the oxygen isotope data indicate that this fluid must have passed through some samples in the Roundstone granite in fairly large quantities down to temperatures <200°C. Such low temperatures would be inconsistent with a fluid originating from a crystallising melt at temperatures >650°C, unless the fluid had been channeled into these rocks from much greater depths.

2. The homogeneity of the fluid δD values and $H_2O/(H_2O+CO_2)$ ratios (fig. 6.5), not only in samples from the same granite, but from samples from two different granite bodies, is not what would be expected if this fluid had been produced by exsolution from a melt. If the fluid had been produced in this manner, then the δD of the fluid would have decreased as as fluid was progressively exsolved (Nabelek *et al.*, 1983), while the $H_2O/(H_2O+CO_2)$ ratio would have increased (Burnham, 1969, p.72), so that these two ratios would be expected to be variable and negatively correlated.

3. Nabelek *et al.* (1983) estimate that the <u>maximum</u> δD of the fluid produced by an exsolution process would be ~20‰ heavier than the initial δD of the melt. Thus fluid with a δD value of ~-20‰ could only have been produced if the Galway granite melts had a δD of -40‰, which is higher than the range thought to be normal for granitic melts.

Thus an internal origin for the high δD fluid in the Galway granites is considered to be highly unlikely and it is concluded that this fluid must have originated from a source external to the granites (i.e. exotic).

The high δD and low $\delta^{18}O$ values estimated for this exotic fluid indicate that this fluid must have contained a surface derived component (fig. 2.19).

Other features of this fluid that are consistent with it originating from a surface derived source include:

1. The homogeneity in fluid δD over a wide area, in two different granite bodies.

2. The continued supply of large volumes of this fluid to some of these rocks down to very low temperatures. No other source can be envisaged which could have produced large quantities of fluid at such low temperatures.

The homogeneity in δD values of this fluid, indicate that the δD of this fluid has probably not been greatly altered by fluid/rock interaction, as would be expected. Thus the δD value of ~-20 to -25‰ for this fluid must indicate that it was of meteoric origin, unless the seawater δD was significantly less than 0‰ at that time. The very low $\delta^{18}O$ value (~0‰) estimated for the fluid in equilibrium with one of the chlorites (GJ.003), even when salt effect were not taken into account (6.4.2), is consistent with this hypothesis. This is because the fluid $\delta^{18}O$ values could only have become ^{18}O enriched during fluid/rock interaction and therefore the fluid $\delta^{18}O$ must have been less than or equal to 0‰ prior to any exchange with rock. The fact that meteoric fluid has unequivocally been identified as the source of the fluid which deposited calcite in the late fault cutting the MGS (GJ.196), indicates that meteoric fluid was present in the country rocks at a late stage in the history of this area, supporting this hypothesis.

6.8 THE ORIGIN OF THE HIGH δD FLUID IN S.W. CONNEMARA.

In 4.7.5 it was suggested that the high δD fluid which caused chlorite/epidote/sericite formation in the Cashel-Recess area could have originated from a surface source and that if this was the case, it could well have been brought down into these rocks by convection around the Galway granites. In 6.1, it was noted that if the fluid causing the alteration within the Galway granites could be shown to be similar to that which caused the alteration in the rocks surrounding these granites, then this would provide very strong support for such an origin for this fluid. Comparison of the features of the fluid causing the alteration within the Cashel-Recess district (4.7.1), with those for the fluid causing alteration in the Galway granites (6.7) shows that these fluids are indeed very similar, in that they both:

a. had distinctive high δD values of ~-25‰.

b. had $\delta^{18}O$ values that were variable, but always lower than that which was in equilibrium with these rocks at high temperatures.

c. had very similar $H_2O/(H_2O+CO_2)$ ratios of 0.98-0.987.

d. were present in these rocks between temperatures of 300°C and 180°C (or even less).

e. can be shown to have been derived from a source external to the rock units in which they have been identified.

With all of these features in common, it is considered logical to conclude that these fluids identified in these different rocks had the same origin, from a common (meteoric - see 6.7) source. This being the case, the time at which this fluid infiltrated the rocks in the Cashel-Recess area can be constrained to be post 400 Ma (the age of the Galway granites), and the possibility of a thrusting related origin for the fluid in the Cashel-Recess area can be eliminated.

In 5.4 it was suggested that the late high δD fluid identified in the Delaney Dome area could be correlated with the high δD fluid identified in the Cashel-Recess district. If this correlation is correct, then it can be concluded that the late high δD fluid in the Delaney Dome area was also derived from a meteoric source after 400 Ma. Thus it can be inferred that meteoric water may have infiltrated the whole of S.W. Connemara after the intrusion of the Galway granites.

In 6.4.2. it was shown that one of the effects of meteoric water infiltration into the Roundstone granite was to variably enrich the feldspars in ^{18}O, by equilibration with this fluid down to low temperatures. Since it is now suggested that this same fluid was also present in the MGS, and it has already been shown from the hydrogen isotope data that this fluid was present down to low temperatures (4.3.3), it would be predicted that such ^{18}O enrichment should also be seen in MGS feldspars. That this is actually the case is demonstrated by the oxygen isotope data for mineral separates from the acid (K-feldspar) gneisses presented by Jagger (1985, p.244). Hydrogen isotope data on the biotite-chlorite separates from these rocks (J.57, J.61,J.86,J.87) has already shown that this meteoric fluid was present in all of these rocks during chloritisation (4.2, 4.3.3). In one of the samples analysed by Jagger the quartz - K-feldspar fractionation is negative, while in another sample the fractionation is <0.6‰, indicating that the K-feldspars in these rocks have been ^{18}O enriched. However it is noted that in the other two samples which Jagger analysed the quartz - K-feldspar fractionations are greater than would be expected if the phases had preserved a high temperature equilibrium. This ^{18}O depletion in the K-feldspars is interpreted as the result of equilibration with the meteoric fluid at higher temperatures than the other K-feldspars (as was predicted would be the case in 6.4.2). The fact that these K-feldspars did not subsequently re-equilibrate with the meteoric fluid at lower temperatures suggests that the fluid supply to these rocks ceased at higher temperatures than in the other rocks which show ^{18}O enrichments. It is notable that Jagger's sample which exhibits the most ^{18}O enrichment in the K-feldspar (J.57) is located very near to the same fault from which sample GJ.196 was obtained (map. 1). This suggests that the fault may have remained an aquifer, supplying fluid to the surrounding rocks, down to low temperatures.

The only plausible mechanism by which meteoric fluid could have been brought down into these rocks is by convective circulation (4.7.5). The Galway granite intrusions must have represented localised heat sources, both during intrusion and after (Feely and Madden, 1987) and could

therefore have provided the thermal gradients necessary to initiate pore fluid convection. Because of this, it is considered most likely that the high δD fluid was infiltrated into the rocks of S.W. Connemara as the result of convection around, and through the Galway granites after intrusion.

The recognition that meteoric fluid with a relatively unshifted $\delta^{18}O$ value deposited the calcite in the fault cutting the MGS suggests that this fault and other lineaments may have acted as the major conduits through which the meteoric fluid was carried down into the presently exposed rocks (c.f. Kerrich *et al.*, 1984). As well as the low $\delta^{18}O$ value inferred for the fluid that deposited this calcite, the presence of the calcite itself in this fault also tends to indicate that this structure was a zone of downward fluid flow. This is because the retrograde solubility of calcite means that calcite is much more likely to be deposited from solutions moving up temperature (i.e. downwards) than solutions that are moving down temperature (upwards) if all other factors remained constant (Holland, 1967).

The association of the alteration in both the granites and the Cashel-Recess area with microcracks and bubble planes suggests that these structures were the conduits by which the meteoric fluid moved into rock masses between major lineaments. Presumably fluid movement could have taken place along grain boundaries over the smaller distances between microcracks (<<1 metre?).

Yardley (1987, pers. comm.) has suggested that the apparently greater degree of alteration within the MGS rocks compared with the Galway granites, might be inconsistent with the hypothesis that convection was centred on the Galway granites. Results from this study indicate that the rocks from the MGS are indeed more altered than the granites. Out of the 21 samples from the MGS in the Cashel-Recess area that were isotopically analysed, only two do not appear to have been exposed to the high δD fluid (fig. 4.7), while out of the 16 samples from the granites that were isotopically analysed, only 9 show the effects of interaction with the high δD fluid. However this does not necessarily indicate that convection was not centred on the Galway granites. For example, Norton and Knight (1977) and Norton and Taylor (1979) have shown, using numerical methods, that fluid convection associated with an intrusive body will initially be confined to the surrounding rocks and that the convective system does not "collapse" into the pluton until crystallisation has ceased. This is primarily the effect of the low permeability of rocks at high temperatures during and just after crystallisation. Thus if convection took place during crystallisation, the effect of this would be that the integrated fluid flux experienced by the country rocks would be expected to be higher than the flux experienced by the intrusion. Thus the country rocks might be expected to be more altered than the the granites[1] . The formation of an impermeable carapace of hornfelsed rocks around the granites, during intrusion would further

[1] The greater degree of alteration observed in the Oughterard granite (1.3.4) compared to the Galway granites might be a reflection of this, because if, as is thought likely, this granite was intruded before the other granites, it would have been altered by fluids within the circulation system around the Galway granite.

restrict the access of fluids to the granites. The non pervasive, possibly joint related nature of the alteration within the Roundstone granite, indicates that the high δD fluid probably did not gain access to this body until fracturing had taken place, which would be consistent with the hypothesis outlined above.

An alternative explanation of the apparent greater degree of alteration of the rocks around the granites might be that the granites may in fact be more altered than they appear, but the more altered zones (possibly around faults and joints - see above) have been preferentially weathered and are not seen. The more altered nature of the MGS rocks might also be partly the result of their different mineralogies, with the calcic plagioclase in the MGS being more reactive with a meteoric fluid than the sodic plagioclase in the granites.

Apart from the fact that infiltration of meteoric water into the rocks of S.W. Connemara must have taken place post 400 Ma, the timing of infiltration is not well constrained. The thermal gradient, and therefore the potential for fluid convection (2.7.6), may well have been highest at the time that the granites were intruded. Therefore it might be suggested that fluid convection occurred soon after granite intrusion at 400 Ma. Convection can also be facilitated by the presence of a strong horizontal thermal gradient. However Ferguson and Al-Ameen (1985) suggest that the thermal gradient around the Omey granite at the time of intrusion was very shallow (a temperature distribution which they somehow, erroneously, attribute to the effects of fluid convection).

Some support for convection taking place soon after granite intrusion might come from the sphene FT ages of ~390-380 Ma for the Roundstone and Galway granites (1.3.7). Because the sphene FT closure temperature is likely to have been ~300°C at the most (Faure, 1986, fig. 20.2) these dates indicate that these samples have not been heated above that temperature since that time. Therefore if the temperature at which the high δD fluid was present in the granites <u>was</u> any greater than 300°C the temperature at which fluid was present in the granite could be constrained to be soon after granite intrusion. Unfortunately the estimate of the upper temperature at which this fluid was present in the granites is rather uncertain, although it is hoped that better estimates will soon be obtained from fluid inclusion filling temperatures.

There are two lines of evidence which indicate that meteoric fluid infiltration could have taken place at a much later date. The first is that the U. Carboniferous dikes identified by Mitchell and Mohr (1987) also show the effects of fluid infiltration. The second is the mostly young (ranging from 399 to 253 Ma) apparent K-Ar ages obtained by Mitchell and Mohr (*ibid.*) from variably altered biotite-chlorite fractions from the Galway granite. Data from both naturally and experimentally chloritised biotites indicate that the process of chloritisation of biotite does not dramatically change the apparent K-Ar age (Criss *et al.*, 1982; Kulp and Engels, 1963). Therefore the low K-Ar ages in most of the biotite-chlorite fractions examined by Mitchell and Mohr (*ibid.*) cannot be attributed to the effects of ~400 Ma chloritisation enhancing the rate of later Ar loss in these biotites, but must reflect heating above the

biotite K-Ar closure temperature (250-300±50°C; Dodson, 1973) as late as 250 Ma. This conclusion directly conflicts with the sphene FT data. Thus the sphene data may not necessarily be accurate and constrain the timing of fluid infiltration. One of the biotite-chlorite fractions analysed by Mitchell and Mohr comes from an outcrop less than 800 m away from the location of GJ.213 and has an apparent K-Ar age of 332 Ma, indicating that the alteration in GJ.213 could easily have taken place at 300°C as late as 330 Ma.

If it is assumed that the δD value of the fluid which caused the alteration at the present level is the same as that of the meteoric water source, then the timing of fluid infiltration can be constrained to those periods when meteoric fluids for the Connemara massif were estimated to be ~-25 to -20‰. Examination of fig. 2.20 shows that meteoric waters of the appropriate isotopic composition were present at the surface both at ~420-390 Ma and 330-300 Ma. Thus the δD data would be consistent with fluid infiltration either just after intrusion, or at this later time.

It is envisaged that fluid convection a significant time after intrusion could have resulted from a combination of

a. re-heating of the granites as a result of indigenous heat generation, perhaps coupled with burial beneath a thick cover (e.g during the Carboniferous?).

followed by

b. a phase of rapid tensional uplift which opened fractures and joints in the granites and country rocks and allowed ingress of surface derived fluids.

That fluid convection can take place within a granite and surrounding country rocks a long time after intrusion, has been clearly demonstrated by the study of Jackson *et al.* (1982) of the 290 Ma Lands End granite. These authors showed that although convection of meteoric water into the granite took place soon (~20 Ma) after emplacement, during the main stage mineralisation, convection of meteoric water into parts of the granite also took place at ~220, 165 and 75 Ma. It has even been suggested (Edmunds *et al.*, 1985) that slow convective circulation of groundwaters is still taking place in parts of the Cornish granites. Thus it is quite possible that convection of meteoric waters into the rocks in S.W. Connemara could have taken place a significant time after the emplacement of the Galway granites, and it cannot be assumed that convection took place soon after emplacement, although this is the most likely possibility. It is hoped that the timing of this alteration event may be constrained by radiogenic isotope measurements of alteration minerals, which are currently being carried out. Interestingly preliminary results from an epidote vein in the MGS from near to the contact of the Galway granite (GJ.226), suggest that Rb-Sr isotope homogenisation took place within the vein at ~320 Ma.

6.9 SUMMARY.

The stable isotope data for the Galway and Roundstone granites have been presented in this chapter. The major conclusions which can be drawn from these data are summarised below.

1. The fluid which caused the alteration of biotite and plagioclase within these granites had a high δD value of ~-25 to -20‰. This fluid was probably not present in these rocks at temperatures greater than 300°C.

2. Analysis of the material contained in fluid inclusions, shows that this fluid had a remarkably restricted range of $H_2O/(H_2O+CO_2)$ ratios of 0.982-0.987 over a wide area. The hydrogen isotope data for the fluid inclusion samples indicates that this fluid was saline to some extent.

3. Whole rock samples which have been altered by this high δD fluid are enriched in ^{18}O relative to unaltered rocks. This enrichment is due to subsolidus ^{18}O enrichment of the feldspars, which is demonstrated by the small positive, or negative values of the quartz-feldspar oxygen isotope fractionations in these rocks. High temperature fractionations between quartz, hornblende and magnetite appear to have been preserved in these rocks, despite this alteration.

4. The chlorite $\delta^{18}O$ values indicate that the fluids which chloritised the biotite had $\delta^{18}O$ values in the range +3 to -5‰, depending on the formation temperature of the chlorite and the magnitude of salt effects. The fluid $\delta^{18}O$ may have varied between samples.

5. The ^{18}O enrichment in the feldspars in the altered rocks can only be explained if the feldspars equilibrated oxygen isotopes, with the same fluid that caused the chloritisation of biotite down to temperatures <180°C, probably under conditions of high fluid/rock ratio. Thus this fluid must have been present in these rocks down to very low temperatures. During the chloritisation of the biotite, the feldspars in these rocks must have been depleted in ^{18}O relative to their initial igneous values.

6. Oxygen isotope data for vein material infilling a fault in the MGS indicates that this material must have been deposited at a temperature >210°C from a fluid with a $\delta^{18}O$ <+3.5‰. The early quartz and baryte in this vein formed from a fluid with a $\delta^{18}O$ value at least 3.7‰ heavier than the fluid which deposited the later calcite in this vein, indicating that the fluid $\delta^{18}O$ decreased with time. The calcite in this vein was almost certainly deposited from a fluid of meteoric origin, and it is likely that this fault was a major conduit through which meteoric fluid infiltrated into the MGS. The $\delta^{34}S$ value of the baryte in this vein is consistent with an origin for the sulphate by oxidation of sulphides in the rocks presently exposed.

7. The large variations in the $\delta^{18}O$ and small variation in $\delta^{13}C$ of calcites from the MGS and Roundstone granites are best interpreted as the result of formation from fluids with similar $\delta^{18}O$ and $\delta^{13}C$ values, with subsequent re-equilibration changing the $\delta^{18}O$ but not the $\delta^{13}C$ values. The carbon in these calcites may well have been derived from a source external to the igneous rocks containing the calcites.

8. The features of the fluid causing the alteration in the Galway granites are not consistent with an internal origin by exsolution during crystallisation and therefore an external source for this fluid is implied. This being the case, the features of this fluid indicate that it must have been derived from a meteoric source.

9. The fluid causing the alteration in the Galway granites is extremely similar in a number of respects to the fluid causing the alteration of in the Cashel-Recess district and it is concluded that these fluids had a common origin from a meteoric source. It is suggested that this fluid infiltrated into the whole of S.W. Connemara as the result of convective circulation around, and through, the thermal anomalies associated with the Galway granites. The timing of this fluid convection is not constrained at present. It is possible that this convection could have taken place as late as 300 Ma or possibly even later in some parts of the Galway granite, although it is most likely that the convection took place within 20 Ma of granite emplacement.

CHAPTER 7.

SYNTHESIS AND IMPLICATIONS OF RESULTS.

7.1 SYNTHESIS.

The stable isotope data presented in the previous four chapters have been interpreted as indicating the following sequence of events that affected stable isotope ratios in S.W. Connemara:

1. Early ^{18}O enrichment of the Dalradian amphibolites, probably prior to the metamorphic peak and possibly pre-metamorphism. The δD values of the metasediments were probably also lowered relative to their initial values as a result of dehydration during progradation, although there is no direct evidence to show this.

2. Intrusion of an OIB- or MORB-like basic magma (the MGS magma) which was in the process of being contaminated with crustal material. The crustal material was most probably partial melt derived from Dalradian metasediments, or similar material at slightly deeper levels.

3. Formation of ^{18}O enriched partial melts in pelitic lithologies in the aureoles of the ultrabasic-basic MGS bodies, followed by loss of melt to the MGS magma. Melt extraction may have taken place before isotopic equilibrium between melt and residuum was achieved.

4. Crystallisation of the contaminated magma, with the precipitation of magmatic hornblende. This was followed by the later replacement of anhydrous minerals by hornblende under subsolidus conditions as the result of reaction with hydrous fluids. These fluids were probably derived from other portions of the MGS that were still crystallising.

5. Crystallisation of the partial melt remaining in the metasediments and the release of small amounts of residual fluid from these melts. Some of this fluid may have caused the coarse muscovite growth in the metasediments.

6. Thrusting in the Delaney Dome area, probably without the infiltration of external fluids into the thrust zone mylonites.

7. Intrusion of the Galway granites, which initiated convection of meteoric waters into the rocks of S.W. Connemara. This infiltration of meteoric fluid caused the development of a. the chlorite/epidote/sericite alteration in the MGS rocks, b. the chlorite (and almost certainly the sericite) in the Dalradian rocks and c. the chlorite and sericite in the Galway granites, together with the reddening of the K-feldspars in these bodies. This convective system was a dynamic system which continued over a time interval during which temperature fell and fluid compositions changed. The duration of convection at moderate temperatures (~300°C) may have been geologically quite short (<1 million years).

Some of the important geological implications of the results from this study are outlined in the following section.

7.2 IMPLICATIONS OF RESULTS.

7.2.1 The interpretation of stable isotope data from geologically complex areas.

It can be seen from the synthesis in 7.1 that this study has been extremely successful in achieving the original aims of this project (1.2). This demonstrates the potential of stable isotope studies in the investigation of fluid-rock interaction, not only in identifying the source of the O and H and to a lesser extent C and S, but also in elucidating the conditions under which fluid-rock interaction took place. For example, in chapter 6., it was not only possible to show that the fluid which caused the chlorite/sericite forming event was from a meteoric source, but also that it was saline, was first present in the rocks at temperatures not much greater than 300°C, and continued to be present down to temperatures <180°C.

It should be noted however that most of the conclusions in this thesis could not have been obtained by examination of the stable isotope data alone. It was only possible to reach the conclusions given above by integrating the stable isotope data with the results of detailed fieldwork and petrographic observation of samples and the large amount of published geological data which was already available for this area.[1] It is important to emphasise also, the necessity of interpreting the results in the light of the the available theoretical evidence for stable isotope behaviour (hence chapter 2.). An understanding of the kinetics of isotope exchange is of utmost importance. Thus it can be seen from 2.6 that it should not be expected that different minerals will exchange stable isotopes with a fluid at the same rates and therefore under most conditions rocks will be disequilibrium assemblages and should be interpreted as such. Identification of equilibrium-disequilibrium relationships between minerals within a single rock can be used to gain information on more than one event in the geological history of the rock. Using this approach of identifying equilibrium-disequilibrium relationships, even the variations in hydrogen[2] isotope ratios between different minerals within a single rock, and between different samples of the same mineral from within a rock unit, can be shown to be attributable to a few simple processes which affected that rock. For example, it was possible to show in chapter 2. that the hydrogen isotope ratios of the MGS hornblendes have been largely unaffected by later events, even though they were exposed to fluids derived from a meteoric source at elevated temperatures. The fact that re-equilibration did not take place was used to constrain the temperature-time relationships of the hydrothermal event (4.2). Similarly the large variation in the hydrogen isotope ratios of the MGS epidotes can be attributed to variable degrees of re-

---

[1] Stable isotopes may provide a key but you have to find the door first!

[2] "A rather squirrely element"- Valley (pers. comm., 1988).

equilibration with the same fluid during cooling below 200°C. Each mineral within a rock has an individual story to tell.

The success of this project bodes well for stable isotope studies of other geologically complex areas where much field and petrographic work have already been carried out. The Lewisian is one such example.

7.2.2 Interaction between basic magma and mid crustal metasediments.

In 4.6.1 it was concluded that the MGS magma probably originated by mixing of a MORB- or OIB-like parental magma with 20-30 wt.% of crustal material which was probably mostly partial melt derived from Dalradian metasediments. These conclusions are in very good agreement with those given by Jagger (1985) on the basis of radiogenic isotope modelling.

Contamination of a basic magma by partial melt material would be expected to have a number of effects on the magma:

1. An increase in the melt in the proportions of "granitic" major elements (Si, Al, K, Na), which would tend to increase the volume of later differentiates produced during fractionation.

2. An increase in the water content of the melt. This would allow hornblende crystallisation and possibly also stabilise calcic feldspar (Bremner and Leake, 1980). Because hornblende is silica undersaturated, the effect of hornblende fractionation would also be to increase the volume of the later quartz bearing differentiates. Hornblende fractionation may also cause the trace element variation that takes place with fractionation to differ from that which would take place in an uncontaminated basaltic melt.

3. Contamination of the melt with "granitic" trace elements including Sr and Nd with crustal isotope ratios.

4. Contamination of the melt with crustal ^{18}O enriched oxygen.

It is be concluded that similar effects must also take place wherever basic magma has been intruded into pelitic lithologies at a mid crustal level.

It is noted that the potential exists for a much more detailed review of the effects of the contamination of the magma by partial melt material than is given above. This is because detailed major and trace element data are now available for both the partial melt material (Ahmed-Said, 1988) and the fractionated sequence of rocks which resulted from this contamination process (Jagger, 1985). However caution must be emphasised, because some trace element abundances may have been affected by later hydrothermal alteration (see below). It is also important to note that there is limited evidence from this study, and that of Jagger (*ibid.*) that isotopic equilibrium between partial melt and residuum may not have been achieved prior to assimilation of the partial melt into the magma. That such a process could occur in a mid-crustal environment has important implications for the interpretation of igneous rocks which may have been contaminated in such an environment and further investigation is warranted.

7.2.3 Hydrothermal alteration in Connemara.

One of the major findings of this thesis has been to conclude that a meteoric convection system operated in S.W. Connemara post 400 Ma. This system must have extended over the entire area which was investigated in this study (an area of 20 × 10 km bounded at four corners by Ballinaboy and Ballyconneely in the west and Recess and Carna in the east, map 1.). The outer limits of this convective system are presently unknown.

The size of a convective system will depend on a number of parameters, especially the permeability (Norton and Knight, 1977). Some estimate of the possible size of this convection system can be gained from examination of the stable isotope variations around intrusives where meteoric water convection is known to have occurred. For example, Taylor (1977) shows that on Mull oxygen isotope depletions of whole rock samples can be recognised up to 4-10 km from the edges of the intrusive bodies in the Tertiary centre. However since fluid/rock ratios for hydrogen are always much larger than for oxygen, it is likely that the hydrogen isotope ratios of these rocks could have been affected much further away from the centre where only small fluid/rock (mass) ratios were experienced during convection. The theoretical study of Norton and Knight (1977) has indicated that for small plutons ~2 km across, fluid flow might take place up to 6 km or more (3 pluton diameters) away from the edge of the pluton, if reasonable rock permeabilities are assumed. If this relationship between the size of the pluton and the size of the convective system can be scaled up to apply to the Roundstone granite, then it is possible that a convective system associated with this granite alone could have extended across nearly all of the Dalradian rocks of Connemara.

Since a number of granitic bodies were intruded at ~400 Ma, including the large radioactive (Feely and Madden, 1987) Galway granite, it is considered likely that convective systems associated with these granites could have easily extended across the whole of the Connemara Dalradian. This conclusion is supported by stable isotope data from the western part of the Oughterard granite and the Maum Valley Fault zone which indicate that these rocks were altered at low temperatures by low $\delta^{18}O$ (+6 to +1‰) and high δD (-10 to -30‰) fluids (N. Reynolds, pers. comm., 1987). Reynolds also notes that retrogression is very intense in some zones around the Omey granite and within the granite itself, strongly suggesting that this granite may have developed a meteoric convection system similar to that identified in the presently studied area.

The recognition that a meteoric convection system developed in Connemara has a number of important implications as a result of the large mass transfer capabilities of such systems. The enormous amount of fluid movement that can take place in such systems is underlined by the calculations of Norton and Taylor (1979). These authors estimated that in the Skaergaard hydrothermal system, between 100 and 5000 kg of water flowed through each square centimetre cross section of rock in the upper part of the intrusion, over the lifetime of the system. Obviously the potential for the transport of various elements in such systems is

enormous. The possible mass transfer effects of such a system are described in the next three sections.

Chemical changes caused by hydrothermal alteration.

It should be seen that the changes in the chemistry and radiogenic isotope ratios of the rocks involved in a convective system are controlled by similar factors to those which control stable isotope variations during fluid-rock interaction described in 2.7. Thus the change in concentration of an element in a rock will depend on:

a. the initial concentrations of the element in the fluid and rock (analogous to δ_{Wi} and δ_{Ri} for stable isotopes -see 2.7)

b. the fluid-rock partition coefficient for that element (analogous to α for stable isotopes).

c. The fluid/rock mass ratio.

d. The kinetics of transfer of the element from the fluid to the rock, or *vice versa*.

It is beyond the bounds of this study to give a detailed account of the effects that infiltration of meteoric fluid may have had on these rocks, but three examples of the possible effects which may have taken place are given here.

Potassium. K is likely to have been released in to the fluid in large quantities as the result of biotite breakdown, so that the fluid is likely to become saturated in K. Whether or not the K content of the rock will be affected depends on the amount of K that is taken up during sericite growth. Thus rocks containing a large amount of chlorite, but little sericite might be expected to be K depleted relative to the unaltered rocks. Rocks which were initially K poor (e.g. the ultrabasic MGS rocks), which were infiltrated by K bearing fluid derived from rocks in which biotite breakdown was taking place may well have had their K contents increased if sericitisation took place in these rocks. Thus the measured K contents of the ultrabasic MGS rocks should be viewed with caution.

Aluminium. Al is often considered to be relatively insoluble in hydrothermal fluids, which together with its high abundance in all rocks indicates that the Al contents of these rocks are unlikely to have been changed during hydrothermal alteration (Brimhall, 1979).

Chlorine. Cl is known to be strongly partitioned into the fluid phase relative to Cl-bearing minerals, such as biotites and amphiboles, at 600°C (Volfinger *et al.*, 1985). If the partition coefficient does not vary greatly with temperature it might be expected that progressive infiltration of biotite and amphibole bearing rocks, even by a Cl rich fluid, will result in the Cl being "washed out" of these minerals. Therefore it is quite possible that the MGS hornblendes have not retained their original Cl contents.

It is suggested that the effect of fluid-rock interaction on the chemistry of these rocks could be investigated in future using similar methods to those employed by Ferry (1985a,b) in his study of the hydrothermal alteration of

the Tertiary centre in Skye. Using these methods Ferry (*ibid.*) suggests that K, Na, Sr, Mg and possibly Fe and Si abundances were changed during the alteration of the gabbros on Skye, while Ca, Fe and probably Na abundances within the granites may have been changed.

Disruption of geochronological systems.

As well as altering the geochemistry of rocks in S.W. Connemara, the convection of meteoric water into the area may have also disrupted various geochronological systems.

Since fluid convection is thought to have occurred at temperatures well below ~550°C, which is often quoted as the closure temperature for Ar diffusion in hornblende, the K-Ar ages measured on hornblendes from Connemara (Elias *et al.*, 1988) should not have been affected by the infiltration of fluid into these rocks. This would only be the case if the hornblendes were stable in this fluid and did not react with it. However, it was noted in 4.3.1 that nearly all of the hornblendes in the MGS appear to contain anomalously high amounts of water and this was attributed to the presence of submicroscopic chlorite growth within these hornblendes as a result of reaction with the meteoric fluid. Onstott and Peacock (1987) have shown that such alteration may well reduce the effective grain size of these hornblendes, which could in turn reduce the closure temperature. However, it is questionable whether the closure temperature of the hornblendes could have been reduced to as much as 300°C by this process. The fact that most of the K-Ar ages determined for hornblendes by Elias *et al.* (1988) are appreciably older than 400 Ma indicates that drastic resetting of the Ar content of the hornblendes has not occurred. The fact that the hornblendes did not equilibrate hydrogen isotopes with the meteoric derived fluid also suggests that Ar loss is unlikely to have occurred, since hydrogen diffuses much faster than Ar in hornblendes (Graham *et al.*, 1984; Harrison, 1981). However some anomalously young ages were determined by Elias *et al.* (1988). It would be interesting to compare the apparent K-Ar ages of hornblendes from Connemara with normal and high water contents, in order to test whether or not the ages are significantly different.

The lower closure temperature for Ar diffusion in biotite (normally quoted as ~250-300°C) means that this mineral could have undergone Ar loss during the hydrothermal event, if the estimates of an upper temperature of ~300°C for fluid presence are correct. Some of the biotites analysed by Elias *et al.* (*ibid.*) do indeed have young apparent ages (<425 Ma), although many of these samples come from N.W. Connemara away from any large granite outcrops. A stable isotope investigation of the rocks containing these biotites might indicate whether or not these rocks had been exposed to the meteoric fluid. However, from the work of Criss *et al.* (1982) and Kulp and Engels (1963) it would appear that reaction with this fluid could not have in itself caused substantial Ar loss from the biotites, but that temperature is the important factor in governing Ar loss. Thus the presence of meteoric fluid in the samples containing these biotites should only have affected the apparent ages of these biotites if the fluid actually heated the rock to temperatures >250-300°C. Heating of a rock in a convective system could only have occurred in an updraft zone, where heated fluids were rising form depth. Downdraft zones will be cooled by the

downward flow of cool fluid. Possibly there is an updraft zone in N.W. Connemara over an unexposed granite body.

Jagger (1988) measured a lower intercept U-Pb age of 454^{+16}_{-14} Ma for zircons from a sample of acid MGS gneiss from Lettershanna Hill. This age is anomalously young, since hornblende K-Ar ages from the same area are 477±9 Ma (Elias *et al.*, 1988). Jagger (1988) suggests that the young age for this zircon sample is due to Pb loss, but could not attribute this Pb loss to any geological event. It is suggested here, that the Pb loss from these zircons could have taken place during alteration of this rock by meteoric derived fluid in the post 400 Ma hydrothermal convective system.

Mineralisation in Connemara.

Because of the large mass transfer capability of hydrothermal convective systems, such systems have the potential to concentrate dispersed metals into economic ore deposits. Indeed one of the most productive mining districts in the world at Butte, Montana (once called the richest hill on earth; Evans, 1980) was formed by a meteoric convective system (Sheppard and Taylor, 1974).

Previous workers have noted that some mineralisation in Connemara does appear to be associated with rocks which have undergone retrograde hydration. N. Reynolds (pers. comm., 1987) has found that fluids with light $\delta^{18}O$ values (+6 to +1‰) and high δD values (-10 to -30‰) which caused retrogression around the western Oughterard granite body were also involved in late vein hosted mineralisation in this area. O'Connor (1985) notes that U showings in the Galway granite are often associated with chloritisation and haematisation along fractures and joints. The similarity in the stable isotope composition of the fluid causing alteration in E. Connemara and the mineralogy of the U showings indicates that it highly likely that both these instances of mineralisation were caused by the same meteoric convection system that has been identified in the present study area, or else another similar system which developed at the same time.

The locations of solution and precipitation of any element within a convective system is a function of the geometry of the convective system and the stabilities of the minerals containing that element. Since different mineral stabilities are functions of temperature, pressure and fluid composition (e.g. Bird and Helgeson, 1981) all of which vary in space and time within a convective system, it is not possible to make any generalisations about the likely locations for ore mineral deposition within such a system. Thus while it is often supposed that mineral deposition is only associated with with the zones of fluid updraft in a convective system, this is not necessarily the case. For example calcite may be deposited in zones of downward fluid movement (Holland, 1967), while Criss and Taylor (1983) noted that Au-Ag deposits within the Idaho batholith show an empirical relationship with the outer zones of intense hydrothermal circulation.

Since there does appear to be some mineralisation that is apparently associated with meteoric convection (see above), it is suggested that future research into mineral deposits in Connemara should concentrate on

finding out what part of the convective system(s) these examples of mineralisation were deposited in. If these mineral deposits are found to be confined to a certain part of the system, then the location of target areas for mineral prospecting could proceed by mapping the geometry of the hydrothermal systems using techniques similar to those outlined in this thesis.

7.3 SUMMARY.

The sequence of events that is recorded in the stable isotope ratios of the rocks in Connemara and some of the geological implications of these events have been reviewed in this chapter. It is concluded that:

1. The major geological events which affected the stable isotope ratios in S.W. Connemara include the contamination of the MGS magma by partial melt derived from Dalradian metasediments during intrusion, followed by the infiltration of the whole area by meteoric derived fluids in a dynamic convective-hydrothermal system.

2. This study has proved that stable isotope studies can be extremely useful in investigating fluid-rock interaction in geologically complex areas. However the importance of integrating the stable isotope data with other available data cannot be over-emphasised.

3. The contamination of the MGS magma by partial melt material must have caused important changes in the chemistry of this magma. Similar changes in the composition of basic magma should take place wherever it is intruded through pelitic metasediments in the mid-crust.

4. The recognition that meteoric water has probably infiltrated the whole of the Dalradian in Connemara in one or more hydrothermal-convective system(s) has important implications for the interpretation of whole rock geochemical data and radiogenic isotope data and for mineral prospection in Connemara.

APPENDIX

A.1. ANALYTICAL TECHNIQUES.

A.1.1 Oxygen Isotope Analysis of Silicate Minerals

Oxygen isotope analyses of silicates was carried out using techniques which have been routinely employed at SURRC for the last five years.

Oxygen was liberated from silicate minerals by oxidation with ClF_3 (Borthwick and Harmon, 1982) using a vacuum extraction line similar to that described by Clayton and Mayeda (1963). The oxygen was then reduced to CO_2 for mass spectrometric analysis.

Analytical procedures used in this study were almost identical to those outlined by Borthwick and Harmon (1982), except that:

a. Between 10-20 mg of powdered sample was used for each analysis.

b. The oxidation reactions were carried out at 700°C for whole rock powders and magnetite, 660°C for quartz and alkali feldspars and 680°C for other minerals.

c. Analyses carried out after August 1987 were performed on the newly built FS12 line. On this line the carbon dioxide yield was measured using a fixed volume capacitance manometer.

The yield of oxygen from mineral separates in each experimental run was compared with the calculated yield for the mineral, if the mineral had a fixed composition, or with the calculated yield for pure end members if it was part of a solid solution series. The experimental yield for minerals with fixed compositions was normally found to be within ±5% of the calculated yield. The yield and $\delta^{18}O$ values measured for runs which gave oxygen yields outside these limits were excluded from the average values calculated for each sample in A.2.2. If the experimental yield for minerals showing solid solution was not within the range calculated for the end members, then data from these runs were excluded from the average in A.2.2.

The carbon dioxide was then analysed using either a VG-Micromass 903E mass spectrometer prior to August 1987 or a VG-SIRA 10 after this time. The 45/44 and 46/44 mass abundance ratios of the sample gas were measured relative to those of a laboratory standard gas calibrated against isotope reference materials. The raw data were corrected for instrumental and isobaric effects following the procedures of Craig (1957).

Delta values obtained by this method have a precision of ±0.2‰ or better. This error value includes combined sampling, analytical and instrumental errors. Using this method repeat analyses of NBS#28 in the SURRC laboratory gives an average delta value of 9.60‰.

A.1.2 Carbon and Oxygen Isotope Analysis of Calcite.

Calcite bearing samples (pure calcite or calcite rich mineral separates) were treated with 100% phosphoric acid at 25.18 ±0.05°C for 3 hours to extract carbon dioxide for isotopic analysis (McCrea, 1950). The yield of CO_2 was measured using a constant volume capacitance manometer accurate to within ±1%.

Oxygen isotope compositions of the calcites were derived from the values for the CO_2 using the value of 1.01025 for the fractionation between carbon dioxide and calcite for the reaction conditions specified (Friedman and O'Neil, 1977). The mass spectrometry of the CO_2 is described in A.1.1.

Values of $\delta^{13}C$ are quoted relative to the PDB standard while $\delta^{18}O$ values are relative to SMOW. $\delta^{18}O$ and $\delta^{13}C$ values have a precision of + 0.13‰ or better. Using this method repeat analyses of NBS#20 in the SURRC laboratory gives an average $\delta^{18}O$ value of $+26.64_{(V\text{-}SMOW)}$ ‰ and a $\delta^{13}C$ value of $-1.06_{(PDB)}$ ‰.

A.1.3 Hydrogen isotope analysis of minerals.

Hydrogen was extracted from minerals using a technique similar to that described by Godfrey (1962). This involves heating samples under vacuum to release the bound hydrogen, either as hydrogen gas or mostly as water vapour. The water is converted to hydrogen by reaction with hot uranium.

Since the procedures used at SURRC for hydrogen extraction are slightly different from those described in the literature, a short description of our procedures where they differ will be given here.

Platinum crucibles are outgassed at ~1400°C under vacuum until the water release from the crucible and extraction vessel was measured to be less then 3-4 μM/hour (usually 2-4 hours). The extraction vessel was then quickly opened to the atmosphere and the dry powdered sample (<200#, 70 μm) is loaded into the crucible. If sufficient sample was available the weight was varied to try to achieve a yield of hydrogen of 100-150 μM (25-120 mg depending on mineral). The sample and extraction vessel are then evacuated and degassed by heating to 120°C overnight (12-14 hour) under vacuum. Blanks due to absorbed moisture on the Pt crucible not removed by this degassing procedure are very small (<1 μM) and have very light δD values of -120 to -140‰[1]. These blanks have a negligible effect on measured

[1] Suzuoki and Epstein (1976) encountered blanks of similar isotopic composition from platinum crucibles. The crucibles had been exposed to the atmosphere and then degassed for 30 minutes at 150-250°C. After this a blank with δD of -120 to -165 ‰ was collected. The size of the blank that they obtained (2-19 μM) is much greater that our own (<1μM) suggesting that the removal of absorbed moisture from the extraction vessel is not only temperature dependent but also time dependent.

The reason for such a deuterium depleted composition for the blank is not clear. Thermodynamic theory predicts that the bonds formed by H are more easily broken than those formed by D. It would therefore be expected that H might be preferentially lost by a kinetic effect during degassing. As a result of this any resultant blank should be more D rich than the starting composition (meteoric water at East Kilbride is ~-40 ‰). Since this is not

δ values of large samples of hydrogen. However as the sample size decreases and the blank makes up a larger proportion of the gas measured, then the δ value will deviate significantly from the actual value of the sample, becoming consistently lower. This effect will be most noticeable for the most deuterium enriched samples (see below).

After overnight degassing the extraction vessel is attached to the extraction line (Godfrey 1962, p.1218). The line is degassed by flaming with a torch while open to the high vacuum. The crucible is then slowly heated under vacuum by means of a high frequency induction coil to ~1400°C and kept at this temperature for 30 minutes. Under these conditions all minerals have melted (except muscovite) and all have completely released their hydrogen content. Random checks on the amount of gas being given off after this 30 minute period revealed that negligible amounts were being evolved.

The liberated gases were passed through a liquid nitrogen trap where water and any carbon dioxide are frozen. The non-condensible gases (non condensible at -196°C i.e. N_2, H_2, Ar etc) are pumped by a Toepler pump into a mercury filled manometer and measured. The yield of free hydrogen is relatively constant for each mineral and an increase in the amount of non condensible gas over that expected was assumed to be due to nitrogen originating from a leak in the line. If this was the case the sample was rerun.

After the extraction of the gas from the sample, the trap containing the water and carbon dioxide is warmed to -78°C with an acetone-dry ice mixture which allows the CO_2 to sublimate. This is measured qualitatively and then pumped away. For some samples yielding a large amount of free hydrogen, the pressure in the line can rise during dehydration of the sample, if the hydrogen cannot be pumped away fast enough. Under a high partial pressure of hydrogen it is conceivable that some hydrogen may be frozen down with the water. If this was the case it would be evolved at this stage and lost. This could possibly increase errors for δD determination in these minerals.

The purified water is then allowed to warm to room temperature so that it evaporates. It is then passed through uranium turnings at ~750°C. This reduces the water to hydrogen which is pumped into the manometer. Once most of the hydrogen has been pumped away the trap and surrounding piping are flamed to release adsorbed water. Any water that passes through the furnace (usually only a fraction of a micromole) is condensed in a second liquid nitrogen trap and then recycled through the U furnace to ensure quantitative conversion. The total yield of hydrogen is then measured with the manometer. The accuracy of the manometer varies with the amount of gas. At best it is ±0.5% and at worse ±3% for normal sized samples. Since weighing errors are small in comparison, this means that

---

the case it can only be surmised that platinum and/or glass surfaces have some preference towards absorption (or adsorption) and retention of H relative to D.

the ratio μM/mg has approximately the same errors. This can be converted to weight % H_2O by multiplying by 1.8015.

The sample is then pumped into an outgassed sample tube and transferred to the mass spectrometer. The hydrogen was analysed using a VG-Micromass 602B with a modified inlet system. This inlet system makes use of mercury pistons to enable very small samples (<1μM) to be introduced into the mass spectrometer.

The 3/2 mass ratio of the sample gas was measured relative to a standard gas of $\delta D \approx -50‰$. The standard gas was calibrated and the relationship of measured 3/2 ratio (sample): 3/2 ratio (standard) was determined for the mass spectrometer by running the standard against hydrogen prepared from standard water samples SLAP (-428‰) and SMOW (0‰). Corrections are made for value mixing and interference of H_3^+ with the HD beam, following Craig (1957).

Delta values obtained by this method have a precision of 2‰ or better. This value includes combined sampling, analytical and instrumental errors. Using these methods repeat analysis of NBS #30 gives an average δD value of -64‰.

The effect of blanks on measured isotopic composition of samples.

The effect on the δD value of a sample which is contaminated by a blank can be calculated using:

$$\delta D_{meas} = ((\delta D_{samp} \times Y_{samp}) + (\delta D_{blank} \times Y_{blank})) / Y_{meas}$$

where δD_{meas} = δD of gas measured at spectrometer, δD_{samp} = δD of uncontaminated gas from sample, δD_{blank} = δD of blank gas, Y_{samp} = moles of gas from sample, Y_{blank} = moles of gas from blank and Y_{meas} = moles of gas measured = $Y_{samp} + Y_{blank}$.

The effect of a constant blank of -140‰, 2 μM on varying sizes of sample gas of different isotopic composition is shown in fig. A.1.

In fig. A.2 δD_{meas} is plotted against Y_{meas} for all samples analysed in this study for hydrogen isotopes. Also shown on this diagram are lines for $\delta D_{samp} - \delta D_{meas} = 2$ for two different blanks. The position of these lines is strongly dependent on the blank composition and amount. Even taking the more pessimistic estimate of blank size only a few samples have been significantly contaminated. Although it is possible to correct for the effects of the blank, this is not done here because of the uncertainty of blank composition and amount.

It is important to note that larger blanks may be obtained from some voluminous samples (see section on results fluid inclusion gas analysis) because of their greater surface area.

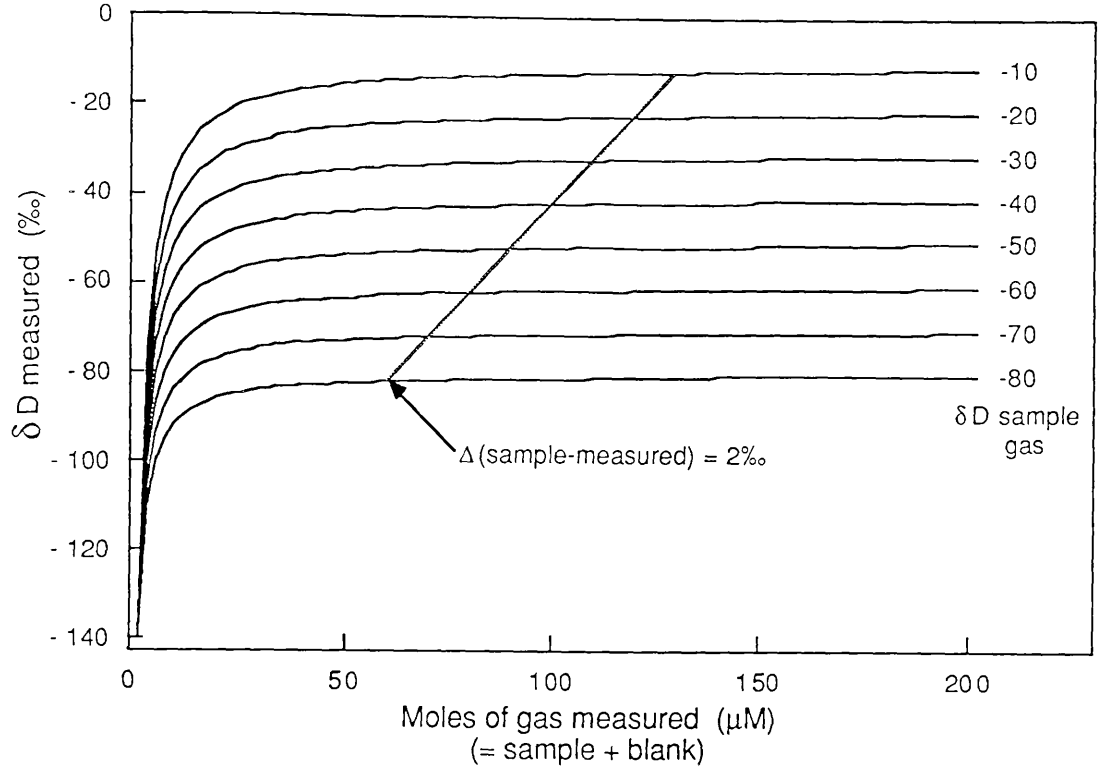

Fig. A.1 Measured yield of hydrogen vs. measured δD value for mixtures of hydrogen between samples of varying size and δD and a blank of constant δD and size (-140‰, 2μM). The dashed line is the limit beyond which smaller amounts of gas from the sample will cause $\delta D_{samp} - \delta D_{meas}$ to increase above 2‰ and therefore become significant.

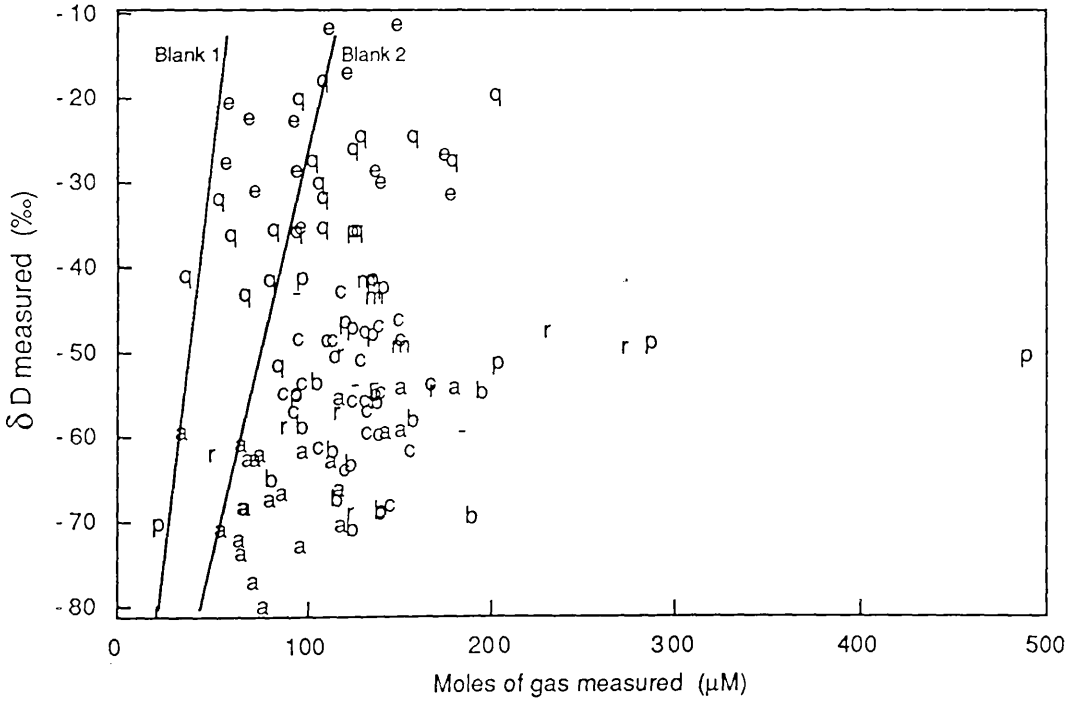

Fig. A.2 Measured yield of hydrogen vs. measured δD value for all individual hydrogen isotope analyses carried out during this study. The lines labeled blank

1 and blank 2 correspond to the points where $\delta D_{samp} - \delta D_{meas} = 2‰$ for blanks of 1μm and 2μm respectively, with $\delta D = -120‰$. Abbreviations used are a = amphibole, b = biotite, c = chlorite, e = epidote, m = muscovite, p = plagioclase, q = quartz, r = whole rock and - = chloritised biotite.

A.1.4 Analysis of fluid inclusion δD and gas composition.

Analysis of the bulk hydrogen isotope composition of quartz samples was carried out using nearly the same procedure as for hydrous minerals (A.1.3), but it was necessary to use a large amount of quartz (1-3 g) to obtain enough hydrogen for analysis. It is possible that these large samples may have larger blanks associated with them because of their large surface area for hydrogen absorption. The quartz samples were heated to ~1100°C and were not fused. The amount of water (as hydrogen) and non-condensible gases were measured manometrically as for hydrous minerals. Because of the increased errors in the measurement of small amounts of gas, the accuracy of measurement of the non-condensibles is only about ±10-20%. The yield of non-condensibles was never enough to allow identification of the species present by mass spectrometry. The carbon dioxide from the sample was collected and the yield was measured with a fixed volume capacitance manometer with an accuracy of ±1%.

A.1.5 Sulphur and oxygen isotope analysis of baryte.

The baryte was reduced to sulphur dioxide for sulphur isotope analysis using a procedure very similar to that described by Coleman and Moore (1978). The only difference in the procedure employed at SURRC is that the gases evolved from the sample are passed through a Cu gauze placed at the end of the main furnace as well as a separate Cu filled furnace. This ensures that SO_3 has been completely reduced to SO_2. The $\delta^{34}S$ value of the SO_2 produced by this procedure was determined using an ISOSPEC 64 mass spectrometer. The $\delta^{34}S$ values obtained by this method have a precision of ±0.3‰. This value includes errors resulting from both analytical and instrumental effects. Twenty complete replicate analyses of the internal laboratory standard gave a reproducibilty of ±0.27‰ (1σ). Using this method, repeat analyses of international standards NBS#123 and NZ-1 gave mean $\delta^{34}S$ values of +17.1 and -0.1‰ respectively.

The oxygen in the baryte was quantitatively converted to CO_2 for determination of the $\delta^{18}O$ value by a method almost identical to that described by Sakai (1977). This method is a modification of the method first devised by Rafter (1967). The only difference between the technique employed in the SURRC laboratory and that described by Sakai (1977), is that in the SURRC laboratory the reduction of baryte with carbon to produce CO_2 and CO was carried out in a platinum crucible heated by a radio frequency induction coil. The measurement of the $\delta^{18}O$ value of CO_2 has already been described in A.1.1. Repeat analyses of the international standard NBS#127 gave a $\delta^{18}O$ of 9.4±0.2‰ (n=5).

The IAEA accepted values for the sulphur and oxygen isotope standards are given below

NBS#123	$\delta^{34}S = +17.09 \pm 0.31$	(average of 13 laboratories)
NZ-1	$\delta^{34}S = -0.34 \pm 0.07$	(one laboratory)
NBS#127	$\delta^{18}O = +9.34 \pm 0.26$	(three laboratories)

A.1.6 Rb-Sr Isotope Analysis

Rb and Sr concentrations and $^{87}Sr/^{86}Sr$ ratios were determined for single aliquots of between 5 and 25 mg of sample powder. The Rb and Sr were separated by conventional cation-exchange chromatography. Rb concentrations were determined by isotope dilution using a VG-Micromass 30B mass spectrometer. Sr concentrations by isotope dilution and isotope ratio measurements were determined on a VG-Isomass 54E mass spectrometer.

$^{87}Rb/^{86}Sr$ is determined to a precision of ±0.6%. $^{87}Sr/^{86}Sr$ values are normalised to $^{86}Sr/^{88}Sr = 0.1194$. Errors quoted on $^{87}Sr/^{86}Sr$ are $\pm 2\ \sigma_n$ and correspond to least significant digits. NBS 987 has a $^{87}Sr/^{86}Sr$ ratio of 0.71027 as measured during this work. The decay constant (λ) of ^{87}Rb is taken to be $1.42 \times 10^{-11}\ y^{-1}$.

A.1.7 Electron microprobe analysis of minerals.

Grain mounts of mineral separates were chemically analysed using a Cambridge Instruments Microscan 5 X-ray microanalyser (microprobe) fitted with a Link Systems Energy Dispersive Analyser. The microprobe operating conditions used were: accelerating potential = 20 kV, probe current = 3 nA and count times of 50-200 seconds. The count times were automatically corrected for dead time. The X-ray spectrum was processed to give peak areas of the elements of interest using an iterative stripping technique (Statham, 1976), with a reference cobalt spectrum. Elemental concentrations were then obtained by calibrating against pure metal or simple mineral standards, followed by a full atomic number absorption and fluorescence correction (ZAF) as described by Sweatman and Long (1969). All oxide percentages quoted are above the detection limits.

A.1.8 Mineral Separation

Mineral separates were prepared using standard techniques including isodynamic magnetic separation, heavy liquid separation with bromoform, tetrabromoethane or methylene iodide, and hand picking of separates. A combination of these techniques was used for most samples. The purity of separates was estimated with the aid of a binocular microscope or by X-ray diffraction. Unless stated otherwise in A.2 the purity of separates is estimated to be better than 98%.

Samples that had been separated in heavy liquid were thoroughly rinsed with Analar grade acetone after separation. The heavy liquids were

frequently washed with water and filtered through a fine filter paper to remove fine mineral particles. Godfrey (1962) states that the use of heavy liquids does not affect the deuterium content of hydrous minerals.

Quartz Separation

Quartz-feldspar mixtures isolated using heavy liquids were boiled with dilute HCl to remove carbonates, chlorite and iron oxide minerals. The mixture was then treated with hydrofluorosilicic acid (H_2SiF_6), this selectively dissolves the feldspar leaving pure quartz (Syers *et al.* 1968). Because the grain size of the quartz-feldspar mixtures (between 355 and 90 μm) was coarser than the material used by Syers *et al.*, the dissolution took longer than the 3-6 days specified by these authors. Most samples took between 6 and 15 days for complete dissolution of the feldspar with the H_2SiF_6 being replenished every 3 days. One sample took 3 weeks. No etching of the quartz grains was observed in any sample. It was found that partial etching of the feldspar altered its specific gravity and mixtures of quartz and feldspar which had originally had the same specific gravity could then be separated using heavy liquids.

One sample of quartz was isolated from a quartz epidote mixture using a pyrosulphate fusion method (Kiely and Jackson, 1965) to remove the epidote.

Quartz separation for fluid inclusion analysis

Because the quantity of water as fluid inclusions in quartz is very small the water evolved from the quartz is very prone to contamination by very small amounts of hydrous minerals in the separate. For example fluid inclusion rich quartz will usually contain < 0.1 wt.% H_2O while chlorite can contain 10 wt.%. Approximately 2 g of quartz is needed to produce enough hydrogen for analysis yet if even 10 mg of chlorite is present in the 2 g (=0.5 wt.% or ~0.4 volume %) then approximately 1/3 of the evolved gas will be from the chlorite. The quartz for fluid inclusion analysis must therefore be especially pure. The following procedure was used to try to attain this. The quartz from rock samples was isolated from quartz feldspar mixtures using H_2SiF_6 as described above. Quartz from veins was not treated with H_2SiF_6. The quartz was then boiled in either concentrated HCl or *aqua regia*. If inclusions of other minerals were still present within the grains the sample was put through the Frantz separator at maximum amperage. The sample was then hand picked.

If it was suspected that the sample might contain organic fragments e.g. tissue from filter papers or hairs then the sample was steeped overnight in 30 % hydrogen peroxide to remove this material. Finally the sample was washed in de-ionised water then Analar acetone.

Throughout all of these procedures, care was taken to minimise as far as possible premature opening or leakage of the inclusions prior to analysis. Thus the quartz sample was never heated above 110°C and heated and cooled as slowly as possible.

In order to test whether any of these treatments could affect the δD of the sample, two splits of a quartz vein were taken; one was put through all of

the procedures outlined above, while the other was only handpicked. No significant difference in the δD values or yield was found.

A.1.9 Computing

All numerical computing was carried out using the Glasgow University Geology department VAX 11/750. Data manipulation was carried out using Fortran 77 programs written during the course of this research or the "S" interactive data analysis system. Diagrams and text were prepared using the "S" system and the Mac Draw, MacAuthor and Microsoft Word programs on the departmental Apple Macintosh micro computers.

A.2 ANALYTICAL RESULTS.

A.2.1 Hydrogen isotope analyses.

Abbreviations:
~ yield only approximate because gas volume was outside calibrated range.
---.--- not measured.
* a low yield for measured δ value may mean that there may be a significant blank contribution to the measured δD of the hydrogen (more than 2‰). In this case the δD is a minimum.
# the yield is significantly lower than the theoretical value, or the values obtained in other runs, so that the δD may be significantly in error.
? prior to δD value indicates that the analytical uncertainty may be greater than ± 2‰ because of various factors.
? after a number indicates that the analytical uncertainty is such that the last digit is not known.
(-) yield or δD value excluded from averaging. The number in brackets after the average is one standard deviation (σ_{n-1}).
WS these analyses were kindly performed by Dr. Ward Scott.
JJ this mineral separate was kindly prepared by Mr J. Jocelyn.
Rock or mineral: am = amphibole, bi = biotite, cc = calcite, cb = partly chloritised biotite, ch = chlorite, ep = epidote, kf = K-feldspar, mt = magnetite, mu = muscovite, pl = plagioclase, pyx = pyroxene, q = quartz, wr = whole rock powder.
Sample numbers not preceded by letters are my own samples (GJ.no).

To obtain weight % H_2O multiply yield by 1.8015.

Sample no.	Rock or mineral with separate no.	Run no. (HMC.)	Yield (μ moles)	Yield (μM mg^{-1})	δD (‰)
001	wr	3860	122.6	0.355	-69.0
002	am	3887	32.2*	1.304	> -59.3
002	bi	3895	79.3	2.306	-64.9
002	cb	3869	183.5	3.495	-59.1
002	ch	3888	123.4	5.792	-55.4
	ch	3897	112.8	5.347	-50.2
				5.570 (0.31)	-52.8 (3.7)
002	kf	3889	32.8*	0.158	> -66.5
002	pl	3898	20.3*	0.900	> -69.9
002	wr	3862	115.3	0.470	-57.1
003	ch 52	3896	111.6	4.536	-48.5
003	q treat.8D	4157	93.4*	0.074	> -19.6

Sample no.	Rock or mineral with separate no.	Run no. (HMC.)	Yield (μ moles)	Yield (μM mg^{-1})	δD (‰)
003	wr	3861	~272.3	~0.778	-49.2
005	wr	3873	49.7*	0.369	> -61.9
008	wr	3871	166.7	1.691	-54.3
009	am .14P	4255	62.9	1.310	-73.6
009	ep .9B	4248	67.9*	1.391	> -22.0
009	wr	3870	87.4	1.486	-58.6
015	bi .10P	4481	137.8	2.989	-68.6
019	ep .4A 355-250 μm pick	3968	138.0	1.337	-29.8
	ep .4A 355-250 μm pick	4011	92.2*	1.370	> -28.4
				1.354 (0.02)	-28.?
025	pl .6B	4407	201.6	0.779	?-51.1
028	am	4062	95.1	1.50?	?-72.7
028	ch .7B	4061	142.9	(6.08?)	(?-67.8)
	ch .7B	4252	153.9	5.637	-61.4
				5.637	-61.4
029	am heavy fraction	3855	66.9	1.333	-62.5
	am heavy fraction	3856	65.1	1.247	-68.2
				1.290 (0.06)	-65.4 (4.0)
029	am light fraction	3858	84.9	1.477	-66.6
	am light fraction	3859	64.5	1.287	-68.2
				1.382 (0.13)	-67.4 (1.1)
029	pl	3863	~489.9	(~1.925)	-50.6
	pl	3872	92.9	1.778	-54.8
				1.778	-52.7 (3.0)
034	ep .2B 355-250μm pick	4010	111.1*	1.180	> -11.4
035	pl .5A	4408	285.2	1.112	(?-48.7)
	pl .5A	4473	138.8	1.261	-42.3
	pl .5A	4486	133.4	1.219	-41.3
				1.196 (0.08)	-41.8 (0.7)
043	ep	4006	147.7	1.120	-10.8
060	am (JJ)	4009	70.4	1.270	-76.9
060	ch (JJ,WS)	4038	198.0	(4.40?#)	(?-75.6)
	ch (JJ)	4059	---.---	5.72?	---.---
	ch (JJ)	4063	164.9	5.686	-53.6
	ch (JJ)	4246	93.4	(3.511#)	(?-48.1)
				5.703 (0.02)	-53.6

Sample no.	Rock or mineral with separate no.	Run no. (HMC.)	Yield (μ moles)	Yield (μM mg^{-1})	δD (‰)
060	ep	4008	175.7	1.320	-31.1
060	pl .6B[1]	4409	123.1	(0.329)	(-35.6)
	pl .6B	4470	96.5	(0.326)	(-41.0)
	pl .6B	4476	123.1	0.392	-46.8
	pl .6B	4477	118.1	0.385	-46.2
				0.389 (0.005)	-46.5 (0.4)
060	q treat	4156	34.3*	0.031	> -40.7
130	am .8B (WS)	4039	63.0*	1.26?	> -60.8
160	q treat 180-125μm	4153	51.2*	0.050	(> -31.6)
	q treat 180-125μm	4154	104.6	0.054	-29.7
				0.052 (0.003)	-29.7
160	q treat 125-90μm	4155	101.6	0.050	-27.2
	q treat 125-90μm	4489	81.3*	0.045	(> -35.3)
				0.048 (0.004)	-27.2
160	q treat 90-45μm	4493	125.0	0.044	-35.4
166	am Band e .9D	4300	72.9	1.031	-61.9
	am Band e .9D	4303	78.9	1.055	-67.2
				1.043 (0.02)	-64.6 (3.7)
168	ch .9A	3969	138.0	(4.058)[2]	-54.5
	ch .9A	4007	129.4	5.280	-55.4
				5.280	-55.0 (0.6)
196	cc picked (vein)	4496	155.3	0.055	-24.4
196	ch .4A (rock)	4305	109.4	4.655	-48.4
196	pl .5B (rock)	4487	133.4	0.917	-47.7
196	q .6 (rock)	4485	176.6	0.064	-27.1
203	am	4349	110.9	1.433	-62.6
206	am .5	4414	178.1	1.542	-54.0
	am .5	4466	149.6	1.580	-54.2
				1.561 (0.03)	-54.1 (0.1)
207	am	4348	95.9	1.149	-61.4

[1] Sample contains ~50 volume % quartz from point count of 450 grains.

[2] Low yield due to jumping in crucible so that δD is probably not in error.

Sample no.	Rock or mineral with separate no.	Run no. (HMC.)	Yield (μ moles)	Yield (μM mg^{-1})	δD (‰)
207	ep	4337	135.4	1.064	-28.3
	ep	4338	172.4	1.086	-26.4
				1.075 (0.02)	-27.4 (1.3)
213	ch	4421	129.0	5.862	-47.4
	ch	4461	147.6	5.468	-45.9
				5.665 (0.28)	-46.7 (1.1)
213	q .11	4478	127.5	0.058	-24.4
	q .11	4490	122.8	0.061	-25.6
				0.060 (0.002)	-25.0 (0.8)
220	ch .7B	4415	127.0	4.980	-50.7
	ch .7B	4463	96.0	4.975	-53.4
				4.978 (0.004)	-52.1 (1.9)
220	q .6	4491	200.4	0.072	-19.1
	q .6 picked	4495	106.3	0.071	-17.6
				0.072	-18.4 (1.1)
226	ep	4330	119.4	1.018	-16.6
234	ch .5A	4302	130.9	5.133	-56.8
238	ch	4422	136.8	4.852	-46.7
	ch	4462	148.6	4.905	-48.4
				4.879 (0.04)	-47.6 (1.2)
AY1	bi	4329	154.9	3.66?	-57.8
	bi	4413	134.9	3.788	-54.8
	bi	4464	135.8	3.881	-55.8
				3.776 (0.11)	-56.1 (1.5)
AY4	bi	4402	122.9	2.289	-70.7
AY10	bi	4412	103.9	2.268	(?-53.4)
	bi	4434	96.0	2.443	-58.5
				2.356 (0.12)	-58.5
AY13	bi	4328	187.9	2.723	-69.5
	bi	4420	140.8	2.902	(?-59.3)
	bi	4451	137.8	3.161	-68.8
				2.929 (0.22)	-69.2 (0.5)
AY50	cb	4411	93.6	3.727	(?-42.7)
	cb	4469	136.3	3.873	-53.3
	cb	4472	125.0	4.033	-53.5
				3.878 (0.15)	-53.4 (0.1)
B1248	am	4060	76.9	1.288	-79.8
B1248	ch .7C pick	4306	130.4	4.234	-59.4

Sample no.	Rock or mineral with separate no.	Run no. (HMC.)	Yield (μ moles)	Yield (μM mg^{-1})	δD (‰)
B1248	ep .9P	4304	56.9*	1.000	> -20.1
B2085	cb .7B	4251	193.4	3.472	-54.7
B2085	ch .7F	4250	116.4	4.477	-42.6
B2085	q .11	4480	16.5*	0.018	> -68.9
E43	am (WS)	4040	61.8	1.28?	-71.9
E44	am	4336	140.4	1.364	-59.3
	am	4347	114.9	1.325	(?-55.3)
	am	4483	149.4	1.377	-59.1
				1.355 (0.03)	-59.2 (0.1)
J001	am .10B (WS)	4037	52.8	1.17?	-70.8
J011	am	3864	114.7	1.443	-66.0
J019	bi .10A (not ground)	4244	111.4	1.904	-61.5
	bi .10A (ground)	4254	114.4	1.990	-67.2
				1.947 (0.06)	-64.4 (4.0!
J019	mu .11AP	4245	128.4	2.119	-41.5
	mu .11AP	4247	132.4	2.259	-43.3
				2.189 (0.10)	-42.4 (1.3)
J057	ch	3891	85.5	3.997	-54.6
J061	ch	3893	104.8	3.823	-60.9
J086	ch	3892	93.0	3.562	-54.5
J087	ch	3894	91.7	4.542	-56.7
J149	ch .3B	4249	136.9	5.166	-59.7
	ch .3B	4256	118.4	(4.700#)	(-63.6)
				5.166	-59.7
J149	mu .1 pick	4253	146.9	2.332	-49.1
T1750	ep .2A pick	4465	71.2*	0.741#	> -30.7
T1750	wr (matrix material)	4396	229.4	0.991	-47.5
	wr (matrix material)	4400	117.4	1.017	-50.0
				1.004 (0.02)	-48.8 (1.8)
T5	q .11 500-350 μm	4479	65.7	0.040	-42.9
	q .11 500-350 μm	4482	106.6	0.039	-34.9
	q .11 500-350 μm	4484	101.7	0.036	-31.4
				0.039 (0.003)	-36.4 (5.9!
T5	q 180-125 μm	4494	86.8	0.031	-35.6

Sample no.	Rock or mineral with separate no.	Run no. (HMC.)	Yield (μ moles)	Yield (μM mg^{-1})	δD (‰)
T6	q .3 350-250 μm	4410	57.6*	0.027	> -36.1
	q .3 350-250 μm	4488	82.8	0.031	-51.2
				0.029 (0.003)	-43.7 (10.6)
T6	q 180-125 μm	4492	74.7*	0.025	>-41.1
T7	am cr.10	4376	70.9	(0.854#)	(-62.5)
	am cr.10	4398	116.9	1.100	-70.3
				1.100	-70.3
T7	bi cr.11	4399	121.9	2.409	-63.1
T7	ep .7 (vein)	4397	55.9*	0.436	> -27.3
	ep .7 (vein)	4401	94.9	0.476	(?-34.9)
	ep .7 (vein)	4452	91.8*	0.460	> -22.3
				0.457[2] (0.02)	> -24.8 (3.5)

A.2.2 Oxygen, carbon and sulphur isotope analyses.

Abbreviations: ---.--- not measured, # the yield is significantly different from the theoretical value, or the values obtained in other runs, so that the $\delta^{18}O$ value may be significantly in error, [a] air detected in CO_2 sample at mass spec., usually in this case the measured $\delta^{18}O$ of the CO_2 differs from that of the mineral, so these runs were excluded from the average, (-) yield or $\delta^{18}O$ value excluded from averaging because they are believed to be erroneous. The number in brackets after the average is one standard deviation (σ_{n-1}).
CB these analyses were kindly performed by Mrs. Claire Behan.
JJ this mineral separate was kindly prepared by Mr J. Jocelyn.
JG-AB this baryte was analysed by Mrs Julie Gerc and Mr Adrian Boyce.
Mineral and rock abbreviations are as given in the previous table. When the mineral has a fixed stoichiometry, or if the mineral has been chemically analysed the yield is also given as a % relative to the theoretical yield.
Sample numbers not preceded by letters are my own samples (GJ.no).

[2] Low yield is due to the presence of significant quantities (~50%) of quartz in the sample. Because of its very low hydrogen content the presence of the quartz should have very little influence on the measured hydrogen isotope composition.

Sample no.	Rock or mineral with separate no.	Run no. (FS)	Yield (μ M mg^{-1})	Yield (%)	$\delta^{18}O$ (‰)
001	wr	B2149	(16.63[a])		(---.---)
	wr	B2150	(12.24[a#])		(+8.69)
	wr	B2185	(12.43[#])		(+7.97)
	wr	B2186	13.45		(---.---)
	wr	B2220	13.33		+8.21
	wr	B2221	13.42		(+8.84)
	wr	B2491	13.48		+8.25
	wr	B2492	13.56		+8.02
			13.45 (0.08)		+8.16 (0.12)
002	am	A3812	13.52		+4.75
	am	A3813	13.96		+4.95
			13.74 (0.31)		+4.85 (0.14)
002	bi	A3810	13.50		+2.01
	bi	A3811	12.67		+3.76
	bi	A3824	12.58		+4.19
			12.91 (0.51)		+3.32 (1.15!)
002	ch	A3806	13.18		+3.03
	ch	A3807	12.55		+3.31
			12.87 (0.45)		+3.17 (0.20)
002	kf	A3804	13.55	94.3	+9.88
	kf	A3805	14.14	98.4	(+8.94)
	kf	A3820	14.04	97.7	+9.87
			13.91 (0.32)		+9.88 (0.007)
002	mt	A3808	8.30	96.1	+1.22
	mt	A3809	---.---	0.0	---.---
	mt	A3815	(1.91)	22.1	(-0.47)
			8.30		+1.22
002	pl 19(1)	A3816	14.23		+8.02
	pl 19(1)	A3817	14.08		+7.93
			14.16 (0.11)		+7.98 (0.06)
002	q .22 180-125 μm	B2507	16.47	99.0	(+9.42)
	q .22 180-125 μm	B2508	(---.---)	?	(+10.46)
	q .22 180-125 μm	B2513	(14.94[#])	89.8	(+9.74)
	q .22 180-125 μm	B2514	16.51	99.2	+10.02
	q .22 180-125 μm	B2519	(14.88[#])	89.4	(+9.63)
	q .22 180-125 μm	B2520	(14.24[#])	85.6	(+9.87)
	q .22 180-125 μm	B2525	16.08	96.6	(+8.81[a])
	q .22 180-125 μm	B2526	16.72	100.5	+10.04
			16.45 (0.27)		+10.03 (0.01)

Sample no.	Rock or mineral with separate no.	Run no. (FS)	Yield (μ M mg^{-1})	Yield (%)	$\delta^{18}O$ (‰)
002	wr	B2151	(17.26#)		(+9.74)
	wr	B2152	13.82		(---.---)
	wr	B2187	13.89		+8.96
	wr	B2188	12.23		+8.76
			13.31 (0.94!)		+8.86 (0.14)
003	cc .8B $\delta^{13}C$ = -5.22	C2257	0.340	3.4	+12.39
003	cc .8A $\delta^{13}C$ = -5.29	C2259	0.536	5.4	+12.23
	cc .8A $\delta^{13}C$ = -5.12	C2260	(---.---)		+12.28
	-5.21 (0.12)		0.536		+12.26 (0.04)
003	cc .8C $\delta^{13}C$ = -5.41	C2261	0.172	1.7	+12.52
	cc .8C $\delta^{13}C$ = -5.41	C2262	0.165	1.7	+12.47
	-5.41		0.169 (0.005)		+12.50 (0.04)
003	ch	A3818	13.32		+0.12
	ch	A3819	13.26		+0.32
			13.29 (0.04)		+0.22 (0.14)
003	kf 6(3)	A3822	14.23	99.0	+11.69
	kf 6(3)	A3823	(15.15#)	105.4	(+10.93)
	kf 6(3) (CB)	A3828	14.04	97.7	+11.71
			14.14 (0.13)		+11.70 (0.01)
003	q .9	B2517	17.06	102.5	+9.57
	q .9	B2518	16.20	97.3	+9.67
			16.63 (0.61)		+9.62 (0.07)
003	wr	B2153	(18.78#)		(+6.76)
	wr	B2154	13.97		(+9.00)
	wr	B2179	13.67		+9.51
	wr	B2180	13.78		+9.96
	wr	B2222	14.03		+9.70
	wr	B2223	14.15		(+8.96)
			13.92 (0.19)		+9.72 (0.23)
004	wr	B2155	(12.54a)		(---.---)
	wr	B2156	(13.12a)		(+11.74)
	wr	B2181	12.75		+8.88
	wr	B2182	12.83		+8.62
			12.78 (0.08)		+8.75 (0.18)
005	wr	B2157	(11.92#)		(---.---)
	wr	B2158	12.70		(+11.20)
	wr	B2183	12.97		+8.85
	wr	B2184	(0.0#)		(---.---)
	wr	B2190	13.40		+8.82
			13.02 (0.35)		+8.84 (0.02)

Sample no.	Rock or mineral with separate no.	Run no. (FS)	Yield (μ M mg^{-1})	Yield (%)	$\delta^{18}O$ (‰)
006	wr	B2159	(12.83#)		(+7.84)
	wr	B2160	13.15		(+5.82)
	wr	B2189	(0.0#)		(---.---)
	wr	B2191	13.54		+8.42
	wr	B2192	13.73		+8.44
			13.59 (0.12)		+8.43 (0.01)
007	wr	B2161	(20.22#)		(+2.83)
	wr	B2162	(15.08#)		(+7.72)
	wr	B2163	(15.03#)		(---.---)
	wr	B2193	13.49		+7.82
	wr	B2224	13.04		+8.28
	wr	B2225	12.84		+7.94
			13.12 (0.33)		+8.01 (0.24)
008	wr	B2194	13.83		+7.54
	wr	B2195	14.66		+7.49
			14.25 (0.59)		+7.52 (0.04)
009	wr	B2165	(16.61[a])		(---.---)
	wr	B2166	14.02		+7.39
	wr	B2226	13.24		+7.10
	wr	B2227	12.90		+7.50
			13.39 (0.57)		+7.33 (0.21)
010	wr	B2167	(14.14[a])		(+8.36)
	wr	B2168	14.82		+9.11
	wr	B2228	13.73		+9.00
	wr	B2229	13.49		+9.20
			14.01 (0.71)		+9.10 (0.10)
011	wr	B2169	14.34		(+13.49)
	wr	B2230	13.94		+11.67
	wr	B2231	13.55		+11.48
			13.94 (0.39)		+11.56 (0.13)
012	wr	B2171	14.34		+9.96
	wr	B2172	13.90		(---.---[a])
			14.12 (0.31)		+9.96
015	kf 4(E) 355-250 μm pick	B2443	(---.---)		(+10.49)
	kf 4(E) 355-250 μm pick	B2444	14.72	102.4	(+10.91)
	kf 4(E) 355-250 μm pick	B2484	14.39	100.1	+9.41
	kf 4(E) 355-250 μm pick	B2485	14.02	97.6	+9.50
			14.38 (0.35)		+9.46 (0.06)

Sample no.	Rock or mineral with separate no.	Run no. (FS)	Yield (μ M mg^{-1})	Yield (%)	$\delta^{18}O$ (‰)
015	q 4 355-250 μm pick	B2445	17.21	103.4	(+10.70)
	q 4 355-250 μm pick	B2446	15.98	96.0	(+11.42)
	q 4 355-250 μm pick	B2486	16.76	100.7	+9.52
	q 4 355-250 μm pick	B2487	17.01	102.2	+9.53
			16.74 (0.54)		+9.53 (0.007)
015	wr	B2377	14.48		+9.54
	wr	B2378	14.76		(+10.41)
	wr	B2499	14.92		+9.48
	wr	B2500	14.32		+9.57
			14.62 (0.27)		+9.53 (0.05)
016	wr	B2379	(13.32)		(+8.84)
	wr	B2380	(13.37)		(+6.37[a])
	wr	B2493	12.87		+8.64
	wr	B2494	12.72		+8.62
			12.80 (0.11)		+8.63 (0.01)
019	ep .4A 350-255 μm	B2515	(14.24[#])	107.7	(+8.94)
	ep .4A 350-255 μm	B2516	13.52	102.3	(+7.69)
	ep .4A 350-255 μm	B2529	13.42	101.5	+8.06
	ep .4A 350-255 μm	B2530	12.68	95.9	+8.16
			13.21 (0.46)		+8.11 (0.07)
028	am .8A 90-45	B2653	(11.32[#])		(+8.33)
	am .8A 90-45	B2654	(6.08[1])		+7.60
	am .8A 90-45	B2659	13.32		(+8.40)
	am .8A 90-45	B2664	13.21		+7.70
	am .8A 90-45	B2665	13.33		+7.52
			13.29 (0.07)		+7.61 (0.09)
029	am heavy fraction	B2199	14.05		+6.97
	am heavy fraction	B2200	13.51		+6.95
	am heavy fraction	B2201	13.83		+6.67
			13.79 (0.27)		+6.86 (0.16)
029	am light fraction	B2176	14.64		+7.05
	am light fraction	B2177	13.68		(---.---[a])
	am light fraction	B2178	14.26		(+6.37)
	am light fraction	B2196	13.91		+6.98
	am light fraction	B2197	13.47		+6.82
			13.99 (0.47)		+6.95 (0.11)

[1] Low yield due to sample spillage on loading, so that the isotopic ratio should not have been affected.

Sample no.	Rock or mineral with separate no.	Run no. (FS)	Yield (μ M mg^{-1})	Yield (%)	$\delta^{18}O$ (‰)
029	pl	B2206	14.57		(---.---)
	pl	B2207	14.57		+8.23
	pl	B2212	14.40		+8.47
	pl	B2213	14.21		+8.38
			14.44 (0.17)		+8.36 (0.12)
029	pyx	B2173	13.05		+6.21
	pyx	B2174	13.24		+6.02
	pyx	B2175	13.50		+6.38
	pyx treated with HNO_3	B2198	12.98		+6.30
			13.19 (0.23)		+6.23 (0.15)
029	q	B2210	13.23#	79.5	+8.72
	q	B2204	14.19#	85.3	+8.56
	q	B2205	14.44#	86.8	+9.45
	q	B2211	14.25#	85.6	+9.03
			14.03 (0.54)		+8.94 (0.39!)
029	wr	B2202	13.71		+6.88
	wr	B2203	(14.13)		(+7.57)
	wr	B2208	12.82		+6.83
	wr	B2209	13.35		+6.78
			13.29 (0.45)		+6.83 (0.05)
034	ep .2B pick	B2509	(---.---)		+6.75
	ep .2B pick	B2510	13.65	103.7	+6.51
			13.65		+6.63 (0.17)
034	q	B2523	(18.47#)	111.0	(+13.98)
	q	B2524	16.28	97.8	+12.99
			16.28		+12.99
035	cc .6C $\delta^{13}C$ = -5.71 (CB)	C????	00.16	1.6	+12.65
043	ep 250-180 μm	B2533	13.12	100.5	(+6.46)
	ep 250-180 μm	B2534	13.54	103.7	+5.95
	ep 250-180 μm	B2535	12.83	98.2	+5.86
			13.16 (0.36)		+5.91 (0.06)
060	am (JJ)	B2531	13.22		+5.93
	am (JJ)	B2532	12.71		+6.10
	am (JJ)	B2536	12.17		+5.86
			12.70 (0.53)		+5.96 (0.12)
060	cc .6A $\delta^{13}C$ = -5.89 (CB)	C	00.13	1.3	+25.67
060	ch (JJ)	B2670	14.06		+4.24
	ch (JJ)	B2671	12.66		+4.37
			13.36 (0.99!)		+4.31 (0.09)

Sample no.	Rock or mineral with separate no.	Run no. (FS)	Yield (μ M mg^{-1})	Yield (%)	$\delta^{18}O$ (‰)
060	ep (JJ)	B2537	12.87	98.9	+5.16
	ep (JJ)	B2538	12.94	99.4	+5.20
	ep (JJ)	B2541	12.65	97.2	+5.30
			12.82 (0.15)		+5.22 (0.07)
060	mt (JJ)	B2539	9.25	107.1	+2.99
	mt (JJ)	B2540	9.46	109.5	+1.29
			9.34 (0.15)		+2.14 (1.2!)
060	q (JJ)	B2650	16.79	100.9	+10.86
	q (JJ)	B2651	15.50	93.1	+10.98
			16.15 (0.91)		+10.92 (0.08)
130	am .6A pick	A4125	(13.53)		(+8.45)
	am .6A pick	A4126	(12.45)		(+7.23)
	am .8B 90-45 µm (CB)	B2603	14.30		+7.60
	am .8B 90-45 µm (CB)	B2604	13.77		+7.58
			14.04 (0.37)		+7.59 (0.01)
160	q	B2479	15.79	94.9	+11.21
	q	B2480	16.47	99.0	+11.13
			16.13 (0.48)		+11.17 (0.06)
168	ch .9A 355-250 µm pick	B2511	13.47		+3.55
	ch .9A 355-250 µm pick	B2512	---.---		+3.58
			13.47		+3.57 (0.02)
168	kf	B2453	13.72	95.5	(+11.77)
	kf	B2454	13.89	96.7	+12.61
	kf	B2496	13.86	96.4	+12.36
			13.82 (0.09)		+12.49 (0.18)
168	q .11	B2521	16.51	99.2	(+11.05)
	q .11	B2522	16.59	99.7	+9.78
	q .11	B2527	16.24	97.6	(+10.44)
	q .11	B2528	16.93	101.7	+9.52
			16.57 (0.28)		+9.65 (0.18)
168	wr	B2375	13.39		(+10.64)
	wr	B2376	13.76		+11.72
	wr	B2449	(14.78#)		(+9.75)
	wr	B2450	12.45		+11.01
	wr	B2461	12.62		+11.42
	wr	B2462	12.56		+11.71
	wr	B2468	13.62		(+10.28)
	wr	B2482	(10.85#)		(+11.08)
	wr	B2483	13.44		+11.03
			13.12 (0.55)		+11.38 (0.35)

Sample no.	Rock or mineral with separate no.	Run no. (FS)	Yield (μ M mg^{-1})	Yield (%)	$\delta^{18}O$ (‰)
169	wr	B2455	13.37		+10.45
	wr	B2456	13.74		+10.47
	wr	B2475	(14.35#)		(+10.07)
			13.56 (0.26)		+10.46 (0.01)
170	wr	B2471	14.33		+8.94
	wr	B2472	14.24		+9.07
			14.29 (0.06)		+9.01 (0.09)
171	wr	B2473	13.59		+9.07
	wr	B2474	(15.95#)		(+10.53[a])
	wr	B2481	13.52		+8.95
			13.56 (0.05)		9.01 (0.08)
172	kf	B2441	13.06	90.8	+11.37
	kf	B2442	13.37	93.0	+11.38
	kf	B2477	13.78	95.9	(+15.63)
	kf	B2478	14.20	98.8	+10.93
			13.60 (0.50)		+11.23 (0.26)
172	q 4(H) >250 μm	B2497	16.32	98.1	+9.78
	q 4(H) >250 μm	B2498	16.49	99.1	+9.80
			16.40 (0.12)		+9.79 (0.01)
172	wr	B2451	12.21		+9.76
	wr	B2452	11.99		(+10.42)
	wr	B2465	13.11		+9.68
	wr	B2466	13.41		+9.86
			12.68 (0.69)		+9.77 (0.09)
173	wr	A3825	14.43		(---.---)
	wr	A3826	14.30		+9.17
	wr	B2457	12.48		+9.10
	wr	B2458	11.97		(+10.35)
	wr	B2469	12.35		+9.05
			13.11 (1.2!)		9.11 (0.06)
196	baryte (vein) $\delta^{34}S$ = +12.6 (JG-AB)				+4.6
196	cc (vein) $\delta^{13}C$ = -4.69 (CB)	C2579	8.24		+5.91
	cc (vein) $\delta^{13}C$ = -4.69 (CB) -4.69	C2580	8.68		+5.95
			8.46 (0.31)		+5.93 (0.03)
196	q	A4803	14.83	89.0	+10.49
	q	A4804	14.25	85.5	+10.11
			14.54[2] (0.41)		+10.30 (0.27)

[2] Low yield may be attributed to a poorly calibrated manometer.

Sample no.	Rock or mineral with separate no.	Run no. (FS)	Yield (μ M mg^{-1})	Yield (%)	$\delta^{18}O$ (‰)
B1248	am (JJ)	B2666	12.73		+6.45
	am (JJ)	B2667	12.70		+6.57
			12.72 (0.02)		+6.51 (0.08)
E43	am +65 -160 mesh (CB)	B2605	13.97		+7.51
	am +65 -160 mesh (CB)	B2606	13.87		+7.61
			13.92 (0.07)		+7.56 (0.07)
J001	am .10B 90-45µm (CB)	B2601	13.08		+7.84
	am .10B 90-45µm (CB)	B2602	13.95		+8.07
			13.52 (0.62)		+7.96 (0.16)
J002	q .3C 250-180 µm	A4124	15.42	92.7	+13.00
	q .3C 250-180 µm (CB)	A4129	15.11	90.8	+13.42
	q .3C 250-180 µm	B2657	16.32	98.1	+13.71
	q .3C 250-180 µm	B2662	15.23	91.5	+12.92
			15.52 (0.55)		+13.26 (0.37)
J003	q .6 pick	A4118	15.60	93.7	(+13.27)
	q .6 pick	A4123	16.16	97.1	+14.60
	q .7	B2644	15.96	95.9	+14.21
	q .7	B2645	16.33	98.1	+14.30
			16.01 (0.311)		+14.37 (0.2)
J011	am	A3814	13.34		+6.02
	am	B2447	11.66		+6.45
	am	B2448	12.73		+6.47
	am	B2489	(8.92#)		(+5.58)
	am	B2490	12.70		+5.99
			12.61 (0.70)		+6.23 (0.26)
J018	q .4A pick	A4112	15.93	95.7	+13.79
	q .4A pick	A4113	(25.66#)	154.2	(+12.38[a])
	q .4A pick	A4127	(14.00#)	84.1	(+12.49)
	q .4A pick	B2649	15.84	95.2	+13.29
	q .7 355-250 µm	B2655	16.37	98.4	+13.53
	q .7 355-250 µm	B2656	16.31	98.0	+13.86
			16.11 (0.27)		+13.62 (0.26)
J018	wr 250 mesh	A4121	13.92		+11.06
	wr 250 mesh	A4122	13.50		(+12.11)
			13.71 (0.30)		+11.06
J019	q .4 pick	A4114	(14.99#)	90.1	(+12.87)
	q .4 pick	A4115	15.90	95.5	+12.74
	q .7	B2647	16.85	101.2	+12.66
	q .7	B2648	16.31	98.0	+12.56
			16.35 (0.48)		+12.65 (0.09)

Sample no.	Rock or mineral with separate no.	Run no. (FS)	Yield (μ M mg^{-1})	Yield (%)	$\delta^{18}O$ (‰)
J019	wr 250 mesh	A4119	14.04		+9.40
	wr 250 mesh	A4120	14.78		+9.28
			14.41 (0.52)		+9.34 (0.08)
J029	q .5 pick	A4116	(26.98#)	162.1	(+13.17)
	q .5 pick	A4117	16.13	96.9	+11.91
	q .6 250-180 μm	B2660	15.95	95.8	+12.17
	q .6 250-180 μm	B2661	15.92	95.7	+12.32
			16.00 (0.11)		+12.13 (0.21)

A.2.3 Fluid inclusion volatile analyses.

Sample no., separate and run no.		H_2O (μM)	CO_2 (μM)	NCs (μM)	sample weight (g)	δD_{H2O} (‰)
GJ.3 Q.8D	BE	90.20	1.17	2.91	1.259	-19.6
HMC 4157	max	90.75	1.18	3.12		
	min	89.64	1.16	2.71		
GJ.60 Q	BE	35.10	0.74	4.16	1.279	-40.7
HMC 4156	max	35.88	0.75	4.45[1]		
	min	34.32	0.74	3.87		
GJ.160 Q.TREAT	BE	51.22	2.00	0.00	1.017	-31.6
180-125 μm	max	51.66	2.02	0.00		
HMC 4153	min	50.79	1.98	0.00		
GJ.160 Q.TREAT	BE	105.16	3.59	2.91	1.964	-29.7
180-125 μm	max	105.74	3.63	3.12		
HMC 4154	min	104.57	3.56	2.71		
GJ.160 Q.TREAT	BE	102.00	3.10	2.08	2.058	-27.3
125-90 μm	max	102.51	3.13	2.23		
HMC 4155	min	101.48	3.07	1.94		
GJ.160 Q.TREAT	BE	77.13	2.28	4.12	1.722	-35.3
125-90 μm	max	79.66	2.31	5.02		
HMC 4489	min	74.58	2.26	3.25		
GJ.160 Q.TREAT	BE	119.54	>2.05	5.49	2.711	-35.4
90-45 μm	max	121.99	2.07	6.65		
HMC 4493	min	117.01	2.03	4.37		
GJ.196 Q.6 (rock)	BE	174.86	2.57	1.76	2.781	-27.1
HMC 4485	max	177.46	2.59	2.22		
	min	172.21	2.54	1.35		
GJ.196 cc pick (vein)	BE	154.47	--.--[2]	0.78	2.822	-24.4
HMC 4496	max	156.38	--.--	1.05		
	min	152.51	--.--	0.56		
GJ.213 Q.11	BE	126.29	2.14	1.18	2.196	-24.4
HMC 4478	max	127.96	2.16	1.52		
	min	124.60	2.12	0.87		

[1] The high fraction of non-condensibles in this analysis is probably due to a minor leak in the extraction line.

[2] Not measured because large amounts of CO_2 produced by breakdown of calcite.

Sample no., separate and run no.		H_2O (μM)	CO_2 (μM)	NCs (μM)	sample weight (g)	δD_{H2O} (‰)
GJ.213 Q.11	BE	121.04	2.20	1.76	2.016	-25.6
HMC 4490	max	122.79	2.22	2.22		
	min	119.24	2.17	1.35		
GJ.220 Q.6	BE	197.63	3.05	2.75	2.769	-19.1
HMC 4491	max	200.93	3.08	3.38		
	min	194.31	3.01	2.14		
GJ.220 Q.6 pick	BE	101.23	1.82	5.10	1.507	-17.6
HMC 4495	max	103.64	1.84	6.19		
	min	98.78	1.80	4.05		
B.2085 Q.11	BE	16.27	0.85	0.20	0.938	-68.9
HMC 4480	max	19.64	0.86	0.35		
	min	12.91	0.84	0.08		
T.5 Q.11	BE	65.67	2.43	0.20	1.628	-42.9
500-350 μm	max	66.71	2.45	0.35		
HMC 4479	min	64.60	2.40	0.08		
T.5 Q.11	BE	106.62	3.86	0.20	2.738	-34.9
500-350 μm	max	108.10	3.90	0.35		
HMC 4482	min	105.11	3.82	0.08		
T.5 Q.11	BE	101.72	3.31	5.10	2.796	-31.4
500-350 μm	max	104.13	3.34	6.19		
HMC 4484	min	99.27	3.28	4.05		
T.5 Q 180-125 μm	BE	86.83	1.52	5.49	2.833	-35.6
HMC 4494	max	89.44	1.54	6.65		
	min	84.18	1.51	4.37		
T.6 Q.3 350-250 μm	BE	57.61	3.31	0.20	2.107	-36.1
HMC 4410	max	58.55	3.34	0.35		
	min	56.64	3.27	0.08		
T.6 Q.3 350-250 μm	BE	82.78	1.97	0.20	2.707	-51.2
HMC 4488	max	84.52	1.99	0.35		
	min	81.00	1.94	0.08		
T.6 Q 180-125 μm	BE	74.73	2.07	4.31	3.046	-41.1
HMC 4492	max	77.32	2.09	5.25		
	min	72.10	2.05	3.41		

abbreviations: BE = best estimate, max = maximum and min = minimum.

The maximum and minimum values take into account the uncertainties associated with the regression lines as well as that associated with reading errors.

A.2.4 Electron microprobe analyses.

Epidotes.

	GJ.19		GJ.34		GJ.43		GJ.60	
	Wt.%	σ_{n-1}	Wt.%	σ_{n-1}	Wt.%	σ_{n-1}	Wt.%	σ_{n-1}
SiO_2	37.00	0.44	36.93	0.32	36.83	0.29	36.63	0.35
Al_2O_3	25.74	1.09	23.97	1.00	22.47	0.42	21.83	1.14
Fe_2O_3	10.71	1.48	13.21	1.32	15.25	0.48	15.56	1.27
Mn_2O_3	0.36	0.18	0.16	0.19	0.17	0.19	0.20	0.16
MgO	0.01	0.04	0.02	0.04	0.04	0.09	0.02	0.07
TiO_2	0.01	0.04	0.05	0.07	0.03	0.07	0.26	0.38
CaO	23.26	0.23	23.16	0.36	22.87	0.28	22.94	0.33
H_2O	2.44	0.04	2.13	-.-	2.02	-.-	2.38	-.-
	99.53		99.64		99.68		99.82	

Number of cations per formula unit of 25 oxygens.

Si	5.893		5.908		5.925		5.921	
$Al_{(tet)}$	0.107		0.092		0.075		0.079	
	6.000		6.000		6.000		6.000	
$Al_{(oct)}$	4.726		4.429		4.186		4.081	
Fe^{3+}	1.284		1.591		1.846		1.893	
	6.010		6.020		6.032	Mn^{3+}	0.025	
							5.999	
Mn^{3+}	0.043		0.019		0.020			
Mg	0.002		0.005		0.010		0.005	
Ti	0.001		0.006		0.004		0.032	
Ca	3.969		3.970		3.942		3.973	
	4.015		4.000		3.976		4.010	
Mol.%	21.35	3.07	26.44	2.77	30.61	1.00	31.80	2.87
pistacite.		(σ_{n-1})		(σ_{n-1})		(σ_{n-1})		(σ_{n-1})
n =		10		19		10		12

Notes: It is assumed that all Fe and Mn ions in these epidotes are present in their trivalent states. The analyses are of the mineral separates which were analysed isotopically. Between one and three spots were analysed per grain and the composition of each grain was averaged prior to finding the mean and standard deviation of a number of grains (n). H_2O contents were calculated from the yield of hydrogen during hydrogen isotope analysis. However they are unusually high probably due to the presence of small amounts of chlorite in the sample (4.3.3). Because of this apparently high H_2O content the hydrogen was excluded when calculating formulae and the cations were calculated to 25 oxygens per formula unit. The mole % of pistacite ($Ca_2Fe_3Si_3O_{12}(OH)$) was calculated from the octahedral site occupancies on the basis of 25 oxygens.

GJ.029 amphibole separates.

	Light fraction		Heavy fraction	
	Wt.%	σ_{n-1}	Wt.%	σ_{n-1}
SiO_2	52.15	2.38	49.21	1.68
Al_2O_3	4.54	2.22	7.35	1.51
TiO_2	0.34	0.27	0.80	0.40
MgO	17.69	1.21	15.90	0.54
FeO	8.90	0.79	10.05	0.50
MnO	0.13	0.05	0.14	0.07
CaO	12.47	0.93	12.34	0.20
Na_2O	0.34	0.35	0.73	0.21
K_2O	0.22	0.17	0.50	0.53
H_2O	2.49	0.23	2.32	0.11
	99.27		99.37	

Number of cations per formula unit of 23 oxygens.

Si	7.469	7.114
Al(tet)	0.531	0.886
	8.000	8.000
Al(oct)	0.236	0.367
Ti	0.037	0.087
Mg	3.776	3.425
Fe^{2+}	0.951	1.121
	5.000	5.000
Fe^{2+}	0.115	0.094
Mn	0.016	0.017
Ca	1.914	1.911
	2.045	2.022
Na	0.094	0.205
K	0.040	0.098
	0.134	0.303
$Mg/(Mg+Fe_{tot})$ =	0.78	0.74

Notes: The analyses are of the mineral separates which were analysed isotopically. Between one and three spots were analysed per grain and the composition of each grain was averaged prior to finding the mean and standard deviation of nine grains. H_2O contents were calculated from the yield of hydrogen during hydrogen isotope analysis. However they are unusually high probably due to the presence of small amounts of chlorite in the sample (4.3.1). Because of this apparently high H_2O content the hydrogen was excluded when calculating formulae and the cations were calculated to 23 oxygens per formula unit. No attempt was made to estimate Fe^{3+} content by recalculation procedures, and all Fe is assumed to be present as Fe^{2+}. Using this assumption the tetrahedral+octahedral total is only just >13 (~13.1 cations/23 oxygens) which would tend to support the proposal that the amount of Fe^{3+} is relatively low. From recalculation of the EDS spectrum the light fraction is estimated to contain ~0.1 wt.% Cl.

A.3 SAMPLE LOCALITIES AND DESCRIPTIONS.

Samples GJ... are my own samples, samples AY... were kindly supplied by Y. Ahmed-Said further information on these samples can be found in Yousef (1988). Samples BL... , E... and J... were kindly supplied by B.E. Leake, E.M. Elias and M.D. Jagger respectively.

The six figure number is the grid reference on the Irish National Grid. Minerals are listed in approximate order of decreasing abundance. Opaque oxides and sulphides were partially identified from their colour in reflected light in an ordinary thin section (i.e. steel coloured grains = opaques, brassy coloured grains = sulphide) and then further identified by means of their magnetic properties during mineral separation (i.e. brassy magnetic grains = pyrrhotite, black metallic grains = magnetite, brassy non-magnetic grains = pyrite) XRD analysis of a few mineral separates supported this identification scheme.

Abbreviations: MX = megacrystic, OX = oikocrystic, PC = a modal analysis by point counting is tabulated in A.n, → = altering to, transg = transgranular, intrag = intragranular, interg = intergranular.

GJ.1 781.425 Roundstone granite. Northeastern side of granite. ~ 500 m down track opposite Sunset Cottage, Cashel, in field on left. ~ 1160 m from granite contact. Orth (faintly turbid, microperthitic), plag (zoned,→ ser), qtz, bi (→ chl), hb, ap, sph, mt. Rock faintly foliated, some rusty stains around some of the mafic minerals, possible miarolitic cavities present.

GJ.2 784.428 Roundstone granite. Northeastern side of granite. On shoreline in small inlet to W of Sunset Cottage. ~ 700 m from granite contact. Orth (faintly turbid, XRD indicates contains celsian), plag (zoned, → ser), qtz, bi (→chl), sph, hb (→chl), mt, ap, zirc. Chlorite-quartz filled transg microcrack.

GJ.3 788.429 Roundstone granite. Northeastern side of granite. Just behind last wall before open country to E of Sunset Cottage. ~ 320 m from granite contact. Orth (OX, strongly turbid, microperthitic, XRD indicates contains celsian), plag (zoned, → ser + cc), qtz (contains abundant bubble planes of 2 and ? 3 phase inclusions - l+v±s), chl (after bi, ilmenite, sphene or TiO_2 inclusions), sph (→ TiO_2+cc), hb (→chl+cc), mt (→chl), ap, cc. Feldspar is bright pinky red in hand specimen. cc-?prehnite filled microcracks (transg, interg, intrag.).

GJ.4 789.431 Roundstone granite. Northeastern side of granite. To NE of Sunset Cottage. ~ 50 m from contact. Orth (MX, faint turbidity), plag (zoned, → ser), qtz (bubble planes), bi (→chl + ep + TiO_2 ± sph + ?prehn), hb (→chl), mt (→?ep), sph, ap. qtz-cc transg microcrack. Small ?miarolitic cavities.

GJ.5 790.431 Roundstone granite. Northeastern side of granite. To NE of Sunset Cottage. ~ 10 m from contact. Orth (faintly turbid, microperthitic), plag (zoned, → ser ± ep), qtz, bi (chl + TiO_2), hb (→ chl), mt, sph, ap.

GJ.6 792.432 Intermediate gneiss (MGS). SW of summit of Cashel Hill. ~ 30 m from contact with Roundstone granite. Plag (MX, strongly → ser ± ep), qtz (bubble planes with 2 phase l-v inclusions), chl (from bi?, ep inclusions), mt (→chl), sulphide. Large transg branching microcracks containing plag, plag-cc, cc-qtz-?prehn, plag-ep-cc assemblages cross cut the strong foliation.

GJ.7 794.431 Intermediate gneiss (MGS). SW of summit of Cashel Hill. ~ 170 m from contact with Roundstone granite. Plag (strongly → ser + ep), qtz, hb (→bi), bi (faintly chloritised, decussate texture indicates may be a thermal effect from the granite), sph (after mt?), mt, ap. Strongly foliated. Contains sheared zones of qtz, ser, opaques, sph, ep.

GJ.8 797.433 Intermediate gneiss (MGS). SW of summit of Cashel Hill. ~ 450 m from contact with Roundstone granite. Plag (strongly → ser + cc), qtz (bubble planes), chl (+TiO_2±ilmenite±cc - after bi), hb (→chl+TiO_2), mt (→chl), sph?, ap, sulphide (→hem?). Large transg cc, cc-qtz microcracks cut strong foliation. Interg cracks filled with sericite occur in areas of polycrystalline quartz.

GJ.9 800.436 Ultrabasic-basic metagabbro (MGS). ~ 30 m on a bearing of 161° from new trig. point on summit of Cashel Hill, at top of gully trending ~080°. Plag (→ ser + ep, ~An_{78}), hb (OX, →ep ± chl), ep (after hb), pyrite, mt (→chl), qtz (interstitial and blebby inclusions in hb), chl (after bi?). Hornblende varies in composition in patches to a pale actinolitic amphibole over a very short distance. This might relate to the former presence of clinopyroxene.

GJ.10 800.438 Hornfelsed psammitic screen of metasediment within the MGS. ~ 30 m on 031° from new trig. point on summit of Cashel Hill. Qtz (bubble planes with 2 and ?3 phase inclusions l-v-s), plag (→ser), bi (→chl + TiO_2), ep, mt (→chl), sulphide. Faint planar fabric. Intrag, interg and transg microcracks present, some filled with epidote, others empty.

GJ.11 806.447 Microcline granite sill (Cashel Sill) on N side of Cashel intrusion. Micr (OX, turbid, perthitic), plag (strongly → ser), qtz (bubble planes 2 and ?3 phase inclusions l-v-s), bi (→chl±ep±TiO_2), ap, sph (→TiO_2), zirc, opaques + sulphides, allanite.

GJ.12 837.450 Contaminated ultrabasic rock (MGS). N side of small island N shore of L. Wheelaun. Plag (zoned, →ser±ep), anthophyllite (after opx?, fibrous, →bi + chl + qtz), bi (only slightly chloritised), mt, sulphide, qtz (odd irregular masses). Rock is well foliated and contains partially assimilated xenoliths of country rock containing green (?pleonaste) spinel and ?diaspore after corundum.

GJ.15 873.397 Galway granite, Murvey phase. NW facing quarry just before bend in Cashel-Screeb road, NE of Benagower. ~ 30 m from contact of Galway batholith. Orth (faint turbidity, perthitic, MX, OX), plag (zoned, →ser), qtz (a few bubble planes with 2 phase l-v inclusions), bi (quite fresh,→chl ± ep ± TiO_2), mt (→ep), ap. Intrag and interg cracks in quartz, mostly empty but sometimes with red colouration = iron oxide?).

GJ.16 872.398 Intermediate gneiss (MGS). ~ 10 m to NE from NE corner of small unnamed lough NW of sample GJ.15. ~110 m from the contact. Plag (→ser or fine acicular hb), hb (→fine acicular hb), qtz (→ acicular hb, some bubble planes with 2 phase l-v inclusions), ep, mt, cc. Well foliated. Narrow cc filled interg microcracks occur in areas of polycrystalline qtz.Fine plag and mt forms veins or shear zones. Much of the early coarse hb appears to be associated with minor shear planes in the rock. Late fractures along these hb rich planes sometimes contain brown iron oxides.

GJ.19 865.412 Altered basic metagabbro (MGS). SE corner of small lough to the SE of L. Curreel. Ep, qtz (large grains strained - smaller ones at margins are not suggesting that grain diminution has taken place), plag (ser + ep), sulphide, zirc. The rock is well foliated consisting of alternating fine bands of qtz and ep. This assemblage must have resulted from the alteration of the basic metagabbro which made up the rest of the outcrop from which this sample was taken. Qtz and qtz-ep veins ~ 50 μm wide cut the foliation.

GJ.25 835.446 Fine grained basic xenolith (MGS) in basic metagabbro (GJ.26). SW of L. Wheelaun. Hb (→ chl+sph), plag (strongly →ser), chl (+?prehn±sph -after bi), pyrite, pyrrhotite, ap, cc. Foliation cut by branching transg microcracks containing cc-act, act, cc-plag, plag-sulphide-act assemblages. Plagioclase contains intrag chlorite filled microcracks.

GJ.28 835.444 Basic metagabbro (MGS) SSW of L. Wheelaun. PC. Hb (OX, contains patches of actinolitic amphibole), plag (→ ser+ep), chl (after bi?), sph, pyrrhotite + pyrite (→hem?), ?mt (→ep), qtz, ep, ap, cc. Plag-chl-act filled transg microcracks occur. Intrag cracks in plag filled with chl.

GJ.29 836.443 Ultrabasic metagabbro (MGS). S of L. Wheelaun. Cpx (→act forming an intimate intergrowth of the two minerals), act (in places some rather browner hb does not contain cpx relics, OX), plag (strongly →ser, flakes up to 200 μm in dia., often has rounded margins against act and may be totally enclosed by it), pyrrhotite+pyrite (→?ep, pyrr by XRD), qtz.

GJ.34 838.442 Ep vein in basic metagabbro (MGS). W of Cahereeshal L. Two parallel veins each ~ 2 mm wide contain eu-subhedral qtz crystals ~ .2 mm dia. × .4 mm long mostly growing from the vein walls and overgrown by larger eu-subhedral ep crystals up to 3 mm long. Some qtz has infilled voids at the centre of the veins, some void space also occurs. V. minor sodic plag may also occur. Qtz contains small ?primary l-v inclusions. Host basic rock is now almost entirely converted to ep + chl (after bi) within 2 mm of the veins. Further away from the vein the

amount of hb increases although it is still being replaced by ep. No plag is observed in the host rock.

GJ.35 841.442 Intermediate rock (MGS). N shore of Cahereeshal L. Plag (almost totally →ser), qtz (abundant bubble planes, inclusions mostly small), ?hb (now totally →chl + cc), bi (totally → chl + TiO_2 + ep), mt (→chl), sulphide, zirc. Rock only weakly foliated.

GJ.43 856.437 Intermediate gneiss (MGS). In gneisses to the E side of L. Wheelaun body. Plag (MX,mildly →ser, twinning easily seen and often kinked or offset along small fractures), qtz (strained, abundant bubble planes with l-v inclusions), bi (→chl + TiO_2). Rock cut by many transg branching ep veins up to 1.5 mm across. Ep in some veins is very fine grained <10 μm while in other grains it is coarse > 100 μm. Transg ep-plag and plag veins also occur. Host rock feldspar often contains many intrag microcracks filled with fresh feldspar or chl.

GJ.60 853.438 Intermediate gneiss (MGS). In gneisses to the E side of L. Wheelaun body. PC. Plag (MX, →ser), qtz (bubble planes with l-v inclusions), hb (OX, some colour zonation), chlorite (with ep after bi?), ep, orth (weakly turbid), ap, mt, zirc, sph, cc.

GJ.130 819.444 Dalradian amphibolite. Lakes Marble Formation to E of Cashel metagabbro mass. Hb (fresh, brown), plag (almost totally fresh in places, →ser near microcracks), mt, sulphide. Well foliated, occasional segregations or veins of coarser plag occur parallel to the foliation. Foliation cut by thin (~ 20 μm across) plag filled microcracks around which the alteration in the plagioclase is much more intense.

GJ.160 807.447 Milky quartz vein cutting microcline granite sill ~ 20 m to NE of sample GJ. 11. The quartz comes from the centre of a composite vein within the microcline granite sill. The outer margins of the vein were composed of coarse K-feldspar (GJ.159). This vein may be a late segregation of residual material from the sill, the relationship of the vein with the country rock was not observed.

GJ.166 (band e) 809.446 Clinopyroxene rich layer from outcrop of layered ultrabasic metagabbros (MGS), locality 42. Northern side of Cashel Hill metagabbro mass. PC. Cpx (→hb), hb (OX, dark brown, intimately replacing and surrounding cpx), opx (→unidentified mineral), plag (→clinozoisite or chl), bi (fresh!, nearly always occurs in hb and may be replacing it), mt, sulphide.

GJ.168 Plagioclase porphyry dyke running along granite contact, on traverse between GJ.169 and GJ.173. Plag (MX,→ser, turbid yellowy colour in t.s. but zoning and twinning still seen), qtz (only a few bubble planes with l-v inclusions), orth (strongly turbid, due to many fine ?microtubes ~10 μm long × 0.25 μm wide), bi (mostly →chl+TiO_2+ilmenite?), cc, opaque, ap, sph (totally pseudomorphed by ?TiO_2). Both plag and K-feldspar are orangy-pink in hand specimen.

GJ.169 793.430 Dalradian psammite ~ 10 m from contact of Roundstone granite, NE of Bolgers public house, Cashel (Doonreaghan). Qtz (abundant bubble planes with l-v inclusions cross cut foliation at ⊥ over whole slide and therefore may run at ⊥ to the granite contact), plag (→ser), bi (mostly →chl), sulphide, opaque. Foliation cut at ~⊥ by 0.6 mm wide calcite vein.

GJ.170 Roundstone granite. ~ 40 m from granite contact, on traverse between GJ.169 and GJ.173. Orth (faintly turbid, microperthitic), plag (good zoning, mostly fresh only a few cores →ser), qtz (contains only a v. few bubble planes), bi (only minor → chl), hb, sph, opaque, ap, zirc. A few open transg cracks occur.

GJ.171 Roundstone granite. ~ 60 m from granite contact, on traverse between GJ.169 and GJ.173. Orth (only weakly turbid and microperthitic), plag (zoned, a few cores →ser), qtz (only a v. few bubble planes), bi (only minor →chl), hb, sph, opaque, ap.

GJ.172 Roundstone granite. ~ 85 m from granite contact, on traverse between GJ.169 and GJ.173. Orth (faintly turbid, pink in hand specimen), plag (MX, zoned, →ser), qtz (a few bubble planes with l-v inclusions), bi (→chl), hb, sph, mt.

GJ.173 792.429 Roundstone granite. ~ 120 m from granite contact. NE of Bolgers public house, Cashel (Doonreaghan). Orth (OX, only turbid in places, microperthitic), plag (zoned, mostly fresh only a few cores →ser), qtz (bubble planes rare), bi (only minor →chl), hb, opaque, sph, ap.

GJ.196 825.437 Intermediate gneiss (MGS). From blasted outcrop on W side of the N-S road from Cashel X to Recess X, just N of turning to Lettershanna and S of L. Nambrackeagh. Plag (strongly →fine ser ± cc, coarse ser developed along plag-plag grain boundaries, twinning sometimes still visible), qtz (undulose extinction indicates is highly strained, contains subparallel bubble planes which run at a high angle to foliation), chl, mt (→ chl), rutile?. Well foliated. In thin section numerous microcracks, some of which branch at high angles, cut rock. These are filled with cc-qtz, cc-TiO_2 and cc-ser assemblages. In the hand specimen foliation in rock is cross cut by a number of veins, one of which is ~ 1 cm thick. Euhedral quartz crystals up to 5 mm long by 2.5 mm dia., but mostly < 1 mm long and tabular platy baryte crystals have grown from the vein wall. The quartz crystals are clear at their tips but often cloudy at the base. Coarse honey coloured calcite infills the remaining space in the vein, growing on top of quartz and baryte, indicating that it may have been deposited later. Some surfaces along the margins of veins and minor joint surfaces in the host rock show slickensides.

GJ.203 632.438 Ballyconneely amphibolite SE of Ballyconneely. Hb (green prismatic, max prism length ~300 μm, av = ~100 μm, →bi in places), plag (very weak →ser even near to ep microcracks), opaque (oblong grains ~80×5 μm), sulphide (subhedral, porphyroblasts? ~200×200 μm ?growing across foliation), sph, ep, qtz. Fine grained, very well

defined almost slaty foliation. Foliation cut by epidote veins with minor qtz ~300-600 μm wide. These veins are themselves cut and sometimes offset by thin (~30 μm wide) ep and chl filled microcracks. The rock for ~10-20 μm around the chlorite vein contains more opaque material and the hb →chl.

GJ.206 644.440 Amphibolite in Delaney Dome Formation. E. of Ballyconneely. Act (prismatic-acicular-fibrous), ?plag (totally →coarse ser + ep, ser flakes ~20 μm dia), sph,ap. Fine grained. Strong foliation. one very thin transg quartz filled microcrack.

GJ.207 642.479 Ballyconneely amphibolite. On S shore of Errislanan peninsula, W of Ballinaboy. Hb (green prismatic, prisms up to ~600 μm long av = ~200 μm), plag (v. weak →ser, even near ep veins), opaque (oblong ~60×10 μm, often rimmed by sph), sph, ep, sulphide (subhedral porphyroblasts? ~200×200 μm. V. fine grained. Amphibole strongly lineated, planar fabric much more difficult to identify. Rock contains patches (?segregations) ~2 mm across containing coarse plag with minor anhedral opaque grains and large subhedral sulphide grains which are sometimes rimmed by hematite. Foliation is disturbed or indistinct around the segregations suggesting that they might haveformed after the foliation. The foliation and segregations are cut by two sets of microcracks. An early microcrack ~1 mm wide contains coarse ep with minor plag + qtz. The opaque material within 10-20 μm of this vein appears to be altering to sphene or rutile. On one side of the microcrack a wedge shaped area of host rock (~1 cm long and 5 mm wide at the microcrack) running parallel to the foliation has been altered to ep + plag + qtz. There is no apparent reason why only this specific area has been altered. The second set of microcracks cuts the first and the altered wedge related to the first and contains ep + fresh plag + act + chl assemblages.

GJ.213 881.392 Galway granite, Errisbeg Townland phase. W of L. Avally, just S of road. Orth (OX-MX grains up to 1×1.5 cm with chl, plag or opaque inclusions, weakly turbid, minor microperthite), plag (→ser mostly fine < 10 μm dia. some flakes up to 500 μm dia. ±cc, twinning still seen in most grains), qtz (occasional bubble planes of l-v inclusions), chl (after bi, minor opaque + rutile inclusions, often surrounded by cc), sphene (euhedral, fresh or totally pseudomorphed by rutile or rutile and cc), mt (→ chl), ap, zirc (zoned!). The orth is bright pink in hand specimen, while the plag is pale greenish. A few cc-qtz-fsp-ser filled microcracks seen in the thin section.

GJ.220 789.340 Galway granite, Murvey phase. ~ 50 m E of Carna road, to E of L. Bola. Orth (OX - up to 5 mm dia., v. strongly turbid in places due to v. fine microtubes, →cc! fine perthite in places), plag (→ v. fine ser±cc±chl, rather turbid, twinning still visible, weakly zoned), qtz (rather undulose extinction, contains many bubble planes of l-v inclusions in a number of orientations), chl (inclusions of minor opaque material), opaque, zirc. All the feldspar is pink in hand specimen. Intrag microcracks present along cleavages in feldspars as well as some transg microcracks, both contain chl or chl-K-fsp-cc assemblages.

GJ.226 784.356 Epidote layer in intermediate member of MGS. N side of quarry to W of Carna road to E of Knockboy Hill. ~400m from contact of Galway granite. Host rock: qtz (bubble planes extremely rare, occasional single l-v inclusions occur), plag (→ser + ep, a few grains seem to be recrystallised to v. fine material and contain many fine < 4μm dia. grains of cubic opaque material), hb, sph, large cubic subhedral sulphide crystals, v. minor chlorite. The rock is gneissose but the bands are v. narrow ~ 0.5 mm. The major epidote layer = ?vein is ~ 7 mm thick and is parallel to the foliation. The outer margins of this ?vein are often rich in altered plag and quartz so that they appear white in hand specimen. Epidote layers occur in host rock on one side of the main ?vein so that it is possible that these layers could be an original layer or segregation rather than a vein. The main ?vein consists mostly of interlocking epidote grains which are rather grainy in appearance, minor qtz, plag sph also occur. Other veins occur cross cutting the main ?vein and foliation, the largest of which consists of less grainy looking, coarser grained epidote with minor cc. The edge of this vein "disappears" when it passes through a quartz rich area. Sph cannot be found within this vein but it is still present in the host rock at its margins. Other veins have similar lithologies and are as difficult to trace across quartz rich regions. Another vein is mostly plag and fine cubic opaque material - similar to that seen in some plag grains, with some ep.

GJ.234 823.464 Dalradian pelitic schist, Lakes Marble Formation. ~ 10 m E of road ~ 300 m S of Recess X. ~ 1 m away from calcite marble band. Bi (→chl), plag (mildly →ser), qtz, musc, pyrite. Segregations of coarse plag and quartz occur. The coarse plag is similar to the groundmass plag, the quartz contains many more bubble planes than the groundmass quartz. All bubble planes are ~ parallel and run at a high angle to the schistosity and are made up of small apparently l-v inclusions. Two late irregular chlorite-sulphide veins cut the schistosity, segregations and possibly the bubble planes.

GJ.238 837.477 Dalradian pelite, Streamstown Formation. On the E side of the Glen Inagh road out of Recess ~ 100 m from junction. Qtz (bubble planes ~ parallel throughout slide), plag (→ser), chl (+TiO_2+ep - after bi), pyrite, ap. A schistosity is not apparent, the rock appears almost isotropic, possibly because of mobilisation during partial melting. A thin ~ 10 μm transg microcrack filled with plag-qtz-cc runs ~ parallel to the bubble planes while a qtz-plag microcrack runs at right angles.

AY.1 813.460 Dalradian migmatite, Cashel Formation. ~300 m S of SE point of Athry L. Bi, plag, qtz, ser, sillim, gt, ap, musc.

AY.4 809.460 Dalradian migmatite, Cashel Formation. ~300 m SSW of SW point of Athry L. Bi, qtz, plag, sillim, gt, ser, zirc, ap.

AY.10 785.462 Dalradian migmatite, Cashel Formation. ~700 m SW of Ballinafad. Bi, plag, qtz, cord, gt, sillim, ser, opaque, zirc, ap.

AY.13 807.454 Dalradian migmatite, Cashel Formation. ~1 km SSW of SW point of Athry L. Bi, plag, qtz, sillim, ser, cord, musc, K-fsp,gt.

AY.50 786.459 Dalradian migmatite, Cashel Formation. ~850 m SSW of Ballinafad. Bi, plag, ser, gt, cord, chl, opaque, ap.

BL.1248 830.435 Intermediate gneiss (MGS). ~ 200 m NNW of the summit of Lettershanna Hill. PC. Plag (MX, →ser + ep, twinning still observed in most grains), qtz (a few bubble planes), bi (nearly all →chl+ep+TiO_2). hb (minor → chl± cc), mt, pyrite, sph, ap.

BL.2085 862.387 Galway granite, Errisbeg Townland phase (NB location according to Leake 1970a puts within outcrop of Murvey phase on Connemara map). N. of summit of Benagower. Sample is described in further detail, with a chemical and modal analysis in Leake (1970a). Plag (zoned, →ser+ep), orth (MX, microperthitic, turbid), qtz (bubble planes fairly abundant, some l-v inclusions are up to 5μm), bi (→chl+ep), hb, mt, ap, zirc, sph.

E.43 809.432 Dalradian amphibolite, Lakes Marble Formation. S of Cashel Hill metagabbro mass. Sample description from Elias (1985): "hornblende, green in places altered to chlorite; plagioclase, sericitised; quartz; clinopyroxene (diopside); iron oxide."

E.44 806.433 Basic metagabbro (MGS). S side of Cashel Hill metagabbro mass. Unfortunately no sample description given by Elias (1985).

J.1 806.444 Contaminated ultrabasic rock (MGS). ~ 1 m away from N margin of Cashel Hill intrusion. PC. Hb (OX - contains cpx + rounded plag, also contains patches of fibrous act which have sharp contacts with the brown hb), plag (→ ep±ser, twinning still observed in many grains), bi (→ ?prehn, mostly still brown), qtz (interstitial, only a few fluid inclusions), pyrrhotite, mt (→chl), ap. On a hand specimen scale the rock contains partially assimilated pelitic xenoliths (Jagger, 1985).

J.2 806.444 Contaminated ultrabasic rock (MGS). ~ 50 cm away from N margin of Cashel Hill intrusion. Same locality as J.1. Plag (→ser +ep, twinning still seen), hb (mostly →fibrous act), bi (→prehn, mostly still brown), pyrrhotite, ?mt, qtz (interstitial), ap. Xenoliths contain ep, ser and opaque material with ?diaspore after corundum?

J.3 806.444 Hornfelsed Dalradian semipelite. ~ 50 cm from the contact with the Cashel Hill metagabbro mass, same locality as J.1. Cord (totally →ser ± chl), qtz (few bubble planes), bi (v. minor →chl + TiO_2), plag (minor →ser), gt (highly fractured, cracks filled with ser + chl), opaque, pyrrhotite.

J.11 843.440 Basic metagabbro (MGS). N shore of Cahereeshal L. This is the locality from which Jagger (1985) obtained a zircon Pb-Pb date of 487±3 Ma and Elias (1985) obtained an amphibole K-Ar date of 486±9 Ma (EL.94). Plag (→ ser ± ep, twinning easily visible), bi (→ chl + prehn), hb (qtz, plag, ap inclusions), qtz (only a few bubble planes), opaque, sulphide, ap, zirc.

J.18 803.452 Semi-pelitic Dalradian migmatite. N of Cashel Hill metagabbro mass. Qtz (few bubble planes), bi (→ fibrolite, also →chl ±

TiO_2 needles), plag (→ ser), orth (faintly turbid, microperthitic), muscovite, opaque, ap, zirc. Garnet occurs in part of the rock but not the t.s.

J.19 803.452 Semi-pelitic Dalradian migmatite. N of Cashel Hill metagabbro mass. Qtz (v. few bubble planes), bi (→fibrolite, also →chl ± TiO_2, also to musc?), plag (mildly → ser), orth (in leucosome, weakly turbid, → large ragged musc flakes), zirc, ap. Leucosomes dominantly qtz + orth, paleosome dominantly bi, qtz, plag.

J.29 806.444 Hornfelsed Dalradian metasediment. ~ 2 m from contact with Cashel Hill metagabbro mass, same locality as J.1. Qtz (v. few bubble planes), ?cord (now totally → ser + cc), plag (→ser), gt (cracked, →chl along cracks in places), bi (v. dark and grainy), opaque, ap, zirc.

J.57 825.419 Acid gneiss (MGS). ~ 700 m ESE of Cashel X. Qtz (few bubble planes), plag (strongly → ser, twinning only just observable in some grains), micr (OX, inclusions of rounded plag and qtz and opaque mineral, weakly turbid, small amount of perthite), chl (+ TiO_2 + ep - after bi), opaque (→ chl or sph), sulphide, sph, zirc. A K-fsp-cc-ep transg microcrack runs across the slide.

J.61 818.424 Acid gneiss (MGS). On E side of road ~ 200 m N of Cashel X. Qtz (contains l-v inclusions although bubble planes are difficult to make out), plag (→ ser, twinning easily seen), orth (OX with plag inclusions, →micr, strongly turbid, minor perthite), chl (+ TiO_2 + ep - after bi), sulphide (→ ?hem). Many ~ parallel transg branching microcracks up to .2 mm wide cut across slide. In the orth megacrysts some of these microcracks change direction slightly to follow cleavage. All of these cracks contain an unusual acicular epidote like mineral with minor new plag and quartz.

J.86 830.431 Acid gneiss (MGS). ~ 250 m SSE of summit of Lettershanna Hill. Qtz (a number of bubble planes, large l-v inclusions), orth (OX with rounded quartz and plag inclusions, some grains strongly turbid, some → micr, minor microperthite), plag (→ ser, twinning mostly still visible), chl (+ TiO_2 + ep - after bi), hb (→ ?bi → chl...), opaque, sulphide (→ ?hem), ap, zirc.

J.87 830.431 Acid gneiss (MGS). Same locality as J.86. Qtz (bubble planes rare), orth (OX with qtz, chl, plag inclusions, strongly turbid, → micr, microperthitic), plag (strongly → ser + ep, no twinning observable), chl (+ TiO_2 + ep - after bi), opaque, ap, zirc. Transg K-fsp-plag-ep filled microcrack runs across slide. K-fsp in this crack is also turbid.

J.149 838.449 Pegmatite vein in ultrabasic rocks S shore of L. Wheelaun. Qtz (bubble planes numerous and in a number of orientations), orth (MX, strongly turbid, perthitic), chl (large flakes up to 8 mm dia. with TiO_2 + minor ep obviously after bi), musc (large flakes up to 10 mm dia., also as

much smaller grains around chl. Plag also occurs in hand specimen but is not observed in t.s. Intrag cracks in orth filled with fresh fsps-qtz-ser.

T.5/T.6 666.478 Quartz veins in Ballyconneely Amphibolite. Quarry on N side of Bog road, just before bend ~600 m E of Ballinaboy. This is locality 1740 of P.W.G. Tanner. Quartz veins ~2 cm (T.6) and ~1 cm (T.5) thick in very fine grained, almost slatey, Ballyconneely Amphibolite. The veins are concordant to the foliation. T.6 is quite milky and opaque in hand specimen, while T.5 is more translucent. T.6 has a thin ~2 mm plag segregation down one side. Both veins are cut at high angles by late cracks, sometimes filled by rusty iron oxide.

T.7 666.478 Epidote vein in Ballyconneely Amphibolite. Same locality as T.5 and T.6. The vein is ~1 cm thick and concordant with the foliation. The vein is v. fine grained and composed of quartz with interstitial epidote. In hand speciment the veins shows a fine banding parallel to its margins, due to variations in the amount of epidote that is present. Small amounts of fine grained magnetic ore mineral ?mt are present in the grain and occasionally large grains of sulphide occur. The outer 0.5-1.5 mm of the vein is composed of qtz with minor plag. The host rock is fine grained and contains qtz/plag, bi (fine in groundmass possibly slightly coarser at vein margin,→chl), fine sph and hb (coarse ?relict porphyroclasts mostly in selvedges with coarse qtz and plag,→chl+cc). The host rock is both foliated and lineated. Adjacent to the vein the hb is rather coarser (up to 2 mm long). Occasional thin (3-5 μm wide) parallel calcite filled cracks are seen to cut the vein at a high angle.

T.1750 662.482 Basic rock (MGS) with boudinaged diopside-clinozoisite layers. ~50 m E of road ~300 m to the N of Ballinaboy. Coarse grained diopside-clinozoisite layers (sometimes banded) up to 1 cm thick are boudinaged and pulled apart in a fine grained matrix of hb and plag. The diopside sometimes encloses the clinozoisite, suggesting that it formed at the same time or earlier. The clinozoisite is sometimes observed to be faintly zoned. Plag, sph and calcite are also present in the layers. The matrix is composed of hb, plag (minor→sauss) with minor sphene and clinozoisite. The areas between the boudins sometimes contain coarse segregations of plag (→ser). The foliation is cut by an irregular qtz-plag-cc filled crack.

A.4 STABLE ISOTOPE FRACTIONATION FACTORS USED IN THIS STUDY.

A.4.1 Choice of fractionation factors

Following the arguments presented in 2.4.6 the oxygen isotope fractionation factors chosen are mostly those determined in the Chicago laboratory by Clayton and co-workers (Matsuhisa *et al.*,1979; Matthews *et al.*, 1983a,b), which have been combined to obtain a self consistent data set (Matthews *et al.*, 1983b).

Other fractionation factors, such as the ^{18}O amphibole-water and chlorite-water fractionations have not been succesfully experimentally determined, because of very low exchange rates. These fractionation factors have been calculated back from the semi-empirical mineral-mineral fractionation equations of Javoy (1977) and Bottinga and Javoy (1973). Matsuhisa *et al.* (1979) point out that some of the original data of Clayton *et al.* (1972) used by Bottinga and Javoy to calculate their quartz-water curve was probably inaccurate. Since the quartz-amphibole and quartz-chlorite curves of Javoy (1977) were calculated using this curve, they must also be suspect. However if the amphibole-water and chlorite-water curves are calculated back from the data of Bottinga and Javoy and Javoy (1977) then the effect of this error will be removed.

Fractionation factors are quoted in the form:

$$1000\ln \alpha_{phase1\text{-}phase2} = (A + (C \times \beta)) \times (10^6\ T^{-2}) + B$$

A.4.2 Oxygen isotope fractionation factors.

mineral (-water)	temperature range (°C)	A	B	data source
amphibole	?	0.95	-3.4	Calculated from the quartz - water fractionation of Bottinga and Javoy (1973) and quartz-amphibole fractionation of Javoy (1977).
biotite	?	0.40	-3.1	Calculated from the empirical feldspar-biotite fractionation of Bottinga and Javoy (1975) and the semi-empirical feldspar-water fractionation of Bottinga and Javoy (1973).
chlorite	?	1.56	-4.70	Empirical estimate (Wenner and Taylor, 1971)

mineral (-water)	temperature range (°C)	A	B	data source
chlorite	100-472	4.57	-1.14	$-6.64(10^3/T)$ Recalculated from reduced partition function coefficients of Onuma*et al.* (1972) SEE on regression is 0.12.
epidote	500-250	1.77	-3.31	C=-1.92, β = mole fraction of pistacite[1] in the molecule. Calculated from the quartz-water fractionation of Matsuhisa *et al.* (1979) and the quartz-epidote fractionation of Matthews and Schliestedt (1984).
quartz	800-500	2.05	-1.14	Matsuhisa *et al.* (1979).
quartz	500-250	3.34	-3.31	Matsuhisa *et al.* (1979).
albite	500-800	1.59	-1.16	Matsuhisa *et al.* (1979).
albite	400-500	2.39	-2.51	Matsuhisa *et al.* (1979).
baryte	110-350	3.01	-7.3	Kusakabe and Robinson (1977).
calcite	200-700	3.22	-3.45	Calculated by regression of 200-700°C equilibrium fractionations of O'Neil, Clayton and Mayeda (1969) after correction of the fractionation to take into account the presence of NH_4Cl mineraliser with the data of Truesdell (1974). SEE of regression line is 0.23‰.

mineral (-mineral)	temperature range (°C)	A	B		data source
quartz-epidote		?	1.56	0.0	C = 1.92, β = mole fraction of pistacite[1] in the molecule. Semi empurical estimate given by Matthews and Schliestedt (1984 based on zoisite data of Matthews *et al.* (1983c) and the grossular-andratite fractionation of Taylor and O'Neil (1977).
quartz-magnetite		6.11	0		Matthews *et al.* (1983b).

[1] $Ca_2Fe_3Al_2Si_3O_{12}OH$

A.4.3 Hydrogen isotope fractionation factors

mineral (-water)	temperature range (°C)	A	B	data source
chlorite	700-500	0.0	~-28	Graham *et al.* (1987).
chlorite	200	0.0	~-38	Graham *et al.* (1987).
epidote	650-260	0.0	-35.9	Graham *et al.* (1980).
epidote	150-260	29.2	-138.8	Graham *et al.* (1980).
hornblende	850-350	0.0	-23.1	Graham *et al.* (1984).
biotite, muscovite, actinolite	850-400	-22.4	26.3[2] +Z	Suzuoki and Epstein (1976) "The Suzuoki-Epstein equation", where Z = (2XAl-4XMg-68XFe) and X is the mole fraction of cations in the octahedral site.

A modified Suzuoki-Epstein equation.

Re-evaluating the data given by Suzuoki and Epstein (*ibid.*) using matrix transformations allows the mole fraction coefficients to be calculated to fit the experimental data more accurately.

Recommended coefficients to use are:

	X_{Al}	X_{Mg}	X_{Fe}
New coefficients	+0.52	-4.92	-65.3
Previous coefficients	+2.0	-4.0	-68.0

The largest differences from the fractionation factor determined using the published coefficients will occur at end member compositions i.e. -1.5 ‰, -1 ‰ and +2.5 ‰ respectively. Using the compositional data provided by Suzuoki and Epstein for their samples the mean error (σ_{n-1}) of the calculated fractionation factor from the experimentally determined value is calculated to be 0.9 ‰ using the original values but only 0.33 ‰ using the new coefficients.

The equation can also be modified to allow for the presence of Ti^{4+} and Fe^{3+} in these minerals by making use of the correlation between fractionation factor and the ratio of atomic mass/charge, (Fig. 6 p.1253). Best fit lines through the experimental data points are:

---

[2] This value was incorrectly given in the original paper as being 28.2. The value given here was calculated assuming that at 650°C -22.4 (10^6 T^{-2}) + B = 0. That this value should be 26.3 has recently been confirmed by Kuroda et al. (1986).

	Intercept on y	Slope	r^2
All data points	+33.1	-3.39	0.9801
All points except muscovite	+42.0	-3.87	0.9999

Since the muscovite data seems to be slightly anomalous and an almost perfect fit is obtained on the other four points the values for this line are used to calculate an approximation to the fractionation factor of the pure Ti^{4+} and Fe^{3+} end members from their atomic mass/charge ratios. These are:

	Fe^{3+}	Ti^{4+}
1000ln α (650°C)	-30.1	-4.4

Incorporating both these modifications, the modified Suzuoki - Epstein equation can be written:

$$1000\ln\alpha = -22.4\,(10^6\,T^{-2}) + 26.3 + (2X_{Al} - 4X_{Mg} - 68X_{Fe2+} - 30.1X_{Fe3+} - 4.4X_{Ti})$$

A.5 DIFFUSION COEFFICIENTS AND RATE CONSTANTS USED IN THIS STUDY.

A.5.1 Diffusion coefficients.

Oxygen.

index no	mineral	orientation	E (kcal/mole)	D_0 (cm^2/sec)	temperature range (°C)	data source
1	β-quartz	\\c	23.4	3.4×10^{-9}	825-600	Elphick *et al.* (1986)
2	α-quartz	\\c	68	190	550-500	Giletti and Yund (1984)
3	β-quartz	⊥c	56	1×10^{-4}	800-600	Giletti and Yund (1984)
4	β-quartz	\\c	34	4×10^{-7}	800-600	Giletti and Yund (1984)
5	magnetite	isot?	17	3.2×10^{-14}	550-302	Castle and Surman (1969)
6	hornblende	\\c	41	1×10^{-7}	800-650	Farver and Giletti (1985)
7	phlogopite	\\c	29	1.03×10^{-9}	800-500	Giletti and Anderson (1974)
8	zoisite	bulk	<11.4	5.3×10^{-13}	700-600	Matthews *et al.* (1983c)[1]
9	microcline	bulk	29.6	2.8×10^{-6}	700-400	Yund and Anderson (1974)
10	anorthite	bulk	26.2	1.39×10^{-7}	800-350	Giletti *et al.* (1978)
11	albite	$\perp_{001}$	21.3	2.3×10^{-9}	805-350	Giletti *et al.* (1978)

Hydrogen

index no	mineral	orientation	E (kcal/mole)	D_0 (cm^2/sec)	temperature range (°C)	data source
12	epidote	\\c	12.5	9.7×10^{-6}	650-450	Graham (1981)
13	epidote	\\c	30.7	9.34	350-200	Graham (1981)
14	epidote	⊥c	13.8	3.3×10^{-6}	650-400	Graham (1981)
15	epidote	⊥c	30.6	1.23	350-200	Graham (1981)
16	hornblende	\\c	19.0	1.58×10^{-7}	550-350	Graham *et al.* (1984)
17	hornblende	⊥c	20.1	2.39×10^{-8}	550-350	Graham *et al.* (1984)
18	biotite	\\c	27.8	3.4×10^{-7}	750-450	Cole and Ohmoto (1986)[2]
19	biotite	⊥c	29.3	7.6×10^{-4}	800-450	Cole and Ohmoto (1986)[2]
20	muscovite	\\c	28.7	1×10^{-7}	750-450	Graham (1981)
21	muscovite	⊥c	29	1.05×10^{-4}	750-450	Graham (1981)
22	chlorite	\\c	39.8	4.79×10^{-4}	700-500	Graham *et al.* (1987)
23	chlorite	⊥c	41	6.17×10^{-2}	700-500	Graham *et al.* (1987)

[1] Calculated from data in this paper. Values are maxima because it is assumed that no solution-reprecipitation is taking place, whereas there may actually be some contribution by this exchange process to the observed degree of exchange.

[2] Calculated in this paper from data given by Suzuoki and Epstein (1976).

A.5.2 Rate constants (oxygen isotope exchange).[3]

index no	mineral	orientation	Ea (kcal/mole)	A_o (cm^2/sec)	temperature range (°C)	data source
24	baryte[x]	bulk	13.4	4.75×10^{-2}	350-110	Kusakabe and Robinson (1977)
25	calcite[y]	bulk	10.4	4.72×10^{-4}	700-305	Anderson and Chai (1974)
26	quartz[y]	bulk	15.0	3.46×10^{-4}	550-350	Clayton *et al.* (1972)
27	parag→mu	bulk	14.8	2.07×10^{-4}	600-350	O'Neil and Taylor (1969)
28	albite→Kfsp	bulk	25.6	1.51×10^{2}	650-350	O'Neil and Taylor (1967)
29	albite[z]	bulk	21.2	3.6×10^{-2}	650-500	O'Neil and Taylor (1967)

Abbreviations: \\c = parallel to c-axis, $\perp$c = right angles to c-axis, $\perp_{001}$ = right angles to the 001 face, isot = isotropic (i.e. spherical model applies), bulk = lack of anisotropy in grains meant that only a "bulk" diffusion coefficient, or rate constant for that sample could be calculated.

To convert kcal/mole to kJ/mole multiply by 4.1812, 1 cm^2/sec = 10^{-4} cm^2/sec.

---

[3] All values for Ea and Ao were were calculated from data given in the sources shown by Cole et al. (1983) and Cole and Ohmoto (1986).

[x] 1m NaCl solution.

[y] 0.7m NaF solution.

[z] 3m NaCl solution.

Age BP	Period	Stage/Epoch	Paleolat.	Climate	$\delta^{18}O$	δD	Comments
0	Present	-----	53°N	Subaerial, maritime, low relief, wet	-6	-38	Mean air temperature ≈ 10°C
-- 0							
	Quaternary		53°N	Subaerial, maritime, low relief, glacial-warm, wet	-6 to -10	-38 to -70	Glacial compositions by analogy with compositions at edge of Greenland ice cap.
-- 2							
	Tertiary	Miocene	49°N (10 Ma) 47°N (20 Ma)	Subaerial, maritime, ?elevated, warm-cold, wet.	-6 to -10.5	-30 to -74	Elevation may have been >1 km due to Mid Tertiary uplift (Dewey and McKerrow, 1963).
	Tertiary	Miocene					
-- 25							
	Tertiary	Oligocene	46°N (40 Ma) 44°N (60 Ma)	Subaerial, maritime, low relief, warm-hot, wet.	-3 to -4	-14 to -22	Subtropical meteoric water compositions by analogy with modern day compositions in Florida. Note that BTVP centres ~60 Ma sampling isotopically light water $\delta^{18}O$ = -10 to -13, δD = -70 to -94 because of high relief.
	Tertiary	Paleocene					
-- 65							
	Cretaceous	Maastrichtian	42°N (80 Ma)	Submarine	0	0	Chalk sea
	Cretaceous	Cenomanian	43°N (100 Ma)				
-- 100							
	Cretaceous	Albian	42°N (120 Ma) 39°N (140 Ma)	Subaerial, maritime-continental, low relief, wet.	-4 to -6	-22 to -38	North Atlantic still very narrow, mainly continental area to south west (direction from which major winds should be coming).
	Cretaceous	Berriasian					
-- 140							
	Jurassic	Tithonian	38°N (160 Ma) 39°N (180 Ma)	Submarine	0	0	
	Jurassic	Hettangian	36°N (200 Ma)				
-- 210							
	Triassic	U.Rhaetic	27°N (220 Ma)	Subaerial-submarine, maritime, low relief, hot dry.	+8 to 0	+20 to -20	Semi-marine lagoons, evaporation of sewater can produce very heavy compositions in restricted basins (Pierre et al., 1984).
	Triassic	L. Rhaetic					
-- 220							

Age BP	Period	Stage/Epoch	Paleolat.	Climate	$\delta^{18}O$	δD	Comments
	Triassic	Norian	12°N (240 Ma)	Subaerial, continental	0	+10	Meteoric water compositions analagous with the
			5°N (280 Ma)	low-high relief?, hot, dry	to	to	Sahara.
	Carboniferous	Stephanian			-3	-14	
-- 295							
	Carboniferous	Westphalian	2°S (320 Ma)	Subaerial, continental-	-2	-6	Meteoric water compositions analagous with equatorial
				maritime, low relief, hot,	to	to	Africa.
	Carboniferous	Namurian		humid.	-4	-22	
-- 335							
	Carboniferous	U. Visean		Submarine	0	0	Although paleogeographical maps of S evastopulo
		(Brigantian)					(1981) do not show Connemara to be submerged the
		(Chadian)					presence of a sub Visean UC (Dewey & McKerrow, 1963)
	Carboniferous	L. Visean					attests to submergence during this time.
-- 350							
	Carboniferous	U.Tournasian	8°S (360 Ma)	Subaerial, maritime, low	-1	+2	Meteoric water compositions analagous with equatorial
		(Courceyan)		relief, hot, dry	to	to	Africa.
	M. Devonian	Eifelian	7°S (M.-U. Dev)		-3	-14	
-- 387							
	L. Devonian	Emsian	27°S (L.Dev)	Subaerial, maritime, med.	-4	-22	Fallick et al. (1985) suggest that meteoric water at ~410
	Silurian	Pridoli		-low relief?, hot, wet.			Ma was -5,-30‰ in the Midland Valley of Scotland.
-- 415							
	Silurian	Ludlow- U. Llandovery		Submarine	0	0	Transgression c. 430 Ma (Bluck and Leake, 1986).
-- 430							
	Silurian	L. Llandovery	15°S (Silur.)	Subaerial, maritime	-1	+2	Expect sea level air temperature at these latitudes
				elevated-low relief,	to	to	to be about 20°C. A major phase of renewed uplift may
				cold-warm, wet	-4	-22	have taken place at ~440 Main which case water values
	Ordovician	Llanvirn	21°S (Ord.)				may have been more negative at this time.
-- 487							
	Ordovician	Arenig	21°S (Ord.)	Subaerial, maritime	-15	-110	Rapid post-metamorphic uplift history recorded in
				elevated, cold, wet	at	3.5 km	Connemara massif suggests that elevated mountain
					possibly	less?	belt possibly 3-5 km could have formed at the peak of
	Ordovician	Arenig					uplift (B.J. Bluck pers. comm.)
-- 488							

Notes for A.6. Most of the paleogeographical information is from either Anderton *et al.* (1979) or Holland (1981), the paleolatitude data is obtained from Smith *et al.* (1981), except for pre-Carboniferous data which is from Torsvik (1985). Dansgaard's (1964) relation of $\delta^{18}O$ to temperature is employed along with an average lapse rate of 6.5°C/km (Oliver and Hidore, 1984) in estimating the isotopic composition of precipitation at altitude. NB. The assumptions are made that seawater has remained constant in stable isotopic composition through time and that the earths atmospheric circulation system in the past was broadly similar.

A.7 REGRESSION OF THE CHLORITE-WATER HYDROGEN ISOTOPE FRACTIONATION DATA DETERMINED BY MARUMO *ET AL.* (1980).

These authors determined the hydrogen isotope fractionation between chlorites and coexisting hydrothermal fluid at different temperatures in an active hydrothermal system (their table 2.). The Fe/(Fe+Mg) ratios of these chlorites, estimated from X-ray diffraction patterns, were also reported. Provided that these chlorite-water fractionation data represent equilibrium fractionations and that variations in fluid salinity (not reported) are small, then these data can be used to evaluate the dependence of the the chlorite-water fractionation on temperature and Fe/(Fe+Mg) ratio.

The coefficients obtained by multiple regressions of different combinations of these data are given below. The standard error of estimate (SEE) is also given as an measure of the fit of the data to the regression surface or line.

K	L	M	N	SEE
-	-	+7.9	-68.3	6.0
-	+33.2	-	-103.1	6.1
-93.2	-	-	+1.4	5.4
-65.4	-	+4.7	-29.2	4.5
-56.1	-271.0	+68.4	+253.0	4.4

where

$$10^3 \ln \alpha_{\text{chlorite-water}} = K\,(Fe/(Fe+Mg)) + L\,(1000/T) + M\,(10^6 T^{-2}) + N$$

in which T = temperature in K.

The SEE is defined as

$$SEE = \sqrt{\frac{\sum Y - \hat{Y}}{\text{deg rees of freedom}}}$$

It can be seen from this table that the variation in measured $10^3 \ln \alpha$ between samples is best described (i.e. the SEE is minimised) by a fractionation equation which takes into account variations in both temperature and chlorite Fe/(Fe+Mg) between samples. This tends to suggest that both factors are important in controlling the magnitude of the chlorite water fractionation. However even when both factors are taken into account the SEE is still rather greater than would be expected if the residual variation was solely due to the analytical uncertainty in the hydrogen isotope analyses alone. Possibly this can be attributed to the analytical error in the Fe/(Fe+Mg) ratio determinations, which are not quoted, but are probably quite large. Alternatively other factors which have not been taken into account may also be important in governing the fractionation.

REFERENCES

AHMED-SAID,Y. (1988). The geochemistry of thermal aureoles at Cashel, Co. Galway, and Comrie, Perthshire. Ph.D. Thesis, University of Glasgow, (unpublished).

ALLEGRE,C.J., STAUDACHER,T., SARDA,P. & KURZ,M. (1983). Constraints on the evolution of the earths mantle from rare gas systematics. Nature. **303.** 762-766.

ALLEN,J.C. & BOETTCHER,A.L. (1978). Amphiboles in andesite basalts II. Stability as a function of P - T - f_{H_2O} - f_{O_2}. Amer. Mineral. 63, 1074-1087.

ANDERSON,T.F. & CHAI,B.T.H. (1974). Oxygen isotope exchange between calcite and water under hydrothermal conditions. In: HOFMANN,A.W., GILETTI,B.J., YODER,H.S. & YUND,R.A. (eds) Geochemical Transport and Kinetics. Carnegie Inst. Washington Publ. **634.** 219-227.

ANDERTON,R., BRIDGES,P.H., LEEDER,M.R., & SELLWOOD,B.W. (1979). A dynamic stratigraphy of the British Isles. Allen and Unwin, London.

ARITA,M., HOSOYA,M., KOBAYASHI,M. & SOMENO,M. (1979). Depth profile measurement by secondary ion mass spectrometry for determining the tracer diffusivity of oxygen in rutile. J. Am. Ceram. Soc. **62.** 443-446.

BARBER.J.P. & YARDLEY, B.W.D. (1985). Conditions of high-grade metamorphism in the Dalradian of Connemara, Ireland. J. Geol. Soc. Lond. **142.** 87-96.

BATZLE,M.L. & SIMMONS,G. (1976). Microfractures in rocks from two geothermal areas. Earth Planet. Sci. Lett. **30.** 71-93.

BECKER,R.A. & CHAMBERS,J.M. (1984). S An interactive environment for data analysis and graphics. The Wadsworth statistics/probability series. California.

BECKER,R.H. & CLAYTON,R.N. (1976). Oxygen isotope study of a Precambrian iron-formation, Hamersley Range, western Australia. Geochim. Cosmochim. Acta **40.** 1153-1165.

BENCE,A.E., HASKINS,L. & RHODES,J.M. (1980). Oceanic intraplate volcanism. Lunar Planet. Inst. Houston Texas.

BENDER,J.F.,HODGES,F.N, & BENCE,A.E. (1980). Petrogenesis of basalts from the project FAMOUS area : Experimental study from 0-15kb. Earth Planet. Sci. Lett., **41**, 277-302.

BENNETT,M.C. & GIBB,F.G.F. (1983). Younging directions in the Dawros Peridotite, Connemara. J. Geol. Soc. Lond. **140**. 63-75.

BERNER,R.A. (1981). Kinetics of weathering and diagenesis. In: LASAGA,A.C. & KIRKPATRICK,R.J. (eds) Kinetics of Geochemical Processes. Reviews in Mineralogy. **8.** 111-134. Mineralogical Society of America.

BIRD,D.K. & HELGESON, H.C. (1981). Chemical interaction of aqueous solutions with epidote-feldspar mineral assemblages in geologic systems II. Equilibrium constraints in metamorphic/geothermal processes. Amer. Journ. Sci., **281,** 576-614.

BIRD,D.K., SCHIFFMAN,P., ELDERS, W.A., WILLIAMS, A.E & McDOWELL, S.D. (1984). Calc-silicate mineralisation in active geothermal systems. Econ. Geol., **79**, 6671-695.

BLUCK,B.J. & LEAKE,B.E. (1986). Late Ordovician to early Silurian amalgamation of the Dalradian and adjacent Ordovician rocks in the British Isles. Geology. **14.** 917-919.

BOETTCHER,A.L. & O'NEIL,J.R. (1980). Stable isotope, chemical and petrographic studies of high pressure amphiboles and micas: evidence of metasomatism in the mantle source regions of alkali basalts and kinberlites. Amer. J. Sci. **280A.** 594-621.

BORTHWICK,J. & HARMON,R.S. (1982). A note regarding ClF_3 as an alternative to BrF_5 for oxygen isotope analysis. Geochim. Cosmochim. Acta **46.** 1665-1668.

BOTTINGA,Y. (1969). Calculated fractionation factors for carbon and hydrogen isotope exchange in the systems calcite-carbon dioxide-graphite, methane-hydrogen-water vapour. Geochim. Cosmochim. Acta **33.** 49-64.

BRACE,W.F. (1984). Permeability of crystalline rocks: new in situ meausrements. J. Geophys. Res. **89** (B6) 4327-4330.

BRADSHAW,R., PLANT,A.G., BURKE,K.C., & LEAKE,B.E. (1969). The Oughterard Granite, Connemara, Co. Galway. Proc. R. Ir. Acad. **68B.** 39-65.

BREMNER,D.L. (1977). The Roundstone ultrabasic complex, Connemara, Ireland. Ph.D. Thesis, University of Glasgow (unpublished).

BREMNER,D.L. & LEAKE, B.E. (1980). The geology of the Roundstone Ultrabasic Complex, Connemara. Proc. R. Ir. Acad. **V80B.** 395-433.

BRIGHAM,R.H. & O'NEIL,J.R. (1985). Genesis and evolution of water in a two-mica pluton: a hydrogen isotope study. Chem. Geol. **49.** 159-177.

BRIMHALL,G.J.Jr. (1979). Lithologic determination of mass transfer mechanisms of multiple-stage porphyry copper mineralisation at Butte, Montana, vein formation by hypogene leaching and enrichment of potassium silicate protore. Econ. Geol. **74.** 556-589.

BROECKER,W.S. & OVERSBY,V.M. (1971). Chemical equilibria in the earth. McGraw-Hill, New York.

BRUTON,C.J. & HELGESON,H.C. (1983). Calculation of the chemical and thermodynamic consequences of differences between fluid and geostatic pressure in hydrothermal systems. Am. J. Sci., **283-A,** 540-588.

BURNHAM,C.W. (1967). Hydrothermal fluids at the magmatic stage. In: BARNES, H.L. (ed). Geochemistry of hydrothermal ore deposits. Holt, Rinehart and Winston. New York.

BURNHAM,C.W. & DAVIS, N.F. (1974). The role of H_2O in silicate melts, II, thermodynamic and phase relations in the system $NaAlSi_3O_8$ - H_2O to 10 kilobars, 700°C to 1100°C. Am. J. Sci., **274,** 902-940.

CARTWRIGHT,I. (1988). Crystallization of melts, pegmatite intrusion and Inverian retrogression of the Scourian Complex, North West Scotland. J. Metamorphic Geol. **6.** 77-93.

CASTLE,J.E. & SURMAN,P.L. (1969). The self diffusion of oxygen in magnetite. The effect of anion vacancy concentration and cation distribution. J. Phys. Chem. **73.** 632-634.

CHAI,B.T.H. (1974). Mass transfer of calcite during hydrothermal recrystallisation. In: HOFMANN,A.W., GILETTI,B.J., YODER,H.S. & YUND,R.A. (eds) Geochemical Transport and Kinetics. Carnegie Inst. Washington Publ. **634.** 205-218.

CHAMBERLAIN,C.P. & RUMBLE,D.III. (1987). Thermal anomalies in a regional metamorphic terrane: evidence for convective heat transport during metamorphism. Geol. Soc. Lond. Newsletter. **16.** (4), 30-31.

CHAPPELL,B.W. & WHITE,A.R.J. (1974). Two contrasting granite types. Pacific Geol. **8.** 173.

CHATTERJEE,N.D. & JOHANNES,W. (1974). Thermal stability and standard thermodynamic properties of synthetic $2M_1$ - muscovite, $KAl_2(AlSi_3)O_{10}(OH)_2$. Contrib. Mineral. Petrol. **48.** 89-114.

CHAUSSIDON,M., ALBARÈDE,F. & SHEPPARD,S.M.F. (1987). Sulphur isotope heterogeneity in the mantle from ion microprobe measurements of sulphide inclusions in diamonds. Nature. **330.** 242-244.

CHO, M. & LIOU, J.G. (1987). Prehnite-pumpellyite to greenschist facies transition in the Karmutsen metabasites, Vancouver Island, B.C. J. Petrol., **28,** 417-443.

CLAYPOOL,G.E., HOLSER,W.T., KAPLAN,I.R., SAKAI,H. & ZAK,I. (1980). The age curves of sulphur and oxygen isotopes in marine sulphate and their mutual interpretations. Chem. Geol. **28.** 199-260.

CLAYTON,R.N. (1981). Isotopic thermometry. In: NEWTON,R.C., NAVROTSKY,A. & WOOD,B.J. (eds) Thermodynamics of Minerals and Melts. Advances in physical geochemistry, volume 1.

CLAYTON,R.N. & MAYEDA,T.K. (1963). The use of bromine pentafluoride in the extraction of oxygen from oxides and silicates for isotopic analysis. Geochim. Cosmochim. Acta **27.** 43-52.

CLAYTON,R.N. & STEINER,A. (1975). Oxygen isotope studies of the geothermal system at Wairakei, New Zealand. Geochim. Cosmochim. Acta. **39,** 1179-1186.

CLAYTON.R.N., FRIEDMAN,I., GRAF,D.L., MAYEDA,T.K., MEENTS,W.F. & SHRIMP,N.F. (1966). The origin of saline formation waters 1. Isotopic composition. J. Geophys. Res. **71.** 3869-3882.

CLAYTON.R.N., MUFFLER,L.J.P. & WHITE,D.E. (1968). Oxygen isotope study of calcite and silicates of the River Ranch No.1. Well, Salton Sea geothermal field, California. Am. J. Sci. **226,** 968-979.

CLAYTON,R.N., O'NEIL,J.R. & MAYEDA,T.K. (1972). Oxygen exchange between quartz and water. J.Geophys. Res. **77.** 3057-3067.

CLAYTON,R.N., GOLDSMITH,J.R., KAREL,K.J., MAYEDA,T.K. & NEWTON,R.C. (1975). Limits on the effect of pressure on isotopic fractionation. Geochim. Cosmochim. Acta **39.** 1197-1201.

COLE,D.R., MOTTL, M.J. & OHMOTO,H. (1987). Isotopic exchange in mineral-fluid systems II. Oxygen and hydrogen isotopic investigation of the experimental basalt-seawater system. Geoch. Cosmo. Acta., **51,** 1523-1538.

COLE,D.R. & OHMOTO,H. (1986). Kinetics of isotopic exchange at elevated temperatures and pressures. In: VALLEY,J.W., TAYLOR,H.P.Jr & O'NEIL,J.R. Stable isotopes in high temperature geological processes. Reviews in Mineralogy. **16.** Min.Soc.Am.

COLE,D.R., OHMOTO,H. & LASAGA,A.C. (1983). Isotopic exchange in mineral-fluid systems. I. Theoretical evaluation of oxygen isotopic exchange accompanying surface reactions and diffusion. Geochim. Cosmochim. Acta **47.** 1681-1693.

COLE,G.A.J. (1922). Memoir and map of localities of minerals of economic importance and metalliferous mines in Ireland. Mem. Geol. Surv. Irel. (reprinted in 1956).

COLEMAN, M.L. & MOORE, M.P. (1978). Direct reduction of sulphates to sulphur dioxide for isotopic analysis. Analytical chemistry, **50 (II)**, 1594-1595.

COX,K.G., BELL,J.D. & PANKHURST,R.J. (1979). The interpretation of igneous rocks. George Allen and Unwin. London.

CRAIG,H. (1957). Isotopic standards for carbon and oxygen and correction factors for mass spectrographic analysis of carbon dioxide. Geochim. Cosmochim. Acva **12.** 133-149.

CRAIG,H. (1961). Isotopic variations in meteoric waters. Science **133.** 1702-1703.

CRAIG,H. (1961). Standard for reporting concentrations of deuterium and oxygen-18 in natural waters. Science **133.** 1833-1934.

CRAIG,H. & GORDON,L.I. (1965). Deuterium and oxygen-18 variations in the ocean and the marine atmosphere. In: Stable isotopes in oceanographic studies and paleotemperatures. Spoleto. July 26-27. Consiglio Nazionale Delle Richerche Laboratorio Di Geologigia Nucleare, Pisa, 1-122.

CRAIG,H. & LUPTON,J.E. (1976). Primordial neon, helium and hydrogen in oceanic basalts. Earth Planet. Sci. Lett. **31.** 369-385.

CRANK,J. (1975). The Mathematics of Diffusion. Oxford University Press, London.

CRISS,R.E. & TAYLOR,H.P.Jr. (1983). An $^{18}O/^{16}O$ and D/H study of Tertiary hydrothermal systems in the southern half of the Idaho Batholith. Geol. Soc. Am. Bull. **94,** 640-663.

CRISS,R.E. & TAYLOR,H.P.Jr. (1986). Meteoric-hydrothermal systems. In:VALLEY,J.W., TAYLOR,H.P.Jr & O'NEIL,J.R. Stable isotopes in high temperature geological processes. Reviews in Mineralogy. **16.** Min.Soc.Am. 373-424.

CRISS,R.E., LANPHERE,M.A. & TAYLOR,H.P.Jr. (1982). Effects of uplift, deformation, and meteoric hydrothermal metamorphism of the K-Ar

ages of biotites in the southern half of the Idaho Batholith. J. Geophys. Res. 87, 7029-7046.

DANSGAARD,W. (1964). Stable isotopes in precipitation. Tellus. **16.** (4) 436-468.

DEBON,F., LeFORT,P., SHEPPARD,S.M.F. & SONET,J. (1986). The four plutonic belts of the Transhimalaya-Himalaya: A chemical, mineralogical, isotopic and chronological synthesis along a Tibet-Nepal section. J. Petrol. **27.** 219-250.

DEINES,P. (1977). On the oxygen isotope distribution among mineral triplets in igneous and metamorphic rocks. Geochim. Cosmichim. Acta. **41.** 1709-1730.

DEINES,P. (1980). The carbon isotopic composition of diamonds: Relationship to diamond shape, colour, occurence and vapour composition. Geochim. Cosmochim. Acta. **44.** 943-961.

DEINES,P. & GOLD,D.P. (1973). The isotopic composition of carbonatite and kimberlite carbonates and their bearing on the isotopic composition of deep-seated carbon. Geochim. Cosmochim. Acta. **37.** 1709-1733.

DEINES,P., LANGMUIR,D. & HARMON,R.S. (1974). Stable carbon isotope ratios and the existenc of a gas phase in the evolution of carbonate groundwater. Geochim. Cosmochim. Acta. **38.** 1147-1164.

DENNIS,P.F. (1984). Oxygen self-diffusion in quartz under hydrothermal conditions. J.Geophys. Res. **89.** (B6). 4047-4057.

DEWEY,J.F. & McKERROW,W.S. (1963). An outline of the geomorphology of Murrish and north west Galway. Geol. Mag. **100.** 260-75.

DEWEY,J.F. & SHACKLETON,R.M. (1984). A model for the evolution of the Grampian tract in the early Caledonides and Appalachians. Nature, 312, 8 Nov. 1984, 115-121.

DODSON,M.H. (1973). Closure temperature in cooling geochronological and petrological systems. Contrib. Mineral. Petrol. **40,** 259-274.

DODSON,M.H. (1979). Theory of cooling ages. In: JAGER,E. & HUNZIKER,J.C. (eds) Lectures in Isotope Geology. Springer-Verlag, Berlin. 194-202.

DODSON,M.H. (1986). Closure profiles in cooling systems. Materials Science Forum. **7,** 145-154.

EDMUNDS,W.M., KAY,R.L.F. & McCARTNEY,R.A. (1985). Origin of saline groundwaters in the Carnmenellis granite (Cornwall): natural processes

and reaction during hot dry rock reservoir circulation. Chem. Geol. 49, 287-301.

ELIAS,E.M., MACINTYRE,R.M. & LEAKE,B.E. (1988). The cooling history of Connemara, Western Ireland, from K-Ar and Rb-Sr Age studies. J. Geol. Soc. Lond. **145**, 649-660.

ELLIOT,D. (1973). Diffusion flow laws in metamorphic rocks. Geol. Soc. Am. Bull. **84.** 2645-2664.

ELPHICK,S.C., DENNIS,P.F., & GRAHAM,C.M. (1986). An experimental study of the diffusion of oxygen in quartz and albite using an overgrowth technique. Contrib. Mineral. Pertrol. **92.** 322-330.

EMRICH,K., EHALT,D.H. & VOGEL,J.C. (1970). Carbon Isotope fractionation during the precipitation of calcium carbonate. Earth Planet. Sci. Lett. **8.** 363-371.

EPSTEIN,S., SHARP,S. & GOW,A.J. (1970). Antarctic ice sheet: Stable isotope analyses of Byrd Station cores and interhemispheric climatic implications. Science. **168.** 1570-1572.

EVANS,A.M. (1980). An introduction to ore geology. Geoscience texts, volume 2. Blackwell Scientific Publications. Oxford.

EVANS,B.W.(1964). Fractionation of elements in the pelitic hornfelses of the Cashel-Lough Wheelaun Intrusion, Connemara, Eire. Geochim et Cosmochim. Acta. **28.** 127-156.

EVANS,B.W. & LEAKE,B.E. (1960). The composition and origin of the striped amphibolites of Connemara, Ireland. J. Petrol. **1.** 337-363.

EWALD,A.H. (1985). The effect of pressure on oxygen isotope exchange in silicates. Chem. Geol. **49,** 179-187.

EWART,A. (1976). Mineralogy and chemistry of modern orogenic lavas - some statistics and implications. Earth Planet. Sci. Lett., **31,** 417-432.

FARVER, J. R. & GILETTI,B.J. (1985). Oxygen diffusion in amphiboles. Geochim et cosmochim Acta **49.** 1403-1411.

FAURE,G. (1986). Principles of isotope geology. 2nd. edn. John Wiley & Sons. New York. 589p.

FEELY,M & MADDEN,J.S. (1987). The spatial distribution of K, U, Th and surface heat production in the Galway granite, Connemara, Western Ireland. Irish. J. Earth Sci. **8,** 155-164.

FERGUSON,C.C. & AL-AMEEN,S.I. (1985). Muscovite breakdown and corundum growth at anomalously low f_{H_2O}; a study of contact

metmorphism and convective fluid movement around the Omey Granite, Connemara, Ireland. Min. Mag. **49.** 505-515.

FERRY,J.M. (1981). Petrology of graphitic sulphide rich schists from South-Central Maine: An example of desulphidation during prograde metamorphism. Am. Mineral. **66.** 908-930.

FERRY,J.M. (1984). A biotite isograd in S-Central Maine, USA: Mineral reactions, fluidtransfer, and heat transfer. J. Petrol. **25.** 871-893.

FERRY,J.M. (1985). Hydrothermal alteration of Tertiary igneous rocks from the Isle of Skye, Northwest Scotland. I Gabbros. Contrib. Mineral. Petrol. **91,** 264-282.

FERRY,J.M. (1985). Hydrothermal alteration of Tertiary igneous rocks from the Isle of Skye, Northwest Scotland. II Granites. Contrib. Mineral. Petrol. **91,** 283-304.

FISHER,G.W. AND ELLIOTT.D. (1974). Criteria for quasi-steady diffusion and local equilibrium in metamorphism. In: HOFMANN,A.W., GILETTI,B.J., YODER,H.S. & YUND,R.A. (eds) Geochemical Transport and Kinetics. Carnegie Inst. Washington Publ. **634.** 231-241.

FLETCHER,R.C. & HOFMANN,A.W. (1974). Simple models of diffusion and combined diffusion-infiltration metasomatism. In: HOFMANN,A.W., GILETTI,B.J., YODER,H.S. & YUND,R.A. (eds) Geochemical Transport and Kinetics. Carnegie Inst. Washington Publ. **634.** 243-259.

FOLAND,K.A. (1974). Alkali diffusion in orthoclase. In: HOFMANN,A.W., GILETTI,B.J., YODER,H.S. & YUND,R.A. (eds) Geochemical Transport and Kinetics. Carnegie Inst. Washington Publ. **634.** 77-98.

FORESTER,R.W. & TAYLOR,H.P.Jr. (1976). ^{18}O-depleted igneous rocks from the Tertiary complex of the Isle of Mull, Scotland. Earth Planet. Sci. Lett. **32,** 11-17.

FRANKS,F. (1972). Water; A comprehensive treatise. Volume 1. The physics and physical chemistry of water. Plenum Press, New York.

FRAPE,S.K., FRITZ,P. & McNUTT,R.H. (1984). Water rock interaction and chemistry of groundwaters from the Canadian Shield. Geochim. Cosmochim. Acta. **48.** 1617-1627.

FREER,R. (1981). Diffusion in silicate minerals and glasses: a data digest and guide to the literature. Contrib. Mineral. Petrol. **76,** 440-454.

FREER,R. & DENNIS,P.F. (1982). Oxygen diffusion studies I. A preliminary ion microprobe investigation of oxygen diffusion in some rock forming minerals. Min. Mag. **45,** 179-192.

FRIEDMAN,I. & SMITH,R.L. (1958). The deuterium content of water in some volcanic glasses. Geochim. Cosmochim. Acta **15,** 218-228.

FUEX,A.N. & BAKER,D.R. (1973). Stable carbon isotopes in selected granitic, mafic and ultramafic rocks. Geochim. Cosmochim. Acta **37.** 2509-2521.

FYFE,W.S. & KERRICH,R. (1985). Fluids and thrusting. Chem. Geol. **49.** 353-362.

GARCIA,M.O., LIU,N.M.K. & MUENOW,D.W. (1979). Volatiles in submarine volcanic rocks from the Mariana island arc and trough. Geochim. Cosmochim. Acta, **43,** 305-312.

GARLICK,G.D. (1966). Oxygen isotope fractionation in igneous rocks. Earth Plan. Sci. Letts **1.** 361-368.

GARLICK,G.D. (1969). Chapter 8B. The stable isotopes of oxygen. In: Handbook of Geochemistry. Wedepohl,K.H. (ed). 1-27. Springer-Verlag.

GILETTI,B.J. (1974b). Studies in diffusion I: argon in phlogopite mica. In: HOFMANN,A.W., GILETTI,B.J., YODER,H.S. & YUND,R.A. (eds) Geochemical Transport and Kinetics. Carnegie Inst.Washington Publ. **634.** 107-115.

GILETTI,B.J. (1985). The nature of oxygen transport within minerals in the presence of hydrothermal water and the role of diffusion. Chem. Geol. **53,** 197-206.

GILETTI,B.J. (1986). Diffusion effects on oxygen isotope temperatures of slowly cooled igneous and metamorphic rocks. Earth Planet. Sci. Lett. **77,** (2) 218-229.

GILETTI,B.J. & ANDERSON,T.F. (1975). Studies in diffusion II. Oxygen in phlogopite mica. Earth Plan. Sci Letts **28.** 225-233.

GILETTI,B.J. & YUND, R.A. (1984). Oxygen diffusion in quartz. J.Geophys. Res. **89,** (B6) 4039-4046.

GILETTI,B.J., SEMET,M.P. & YUND,R.A. (1978). Studies in diffusion - III. Oxygen in feldspars, an ion microprobe determination. Geochim. Cosmochim. Acta. **42,** 45-57.

GLEADOW,A.J.W. (1978). Fission-track evidence for the evolution of rifted continental margins. Proc. 4th Int. Conf. Geochron. Cosmochron. Isotope geology. 1978 Colorado. 146-147.

GODFREY,J.D. (1962). The deuterium content of hydrous minerals from the east-central Sierra Nevada and Yosemite National Park. Geochim. Cosmochim. Acta **26,** 1215-1245.

GRAHAM,A.M., GRAHAM,C.M. & HARMON,R.S. (1982). Origins of mantle waters: Stable isotope evidence from amphibole-bearing plutonic cumulate blocks in calc-alkaline volcanics Granada, Lesser Antilles. Proc. 5th Int. Conf. Geochron. Cosmochron. Isotope geology. 119-120.

GRAHAM,C.M. (1976). Petrochemistry and tectonic significance of the Dalradian metabasaltic rocks of the south-west Scottish Highlands. J. Geol. Soc. Lond. **132.** 61-84.

GRAHAM,C.M. (1981). Experimental hydrogen isotope studies III: Diffusion of hydrogen in hydrous minerals, and stable isotope exchange in metamorphic rocks. Contrib. Mineral. Petrol. **76,** 216-228.

GRAHAM,C.M. & HARMON,R.S. (1983). Stable isotope evidence on the nature of crust mantle interactions. In: HAWKESWORTH,C.J. & NORRY,M.J. (eds). Continental basalts and mantle xenoliths. Shiva, Nantwich. 20-45.

GRAHAM,C.M., & SHEPPARD,S.M.F. (1980). Experimental hydrogen isotope studies II : Fractionation in the systems epidote NaCl-H_2O, epidote- $CaCl_2$-H_2O and epidote-seawater, and the hydrogen isotope compositions of natural epidotes. Earth Plan. Sci, Letts. **49.** 237-251.

GRAHAM,C.M., HARMON,R.S. & SHEPPARD, S.M.F. (1984). Experimental hydrogen isotope studies: hydrogen isotope exchange between amphibole and water. Amer. Min. **69.** 128-138.

GRAHAM,C.M., FALLICK,A.E., ROBERTS,I. & GREIG,K.M. (1987). Metabasites as fluid aquifers during regional metamorphism. Terra Cognita. **7.** 136.

GRAHAM,C.M., SHEPPARD,S.M.F. & HEATON,T.H.E. (1980). Experimental hydrogen isotope studies I: systematics of hydrogen isotope fractionation in the systems epidote-H_2O, zoisite-H_2O and AlO(OH)-H_2O. Geochim et Cosmochim Acta. **44.** 353-364.

GRAHAM,C.M., VIGLIANO,J.A. & HARMON,R.S. (1987). An experimental study of hydrogen isotope exchange between aluminous chlorite and water, and of hydrogen diffusion in chlorite. Am. Mineral. **72.** 566-579.

GREGORY,R.T. & CRISS,R.E. (1986). Isotopic exchange in open and closed systems. In:VALLEY,J.W., TAYLOR,H.P.Jr & O'NEIL,J.R. Stable isotopes in high temperature geological processes. Reviews in Mineralogy. **16.** Min.Soc.Am. 91-127.

GREGORY,R.T. & TAYLOR,H.P.Jr. (1981). An oxygen isotope profile in a section of Cretaceous oceanic crust, Samail Ophiolite, Oman: Evidence

for $\delta^{18}O$-buffering of the oceans by deep (>5km) seawater-hydrothermal circulation in mid ocean ridges. J. Geophys. Res. **86.** 2737-2755.

GREGORY,R.T. & TAYLOR,H.P.Jr. (1986a). Possible non-equilibrium oxygen isotope effects in mantle nodules, an alternative to the Kyser-O'Neil-Carmichael $^{18}O/^{16}O$ geothermometer. Contrib. Mineral. Petrol. **93.** 114-119.

GRINENKO,V.A. & GRINENKO,L.N. (1967). Fractionation of sulphur isotopes in high temperature decomposition of sulphides by water vapour. Goekhimiya. **9.** 1049-1055.

GUIDOTTI,C.V. (1984). Micas in metamorphic rocks. Reviews in mineralogy **13.** Bailey, S.W. (ed) Min. Soc. Am.

HAAS,J.L. (1971). The effect of salinity on the maximum thermal gradient of a hydrothermal system at hydrostatic pressure. Economic Geology, **66,** 940-946.

HALL,A.J., BOYCE,A.J. & FALLICK,A.E. (1988). Iron sulphides in the late Precambrian Dalradian Easdale Slate Formation, Argyll, Scotland. Min. Mag. (in press).

HALLIDAY,A.N. & MITCHELL, J.G. (1983). K-Ar ages of clay concentrates from Irish orebodies and their bearing on the timing of mineralistion. Trans R. Soc. Edinb. Earth Sci. **74.** 1-14.

HALTER,G., SHEPPARD,S.M.F., WEBER,F., CLAUER,N. AND PAGEL,M. (1987). Radiation-related retrograde hydrogen isotope and K-Ar exchange in clay minerals. Nature **330,** 638-640.

HAMILTON,D.L., BURNHAM,C.W. & OSBORN,E.R. (1964). The solubility of water and effects of oxygen fugacity and water content on crystallisation in mafic magmas. J. Petrol., **5,** 21-39.

HARLAND,W.B., COX,A.V., LLEWELLYN,P.G., PICKTON,C.A.G., SMITH,A.G. & WALTERS,R. (1982). A geologic time scale. Cambridge University Press.

HARRIS,A.L. & PITCHER,W.S. (1975). The Dalradian Supergroup. In: A correlation of the Precambrian rocks in the British Isles. HARRIS, A.L., SHACKLETON,R.M., WATSON,J., DOWNIE,C., HARLAND,W.B., & MOORBATH,S. (eds). 52-75. Geol. Soc. Lond. Spec. Rep. **6.**

HARRISON,T.M. (1981). Diffusion of ^{40}Ar in hornblende. Contrib. Mineral. Petrol. **78,** 324-331.

HARVEY,P.K. (1967). The geology of the Glinsk district, Connemara, Eire. Ph.D. thesis, University of Bristol. (unpublished).

HAWTHORNE,H.C. (1981). The crystal chemistry of the amphiboles. In VEBLEN,D.R. (ed.): Amphiboles and other hydrous pyroboles. Reviews in Mineralogy, **9A**, Min. Soc. Am.

HAY,S.J., HALL,J., SIMMONS,G. & RUSSELL,M.J. (1988). Sealed microcracks in the Lewisian of NW Scotland: a record of two billion years of fluid circulation. J. Geol. Soc. Lond., (in press).

HEATON,T.H.E. & SHEPPARD,S.M.F. (1977). Hydrogen and oxygen isotope evidence for seawater-hydrothermal alteration and ore deposition, Troodos Complex, Cyprus. In: Volcanic processes in ore genesis. Inst. Mining Metall. & Geol. Soc. Lond. 42-57.

HELZ,R.T. (1973). Phase relations of basalts in their melting range at P H_2O = 5 kb as a function of oxygen fugacity. Part I. Mafic phases. J. Petrol. **14.** 249-302.

HELZ,R.T. (1982). Phase relations and compositions of amphiboles produced in studies of the melting behaviour of rocks. In VEBLEN,D.R. & RIBBE,P.H. (eds): Amphiboles: petrology and experimental phase relations. Reviews in mineralogy, **9B**, Min. Soc. Am.

HODGES,F.N. (1974). The solubility of H_2O in silicate melts. Carnegie Inst. Washington Yearb., **73**, 251-255.

HOEFS,J. (1978). Chapter 6E. Abundance in common igneous rocks (carbon). In: Handbook of Geochemistry. Volume II/1. WEDEPOHL,K.H. (ed.). Springer-Verlag.

HOLDWAY,M.J. (1972). Thermal stability of Al-Fe epidote as a function of fO_2 and Fe content. Contr. Mineralogy Petrology, **37**, 307-340.

HOLLAND, C.H. (1981) (Ed.). A geology of Ireland. Scottish Academic Press Ltd. Edinburgh.

HOLLAND,H.D. (1967). Gangue minerals in hydrothermal ore deposits. In: H.L.BARNES (ed.). Geochemistry of hydrothermal ore deposits. Holt, Rinehart and Winston. New York.

HOLLOWAY,J.R. & BURNHAM,C.W. (1972). Melting relations of basalt with equilibrium water pressure less than total pressure. J. Petrol. **13**, 1-30.

HUBBERT,M.K. & RUBEY,W.W. (1959). Role of fluid pressure in mechanics of over-thrust faulting. Geol. Soc. Am. Bull. **70 (2)**, 115-166.

JACKSON,N.J., HALLIDAY,A.N., SHEPPARD,S.M.F. AND MITCHELL,J.G. (1982). Hydrothermal activity in the St. Just mining district Cornwall,

GB. In:EVANS, A.M. (ed.). Metallisation associated with acid magmatism. John Wiley & Sons. Chichester, N.Y.

JAGGER,M.D. (1985). The Cashel district of Connemara, Co. Galway, Eire: An isotopic study. Ph.D. Thesis (unpubl.). University of Glasgow.

JAGGER,M.D., MAX,M.D., AFTALION,M & LEAKE,B.E. (1988). U-Pb zircon ages of basic rocks and gneisses intruded into the Dalradian rocks of Cashel, Connemara, Western Ireland. J. Geol. Soc. Lond. **154,** 645-648.

JOHANNES,W. (1985). The significance of experimental studies in the formation of migmatites. In Ashworth,J.R. (ed.) Migmatites, 36-85, Blackie, Glasgow.

JOSWIG,W., FUESS,H., ROTHBAUER,R., TAKEUCHI,Y. AND MASON,S.A. (1980). A neutron diffraction study of a one-layer triclinic chlorite (penninite). Amer. Mineral. **65,** 349-352.

JOY,H.W. & LIBBY,W.F. (1960.) Size effects among isotopic molecules. J.Chem.Phys. **33,** 1276.

KANARIS-SOTIRIOU,R. & ANGUS,N.S. (1976). The Currywongaun-Doughruagh syntectonic intrusion, Connemara, Ireland. J. Geol. Soc. Lond. **132,** 385-508.

KAY,L.F. (1979). Oxygen and hydrogen isotope ratio-studies in Caledonian rocks of Northeast Scotland. Ph.D. Thesis (unpubl.). University of Aberdeen.

KAZAHAYA,K. & MATSUO,S. (1986). D/H and $^{18}O/^{16}O$ fractionations in NaCl aqueous solution-vapour systems at elevated temperatures. Terra Cognita **6** (2), 262.

KEENAN,J.H., KEYES,F.G., HILL,P.G., & MOORE,J.G. (1978). Steam tables, thermodynamic properties of water including vapour, liquid and solid phases. Wiley-Interscience New York.

KELL,G.S., McLAURIN,G.E. & WHALLEY,E. (1985a). The PVT properties of water V. The fluid to 1 kbar at 350-500°C and along the saturation line from 150-350°C. Phil. Trans. Roy. Soc. **A315,** 235-246.

KELL,G.S., McLAURIN,G.E. & WHALLEY,E. (1985b). The PVT properties of water VI. Deuterium oxide in the range 150-500°C and 1-100 MPa. Phil. Trans. Roy. Soc. **A315,** 247-258.

KENDALL,C., CHOU,I.-M. & COPLEN,T.P. (1983). Salt effect on oxygen isotope equilibria. Eos Trans. Am. Geophys. Union **64,** 334-335.

KENNAN,P.S. & MURPHY,FC. (1987). Tectonically reset Rb-Sr system during late Ordovician terrane assembly in Iapetus, western Ireland. Geology **15.** 1155-1158.

KENNAN,P.S., FEELY, M., & MOHR,P. (1987). The age of the Oughterard Granite, Connemara, Ireland. Geol. J. **22.** 273-280.

KERRICH,R., LATOUR, T.E. & WILLMORE, L. (1984). Fluid participation in deep fault zones : evidence from geological, geochemical and $^{18}O/^{16}O$ relations. J. Geophys. Res., **89.** 4331-4343.

KIEFFER,S.W. (1982). Thermodynamics and lattice vibrations of minerals: 5. Applications to phase equilibria, isotopic fractionation, and high pressure thermodynamic properties. Rev. Geophys. Space Phys. **20,** 827-849.

KITTEL,C. (1956). Introduction to solid state physics. Second edn. Wiley, New York.

KOKUBU,N., MAYEDA,T. & UREY,H.C. (1961). Deuterium content of minerals, rocks and liquid inclusions from rocks. Geochim. Cosmochim. Acta. **21.** 247-256.

KOVALEV,G.N. (1971). O diffuzii po granitsam zeren v gorny v prisutstvii vody. (On diffusion through the boundaries of grains in a rock in the presence of water). Dokl. Akad. Nauk. SSSR. **197.** (6), 1410-1412.

KOZLOVSKY,A. (1981). The words deepest well. Scient. Amer. **251.** 106-113.

KRONENBERG,A.K., YUND,R.A. & GILETTI,B.J. (1984). Carbon and oxygen diffusion in calcite: effects of Mn content and P_{H_2O}. Phys. Chem. Minerals. **11,** 101-112.

KULP,J.L. & ENGELS,J. (1963). Discordances in K-Ar and Rb-Sr isotopic ages. In: Radioactive dating. IAEA, Vienna. 219-238.

KURODA,Y., SUZUOKI,T. & MATSUO,S. (1977). Hydrogen isotope composition of deep seated water. Contrib. Mineral. Petrol. **60.** 311-315.

KURODA,Y., YAMADA,T., KOBAYASHI,H., OHMOTO,Y., YAGI,M. & MATSUO,S. (1986). Hydrogen isotope study of the granitic rocks of the Ryoke Belt, Central Japan. Chem. Geol. (Isotope geoscience) **58.** 283-302

KUSAKABE,M & ROBINSON,B.W. (1977). Oxygen and sulphur isotope equilibria in the $BaSO_4$-HSO_4^--H_2O system from 110 to 350°C and applications. Geochim. Cosmochim. Acta. **41.** 1033-1040.

LAMBERT,R.St. J. & MCKERROW,W.S. (1976). The Grampian Orogeny. Scott. J. Geol., **12**, 271-292.

LAOUAR,R. (1987). A sulphur isotope study of the Caledonian granites of Britain and Ireland. M.Sc. Thesis (unpubl.). University of Glasgow.

LASAGA,A.C. (1981a). Rate laws of chemical reactions. In: LASAGA,A.C. & KIRKPATRICK,R.J. (eds) Kinetics of Geochemical Processes. Reviews in Mineralogy. **8.** 1-68. Mineralogical Society of America.

LASAGA,A.C. (1981b). Dynamic treatment of geochemical cycles: global kinetics. In: LASAGA,A.C. & KIRKPATRICK,R.J. (eds) Kinetics of Geochemical Processes. Reviews in Mineralogy. **8.** 69-110. Mineralogical Society of America.

LASAGA,A.C. (1981c). Transition state theory. In: LASAGA,A.C. & KIRKPATRICK,R.J. (eds) Kinetics of Geochemical Processes. Reviews in Mineralogy. **8.** 135-169. Mineralogical Society of America.

LASAGA,A.C. (1981d). The atomistic basis of kinetics: defects in minerals. In: LASAGA,A.C. & KIRKPATRICK,R.J. (eds) Kinetics of Geochemical Processes. Reviews in Mineralogy. **8.** 261-319. Mineralogical Society of America.

LAWRENCE,J.R. & GIESKES,J.M. (1981). Constraints on water transport and alteration in the oceanic crust from the isotopic composition of pore water. J. Geophys. Res. **86.** (B9), 7924-7934.

LAZARUS,D. & NACHTRIEB,N.H. (1963). Effect of high pressure on diffusion. In: PAUL,W. & WARSCHAUER,D.M. (eds) Solids under pressure. 43-69 Mc Graw-Hill, New York.

LEAKE,B.E. (1958). The Cashel-Lough Wheelaun intrusion, Co. Galway. Proc. R. Ir. Acad. **59.** (B9), 155-203.

LEAKE,B.E. (1970a). The origin of the Connemara Migmatites of the Cashel district, Connemara, Ireland. Q. Geol. Soc. Lond. **125.** 219-276.

LEAKE,B.E (1970b). The fragmentation of the Connemara basic and ultrabasic intrusions. In Newall,G. & Rast.N. (eds), Mechanics of igneous intrusion, 103-122. Seel House Press, Liverpool. Geol. J. Spec. Iss. **2.**

LEAKE,B.E (1978a). Granite emplacement: the granites of Ireland and their origin. In Bowes,D.R. & Leake,B.E. (eds), Crustal evolution in northwestern Britain and adjacent regions. Geol. J. Spec. Iss. **10.** 221-248.

LEAKE,B.E (1978b). Nomenclature of amphiboles. Min Mag. **42.** 533-63.

LEAKE,B.E (1986). The geology of SW Connemara, Ireland : a fold and thrust Dalradian and metagabbroic-gneiss complex. J. Geol. Soc. Lond. **143.** 221-236.

LEAKE,B.E (1988). Comment on the age of the Oughterard Granite, Connemara, Ireland. J. Geol. Soc. Lond. (in press).

LEAKE,B.E & SINGH,D. (1986). The Delaney Dome Formation, Connemara, W. Ireland, and the geochemical distinction of ortho- and para-quartzofelspathic rocks. Min. Mag. **50.** 205-215.

LEAKE,B.E & SKIRROW,G. (1960). The pelitic hornfelses of the Cashel-Lough Wheelaun Intrusion, Co. Galway, Eire. J. Geol. **68.** 24-40.

LEAKE,B.E, TANNER,P.W.G. & SENIOR, A. (1981). The geology of Connemara (Map, scale 1: 63,360), University of Glasgow.

LEAKE,B.E, TANNER,P.W.G., MACINTYRE,R.M. & ELIAS,E. (1984). Tectonic position of the Dalradian rocks of Connemara and its bearing on the evolution of the Midland Valley of Scotland. Trans R. Soc. Edinb. Earth Sci. , **75,** 165-171.

LEAKE,B.E, TANNER,P.W.G., SINGH,D. and HALLIDAY,A.N. (1983). Major southward thrusting of Dalradian rocks of Connemara, Western Ireland. Nature, **305,** (5931), 210-213.

LIOU,J.G., KIM,H.S. & MARUYAMA,S. (1983). Prehnite-epidote equilibria and their petrologic applications. J. Petr., **24,** 321-342.

LIOU,J.G., MARUYAMA,S. & CHO,M. (1985). Phase equilibria and mineral paragenesis of metabasalts in low grade metamorphism. Min. Mag. **49,** 321-333.

LIVINGSTON,D.A. (1963). Chemical composition of rivers and lakes. In: Data of geochemistry. FLEISHER,M. (ed.). 6th edn. U.S. Geol. Surv. Prof. Pap. **440-G,** 64p.

MANNING,J.R. (1968). Diffusion kinetics for atoms in crystals. Van Nostrad, New York.

MANNING,J.R. (1974). Diffusion kinetics and mechanisms in simple crystals. In HOFMANN,A.W., GILETTI,B.J., YODER,H.S. & YUND,R.A. (eds) Geochemical Transport and Kinetics. Carnegie Inst. Washington Publ. **634.** 3-13.

MARUMO,K., NAGASAWA,K. & KURODA,Y. (1980). Mineralogy and hydrogen isotope geochemistry of clay minerals in the Ohnuma geothermal area, northeast Japan. Earth Planet. Sci. Lett. **47,** 255-262.

MATSUHISA,Y., GOLDSMITH.J.R. & CLAYTON,R.N. (1979). Oxygen isotope fractionation in the system quartz-albite-anorthite-water. Geochim. Cosmochim. Acta **43,** 1131-1140.

MATTHEWS,A. & KOLODNY,Y. (1978). Oxygen isotope fractionation in decarbonation metamorphism: The Mottled Zone event. Earth Planet. Sci. Lett. **39.** (1), 179-192.

MATTHEWS,A., GOLDSMITH,J.R. & CLAYTON,R.N. (1983a). On the mechanisms and kinetics of oxygen isotope exchange reactions at elevated temperatures and pressures. Geol. Soc. Am. Bull. **94,** 396-412.

MATTHEWS,A., GOLDSMITH,J.R. & CLAYTON,R.N. (1983b). Oxygen isotope fractionations involving pyroxenes: the calibration of mineral-pair geothermometers. Geochim. Cosmochim. Acta **47,** 631-644.

MATTHEWS,A., GOLDSMITH,J.R. & CLAYTON,R.N. (1983c). Oxygen isotope fractionation between zoisite and water. Geochim. Cosmochim. Acta **47,** 645-654.

MATTHEWS,A., & SCHELIESTEDT,T.M. (1984). Evolution of the Blueschist and Greenschist facies rocks of Sifnos, Cyclades, Greece. A stable isotope study of subduction-related metamorphism. Contrib. Mineral. Petrol., **88,** 150-163.

MAYEDA,T.K., GOLDSMITH,J.R. & CLAYTON,R.N. (1986). Oxygen isotope fractionation at high temperature. Terra Cognita **6,** 261 (abstract).

MAX,M.D., LONG,C.B. and GEOGHEGAN,M.A. (1978). The Galway Granite. Bull. Geol. Surv. Ireland, **2,** 223-233.

McCREA,J.M. (1950). On the isotope chemistry of carbonates and a paleotemperature scale. J.Chem.Physics **18,** 849-857.

McKERROW,W.S. & CAMPBELL, C.J. (1960). The stratigraphy and structure of the Lower Palaeozoic rocks of North West Galway. R. Dubl. Soc. Sci. Proc. Ser. A, **1,** 27-52.

MISENER, D. J. (1974). Cationic diffusion in olivine to 1400°C and 35 kbar. In: HOFMANN,A.W., GILETTI,B.J., YODER,H.S. & YUND,R.A. (eds) Geochemical Transport and Kinetics. Carnegie Inst. Washington Publ. **634.** 117-129.

MITCHELL,J.G. & MOHR,P. (1986). K-Ar systematics in Tertiary dolerites from West Connacht, Ireland. Scott. J. Geol. **22 (2),** 225-240.

MITCHELL,J.G & MOHR,P (1987). Carboniferous dikes of West Connacht, Ireland. Trans R. Soc. Edinb. Earth Sci., **78,** 133-151.

MONGKOLTIP,P. AND ASHWORTH,J.R (1986). Amphibolitisation of metagabbros in the Scottish Highlands. J. Met. Geol., **4**, 261-283.

MUEHLENBACHS,K. & CLAYTON,R.N. (1972). Oxygen isotope geochemistry of submarine greenstones. Can.J. Earth Sci. **9.** 471-478.

MUEHLENBACHS,K. & KUSHIRO,I. (1974). Oxygen isotope exchange and equlibrium of silicates with CO_2 or O_2. Carnegie Inst. Wash. Ybk. **73,** 232-236.

MYERS,O.E. AND PRESTWOOD,R.J. (1951). Chapter 1 - Isotopic exchange reactions. In: Radiochemistry applied to chemistry. WAHL, A.C. (ed), 6-43.

NABELEK,P.I., O'NEIL,J.R. & PAPIKE,J.J. (1983). Vapour phase exsolution as a controlling factor in hydrogen isotope variation in granitic rocks: The Notch Peak granitic stock, Utah. Earth Planet. Sci. Lett. **66.** 137-150.

NABELEK,P.I., LABOTKA,T.C., O'NEIL,J.R. & PAPIKE,J.J. (1984). Fluid/rock interaction between the Notch Peak granitic intrusion and argillites and limestones: Evidence from stable isotopes and phase assemblages. Contrib. Mineral. Petrol. **86.** 25-34.

NEGGA,H.S., SHEPPARD,S.M.F., ROSENBAUM,J.M. & CUNEY,M. (1986). Late Hercynian U-vein mineralisation in the Alps: fluid inclusion and C, O, H isotopic evidence for mixing between two externally derived fluids. Contrib. Mineral. Petrol. **93.** 179-186.

NORTHROP,D.A. & CLAYTON,R.N. (1966). Oxygen isotope fractionations in systems containing dolomite. J.Geol. **74,** 174-196.

NORTON,D. & KNIGHT,J. (1977). Transport phenomena in hydrothermal systems: cooling plutons. Am. J. Sci. **277,** 937-981.

NORTON,D. & TAYLOR,H.P.Jr. (1979). Quantitative simulation of the hydrothermal systems of crystallising magma on the basis of transport theory and oxygen isotope data: an analysis of the Skaerrgaard intrusion. J. Petrol. **20** (3), 421-486.

O'CONNOR,P.O.J. (1985). Geochemical and isotopic studies of the late Caledonian granitoids in Ireland. Ph.D. thesis. University of Utrecht.

OHMOTO,H. (1986). Stable isotope geochemistry of ore deposits. In: VALLEY,J.W., TAYLOR,H.P.Jr & O'NEIL,J.R. Stable isotopes in high temperature geological processes. Reviews in Mineralogy. **16.** Min.Soc.Am. 491-559.

OHMOTO,H. & RYE,R.O. (1979). The isotopes of sulphur and carbon. In: Geochemistry of hydrothermal ore deposits. BARNES,H.L. (ed.). 2nd edn. Wiley & Sons, New York. 509-567.

OLIVER,J.E. & HIDORE,J.J. (1984). Climatology. Merrill Publishing Co. Columbus, London.

O'NEIL,J.R. (1986a). Theoretical and experimental aspects of isotopic fractionation. In: VALLEY,J.W., TAYLOR,H.P.Jr & O'NEIL,J.R. Stable isotopes in high temperature geological processes. Reviews in Mineralogy. **16.** Min.Soc.Am.

O'NEIL,J.R. (1986b). Appendix: terminology and standards. In: VALLEY,J.W., TAYLOR,H.P.Jr & O'NEIL,J.R. Stable isotopes in high temperature geological processes. Reviews in Mineralogy. **16.** Min.Soc.Am.

O'NEIL,J.R. & GHENT,E.D. (1975). Stable isotope study of coexisting metamorphic minerals from the Esplanade Range, British Columbia. Geol. Soc. Am. Bull., **86,** 1708-1712.

O'NEIL,J.R. & TAYLOR,H.P.Jr. (1967). The oxygen isotope and cation exchange chemistry of feldspars. Am. Mineral. **52,** 1414-1437.

O'NEIL,J.R. & TAYLOR,H.P.Jr. (1969). Oxygen isotope equilibrium between muscovite and water. Journ. Geophys. Research, **74,** 6012-6022.

O'NEIL,J.R., CLAYTON,R.N. AND MAYEDA,T.K. (1969). Oxygen isotope fractionation in the divalent metal carbonates. J. Chem. Physics. **51,** 5547-5558.

O'NEIL,J.R., SHAW,S.E. & FLOOD,R.H. (1977). Oxygen and hydrogen isotope compositions as indicators of granite genesis in New England Batholith, Australia. Contrib. Mineral. Petrol. **62.** 313-328.

ONSTOTT,T.C. & PEACOCK,M.W. (1987). Argon retentivity in hornblendes: a field experiment in a slowly cooled metamorphic terrane. Geochim et Cosmochim Acta, **51,** 2891-2903.

ONUMA,N., CLAYTON,R.N. & MAYEDA,T.K. (1972). Oxygen isotope cosmothermometer. Geochim. Cosmochim. Acta. **36,** 169-188.

OSTWALD,W. (1900). Uber die vermeintliche Isomeric des roten und gelben Quecksilberoxyds und die Oberflachenspannung fester Korper. Z. Phys. Chem. Stoechiom. Verwandschaftslehre **34,** 495-503.

PIDGEON,R.T. (1969). Zircon U-Pb ages from the Galway granite and the Dalradian, Connemara, Ireland. Scott. J. Geol. **5 (4),** 375-392.

PIERRE,C., ORTLIEB, L. & PERSON, A. (1984). Supratidal evaporitic dolomite at Ojo de Liebre Lagoon: Mineralogical and isotopic arguments for primary crystallisation. J. Sed. Pet., **54**, 1049-1061.

POREDA,R. (1985). Helium-3 and deuterium in back-arc basalts: Lau Basin and the Mariana Trough. Earth Planet. Sci. Lett. **73.** 244-254.

POREDA,R., SHILLING,J.G. & CRAIG,H. (1986). Helium and hydrogen isotopes in ocean ridge basalts north and south of Iceland. Earth Planet. Sci. Lett. **78.** 1-17.

POWELL,R. (1978). Equlibrium thermodynamics in petrology. Harper and Row, London.

RAFTER,T.A. (1967). Oxygen isotopic composition of sulphates, part I. A method for the extraction of oxygen and its quantitative conversion to carbon dioxide for isotope ratio measurements. New Zealand J. Sci. **10**, 493-510.

RAITH,M. (1976). The Al-Fe (III) epidote miscibility gap in a metamorphic profile through the Penninic Series of the Tauern Window, Austria. Contr. Mineral. Petrol. **57**, 99-117.

RICE,J.M. & FERRY,J.M. (1982). Buffering, infiltration and the control of intensive variables during metamorphism. Reviews in Mineralogy, **10**, 263-324.

RICHET,P., BOTTINGA,Y. & JAVOY,M. (1977). A review of hydrogen, carbon, nitrogen, oxygen and chlorine stable isotope fractionation among gaseous molecules. Ann. Rev. Earth Planet. Sci. **5**, 65-110.

RICHTER,R.D. & SIMMONS, G. (1977a). Microscopic tubes in igneous rocks. Earth Plan. Sci. Lett., **34**, 1-12.

ROEDDER,E. (1984). Fluid Inclusions. Reviews in Mineralogy. **12.** Min. Soc. Am.

RUSSEL,M.J. (1978). Downward-excavating hydrothermal importance of an underlying thick Caledonian prism. Trans. Inst. Min. Metal., **87B**, 168-171.

RYE,D.M. & WILLIAMS,N. (1981). Studies of the base metal sulphide deposits at McArthur River, Northern Territory, Australia: III. The stable isotope geochemistry of the H.Y.C. Ridge and Cooley deposits. Econ. Geol. **76**, 1-26.

RYE,R.O., SCHUILING,R.D., RYE,D.M. & JANSEN,J.B.H. (1976). Carbon, hydrogen, and oxygen isotope studies of the regional metamorphic complex at Naxos, Greece. Geochim. Cosmochim. Acta, **40**, 1031-1049.

SAKAI,H. (1968). Isotopic properties of sulphur compounds in hydrothermal processes. Geochem. J. **2.** 29-49.

SAKAI,H. (1977). Sulfate - water isotope thermometry applied to geothermal systems. Geothermics, **5,** 67-74.

SCHIDLOWSKI,M., HAYES,J.M. & KAPLAN,I.R. (1983). Isotopic inferences of ancient biochemistries: carbon, sulphur, hydrogen and nitrogen. In: Earth's earliest biosphere, its origin and evolution. SCHOPF,J.W. (ed.). 149-186.

SCHLIESTEDT,M., MATTHEWS,A. & JOHANNES,W. (1986). Oxygen isotope and cation exchange systematics between plagioclase and aqueous chloride solution. Terra Cognita **6,** 262.

SEVASTOPULO, G.D. (1981). Chapter 9, Lower Carboniferous. In Holland, C.H. (ed). A Geology of Ireland. Scottish Academic Press. Edinburgh.

SHEPHERD,T.J., RANKIN,A.H. & ALDERTON,D.H.M. (1985). A practical guide to fluid inclusion studies. Blackie and Son, Glasgow.

SHEPPARD,S.M.F. (1986a). Characterisation and isotopic variations in natural waters. In: VALLEY,J.W., TAYLOR,H.P.Jr & O'NEIL,J.R. Stable isotopes in high temperature geological processes. Reviews in Mineralogy. **16.** Min.Soc.Am. 165-183.

SHEPPARD,S.M.F. (1986b). Igneous rocks: III. Isotopic case studies of magmatism in Africa, Eurasia and Oceanic islands. In: VALLEY,J.W., TAYLOR,H.P.Jr & O'NEIL,J.R. Stable isotopes in high temperature geological processes. Reviews in Mineralogy. **16.** Min.Soc.Am. 319-371.

SHEPPARD,S.M.F. & CHAREF,A. (1986). Eau oganique: caractérisation isotopique et évidence de son rôle dans le gisement Pb-Zn de Fedj-el-Adoum, Tunisie. C. R. Acad. Sci. Paris. **t302.** Série II, (19), 1189-1192.

SHEPPARD,S.M.F. & HARRIS,C. (1985). Hydrogen and oxygen isotope geochemistry of Ascension Island lavas and granites: variation with crystal fractionation and interaction with seawater. Contrib. Mineral. Petrol. **91.** 74-81.

SHEPPARD,S.M.F. & TAYLOR,H.P.Jr. (1974). Hydrogen and oxygen evidence for the origins of water in the Boulder Batholith and the Butte ore deposits, Montana. Econ. Geol. **69,** 926-946.

SHEPPARD,S.M.F., BROWN,P.E., & CHAMBERS, A.D. (1977). The Lilloise Intrusion, East Greenland: Hydrogen isotope evidence for the efflux of magmatic water into the contact metamorphic aureole. Contrib. Mineral. Petrol., **63,** 129-147.

SHEPPARD,S.M.F, NIELSON,R.L. & TAYLOR,H.P.J. (1971). Hydrogen and oxygen isotope ratios in minerals from porphyry copper deposits. Econ. Geol., **66**, 515-542.

SIMMONS,G. & RICHTER, D. (1976). Microcracks in rocks. In: The physics and chemistry of minerals and rocks. STRENS,R.G.J. (ed). 105-137.

SMITH,A.G., HURLEY, A.M. & BRIDEN, J.C. (1981). Phanerozoic paleocontinental world maps. Cambridge Earth Science Series. Cambridge University Press.

SMITH,D.L. & EVANS,B. (1984). Diffusion crack healing in quartz. J. Geophys.Res. **89**, (B6), 4125-4135.

SOFER,Z. & GAT,J.R. (1972). Activities and concentrations of oxygen-18 in concentrated salt solutions: analytical and geophysical implications. Earth Planet. Sci. Lett. **15**, 232.

SPRUNT,E.S. & NUR,A. (1979). Microcracks and healing in granites: new evidence from cathodoluminescence. Science **205**, (4405), 495-497.

STAKES,D.S. & O'NEIL,J.R. (1982). Mineralogy and stable isotope geochemistry of hydrothermally altered oceanic rocks. Earth Planet. Sci. Lett. **57.** 285-304.

STATHAM,P.J. (1976). A comparative study of the techniques for the quantitative analysis of the X-ray spectra obtained with a Si (Li) detector. X-Ray Spectrometry, **5**, 16-28.

SUZOUKI,T. & EPSTEIN,S. (1976). Hydrogen isotope fractionation between OH-bearing minerals and water. Geochim. Cosmochim. Acta **40**, 1229-1240.

SWEATMAN,T.R. & LONG,J.V.P. (1969). Quantitative electron-probe microanalysis of rock forming minerals. J. Petrol., **10**, 332-379.

SYERS,J.K., CHAPMAN,S.L., JACKSON,M.L., RED,R.W. & CLAYTON,R.N. (1968). Quartz isolation from rocks, sediments and soils for determination of oxygen isotope composition. Geochim. Cosmochim. Acta **32**, 1022-1025.

TAYLOR,B.E. & O'NEIL,J.R. (1977). Stable isotope studies of metasomatic Ca-Fe-Al-Si skarns and associated metamorphic and igneous rocks, Osgood Mountains, Nevada. Contib. Mineral. Petrol., **63**, 1-49.

TAYLOR,H.P.Jr. (1974b). Oxygen and hydrogen isotope evidence for large-scale circulation and interaction between groundwaters and igneous intrusions, with particular reference to the San Juan volcanic field, Colorado. In: HOFMANN,A.W., GILETTI,B.J., YODER,H.S. &

YUND,R.A. (eds) Geochemical Transport and Kinetics. Carnegie Inst. Washington Publ. **634.** 299-324.

TAYLOR,H.P.Jr. (1977). Water/rock interactions and the origin of H_2O in granitic batholiths. J. Geol. Soc. Lond. **133.** 509-558.

TAYLOR, H.P. & FORESTER, R.W. (1971). Low ^{18}O igneous rocks from the intrusive complex of Skye, Mull and Ardnamurchan, western Scotland. J. Petrol., **12**, 465-497.

TAYLOR,H.P.Jr. & FORESTER,R.W. (1979). An oxygen and hydrogen isotope study of the Skaergaard intrusion and its country rocks: a description of a 55-my old fossil hydrothermal system. J. Petrol. **20.** 355-419.

TAYLOR,J.R. (1982). An introduction to error analysis. The study of uncertainties in physical measurements.

THODE,H.G., MONSTER,J. & DUNFORD, H.B. (1961). Sulphur isotope geochemistry. Geochim. Cosmochim. Acta. **25.** 159-174.

THOMPSON,R.N. (1985). A model for Grampian tract evolution. Nature, **314** (11 April), 562.

TORSVIK, T.H. (1985). Magnetic properties of the Lower Old Red Sandstone lavas in the Midland Valley, Scotland; Paleomagnetic and tectonic considerations. Physics of the Earth and Planetary Interiors, **39**, 194-207.

TOURET,J. & DIETVORST, P. (1983). Fluid inclusions in high grade anatectic metamorphites. J. Geol. Soc. Lond. **140,** 635-649.

TRELOAR,P.J. (1981). Garnet-biotite-cordierite thermometry and barometry in the Cashel thermal aureole, Connemara, Ireland. Min. Mag., **44,** 183-189.

TRELOAR, P.J. (1985). Metamorphic conditions in central Connemara, Ireland. J. Geol. Soc. Lond., **142,** 77-86.

TRUESDELL,A.H. (1974). Oxygen isotope activities and concentrations in aqueous salt solutions at elevated temperatures: consequences for isotope geochemistry. Earth Planet. Sci. Lett. **23,** 387-396.

TRUESDELL,A.H., NATHENSON,M. & RYE,R.O. (1977). The effects of subsurface boiling and dilution on the isotopic compositions of Yellowstone thermal waters. J. Geophys. Res. **82.** 3694-3704.

VALLEY,J.W. (1986). Stable isotope geochemistry of metamorphic rocks. In: VALLEY,J.W., TAYLOR,H.P.Jr & O'NEIL,J.R. Stable isotopes in high temperature geological processes. Reviews in Mineralogy. **16.** Min.Soc.Am. 445-489.

VALLEY,J.W. & O'NEIL,J.R. (1981). $^{13}C/^{12}C$ exchange between calcite and graphite: a possible thermometer in Grenville marbles. Geochim. Cosmochim. Acta. **45.** 411-420.

VEBLEN, D.R. AND FERRY,J.M. (1983). A TEM study of the biotite-chlorite reaction and comparison with petrological observations. Amer. Mineral., **68,** 1160-1168.

VEIZER,J. (1983). Chemical diagenesis of carbonates: theory and application of trace element technique. In: Stable isotopes in sedimentary geology, ARTHUR,M.A. (ed.). SEPM short course notes 10.

VEIZER,J., HOLSER,W.T. & WILGUS,C.K. (1980). Correlation of $^{13}C/^{12}C$ and $^{34}S/^{32}S$ secular variation. Geochim. Cosmochim. Acta. **44.** 579-587.

VOLFINGER,M., ROBERT,J.L., VIELZEUF,D., NIEVA,A.M.R. (1985). Structural control of the chlorine content of OH-bearing silicates (micas and amphiboles). Geochim. Cosmochim. Acta. **49** (1), 37-48.

WADA,H. (1988). Microscale isotopic zoning in calcite and graphite crystals in marble. Nature **331,** 61-63.

WAGER,L.R. (1932). The geology of the Roundstone District, Co. Galway. Proc. R. Irish Acad., **41B,** 46-72.

WAGER,L.R., BROWN, C.M. & WADSWORTH, W.J. (1960). Types of igneous cumulates. J. Pet, **1,** 73-85.

WALTHER,J.V. & HELGESON,H.C. (1977). Calculation of thermodynamic properties of aqueous silica and solubility of quartz and its polymorphs at high pressures and temperatures. Am. J. Sci. **277,** 1315-1353.

WENNER,D.B. & TAYLOR,H.P.Jr. (1971). Temperatures of serpentinisation of ultramafic rocks based on $^{18}O/^{16}O$ fractionation between coexisting serpentine and magnetite. Contrib. Mineral. Petrol. **32,** 165-185.

WENNER,D.B. & TAYLOR,H.P.Jr. (1976). Oxygen and hydrogen isotope studies of a Precambrian granite-rhyolite terrane St. Francois Mountains, southeastern Missouri. Geol. Soc. Am. Bull. **87,** (11) 1587-1598.

WICKHAM,S.M. & TAYLOR,H.P.Jr. (1985). Stable isotope evidence for large scale seawater infiltration in a regional metamorphic terrane; the Trois Seigneurs Massif, Pyrenees, France. Contrib. Mineral. Petrol. **91,** 122-137.

WHITE,W.M. & PATCHETT,J. (1984). Hf-Nd-Sr isotopes and incompatible element abundances in island arcs: implications for magma origins and crust-mantle evolution. Earth Planet. Sci. Lett. **67.** 167-185.

YARDLEY,B.W.D., BARBER,J.P. & GRAY,J.R. (1987). The metamorphism of the Dalradian rocks of Western Ireland and its relation to the tectonic setting. Phil. Trans. R. Soc., **A321**, 243-270.

YARDLEY,B.W.D. & SENIOR,A (1982). Basic magmatism in Connemara, Ireland: evidence for a volcanic arc. J. Geol. Soc. Lond., **139**, 67-70.

YODER.H.S.J. & TILLEY,C.E. (1962). Origin of basalt magmas: an experimental study of natural and synthetic rock systems. J. Petrol., **3**, 342-532.

YUND,R.A. & ANDERSON,T.F. (1974). Oxygen isotope exchange between potassium feldspar and KCl solution. In: Geochemical transport and kinetics. HOFMANN,A.W., GILETTI, B.J., YODER,H.S. & YUND, R,A. (eds). Carnegie Inst. Washington Publications, **634**, 99-105.

YUND,R.A. & ANDERSON,T.F. (1978). The effect of fluid pressure on oxygen isotope exchange between feldspar and water. Geochim. Cosmochim. Acta **42**, 235-239.

YURTSEVER,Y. & GAT,J.R. (1981). Atmospheric waters. In: Stable isotope hydrology: deuterium and oxygen-18 in the water cycle. GAT,J.R. & GONFIANTINI (eds). Technical Reports Series No. **210**. IAEA, Vienna. 103-142.

ZINDLER,A., STAUDIGEL,H. & BATIZA,R. (1984). Isotope and trace element geochemistry of young Pacific seamounts: implications for the scale of upper mantle heterogeneity. Earth Planet. Sci. Lett. **70**. 175-195.

MAP. 2 REPRODUCED FROM LEAKE (1970a) WITH PERMISSION.

Geology of the Cashel District, Co. Galway

ADDITIONAL REFERENCES.

ARCULUS,R.J. & WILLS,J.A. (1980). The petrology of plutonic blocks and inclusions from the Lesser Antilles island arc. J. Petrol., **21**, 743-799.

BOTTINGA,Y. & JAVOY,M. (1973). Comments on oxygen isotope geothermometry. Earth Planet. Sci. Lett., **20**, 250-265.

BOTTINGA,Y. & JAVOY,M. (1975). Oxygen isotope partitioning among the minerals in igneous and metamorphic rocks. Rev. Geophys. Space Physics., **13**, 401-418.

BRACE,W.F. (1980). Permeability of crystalline and argillaceous rocks. Int. J. Rock Mech. Min. Sci. **17**, 241-251.

CLAYTON,R.N. & EPSTEIN,S. (1961). The use of oxygen isotopes in high temperature geological thermometry. J. Geol., **69**, 447-452.

CRISS,R.E., GREGORY,R.T. & TAYLOR,H.P.Jr. (1987). Kinetic theory of oxygen isotope exchange between minerals and water. Geochim. Cosmochim. Acta, **51**, 1099-1108.

ETHERIDGE,M.A., WALL,V.J. & VERNON,R.H. (1983). **The role of the fluid phase during regional metamorphism and deformation.** J. Met. Geol., **1** (3), 205-226.

[illegible] (1984). High fluid [illegible] regional metamorphism and deformation: Implications for mass transport and deformation mechanisms. J. Geophys. Res., 89 (B6), 4344-4358.

FLECK,R.J. & CRISS,R.E. (1985). Strontium and oxygen isotopic variations in Mesozoic and Tertiary plutons of central Idaho. Contrib. Mineral. Petrol., **90**, 291-308.

FRIEDMAN,I., SMITH,R.L., LEVIN,B. & MOORE,A. (1964). The water and deuterium content of phenocrysts from rhyolitic lavas. Chapter 15. In: Isotopic and cosmic chemistry. H.CRAIG ET AL. (eds). North Holland Publishing Co. Amsterdam. 200-204.

HERMON,R.S. (1984). Stable isotope geochemistry of Caledonian granitoids from the British Isles and East Greenland. Phys. Earth Planet. Int., **35**, 105-120.

HARRIS,A.L. (1984). The nature and timing of orogenic activity in the Caledonian rocks of the British Isles. Mem. Geol. Soc. Lond., **9**, 64p.

HATTORI,K. & MUEHLENBACHS,K. (1982). Oxygen isotope ratios of the Icelandic crust. J. Geophys. Res., **87** (B8), 6559-6565.

ADDITIONAL REFERENCES.

ARCULUS,R.J. & WILLS,J.A. (1980). The petrology of plutonic blocks and inclusions from the Lesser Antilles island arc. J. Petrol., **21**, 743-799.

BOTTINGA,Y. & JAVOY,M. (1973). Comments on oxygen isotope geothermometry. Earth Planet. Sci. Lett., **20**, 250-265.

BOTTINGA,Y. & JAVOY,M. (1975). Oxygen isotope partitioning among the minerals in igneous and metamorphic rocks. Rev. Geophys. Space Physics., **13**, 401-418.

BRACE,W.F. (1980). Permeability of crystalline and argillaceous rocks. Int. J. Rock Mech. Min. Sci. **17**, 241-251.

CLAYTON,R.N. & EPSTEIN,S. (1961). The use of oxygen isotopes in high temperature geological thermometry. J. Geol., **69**, 447-452.

CRISS,R.E., GREGORY,R.T. & TAYLOR,H.P.Jr. (1987). Kinetic theory of oxygen isotope exchange between minerals and water. Geochim. Cosmochim. Acta, **51**, 1099-1108.

ETHERIDGE,M.A., WALL,V.J. & VERNON,R.H. (1983). **The role of the fluid phase during regional metamorphism and deformation.** J. Met. Geol., **1** (3), 205-226.

[illegible] (1984). High fluid [illegible] regional metamorphism and deformation: Implications for mass transport and deformation mechanisms. J. Geophys. Res., 89 (B6), 4344-4358.

FLECK,R.J. & CRISS,R.E. (1985). Strontium and oxygen isotopic variations in Mesozoic and Tertiary plutons of central Idaho. Contrib. Mineral. Petrol., **90**, 291-308.

FRIEDMAN,I., SMITH,R.L., LEVIN,B. & MOORE,A. (1964). The water and deuterium content of phenocrysts from rhyolitic lavas. Chapter 15. In: Isotopic and cosmic chemistry. H.CRAIG ET AL. (eds). North Holland Publishing Co. Amsterdam. 200-204.

HERMON,R.S. (1984). Stable isotope geochemistry of Caledonian granitoids from the British Isles and East Greenland. Phys. Earth Planet. Int., **35**, 105-120.

HARRIS,A.L. (1984). The nature and timing of orogenic activity in the Caledonian rocks of the British Isles. Mem. Geol. Soc. Lond., **9**, 64p.

HATTORI,K. & MUEHLENBACHS,K. (1982). Oxygen isotope ratios of the Icelandic crust. J. Geophys. Res., **87** (B8), 6559-6565.

JAVOY,M. (1977). Stable isotopes and geothermometry. J. geol. Soc. Lond., **133,** 609-636.

KAWABE,I. (1978). Calculation of oxygen isotope fractionation in quartz-water system with special reference to the low temperature fractionation. Geochim. Cosmochim. Acta, **42,** 613-621.

KYSER,T.K. (1986). Stable isotope variations in the mantle. In: VALLEY,J.W., TAYLOR,H.P.JR & O'NEIL,J.R. (eds.) Stable isotopes in high temperature geological processes. Reviews in Mineralogy. **16.** Min. Soc. Am. 141-164.

KYSER,T.K. & O'NEIL,J.R. (1984). Hydrogen isotope systematics of submarine basalts. Geochim. Cosmochim. Acta, **48,** 2123-2133.

KYSER,T.K., O'NEIL,J.R. & CARMICHAEL,I.S.E. (1982). Oxygen isotope thermometry of basic lavas and mantle nodules. Contrib. Mineral. Petrol., **77,** 11-23.

LEGGO,P.J., COMPSTON,W. & LEAKE,B.E. (1966). The geochronology of the Connemara granites and its bearing on the antiquity of the Dalradian series. Q. J. Geol. Soc. Lond., **122,** 91-118.

MONSTER,J., APPEL,P.W.U., THODE,H.G., SCHIDLOWSKI,M. & CARMICHAEL,C.M. (1979). Sulphur isotope studies in early Archaean sediments from Isua, West Greenland: Implications for the antiquity of bacterial sulphate reduction. Geochim. Cosmochim. Acta, **43,** 405-413.

MUEHLENBACHS,K. (1986). Alteration of the oceanic crust and the ^{18}O history of seawater. In: VALLEY,J.W., TAYLOR,H.P.JR & O'NEIL,J.R. (eds.) Stable isotopes in high temperature geological processes. Reviews in Mineralogy. **16.** Min. Soc. Am. 425-444.

OHMOTO,H. (1972). Systematics of sulphur and carbon isotopes in hydrothermal ore deposits. Econ. Geol. **67,** 551-579.

PATCHETT,P.J. (1980). Thermal effects of basalt on continental crust and crustal contamination of magmas. Nature, **283** (5747), 559-561.

SHACKLETON,N.J. & KENNET,J.P. (1975). Paleotemperature history of the Cenozoic and the initiation of Antarctic glaciation: oxygen and carbon isotope analyses in DSDP sites 277, 279 and 281. In: J.P. KENNET, R.E. HOUTZ *ET AL.* (eds.), "Initial reports of the Deep Sea Drilling Project", **XXIX**, Washington (U.S. Government Printing Office), 743-755.

SHIRO,Y. & SAKAI,H. (1972). Calculation of the reduced partition function ratios of alpha-beta quartz and calcite. Japan Chem. Soc. Bull., **45,** 2355-2359.

TAYLOR,B.E. (1986). Magmatic volatiles: Isotopic variation in C, H and S. In: VALLEY,J.W., TAYLOR,H.P.JR & O'NEIL,J.R. (eds.) Stable isotopes in high temperature geological processes. Reviews in Mineralogy. **16.** Min. Soc. Am. 185-225.

TAYLOR,H.P.Jr. & SHEPPARD,S.M.F. (1986). Igneous rocks: I processes of isotope fractionation and isotope systematics. In: VALLEY,J.W., TAYLOR,H.P.JR & O'NEIL,J.R. (eds.) Stable isotopes in high temperature geological processes. Reviews in Mineralogy., **16.** Min. Soc. Am. 227-271.

YARDLEY,B.W.D., SHEPHERD,T.J. & BARBER,J.P. (1983). Fluid inclusion studies of high-grade rocks from Connemara, Ireland. In: ATHERTON & GRIBBLE (eds.), High grade metamorphism and migmatites. Shiva, Nantwich.

YODER,H.S.Jr. (1976). Generation of basaltic magma. National Academy of Sciences. Washington, D.C.